

Disrupting inhibitory-kappaB kinase (IKK)-Aurora kinase signalling in prostate cancer cells.

Stuart McEwan

A Thesis submitted for the fulfilment of the requirements for the
degree of Doctor of Philosophy.

2021

Strathclyde Institute of Pharmacy and Biomedical Sciences
(SIPBS)
Glasgow, UK

This thesis is the result of the author's original research. It has been composed by the author and has not been previously submitted for examination which has led to the award of a degree.

The copyright of this thesis belongs to the author under the terms of the United Kingdom Copyright Acts as qualified by University of Strathclyde Regulation 3.50. Due acknowledgement must always be made of the use of any material contained in, or derived from, this thesis.

Signed:

Date: 30/04/2021

Stuart McEwan

ACKNOWLEDGEMENTS

Firstly, I would like to thank my supervisor, Dr Andrew Paul for all his help and patience with me over the years. I am very grateful for the opportunity to carry out this PhD in the 1st place and I will be forever appreciative for everything. I would also like to thank my 2nd Supervisor Robin Plevin for the support too. A special mention has to go to Dr Kathryn McIntosh for her help with experiments in the lab and Calum McMullen who helped me get through when times seemed tough. I'd also like to thank the level 4 lab area for making the whole experience enjoyable on a day to day basis. A big hand also has to go to my family and friends for the support in getting through my PhD as well as putting up with me during the writing up period. Lastly, I would like to thank my girlfriend Chloe for helping pick me up every day and continue to encourage me to finish my PhD, it's the little things like this that mean a lot.

Contents

Abstract	1
Chapter 1: Introduction	2
1.1. Cancer	3
1.2. Prostate cancer	5
1.3 Current treatments of Prostate Cancer	7
<u>1.3.1. Active surveillance/Watchful waiting</u>	8
<u>1.3.2. Radical prostatectomy (surgery)</u>	8
<u>1.3.3. External beam radiation therapy (EBRT)</u>	8
<u>1.3.4. Brachytherapy</u>	9
<u>1.3.5. Cryotherapy</u>	10
<u>1.3.6. High Intensity Focal Ultrasound (HIFU)</u>	10
<u>1.3.7. Immunotherapy</u>	10
<u>1.3.8. Prostate cancer vaccine</u>	12
<u>1.3.9. Androgen deprivation therapy (ADT)/Hormone deprivation therapy (HDT)</u>	13
1.4. Genetic and molecular basis of prostate cancer	14
1.5. Regulation of the NF-κB signalling pathway	15
<u>1.5.1. NF-κB family members</u>	15
<u>1.5.2. Inhibitory kappa B Kinases (IKKs) in regulation of the canonical and non-canonical NF-κB pathways</u>	16
1.6. NF-κB signalling in the regulation of cancer hallmarks	19
1.7. IKK-NF-κB in prostate cancer	21
1.8. IKK inhibitors	22
<u>1.8.1. ATP-competitive inhibitors</u>	22
<u>1.8.2. Allosteric inhibitors</u>	24
<u>1.8.3. Targeting protein-protein interactions of the IKKs – the use of cell-permeable peptides (CPPs) challenging IKK-NEMO binding</u>	25
1.9. NF-κB-independent IKK-dependent substrates	28
1.10. Aurora Kinase Family	29
<u>1.10.1. AURKA</u>	30
<u>1.10.1.1 TPX2</u>	32
1.10.2. AURKB.....	34
<u>1.10.3. AURKC</u>	35
1.11. AURKs and cancer	36
<u>1.11.1 AURKA in prostate cancer</u>	38
1.12. Aurora kinase inhibitors	39
<u>1.12.1. ATP-competitive inhibitors</u>	39
1.13. AURKA/TPX2 in cancer	42

1.13.1. Allosteric inhibitors (of the AURKA/TPX2 complex).....	44
1.14. Cross-talk between IKKs and AURKA.	46
1.14.1 Mapping of the PPIs of the IKKs and the AURKs.	47
1.15. Aims of the study.	47
Chapter 2: Materials and Methods.	50
2.1. Materials	51
2.1.1. Antibodies.	51
2.1.2. Reagents.....	53
2.1.2.1. Reagents for cell culture and transfection.	54
2.1.2.2. Small molecule kinase inhibitors targeting IKKs and Aurora kinases.	54
2.1.2.3. Reagents for targeted rundown of expression.....	57
2.1.2.4. Reagents/equipment for phenotypic assays.....	57
2.1.2.5. NEMO-Binding Domain Peptides derived from IKK β	57
2.2.1. Cell Culture.	59
2.2.1.1. Cell lines.	59
2.2.1.2. Cell culture.	60
2.2.1.3. Cell subculture.	60
2.2.2. Cell synchronisation.	60
2.2.2.1. Nocodazole trap: arresting cells at pro-metaphase in the cell cycle	60
2.2.3. Western Blotting and Sample Preparation (whole cell extracts (WCEs)).	61
2.2.3.1. Sample Preparation.	61
2.2.3.2. SDS-Polyacrylamide Gel Electrophoresis.	61
2.2.3.3. Electrophoretic Transfer of Proteins to a Nitrocellulose Membrane.	62
2.2.3.4. Immunological Detection of Protein through Antisera.	62
2.2.3.5. Nitrocellulose membrane stripping and reprobing.	63
2.2.4. Fluorescence-Activated Cell Sorting to assess cell cycle status.	63
2.2.5. Pharmacological and molecular techniques used to target the IKK-NF-κB and AURKA-TPX2 signalling pathways.	64
2.2.5.1. Targeting IKK-NF- κ B and IKK-AURKA protein-protein interactions using cell permeable short-length NBD peptide.....	64
2.2.5.2. Targeting cellular IKK catalytic activity using small molecule (SM) isoform selective IKK inhibitors.....	64
2.2.5.3. Cellular depletion of IKK α / β protein expression using transfection of short-inhibitory RNA (siRNA) sequences transfection.	65
2.2.5.4. Targeting of PPIs and protein expression in cells using NBD CPPs and siRNA IKK α and IKK β alone or in combination.....	65
2.2.6. Pharmacological techniques used to target IKK-NF-κB and IKK-AURKA signalling	66
2.2.6.1. NBD CPPs as agent alone or in combination with ATP-competitive Aurora kinase inhibitors.	66

2.2.7. Phenotypic assays to assess dual targeting of IKK/AURK signalling.	66
2.2.7.1. Cell viability assay	66
2.2.7.2. Clonogenic survival assay	67
2.2.7.3. Apoptosis assay	67
2.8 Statistical Analysis.	68
2.8.1. Data Analysis	68
2.8.2. Combination Index Analysis (CIA)	68
2.8.3. Image processing and analysis	68
Chapter 3: Characterising the mechanism of cross-talk between IKK-AURKA signalling in PCa cells – examining the impact of a NBD-derived cell permeable peptide.	70
3.1. Introduction.	71
3.2. Examining the status of AURKs and NF-κB components in PC3 cells through mitosis	74
3.2.1. Assessment of the status of AURKA and cell cycle components following Nocodazole mediated cell cycle arrest/trap and release	74
3.2.2. Status of NF- κ B components in PC3 cells following Nocodazole mediated trap and release	81
3.3. Elucidating the relationship between IKK and AURK signalling in PC3 cells via the use of pharmacological interventions.	83
3.3.1. Effects of NBD WT CPP on the status of AURKA and cell cycle markers following nocodazole trap and release in PC3 cells	83
3.3.2. Effects of the NBD WT CPP on agonist-stimulated canonical NF- κ B activation	87
3.3.3. Effects of NBD WT CPP on agonist-stimulated non-canonical NF- κ B activation	88
3.3.4. Effects of small molecule IKK-kinase inhibitors on agonist-stimulated NF- κ B signalling	92
3.3.5. Effect of a small molecule IKK α -selective kinase inhibitor on agonist-stimulated canonical NF- κ B signalling	96
3.3.6. Effect of a small molecule IKK β -selective kinase inhibitor on agonist-stimulated non-canonical NF- κ B signalling	97
3.3.7. Effects of small molecule IKK α and IKK β inhibitors on the status of AURKA and cell cycle markers in synchronised PC3 cells	99
3.3.8. Effects of siRNA IKK α and IKK β on agonist-stimulated NF- κ B signalling	105
3.3.9. Effects of siRNA run-down of IKKs on AURKA and cell cycle markers status following nocodazole trap and release in PC3 cells	109
3.3.10. Effects of NBD CPPs in the absence and presence of siRNA IKKs on the status of AURKA and cell cycle markers in synchronised PC3 cells	114
3.4. Examining the status of AURKs and related markers in MEF cells through mitosis.	121
3.4.1. Assessment of the status of AURKA and cell cycle components following Nocodazole mediated cell cycle arrest/trap and release in Double-knockout (DKO) MEF cells	121

3.4.2. Effects of NBD WT CPP on the status of AURKA and cell cycle markers following nocodazole trap and release in DKO MEF cells.	126
3.4.3. Assessment of the status of AURKA and cell cycle components following Nocodazole mediated cell cycle arrest/trap and release in Wild-type (WT) MEF cells. .	129
3.4.4. Effects of NBD WT CPP on the status of AURKA and cell cycle markers following nocodazole trap and release in WT MEF cells.	133
3.5. Discussion.	137
3.5.1. IKK/Aurora signalling in the cell cycle.	138
3.5.2. Pharmacologically challenging the IKK-Aurora interaction.	140
3.5.3. Determining the impact of the NBD CPPs on IKK-AURK signalling in a ‘double knock-out’ model.	143
3.5.4. Conclusions.	146
Chapter 4: The effect of NBD CPP-mediated targeting of AURKA and associated proteins and potential impact phenotypically in a variety of solid tumour cell lines.	148
4.1. Introduction.	149
4.2. Determining the effect of the NBD WT CPP mechanistically on AURKA signalling and phenotypically on cell viability in solid tumour cell lines.	150
4.2.1. Optimisation of Nocodazole-mediated cell synchronisation conditions in different cancer cell lines (LNCaP AI, MCF7 and T98G cells).	150
4.2.2. Assessment of the status of AURKA and cell cycle components following Nocodazole mediated cell cycle arrest/trap and release in LNCaP AI, MCF7 and T98G cells.	152
4.2.3. Effects of the NBD WT CPP on the status of AURKA and cell cycle markers following nocodazole trap and release in LNCaP AI, MCF7 and T98G cells.	161
4.2.4. Effects of the NBD CPPs on cell viability in PC3, LNCaP AI, MCF7 and T98G cells.	172
4.3. Discussion.	176
4.3.1. NBD CPP targeting of AURKA signalling in other solid tumour cell lines.	176
4.3.2. NBD CPP targeting of cell growth in different cancers.	178
4.3.3. Conclusions.	179
Chapter 5: Characterisation of pharmacological targeting of AURK phosphorylation and expression with small molecule AURK kinase inhibitors in the absence or presence of NBD CPPs in PCa cells.	181
5.1. Introduction.	182
5.2. Effect of AURK inhibitors and NBD CPPs alone or in combination on the status of p-AURKs, AURKA and TPX2.	184
5.2.1. Assessment of the efficacy of ATP-competitive AURK inhibitors on AURK signalling following nocodazole trap and release in PC3 cells.	184
5.2.2. Effect of AURK inhibitor II alone or in combination with NBD WT CPP on AURKA status/signalling.	196
5.2.3. Effect of AURK inhibitor III alone and in combination with NBD WT CPP on AURKA signalling.	201

5.2.4. Effect of Aurora kinase/CDK inhibitor alone or in combination with NBD WT CPP on AURKA-TPX2 signalling.	207
5.2.5. Effect of VX-680 alone and in combination with NBD WT CPP on AURKA-TPX2 signalling.	213
5.2.6. Effect of ZM 447439 alone and in combination with NBD WT CPP on AURKA signalling.	219
5.3. Discussion.	225
5.3.1. Single-agent pharmacological targeting of AURK signalling.	225
5.3.2. Dual pharmacological targeting of AURKA-TPX2 signalling.	227
5.3.3. Conclusions.	228
Chapter 6: Characterising the phenotypic outcomes of disrupting AURKA-TPX2 signalling in PCa cells.	231
6.1. Introduction.	232
6.2. Effect NBD CPPs or AURK inhibitors alone and in combination on phenotypic characteristics of prostate cancer cells.	234
6.2.1. Effect of NBD WT CPPs on cell viability and clonogenic survival in PC3 cells.	234
6.2.2. Effect of AURK inhibitor II and NBD WT CPP alone and in combination on cell viability and clonogenic survival of prostate cancer cells.	237
6.2.3. Effect of AURK inhibitor III and NBD WT CPP alone and in combination on cell viability and clonogenic survival of prostate cancer cells.	243
6.2.4. Effect of Aurora kinase/CDK inhibitor and NBD WT CPP alone and in combination on cell viability and clonogenic survival of prostate cancer cells.	249
6.2.5. Effect of ZM 447439 and NBD WT CPP alone and in combination on cell viability and clonogenic survival of prostate cancer cells.	255
6.2.6. Effect of VX-680 and NBD WT CPP alone and in combination on cell viability and clonogenic survival of prostate cancer cells.	261
6.2.7. Effect of VX-680 and NBD WT CPP alone and in combination on the induction of apoptosis in prostate cancer cells.....	267
6.3. Discussion.	269
6.3.1. Dual pharmacological targeting and the impact on cancer cell viability and survival.	269
6.3.2. Combination treatment and the impact on the growth of 3D cultures and the induction of cell death.	271
6.3.3. Conclusions.	272
Chapter 7: GENERAL DISCUSSION.	273
7.1. Targeting IKK-AURKA interactions.	274
7.2. Targeting IKK-AURKA-TPX2 signalling.	278
7.3. Additional future work.	280
7.4. Conclusions.	282
References	284

LIST OF FIGURES.

Chapter 1

Figure 1.1.	Androgen receptor (AR) signalling.	6
Figure 1.2.	The canonical (classical) and non-canonical (alternative) NF- κ B signalling pathways.	17
Figure 1.3	NF- κ B independent IKK dependent substrates.	28
Figure 1.4.	Schematic representing the structure of all three Aurora kinase family members.	29

Chapter 3

Figure 3.1.	Effect of nocodazole trap and release on cell cycle distribution in PC3 cells.	78
Figure 3.2	Effect of Nocodazole trap and release on AURKs and related protein markers of mitosis in PC3 cells.	80
Figure 3.3.	Effect of Nocodazole trap and release on NF- κ B markers in PC3 cells	81
Figure 3.4.	Impact of NBD WT CPP on AURKs and related protein markers of mitosis in PC3 cells.	85
Figure 3.5.	Impact of the NBD WT CPP on canonical NF- κ B markers in PC3 cells.	87
Figure 3.6.	Impact of NBD WT CPP on non-canonical NF- κ B markers in PC3 cells.	90
Figure 3.7.	Impact of small molecule isoform-selective IKK α and IKK β kinase inhibitors on non-canonical and canonical NF- κ B markers in PC3 cells.	93
Figure 3.8.	Impact of an IKK α -selective kinase inhibitor on canonical NF- κ B cellular markers.	96
Figure 3.9.	Impact of a small molecule IKK β -selective kinase inhibitor on non-canonical NF- κ B cellular markers in PC3 cells.	98
Figure 3.10.	Impact of small molecule isoform-selective IKK inhibitors on AURKs and related protein markers of mitosis and IKK proteins	101

in PC3 cells.	
Figure 3.11. Impact of isoform-selective IKK α and IKK β siRNA on non-canonical and canonical NF- κ B markers in PC3 cells.	105
Figure 3.12. Impact of isoform-selective siRNA targeting of IKKs on AURKs and related protein markers of mitosis and IKK proteins in PC3 cells.	111
Figure 3.13. Impact of siRNA targeting IKKs and NBD CPPs alone or in combination on AURKs and related markers in synchronised PC3 cells.	115
Figure 3.14. Effect of Nocodazole trap and release on AURKs and related protein markers of mitosis in DKO MEFS.	122
Figure 3.15. Impact of NBD CPPs on AURKs and related protein markers of mitosis in DKO MEF cells.	126
Figure 3.16. Effect of Nocodazole trap and release on AURKs and related protein markers of mitosis in WT MEF cells.	130
Figure 3.17. Impact of NBD WT CPP on AURKA and related protein markers of mitosis in WT MEF cells.	133

Chapter 4

Figure 4.1. Effect of different concentrations of Nocodazole trap and release on p-AURKs in LNCaP AI, MCF7 and T98G cells.	150
Figure 4.2. Assessment of the status of cell cycle markers following Nocodazole trap and release in LNCaP AI, MCF7 and T98G cells.	154
Figure 4.3. Impact of NBD WT CPP on AURKs and related protein markers of mitosis in LNCaP AI, MCF7 and T98G cells.	164
Figure 4.4. Impact of NBD CPPs on cell viability of solid tumour cell lines.	172

Chapter 5

Figure 5.1. Effect of different concentrations of AURK inhibitors (AURK inhibitor II, AURK inhibitor III, Aurora kinase/CDK inhibitor, VX-680 or ZM 447439) on phosphorylation of Aurora kinases.	186
Figure 5.2. Effect of AURK inhibitor II alone or in combination with NBD WT CPP on AURKs and related protein markers of mitosis in PC3 cells.	194
Figure 5.3. Effect of AURK inhibitor III alone or in combination with NBD WT CPP on AURKs and related protein markers of mitosis in PC3 cells.	200

Figure 5.4. Effect of Aurora kinase/CDK inhibitor alone and in combination with NBD WT CPP on AURKs and related protein markers of mitosis in PC3 cells.	206
Figure 5.5. Effect of VX-680 alone and in combination with NBD WT CPP on AURK and related protein markers of mitosis in PC3 cells.	211
Figure 5.6. Effect of ZM 447439 alone and in combination with NBD WT CPP on AURK and related protein markers of mitosis in PC3 cells.	218

Chapter 6

Figure 6.1. Effect of NBD CPPs treatment on clonogenic survival of PC3 cells.	231
Figure 6.2. Effect of NBD MT/WT CPP and AURK inhibitor II alone or in combination on cell viability and clonogenic survival of PC3 cells.	235
Figure 6.3. Effect of NBD MT/WT CPP and AURK inhibitor III alone or in combination on cell viability and clonogenic survival of PC3 cells.	241
Figure 6.4. Effect of NBD MT/WT CPP and Aurora kinase/CDK inhibitor alone or in combination on cell viability and clonogenic survival of PC3 cells.	247
Figure 6.5. Effect of NBD MT/WT CPP and ZM447439 alone or in combination on cell viability and clonogenic survival of PC3 cells.	253
Figure 6.6. Effect of NBD MT/WT CPP and VX-680 alone or in combination on cell viability and clonogenic survival of PC3 cells.	259
Figure 6.7. Effect of NBD MT/WT CPP and VX-680 alone or in combination on induction of apoptosis in PC3 cells.	264

Chapter 7

Figure 7.1. Molecular and Pharmacological techniques to investigate mechanisms of IKK-AURKA through different features of the IKK proteins.	272
--	-----

List of Tables

Table 1.1. Aurora kinases localisation and function and cancers which they are expressed in.	37
---	----

Abbreviation List

ABIN	- A20-Binding Protein
ADP	- Adenosine Diphosphate
ADT	- Androgen Deprivation therapy
ALL	- Acute Lymphoblastic Leukaemia
AKT	- Protein kinase B
AML	- Acute Myeloid Leukaemia
ANOVA	- Analysis of variance
ANTP	- Antennapedia
APC	- Adenomatous polyposis coli
APC/C	- Anaphase Promoting Complex/Cyclosome
APS	- Ammonium Persulfate
AR	- Androgen Receptor
ATM	- Ataxia telangiectasia mutated
ATP	- Adenosine triphosphate
AURKA/B/C	- Aurora kinase A/B/C
Bax	- Bcl-2-associated X protein
βTrCP	- β-transducin repeat-containing protein
Bcl2	- B-cell leukemia 2
Bcl-xL	- B-cell lymphoma-extra Large
Bim	- Bcl-2-like protein 11
BMS	- Bristol Myers Squibb
BSA	- Bovine Serum Albumin
CBP	- CREB Binding Protein
CD28	- Cluster of Differentiation 28
CDE	- Cell cycle-Dependent Element
CDK	- Cyclin Dependent Kinase
CHR	- Cell cycle gene homology region
CML	- Chronic Myeloid Leukaemia
CIA	- Collagen-Induced Arthritis
c-IAP	- c-Inhibitor of Apoptosis
CIKS	- Connection to IKK and SAPK xiv
CO-IP	- co-Immunoprecipitation

COPD	- Chronic Obstructive Pulmonary Disease
COX	- Cyclo-oxygenase
CPP	- Cell Permeable Peptide
CRPC	- Castration-resistant prostate cancer
CTLA-4	- Cytotoxic T-lymphocyte-associated protein 4
DHT	- Dihydrotestosterone
DNA	- Deoxyribonucleic Acid
DRE	- Digital rectal examination
DS	- Disulfiram
DSS	- Dextran Sulfate Sodium
DTT	- Dithiothreitol
EAE	- Experimental allergic encephalomyelitis
EBRT	- External-beam radiation therapy
ECL	- Enhanced Chemiluminescence
EGF	- Epidermal Growth Factor
EGFR	- Epidermal Growth Factor Receptor
EMT	- epithelial–mesenchymal transition
ER α	- Oestrogen Receptor- α
ERK	- Extracellular signal-regulated kinases
ETS	- E-twenty six
FCS	- Foetal Calf Serum
FDA	- Food and Drug Administration
FLT3	- Fms-related tyrosine kinase 3
FOXO3a	- Forkhead Box O3a
FSH	- Follicle Stimulating Hormone
GAB-P	- GA-Binding Protein
GFAP	- Glial fibrillary acidic protein
GM-CSF	- Granulocyte-Macrophage Colony-Stimulating Factor
HCC	- Hepatocellular Carcinoma cells
HDR	- High dose rate
HDT	- Hormone deprivation therapy
HEK	- Human Embryonic Kidney
HEPES	- 4-(2-hydroxyethyl)-1-piperazineethanesulfonic acid
HER-2	- Human epidermal growth factor receptor 2
HLA-A2	- Human leukocyte antigen-A2

HLH	- Helix-loop-Helix xv
HNSCC	- Head and Neck Squamous Cell Carcinoma
HPV	- Human Papilloma Virus
HRT	- Hormone replacement therapy
Hsps	- Heat-Shock Proteins
HTS	- High-Throughput Screening
IAP	- Inhibitor of Apoptosis
IBD	- Inflammatory Bowel Disease
IC50	- Inhibitory Concentration (50%)
IgG	- Immunoglobulin G
IKIP	- IKK Interacting Protein
IKK	- Inhibitory κ B Kinase
I κ B	- Inhibitor of κ B
IL-1	- Interleukin-1
IL-2	- Interleukin-2
IL -6	- Interleukin-6
IMRT	- Intensity modulated radiation therapy
INCENP	- Inner Centromere Protein
IRFs	- Interferon Regulatory Factors
JNK	- c-Jun N-terminal Kinase
KO	- Knockout
KRAS	- Kirsten rat sarcoma viral oncogene homolog
kDa	- Kilo-Dalton
LDR	- Low dose rate
LH	- Luteinizing hormone
LH-RH	- Luteinizing hormone-releasing hormone
LPS	- Lipopolysaccharide
LT- α	- lymphotoxin- α
MAB	- Maximal androgen blockade
MAPK	- Mitogen-activated protein kinases
MCAK	- Mitotic Centromere-Associated Kinesin
MCL-1	- Induced myeloid leukemia cell differentiation protein 1
MDM2	- Murine double minute 2
MEFs	- Murine Embryonic Fibroblasts
MMP	- Matrix Metallo-Proteinase

NBD	- NEMO-Binding Domain
NDEL 1	- Nuclear distribution protein nudE-like 1
NEMO	- NFκB Essential Modulator
NIK	- NFκB inducing kinase
NF-κB	- Nuclear Factor kappa B
NLS	- Nuclear Localisation Sequence
NNK	- Nicotine-derived nitrosamine ketone
NSAIDs	- Non-Steroidal Anti-Inflammatory Drugs
OCT4	- octamer-binding transcription factor 4
ORF	- Open Reading Frame
PAGE	- Polyacrylamide gel electrophoresis
PAH	- Polycyclic aromatic hydrocarbons
PAK1	- Protein Activated Kinase 1
PAP	- Protein acid phosphatase
PBS	- Phosphate Buffered Saline
PCM	- Pericentriolar Material
PDGF	- Platelet Derived Growth Factor
PD-L1	- Programmed death ligand 1
PEI	- Polyethylenimine
PGE	- Prostaglandin E
PI3K-Akt	- phosphatidylinositol 3-kinase-Akt
PIN	- Prostatic Intraepithelial Neoplasia
PLK1	- Polo-like kinase 1
PMA	- Phorbol Myristoyl Acetate
PMBC	- Peripheral Blood Mononuclear Cells
PPI	- Protein-Protein Interaction
PP1A	- Protein Phosphatase 1A
PRE	- Positive Regulatory Element
PUMA	- p53 upregulated modulator of apoptosis
PSA	- Prostate Specific Antigen
RA	- Rheumatoid Arthritis
RAN	- RAS-related Nuclear protein
RANK	- Receptor Activator for Nuclear Factor κB
RANKL	- RANK ligand

RANTES	- Regulated upon Activation, Normal T cell Expressed and Secreted
RCC1	- Regulator of chromosome condensation 1
RHD	- Rel Homology Domain
RNA	- Ribonucleic Acid
ROS	- Reactive Oxygen Species
SAR	- Structure Activity Relationship
SAC	- Spindle Assembly Checkpoint
SDS	- Sodium dodecyl sulphate
siRNA	- Small interfering RNA
SLUG	- Zinc finger protein SNAI2 (chicken homolog)
SMC	- Structural Maintenance of Chromosomes
SMRT	- Silencing Mediator for Retinoic Acid and Thyroid Hormone Receptor
SOD	- Superoxide Dismutase
SSC	- Sodium Sodium Citrate
TACC3	- Transforming Acidic Coiled-coil-Containing protein 3
TAD	- Transcriptional Activation Domains
TAMS	- Tumour-Associated Macrophages
TAT	- Trans-Activator of Transcription
TNBS	- Trinitrobenzene sulphonic acid
TPX2	- Targeting protein for Xklp2
TRAFs	- TNF-Receptor-Associated Factors
TBK1	- TANK-Binding Kinase 1
TLR	- Toll Like Receptor
TNF- α	- Tumour Necrosis Factor- α
TRAMP	- Transgenic Adenocarcinoma of Mouse Prostate
UVR	- Ultraviolet radiation.
VEGF	- Vascular Endothelial Growth Factor
WT	- Wild Type

Abstract

Prostate cancer (PCa) is the second most common cause of cancer-related death in men. Aurora kinase A (AURKA) is commonly overexpressed in PCa and when active is bound to its activating cofactor, Targeting protein for Xklp2 (TPX2), preventing the dephosphorylation and degradation of AURKA. AURKA interacts with the I κ B kinase (IKK) proteins, IKK α , IKK β , and IKK γ or NF-kappa-B essential modulator (NEMO). From mapped binding studies an IKK β -derived NEMO-binding domain (NBD) peptide was developed as a competitive disruptor of IKK-AURKA signalling and was hypothesised to allosterically modulate AURKA-TPX2 status. The NBD peptide in a cell-permeable (CPP) Wild-type form (WT; 100 μ M), also known to inhibit canonical NF- κ B activation, was identified to significantly ($p < 0.05$) accelerate AURKA dephosphorylation/degradation through mitosis and had a similar effect on TPX2, Polo-like kinase-1 (PLK1) status in PC3 prostate cancer cells. Pharmacological and molecular techniques alongside genetically modified cell models (wild type and *ikka*^{-/-}/*ikkb*^{-/-}-double 'knockout' (KO) murine embryonic fibroblasts (MEFs)) were used to target/characterise different aspects of IKK signalling and so elucidate the mechanism of disrupting IKK-AURKA signalling. Small molecule inhibitors and siRNA targeting IKK α/β had minimal effect upon AURKA and TPX2 status. The NBD WT CPP caused mechanistic disruption of AURKA-TPX2-PLK1 status and phenotypic characteristics in different solid tumours; LNCaP AIs (AR+ve prostate cancer); MCF7 (ER+ve breast cancer), T98G (glioblastoma). NBD WT CPP plus ATP-competitive AURK inhibitors significantly ($p < 0.05$) accelerated AURK dephosphorylation/degradation and TPX2 degradation in PCa cells which correlated with a synergistic (CI < 1) inhibition of phenotypic outcomes - rank order of potency: VX-680 > ZM447439 > Aurora kinase/CDK inhibitor > Aurora kinase inhibitor II > Aurora kinase inhibitor III. Hence, the NBD peptide may support two-site targeting of AURKA-TPX2 signalling, potentially improve access to the AURKA catalytic site and therefore be an advance towards pre-clinical molecules/mimetics that can potentially enhance the efficacy and clinical outcome of AURK inhibitors.

Chapter 1: Introduction

1.1. Cancer.

Cancer is an illness which affects around 18.1 million people and causes around 9.6 million deaths each year (based on studies by the WHO in 2018). It is defined by the aberrant division of cells in the body and this can affect a host of different organs of the body with the most prevalent being lung, bowel, breast and prostate (Bray et al., 2018). Cancer was classified as displaying six distinct features which were known as the six hallmarks of cancer. These involve; avoiding growth suppressors, sustaining proliferative signalling, permitting replicative immortality, promoting angiogenesis, resisting cell death and activating invasion and metastasis (Hanahan and Weinberg, 2000). These were later re-established as the 10 hallmarks of cancer with the aforementioned above plus additional characteristics; Genome instability and mutation, deregulated cellular energetics, avoiding immune destruction and tumour promoting inflammation (Hanahan and Weinberg, 2011). Cancers can be termed as either benign or malignant tumours with both possessing the ability of uncontrolled growth, but malignant tumours differ by their capacity to dedifferentiate, invade and undergo metastasis (i.e. move to other bodily tissues to form secondary independent tumours). It is this process that is the main cause of death due to cancerous tumours spreading to vital organs and resulting in subsequent failure of organ function (Bray et al., 2018, Hanahan and Weinberg, 2011).

There is no definitive cause of cancer, although there are a variety of elements which predispose for or increase the risk. There are also a wide range of cancers each of which differ in their biology and pathophysiology (Hanahan and Weinberg, 2011). There has been for example, strong relationship between the smoking and lung cancer as well as external UV radiation (e.g. from direct sunlight, tanning beds, etc.) and skin cancer (Narayanan et al., 2010, Sasco et al., 2004). Although cancer can also be caused externally by so-called chemical carcinogens and biological agents each can lead to the advancement of other independent tumours (Bansal et al., 2016, Wogan et al., 2004).

Ultraviolet radiation (UVR) and ionising radiation are what are known as physical risk factors which can lead to cancer (Narayanan et al., 2010). In particular UVR is the main agent responsible for the progression of skin cancer; ~ 99% of non-melanoma skin cancers and 95% of melanoma (Narayanan et al., 2010). Exposure to ionising radiation can cause a disruption of stable atoms, leading to an imbalance of charge (ionisation), leading to chemical changes (formation of free radicals and reactive oxygen species) and damage to genetic material present in cells, both of which can cause damaging mutations (Gilbert, 2009). Also, radiation therapy used to treat cancer may also cause another type of cancer, e.g. chest radiation therapy for lymphomas can lead to the development of breast cancer (De Bruin et al., 2009).

Various chemical agents such as, those found in tobacco smoke, arsenic (water contamination) and aflatoxin (found in certain moulds on food) are what's known as chemical carcinogens and can lead to the onset of cancer. Tobacco smoke is believed to contain over 4000 chemicals with Nicotine-derived nitrosamine ketone (NNK) and Polycyclic aromatic hydrocarbons (PAH) as specific tobacco carcinogens, although many of the chemicals are believed to be able to cause cancer (Sasco et al., 2004, Wogan et al., 2004). Aflatoxin on the other hand is a highly carcinogenic mould that can increase the risk of primary liver cancer (Wogan et al., 2004).

Lastly, cancer can also be caused biologically through viral/bacterial infection (Radosevich, 2012). A well-known example of this is by infection with the Human Papilloma Virus (HPV) (Butz et al., 1999). HPV is a virus which affects the skin and mucosa and can be associated with cancer of the; cervix, vulva, vagina, anus, penis, head and neck (Radosevich, 2012). There are also several other viral infections which can lead to different types of cancers such as Hepatitis B and C and the Epstein-Barr Virus (Liao, 2006).

As well as these external risk factors, there are also genetic risk factors which elevate the risk of cancer in an individual. There are two important genetic changes in cancer. Firstly, the conversion of a proto-oncogene into an oncogene, these are genes that control normal cell division, apoptosis, etc. and can be induced to undergo malignant action through endogenous mutation (Chial et al., 2008, Vogelstein et al., 2000). Examples of these include the mutant K-RAS in pancreatic cancer and Human epidermal growth factor receptor 2 (HER-2) in breast cancer (Chial et al., 2008). Secondly, the inactivation of tumour suppressor genes (also known as anti-oncogenes) and this loss of function can be the vital incident leading to the formation of cancer. These include the BRCA1 and BRCA2 genes (loss of which leads to impairment of homologous recombination, a normally accurate repair process which fixes breaks in DNA) which when present in an inactive form drastically increase the risk of developing breast cancer as well as mutation of the p53 gene (which leads to loss of cell cycle checkpoint control and inhibition of apoptosis which then leads to uncontrollable cell growth) which is involved in a variety of cancers including bone and brain cancer among others (King et al., 2003, Vogelstein et al., 2000).

Profoundly, cancer is a combination of environmental risk factors, which contribute to a lesser degree, with genetic mutations and these tend to work in tandem over a long period of time and eventually lead to the development of cancer. Different cancers have different risk factors and introduction to one or a combination of these factors leads to detrimental genetic mutation and eventual development of carcinogenesis (Hanahan and Weinberg, 2011).

Cancer is divided into two main subcategories, blood cancers and solid tumours. Firstly, blood cancers are divided into 3 main categories: Leukemia (a cancer which is found in the blood and bone marrow, Lymphoma (a blood cancer which affects the lymphatic system) and Myeloma (a cancer that affects the plasma cells in the blood) (Allart-Vorelli et al., 2015). Solid tumours on the other hand can be classified as either benign (non-cancerous) or

malignant and can be categorised into two cancer types based on where the cancer originates from. These are; carcinoma (when a cancer starts in the cells that line or cover internal organs) or sarcoma (this is a tumour that manifests itself in bone, cartilage, fat, muscle, blood vessels or other connective or supportive tissue) (El-Deiry et al., 2019). The 5 main solid tumours by incidence and death rate are; Lung, Colorectal/Bowel, Prostate, Breast and skin cancer (Priestley et al., 2019). Of these, this thesis will mainly focus on Prostate cancer.

1.2. Prostate cancer.

Cancer of the prostate is characterised as an adenocarcinoma or glandular malignant neoplasm which occurs most commonly in the peripheral zone of the prostate as a result of ordinary semen-secreting prostate gland cells mutating into cancer cells (Algaba et al., 2007). Prostate cancer is the 2nd most common cause of cancer-related mortality, behind only lung cancer. In the initial stages, there is an imbalance between the level of proliferation and the rate of cell death, and this leads to tumorigenesis. This manifests itself in patients as; urinary incontinence, blood in the urine, blood in the seminal fluid, erectile dysfunction, pain during urination and discomfort/pain when seated due to an enlarged prostate (Cuzick et al., 2014). The cancer is termed androgen-dependent and is localised to the prostate and is therefore easily treatable (Ghosh et al., 2005). This is due to an increase in a protein called Prostate-Specific Antigen (PSA) which allows the cancer to be easily identifiable in its initial stages when it is localised within the gland with a typical 5-year survival in 100% of patients (Ammirante et al., 2010, Ghosh et al., 2005). Once Prostate cancer progresses or reoccurs it is recognised to often be independent of androgen for growth and if develops to sites beyond the prostate gland itself is known as metastatic prostate cancer (castration-resistant) and is incurable with an average poor prognosis of 16-18 months (Karantanos et al., 2013).

In its early stages, prostate cancer is driven primarily through one main mechanism, activation of the gonadal-testosterone-androgen receptor (AR) as it is a hormone-dependent cancer. The prostatic epithelial cells which mainly comprise the tumours in prostate cancer are reliant on the presence of androgens which activate the AR (Lu et al., 1997, Sharifi, 2013). Prostate cancer cells are reliant on a balance between the rate of cell proliferation and a number of cells undergoing apoptosis and a transcriptional pathway is activated by the AR which has an important role in maintaining this balance for a healthy prostate as well as being involved in cancerous prostate tissue (Dehm and Tindall, 2006, Feldman and Feldman, 2001). Shown in Figure 1.1 is the pathways underlying AR signalling.

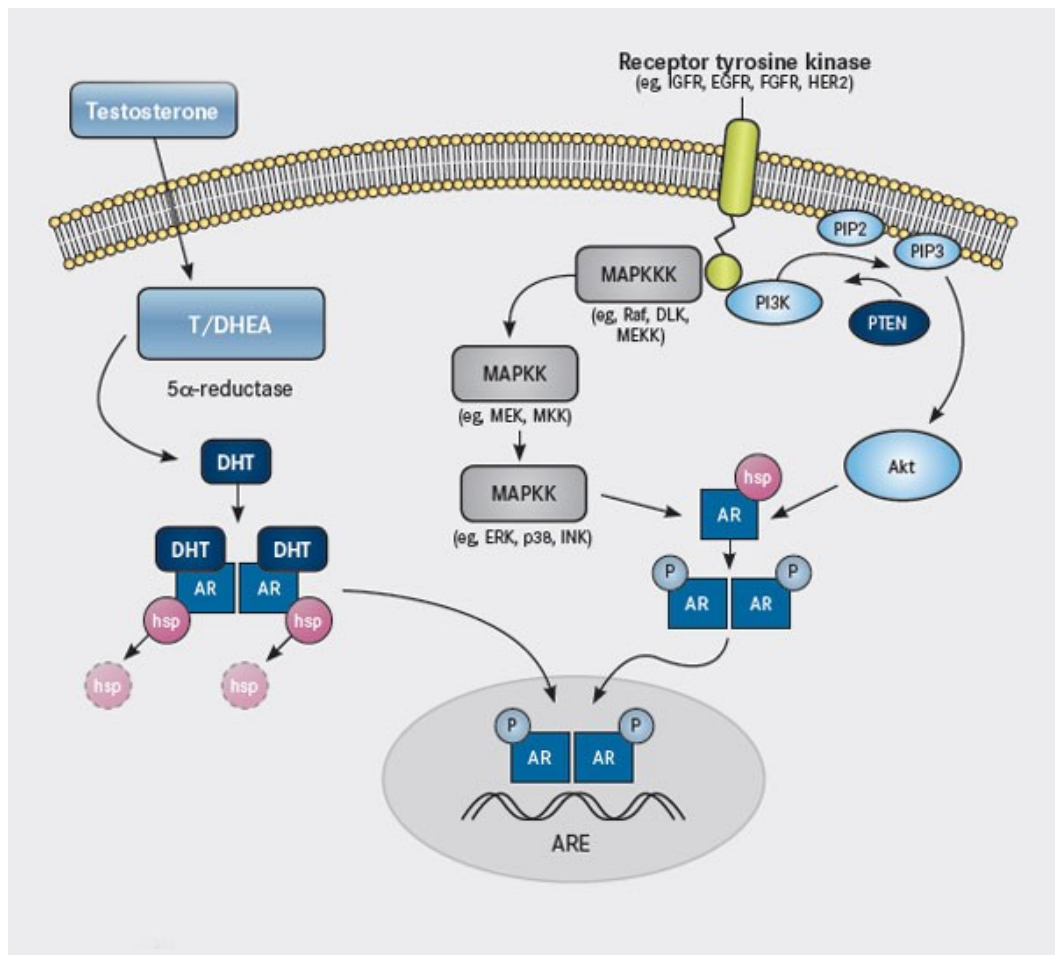


Figure 1.1. Androgen receptor (AR) signalling (Girling et al., 2007). Testosterone/DHT binds to the AR with high affinity and induces dimerisation of the receptor and subsequent translocation to the nucleus and binding to target genes in order to regulate expression. In androgen-independent activation the AR can also be transactivated in the absence, or in very low levels of circulating androgens. Activating signals arise from several, non-mutually exclusive mechanisms including alternative signalling pathways such as the MAPK pathway and PI3K-Akt pathway. (AR – Androgen receptor, DHT – dihydrotestosterone, MAPK – Mitogen-Activated Protein Kinase, PI3K-Akt - phosphatidylinositol 3-kinase- protein kinase B).

Progression of prostate cancer to the latter stages, i.e. establishment of metastatic castration-resistant prostate cancer (CRPC), can be characterised by one or a combination of the subsequent features; increase in PSA present in serum, development of pre-existing disease and/or the presence of new metastases (Hotte and Saad, 2010). Activation of the AR signalling axis can also otherwise transpire through an androgen independent mechanism of modulating AR activity which involves the autocrine synthesis of growth factors and/or their receptors, tumour-suppressor gene inhibition and stimulation of oncogenes (Mahato et al., 2011, Soucek et al., 2007). Ras and MAPK, which are oncogenes, have been shown to trigger altering of the tumour microenvironment through; recruitment of leukocytes,

upregulation in tumour-promoting chemokines and cytokine expression and/or initiation of angiogenesis (Mahato et al., 2011, Soucek et al., 2007, Sparmann and Bar-Sagi, 2004). The Ras-MAPK (both Ras and MAPK are oncogenes) pathways, as well as the phosphatidylinositol 3-kinase-Akt (PI3k-Akt) pathways (shown in Fig 1.1), are phenotypically linked to invasive cell signalling (Gao et al., 2005, Mahato et al., 2011). There is an immediate inflammatory response where the tumour starts to die when the androgens are removed and IKK β has a role in the production of cytokines like lymphotoxin- α (LT- α), B₂ and Receptor activator of nuclear factor kappa-B ligand (RANKL). This results in the reactivation of the tumour through a switch over from IKK β to IKK α . In this study by Ammirante et al. (2010) the androgens are removed surgically by castration of the male gonads whereas in the clinic via androgen deprivation strategies delivered pharmacologically. A study (Shu et al., 2010) also suggested that the AR is a substrate for Aurora-kinase A (AURKA) and is trans-activated through phosphorylation at Thr 282 and Ser 293. An increase in expression of AURKA results in induction of PSA expression and cell survival whilst knocking it down (by siRNA silencing) sensitises cells to apoptosis and the halting of cell growth. These studies mentioned above indicate that prostate cancer cells grow and survive through utilising a diverse range of mechanisms of AR stimulation and in the case of CRPC without the requirement of androgens. As a result of this, there is substantial therapeutic potential in the AR signalling axis, and this may be extended to Aurora kinases-IKK/NF- κ B signalling.

1.3 Current treatments of Prostate Cancer

Early Prostate Cancer is diagnosed by a variety of factors including; an increased serum PSA level, digital rectal examination (DRE) and by the Gleason score (2-10) method (Ghosh et al., 2005). Firstly, patients undergo blood tests, usually prompted due to age (as a check-up) or by displaying urinary symptoms, to determine the amount of PSA present in the blood, this is a protein which is produced both by healthy prostate cells and cancer cells. The amount of PSA in the blood normally increases with Prostate Cancer, a level of 4ng/ml or more and patients may be referred for other tests such as biopsy of the prostate (Hayes and Barry, 2014). Next, in DRE, this involves the doctor gently inserting a lubricated finger into the rectum and feeling the prostate to check that it is smooth. DRE is an essential medical test when assessing for Prostate Cancer and can predict prostate cancer independently in the situation of a normal PSA level (Walsh et al., 2014). Lastly, the Gleason score method links to analysis of patients samples and grades tumours on whether they are; well-differentiated (score 2-4), moderately differentiated (score 5-7) or poorly differentiated (score 8-10) and a score of ≥ 7 indicates a lowly outlook for disease progression (Algaba et al., 2007, Ghosh et al., 2005, Hayes and Barry, 2014). In the early stages of prostate, the first-line treatments consist of; active surveillance or watchful waiting, radical prostatectomy, external-beam radiation therapy (EBRT), Brachytherapy or Cryotherapy. Androgen Deprivation therapy (ADT) is also used as

soon as the patient is diagnosed (Shafi et al., 2013, Shore, 2014).

1.3.1. Active surveillance/Watchful waiting.

Watchful waiting and active surveillance are both preventative forms of treatment which aim to avoid other potentially more invasive forms of treatments or interventions such as EBRT or radical prostatectomy (Shore, 2014). It involves waiting for those patients whose cancer is unlikely to progress and waiting for them to present with any advanced signs of disease (Shore, 2014). Active surveillance on the other hand is the extra observation of patients (normally with PSA, DRE and re-biopsy) towards the aim of curing the disease should it progress (Dall'era et al., 2008). It was shown by (Xia et al., 2012) that by remaining on active surveillance for a number of years compared to receiving immediate surgery, possibly conserved the quality of life.

1.3.2. Radical prostatectomy (surgery).

An alternative method of treatment is what is known as radical prostatectomy, this is defined as the comprehensive removal of the prostate gland by means of surgery (Bill-Axelson et al., 2005, Shore, 2014, Xia et al., 2012). The surgical procedure can be performed in a number of ways; open perineal (incision made in the perineum between the anus and the scrotum), open retropubic (incision made in the lower stomach) and more emerging procedures such laparoscopic (small incisions made in the stomach and prostate viewed using a laparoscope) and robotic-assisted techniques (robotic arms are used to assist the surgeon and make his actions more precise) (Shore, 2014). Due to it being an invasive surgical procedure there are a variety of risks and complications associated with it. These include; erectile dysfunction, urinary incontinence, risk of bleeding, risk of infection at the incision site and a risk of blood clot (Bill-Axelson et al., 2005, McCullough, 2005, Zhang et al., 2014). A study by (Wilt et al., 2012) showed that radical prostatectomy had no advantage over watchful waiting when treating low-risk prostate cancer and in comparison radical prostatectomy was associated with a statistically significant rise in erectile dysfunction ($p < 0.01$) and urinary incontinence ($p < 0.01$).

1.3.3. External beam radiation therapy (EBRT).

EBRT is the delivery of multiple quantities of radiation and this is done across numerous days to weeks in order to destroy the prostate cancer cells. EBRT includes conventional radiation therapy and the more specific intensity modulated radiation therapy (IMRT) (Shore, 2014). This technique permits the application of multiple doses of radiation locally to tumour as the

radiation beams are matched specifically to the shape, position and size of the prostate and this helps to reduce any potential harmful side effects (Bauman et al., 2012, Shore, 2014). Common side effects include, gastrointestinal and genitourinary toxicity (Bauman et al., 2012). In order to improve response in those patients with more advanced prostate cancer that are still localised to the prostate, radiation can be used in combination with hormone therapy (Bauman et al., 2012, Shore, 2014). The hormone therapy can be used to shrink the tumour and make the radiation treatment more effective. (Sooriakumaran et al., 2014) showed that in patients with localised prostate cancer the survival rate was greater in patients treated with radical prostatectomy rather than radiation therapy alone. Therefore, the combination approach has been recommended as one of two treatment options (the other being radical prostatectomy) to be used with intention to cure the disease (Bohmer et al., 2016). So, the combination approach with EBRT and ADT or treatment with radical prostatectomy are the best interventions in patients with localised prostate cancer.

1.3.4. Brachytherapy.

Another method used in the treatment of prostate cancer (as well as other cancers such as; cervical, breast and skin) is what is called brachytherapy, which involves the use of radioactive implants that release radiation to cancer cells (Shore, 2014, Zhang et al., 2014). This can either be in the form of Permanent, low dose rate (LDR) or temporary, high dose rate (HDR) brachytherapy and can be used in combination with EBRT and chemotherapy (Pieters et al., 2009). The actual technique of brachytherapy involves injection of a radioisotope which is enclosed in protective capsule and placed precisely at the site of the tumour. The purpose of the capsule allows the radiation to escape to destroy the surrounding cancerous tissue but prevents it from dissolving in bodily fluids or moving and therefore reducing potential harm to healthy tissues (Challapalli et al., 2012). Common side effects when treating prostate cancer with brachytherapy include; localised bruising, swelling and bleeding within the region of implantation as well as urinary and digestive problems such as; urinary retention, urinary incontinence, diarrhoea, constipation and minor rectal bleeding (Doust et al., 2004, Fieler, 1997, Frank et al., 2007). Brachytherapy displayed a similar effect on controlling tumour growth and survival rates to EBRT but has the advantage due its focussed effect at the prostate, which reduces the risk of side effects (Chao et al., 2015). Although this localised approach has the disadvantage in that it is ineffective if the cancer has spread beyond the prostate (Chao et al., 2015). This is an effective and minimally invasive therapy for treating localise prostate cancer but also further highlights the lack of treatments for advanced metastatic prostate cancer.

1.3.5. Cryotherapy.

An additional technique is what is known as cryotherapy, rapid freeze-thawing to destroy cancer cells and is used in localised prostate cancer (Shore, 2014). Cryotherapy works by essentially causing the cells to become “dehydrated” by drawing water from the cell and given enough time in this dehydrated state, the resultant increase in intracellular electrolyte concentration is normally enough to destroy the cells (Theodorescu, 2004). If this does not kill the cells then the development of intracellular ice which occurs at temperatures below -20°C, is nearly always fatal for target cells (Mazur, 1984, Theodorescu, 2004). During the thawing out, a process called recrystallisation occurs, which is essentially ice crystals fusing to form large crystals. These are able to disrupt the cell membrane and cause added damage to the cell (Theodorescu, 2004). There are also several side effects when it comes to the use of cryotherapy in prostate cancer, including; erectile dysfunction, frequent difficulty or pain in passing urine, blood in urine, urinary incontinence and bleeding or infection in the area treated (Aus, 2008, Cho and Kang, 2014). Again, like brachytherapy, this treatment is minimally invasive and can be used in the treatment of localised prostate cancer but is ineffective once the cancer has metastasised and further highlights the lack of treatment options in this disease setting.

1.3.6. High Intensity Focal Ultrasound (HIFU).

This is a technique which involves the application of high energy sound waves that are used to heat and destroy cancer cells. It is also used in the treatments of other cancer types including; bladder, liver, pancreatic and kidney and has the advantage that it is minimally and locally invasive (Hu et al., 2016). It was also shown in the study by (Hu et al., 2016) that High Intensity Focal Ultrasound can be useful in treating patients who have relapsed and their prostate cancer has re-occurred following treatment with external beam radiation therapy.

1.3.7. Immunotherapy.

Immunotherapy is a technique which uses the body's own immune system to attack cancer cells and is normally used in the treatment of advanced prostate cancer. The immunotherapies currently under investigation and use to treat different types of cancer are; administration of immunomodulatory cytokines/effectors, vaccines as well as antibody therapies (Risk and Corman, 2009).

The 1st method, immunomodulatory therapy, involves administration of cytokines or other immunomodulatory agents to illicit an immune response. The main advantage of this is the fact that it is relatively easy and quick to administer (Risk and Corman, 2009). Various clinical trials have used Granulocyte-Macrophage Colony-Stimulating Factor (GM-CSF), due to its stimulation of antigen uptake and processing by dendritic cells, which recruits more T

cells and brings about an anti-tumour response (Risk and Corman, 2009). A trial by (Small et al., 1999) demonstrated decreases in prostate-specific antigen (PSA) levels at the end of two 14-day cycles in a 28 day period. It has also been demonstrated in both pre-clinical and human studies that Fms-related tyrosine kinase 3 (FLT3) ligand can increase levels of a variety of haematopoietic cell types, including dendritic cells (Higano et al., 2004). In this study by (Higano et al., 2004), all patients who completed the trial showed increased levels of dendritic cells and 50% showed disease stabilisation. The last immunomodulatory therapy to mention is the utilisation of interleukin-2 (IL-2), a key cytokine for the recruitment and activation of T-cells and which has been well studied in the therapy of renal cell carcinoma (Risk and Corman, 2009). A study by (Dieli et al., 2007) demonstrated a combination therapy of IL-2 and zoledronate (novel therapy targeting stimulation of the $\gamma\delta$ T-cell subset) in the treatment of advanced castration-resistant prostate cancer (CR-PC). 18 patients were involved in the trial, 9 received zoledronate alone and the other 9 received zoledronate plus low-dose IL-2. Of the 9 in the single agent therapy, only 3 survived and only 2 remained free from disease progression. Whereas in the combination therapy, 7 of the 9 survived and 6 were free from progression.

As opposed to immunomodulatory agents, which cause a general stimulation of the immune system, a vaccine-based approach causes an immune response against a specific antigen(s) (Risk and Corman, 2009). A trial by (Perambakam et al., 2006) used a prostate-specific antigen peptide to bind human leukocyte antigen (HLA)-A2 and cause a T-cell response *in vitro*. It was then used in 28 patients, in which delayed-type hypersensitivity was observed in 50% of the patients and this was indicative of the mechanism being feasible for immunotherapy. In contrast, tumour vaccines use autogenic (isolating tumour cells and formulating into a vaccine before administering to the same person the cells were isolated from) or allogenic (isolating tumour cells from one person and formulating into a vaccine before administering to another person to which the cells were isolated from) tumour cells to illicit an immune response (Risk and Corman, 2009). An early study involved the use of autologous tumour cells which had been harvested during a radical prostatectomy (Simons et al., 1999). These cells were expanded and transfected with GM-CSF complementary DNA which was irradiated and administered intra-dermally. Of the 11 patients that were engaged with in the trial, 8 had successful cultures that were eligible for analysis and at least 7 of these went on to develop some sort of hypersensitivity, which allowed them to determine that the results were viable.

Lastly, an area of immunotherapy which is attracting great attention nowadays, is antibody therapies. In this setting antibodies can be used to direct destruction of the tumours cells through macrophages and neutrophils or alternatively conjugate toxins or radioactive substances that lead to cell death (Risk and Corman, 2009). The 1st example of this is an antibody therapy directed against HER-2/neu (trastuzumab) which has shown clinical benefit in patients with advanced breast cancer, may be of use in advanced prostate cancer (HER-

2/neu is expressed in some). Two studies, (Lara et al., 2004) and (Ziada et al., 2004), demonstrated this antibody therapy in HER-2/neu positive advanced prostate cancer had limited benefit. The mechanism behind the therapy was to use a chimeric antibody known as MDXH210 which recognises HER-2/neu and the IgG Fc receptor and try and recruit the Fc-expressing cells (monocytes, neutrophils) to the HER-neu positive cancer cells. Cytotoxic T-lymphocyte-associated protein 4 (CTLA-4) antibody therapy is different from conventional antibody therapies in that instead of trying to bring about the induction of cell death, it's aim is to improve the immune response (Risk and Corman, 2009). Antibody therapies to CTLA-4 aim to prevent Cluster of Differentiation 28 (CD28) from blocking the CTLA-4 receptor that is expressed in T cells from binding to B7-1 on the Adenomatous polyposis coli (APC) and thus allowing T-cell activation (Risk and Corman, 2009). An anti-CTLA-4 antibody (ipilimumab) was trialled by (Small et al., 2007) in 14 patients with CR-PC, these showed promising results with up to 50% decrease in PSA levels. Lastly and probably the most recent discovery (November 2019) in terms of antibody therapies, is the use of the humanised antibody Pembrolizumab against programmed death ligand 1 (PD-L1). The study by (Antonarakis et al., 2020) in advanced metastatic castration-resistant prostate cancer patients showed an increased survival time of 2 years in 1 in 20 patients. This is FDA approved in advanced prostate cancer and immunotherapy represents a more targeted approach to specifically kill cancer cells compared to the unspecific nature of chemotherapy in targeting dividing cells.

1.3.8. Prostate cancer vaccine.

Following on from the vaccine immunotherapy mentioned previously, the FDA approved a cancer vaccine specifically to target prostate cancer cells in 2010. This is used differently from a traditional vaccine in that it is used therapeutically to stimulate an immune response rather than prevent an infectious disease (Drake, 2011). The drug which was approved is Sipuleucel-T (Provenge) and it is made specifically for each prostate cancer patient by harvesting the patient's blood leukocytes and mixing with an antigen known as protein acid phosphatase (PAP). The mixture is then given intravenously back into the blood and this is then used to bring about an immune response in the patient (Drake, 2011). It is approved to treat people with asymptomatic or minimally symptomatic metastatic castration-resistant prostate cancer, it's not been shown to prevent the growth of the tumour but only prolong the life of the patient by several months (Drake, 2011). This is one of only two FDA approved immunotherapy treatments along with Pembrolizumab. Unlike the substantial clinical improvement observed in some patients treated with Pembrolizumab, treatment with Sipuleucel-T (Provenge) produced minimal improvement and is less likely to serve as a choice of treatment in prostate cancer.

1.3.9. Androgen deprivation therapy (ADT)/Hormone deprivation therapy (HDT).

The most commonly utilised and best recognised treatment management strategy is hormone replacement therapy (HRT) or androgen deprivation therapy (ADT). This technique involves either the surgical removal of the testicles or injection of 'anti-androgens' to lower the levels of circulating androgens (Schrijvers, 2007, Sharifi et al., 2005, Shore, 2014). The objective of this technique is to reduce the amount of testosterone and other androgens to castration levels (i.e. loss of ability to produce testosterone) as androgens are one of the main elements that progress prostate cancer (Sharifi, 2013). ADT can be tackled in two ways, either by surgical castration (i.e. removal of the testes) or by drugs based methods such as luteinizing hormone (LH) releasing hormone (LHRH) agonist and antagonists which both act to reduce the amount of testosterone released from the testes (Huggins et al., 1941, Perlmutter and Lopor, 2007). The LHRH agonists act by reducing the amount of LH released by the pituitary gland whereas LHRH antagonist have a direct effect on decreasing the amount of testosterone (Perlmutter and Lopor, 2007). The LHRH agonist can also be used in combination with a drug known as an anti-androgen to achieve maximal androgen blockade (MAB) in patients with advanced prostate cancer (Chodak, 2005, Perlmutter and Lopor, 2007). This is because androgens are produced by both testes (90-95%) and the adrenal gland (~5-10%). LHRH agonists act on reducing the levels of androgens produced by the testes, whereas anti-androgens act on the AR blocking the effects of adrenal androgens and thus these in combination can pharmacologically produce MAB (Perlmutter and Lopor, 2007). There are numerous side effects that are associated with ADT such as; reduction in libido, erectile dysfunction, osteopenia with an increased risk of fracture, metabolic alterations and changes in mood and cognition (Kumar et al., 2005, Perlmutter and Lopor, 2007, Shore, 2014).

Unfortunately the majority of patients treated with ADT eventually progress to CRPC within 2-3 years of treatment, this involves reengagement of AR signalling pathway (indicated by a rise in PSA) but it is now insensitive to androgens and therefore ADT (Augello et al., 2014, Hotte and Saad, 2010, Sridhar et al., 2014, Sundararajan and Vogelzang, 2014). The exact mechanisms of resistance are debated but there is substantial evidence from a variety of studies that the AR persists and is upregulated despite resistance to ADT (Dehm and Tindall, 2006, Hotte and Saad, 2010, Marques et al., 2010, Shafi et al., 2013, Sharifi et al., 2005). This post-castration stimulation of AR involves a number of cellular and molecular modifications including; inadequate blockage of AR-ligand signalling, AR amplifications, AR mutations, abnormal AR co-regulator activities and AR splice-variant expression (Karantanos et al., 2013).

1.4. Genetic and molecular basis of prostate cancer.

Whilst the AR has been recognised as a key driver the development of molecular studies at the genetic level have allowed the further development of knowledge regarding the genetic background(s) that underlie these well recognised characteristics. Prostate cancer is recognised to have an extremely complicated genetic makeup including; somatic copy number alterations, point mutations, structural rearrangements and changes in chromosomal number (Wallis and Nam, 2015). Somatic copy number alterations (SCNAs) cause a gain or loss of genetic material that plays a role in activation of oncogenes and the inactivation of tumour suppressor genes (Wallis and Nam, 2015). This includes genes like phosphatase and tensin homologue (PTEN) tumour suppressor gene in which loss of function is associated with activation of the PI3K-Akt pathway and tumorigenesis in 20% of primary tumours and 50% of castration-resistant prostate cancers (Jamaspishvili et al., 2018, Wallis and Nam, 2015). In primary prostate cancer tumours, loss of function of the p53 tumour suppressor is associated with avoidance of apoptosis and oncogenic activity. Conversely, the oncogene MYC was frequently overexpressed at the transcriptional level in the majority of metastatic-castration resistant prostate cancer (mCRPC) cases (Rebello et al., 2017) The activity of MYC cooperates with the aberrant signalling in the PI3K/AKT/mTOR pathway to promote the survival of prostate cancer cells (Rebello et al., 2017). Improper repair of DNA breaks can result in both intra- and inter- chromosome rearrangements, with transmembrane protease serine 2:v-ets erythroblastosis virus E26 oncogene homolog gene (TMPRSS2-ERG) being the most frequently occurring in prostate cancer, present in about 40-80% of cancers in humans (Wallis and Nam, 2015). TMPRSS2-ERG has been demonstrated to be linked to AR signalling and is aberrantly expressed in androgen-dependent prostate cancer but down-regulated in androgen-independent prostate cancer cells (Wallis and Nam, 2015). It was also recently demonstrated by (Zhou et al., 2019) that TMPRSS2-ERG gene fusion causes aberrant activity in the ERG pathway which impacts on nitric oxide (NO)-cGMP signalling, causing an elevation in cGMP synthesis, leading to an increase in Protein kinase G (PKG) activity/expression and cell proliferation. It was also shown in this study that an sGC (the major mediator of NO-cGMP signalling) inhibitor in combination with the potent AR antagonist enzalutamide synergistically reduced tumour growth in TMPRSS2-ERG-positive prostate cancer xenograft models (Zhou et al., 2019). The studies detailed above highlight the diverse and complex nature of the genetic background and signalling pathways involved in prostate cancer and the increased need to target multiple markers to improve clinical outcome. The signalling pathways can include; RAS, PI3K-Akt, integrin-FAK, MAPK, STAT3 and NF- κ B signaling.

1.5. Regulation of the NF- κ B signalling pathway.

1.5.1. NF- κ B family members.

Nuclear Factor kappa B (NF- κ B) proteins are a family of transcriptional factors that play a vital role in regulating a variety of cellular procedures including; inflammation, cell survival/death and the cell cycle (Gamble et al., 2012a, Liu et al., 2017). There are five constituents of the NF- κ B family recognised in mammalian cells; p65 (Rel A), c-Rel, RelB, NF- κ B1 (p50) and NF- κ B2 (p52) (Gamble et al., 2012a, Liu et al., 2017). These 5 proteins share a common domain of high sequence homology, called the Rel Homology Domain (RHD), which is a vital element in the dimerisation process as well as DNA binding, inhibitor binding and nuclear localisation (Hoesel and Schmid, 2013). This RHD domain is approximately 300 residues long and positioned near the N-terminus and its immunoglobulin-like C-terminal, which is around 100 amino acids in length, is solely responsible for the process of dimer formation (Hoesel and Schmid, 2013). NF- κ B activity is primarily controlled through its ability to bind DNA and in most cells which are unstimulated the NF- κ B subunit dimers are situated in the cytoplasm as they are bound to a family of inhibitors known as inhibitors of NF- κ B (I κ Bs), which prevents translocation of the NF- κ B complex to the nucleus, rendering them inactive (Hoesel and Schmid, 2013). These inhibitors possess several copies of the Ankyrin repeat domain. These permit the I κ Bs to mask the nuclear localisation sequences (NLS) by association with the DNA-binding domains of the NF- κ B proteins and thus they remain transcriptionally inactive in the cytoplasm (Hoesel and Schmid, 2013). Both p105 and p100, which act as precursors for p50 and p52 respectively, also contain Ankyrin repeats and these are removed by cleavage upon processing – therefore they function as their own inhibitors (Gamble et al., 2012a, Hoesel and Schmid, 2013). Perhaps more crucially though is the fact that both p50 and p52 do not have a transactivation domain (TAD) and are therefore transcriptionally inactive and as such p50-p52 homodimers are said to be repressors of transcription (Gamble et al., 2012a, Liu et al., 2017). On the other hand, when p50 or p52 form hetero-dimers with p65 or RelB respectively, which both contain a TAD, they form a transcriptional activator (Hoesel and Schmid, 2013). These TAD and RHD domains can also both undergo post-translation modifications and this is important for activation and potential cross-talk with other pathways (Gamble et al., 2012a, Liu et al., 2017). In a grander scheme, activation occurs following the release of NF- κ B from the I κ B proteins (these act as gatekeepers of the pathway) or by removal of Ankyrin repeats from p100 and p105 (Hayden and Ghosh, 2012). This is mediated either by proteasomal degradation of I κ B by the 26S proteasome or by partial processing (degradation) of the precursors to p52 and p50 respectively (Hoesel and Schmid, 2013). The ubiquitination and subsequent degradation which these proteins are subjected to is initially driven by phosphorylation by the inhibitory kappa B kinases (IKK) as part of IKK complexes, allowing NF- κ B to translocate to the nucleus and be able to bind DNA (Gamble et al., 2012a, Liu et al., 2017).

1.5.2. Inhibitory kappa B Kinases (IKKs) in regulation of the canonical and non-canonical NF- κ B pathways.

IKK α and IKK β (catalytic kinases) as well as the regulatory NF- κ B essential modulator (NEMO)/IKK γ are the three subunits that form the proto-typical catalytically active multimeric IKK complex and this 700-900kDa multiprotein is believed to act as the “master co-ordinator” controlling NF- κ B activation (Rushe et al., 2008). Both kinases, IKK α and IKK β share around 52% homology and contain a leucine zipper (LZ) motif through which both IKKs dimerise and form different combinations of either homo- or heterodimers. They also both possess a helix-loop-helix domain, followed by a C-terminal tail, which unphosphorylated, interacts with NEMO (Rushe et al., 2008, Zandi et al., 1997). Common to both IKK α and IKK β is a conserved sequence which is known as the NEMO-binding domain (NBD), which has the following sequence: L-D-W-S-W-L (Leu-Asp-Trp-Ser-Trp-Leu) and this sequence is used to control the interaction between IKK α /IKK β and NEMO (IKK complex) (May et al., 2000a).

Whether the IKK complex forms a homo- or hetero- dimer between IKK α and IKK β determines which pathway is taken as the route to the liberation of activated NF- κ B complex (Gamble et al., 2012a, Liu et al., 2017) – (see Figure 1.2). In canonical (classical) NF- κ B signalling, the IKK complex is believed to exist predominantly in a ratio of 1:1:2 (IKK α :IKK β :NEMO) – and this enhances the idea that the catalytic IKKs exist in a hetero-dimer with dimers of NEMO bound (Hacker and Karin, 2006, Liu et al., 2012). Activation of the canonical pathway can occur through the action of a variety of stimuli, including; Tumour Necrosis Factor α (TNF α), lipopolysaccharides, found in bacterial cell walls and interleukin-1 β (IL-1 β) (Hoesel and Schmid, 2013, Schmid and Birbach, 2008).

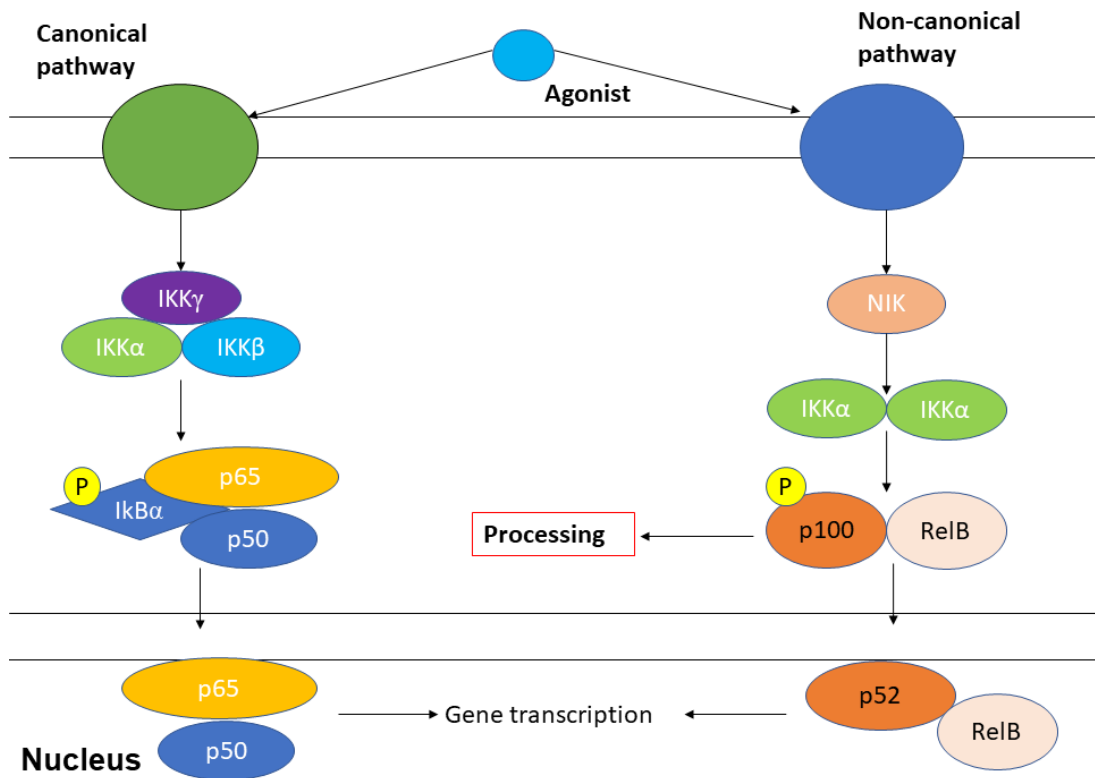


Figure 1.2. The canonical (classical) and non-canonical (alternative) NF- κ B signalling pathways. Adapted from (Jost and Ruland, 2007).

Upon activation of Toll-like receptors (TLRs), Tumour Necrosis Factor Receptor (TNFR) and IL-1R by these stimuli leads to subsequent activation of the IKK complex, primarily through phosphorylation of both IKK α (S176 and S180) and IKK β (S177 and S181), which in turn leads to a conformational change that drives kinase domains to a catalytically active confirmation (Liu et al., 2012, Mercurio et al., 1997). The active IKK complex then phosphorylates I κ B α at two critical serine residues (S32 and S36) which are located in the NH $_2$ -regulatory domain of I κ B α (Brasier, 2006). This leads to polyubiquitination and subsequent degradation by the 26S proteasome. Upon degradation, the NF- κ B complex can then rapidly translocate to the nucleus and activate specific genes that possess NF- κ B DNA-binding sites by recruiting coactivators and inducing assembly of active promoters to the gene promoters and therefore upregulate gene expression (Brasier, 2006, Hoesel and Schmid, 2013, Sheppard et al., 1999). IKK β has a crucial role in canonical NF- κ B signalling but in its absence IKK α can in specific scenarios (e.g. Il1b-stimulated Murine Embryonic Fibroblasts (MEFs)) substitute for its functions but in the majority is not required to activate the pathway. This has been demonstrated in a variety of animal and cellular knockout (KO) models that have lethal phenotypes, which are then used to generate cells. Cell-based studies in MEFs generated IKK α KO, IKK β KO and IKK α / IKK β double KO with varying end results in terms of phenotypic

outcome Firstly, in the IKK β KO mouse model it was shown that they underwent massive liver apoptosis which ultimately led to death in the embryonic stage as is the case in both RelA and ikky KO mice (Beg et al., 1995, Liu et al., 2012). Whereas, in ikka KO mice the embryonic mice survive up to a month but they have severe developmental defects including underdeveloped limbs (Liu et al., 2012). Lastly, in ikka/ikkb double KO mice they experience mortality fairly early on in the embryonic stage (E12) as a result of greater apoptosis and liver defects and they did not display any measurable NF- κ B activity (Liu et al., 2012). These studies detailed above indicate that the two catalytic IKK proteins show some crossover in terms of function but in general play different roles in transcription and resultant physiological and pathological response. It was also demonstrated in Mouse Embryonic Fibroblasts (MEFs) cells lacking IKK α /b/ γ that IKK β and NEMO were required in a 'full IKK complex' for TNF α induced NF- κ B activation (Solt et al., 2007). In contrast, it was also shown by (Solt et al., 2007) that following IL-1 induced NF- κ B activation in ikkb KO MEFs, IKK α and NEMO form a functional IKK complex in which IKK α rescues IL-1 induced NF- κ B activation.

However, in non-canonical (alternative) NF- κ B signalling both IKK β and NEMO (key components in canonical activation) are not required for activation of this pathway (Paul et al., 2018). Activation occurs through exposure of cells to the following stimuli; B-cell activation factor (BAFF), lymphotoxin β (LT β), CD40 ligand (CD40L), receptor activator for nuclear factor kappa B ligand (RANKL), TNF and Tumor necrosis factor ligand superfamily member 12 (TNFSF12) also known as TNF-related weak inducer of apoptosis (TWEAK)(Hoesel and Schmid, 2013, Paul et al., 2018). In this pathway, p100 is the main component and binds to RelB and acts like an I κ B molecule by virtue of its C-terminal tail having a sequence of Ankyrin repeats, preventing RelB from translocating to the nucleus (Hoesel and Schmid, 2013, Paul et al., 2018). Upon agonist binding to one of the receptors listed above, NF- κ B inducing kinase (NIK) is stabilised (as a result of TNF receptor-associated factor 3 (TRAF3) degradation) and activated, leading to the phosphorylation and activation of IKK α . This leads to phosphorylation of p100 and resultant ubiquitination and partial degradation to its mature form – p52 (Hoesel and Schmid, 2013, Paul et al., 2018). This then localises to the nucleus where it interacts with promoter regions on DNA to increase expression of genes regulated by NF- κ B (Paul et al., 2018). It was also demonstrated by (Gray et al., 2014) in the relevant KO MEF models that binding of NEMO to IKK α was not required for the ligand-dependent stabilisation of NIK and consequent non-canonical NF- κ B activation. However, an intact IKK complex was required to suppress basal NIK activity in cells which hadn't undergone agonist stimulation and hence highlighted a role for the classical NF- κ B pathway in suppressing basal non-canonical NF- κ B signalling (Gray et al., 2014).

1.6. NF- κ B signalling in the regulation of cancer hallmarks.

The roles of the NF- κ B signalling pathways in cancer are an area in which a large amount of research has already taken place and is still ongoing (Gamble et al., 2012a). The NF- κ B pathway has shown to be overexpressed in the most common solid tumours; lung (Chen et al., 2011), prostate (Jin et al., 2013), breast (Smith et al., 2014), colorectal (Wang et al., 2009) and blood cancers such as leukaemia, multiple myeloma (MM) and lymphoma (Jost and Ruland, 2007, Liu et al., 2011). Increased activity of the NF- κ B pathway has shown to be involved in both the formation and growth of tumours by virtue of the diverse number of gene transcription events the pathway regulates, ones that underpin the development of key critical phenotypes; stimulation of cell proliferation, prevention of apoptosis, tumour angiogenesis and metastasis as well as remodelling of the tumour metabolism (Dolcet et al., 2005, Xia et al., 2014) – thus the increase in activity of the NF- κ B pathways has bearing on what are defined by (Hanahan and Weinberg, 2011) as the hallmarks of cancer, considered below.

Angiogenesis is the process of new blood vessels forming from the vasculature which is already present (Nishida et al., 2006). This is an essential part of both the growth and the progression of the tumour because due to the increase in cell mass, the tumour eventually surpasses the capacity of the body's blood supply and hence must supply new vasculature for adequate blood supply and therefore nutrients and oxygen (Naugler and Karin, 2008). The cytokines TNF- α , IL-1 and IL-6 (which can activate the NF- κ B pathway) can also stimulate the expression of what is known as the main regulator of angiogenesis, vascular endothelial growth factor (VEGF) – due to it being a target gene for NF- κ B (Bassères and Baldwin, 2006, Naugler and Karin, 2008). The expression of VEGF is also regulated by HIF-1 α under hypoxic conditions and basic fibroblast growth factor (bFGF), IL-8, matrix metalloproteinase-9 (MMP-9) among other NF- κ B target genes, play a role in various steps of angiogenesis (Huang et al., 2001, Xia et al., 2014).

Evasion and prevention of apoptosis is probably the best characterised and most apparent way in which the NF- κ B pathway is involved in the development of cancer and has long been recognised to inhibit apoptosis (Van Antwerp et al., 1996). Apoptosis is the process by which cells die as a regulated, controlled part of an organism's growth and development (Elmore, 2007). This is the normal mechanism by which the body's surveillance eradicates pre-cancerous or cancerous cells and there are a number of NF- κ B target genes which prevent tumour death (or in cancer, support survival); inhibitors of apoptosis proteins (IAPs), c-IAP1/2 and XIAP, the caspase-8 inhibitor FLIP and Bcl-2 family of apoptosis regulators such as Bcl-xL (Karin, 2006, Xia et al., 2014). Collectively, the regulatory influence of NF- κ B signalling upon the evasion and prevention of apoptosis highlights another way by which the signalling of this family of transcription factors is closely linked with tumour progression.

Cancer is recognised to have progressed from the early local stage to the more

progressive late-stage when it becomes metastatic (Xia et al., 2014). Activation of the canonical NF- κ B pathway is involved in an initial incident in metastasis known as Epithelial-Mesenchymal Transition (EMT) and this event is thought to lead to invasion of tissue and bring about metastasis (Kang and Massagué, 2004). A key transcriptional regulator, which regulates EMT, is known as Twist-related protein 1 (Twist1) and NF- κ B has been detailed to promote metastasis through transcriptional activation of this protein (Horikawa et al., 2007). Stimulation of what is known as the mesenchymal program, which involves cell adhesion molecules; selectins, integrins and the ligands they bind too (MMP2/9, VCAM-1, ICAM-1, Cathepsins B and Z). These were found to be NF- κ B dependent, especially in the breast cancer model (Collins et al., 1995, Huber et al., 2004, Naugler and Karin, 2008). These are vital in promoting the extravasation of cancer cells to distant sites (Naugler and Karin, 2008).

An hallmark that has emerged over the last 10 years in the fight against cancer is the ability of the tumour to re-model its energy metabolism (Hanahan and Weinberg, 2011, Xia et al., 2014). Several studies have discussed the role of the NF- κ B pathway in direct regulation of cell energy metabolism and it has been shown that both non-canonical and canonical NF- κ B pathways are involved in energy metabolism, as demonstrated in sarcoma cells (Londhe et al., 2018).

Inflammation acts as a key defence mechanism in the immune response's weaponry but chronic inflammation is also involved in promoting tumorigenesis through altering genetic sequences and its microenvironment (Xia et al., 2014). At the heart of this is NF- κ B, the so-called "master regulator", which controls cross-talk between innate immunity/inflammation and cancer at a variety of levels and in tumours with an elevated NF- κ B level, accumulation of pro-inflammatory cytokines at the tumour site has an influence on the pro-tumorigenic microenvironment (Xia et al., 2014).

Another hallmark that has emerged over the last few years is the ability of cancer cells to avoid detection and destruction by our immune system. This is also built on the hypothesis that the tumour is creating this chronic inflammatory environment but as well as this inflammation driving tumour growth, it also allows the tumour to suppress the immune system and evade detection – a sort of 'double-edge sword' of inflammation (Xia et al., 2014). A cancer-related chronic inflammatory microenvironment can also promote tumour infiltrating macrophages (TAM) to switch state from M1 to M2-polarised (this state favours low tumouricidal activity, increased angiogenesis and tissue re-modelling). Alternatively, downregulating NF- κ B in TAMs can cause them to shift back to the M1-polarised state (Hagemann et al., 2008). The NF- κ B family member, p50 has been known to inhibit M1- and encourage M2-polarisation of TAMs, therefore promoting a microenvironment that is immune suppressed (Porta et al., 2009) and represents a good target in this setting.

Another consequence of chronic inflammation that promotes tumorigenesis is genomic instability and mutation (Elinav et al., 2013). At the inflammation site, neutrophils and macrophages release reactive oxygen species (ROS) and this can lead to DNA damage.

These cells of the immune system can also activate the NF- κ B pathway by releasing ROS and cytokines and creating a positive feedback loop to enhance NF- κ B levels in cells at the inflammation site (Xia et al., 2014). A study by (Matsumoto et al., 2007) demonstrated that activating NF- κ B induced the expression of activation-induced cytidine deaminase (AID), this is an enzyme that causes mutations in multiple cellular genes including p53 and Myc and again promotes the tumour development process.

The upregulation of growth which is uncontrolled and is widely associated with cancer occurs through either; stimulation of so called “pre-malignant” cells to undergo development into cancerous cells or microenvironment cells which are recruited to the tumour microenvironment where a combination of cytokines, growth factors, proteases, etc. work to degrade the extracellular matrix and shift towards malignant progression (Inoue et al., 2007). Pre-malignant cells are acted on by circulating cytokines such as TNF- α and IL-1 β and this causes activation of the NF- κ B pathway and expression of genes involved in prevention of apoptosis and upregulation of proliferation (Inoue et al., 2007). Examples of these genes and their protein products include; Cyclin D1, Cyclin E, CDK2 and c-Myc and these are vital for correct cell cycle regulation (Naugler and Karin, 2008). Genes which are targeted by NF- κ B also include growth signals such as; Granulocyte macrophage colony-stimulating factor (GM-CSF) and interleukin-6 (IL-6). Also, in breast cancer, growth and development of the mammary gland is reliant on Cyclin D1 expression which is dependent on the activation of IKK α . In this setting, an ErbB2/Her2 model with inactive IKK α showed inhibition of breast cancer development (Cao et al., 2007).

The wide scope of literature gathered above serves to highlight the distinct and complex role that both the IKKs and the NF- κ B pathways play in both the development and progression of cancer.

1.7. IKK-NF- κ B in prostate cancer.

As mentioned earlier, the NF- κ B pathway and in particular IKK α and IKK β have a role in the re-emergence of prostate cancer recognised as the transition from hormone responsive– to castrate resistant-disease through an inflammatory response. As part of the inflammatory response the key participants are B cells (Ammirante et al., 2010). Upon hormone deprivation there is an immediate inflammatory response where the tumour starts to die undergoing apoptosis and as a rebound response IKK β has a role in the production of cytokines like lymphotoxin- α (LT- α _{1 β 22} and Receptor activator of nuclear factor kappa-B ligand (RANKL). This results in the reactivation of the tumour through a switch over from IKK β - to IKK α -mediated signalling (Ammirante et al., 2010). This inflammation is an important factor in the progression of growth in the absence of androgens and eventually CRPC (Ammirante et al., 2010). This occurs through activation of a transcription factor known as STAT3 which

possesses pro-tumorigenic and anti-apoptotic properties and is induced by IKK α (Abdulghani et al., 2008). In a study by (Jain et al., 2012), it was shown that reduced *in vivo* AR phosphorylation following treatment with the IKK inhibitor BMS345541 and *in vitro* AR phosphorylation by IKK α or IKK β , implicates the AR as an IKK target in prostate cancer cells. In prostate cancer cell lines where the AR wasn't present, constitutive activation of NF- κ B was observed, whereas AR positive prostate cancer cell lines have a very low basal level of NF- κ B activity (Suh et al., 2002). This suggests that the presence of the AR potentially inhibits NF- κ B activity in prostate cancer cells or alternatively, there is a correlation between constitutive NF- κ B activity and loss of AR and this may play a role in compensatory cellular changes which allow cell survival and growth in absence of AR activation (Suh et al., 2002). Furthermore it was demonstrated that constitutive activation of NF- κ B *in vivo*, by the absence of I κ B α , alleviates the regression of the prostate post-castration by sustaining high nuclear levels of AR, which maintains differentiated function and renewed proliferation of the epithelium (Jin et al., 2008). This was achieved through activation of the NF- κ B pathway in the prostate of an ARR2PB-myc-PAI (Hi-myc) mouse model which was cross-bred into a *ikba*^{+/-} haploid insufficient line (Jin et al., 2008). In this disease model, the mouse prostate continued to proliferate post-castration and this implicates that NF- κ B activation is sufficient to maintain androgen-independent growth of the prostate and prostate cancer through regulation of the AR and highlights the NF- κ B pathway as a potential target for therapy (Jin et al., 2008). The downstream catalytic IKK proteins represent attractive targets for therapeutic intervention with small molecule ATP-competitive inhibitors and furthermore the emergence of potential Protein-protein interactions (PPIs) inhibitors/mimetics which disrupt the PPIs within the IKK complex (Gamble et al., 2012a, Prescott and Cook, 2018). Because of this, the full IKK complex has been considered as a prime target for pharmacological inhibition in drug development and as such a wealth of research has been pursued and remains ongoing into potential therapeutics. Unfortunately, despite these treatments the disease does still tend to progress and therefore other pathways may act as targets (Hagemann et al., 2008). These studies highlight the shortage of pharmacological target-based treatments associated with CRPC.

1.8. IKK inhibitors.

1.8.1. ATP-competitive inhibitors.

As described in the previous section, the NF- κ B pathway is involved in almost all aspects of tumorigenesis both in terms of tumour initiation and development. It is for these reasons that

the NF- κ B pathway, and the IKKs (IKK α and IKK β) that regulate them, make for attractive therapeutic targets.

The best recognised inhibitors that have received significant resource in terms of development are ATP-competitive IKK inhibitors, molecules that competitively interfere with binding of ATP at the ATP-binding site in close proximity to the 'gatekeeper' residue within the kinase domain. Bayer 'Compound A', one of the first described inhibitors was identified an ATP-competitive compound that has been tested both in immortalised cell lines as well as *in vivo* and targets both IKK α (IC₅₀ 135nM) and IKK β (2nM) (Gamble et al., 2012a). It was demonstrated in a study by (Ziegelbauer et al., 2005) that 'Compound A' inhibited NF- κ B transactivation, expression of chemokines, cytokines and adhesion molecules as well as the proliferation of T cells and B cells. It was also shown to terminate carrageenan-induced leukocyte trafficking in mice and dampened down the formation of oedema in response to arachidonic acid. A study by (Yemelyanov et al., 2006) showed that the potent IKK β inhibitor (IC₅₀ 150nM) PS-1145, blocked both basal and induced NF- κ B activity in prostate cancer cells. They also showed that the inhibitor prevented cell proliferation as well as cell invasion in a highly invasive prostate cancer cell line and was a chemical forerunner to the Millennium Pharmaceuticals compound, ML120B, a selective, reversible ATP-competitive IKK β inhibitor (IC₅₀ 50nM) (Lee and Hung, 2008). It was shown in a study by (Wen et al., 2006) that ML120B inhibited TNF α -induced I κ B α phosphorylation and NF- κ B transcriptional activity and was also found to disrupt TNF α and IL-1 β -induced IL-6, RANTES and MCP-1 expression. It also had no real effect on other kinases, including IKK α (>100 μ M) (Lee and Hung, 2008). Lastly, SC-514 is selective, reversible, weak ATP-competitive inhibitor of IKK β (IC₅₀ 6.9-15.9 μ M) and has little effect on other IKK isoforms or any other cellular protein kinases (Lee and Hung, 2008). A study by (Kishore et al., 2003) indicated that SC-514 inhibits the phosphorylation and degradation of I κ B α and thus the production of IL-6 and IL-8 through blocking induction of IL-1 β . SC-514 was also shown to inhibit RANKL-induced osteoclastogenesis and NF- κ B activation and has also been suggested as a ROS-inducing IKK β inhibitor with potential implications in the treatment of melanoma (Liu et al., 2013, Tse et al., 2017). The various studies detailed above of different IKK β inhibitors highlights their benefits in off-setting pro-inflammatory responses. Unfortunately IKK β targeting with KIs generates normal cell death and sensitisation to TNF α -stimulated apoptosis, so not a good target in cancer as will impact on normal cells, no differential between cancer and normal cells.

To date, there are currently no selective IKK α inhibitors used clinically or published in the literature towards that goal apart from the "in-house" selective inhibitors of IKK α which are currently under development at the University of Strathclyde. Early generation molecules considered pharmacological tools have been generated which are selective for IKK α and able to inhibit key markers of the IKK α -driven non-canonical NF- κ B signalling in the U2OS cancer cell line (Anthony et al., 2017a).

The issues with these inhibitors that hamper their progress, like all ATP-competitive inhibitors, is they have certain limitations in a disease setting. Even though most have good oral bioavailability and block the protein they are intended to target, due to the high sequence homology between individual kinases or families of kinases through the kinome, they can 'hit' other kinases generating 'off-target' effects (Gamble et al., 2012a, Garber, 2006). It also been observed that in cancer, ATP-competitive inhibitors as a treatment strategy can be ineffective as tumours and their kinases develop resistance. This can occur through mutation of the ATP binding pocket which prevents drug binding and stops its effects (Gamble et al., 2012a). An example of this being the emergence of drug resistance by the epidermal growth factor receptor in response to tyrosine kinase inhibitors (TKIs) (Minnelli et al., 2020, Yun et al., 2008). There are two mutations involved here; the oncogenic L858R mutation which causes aberrant activation of tyrosine kinase domain and the T790M mutation which is the one which confers resistance to TKIs and also increases the affinity of the oncogenic L858R mutant (Minnelli et al., 2020, Yun et al., 2008). That said, there is no data available to appraise this with respect to assessing the targeting of IKKs.

1.8.2. Allosteric inhibitors.

To overcome the limitations which are associated with ATP-competitive IKK inhibitors, one method which is explored to try and overcome this is the use of so-called "allosteric inhibitors". The advantages of these over conventional ATP-competitive inhibitors is the fact that they offer a higher degree of selectivity and avoid competition with high concentrations of substrates and ligands such as ATP (Liu et al., 2018).

The first allosteric inhibitor and probably the most well-known and well researched in relation to targeting the catalytic activity of IKKs is the BMS-345541 (4(2'-aminoethyl) amino-1,8-dimethylimidazo(1,2-a) quinoxaline) compound. This shows an average selectivity for IKK β over IKK α (IC_{50} = 0.3 μ M vs 4 μ M), an around 13-fold difference in selectivity (Burke et al., 2003, Prescott and Cook, 2018). BMS-345541 binds to IKK β in a mutually exclusive manner to phosphorylated I κ B α and in a non-mutually exclusive manner with regards to ADP. The opposite effect was seen on IKK α (Burke et al., 2003, Prescott and Cook, 2018). Collectively, this is viewed as an allosteric inhibitor. Another example of an allosteric inhibitor is the natural product ainsliadimer. This covalently binds to a conserved cysteine residue (C46) that is present in both IKK α and IKK β , resulting in inhibition of both through what is known as a putative novel allosteric effect with an IC_{50} = 30nM (Dong et al., 2015, Prescott and Cook, 2018). Ainsliadimer also caused the inhibition of the LPS-induced inflammatory response and tumour growth in an *in vivo* setting and therefore has therapeutic potential in the treatment of cancer and inflammatory disorders (Dong et al., 2015, Prescott and Cook, 2018). In a study by (Liu et al., 2018) using a virtual screening approach, a library of inhibitors which

targeted a potential novel allosteric domain situated between the kinase domain (KD) and the ubiquitin-like domain (ULD) in IKK β was identified. There were a total of 133 inhibitors tested in the screen and 16 of these were identified to block NF- κ B activity by >50% at a concentration of 50 μ M in a NF-kappaB-linked luciferase reporter assay. Following on from this, additional quantitative and cytotoxic studies allowed the discovery of a 'lead compound' – compound 124 v(3,4-dichloro-2-ethoxy-N-(2,2,6,6-tetramethylpiperidin-4-yl)benzenesulfonamide), which displays a specificity for targeting IKK β in its inactive form (Liu et al., 2018). Through this selective targeting of the inactive form of IKK β by blocking IKK β S177/S181 phosphorylation, this results in the inhibition of I κ B α phosphorylation and TNF α -induced NF- κ B transcriptional activity with an IC₅₀ of 35 μ M in cells (Liu et al., 2018, Prescott and Cook, 2018). Lastly and most recently in terms of discovery, (Elkamhawy et al., 2020) optimised the development of thiazolidine-2,4-dione lead compounds into potential *in vivo* anti-inflammatory therapeutics with the most potent compound producing an IC₅₀ = 0.2 μ M. These lead compounds were first assessed *in vitro* in macrophages which were stimulated with LPS before then studying further *in vivo* in a murine model of LPS-stimulated septic shock, in which compound 7a demonstrated that it could protect against death from septic shock in mice (Elkamhawy et al., 2020). So, collectively the benefits of pursuing an allosteric mechanism is they confer a higher degree of specificity in comparison to conventional ATP-competitive inhibitors and also have less ligands to compete with for binding.

1.8.3. Targeting protein-protein interactions of the IKKs – the use of cell-permeable peptides (CPPs) challenging IKK-NEMO binding.

Protein-protein interactions (PPIs) are important in signalling and are involved in a wide range of biological functions including; cell-to-cell interactions and metabolic and development control (Braun and Gingras, 2012, Rao et al., 2014). Non-covalent bonding between residue side chains form the basis of PPIs and these bonds introduce a variety of interactions which PPIs can be classified based on these contacts (Nooren and Thornton, 2003, Rao et al., 2014). These include; based on their interaction surface, they can be homo- or heterooligomeric; as judged by their stability, they may be obligate or nonobligate; as measured by their persistence, they may be transient or permanent (Nooren and Thornton, 2003, Rao et al., 2014). Transient interactions form signalling pathways, while permanent interactions will form stable protein complexes (Nooren and Thornton, 2003, Rao et al., 2014) PPIs play a role in; modifying the kinetic properties of enzymes, acting as a general mechanism to allow for substrate channelling, constructing a new binding site for small effector molecules, inactivation or suppression of a protein, changing the specificity of a protein for its substrate through interaction with different binding partners and serving a regulatory role in either an upstream

or downstream signalling level (Padamallu and Posfai, 2010, Rao et al., 2014). PPIs can also inform in the identification of potential drug targets (Padamallu and Posfai, 2010, Rao et al., 2014). Disruption of PPIs are considered an alternative, though challenging approach to generating inhibition. A well-characterised approach in the literature is the disruption of the p53-Mdm2 interaction using the nutlin molecules. Murine double minute 2 (Mdm2) negatively regulates the tumour suppressor protein p53 and it has been shown that nutlins can displace p53 from Mdm2 *in vitro* with nanomolar potency by occupying the p53-binding pocket of Mdm2 in a way that mimics the molecular interactions of p53 (Shen and Maki, 2011, Trino et al., 2016, van Leeuwen et al., 2012). Although nutlin molecules represented a promising alternative approach, they do have a number of disadvantages; they haven't been approved for clinical use, have low efficacy *in vivo*, high doses required to exert an effect in mice (200 mg/kg orally administered nutlin-3) and its selectivity for p53 is linked to a narrow therapeutic window, with doses above 10 μ M leading to DNA damage and doses below 2 μ M causing no measurable effect (Trino et al., 2016, van Leeuwen et al., 2012).

This approach of targeting PPIs has also been utilised for the IKK-NF- κ B signalling and the IKKs directly using a peptide-based approach. An example of this has been demonstrated by (Collins et al., 2015) which described the development of a peptide mimetic which mimicked the I κ B family protein BCL3 causing a stabilisation of the NF- κ B p50 homodimer complex through inhibition of the ubiquitination of p50. This leads to inhibition of Toll-like receptor induced cytokine expression *in vitro* and the prevention of inflammation *in vivo* (Collins et al., 2015). Another example and with particular relevance to this thesis, is the use of cell-permeable peptides (CPPs) derived from the NEMO-binding domain (NBD) of IKK α /IKK β which can disrupt the interaction between the IKKs and NEMO as mentioned but also has a non-selective effect on inhibiting IKK α and IKK β (Prescott and Cook, 2018). It was first shown by (May et al., 2000b) that the catalytic IKK proteins (IKK α and IKK β) contain a carboxyl-terminal segment within their NEMO-binding domain (NBD) which associates with NEMO through an amino terminal α -helical region. They also demonstrated that using the hexapeptide (6 amino acid sequence) sequence derived from the NBD of IKK β to design cell-permeable peptides (CPPs), they could disrupt the interaction between the IKK complex and NEMO and hence block NF- κ B activation. NBD CPPs also caused inhibition of cytokine-stimulated NF- κ B activation, NF- κ B-dependent gene expression and off-set inflammatory responses in murine models of acute inflammation (May et al., 2000a).

Since their seminal discovery and use, the NBD CPPs have been shown to inhibit NF- κ B activation in a variety of different disease models, mostly linked to inflammatory diseases but also including cancer. In the cancer setting, NBD peptides have shown useful treatment results in both human melanoma (Ianaro et al., 2009) and an aggressive form of canine cancer known as Activated B-cell Diffuse Large B-Cell Lymphoma (ABC-DLBCL) (Gaurnier-Hausser et al., 2011, Habineza Ndikuyeze et al., 2014). In the melanoma setting, the NF- κ B pathway has been demonstrated to be constantly aberrantly expressed and it was shown that a short

NBD CPP derived from IKK β inhibited the proliferation of A375 human melanoma cell line which show increased NF- κ B activity (Ianaro et al., 2009). This was also linked to direct blockade of NF- κ B DNA-binding activity and induction of apoptosis by caspase-3 activation (Ianaro et al., 2009). It was also demonstrated that, in dogs with relapsed B-cell lymphoma, the NBD causes inhibition of NF- κ B target gene expression as well as a reduction in tumour burden (Gaurnier-Hausser et al., 2011). Finally, in a Phase 1 clinical trial conducted by (Habineza Ndikuyeze et al., 2014) it was shown that systemic administration of NBD CPP is safe and inhibits aberrant NF- κ B activity and reduces malignant B cell proliferation in canines with ABC-DLBCL and this could potentially be translated to humans.

The NBD is also shown to be effective in a variety of models of inflammation and disease both cellular and *in vivo*. Firstly, it was shown in a study by (Dai et al., 2004) that a NBD peptide may block NF- κ B stimulated osteoclastogenesis and bone erosion in inflammatory arthritis. They demonstrated that the peptide may inhibit osteoclast formation stimulated by cytokines and it was also shown in a murine arthritic inflammatory model that administration of NBD 'wild type' peptide before inducing inflammatory arthritis, caused a blockade in osteoclastogenesis, focal bone erosion and amends inflammatory responses in the joints (Dai et al., 2004). A 'mutant type' NBD peptide did not exert any of these effects. A study by (Dave et al., 2007) demonstrated the effects of a NBD peptide in a IL-10 knockout (IL-10^{-/-}) mouse model of spontaneously occurring chronic murine colitis. This study used an "8K" (8 lysine residues in transduction domain to enable entry into cells) NBD peptide which inhibited both the TNF α stimulated activation of NF- κ B and the translocation to the nucleus of NF- κ B family members. Systemic treatment of the mouse models with the 8K-NBD resulted in improvement of established colitis and a reduction in NF- κ B activation in the lamina propria and hence the 8K-NBD could be of therapeutic value in the treatment of inflammatory bowel disease (IBD) (Dave et al., 2007). Most recently, a group (Zhao et al., 2018a) used virtual screening to identify so-called "NBD mimetics" of the original 11-amino acid NBD peptide derived from IKK β . From this screen, two lead "hit" NBD mimetics were produced, SR12343 and SR12460, both of which caused inhibition of TNF- α and LPS-stimulated activation of NF- κ B by disrupting the IKK β -NEMO interaction (Zhao et al., 2018a). They also downregulated LPS-stimulated pulmonary inflammation in a murine model (Zhao et al., 2018a). Treatment with both 'hit mimetics' for a chronic period in a murine model of Duchenne muscular dystrophy (DMD) resulted in a reduction in inflammatory mediators, necrosis and muscle degeneration, implicating a role for these NBD mimetics in different disease types (Zhao et al., 2018a).

To summarise, CPPs offer an alternative approach to targeting PPIs and may present greater specificity than the more often targeted kinase domain and this method could be explored further in the targeting of other PPIs, though it is recognised that there is a required development process to in build drug-like features to make them effective *in vivo*.

1.9. NF- κ B-independent IKK-dependent substrates.

As well as in the NF- κ B pathway, IKKs have shown to be involved in regulation of alternative cellular substrates beyond I κ B molecules– so called NF- κ B-

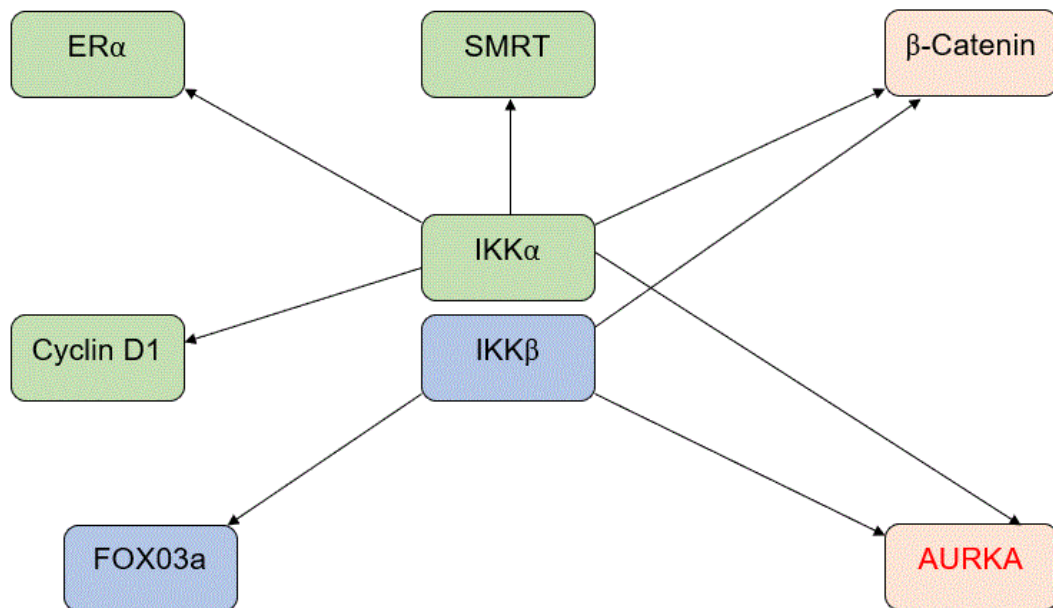


Figure 1.3. NF- κ B independent IKK dependent substrates. Diagram showing some of the NF- κ B independent proteins which are regulated by the catalytic IKK proteins. **IKK α activation phosphorylates/stimulates** – SMRT (De-repression of NF- κ B target genes, increases NF- κ B dependent transcription), ER α (Enhances estrogen receptor-mediated gene activation, hormone response) and cyclin D1 (Triggers cyclin D1 degradation, cell cycle regulation). **IKK β activation phosphorylates/stimulates**– FOXO3a (Promotes degradation of FOXO3a, growth control/cancer) and AURKA (Induces proteasomal degradation, Genome integrity). **IKK α and IKK β phosphorylate/stimulate** - β -catenin (Interferes with ubiquitination mediated degradation and increases β -catenin-dependent transcription respectively, cell cycle regulation/cancer) (Hinz and Scheidereit, 2014).

independent substrates. These are shown above in Figure 1.3 with the role IKK α and IKK β plays in the regulation of each protein detailed along with their biological function. IKK α has also been shown to regulate a number of downstream molecules - including; ER α (Estrogen receptor alpha), β -catenin and depression of silencing mediator for retinoic acid and thyroid hormone receptor (SMRT), Forkhead box O3 (FOXO3) and by phosphorylating cyclin D1 – and these cellular regulators changes are also implicated in prostate cancer prognosis (Mahato et al., 2011, Perkins, 2007). As well as targeting the IKK proteins and the IKK complex in the NF- κ B pathway, NF- κ B-independent substrates are also emerging as pharmacological targets, such as the Aurora kinases. These are regularly overexpressed in a variety of different cancers due to their vital role in the regulation of mitosis and cell

proliferation (Tang et al., 2017b).

1.10. Aurora Kinase Family.

The Aurora kinase family of cell cycle proteins are a group of conserved mitotic serine/threonine kinases which are involved in several steps in cell division by controlling the segregation of chromatids (Bolanos-Garcia, 2005, Tang et al., 2017a). These proteins were discovered over 20 years ago (1998) and give the names Aurora A, B and C in *Drosophila* (Bischoff et al., 1998). In humans and other mammals their genomes encode for three Aurora kinases (AURKs), while in other animals including *Xenopus* and *Drosophila* and the nematode, AURKA and AURKB are only present. In yeast, both *S. cerevisiae* and *S. pombe* they contain only one Aurora-like homolog, which suggests that the functions that Auroras deliver have evolved and diverged from one common ancestor (Bolanos-Garcia, 2005, Brown et al., 2004). The mammalian Aurora kinase subtypes vary in amino acid length from 309-403aa long and they share around 71% sequence homology in their catalytic domain, which is approximately 251 residues long. They also share across the three kinases, a C terminal domain of 15-20 residues long and an N-terminal domain of 39-129 residues long (Bolanos-Garcia, 2005, Kollareddy et al., 2008), as shown in Figure 1.4.

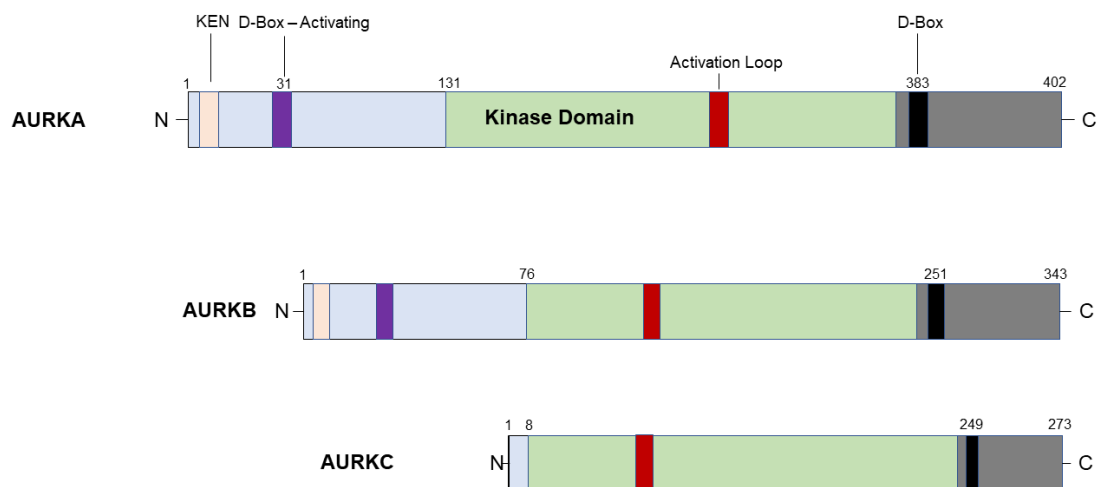


Figure 1.4. Schematic representing the structure of all three Aurora kinase family members. N and C terminal domains contain most of the regulatory sequences. The central domain consists of the kinase domain and activation loop. KEN box is a sequence motif targeted by the APC with the consensus KENxxxN (K is lysine and E is glutamate). D-Box at the C-terminal domain is the destruction box. The D-Box-activating domain within the N-terminal domain of AURKA confers the functionality to the second, a silent D-Box, present within the C-terminus of the kinase. Two different degradation signals which are required for the

proteolysis of AURKA (Kollareddy et al., 2008). TPX2 binding site: TPX2 binds to AURKA at two different sites in the catalytic core [aa 123 – 387]; at the N-terminal lobe [aa 7-21^{TPX2}] and between the N- and C-terminal lobes [aa 30-43^{TPX2}] (Bayliss et al., 2003).

The conserved catalytic domain also contains a very important structure known as the activation segment or loop and is necessary for these enzymes to carry out their function. Each member of the AURK family contains a key threonine residue in the activation segment which is vital for complete activation of the kinase Thr288 (AURKA), Thr232 (AURKB) and Thr195 (AURKC), through auto-phosphorylation of each of these residues (Bayliss et al., 2003, Tang et al., 2017a). On the other hand, the N-terminal domain of the AURKA-C is of very low sequence conservation and it has been proposed that this is a part of the protein structure that may confer selectivity towards regulation of protein-protein interactions, differing for each subtype (Bolanos-Garcia, 2005, Carmena and Earnshaw, 2003). In AURKA and B, both contain an A-box (or D-activating box) in the N-terminus and in the C-terminus there is a destruction box (D-box) – both of these work in tandem for recognition of AURKA by the E3 ubiquitin ligase, Anaphase Promoting Complex/cyclosome and its partner Cdh1(APC/cdh1). This maintains the low level of AURKA in G₁ phase at the start of the cell cycle and then again upon mitotic exit (Katayama H, 2003, Tang et al., 2017a). Lastly, in all three subtypes, the ATP binding site is of very high sequence homology in the 26 amino acids that it is composed of, with only three differences present which are unique to AURKA and occur at the residues L215, T217 and R220 (Brown et al., 2004, Kollareddy et al., 2008). Although the AURKs have high sequence homology, they differ in both their cellular localisation and functions. AURKA is expressed in many different tissues in the body including; thymus, testis, and fetal liver as well as lower expression in bone marrow, lymph node and spleen among many others - expressed ubiquitously in a cell cycle-dependent manner (Bischoff et al., 1998)

1.9. Regulation and function of Aurora kinases

1.10.1. AURKA.

The cellular levels of the AURKs are regulated mainly by phosphorylation and dephosphorylation by various interacting protein kinases and phosphatases (Katayama H, 2003).

The expression profile of AURKA is at a low level through the start of the cell cycle in G₁ and S phase before it peaks during the G₂/M. Its protein expression then returns to a low level again upon exit from mitosis, when degradation by the APC/C complex occurs (Farruggio et al., 1999, Katayama H, 2003). AURKA is localised to the centrosomes during duplication of centromeres until final exit from mitosis (Carmena and Earnshaw, 2003). This was demonstrated by (Bischoff et al., 1998) who utilised antibody-based indirect

immunofluorescence to determine the exact localisation of AURKA. In the mitotic phase of the cell cycle, AURKA is localised to the centrosomes, spindle poles and spindle during transition from prophase to metaphase but primarily to the spindle in telophase (Bischoff et al., 1998, Kollareddy et al., 2008).

Upon localisation to the centrosomes, AURKA undergoes activation by the LIM protein ajuba at the N-terminus (Carmena and Earnshaw, 2003, Tang et al., 2017a). This protein is phosphorylated by AURKA and this causes AURKA to undergo autophosphorylation and hence complete activation (Hirota et al., 2003). After peaking at G₂/M phase, the activated AURKA recruits pericentriolar proteins including γ -tubulin and TACC/MAP215 to microtubule organising centres (MTOCs) where they are involved in the maturation of centrosomes and speedy microtubule nucleation (Giet et al., 2002, Tang et al., 2017a). Following this, the breakdown of the nuclear membrane occurs in prometaphase and activation of AURKA by TPX2 occurs (Kufer et al., 2002). TPX2 is the best known and researched cofactor or co-activator of AURKA where it targets it to the mitotic spindle and activates it. This is also necessary for spindle assembly and correct confirmation of bipolar spindle microtubules (Tang et al., 2017a). Once bound, TPX2 has two roles in the activation of AURKA. The N terminal region of TPX2 binds the AURKA, causing a change in confirmation that induces the auto-phosphorylation of the critical Thr288 residue in the T-loop of the activation segment (Kufer et al., 2002). TPX2 also protects this phospho-threonine residue from dephosphorylation and consequent deactivation by the phosphatase PP1a upon entry into mitosis (Carmena and Earnshaw, 2003, Kufer et al., 2002). A study by (Bayliss et al., 2017) and (Xu et al., 2011) elaborated further on the mechanism of AURKA-TPX2 binding. The Bayliss group described AURKA as closely related to a group of kinases known as the AGC family of Ser/Thr kinases. A feature of their activation is through a hydrophobic (HF) motif in a C-terminal extension to the kinase domain, this then fits into a hydrophobic surface on the N-lobe which is situated between the β -sheet and C-helix called the PDK1 interacting fragment (PIF) pocket (Bayliss et al., 2017). In the case of AURKA, the hydrophobic (HF) motif is provided by a binding partner, TPX2, where short extended peptides interact with the hydrophobic pocket in AURKA (Bayliss et al., 2017). It was also shown that there are two TPX2-dependent “switches” that are closely associated with the activation of AURKA (Xu et al., 2011). These are; switch 1 (Lys-143) and switch 2 (Arg-180) which are bound via hydrogen bonds to ADP, upon TPX2 binding, the forced “opening” of the binding site through switch 1 occurs, pulling ADP away from AURKA (Xu et al., 2011). No TPX2 binding causes the switch to exist in an “open” confirmation which allows for this described outward flipping motion of the phosphothreonine residue (p-Thr288) in the active conformation, this leaves the p-Thr288 residue exposed readily accessible for deactivation by protein phosphatases (Xu et al., 2011). On the other hand, once TPX2 is bound to AURKA, switch 2 is enforced to a “closed” motion, capturing and burying the crucial phosphothreonine (p-Thr288) residue into its locked active confirmation (Xu et al., 2011). Lastly and crucially, a study by (McIntyre et al., 2017) quantified the binding

contributions of individual residues of TPX2 in the AURKA-TPX2 interaction. They detailed there were four key residues found to be crucial for AURKA/TPX2 complex formation: Tyr8, Tyr10, Phe16 and Trp34 and they hypothesised that the binding could be disrupted by blocking any of the pockets that correspond to these residues (McIntyre et al., 2017). There are also other proteins which interact with AURKA and control its activation and expression. Another important cofactor is the protein Bora, which like AURKA was originally discovered in *Drosophila* for its role in this context in asymmetric cell division (Hutterer et al., 2006). The binding of Bora to AURKA and the subsequent phosphorylation of Bora is similar with that of TPX2, and is also required for complete activation of AURKA (Carmena et al., 2009).

Both Bora and AURKA are also involved in the regulation of another important cell cycle kinase known as Polo-like kinase 1 (PLK1), which is activated at the centrosome in the G₂ phase of the cell cycle (Bruinsma et al., 2014, Carmena et al., 2009). Bora controls the access of AURKA to the T-loop (activation loop) of PLK1, where it undergoes phosphorylation by AURKA (Thr210), resulting in complete activation (Seki et al., 2008). Upon degradation of Bora, this instigates a negative feedback loop where phosphorylation of Bora by PLK1 generates a site on Bora which can be recognised by the E3 ubiquitin ligase SCF-betaTrCP (Chan et al., 2008). There are also three further proteins which have been shown to localise with and regulate AURKA and these normally play a role in focal adhesion (Carmena et al., 2009). Firstly, the binding of HEF-1 activates AURKA and this causes activation of HDAC6 through phosphorylation – this protein is a tubulin deacetylase and its role is in the upregulation of ciliary assembly (Pugacheva et al., 2007). This highlights a role for AURKA out with mitosis. The remaining two focal adhesion proteins which are involved in the regulation of AURKA are protein kinases (Carmena et al., 2009). The first of the two, Integrin-like kinase (ILK), when suppressed, results in faults in mitotic spindle assembly by interfering with the interaction between AURKA and TACC3/ch-TOG (Fielding et al., 2008). The last of these focal adhesion proteins, PAK1, forms part of the PAK-PIX-GIT complex which is required for centrosome maturation and becomes activated here and stimulates activation of AURKA by phosphorylating it at Thr288 and Ser342 (Zhao et al., 2005). Lastly, the tumour suppressor p53 also can regulate the expression of AURKA by localising along with AURKA at the centrosome and inhibiting it directly (Carmena et al., 2009), although, AURKA is protected from p53 inhibition by TPX2 binding by hiding the activation loop (Eyers and Maller, 2004).

1.10.1.1 TPX2.

TPX2 is a microtubule-associated protein that was 1st discovered as a factor in the extracts from mitotic eggs, where it was required for dynein-dependent localisation of Xklp2 (a plus-end kinesin) to the spindle poles (Wadsworth, 2015). Thus, the name Targeting Protein for

Xklp2, or TPX2, was coined (Wadsworth, 2015). Although, ironically we still don't understand fully how TPX2 actually targets Xklp2 (Wadsworth, 2015).

The TPX2 protein possesses a nuclear localisation sequence (NLS) and is therefore localised to the nucleus during interphase prior to its localisation at the spindle microtubules during mitosis (Wadsworth, 2015). Indeed, TPX2 possesses two NLS-containing domains that controls its localisation to the microtubules; an amino (N) terminal domain and another in the carboxy (C) terminal domain (Vos et al., 2008). The N-terminal region of human TPX2 [aa 1-480] binds directly to microtubules and also consists of the 43aa sequence that binds and activates AURKA (Brunet et al., 2004). The C-terminus crosses over with the N-terminus slightly (aa 319-715) and is essential but not sufficient on its own to encourage microtubule nucleation (Brunet et al., 2004). However, the C-terminal region does function in spindle assembly and can rescue depleted levels of TPX2 in egg extracts (Brunet et al., 2004). The C-terminal domain of TPX2 also contains tandem repeats that are predicted *in silico* to be comprised mostly of α -helical structures (Sanchez-Pulido et al., 2016). This region of the C-terminal domain can be further sub-divided into five clusters of conserved residues which are separated by unstructured regions (Alfaro-Aco et al., 2017). TPX2 also contains a KEN box motif at amino acid 87 and three D-box (R-X-X-L) motifs at amino acids 119, 341 and 708 (Alfaro-Aco et al., 2017). These motifs are said to be involved in the regulation and degradation of the TPX2 protein by the APC/C, as mutations in these motifs tend to render substrates resistant to APC/C-dependent ubiquitination (Alfaro-Aco et al., 2017, Stewart and Fang, 2005). Furthermore, it has been shown *in vitro* that only the first 83 amino acids [aa 1-83] of the N-terminal region of TPX2 as well as the KEN box were required for recognition by cdh1, a well-known activator of the APC/C (Alfaro-Aco et al., 2017, Stewart and Fang, 2005). Finally, the last 35 amino acids [aa 680-715] of the C-terminal region of TPX2 are involved in its interaction with the kinesin Eg5 (Alfaro-Aco et al., 2017, Stewart and Fang, 2005).

The naming of TPX2 as a 'targeting factor' is appropriate as the TPX2 has now been shown to target several proteins to the spindle, suggested to be like spindle flypaper (Wadsworth, 2015). TPX2 is a mitotic microtubule-associated protein (MAP) that is found to be localised to the nucleus during interphase before migration to the spindles in mitosis, with a particular abundance near the spindle poles (Balchand et al., 2015). During the process of spindle formation, TPX2 is essential for microtubule formation near kinetochores, this requires GTP-bound Ras-related Nuclear protein (Ran), results in the inhibitory action of importin α/β on TPX2 being abolished (Balchand et al., 2015). It has also shown that TPX2 targets the bipolar kinesin Eg5 to microtubules and this has an essential role in the establishment of spindle bipolarity (Balchand et al., 2015). Indeed, TPX2 protein with the 35 C-terminal amino acids critical for Eg5 binding absent, causes defects in spindles with a reduction in Eg5 accumulation on spindle microtubules, unfocussed spindle poles and distorted microtubules (Balchand et al., 2015, Ma et al., 2011).

The N-terminal domain of TPX2 is responsible for the binding and activation of AURKA and is also required to localise AURKA to microtubules (Balchand et al., 2015). TPX2 binds to AURKA in the presence of RanGTP (Brunet et al., 2004). It was firstly demonstrated by Bayliss et al. (2003) that the first 43 amino acids (aa 1-43) of the N-terminal domain of human TPX2 could be characterised as the AURKA binding domain. Furthermore, this was expanded on and the binding of TPX2 to AURKA was shown to be required for full activation of the kinase and protection from dephosphorylation (Bayliss et al., 2003). When TPX2 isn't present, the AURKA activation domain remains in an inactive conformation, where the critical phosphothreonine residue (T288) is exposed and readily available for dephosphorylation (Bayliss et al., 2017). Following TPX2 binding, conformational changes in AURKA pulls on the activation domain, swinging the T288 residue into buried position and locking in an active conformation (Bayliss et al., 2017). TPX2 has been shown to bind AURKA at two distinct sites: amino acids 7-21 of TPX2 bind at the N-terminal lobe of AURKA, whereas amino acids 30-43 bind in an α -helical conformation between the N- and C-terminal lobes (Bayliss et al., 2017). In short, the two proteins exist as a polypeptide model composed of the catalytic core of AURKA [aa 123-387] and two sections of TPX2 [aa 7-21 and aa 30-43] (Bayliss et al., 2017). Furthermore, the N-terminal lobe [aa 123-210] consists of a β -sheet and two α -helices, including the prominent helix α C whereas the C-terminal [aa 217-387] is mostly α -helical and as such the active site is situated at the interface between these two lobes (Bayliss et al., 2017). Moreover, it was also demonstrated that a single amino acid difference in AURKA (G198) and the correspondent in AURKB (N142) determined their subcellular localisation function and respective binding partners/co-factors (Fu et al., 2009).

1.10.2. AURKB.

As the second isoform of the family the expression of AURKB like AURKA peaks at G₂/M phase and then similarly is degraded by the APC/cdh1 complex upon exiting mitosis (Sorensen et al., 2000). In mitosis, AURKB displays flexible changes in localisation (Katayama H, 2003). In prophase, AURKB is associated with chromosomes before it is focussed to inner centromeres until metaphase. AURKB then transfers to the central spindle upon the start of anaphase, where the formation of the cleavage furrow occurs and remains in the mid-zone of the cell until cytokinesis and subsequent degradation by the APC/cdh1 (Katayama H, 2003). AURKB is known as a "chromosome passenger protein" in this context (Kollareddy et al., 2008). AURKB again like AURKA is expressed in most bodily tissues with examples including but not limited to; the thymus and fetal liver, where the expression level is high in both (Kollareddy et al., 2008)

Regulation of AURKB expression relies on the chromosome passenger complex (CPC), which AURKB is a member of along with three other regulators; Inner centromere

protein (INCEP), survivin and borealin in a complex with a ratio 1:1:1 (Jeyaprkash et al., 2007). The binding of INCEP to AURKB cause an increase in activation of the kinase and this goes on to full activation through a feedback loop once the bound INCEP is phosphorylated (Sessa et al., 2005). It has been proposed that borealin promotes localised clustering that leads to the auto-activation of AURKB at the centromere and Mps1 (checkpoint kinase) phosphorylates borealin and causes an increase in the activation of AURKB at the centromere via an unknown mechanism (Jelluma et al., 2008). Lastly, survivin has been suggested to be involved in targeting the CPC to the centromeres (Vader et al., 2006). AURKB is also involved in the control of chromosome condensation through phosphorylation of histone His3 on Ser10 and variant centrosome protein A (CENP-A) at Ser7 (Zeitlin et al., 2001). Lastly, AURKB has also been shown to regulate the spindle assembly checkpoint (SAC), correcting the defective attachment between spindle and kinetochore, maintenance of appropriate chromosome alignment and chromosomal segregation (Tang et al., 2017a). In anaphase, AURKB carries out the phosphorylation of a number of downstream substrates; mitotic kinesin-like protein 1 (MKLP1) and RacGAP1 – this enables the deposition of these proteins at the mid-body and maintains stabilisation of the central spindle (Carmena et al., 2012) and so is key to the process of normal mitotic division.

1.10.3. AURKC.

The third and last member of this family of kinases is AURKC and like both its family members before, also peaks in expression at the G₂/M phase of the cell cycle. During transition from anaphase through to cytokinesis, AURKC is localised on the centrosome (Kimura et al., 1999). In the body, AURKC is found to be predominantly expressed in the testis (proposed to play a role in spermatogenesis) but it is also found to be upregulated in many cancer cell lines (Katayama H, 2003, Kimura et al., 1999, Yang et al., 2015a). The diverse subcellular localisations and mitotic functions of each individual kinase are linked to their relationship with their specific regulatory proteins that are specific to each subtype.

Functionally AURKC is suggested to play an important role in chromosomal segregation. (Li et al., 2004) showed that expression of AURKC in mouse oocytes caused cell cycle arrest and formed eggs displaying aneuploidy. AURKC has also been shown to be a part of the CPC and hence has crosslinks with the functions of AURKB in mitosis (Sasai et al., 2004). A study by (Gabillard et al., 2011) showed that AURKC localised to the mid-body of HeLa cells in cytokinesis as result of its interaction with transforming acid coiled-coil 1 (TACC1).

AURKC is upregulated in several different cancers (Table 1) but as we know little about its function in normal cells, it is difficult to predict the biological significance of the aberrant expression in cancer. The variety of studies mentioned above demonstrate that AURKA as well as the other two AURK family members, play a multi-functional role in mitosis and even some functions out-with mitosis. The research ongoing presently in this area will, going forward, provide a better understanding of AURKs in the cell cycle and in disease states like cancer.

1.11. AURKs and cancer.

During the cell cycle, the AURKs are involved in the regulation of a host of vital roles and their overexpression can cause the cell to change morphology and become cancerous (Kollareddy et al., 2008). This can lead to genetic instability (aneuploidy), which can cause cancer. In this condition, altered DNA content in these cells can arise from defects in centrosome duplication, centrosome separation, cytokinesis and chromosomal bi-orientation errors. Thus, Aurora genes have been classified as oncogenes (Kollareddy et al., 2008). When it was first discovered, the AURKA gene was originally identified as Breast Tumour Activated Kinase (BTAK) because at the translational level AURKA has been shown to be amplified in the transformation of breast cancer cells (Kollareddy et al., 2008, Sen et al., 1997).

The Aurora kinases are mapped to chromosomes which have been recognised to be genetically unstable and frequently mutated; 20q13.2 (AURKA), 17p13.1 (AURKB) and 10q13 (AURKC) respectively and this may partly explain the abnormal expression of AURKs in human cancers (Tang et al., 2017a). Each of the AURK family members has been recognised to be overexpressed in a variety of different cancers (Table 1). It has been shown that AURKA can also be amplified and distributed out with the nucleus in tumour cells (Borum-Auensen et al., 2007). The Ras-association domain family 1, isoform A (RASSF1A) – a tumour suppressor which is phosphorylated by AURKA, to cause disruption of microtubule stabilisation mediated by RASSF1A and M-phase cell cycle arrest, results in uncontrolled cell division in cancer (Rong et al., 2007). AURKA also regulates the NF- κ B pathway in tumorigenesis through phosphorylation of I κ B α and thus activates canonical NF- κ B signalling. AURKA also has a role in the control of apoptosis, where it upregulates anti-apoptotic proteins such as B-cell leukemia-2 (Bcl-2) and Induced myeloid leukemia cell differentiation protein 1 (MCL-1) and downregulates pro-apoptotic proteins such as Bcl-2-associated X protein (Bax), Bcl-2-like protein 11 (Bim) and p53 upregulated modulator of apoptosis (PUMA) (Tang et al., 2017a). It also inhibits the process of autophagy through upregulation of the mammalian Target of Rapamycin (mTOR) pathway (Zou et al., 2012). In patients with cancer, a poor prognosis is normally as a result of metastasis which is mediated by EMT. AURKA has a role in the increased expression of the EMT transcription factor, SLUG, as well as fibrillin 1 (FBN1), which is important in regulation of the tumour microenvironment (Sengle et al., 2012). Increased

expression of proteins which regulate cell-cell adhesion, such as E-cadherin and β -catenin, are downregulated by AURKA, thus stimulating EMT and this was determined by treatment with the AURK inhibitor MLN8237. Also, oncogenic signalling proteins such as; Raf-1, Myc and octamer-binding transcription factor 4 (OCT4) stimulate the progression of EMT through AURKA accumulation (Liu et al., 2016, Tang et al., 2017a). Furthermore, amplification of AURKA expression can also markedly increase the expression of the matrix metalloproteinases (MMP)-2, MMP-7 and MMP-10, causing the degradation of proteins in the extracellular matrix and this leads to the stimulation of tumour mobility and metastasis (Noh et al., 2015). It has been well characterised that AURKA is involved in the regulation of p53, a well-recognised and researched tumour suppressor, by phosphorylating it at Ser215 and Ser315 – this inhibits the transcriptional activity of p53 and leads to an increase in the degradation of p53 which is mediated by Mdm2 (Katayama et al., 2004, Tang et al., 2017a). It was also shown by (Huang et al., 2016) that lack of miR-137 expression in colon polyps can act as a biomarker to predict the disease progression of colorectal cancer (gradually decreases as disease progresses). In human colorectal cancer, miR-137 negatively correlates with AURKA expression, i.e. as AURKA is over-expressed there is a loss of miR-137 (Huang et al., 2016). AURKA is also shown to be abrogated or dysregulated in 5 different types of gynaecological cancers (Suman and Mishra, 2018), non-small cell lung cancer (NSCLC) (Lo lacono et al., 2011) and gastrointestinal cancer (Katsha et al., 2015). So, collectively AURKA has a role in underpinning aspects of the development of recognised hallmarks across multiple cancer types via different cellular mechanisms.

Kinases	Localisation	Function	Tumour Types
AURKA	Centrosome, Spindle microtubule, Midbody	Centrosome maturation/separation; Mitotic entry; Microtubule nucleation; Spindle assembly; Bipolar spindle microtubule formation; cytokinesis; Mitosis exit	Breast cancer; Ovarian cancer; Gastric/Gastrointestinal cancer; Colorectal cancer; Esophageal squamous cell carcinoma; Lung cancer; Cervical cancer; Prostate cancer; Glioma; Acute myeloid leukemia(AML); Oral cancer
AURKB	Chromosome Kinetochore, Midbody	Chromosome condensation; Microtubule-kinetochore attachment; Chromosomal	Breast cancer; Ovarian cancer; Gastric/Gastrointestinal cancer; Colorectal cancer; Lung cancer; Cervical cancer;

		alignment; Chromosomal segregation; Regulating SAC cytokinesis	Prostate cancer; Glioma; Acute myeloid leukemia(AML); Oral cancer
AURKC	Chromosome, Midbody	Meiotic chromosome segregation; Similar to AURKB, e.g. Cytokinesis	Breast cancer; Colorectal cancer; Cervical cancer; Prostate cancer; Glioma

Table 1: Aurora kinases localisation and function and cancers which they are expressed in (adapted from Tang et al., 2017).

1.11.1 AURKA in prostate cancer.

The AURKs and AURKA particularly have been highlighted by a variety of studies to play a part in the development of prostate cancer. AURKA is overexpressed in 98% prostate cancer lesions and 96% of the high-grade prostatic intraepithelial neoplasia (PIN) lesions and this is thought to be an early event in the tumorigenesis within prostate tissue (Buschhorn et al., 2005). AURKA has also been shown to drive tumorigenesis by regulation of the AR by phosphorylating it in absence of agonist binding, causing its activation. It has been proposed this may lead to growth of the tumour through an androgen-independent mechanism (Shu et al., 2010). AURKA also phosphorylated and activated the C-terminus of HSP70-interacting protein (CHIP) through 2-methoxyestradiol (2-ME) stimulation (Sarkar et al., 2017). Inhibition of AURKA resulted in inhibition of CHIP phosphorylation and degradation of the androgen receptor (AR) (Sarkar et al., 2017). AURKA phosphorylated CHIP at Ser273 and it was shown that in prostate cancer cells expressing a S273A mutant version of CHIP, this abolished AR degradation following 2-ME treatment compared to the wild-type (Sarkar et al., 2017). In advanced, late stage CRPC, AR variants (AR-V) are a mechanism by which the cancer develops resistance to established treatments (Jones et al., 2017). In models of CRPC, reduction in the levels of AURKA results in a loss of AR-V target gene expression. AURKA levels are aberrantly expressed in the advanced stages of the disease and due to AR-V being a target gene for AURKA, this demonstrates a positive feedback mechanism in androgen signalling in CRPC (Jones et al., 2017). AURKA is involved in the majority of the recognised hallmarks of cancer as defined by (Hanahan and Weinberg, 2011) and the progression of prostate cancer. This again, like IKK-NF- κ B signalling, serves to highlight the therapeutic potential for AURKA being a target for pharmacological inhibition in the treatment of prostate cancer. Targeting of AURKA therapeutically in prostate cancer presents a serious challenge as it does in other cancer cell types. Again, as with all targeted approaches, there is the challenge to distinguish cancer cells from normal cells which also possess and rely upon the normal physiological function of AURKs. This can give rise to high toxicity (Tang et al., 2017a). AURKA has been suggested in some instances to promote AR degradation in CRPC (Sarkar

et al., 2017) and has also been proposed to increase in expression following androgen stimulation in prostate cancer cells that express high levels of AR (Kivinummi et al., 2017). Inhibition of AURKA has also been shown to overcome the chemo-resistance that is conferred by AURKA (Tang et al., 2017a). Indeed, inhibition of AURKA in the DU145 prostate cancer cell line sensitised cells to treatment with the chemotherapeutic docetaxel (He et al., 2013). This has presented the hypothesis that targeting AURKA with a monotherapy or so-called combination approach with chemotherapeutics, or upon discovery of other potential targets that correlate with AURKA and its involvement in prostate cancer, will bring clinical benefit. Taken together, these studies highlight the therapeutic potential in targeting AURKA in prostate cancer.

1.12. Aurora kinase inhibitors.

1.12.1. ATP-competitive inhibitors.

As mentioned in the previous section, the AURKs and in particular AURKA with its co-activator TPX2 are involved in many aspects of tumorigenesis, particularly when overexpressed/overactive. It is for these reasons that targeting AURKA and more recently, the AURKA/TPX2 complex make for attractive therapeutic targets in the treatment of cancer.

Targeting AURKs has, as for a diversity of kinases in the human kinome, again been pursued via the development of ATP-competitive inhibitors. It has been increasingly demonstrated in the literature that inhibition of AURKs through the use of ATP-competitive Aurora kinase inhibitors caused repression of the progression and growth of tumours *in vitro* and *in vivo* and can also enhance the effect of chemotherapeutics, suggesting the AURKs could potentially be therapeutic targets (Tang et al., 2017a). In one study (Helfrich et al., 2016) barasertib (AZD1152) was assessed in a panel of 23 Small-cell lung cancer (SCLC) cell lines with and without MYC gene amplification. Nine cell lines were highly sensitive to growth inhibition (>75% at 100nM) and this correlated to an increase in sensitivity when c-MYC was amplified (Helfrich et al., 2016). Barasertib, is administered as a phosphate-based prodrug which is then rapidly converted into barasertib-hQPA upon entering a system *in vivo* (Bavetsias and Linardopoulos, 2015b). The barasertib-hQPA displays selectivity for AURKB ($IC_{50} < 0.001\mu M$) over AURKA ($IC_{50} = 1.4\mu M$) (Bavetsias and Linardopoulos, 2015b).

An alternative inhibitor with greater selectivity between AURK isoforms than barasertib is Alisertib (MLN8237) which is a potent, selective inhibitor of AURKA ($IC_{50} = 1.2nM$) vs. AURKB, with a near-400 fold selectivity (Bavetsias and Linardopoulos, 2015b). In a study by Wang et al. (2017) it was demonstrated that alisertib alone or in combination with cisplatin, which crosslinks with the purine bases on DNA to form DNA adducts, preventing repair of the DNA, leading to DNA damage and induction of apoptosis within cancer cells, inhibited AURKA and significantly reduced the viability of cisplatin-resistant cells, a common challenge in the

treatment of gastric cancer. This has been used broadly both *in vitro* and *in vivo* and a recent study (Beltran et al., 2019) detailed its use in a Phase II clinical trial involving castrate-resistant and Neuroendocrine prostate cancer. The rationale behind the trial was that, N-myc tends to drive Neuroendocrine prostate cancer and alisertib disrupts the interaction between N-myc and AURKA which stabilises N-myc, causing inhibition of N-myc signalling and results in a decrease in tumour growth (Beltran et al., 2019). The end result of the trial did not meet its initial end target of 6-months progression-free survival but a set of 'Exceptional responder' patients who had advanced prostate cancer and displayed molecular and/or cellular signs of upregulated expression levels of AURKA and N-myc showed great benefit of single agent treatment with alisertib which resulted in six-month progression-free survival in 13.4% of the cohort (Beltran et al., 2019).

Danuserib is a potent pan-Aurora kinase inhibitor (i.e. it inhibits all three isoforms) – AURKA $IC_{50} = 13nM$, AURKB $IC_{50} = 79nM$, AURKC $IC_{50} = 61nM$ (Bavetsias and Linardopoulos, 2015b). Of note however, this inhibitor also caused a number of 'off-target' effects *in vitro* against a few kinases which have been shown to have anti-tumour activity such as; ABL, RET, and TRK-A (Bavetsias and Linardopoulos, 2015b). For example, it was shown in a study by Borthakur et al. (2015) that Danuserib was used in a Phase I clinical trial of patients with Tyrosine kinase inhibitor (TKI) - resistant chronic myeloid leukemia (CML) and Philadelphia chromosome-positive acute lymphoblastic leukemia (Ph+ ALL) and demonstrated early promising anti-tumour activity in 20% of the evaluated patients, all of which contained the Thr315I BCR-ABL mutation (Bavetsias and Linardopoulos, 2015b).

Probably the best characterised of all the Aurora kinase inhibitors available currently is VX-680, or Tozasertib (MK-0457). VX-680 generated by Vertex, inhibits all three AURK isoforms with a high degree of potency (AURKA $IC_{50} = 0.6nM$, AURKB $IC_{50} = 18nM$ and AURKC $IC_{50} = 4.6nM$) (Gizatullin et al., 2006). It was shown that VX-680 could potentially be used as a novel approach in combination with chemotherapies for metastases from NSCLC or alternatively as a second-line treatment in metastatic adrenocortical carcinomas (ACC) since VX-680 acts specifically on the SW13 (human adrenal carcinoma cell line) cell line and metastatic cells (Gizatullin et al., 2006). Another study by (Sun et al., 2019) demonstrated the effect of the VX-680 inhibitor in human umbilical vein endothelial cells (HUVECs). This was used as a model cell line to demonstrate the inhibitors effect on angiogenesis. The VX-680 inhibitor was shown to inhibit proliferation of HUVECs and promote apoptosis (31% and 64% increase in apoptotic cells when treated with 1.5 μ M and 2.5 μ M respectively) as well cause a marked decrease in migration (~ 2-fold and 4-fold reduction in migration index when treated with 1.5 μ M and 2.5 μ M respectively in comparison to the control) and tube formation (1.5 μ M and 2.5 μ M of VX-680 caused a 1.5- and 2.5- fold reduction in tube formation) of HUVECs (Sun et al., 2019). It was also shown, via an *in vivo* assay technique known as a chicken embryo chorioallantoic membrane assay, that VX-680 significantly reduced the formation of blood vessels and to inhibited the expression of vascular endothelial growth factor (VEGF) and RAC-

α (serine/threonine protein kinase, also called AKT1) (Sun et al., 2019), that support the development of angiogenesis. Thus, the VX-680 is a potential anti-angiogenic agent and targets several of the hallmarks of cancer, including; Angiogenesis, prevention of apoptosis, cell proliferation and migration. The halt to the development of VX-680 occurred after a Phase I trial in advanced ovarian cancer in which it produced QT prolongation (a measure of delayed ventricular response which means the heart muscle takes longer than normal to recharge between beats) in one patient (Traynor et al., 2011). It was then re-entered into a Phase II trial in BCR-ABL T315I mutant chronic myelogenous leukemia and Philadelphia chromosome-positive acute lymphoblastic leukemia but only produced minimal efficacy at higher, intolerable doses (Seymour et al., 2014).

The Aurora kinase inhibitor ZM447439 is used as a pharmacological tool to target all three Aurora isoforms but with selectivity for AURKB over AURKA/C (AURKA IC_{50} = 1000nM, AURKB IC_{50} = 50nM and AURKC IC_{50} = 250nM) (Crispi et al., 2010). ZM447439 was shown to inhibit proliferation of all malignant mesothelioma (MM) cells and this is thought to be due mainly to inhibition of AURKB in MSTO-211H and MPP89 cell lines (Crispi et al., 2010). Another study by Georgieva et al. (2010) demonstrated that ZM447439 had an anti-proliferative effect in three Gastroenteropancreatic Neuroendocrine cancer cell lines (BON, QGP-1 and MIP-101). The anti-proliferative effects produced an IC_{50} in the nanomolar to low micromolar range and ZM447439 potently induced apoptosis as well as brought about cell cycle arrest (G_0/G_1 phase) and blocked G_2/M transition (Georgieva et al., 2010). This anti-proliferative effect of ZM447439 in Gastroenteropancreatic Neuroendocrine cancer cell lines is amplified when in combination with chemotherapeutics and hence ZM447439 could be a novel treatment approach in Gastroenteropancreatic Neuroendocrine cancer (Georgieva et al., 2010). It is therefore currently suggested that ZM447438 should be investigated further in future clinical trials involving Gastroenteropancreatic Neuroendocrine tumours.

PF-03814735 is an orally bioavailable inhibitor of both AURKA (IC_{50} = 0.8nM) and AURKB (IC_{50} = 5nM) and inhibits several other kinases by >90% at 100nM (FLT3, JAK2, TrkB, RET, MST3) (Bavetsias and Linardopoulos, 2015b). A study by Dalva-Aydemir et al. (2019) showed that PF-03814735 caused a potent inhibition of cell growth in KTC2 thyroid cancer cells which possess a mutation (C228T) in the telomerase reverse transcriptase gene promoter (TERTp).

Lastly, AMG-900 is potent, orally bioavailability, AURK inhibitor which inhibits all three isoforms with a relatively similar degree of potency (AURKA IC_{50} = 5nM, AURKB IC_{50} = 4nM and AURKC IC_{50} = 1nM) (Bavetsias and Linardopoulos, 2015b). A recent Phase 1 clinical trial conducted by Carducci et al. (2018) demonstrated a dose expansion study of AMG-900 in three different solid tumour types; taxane- and platinum-resistant ovarian cancer, taxane-resistant triple-negative breast cancer (TNBC), and castration-resistant and taxane- or cisplatin/etoposide-resistant prostate cancer (CRPC). The results produced indicated that a 40mg/day dose with a prophylactic treatment of Granulocyte colony-stimulating factor (G-CSF)

produced a manageable toxicity and showed single-agent activity in patients with heavily pre-treated, chemotherapy-resistant ovarian cancer (Carducci et al., 2018). This could be a potential pre-treatment strategy in patients with heavily pre-treated chemotherapy-resistant ovarian cancer.

Again, as mentioned before in Section 1.11.1, the problems and limitations with ATP-competitive inhibitors remain more or less the same when seeking to target individual kinases. In the case of the AURKs the high sequence homology between the catalytic domain of the three isoforms (McIntyre et al., 2017) makes it a challenge to specifically target each individual AURK isoform using ATP-competitive inhibitors. In targeting AURK there also seems to be a problem where the use of ATP-competitive molecules produce limited efficacy or are ineffective in solid tumours (Bavetsias and Linardopoulos, 2015b). The most popular hypothesis in the field for this is the need to expose the tumour to the drug through a number of cell cycles or for a prolonged time in mitosis, in order to exert their maximum effect in cancer cells before severe toxic side effects manifest in patients (Bavetsias and Linardopoulos, 2015b). Also, molecules with extended chemical space that possess better selectivity for AURKA in isolation are perhaps less able to engage the active site in a cellular setting due to how TPX2 modulates accessibility to the active/ATP-binding site. So strategies are required to either disrupt the binding of TPX2 to make the active site more accessible or develop alternative allosteric inhibitors. Could it be the high levels of TPX2 that are present in solid tumours and its protection of the active site/Thr288 phosphorylation could be rendering currently available ATP-competitive inhibitors less potent? The majority of ATP-competitive inhibitors have been screened for and assayed against AURKA in isolation, not as an AURKA-TPX2 complex (Anderson et al., 2007). The points above highlight the need to target the AURKA in alternative ways rather than targeting the ATP binding site and therefore perhaps there is now the requirement to develop inhibitors targeting the AURKA-TPX2 complex rather than AURKA alone.

1.13. AURKA/TPX2 in cancer.

TPX2, the main regulator of AURKA, has also been considered as an oncogenic marker, both independently and in concert with AURKA. As such it is worth considering its role individually in cancer as well as a key component of the AURKA/TPX2 complex.

TPX2 has been shown to have a pathological effect in a variety of different cancer types including; prostate cancer (Zou et al., 2018a), hepatocellular carcinoma (Hsu et al., 2017), breast cancer (Jiang et al., 2019), gastric cancer (Tomii et al., 2017, Jiang et al., 2019) and colon cancer (Wei et al., 2013). TPX2 is highly expressed in most cancer types but it being considered as a prognostic indicator of disease has been controversial, even though in most cases upregulation of TPX2 had a negative impact on prognosis (Wang et al., 2018). A

conflicting study by Pan et al. (2017) indicated that TPX2 expression in prostate cancer patients was not related to survival time and its decrease, so a meta-analysis by Wang et al. (2018) was carried to gather a better understanding of TPX2's potential prognostic significance across a panel of cancer cell types (Gastric, hepatocellular cancer, malignant astrocytoma, prostate, epithelial ovarian cancer, bladder carcinoma, colon cancer, esophageal squamous cell carcinoma, renal cell cancer and squamous cell lung carcinoma). It was concluded that TPX2 overexpression indicated poor survival in most solid tumours and hence TPX2 expression is a significant prognostic indicator (Wang et al., 2018). The overexpression of TPX2 in human breast cancer was linked to the proliferation, invasion and migration of breast cancer cells through MMP 2 and 9 (Yang et al., 2015b). In another study by (Jiang et al., 2019) TPX2 was indicated as a novel prognostic marker and therapeutic target in human triple-negative breast cancer. The study showed that TPX2 could be a prognostic biomarker of progression free survival and overall survival following initial treatment in triple-negative breast cancer and could also act as an indicator of overall survival and potential therapeutic intervention (Jiang et al., 2019). In colon cancer cells and tissues, TPX2 is aberrantly expressed and is suggested to upregulate the PI3K/AKT pathway, MMP2 expression and hence tumorigenesis, invasiveness and metastasis (Wei et al., 2013). TPX2 is also suggested as a good indicator of prognosis and target for therapeutic intervention in gastric cancer (Liang et al., 2016) as well as being associated with poor survival (Tomii et al., 2017). TPX2 was shown to be aberrantly expressed in gastric cancer compared to the normal epithelia (Liang et al., 2016). Upregulation of TPX2 expression resulted in tumour cell migration and invasion as well as downregulating several genes including; cyclin B1, cdk4, p53, Bax, caspase-3 and E-cadherin but elevating the levels of cyclin D1, cdk2, N-cadherin, slug, MMP-2 and MMP-9, suggesting a link between TPX2 overexpression and tumour cell epithelial–mesenchymal transition (EMT) (Liang et al., 2016). Hepatocellular carcinoma (HCC) is one of the hardest cancers to treat with chemotherapeutics largely having no effect and TPX2 was shown by (Hsu et al., 2017) to be upregulated in 42% of primary HCCs and was linked to advanced stage distant metastases and poor prognosis. Inhibition of TPX2 lead to cell cycle arrest, apoptosis, senescence and a rise in polyploidy in cells in HCC (Hsu et al., 2017). Other research by (Liu et al., 2014b) demonstrated that the level of TPX2 in normal liver cells (hepatocytes) was much reduced compared to that of HCC cells. They also suggested that overexpression of TPX2 may be involved in cancer cell invasion in HCC cells, through activation of the AKT and subsequent increased expression of MMP-2 and MMP-9 (Liu et al., 2014b). Lastly, the upregulation of TPX2 was shown to increase proliferation, invasiveness and migration and inhibit apoptosis in prostate cancer cell lines (Zou et al., 2018a). Increased TPX2 expression was found to be associated with high tumour node metastases (TNM), clinicopathological staging and also with high Gleason scores, metastasis and a rise in PSA after treatment (Zou et al., 2018a). This indicated the potential of TPX2 as a biomarker for the prognosis and diagnosis of prostate cancer (Zou et al., 2018a). In a study by (Pan et al., 2017) it was shown

that the targeted inhibition of TPX2 results in the downregulation of genes associated with regulation of the cell cycle and chromosome segregation (securin, seprase, AURKA, AURKB, Cyclin B1, Cyclin B2, MPS1, BUB1, BUB3, MAD1 and MAD2) in prostate cancer cells.

As well as examining the roles of AURKA and TPX2 in cancer individually, the two must also be considered as a single functional complex in an oncology setting. A paper by (Asteriti et al., 2010) suggested the role of the AURKA/TPX2 complex co-expressed as a functional unit or so-called “holoenzyme” - a biochemically active compound that is composed of an enzyme with a coenzyme - in cancer. This was further enhanced by (Kadara et al., 2009) who highlighted the correlation between AURKA and TPX2 overexpression in a study comparing lung cancer cells to normal cells and similarly upregulation of both AURKA and TPX2 was observed in carcinoma ovarian cancer in comparison to adenoma ovarian cancer (Scharer et al., 2008). Thus, AURKA, TPX2 and the AURKA/TPX2 complex make attractive therapeutic targets. For example, it was shown in a study (van Gijn et al., 2019) that BRCA2-deficient cancer cells become genomically unstable and more susceptible to targeting of both AURKA and TPX2. This was achieved using short-hairpin RNA (shRNA) to produce BRCA2 deficient cancer cell lines and depleting AURKA and TPX2 using siRNA rundown (van Gijn et al., 2019). In pancreatic cancer, specifically pancreatic ductal adenocarcinomas (PDAC) AURKA and TPX2 are suggested to be regulated by KRAS in what is a largely KRAS-driven cancer subtype (Gomes-Filho et al., 2020a). They are both associated with a worsening prognosis and it is hypothesised in this study that AURKA and TPX2 act as targets for KRAS and targeted inhibition of the AURKA/TPX2 signalling axis may be a beneficial therapeutic intervention in KRAS-driven PDAC (Gomes-Filho et al., 2020a).

1.13.1. Allosteric inhibitors (of the AURKA/TPX2 complex).

To overcome the limitations which are associated with ATP-competitive AURKs inhibitors and appreciating AURKA-TPX2 functions as a ‘holoenzyme’, as described above (Section 1.12.1), targeting kinases through an allosteric mechanism may be an alternative and more selective approach. There are currently no potent allosteric AURK inhibitors available. Development of these could be based on targeting the inactive conformation of AURKA or targeting of upstream activator proteins (McIntyre et al., 2017). The most promising and well-researched is development of a compound that would block/disrupt AURKA/TPX2 binding (McIntyre et al., 2017). The benefit of this being that these so-called protein-protein interaction (PPI) inhibitors/mimetics would disrupt AURKA localisation as well as affect its activity. This would serve as a useful validation of the role of the AURKA/TPX2 complex as a target in cancer and also these compounds would display a much higher degree of selectivity compared to ATP-competitive inhibitors (McIntyre et al., 2017). Interestingly, and as eluded to previously

(Section 1.12.1), the majority of Pharma-driven high throughput screening programmes designed to develop ATP-competitive inhibitors typically have screened for inhibition against the AURKA protein in isolation *in vitro* in the absence of TPX2, hence generating molecules with high potency against said AURKA as a target without any insight into potential impact of TPX2 on modulation of catalytic activity and therefore making it a more challenging target.

So, as we move forward, the design of molecules for targeted disruption of the AURKA/TPX2 complex, be it with physical compounds or through computational screening *in silico*, has grown in terms of research in the last 10 years. Initial studies (Widodo et al., 2010) identified TPX2 as a target for Withanone (an alcoholic extract from *Ashwagandha* leaves that has been shown to kill cancer cells), which was shown through a combination of both computational and experimental studies to alter AURKA signalling in an ATP-independent manner through inactivation of the AURKA/TPX2 complex (Grover et al., 2012). This was first based on computational predictions but then was further validated by means of RT-PCR, Western blotting and immunocytostaining in human cancer cell lines.

A study by (Burgess et al., 2016) used what is known as a single variable domain antibody (Nanobodies) or vNAR domain, derived from a shark heavy chain antibody, that binds a specific target, to perturb the AURKA-TPX2 complex. A synthetic vNAR domain, vNAR-D01 was demonstrated to disrupt the binding between AURKA and TPX2 by binding to AURKA in the same hydrophobic pocket that TPX2 occupies (Burgess et al., 2016). vNAR-D01 was shown, through its CDR3 loop to overlap with two key residues of TPX2 (Tyr8 and Tyr10) which are critical for binding in the hydrophobic pocket of AURKA and it inhibited AURKA with an IC₅₀ of 6.76µM (Burgess et al., 2016).

Using a similar experimental rationale, (Zorba et al., 2019) described the use of monobodies, also known as 'antibody mimetics' to bind to an allosteric pocket on AURKA and can cause both strong inhibition or activation. This is a simple alternative to antibodies that are formed of a fibronectin type III (FT3) domain backbone and offer the benefit of strong selectivity, can inhibit or activate (with activation being a particularly powerful and new tool, rarely seen with ATP-competitive inhibitors) and avoid competing with the high levels of endogenous ATP (Zorba et al., 2019). For the monobodies screened in this study, there was a 15-fold activation and 20-fold inhibition in terms of shift in AURKA activity (Zorba et al., 2019). This was measured through use of a ADP/NADH coupled assay which was used to measure phosphorylation of the Lats2 peptide by AURKA in the presence or absence of TPX2 (Zorba et al., 2019). These examples of strong allosteric modulators open the possibility of a new avenue of drug design though it is recognised that they will need to be developed further to make them more drug-like for effective delivery *in vivo*.

An alternative approach has utilised a stapled TPX2 proteomimetic, spanning residues 1-43 (crucial residues for binding to AURKA), has also been used as an additional strategy (Rennie et al., 2016) to understand better the binding between TPX2 and AURKA. This proteomimetic was shown via isothermal titration calorimetry to be bound tighter and with

higher affinity to AURKA than the native TPX2 protein and mimicked it by inducing the autophosphorylation and subsequent activation of AURKA (Rennie et al., 2016). This could have potential therapeutic value in perhaps developing a TPX2 proteomimetic that is 'inactive' but competes with the native TPX2 for AURKA binding and therefore stops the complex from forming and so 'switches off' AURKA activity.

Important to add is that there has been some limited yet significant development of small-molecule inhibitors of the AURKA/TPX2 protein-protein interaction. Following a high-throughput screen of around 17,000 compounds in a fluorescence anisotropy (FA) assay between recombinant AURKA and a tagged TPX2 fragment, a compound known as AurkinA ($K_d = 3.77\mu\text{M}$) was generated (Janecek et al., 2016). This AurkinA compound was able to, bind AURKA in this same hydrophobic "Y-pocket" which is normally inhabited by the critical Y8 and Y10 residues of TPX2 (Janecek et al., 2016), comparable to the vNAR domain approach mentioned earlier. In cell-based assays, AurkinA caused a concentration-dependent shift in mislocalisation of AURKA from the mitotic spindles, which TPX2 normally recruits it to and it also inhibited the AURKA autophosphorylation (p-T288) in a concentration-dependent manner (Janecek et al., 2016) and so represents a first step towards development of potential allosteric inhibitors of AURKA activity.

These studies highlight the potential therapeutic value in targeting protein-protein interactions as an alternative, potent and potentially selective approach to inhibiting kinases whilst avoiding the targeting of the kinase ATP-binding site without the problem of competing with the endogenous ATP.

1.14. Cross-talk between IKKs and AURKA.

A more recently proposed substrate of the IKK complex, distinct from classical IKK substrates, is AURKA, which is proposed to be regulated in a NF- κ B independent but IKK-dependent manner. This suggests that the IKK proteins may be able to regulate AURKA and cell cycle progression. For instance, it was shown in a study by Prajapati et al. (2006) that IKK α has been found to regulate the M phase of the cell cycle by phosphorylating the critical Thr288 residue in the activation loop of AURKA, which renders it in its active conformation. Also, (Irelan et al., 2007) showed there is an interaction between AURKA and β -TRCP which is IKK β -dependent. This suggests that IKK β -regulated AURKA phosphorylation may control or contribute to the regulation of the expression of AURKA through mitosis. These studies suggested a potential role of both IKK α and IKK β in regulation of AURKA in the cell cycle, particularly during the mitotic phase of cell doubling (Irelan et al., 2007, Prajapati et al., 2006). It was also shown that AURKA decreased TNF α -induced I κ B α degradation and AURKA regulated NF- κ B activity by binding directly and phosphorylating I κ B α in gastric cancer cells (Briassouli et al., 2007, Katsha et al., 2013). It was also shown in Multiple myeloma (MM) cells

that blockage of the AURKA by pan-Aurora small molecule kinase inhibitors, decreases AURKA--IKK interaction and subsequently reduces activation of NF- κ B pathway and switching on of anti-apoptotic NF- κ B target genes, thus sensitising cells to apoptosis (Mazzera et al., 2013a). Thus, the studies detailed above implicate the potential role of the catalytic IKK proteins and potentially other NF- κ B components in regulating AURKA and hence a potential PPI between these proteins that needs to be elaborated on.

1.14.1 Mapping of the PPIs of the IKKs and the AURKs.

Both AURKA and its co-activator TPX2 peak in terms of protein expression and functional activity at prometaphase and as mitosis progresses, they are degraded with similar kinetics. Previous work in the lab confirmed, using peptide array techniques and recombinant purified proteins, that AURKA and IKK α/β interact directly. This was demonstrated by bidirectional mapping approaches (recombinant AURKA on IKK $\alpha/\beta/\gamma$ peptide arrays and recombinant IKK β on AURK A/B/C arrays) to highlight two key regions of binding within the amino acid sequences of the IKK proteins, the kinase domains in each isoform and the NEMO binding domain common to each isoform (Wilson 2013). A cell-permeable peptide (CPP) containing the conserved hexapeptide sequence (L-D-W-S-W-L) [aa 737 – 742] derived from IKK β was taken forward as a pharmacological tool. This contained the two key tryptophans (W739 and W741), which were identified by both alanine scanning and truncation (both N- and C-term) analyses and were deemed critical for binding. A NBD CPP peptide was used to disrupt IKK-AURKA binding during mitosis and was shown decrease phosphorylation of AURKA and accelerate degradation of total AURKA protein expression. In quiescent cells, pre-treatment with NBD CPP caused inhibition of TNF α -stimulated NF- κ B-p65 phosphorylation in a cellular setting (Wilson 2013). It was also shown via *in silico* modelling that there was a possibility of the NBD CPP binding to AURKA at the sites engaged by TPX2, therefore explaining a possible mechanism for impacting on AURKA status. Whether this mechanism of Aurora degradation is as a result of a direct effect IKK complex disruption or an independent mechanism (i.e. direct effect on AURKA/TPX2 binding) is unclear and understanding this will lead to the development of novel therapeutics to disrupt IKK-AURKA interactions.

1.15. Aims of the study.

The studies described in Section 1.13 above have to varying degrees illustrated the ability of the IKK proteins to regulate AURKA, where it has been suggested that AURKA is a substrate of the IKKs distinct from activation of the NF- κ B pathways. Previous preliminary data in the lab also suggested that a CPP derived from the NBD of IKK β (with a primary function of

disrupting NF- κ B activation) could impact on the phosphorylation and total expression of AURKA as well as the phosphorylation of the other two AURK family members in a cell cycle-dependent manner (Wilson 2013). Up until now, work carried out previously in the lab and in the literature has not fully tested nor characterised the mechanistic relationship between IKK signalling and AURKA-TPX2 function/activity through the mitotic phase of the cell cycle. Furthermore, the mechanism by which the NBD WT CPP can modulate both IKK-NF κ B and AURKA signalling status remains to be fully explored and raises the question as to whether pharmacological modulation of these signalling proteins has any bearing on the classic markers of cellular mitosis associated with AURKA activation, inactivation and degradation, such as TPX2 PP1A, PLK1 etc..

The objectives of this study are to target IKK signalling comparatively using the identified NBD-derived peptide in parallel to small molecule IKK kinase inhibitors and siRNA protein 'run-down' strategies to explore the potential contribution of the different features of structure and/or activity of the IKKs to the regulation of AURKA-TPX2 status in mitotic cells. This will allow the identification of the effect of different molecular and pharmacological techniques to target different aspects of IKK-AURKA signalling towards elucidating the mechanism of action of the NBD WT CPP and its ability to impact on the status of AURKA and its key related markers, TPX2 and PLK. Following on, could this be extended to different solid tumour cell lines as well as the main focus of prostate cancer and the pharmacological targeting/disruption of AURKA/TPX2 to investigate the effect phenotypically on different cancer hallmarks to determine their role. This would then be extended to use of the NBD WT CPP in combination with previously ineffective ATP-competitive AURK inhibitors to target/disrupt AURKA/TPX2 and subsequent impact on phenotypic cancer hallmarks. It is hypothesised that the NBD WT CPP may support two-site targeting of AURKA-TPX2 signalling by improving access to the catalytic site and therefore an advance towards more effective combination targeting along with previously ineffective ATP-competitive AURK inhibitors.

The aims of this study are therefore to:

1. To establish a cell-based approach to analysing the cellular status of AURKA-TPX2, and IKKs, during mitosis using a nocodazole-mediated cell synchronisation protocol.
2. Characterise the kinetics of mitosis to enable the assessment of signalling proteins in mitotic cells following nocodazole arrest/trap and release.
3. Examine the impact of the NBD peptide on AURKs and related markers that are associated with cell cycle progression.
4. To use different molecular and pharmacological techniques and MEF cells lacking IKKa/b (vs. wild-type) to differentially/simultaneously target IKK proteins and examine the impact on the IKK-AURKA cross-talk.

5. To assess the impact of the NBD WT CPP in the cell cycle/mitotic beyond AURKA status in prostate cancer cells and extended to other solid tumour cell lines.
6. Examine potential utility of NBD WT CPP-mediate perturbation of IKK-AURKA-TPX2 signalling in different tumour settings and its impact on phenotypic outcomes.
7. To pharmacologically target AURKA/TPX2 binding with ATP competitive inhibitors and the NBD WT CPP to assess whether there is an improved efficacy with the combination vs monotherapy to impact on AURKA and TPX2 status and whether this can be correlated to phenotypic outcomes (cell viability, clonogenic survival and apoptosis).

Chapter 2: Materials and Methods.

2.1. Materials.

2.1.1. Antibodies.

A number of antibodies raised in various species were used for detection purposes as detailed below;

Name	Company	Catalog#	Dilution factor	Blocking	Washing method
Rabbit monoclonal IgG anti-Phospho-AURKA (Thr288)/AURKB (Thr232)/AURKC (Thr198) (D13A11)	Cell signalling Technology Inc. (MA, USA)	2914S	1:6000	5% BSA (0.5% 1 ^o Ab)	3x5 mins TBST (0.1%), 2 ^o Ab 0.5% BSA 1hr 30 mins, 3x5 mins TBST (0.1%)
Mouse monoclonal IgG anti – Aurora A (35C1)	Abcam Inc (MA, USA)	ab13824	1:6000	5% BSA (0.5% 1 ^o Ab)	3 x 5 mins TBST (0.1%), 2 ^o Ab 0.5% BSA 1hr 30 mins, 3 x 5 mins TBST (0.1%)
Rabbit Polyclonal IgG anti-TPX2 antibody.	Novus biologicals (Abingdon, UK).	ND500-179SS	1:20000	5% BSA (0.5% 1 ^o Ab)	3 x 10 mins TBST (0.1%), 2 ^o Ab 0.5% BSA 1hr 30 mins, 3 x 10 mins TBST (0.1%)
TPX2 (H-300) rabbit polyclonal antibody.	Santa Cruz Biotechnology Inc (CA, USA)	sc-32863	1:10,000	5% BSA (0.5% 1 ^o Ab)	3x10 mins TBST (0.1%), 2 ^o Ab 0.5% BSA 1hr 30 mins, 3x10 mins TBST (0.1%)
Rabbit Polyclonal IgG anti- Phospho-PLK1 (Thr210) (D5H7)	Cell signalling Technology Inc. (MA, USA)	9062S	1:1000	5% BSA (0.5% 1 ^o Ab)	3x5 mins TBST (0.1%), 2 ^o Ab 0.5% BSA 1hr 30 mins, 3x5 mins TBST (0.1%)
Mouse monoclonal IgG anti-PLK1 (F-8)	Santa Cruz Biotechnology Inc (CA, USA)	sc-17783	1:500	5% BSA (0.5% 1 ^o Ab)	3x5 mins TBST (0.1%), 2 ^o Ab 0.5% BSA 1hr 30 mins, 3x5 mins TBST (0.1%)
Rabbit Polyclonal IgG anti-PP1 α	Cell signalling Technology Inc. (MA, USA)	2582S	1:1000	5% BSA (0.5% 1 ^o Ab)	3x5 mins TBST (0.1%), 2 ^o Ab 0.5% BSA 1hr 30 mins, 3x5 mins TBST (0.1%)

Mouse monoclonal IgG anti-IKK α (14A231)	Merck Chemicals Limited (Nottingham, UK)	OP133	1:3000	5% BSA (0.5% 1 ^o Ab)	3x5 mins TBST (0.1%), 2 ^o Ab 0.5% BSA 1hr 30 mins, 3x5 mins TBST (0.1%)
Phospho-NF- κ B2 p100 (Ser866/870) Rabbit Antibody	Cell signalling Technology Inc. (MA, USA)	4810S	1:1000	1% milk (3% BSA 1 ^o Ab)	3x5 mins TBST (0.1%), 2 ^o Ab 1% milk 1hr 30 mins, 3x5 mins TBST (0.1%)
Mouse monoclonal Anti-NF κ B p52 Antibody	Merck Chemicals Limited (Nottingham, UK)	05-361	1:15000 (RT)	5% BSA (0.5% 1 ^o Ab)	3x5 mins TBST (0.1%), 2 ^o Ab 0.5% BSA 1hr 30 mins, 3x5 mins TBST (0.1%)
Rabbit monoclonal IgG anti-IKK β (Y466)	Abcam Inc (MA, USA)	ab32135	1:1000	5% BSA (0.5% 1 ^o Ab)	3x5 mins TBST (0.1%), 2 ^o Ab 0.5% BSA 1hr 30 mins, 3x5 mins TBST (0.1%)
Rabbit Polyclonal IgG anti – p-p65 (Ser536)	Cell signalling Technology Inc. (MA, USA)	3031S	1:3000	5% BSA (0.5% 1 ^o Ab)	3x5 mins TBST (0.1%), 2 ^o Ab 0.5% BSA 1hr 30 mins, 3x5 mins TBST (0.1%)
Rabbit Polyclonal IgG anti-NF- κ B p65 (C-20)	Santa Cruz Biotechnology Inc (CA, USA)	sc-372-G	1:500	5% BSA (0.5% 1 ^o Ab)	3x5 mins TBST (0.1%), 2 ^o Ab 0.5% BSA 1hr 30 mins, 3x5 mins TBST (0.1%)
I κ B α Rabbit Antibody	Cell signalling Technology Inc. (MA, USA)	9242S	1:3000	5% BSA (0.5% 1 ^o Ab)	3x5 mins TBST (0.1%), 2 ^o Ab 0.5% BSA 1hr 30 mins, 3x5 mins TBST (0.1%)
PARP Rabbit Antibody	Cell signalling Technology Inc. (MA, USA)	9542S	1:1000	5% BSA (0.5% 1 ^o Ab)	3x5 mins TBST (0.1%), 2 ^o Ab 0.5% BSA 1hr 30 mins, 3x5 mins TBST (0.1%)
Caspase-9 Rabbit Antibody (Human Specific)	Cell signalling Technology Inc. (MA, USA)	9502S	1:1000	5% BSA (0.5% 1 ^o Ab)	3x5 mins TBST (0.1%), 2 ^o Ab 0.5% BSA 1hr 30 mins, 3x5 mins TBST (0.1%)
Purified Rabbit Polyclonal anti-Caspase 3 Ab	Biologend	B132165	1:3000	5% BSA (0.5% 1 ^o Ab)	3x5 mins TBST (0.1%), 2 ^o Ab 0.5% BSA 1hr 30

					mins, 3x5 mins TBST (0.1%)
Rabbit XIAP Ab	Cell signalling Technology Inc. (MA, USA)	2042S	1:1000	5% BSA (0.5% 1 ^o Ab)	3x5 mins TBST (0.1%), 2 ^o Ab 0.5% BSA 1hr 30 mins, 3x5 mins TBST (0.1%)
Rabbit monoclonal IgG anti-GAPDH (14C10)	Cell signalling Technology Inc. (MA, USA)	2118S	1:20,000 (RT)	5% BSA (0.5% 1 ^o Ab)	3x5 mins TBST (0.1%), 2 ^o Ab 0.5% BSA 1hr 30 mins, 3x5 mins TBST (0.1%)
Horseradish peroxidase (HRP)-conjugated sheep anti-mouse IgG	Stratech Scientific Limited, Oaks Drive, Newmarket, Suffolk, CB8 7SY	515-035-003	1:15000 (RT)	0.5% BSA / 1% milk (2 ^o Ab)	N/A
HRP-conjugated donkey anti-rabbit IgG	Stratech Scientific Limited, Oaks Drive, Newmarket, Suffolk, CB8 7SY	711-035-152	1:15000 (RT)	0.5% BSA / 1% milk (2 ^o Ab)	N/A

(RT) = Room temperature.

2.1.2. Reagents.

All materials used in this project were of the highest commercial purity available and were supplied by Sigma-Aldrich Co Ltd. (Poole, Dorset, UK) unless otherwise stated.

Pre-stained SDS-PAGE molecular weight markers (Broad and low): **Biorad Laboratories (Hertfordshire, UK).**

Bovine serum albumin (BSA): **Gibco BRL (Paisley, UK).**

Dithiothreitol (DTT): **Boehringer Mannheim Ltd (East Sussex, UK).**

Ethanol: **Bamford Laboratories.**

Hydrochloric acid: **Fisher Scientific (Leicestershire, UK).**

Methanol: **Bamford Laboratories.**

Nitrocellulose membrane (Protran): **Schleicher & Schuell (Surrey, UK).**

3MM filter/blotting paper: **Whatman (Kent, UK).**

Rotiphorese® Gel (37.5:1) Acrylamide: **Carl Rothe GmbH + CO.KG (Karlruhe, Germany).**

Lipofectamine RNAiMax: **Invitrogen Ltd (Paisley, UK).**

2.1.2.1. Reagents for cell culture and transfection.

Corning B.V. (Netherlands).

Cell culture plastic ware;

25cm³ flask.

75cm³ flask.

6-well plate.

12-well plate.

96-well plate.

10mm, sterile, tissue-culture treated dishes.

30mm, sterile, tissue-culture treated dishes.

STARLAB Ltd (Milton Keynes, UK).

2µl single channel pipette.

10µl single channel pipette.

20µl single channel pipette.

200µl single channel pipette.

1000µl single channel pipette.

200µl multi-channel pipette.

Invitrogen GIBCO BRL. (Paisley, UK).

Antibiotics (Penicillin, streptomycin), Foetal calf serum (FCS), Charcoal-stripped FCS, L-glutamine, Dulbecco's Modified Eagles Medium (DMEM), RPMI 1640, Trypsin, Opti-MEM reduced serum Medium, Non-essential amino acids (NEAA), sodium pyruvate.

Sarsredt AG & Co LTD (Leicester, UK).

Serological pipette 5ml.

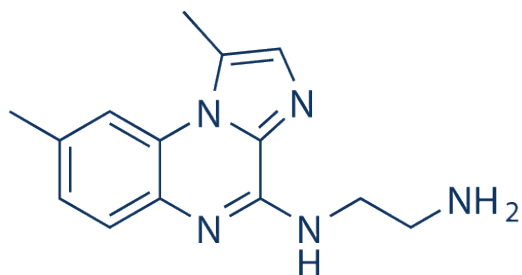
Serological pipette 10ml.

Serological pipette 25ml.

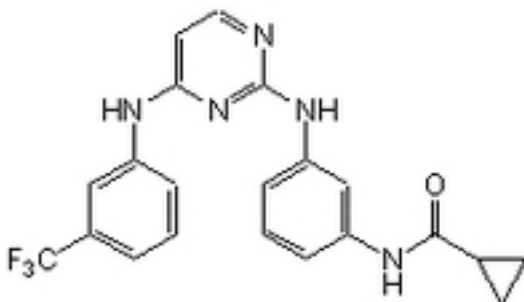
2.1.2.2. Small molecule kinase inhibitors targeting IKKs and Aurora kinases.

Proprietary "in-house" small-molecule IKK α inhibitor (SU1433).

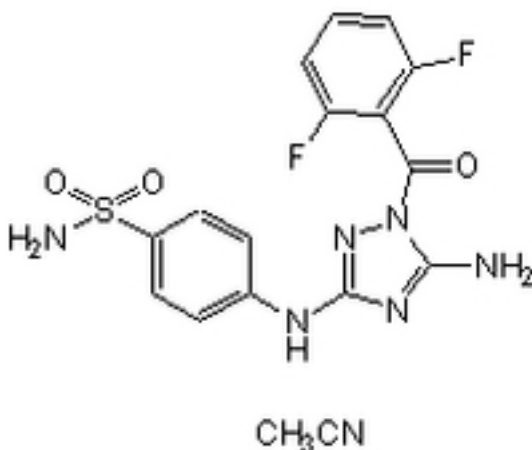
BMS-345541(N-(1,8-Dimethylimidazo[1,2-a]quinoxalin-4-yl)-1,2-ethanediamine hydrochloride) **Sigma-Aldrich Co Ltd. (Poole, Dorset, UK).**



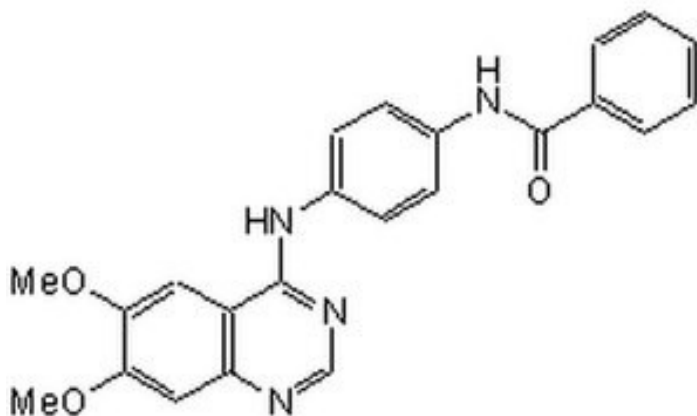
Aurora Kinase inhibitor III (Cyclopropanecarboxylic acid-(3-(4-(3-trifluoromethylphenylamino)-pyrimidin-2-ylamino)-phenyl)-amide)) (Catalog No. S2931) (**Selleckchem, Cambridgeshire, UK**).



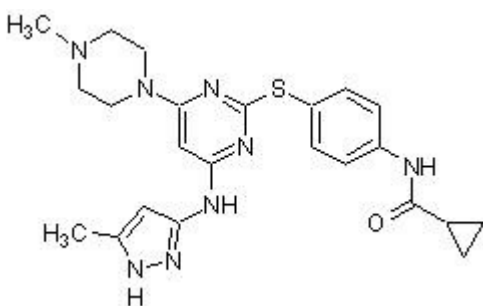
Aurora Kinase/CDK inhibitor (4-(5-Amino-1-(2,6-difluorobenzoyl)-1H-[1,2,4]triazol-3-ylamino)-benzenesulfonamide) (Catalog No.189406) (**Merck KGaA, Darmstadt, Germany**).



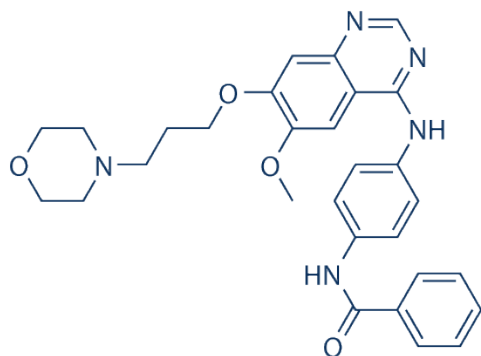
Aurora Kinase inhibitor II: (4-(4'-Benzamidoanilino)-6,7-dimethoxyquinazoline) (Catalog No. sc-203827) (**Santa Cruz Biotechnology Inc (CA, USA)**).



VX-680 (MK-0457): Aurora kinase inhibitor (N-[4-[[4-(4-Methyl-1-piperazinyl)-6-[(5-methyl-1H-pyrazol-3-yl)amino]-2-pyrimidinyl]thio]phenyl]cyclopropanecarboxamide) (Catalog No. ab120799) (**Abcam, Cambridge, UK**).



ZM447439:(N-[4-[[6-methoxy-7-[3-(4-morpholinyl)propoxy]-4-quinazolinyl]amino]phenyl]-benzamide) (Catalog No. S1103) (**Selleckchem, Cambridgeshire, UK**).



2.1.2.3. Reagents for targeted rundown of expression.

Horizon Discovery Ltd (Cambridge, UK)

To run-down IKK α and IKK β in the cell the following siRNA target sequences were used:

IKK α (GCGUGAAACUGGAAUAAAU) (Cat. No. J-003473-08-0050).

IKK β (GAGCUGUACAGGAGACUAA) (Cat. No. J-003503-14-0050).

Non-targeting (Cat. No. D001810-01-05).

2.1.2.4. Reagents/equipment for phenotypic assays.

96 Well Black Assay Plate Clear Bottom With Lid, Catalogue number 3603 (**Corning B.V. Netherlands**).

NucView 488 Caspase-3 substrate solution (**Biotium, Inc. California, USA**).

Nunclon U-bottom ultra-low attachment sphere 96-well plates (**Thermo Scientific Leicestershire, UK**).

Giemsa stain, modified (GS1L) (**Sigma-Aldrich Co Ltd. (Poole, Dorset, UK)**).

2.1.2.5. NEMO-Binding Domain Peptides derived from IKK β .

All NEMO binding domain peptides as depicted below were obtained from **Genscript USA Inc., New Jersey, USA** at >95% purity. Custom synthesis was achieved by liquid phase peptide synthesis (LPPS) or solid phase peptide synthesis (SPPS). HPLC traces below indicate the purity of the peptides.

NEMO-binding domain 'wild-type' cell-permeable peptide **NBD WT CPP**: Sequence - YGRKKRRQRRRFTALD**WSWL**QT-.

NEMO-binding domain 'wild-type' cell-permeable peptide **NBD MT CPP**: Sequence - YGRKKRRQRRRFTALD**ASAL**QT-.

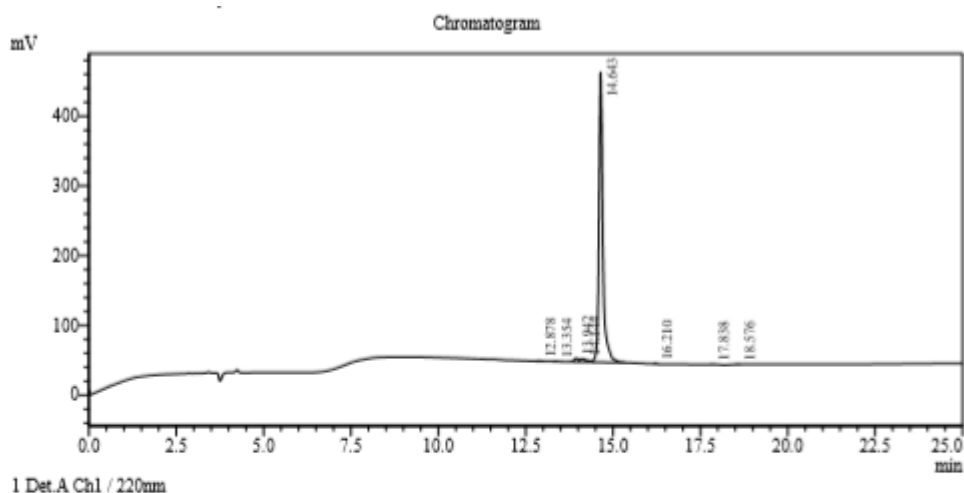
Leader sequence derived from HIV TAT protein in the HIV transduction domain to allow peptide to get across cell membrane (Yang et al., 2013).

11mer peptide sequence – this is the 11 amino acid sequence derived from the C-terminal NBD of IKK β (F734 to T744) which forms the NBD WT CPP and contains the **hexapeptide**

sequence derived from the NBD of IKK β and contains the two key tryptophan (W) residues that are critical for binding. In the NBD MT CPP, the two key residues are changed to alanine (A), which renders the peptides binding inactive (May et al., 2000b).

Peptides were dissolved in DMSO and diluted in the appropriate cell culture media ([1:1(50% v/v) addition to wells, final well concentration of 0.5%] before being mixed vigorously to solubilise the peptides for use in cells *in vitro*.

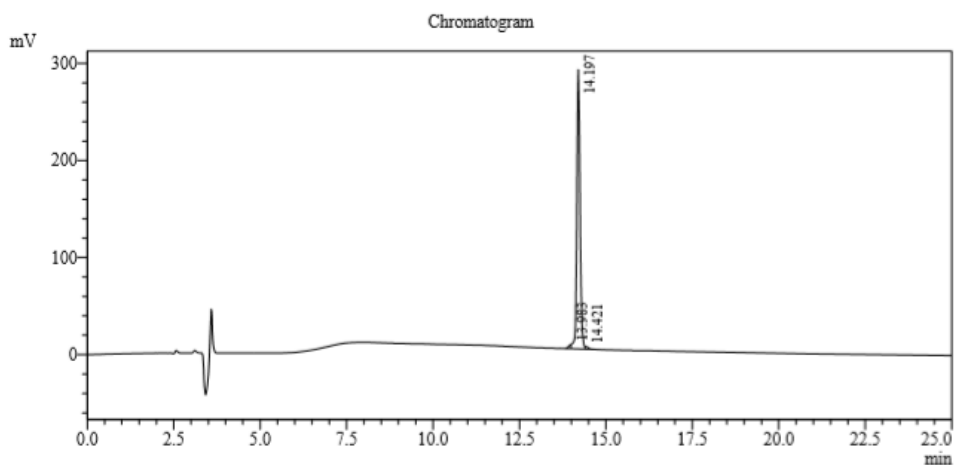
NBD WT CPP (HPLC trace).



Detector A Ch1 220nm

Peak#	Ret. Time	Area	Height	Area %
1	12.878	6236	807	0.183
2	13.354	4648	545	0.136
3	13.942	43126	5076	1.265
4	14.144	61380	4313	1.800
5	14.643	3281697	415590	96.248
6	16.210	6834	1227	0.200
7	17.838	3277	480	0.096
8	18.576	2441	438	0.072
Total		3409639	428475	100.000

NBD MT CPP (HPLC trace).



Peak Table

Peak#	Ret. Time	Area	Height	Area %
1	13.983	21049	4229	1.117
2	14.197	1846364	287695	98.001
3	14.421	16605	2696	0.881
Total		1884018	294620	100.000

2.2 METHODS.

2.2.1. Cell Culture.

Cell culture was carried out under aseptic conditions in a Class II cell culture hood.

2.2.1.1. Cell lines.

Human Caucasian prostate adenocarcinoma (PC3), a kind gift from Prof. H. Leung (Beatson Cancer Institute, Glasgow).

Wild-type and Double-knockout Mouse embryonic fibroblasts (DKO MEFs), a kind gift from Prof. Inder Verma (Salk Institute for Biological Studies, San Diego, USA) and Dr. Michael May (School of Veterinary Medicine, University of Pennsylvania, USA).

T98G Human Caucasian glioblastoma, Catalogue No. 92090213 were obtained from European Collection of Cell Cultures (ECACC), United Kingdom.

MCF7 Human Caucasian breast adenocarcinoma, Catalogue No. 86012803 were obtained from European Collection of Cell Cultures (ECACC), United Kingdom.

LNCaP androgen-insensitive (AI) cells were gifted kindly by Prof. H. Leung (Beatson Cancer Institute, Glasgow).

2.2.1.2. Cell culture.

PC3 and LNCaP AI cells were grown in RPMI 1640 media and MCF7 cells and MEFs were grown in Dulbecco's modified eagles media (DMEM) which was supplemented with 10% (v/v) FCS (Charcoal-stripped for LNCaP AIs), L-glutamine (27mg/ml) and penicillin/streptomycin (250 units/ml; 100µg/ml). T98G cells were grown in Minimum Essential Media (MEM) which was supplemented with 10% (v/v) FCS, non-essential amino acids (1%) and sodium pyruvate (1%). All cells were incubated in a humidified atmosphere at 37°C and 5% CO₂. Cells were cultured as a monolayer in 10ml media in 75cm³ vented flasks and grown until subculture was required.

2.2.1.3. Cell subculture.

Cells were grown as a monolayer until approximately 70-85% confluent, the media was then aspirated, and the cells washed twice with 1.5ml sterile 5% (w/v) trypsin solution. The trypsin was aspirated, and the flasks were given a gentle tap to ensure cells were fully detached. The flask was then washed with 10ml media to re-suspend the recovered cells for passage into flasks and plates with fresh media as appropriate.

2.2.2. Cell synchronisation.

2.2.2.1. Nocodazole trap: arresting cells at pro-metaphase in the cell cycle

Cells were grown in 10mm petri dishes until about 70-80% confluent. Based on the method demonstrated by Zieve et al. (1980), treatment of cells was optimised with the appropriate concentration of Nocodazole depending on each cell type (50ng/ml unless stated otherwise). Cells were treated with Nocodazole overnight for 16-20 hours to trap the cells at prometaphase and then released back through the cell cycle by washing with media that enabled exit through G₂/M phase and subsequently mitosis. After their release from the nocodazole trap, cells were incubated as deemed appropriate for individual experiments. After each time point cells were removed from the incubator and the procedure for preparation of WCEs was carried out as described in Section 2.2.3.1.

2.2.3. Western Blotting and Sample Preparation (whole cell extracts (WCEs)).

2.2.3.1. Sample Preparation.

Whole cell extracts were prepared using a 1x sample buffer (DTTSB) as detailed by Laemmli (1970) (63mM Tris/HCl [pH 6.8], 2mM Na₄P₂O₇, 5mM EDTA, 10% (v/v) Glycerol, 2% (w/v) SDS, 0.007% (w/v) Bromophenol and Blue, 50mM DTT). The bathing medium was firstly aspirated, and the cells were washed once with 1ml of cold PBS. 250µl of DTTSB was added to each well to lyse the cells and cellular material was recovered using a cell scraper. Samples were passed through a 21g needle 3-5 times to shear genomic DNA. Samples were then placed in eppendorfs with a hole pierced in the lid and boiled for 5 min (to denature the protein polypeptides). Samples were either used immediately or frozen at -20°C for future use.

2.2.3.2. SDS-Polyacrylamide Gel Electrophoresis.

Prepared protein samples were separated based on their electrophoretic mobility using SDS-Polyacrylamide Gel electrophoresis (SDS-PAGE). Resolving gels were prepared using: N-methylenebis-acrylamide (30:0.8) to final differing percentages of 10% (v/v) or 7.5% (v/v) acrylamide containing 0.375M Tris (pH 8.8), 0.1% (w/v) SDS and 10% (w/v) ammonium persulfate (APS) and 10% (v/v) glycerol. The acrylamide gel polymerised at room temperature following the addition of N,N,N,N-tetramethylethylenediamine (TEMED) 0.05% (v/v). The solution was poured between two glass plates with 0.05mm spacing (Biorad Protean III setup) and this was assembled in a vertical slab orientation, leaving a 1-1.5cm space and overlaid with 0.1% (w/v) SDS until polymerisation had taken place. After the gel had polymerised, the 0.1% (w/v) SDS was removed and a stacking gel added. The stacking gel was composed of: 10% (v/v) acrylamide: N, -methylenebis-acrylamide (30:0.8) in 125mM Tris, (pH 6.8) 0.1% (w/v) SDS, 0.05% (w/v) ammonium persulfate and 0.05% (v/v) TEMED. Immediately following the addition of the stacking gel, a teflon comb (10 or 15 wells) was inserted prior to polymerisation (~10-15 mins) to mould the wells for loading. After polymerisation, the combs were removed from the wells, gels assembled in a Protean III™ (Bio-Rad) electrophoresis tank (Bio-Rad) and filled with electrophoresis running buffer (25mM Tris, pH 7.5, 129mM glycine, 0.1% (w/v) SDS). Using a Hamilton™ microsyringe, a volume (2-5µl) of pre-stained molecular weight (MW) markers of known molecular weights was loaded into a well in parallel to prepared cell lysates. Samples underwent gel electrophoresis at a constant voltage of 130V until the bromophenol dye present in the sample buffer and off the bottom of the gel.

2.2.3.3. Electrophoretic Transfer of Proteins to a Nitrocellulose Membrane.

Gels containing separated protein polypeptides were transferred following electrophoresis onto nitrocellulose membranes by an electrophoresis blotting procedure described previously Towbin et al. (1979). Each gel was placed firmly onto a nitrocellulose sheet between two 3MM sheets of blotting paper and two outer sponges and assembled in a transfer cassette. This was submerged in transblot buffer (25M Tris, 19mM glycine, 20% (v/v) methanol) in a Bio-Rad Mini Trans-Blot™ tank with the nitrocellulose facing towards the anode. A constant current of 300mA (0.3A) was applied for 1 hour 45 minutes and this was cooled by the addition of an ice pack to the tank.

2.2.3.4. Immunological Detection of Protein through Antisera.

Following transfer of the proteins to the nitrocellulose membrane, the membrane was then 'blocked' for non-specific binding by incubation in 5% (w/v) Bovine Serum Albumin (BSA) in Tris-buffered saline, 0.1% Tween (TBST) buffer blocking solution (150mM NaCl, 20mM Tris, pH7.4, 0.1%(v/v) Tween-20) and gently rocked back and forth on a platform shaker for 2 hours. The 5% (w/v) BSA blocking buffer was then discarded and replaced with 0.5% (w/v) BSA TBST pH 7.4 solution containing an appropriate concentration of antisera (1° antibody) specific to the target protein. This was left overnight on a roller at 4°C in the cold room. The next day, the membranes were washed every 5 minutes in TBST for 15 minutes on a platform shaker. After this wash cycle, the membranes were incubated with a 2° antibody, an IgG antibody which is raised against the species of the primary antibody and had horseradish peroxidase conjugated to it. This was added (1:10,000) to 0.5% BSA in TBST buffer (pH 7.4) and left on the platform shaker at room temperature for 1 hour 30 minutes. Following this, the membrane was then washed every 5 minutes for 15 minutes with TBST as described before. After this second wash cycle, the membrane was then developed using enhanced chemiluminescence (ECL) reagents. The TBST buffer from the final wash was discarded and 5ml of both ECL solution 1 (2.5mM Luminol, 1.2mM Cumeric acid and 100mM Tris/HCl solution [pH 8.5]) and 5ml ECL solution 2 (100mM Tris/HCl solution [pH8.5] and 6.27 mM H₂O₂) were added and washed over the membrane for 2 mins. The membranes were then blotted on tissue (to remove an excess ECL solution) before placed in an exposure cassette and covered with cling film. Lastly, the membranes were developed in the dark room where Kodak X-OMAT LS film was exposed to the membranes for an appropriate amount of time, dependent on the sensitivity of the antibody used. The film was developed by a Kodak M35-M-X-OMAT

processor. The films were then scanned and quantified by densitometry using Scion image software (Scion Corp, Maryland, USA).

2.2.3.5. Nitrocellulose membrane stripping and reprobing.

To re-probe nitrocellulose membranes for detection of additional proteins/protein species said membranes after initial exposure, were removed from film cassettes and were stored at 4°C in TBST prior to stripping of antibody and re-probing for the detection of other proteins using a different antibody. Stripping of antibodies from the nitrocellulose membrane involved incubating in 15 ml stripping buffer (0.05 M Tris-HCl, 2% (w/v) SDS, and 0.1 M β -mercaptoethanol) for around 60 minutes at 60°C in an incubator/shaker (Stuart Science Equipment). After the incubation period was complete, the stripping buffer was discarded in a fume cupboard and the membranes were washed three times with TBST buffer (pH 7.4), changed every 5-10 min to remove any excess stripping buffer/ β -mercaptoethanol remaining. Once the washing periods were finished, the membranes were incubated with primary antibody and detection pursued as described previously using the Western blotting procedure detailed in Section 2.2.3.4.

2.2.4. Fluorescence-Activated Cell Sorting to assess cell cycle status.

Fluorescence-Activated Cell Sorting (FACS) was utilised to enable the sorting of heterogeneous cell populations and identify the distribution of sub-populations of cells in the different phases of the cell cycle (G_1 , S, G_2/M , sub G_0). Cells were plated in 30mm dishes and grown to approximately 70-80% confluency prior to treatment with nocodazole for 16-20 hours and released as described previously in Section 2.2.2.1. FACS tubes were labelled and 2ml fresh media added to each tube. The media was aspirated in each dish and replaced with 1ml trypsin and placed in the incubator for 1-2 mins until the cells detached. The cells were collected and transferred to the FACS tubes with the media and centrifuged for 5 mins at 13,000rpm. The supernatant was aspirated (being careful not to disturb the pellet), 150 μ l PBS added and the pellet resuspended and vortexed. Then, 350 μ l of ice cold 70% (v/v) ethanol was added dropwise with vortexing. The samples were then stored at 4°C for 20 minutes or overnight prior to use. In preparation for analysis, 1ml of PBS was added to each FACS tube and centrifuged at 3000rpm for 10 mins. The supernatant was discarded and 250 μ l of PBS added and samples vortexed. Each sample was vortexed again prior to the addition of RNAase A (final conc. 50 μ g/ml) and tubed incubated at 37°C, wrapped in aluminium foil (to protect from light) for 30min-1h prior to flow cytometry. Next, Propidium iodide (final conc.

50µg/ml) was added to each sample and vortexed. Samples were run on FACScanto Flow cytometer at 10,000 events measured for each sample. The data was analysed with FACSDiva software (FACS scan, Becton Dickinson, Oxford, UK). PI stained populations were used to determine the gating and cell cycle events were gated on G₁, S phase and G₂/M, with a % total events identified in each phase.

2.2.5. Pharmacological and molecular techniques used to target the IKK-NF-κB and AURKA-TPX2 signalling pathways.

2.2.5.1. Targeting IKK-NF-κB and IKK-AURKA protein-protein interactions using cell permeable short-length NBD peptide.

To disrupt the binding interactions of the IKKs with NEMO (May et al., 2000b) and IKKs with AURKA (A Wilson, PhD thesis), all mediated by the NBD, cell permeable short-length NBD mimetic peptides derived from IKKβ (as described in Section 2.1.2.6 in Materials) were utilised in cell based experiments. Cells were grown in 12 x 1ml dishes until they were approximately 70-80% confluent. Cells were pre-treated overnight with nocodazole for 16-20 hours and the next day each dish underwent the normal 'wash and release' procedure as described previously in Section 2.2.2.1. Following release from the nocodazole-mediated arrest, DMSO, cell-permeable peptide (CPP) NBD wild-type (WT) or mutant-type (MT) (both 100µM) were added to each dish and then incubated for the appropriate time points, as appropriate (e.g. 0, 30min, 1h and 2h) and dishes then removed from the incubator, WCEs prepared as described in Section 2.2.3.1.

2.2.5.2. Targeting cellular IKK catalytic activity using small molecule (SM) isoform selective IKK inhibitors.

To challenge pharmacologically the endogenous cellular activity of IKKα and IKKβ and examine its resultant effect on IKK-AURKA signalling, cells were treated with molecules targeting the ATP-binding component of the kinase domain of IKKα and IKKβ. Cells were grown in 12 x 1ml dishes until they were approximately 70-80% confluent and then pre-treated overnight with nocodazole for 16-20 hours. The next day each dish underwent the normal 'wash and release' procedure as described previously in Section 2.2.2.1. Following release from nocodazole-mediated arrest, DMSO, a proprietary novel "in-house" IKKα-inhibitor (SU1433) related to those reported in Anthony et al. (2017b) or an IKKβ-inhibitor (BMS-345541) were added to each dish and then incubated for the appropriate time points (e.g.0,

30min, 1h and 2h), the dishes were then removed from the incubator and WCEs prepared as described in Section 2.2.3.1.

2.2.5.3. Cellular depletion of IKK α / β protein expression using transfection of short-inhibitory RNA (siRNA) sequences transfection.

To run-down the protein expression of IKK α and IKK β in the cell transfection of siRNA targeting sequences was used. Non-targeting control and isoform specific sequences targeting IKK α or IKK β were utilised to test aspects of the IKK-Aurora interaction at the transcriptional level.

Cells were plated into 12-well plate or 12 x 1ml dishes and grown until they were about 50% confluent on the day of transfection. For the transfection of cells with siRNA, two separate tubes were prepared per well – Tube A and Tube B. In Tube A 100 μ M siRNA was added and the total volume made up to 100 μ l with Optimem media. In Tube B, 5 μ l of Lipofectamine RNAiMAX was made up to 100 μ l in Optimem cell media. Tube B was added to Tube A and mixed together (200 μ l) by hand before being left for 15-20 mins at room temperature to allow siRNA and lipofectamine to form a complex. During this incubation period, the full RPMI 1640 media bathing the cultured cells was removed by aspiration and the monolayer washed with Optimem (to remove any residual media containing antibiotics). The media was then replaced with 800 μ l of Optimem per well. Following the incubation period, the siRNA transfection mixture was added drop by drop using a pipette and agitated before being placed in an incubator overnight at 37 $^{\circ}$ C in a humidified atmosphere of air/CO₂ (19:1). The following morning, the media containing the transfection mixture was removed by aspiration and replaced with full RPMI 1640 media. Cells were then placed back in the incubator for 48 hours (after approximately 30-32 hours cells were treated overnight with nocodazole for 16-20 hours), when maximal rundown was observed (see later results section) to have been achieved.

2.2.5.4. Targeting of PPIs and protein expression in cells using NBD CPPs and siRNA IKK α and IKK β alone or in combination.

To use siRNA targeting both IKK α and IKK β to simultaneously rundown the endogenous levels of both IKK α and IKK β proteins at the transcriptional and investigate the effect on IKK-AURKA interaction and whether the NBD WT CPP can still exert it's effect on AURKA in combination with targeted rundown of the IKK proteins. Transfection of siRNA was carried out as mentioned in Section 2.2.5.3. After 28-32 hours of transfection cells were treated with

nocodazole overnight prior to release and treatment with NBD peptides as detailed in Section 2.2.5.1.

2.2.6. Pharmacological techniques used to target IKK-NF- κ B and IKK-AURKA signalling.

2.2.6.1. NBD CPPs as agent alone or in combination with ATP-competitive Aurora kinase inhibitors.

To examine the effect of the NBD WT CPP (to disrupt the binding interactions of the IKKs with NEMO (May et al., 2000b) and IKKs with AURKA (A Wilson, PhD thesis)) in combination with commercially available AURK inhibitors (Aurora Kinase inhibitor III, AURK inhibitor II, AURK/CDK inhibitor, VX-680 and ZM 447439) to improve the overall efficacy of the ATP-competitive inhibitors, cells were grown in 12 x 1ml dishes until they were approximately 70-80% confluent. Cells were pre-treated overnight with nocodazole for 16-20 hours and the next day each dish underwent the normal wash and release procedure as described previously in Section 2.2.2.1. Following release from nocodazole-mediated arrest, vehicle (DMSO, 0.5% (v/v)), cell-permeable peptide (CPP) NBD wild-type (WT) or mutant-type (MT) (both 100 μ M) were added to each dish and/or AURK inhibitors (AURK inhibitor III, AURK inhibitor II, AURK/CDK inhibitor, VX-680 and ZM 447439) and then incubated for appropriate time points (e.g.0, 10min, 20min and 30min) the dishes removed from the incubator and the WCEs prepared as described in Section 2.2.3.1.

2.2.7. Phenotypic assays to assess dual targeting of IKK/AURK signalling.

2.2.7.1. Cell viability assay.

To determine cell viability a 3-(4,5-dimethylthiazol-2-yl)-2,5-diphenyltetrazolium bromide (MTT) assay was carried out as described previously (Zhang *et al.*, 2019). Cells were seeded in 96-well plates and incubated until they reached approximately 40-60% confluency. The media was removed and 100 μ l of full media containing vehicle (DMSO 0.5% (v/v)), different concentrations of NBD CPPs and/or AURK ATP competitive inhibitors (AURK inhibitor III, AURK inhibitor II, AURK/CDK inhibitor, VX-680 and ZM 447439) were added and incubated at 37°C for 72h. Cells with no treatment were used as a positive control and cells in water instead of media to indicate non-viable cells, were used as a negative control. The treatments were terminated by aspirating the media from each well and 90 μ l of full media and 10 μ l of MTT

agent (stock concentration 10mg/ml) were added and plates incubated in the dark at 37°C for 2 hours. After this, the media was removed and 100µl volume of dimethylsulfoxide (DMSO) was added and cells were incubated at 37°C for a further 10-15mins to dissolve the formazan crystals. The plates were then read and quantified using the POLARstar Omega plate reader (BMG LABTECH Ltd, Aylesbury, UK) at wavelength 570nm.

2.2.7.2. Clonogenic survival assay.

Clonogenic assay was carried out based on a method described previously (Carlin *et al.*, 2000) to assess cellular replicative potential. PC3 cells were seeded in 6-well plates at 900 cells per well and allowed to attach for 24 hours. After 24 hours, media was changed to media containing vehicle, different concentrations of NBD CPPs and/or AURK ATP competitive inhibitors and incubated at 37°C for a further 72h. Cells with no treatment were used as a survival control and cells treated with 600µM Hydrogen peroxide (H₂O₂) used as a positive control for inhibition of clonogenic survival. After this incubation period, “drug containing” media was changed to 3ml full media and the cells were incubated for 10-14 days to assess clonogenic survival. Cells were then washed with PBS, fixed with methanol (5ml) for 15min and stained with Giemsa 10% (v/v) stain for 5-10min. The excess stain was then poured off and the dishes washed in tap water, left to dry and the colonies counted by eye.

2.2.7.3. Apoptosis assay.

Cellular apoptosis was assessed by the ability of the treatment groups to cause activation of caspase 3 (protease involved in the execution of apoptosis) which cleaves the caspase 3 recognition sequence bound to a fluorogenic dye, acting as a substrate in the assay and hence releasing a green fluorescent signal upon cleavage. Caspase-3 substrate assay was performed based on a method described previously (Shafran *et al.*, 2017). PC3 cells were plated in a 96-Well Black Assay Plate, Clear Bottom, at a density of 5x10⁴ cells per well. Cells were grown until 40-60% confluent prior to treatment with vehicle, different concentrations of NBD CPPs and/or Aurora kinase ATP competitive inhibitors and incubation at 37°C for 72h. Cells with no treatment were used as a positive control and cells treated with 600µM hydrogen peroxide (H₂O₂) used as a negative control for induction of apoptosis. After this incubation period, the treatments were terminated by aspiration of the media. NucView® 488 caspase-3/7 substrate solution (5µM) was then added to each well in a working volume of 100µl. Cells were incubated with the substrate in the dark at room temperature for 30min. After 30 minutes, the media was removed and replaced with PBS (as the phenol red in the media causes a high

background when imaging). Cells were observed by fluorescence microscopy using the EVOS®FL Auto microscope (Thermo Scientific (Leicestershire, UK)) with filter sets for green fluorescence (excitation/emission: 485/515nm) at x10 magnification and 25% coverage (12 images in total, 4x3 images). Images were processed and analysed using ImageJ (NIH, Rockville, USA).

2.8 Statistical Analysis.

2.8.1. Data Analysis.

Data representative of three independent experiments are shown as percentage mean \pm S.E.M unless stated otherwise. The statistical significance of differences between means was determined by a two-tailed one-way analysis of variance (ANOVA) with post-hoc Dunnet's test to 95% confidence levels ($P < 0.05$) unless stated otherwise.

2.8.2. Combination Index Analysis (CIA).

As well as the general data analysis in Section 2.8.1, experiments which involved using the NBD CPPs and the AURK inhibitors (AURK inhibitor III, AURK inhibitor II, AURK/CDK inhibitor, VX-680 and ZM 447439) in combination also used the CIA algorithm and Compusyn software (Paramus, NJ, USA) which was first pioneered by Chou et al. (1994). This determines, based on a value (combination index (CI)), whether a drug combination is additive ($CI = 1$), synergistic ($CI < 1$) or antagonistic ($CI > 1$). The data was converted to the form 1-normalised results (Compusyn can only process values < 1). Once data was in the correct format, results were entered into Compusyn for each concentration of each single drug before analysing as a "new drug combo" at a non-constant ratio. The results from the drug comb were then generated into a report, from which one of the graphs generated is Fraction affected (Fa)-CI plot. This determines the percentage of cells affected/inhibited by the drug combination and if it is synergistic, additive or antagonistic. The results were then plotted in GraphPad prism (GraphPad Software, San Diego, USA).

2.8.3. Image processing and analysis.

In Section 2.2.7.3, the images that were acquired as a result of the apoptosis substrate assay then underwent image processing and analysis using ImageJ software (NIH, Rockville, USA). To begin with, a region of interest (ROI) was selected using the rectangular tool and duplicated,

one for processing the image for presentation and the other for image analysis and quantification. The ROI was then locked and saved in order to keep it consistent across the different treatment groups. Firstly, for the image processing, the image was kept in Red, green, blue (RGB) colour format and the background was subtracted to give a black background with any observed fluorescent a reflection of the treatments themselves. Scale bars were then fitted, and this again was kept consistent across all images. Next, for analysis the RGB image was 'Split' into three separate channels (red, green and blue), with only the green 8-bit grayscale image kept. Following on from this, the image then underwent a process known as thresholding (this was a way of creating a binary image from a grayscale image and allowed us to separate the "object" pixels from the background pixels). Five ROI from the image were then selected and analysed, and these gave an 'integrated density' value from which an average was taken. This was then used to calculate the Corrected Total Cell Fluorescence (CTCF) for each treatment group based on the following equation: **CTCF = Integrated Density – (Area of selected cell x Mean fluorescence of background readings)**. This was repeated three times in each treatment group for different ROI of identical size to give a fair representation of the images being portrayed before plotting the results in GraphPad Prism (GraphPad Software, San Diego, USA).

Chapter 3: Characterising the mechanism of cross-talk between IKK-AURKA signalling in PCa cells – examining the impact of a NBD-derived cell permeable peptide.

3.1. Introduction.

In the NF- κ B pathway, the large molecular weight (~700kDa) multi-subunit IKK complex, first identified by (Chen et al., 1996), has been shown to regulate the activation of the pathway via phosphorylation of Serine 32 and Serine 36 of I κ B α , leading to its targeted ubiquitination and subsequent degradation. This serves as a molecular switch for the liberation of NF- κ B complexes in their active forms. The regulatory phosphorylation event is mediated specifically by the two catalytic IKK proteins (IKK α and IKK β) which dimerise and interact with IKK γ /NEMO to form the functional IKK complex. It is the interaction of these proteins within the complex which governs its catalytic activity (Israel, 2010). As described previously, IKK α and IKK β both possess within their protein structure a conserved amino acid sequence known as the NEMO-binding domain (NBD), and as such enables each of these two catalytic proteins to bind to the regulatory/scaffolding protein, NEMO. The NBD contains a conserved hexapeptide (six amino acids; IKK α [738–743], IKK β [737–742]) sequence: L-D-W-S-W-L (Leu-Asp-Trp-Ser-Trp-Leu) and this sequence, particularly the two hydrophobic tryptophans, dictates the interaction between IKK α /IKK β and NEMO (May et al., 2000) – thus forming the prototypical IKK complex.

It was shown by May et al. (2000b) that any mutations to the central tryptophan residues (W) in this conserved sequence of the NBD, resulted in a critically detrimental effect on the interaction of the IKK proteins with NEMO. This was consistent with the work of Zhao et al. (2018b) who showed that the residues crucial for binding were; W739, W741 and L742 and substituting arginine for the two tryptophans resulted in the loss of binding.

Subsequently, these interactions have been targetable using competitive peptides derived from the NBD of IKK β synthesised in cell permeable forms using various membrane transduction leader sequences derived from *Drosophila antennapedia* (ANTP) or HIV Tat proteins (Gamble et al., 2012a). In these various forms the common element has been the incorporation of the core hexapeptide sequence of IKK β into an already well-established pharmacological tool which has been shown to interfere with IKK/NEMO binding and so disrupt IKK complex formation/function.

As mentioned earlier, both Ireland et al. (2007) and Prajapati et al. (2006) reported that both IKK α and IKK β could phosphorylate and regulate the mitotic kinase AURKA, suggesting it to be a new substrate for these kinase isoforms. It was also shown previously, using scanning peptide array studies (Wilson 2013) that interaction of AURKA with both IKK α and IKK β *in vitro* and in reverse mapping studies IKK β with AURKA/B/C. These interactions (IKKs-AURKA) were also replicated in co-immunoprecipitation studies pursuing endogenous IKKs/AURKA or those overexpressed following plasmid-mediated delivery and expression

(Wilson 2013). Furthermore, interaction between the IKKs and AURKA *in vitro* was identified to be mediated in part via interaction with the NBD of the IKKs and the central hydrophobic residues of the hexapeptide NBD were critical in mediating interactions, in a similar manner to that reported by others for IKKs with NEMO (May et al., 2000b). Translating the results of the scanning peptide array mapping experiments with recombinant proteins *in vitro* Wilson also identified in preliminary cell-based studies that a membrane permeable peptide (22mer) containing a sequence (11aa) derived from the IKK β NBD structure could modulate AURKA status; phosphorylation, expression/degradation. However, these preliminary experiments didn't inform fully on the mechanism of impact of the NBD CPP upon AURKA status, its effect upon other associated markers of cellular mitosis nor the recognised classic phenotypic outcomes associated with AURKA activity within the cell cycle. Taking these experimental observations into account it was hypothesised that the treatment of mitotic cancer cells with the NBD CPP would result in the targeting of AURKA signalling and functioning, have a bearing on the regulatory binding protein TPX2 and other related markers of the progression through the mitotic process. This includes the cellular kinase PLK1. Furthermore, given the ability of IKK α/β to interact with AURKA via the NBD in peptide array mapping experiments it was hypothesised that the effect of the NBD CPP on the AURKA-TPX2 complex would be a direct one to manifest the previously observed reduction in phosphorylation and increased rate of proteolytic degradation.

Therefore, in this first component of the project, the experimental aims were generally to explore further the impact of the NBD CPP peptide on the status of AURKA, IKKs and related proteins in mitotic prostate cancer cells and to examine whether targeting the IKKs with different molecular and pharmacological strategies would generate insight into the mechanism of action of the peptide and thus determine whether it indeed was a direct modulatory effect upon AURKA or an indirect result of prior disruption of the IKK complex, specifically IKK α/β -NEMO interactions mediated by the NBD.

Thus, the specific aims of this chapter, towards elucidating the mechanism(s) of action of the NBD CPP and its impact on IKK α/β -AURKA crosstalk, were to:

1. Establish a cell-based assay system, using nocodazole arrest/trap and release, to enable the assessment of signalling proteins in mitotic PC3 prostate cancer cells.
2. Confirm the effect of the NBD peptide on the Aurora kinases in PC3 cells and examine its potential effect on related regulatory proteins associated with cell cycle progression.

3. Determine the impact of siRNA mediated cellular depletion of IKK α/β protein expression on the status of AURKA and related mitotic markers,
4. Determine the impact of small molecule IKK-selective kinase inhibitors (and absence of IKK α/β catalytic activity) on AURKA and related mitotic markers,
5. Determine the impact of prior siRNA-mediated cellular depletion of IKK α/β protein expression on the effect of the NBD WT CPP on the status of AURKA and related mitotic markers,
6. Examine comparatively the impact of the CPP WT NBD on the status of AURKA and related mitotic markers in murine embryonic fibroblasts, either wild-type or null for IKK α and IKK β (ikka^{-/-}/ikkb^{-/-}) expression.

Collectively, these experiments aimed to determine whether the NBD CPP impacts AURKA-TPX2 status directly, independent of IKK α/β protein expression/activity, IKK $\alpha/\beta/\gamma$ protein-protein interactions and in a 'knockout model' lacking IKK α and IKK β .

3.2. Examining the status of AURKs and NF- κ B components in PC3 cells through mitosis.

3.2.1. Assessment of the status of AURKA and cell cycle components following Nocodazole mediated cell cycle arrest/trap and release.

In order to examine cells at the mitotic phase of the cell cycle a nocodazole based strategy was instigated to arrest growing cells in mitosis, specifically at prometaphase shortly after the G₂/M transition. Nocodazole is recognised as an antineoplastic poison that acts to destabilise the dynamics of microtubules, arresting cells at the G₂/M checkpoint (Kallas et al., 2011). To establish optimal conditions for nocodazole treatment, PC3 cells were treated with various concentrations of nocodazole for 16-20 hours and both AURKA expression and phosphorylation of AURKA, AURKB and AURKC examined in synchronised vs non-synchronised cells via immunoblotting (data not shown). Following on from this an optimal treatment concentration was determined as 50ng/ml and in preparation for experiments cells were treated routinely for 16-20 hours to establish cell cycle arrest or 'trap'. Following treatment with nocodazole for 16-20 hours, cells were washed and released from the arrest/'trap' for varying time periods (up to 6 hours) prior to trypsinisation, fixation with 70% (v/v) ethanol and analysis via flow cytometry (n=3). In Figure 3.1(A), the percentage of cells at each stage of the cell cycle following treatment with nocodazole was assessed based on the DNA content of the cells through propidium iodide staining and compared the 'Non-trapped' controls (NT0 and NT6). In the cells treated with nocodazole at the 0h time point (TR0; i.e. not released from the trap), 77.2% of the cells were arrested in the G₂/M stage of the cell cycle in comparison to 13.1% at G₁ and 9.7% at S phase. This indicated that the nocodazole treatment successfully synchronised the majority of cells treated at the G₂/M stage of the cell cycle. In comparison, samples from cells which weren't treated with nocodazole (NT0 and NT6), or cells which had been released from arrest, 4 hours or greater, displayed a ratio of 60% G₁ to 30% G₂/M. This mapped how the cells progressed through the cell cycle, from G₂/M, prometaphase, through mitosis and return to G₁. Following release from arrest cells had fully exited mitosis by 4 hours.

In Figure 3.2 immunoblotting was used to assess the cell cycle status of total AURKA and its phosphorylation, as well as the outcome of important cell cycle markers (TPX2, p-PLK1, PLK1) in relation to AURKA following nocodazole trap and release at the appropriate time points (up to 6 hours) and these markers were subsequently quantified (C). The phosphorylation of the AURKA (Thr288) / AURKB (Thr232) / AURKC (Thr198) were expressed at an elevated and maximum level at the 0 hour time point (TR0), which compared consistently

with the positive control (TR_{NR}) in which the cells had been trapped with nocodazole and not released while incubated for 6 hours. In Figure 3.2 there was a significant ($p < 0.05$) decrease in phosphorylation of AURKA following release at 1h, TR1 ($48.9 \pm 4.7\%$; $n=3$, $p < 0.001$), 2h (TR2) ($59.9 \pm 7.0\%$; $n=3$, $p < 0.001$), 4h (TR4) ($89.5 \pm 2.7\%$; $n=3$, $p < 0.001$) and 6h (TR6) ($91.1 \pm 3.6\%$; $n=3$, $p < 0.001$) respectively, in comparison to the samples from synchronised cells at the 0 time point (TR0). The phosphorylation of AURKB was also significantly ($p < 0.05$) reduced after 2 hours (TR2) ($38 \pm 3.1\%$; $n=3$, $p < 0.05$), 4 hours (TR4) ($66 \pm 5.6\%$; $n=3$, $p < 0.001$) and 6 hours (TR6) ($68.3 \pm 10.6\%$; $n=3$, $p < 0.001$) relative to the normalised TR0 sample. For the last of the AURK family, AURKC, phosphorylation reduced significantly ($p < 0.05$) in a time-dependent manner after 1 hour (TR1) ($53.7 \pm 13.3\%$; $n=3$, $p < 0.01$), 2 hours (TR2) ($56.8 \pm 5.9\%$; $n=3$, $p < 0.01$), 4 hours (TR4) ($82.3 \pm 6.1\%$; $n=3$, $p < 0.001$) and 6 hours (TR6) ($88.0 \pm 6.9\%$; $n=3$, $p < 0.001$) in comparison to the TR0 sample.

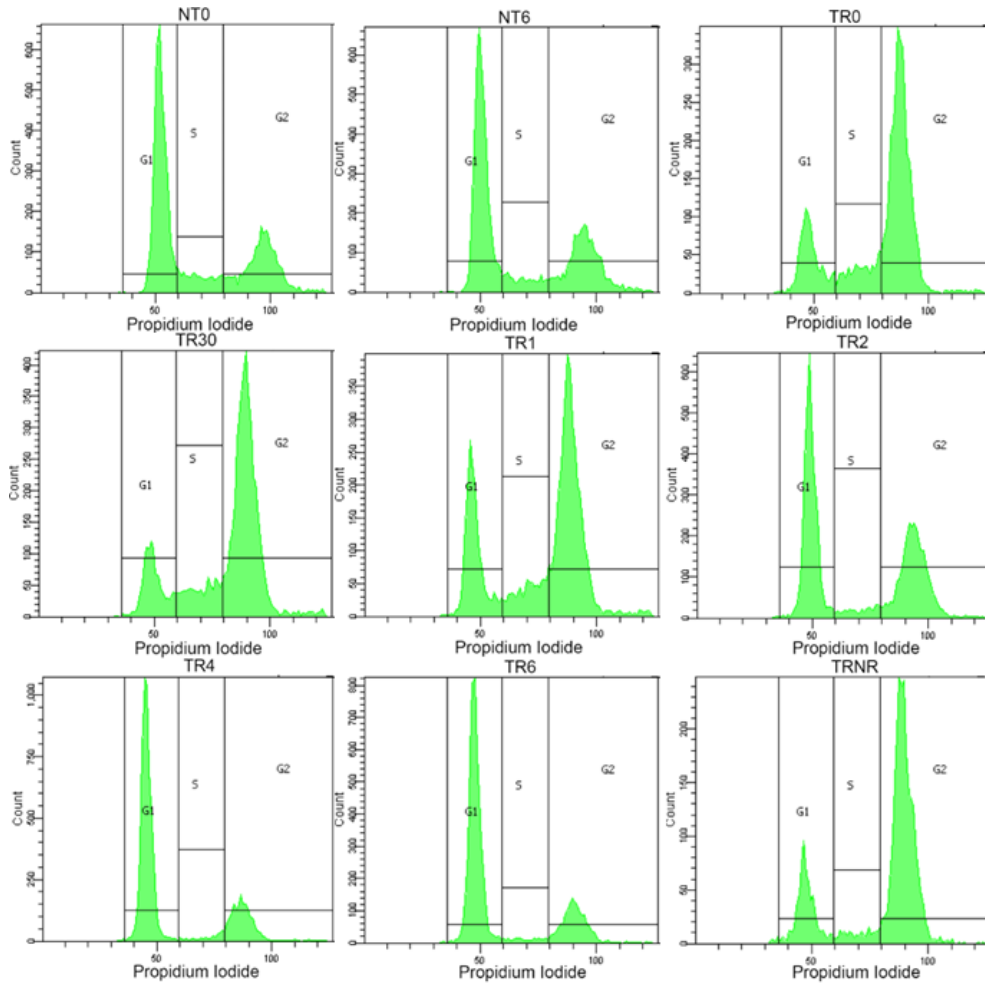
The total expression of AURKA was also analysed and was shown to be significantly reduced after 2 hours (TR2) ($62.7 \pm 14.4\%$; $n=3$, $p < 0.05$), 4 hours (TR4) ($72.9 \pm 2.6\%$; $n=3$, $p < 0.01$) and 6 hours (TR6) ($70.1 \pm 10.2\%$; $n=3$, $p < 0.05$) relative to the TR0 sample. As the cells were released and progressed through mitosis, AURKA expression and phosphorylation (Thr288) was reduced to basal level by the 4 and 6 hour time points as compared to the negative controls (NT₀ and NT₆) – cells which were not trapped with nocodazole 0 and 6 hour time points. By the quantification indicated in Figure 3.1 (C), the detected phosphorylation of AURKA decreased faster kinetically than the total AURKA protein expression e.g. significant reduction in AURKA phosphorylation (Thr288) after 1 hour compared to 2 hours for total AURKA protein expression. This was perhaps not unexpected given the phosphorylation of the protein, an indicator of catalytic activity, would firstly need to be 'switched off' prior to degradation of the protein. A similar pattern was also seen for the phosphorylation of AURKB (Thr232), which declined significantly after 2 hours and this may have reflected the role of AURKB as being later in the cell cycle and into cytokinesis compared to AURKA. Phosphorylation of AURKC (Thr198) declined much quicker, which may suggest a role for AURKC in the earlier stages of mitosis rather the latter. Total protein expression of AURKB and AURKC weren't measured in this study due to time constraints. Understanding the relationship between phosphorylation and total protein expression for each of these isoforms would require further work.

As well as the phosphorylation of the AURKs and total expression of AURKA, the expression of the critical co-activator of AURKA, TPX2, was also measured. The expression levels of TPX2 were significantly reduced at 1 hour (TR1) ($49.9 \pm 7.2\%$; $n=3$, $p < 0.05$), 2 hours (TR2) ($56.2 \pm 5.3\%$; $n=3$, $p < 0.05$), 4 hours (TR4) ($60.5 \pm 5.9\%$; $n=3$, $p < 0.01$) and 6 hours (TR6) ($71.7 \pm 7.5\%$; $n=3$, $p < 0.01$) post release from the nocodazole-mediated trap, compared to the

TR0 sample. As expression of TPX2 remains higher for longer than AURKA, this could suggest that TPX2 could be dissociated from AURKA but not necessarily degraded in the cell. Lastly, the phosphorylation and total expression of another G₂/M cell cycle marker, Polo-like kinase 1 (PLK1), was measured, which is also phosphorylated and regulated by AURKA (Gheghiani et al., 2017). Firstly, with regards to the phosphorylation of PLK1, it was found to be significantly decreased after 4 hours (TR4) ($84.3 \pm 6.3\%$; n=3, p<0.001) and 6 hours (TR6) (81.7 ± 9.3 ; n=3, p<0.001) following release from nocodazole arrest relative to the TR0 sample. A similar pattern was observed for the total expression of PLK1 which was also significantly reduced after 4 hours (TR4) ($69.0 \pm 15.1\%$; n=3, p<0.05) and 6 hours (TR6) ($72.9 \pm 11.1\%$; n=3, p<0.01) relative to the TR0 sample. This late reduction in PLK1 levels is consistent with data observed in the literature in which it was shown in a study by Gheghiani et al. (2017) that PLK1 is activated in late G₂ phase and was then required for entry into mitosis before being degraded upon exit from mitosis.

Collectively, these experimental outcomes demonstrated overall that nocodazole treatment of cells resulted in the arrest of the majority of cells at prometaphase and so could be used in future experimental work when assessing cellular interventions in mitotic cells, particularly in examining the potential effects of the NBD WT CPP on IKK-AURK signalling following trap and release.

(A)



(B)

	NT0	NT6	TR0	TR30	TR1	TR2	TR4	TR6	TRNR
G1	57.5	50.6	13.1	12.1	19.4	54.3	73.3	63.5	12.0
S	12.4	12.8	9.7	9.6	9.5	5.0	4.1	4.4	8.0
G2/M	28.9	28.6	77.2	78.0	70.8	40.3	22.3	32.0	79.0

(C)

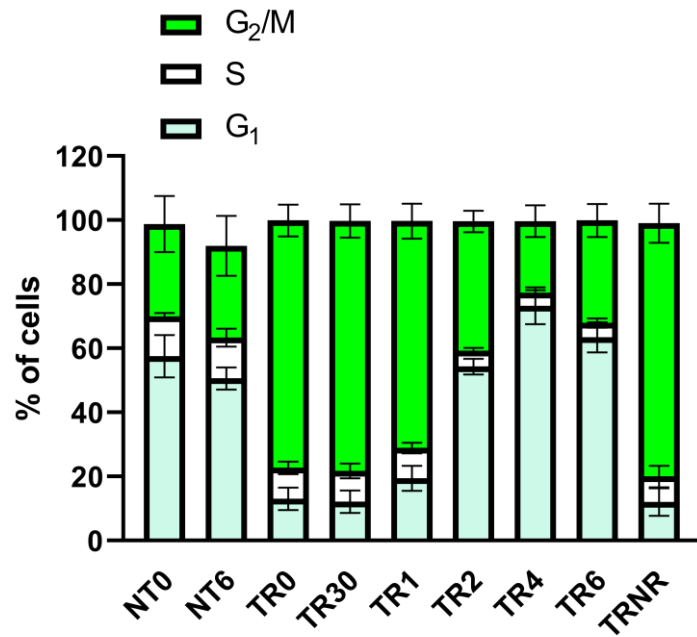
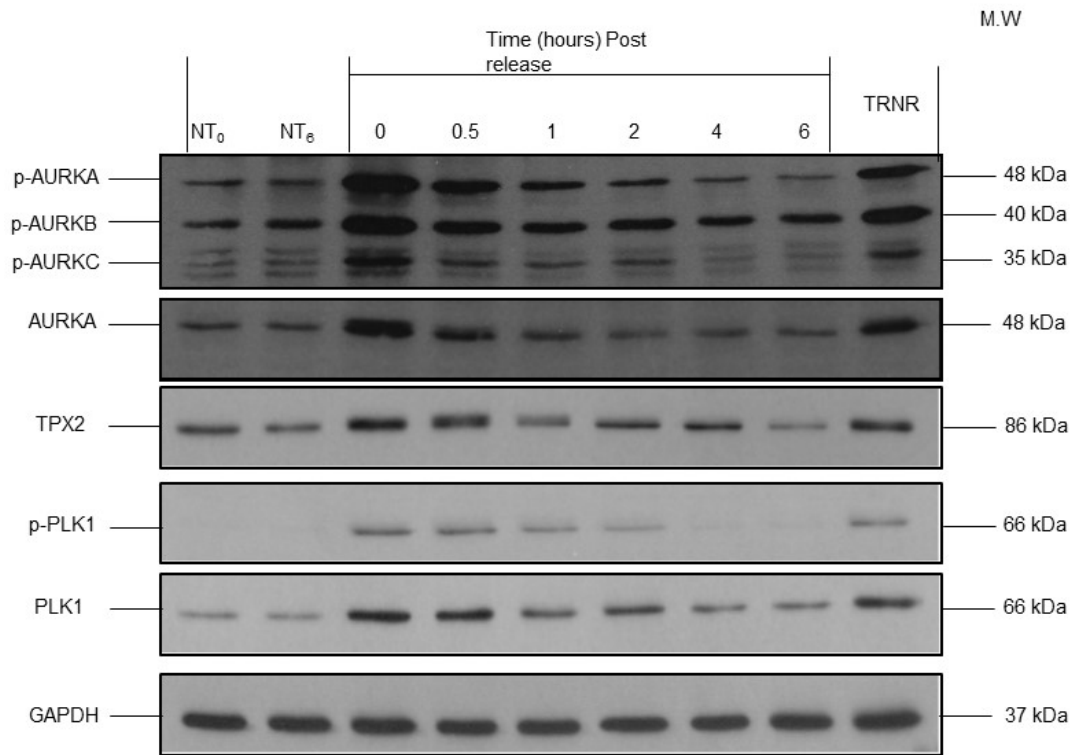


Figure 3.1. Effect of nocodazole trap and release on cell cycle distribution in PC3 cells.

PC3 cells were grown on 30mm dishes and treated with 50ng/ml Nocodazole (16-20 hours) and these were then released by washing twice with fresh media, times indicated as hours post-release from Nocodazole trap. Non-trapped cells at 0 and 6h (NT₀ and NT₆) represent the negative control. Cells treated with Nocodazole but not washed and released represented the positive control (Trap and non-released, TR_{NR}). **(A, B and C)** Fluorescence activated cell sorting (FACS) analysis of percentage of cells (% cells) at each stage (G₁, S, G₂/M) of the cell cycle following treatment with nocodazole and subsequent release (n=3) DNA content measured using a PE filter at excitation wavelength 488nm with FACSCANTO Flow cytometer.

(A)



(B)

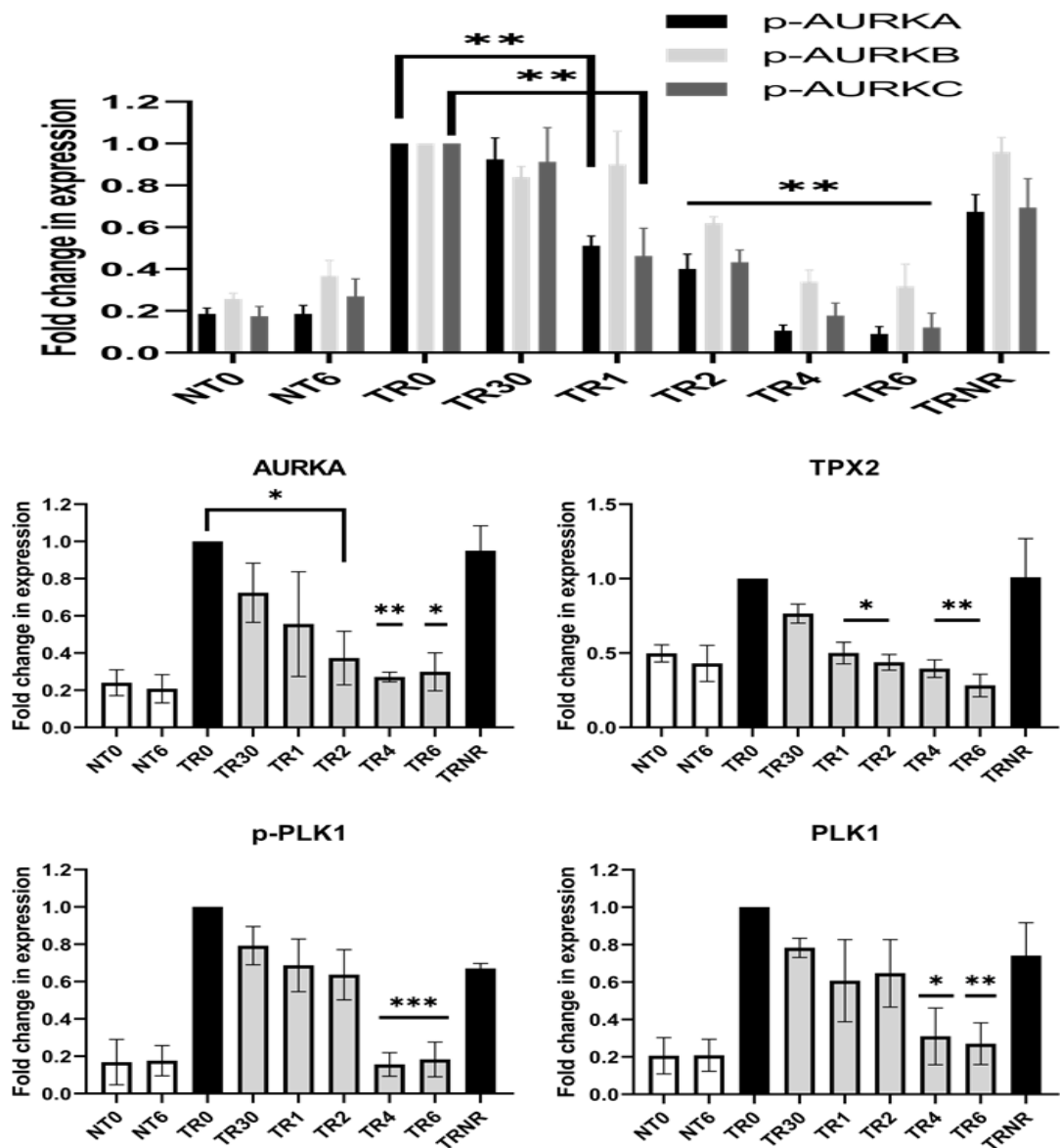
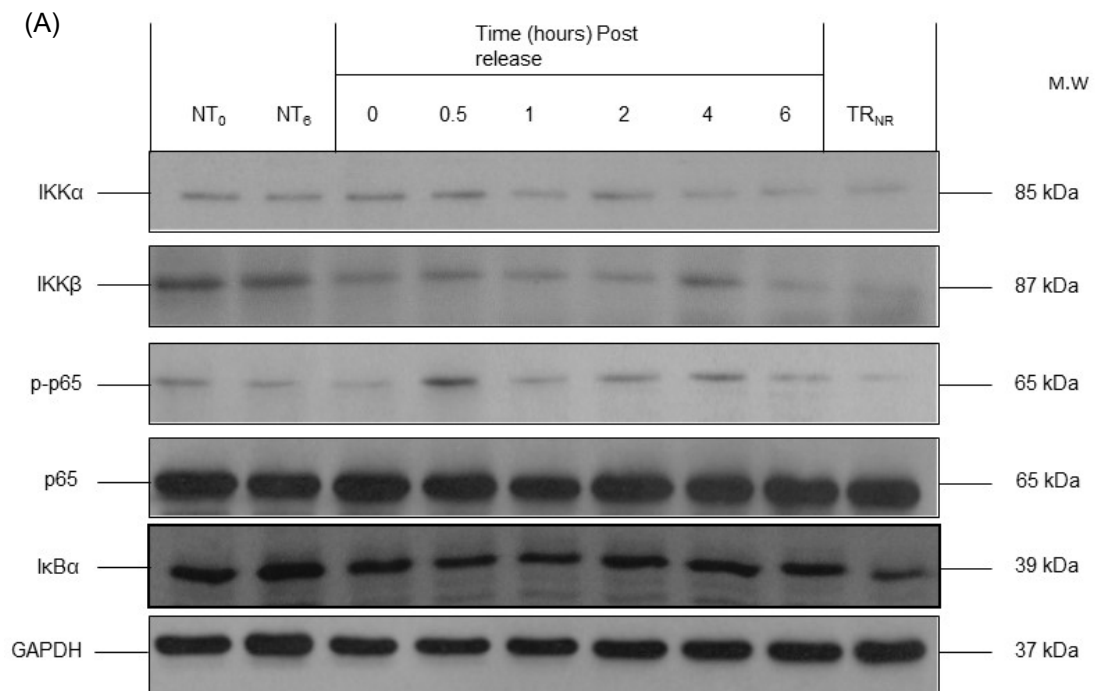


Figure 3.2. Effect of Nocodazole trap and release on AURKs and related protein markers of mitosis in PC3 cells.

PC3 cells were grown on 10mm dishes and treated with 50ng/ml Nocodazole (16-20 hours) and these were then released by washing twice with fresh media, times indicated as hours post-release from Nocodazole trap. Non-trapped cells at 0 and 6h (NT₀ and NT₆) represent the negative control. Cells treated with Nocodazole but not washed and released represented the positive control (Trap and non-released, TR_{NR}). (A) Whole cell lysates were prepared for separation using SDS-PAGE and analysed by Western Blotting using the above antibodies (n=3). GAPDH was used as a loading control. (B) Data was normalised to synchronised sample before release at the zero time point (TR₀) and represents mean \pm S.E.M. One-way ANOVA with post-hoc Dunnett's test was used to determine statistical significance ($p < 0.05$) of observed changes relative to TR₀ synchronised sample at 0 min. (*= $p < 0.05$, **= $p < 0.01$, ***= $p < 0.001$). All results indicated on graphs represent fold change in expression post-release from mitotic arrest compared to the TR₀ sample.

3.2.2. Status of NF- κ B components in PC3 cells following Nocodazole mediated trap and release.

To assess the status of NF- κ B components (IKK α , IKK β , I κ B α , p-p65 and p65) through mitosis, to parallel that for AURKA, TPX2 and PLK1. PC3 cells were again cultured in 10mm dishes and treated with 50ng/ml of nocodazole for 16-18 hours in order to arrest cells at the G₂/M phase of the cell cycle. Cell were then washed with full culture media and released from arrest. Figure 3.3 (A) and (B) depict the outcomes from the immunoblotting and subsequent quantification (B) for each of the cellular components at the described time points up to 6 hours. At the time point of 30min post-release, phosphorylation of p65 appears to be higher. In general though, the expression of the NF- κ B components remained constant throughout nocodazole trap and release with no significant change in expression ($p > 0.05$). As the NF- κ B components mainly showed no significant change in expression through mitosis it suggested that these proteins are not regulated in a cell cycle-dependent manner.



(B)

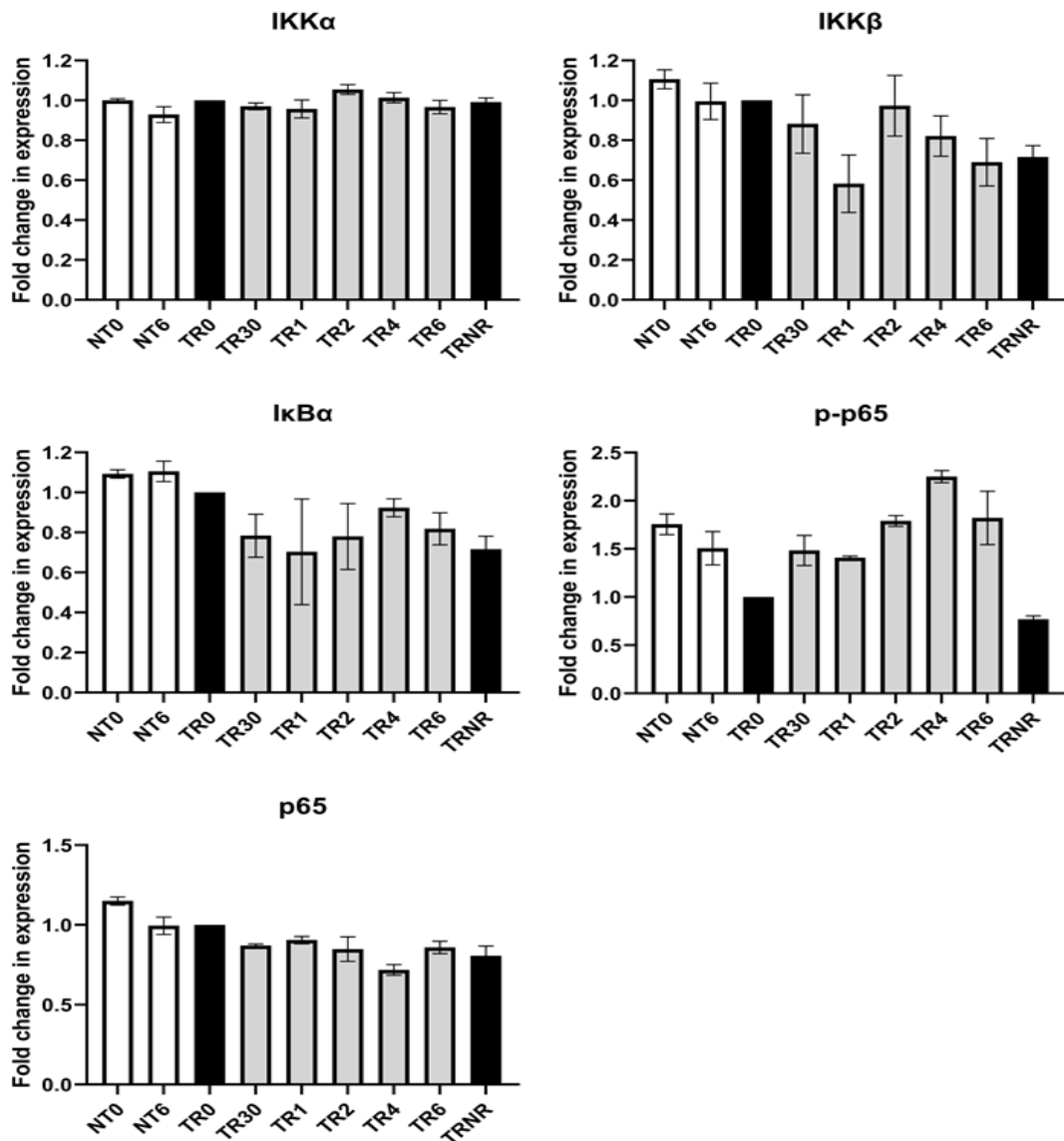


Figure 3.3. Effect of Nocodazole trap and release on NF- κ B markers in PC3 cells.

PC3 cells were grown on dishes and treated with 50ng/ml nocodazole (16-20 hours) and these were then released by washing twice with fresh media, times indicated as hours post-release from nocodazole trap. Non-trapped cells at 0 and 6h (NT0 and NT6) represent the negative control. Cells treated with nocodazole and then not released represented the positive control (Trap and release; non-release, TRNR). (A) Whole cell lysates were prepared for separation using SDS-PAGE and analysed by Western Blotting using the above antibodies (n=3). GAPDH was used as a loading control. (B) Data was normalised to synchronised sample before release at the zero time-point (TR0) and represents mean \pm S.E.M. One-way ANOVA with post-hoc Dunnett's test was used to determine statistical significance ($p < 0.05$) of observed changes relative to TR0 synchronised sample at 0 min. All results indicated on graphs represent fold change in expression post-release from mitotic arrest compared to the TR0 sample.

3.3. Elucidating the relationship between IKK and AURK signalling in PC3 cells via the use of pharmacological interventions.

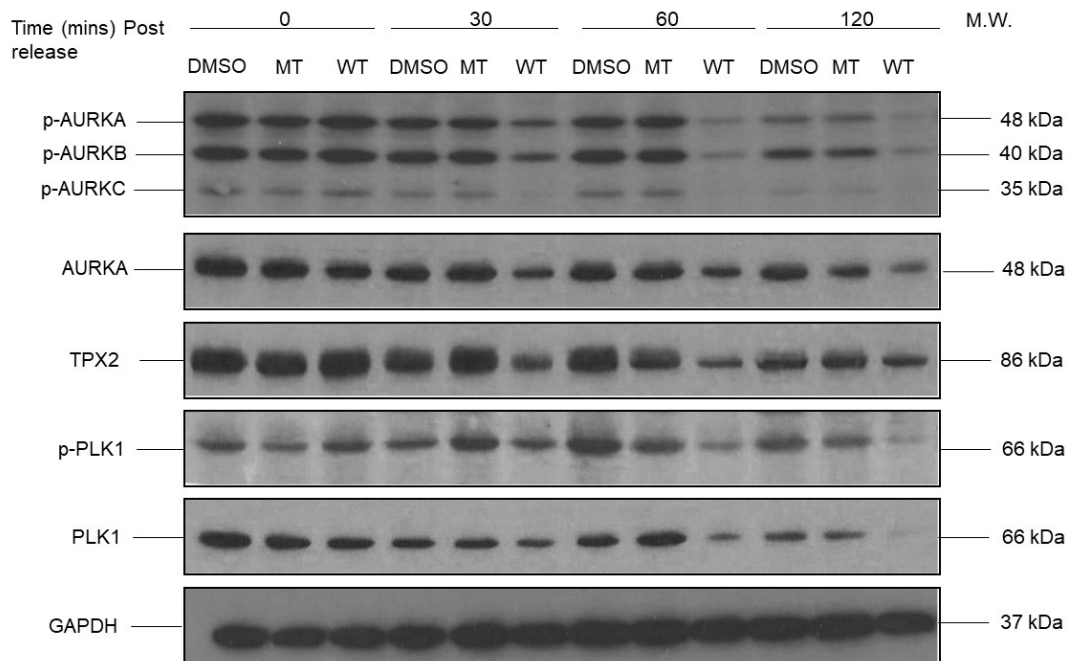
3.3.1. Effects of NBD WT CPP on the status of AURKA and cell cycle markers following nocodazole trap and release in PC3 cells.

As described previously, the NBD peptides are 11-mer long sequence and coupled to a HIV TAT-derived sequence (YGRKKRRQRRR) which is highly charged and allows the peptide to cross the cell plasma membrane. The NBD Wild-type (WT) peptide contained a conserved hexapeptide sequence - L-D-W-S-W-L (Leu-Asp-Trp-Ser-Trp-Leu) and this was used to competitively disrupt the interaction between the IKKs and NEMO. A mutated peptide (NBD MT) acted as a negative control as it possessed the same conserved parental sequence but with the key tryptophan residues (W) changed to alanine (A). This rendered the peptide less hydrophobic, unable to disrupt the interaction between the IKKs and NEMO (May et al., 2000b) and therefore inactive in a cellular setting. These peptides were then utilised side-by-side. Cells were again treated with nocodazole (50ng/mL) for 16-20 hours prior to being washed and released as described previously – Section 2.2.2.1, before NBD MT or NBD WT peptides (100µM) were added upon release and samples prepared thereafter at appropriate time points. The peptides were dissolved in 100% DMSO [1:1(50% v/v) addition to wells, final well concentration of 0.5%] to maintain solubility and as a result all experiments involving the NBD CPPs used DMSO as a vehicle control. The effect of the NBD CPPs on AURKA and its related mitotic markers in terms of their expression and/or phosphorylation were examined by Western blotting at 30, 60 and 120-minute time points.

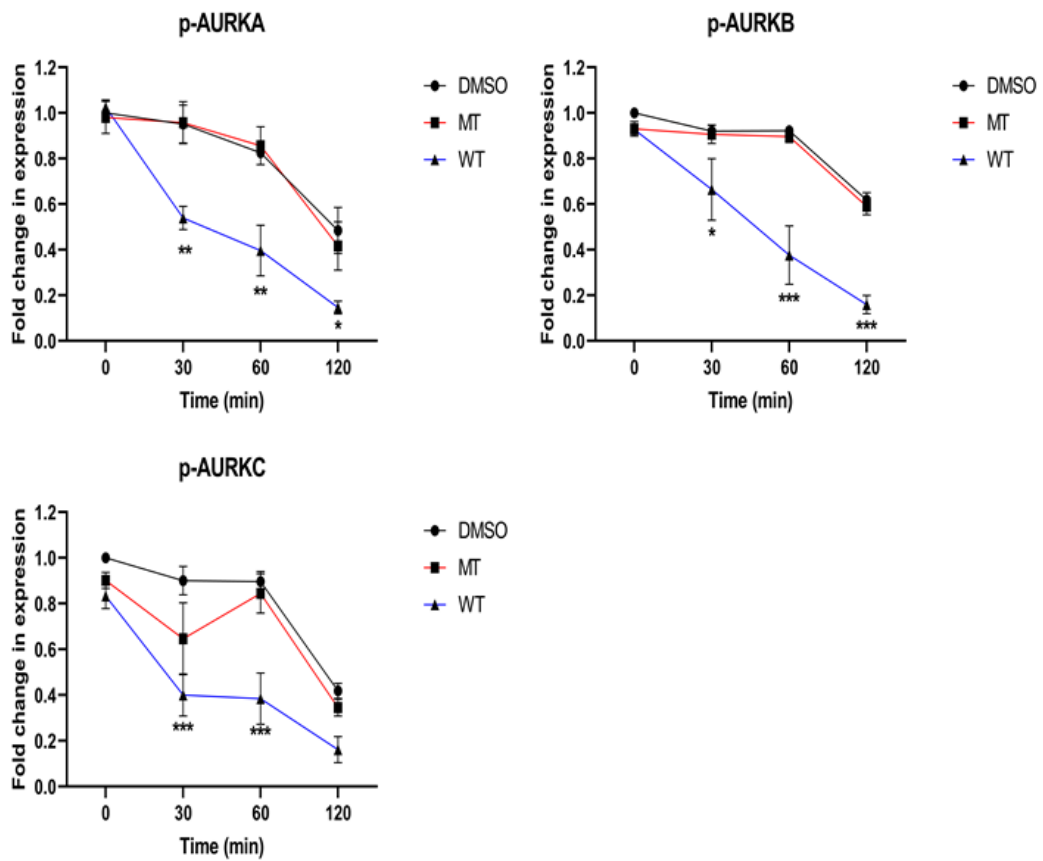
Figure 3.4 (A) shows by immunoblotting the effect of the MT and WT NBD CPP relative to vehicle on the status of p-AURKs, AURKA, TPX2 and p-PLK1/PLK1 post-trap and release. In Figure 3.4, from immunoblotting (A) and the retrospective quantification (B), the NBD WT CPP caused a significant ($p < 0.05$) reduction in phosphorylation of AURKA relative to the vehicle control at each of the time points examined. The phosphorylation of AURKA at each time point post-release was reduced significantly after treatment with the NBD WT CPP at 30 min ($95.1 \pm 8.3\%$ vs $54.0 \pm 5.1\%$; $n=3$, $p < 0.01$), 60 min ($82.6 \pm 1.4\%$ vs $39.6 \pm 11.1\%$; $n=3$, $p < 0.001$) and 120 min ($48.4 \pm 10.1\%$ vs $14.7 \pm 2.8\%$; $n=3$, $p < 0.05$) relative to the vehicle control at each of the measured time points. The AURKA phosphorylation decreased naturally over time and this decrease in phosphorylation was accelerated by the NBD WT CPP. The reduction in total AURKA expression was also assessed to determine whether the kinetics of protein degradation were comparable to the NBD WT CPPs effect on AURKA phosphorylation. In Figure 3.4 (B), the NBD WT CPP caused a significant reduction in

expression of total AURKA at 60 min ($79.0 \pm 6.8\%$ vs $41.1 \pm 0.7\%$; $n=3$, $p<0.05$) and 120 min ($69.1 \pm 13.9\%$ vs $21.7 \pm 5.7\%$; $n=3$, $p<0.01$) relative to the vehicle treated controls at each of those time points. There was also a significant reduction in AURKB phosphorylation by the NBD WT CPP at 30 min ($92.1 \pm 2.7\%$ vs $66.4 \pm 13.5\%$; $n=3$, $p<0.05$), 60 min ($92.3 \pm 0.5\%$ vs $37.7 \pm 12.8\%$; $n=3$, $p<0.001$) and 120 min ($61.9 \pm 3.2\%$ vs $16.0 \pm 4.1\%$; $n=3$, $p<0.001$) when compared with the vehicle control at the relative time points. Phosphorylation of AURKC showed a similar pattern of a statistically significant ($p<0.05$) reduction in phosphorylation to AURKA and B. There was a significant reduction in AURKC phosphorylation by the NBD WT CPP at 30 min ($90.1 \pm 6.3\%$ vs $40.1 \pm 9.3\%$; $n=3$, $p<0.001$) and 60 min ($89.6 \pm 4.4\%$ vs $38.4 \pm 11.2\%$; $n=3$, $p<0.001$). Expression of total AURKB and C were not measured and therefore it remains to be seen if the NBD WT CPP has an inhibitory effect on total protein expression across all AURKs. In Figure 3.4, the effect of the NBD WT CPP on the expression of the critical AURKA co-activator, TPX2 was also assessed. The NBD WT CPP reduced levels of TPX2 at 60 min ($91.9 \pm 3.1\%$ vs $50.2 \pm 14.1\%$; $n=3$, $p<0.01$) and 120 min ($71.9 \pm 8.6\%$ vs $31.5 \pm 7.5\%$; $n=3$, $p<0.01$) compared to each of the vehicle treated control. In Figure .4 (B), the NBD WT CPP significantly reduced phosphorylation of PLK1 after 60 min ($78.8 \pm 11.2\%$ vs $34.8 \pm 8.8\%$; $n=3$, $p<0.05$) and 120 min ($71.6 \pm 9.9\%$ vs $26.8 \pm 2.3\%$; $n=3$, $p<0.05$) post-release, relative to the vehicle controls at the same time points. Total expression of PLK1 was then assessed to see if the effect of the NBD WT CPP on total protein levels of PLK1 was comparable to its effect on phosphorylation. Figure 3.4 (B) shows that there was a significant reduction in total PLK1 expression induced by the WT peptide at 60 min ($75.9 \pm 4.7\%$ vs $43.1 \pm 2.0\%$; $n=3$, $p<0.001$) and 120 min ($54.1 \pm 3.6\%$ vs $20.3 \pm 0.8\%$; $n=3$, $p<0.001$) in comparison to the vehicle control at the same time points. PLK1 expression decreased naturally over time and the decrease in protein expression was accelerated by the NBD WT CPP. This suggest that the NBD WT CPP caused PLK1 to be degraded, as observed in the nocodazole trapped cells (Figure 3.4 A and B) and promoted inhibition of phosphorylation of PLK1. Mechanistically this may have been either as a result of the impact of the NBD WT CPP on upstream AURKA-TPX2 or a direct effect on PLK1 itself.

(A)



(B)



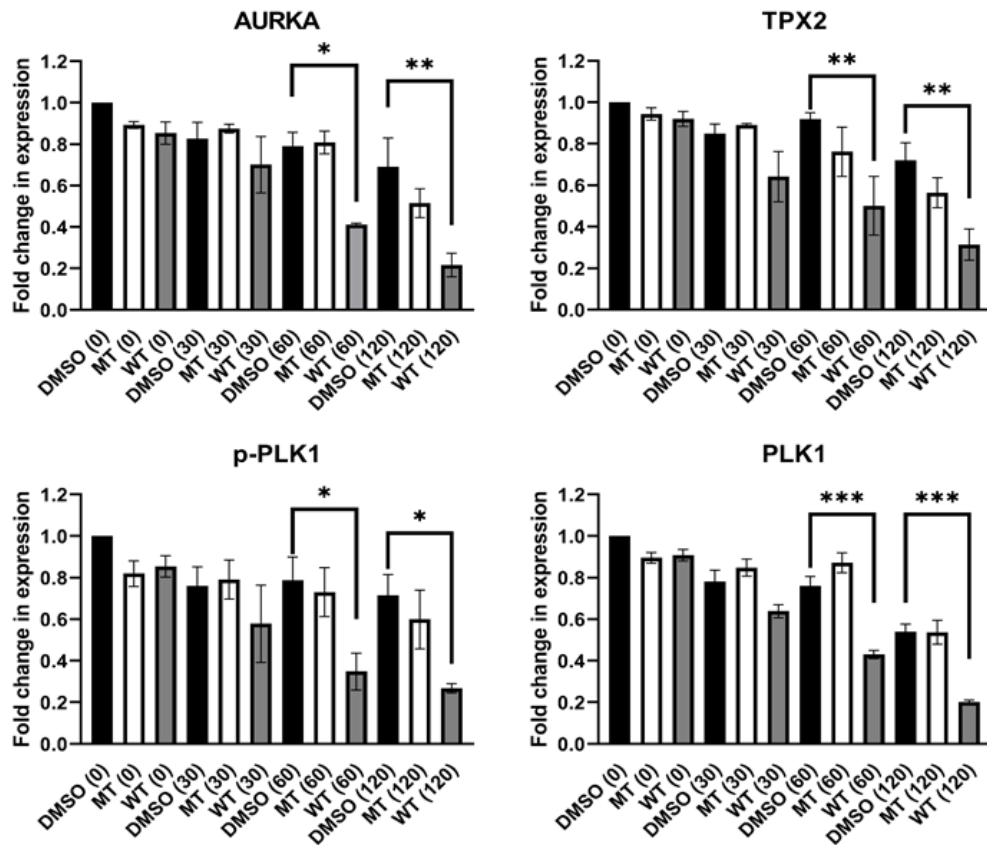
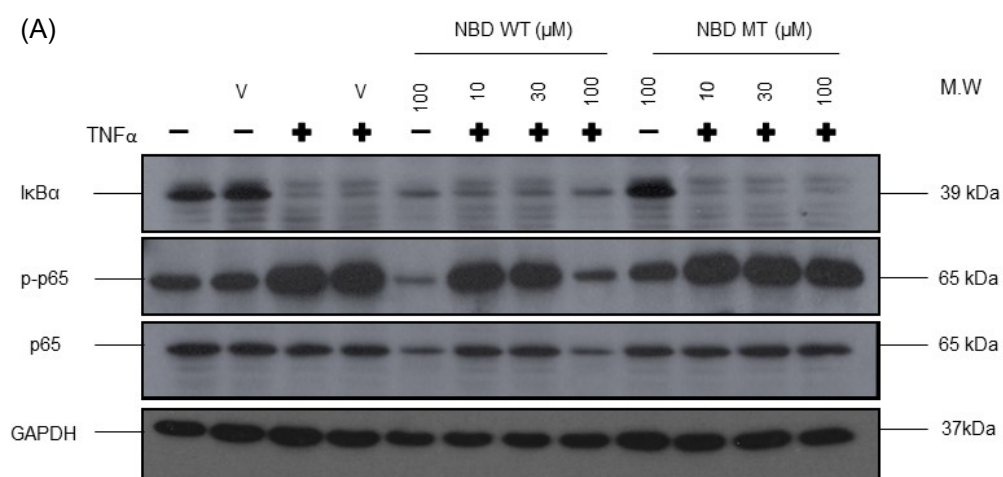


Figure 3.4. Impact of NBD WT CPP on AURKs and related protein markers of mitosis in PC3 cells.

PC3 cells were grown on 10mm dishes and treated with 50ng/ml nocodazole (16-20 hours) prior to treatment with either NBD WT or MT (100 μ M) or DMSO as a vehicle control (0.5% (v/v)) upon release from trap at 30min, 60min and 120min. **(A)** Whole cell lysates were prepared for separation using SDS-PAGE and analysed by Western Blotting using the above antibodies (n=3). GAPDH was used as a loading control. **(B)** Data was normalised to the vehicle treated control at 0 min (DMSO 0) and represents mean \pm S.E.M. One-way ANOVA with post-hoc Dunnett's test was used to determine statistical significance ($p < 0.05$) of observed changes induced by the peptides relative to vehicle control at the same time point of treatment (*= $p < 0.05$, **= $p < 0.01$, ***= $p < 0.001$). p-AURKA: WT(30) vs DMSO(30), ** $p < 0.01$; WT(60) vs DMSO(60), ** $p < 0.01$; WT(120) vs DMSO(120), * $p < 0.05$. p-AURKB: WT(30) vs DMSO(30), * $p < 0.05$; WT(60) vs DMSO(60), *** $p < 0.001$; WT(120) vs DMSO(120), *** $p < 0.001$. p-AURKC: WT(30) vs DMSO(30), *** $p < 0.001$; WT(60) vs DMSO(60), *** $p < 0.001$.

3.3.2. Effects of the NBD WT CPP on agonist-stimulated canonical NF-κB activation.

A NBD peptide was first demonstrated to competitively inhibit canonical NF-κB activation through the disruption of the interactions between NEMO and the IKKs by May et al. (2000b). Prior to use of a related peptide and examination of its ability to impact AURKA-TPX2 status, preliminary experiments were constructed to confirm the ability of the NBD peptide, in a cell permeable form, to inhibit NF-κB activation in PC3 cells. This focussed on measuring recognised markers of canonical NF-κB activation, namely IκBα degradation and phosphorylation of p65 (Ser536), and their blockade following pre-treatment with inhibitory peptide (Zhao et al., 2018b). PC3 cells were cultured in 12-well plates until 70-80% confluent prior to being rendered quiescent in serum-free media for 24 hours to downregulate all growth signalling pathways in cells. Following this, cells were pre-treated with NBD WT or MT CPP (both 100μM) and then exposed to the agonist TNFα (20ng/ml) for 30 min to activate canonical NF-κB signalling. In Figure 3.5, from immunoblotting (A) and subsequent quantification (B) there was a significant ($p < 0.05$) decrease in both the high initial basal expression and the TNFα-stimulated phosphorylation of p65 ($68.8 \pm 10.5\%$; $n=3$, $p < 0.01$) and total p65 protein expression ($77.1 \pm 14.7\%$; $n=3$, $p < 0.05$) in the TNFα stimulated sample that had been treated with 100μM of the NBD WT peptide. This was a hallmark of inhibition of canonical NF-κB signalling. There was no significant reversal of TNFα stimulated IκBα degradation observed following treatment with the NBD WT CPP even though we would expect this to be reversed similarly to the status of p65 phosphorylation and/or expression.



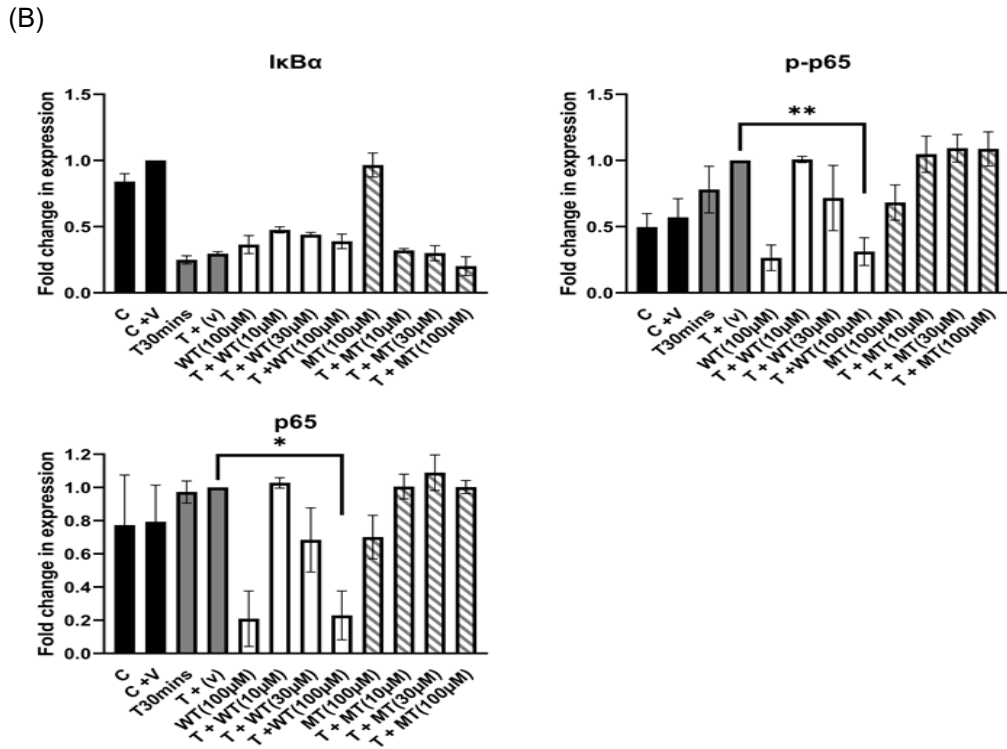


Figure 3.5. Impact of the NBD WT CPP on canonical NF-κB markers in PC3 cells.

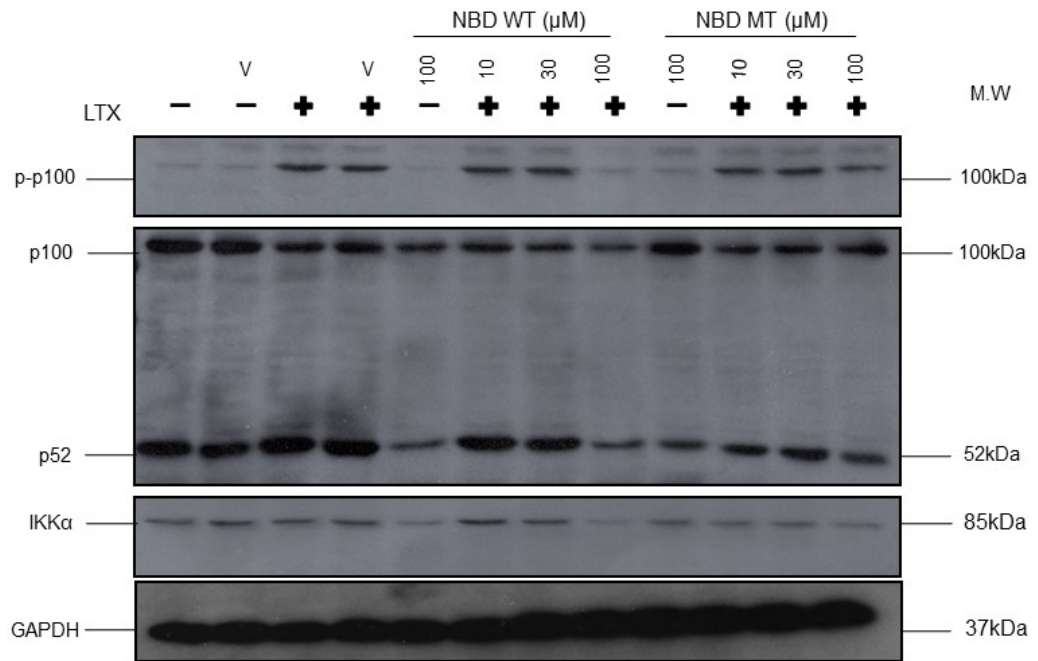
PC3 cells were grown in 12-well plates and serum starved for 24h prior to treatment. After serum starvation, cells were pre-treated with 0.5% (v/v) DMSO (V) or NBD mutant-type (MT) / wild-type (WT) CPPs (100μM, 30μM and 10μM) for 2 hours prior to stimulation with TNF-α (20ng/ml) for 30min (T30min). (C) and (C + V) represents the non-treated and vehicle treated control respectively in non-stimulated cells. **(A)** Whole cell lysates were prepared for separation using SDS-PAGE and analysis by Western Blotting using the above antibodies (n=3). GAPDH was used as a loading control. **(B)** Data was normalised to the vehicle treated stimulated control (T(v)) and represents mean ± S.E.M. One-way ANOVA with post-hoc Dunnet's test was used to determine statistical significance ($p < 0.05$) of observed changes in agonist-stimulated canonical NF-κB activation induced by the mutant-type (T + MT) or wild-type (T + WT) NBD peptide respectively, relative to the agonist-stimulated vehicle control (T + v). (*= $p < 0.05$, **= $p < 0.01$).

3.3.3. Effects of NBD WT CPP on agonist-stimulated non-canonical NF-κB activation.

Extensive research (see Section 3.3.2) has demonstrated the ability of NBD peptides to disrupt the association between the IKK complex and NEMO and consequently inhibit agonist-stimulated canonical NF-κB activation (May et al., 2000b). However, no reported literature investigating the potential effects of NBD peptides on the non-canonical NF-κB pathway exists. As described by Gamble et al. (2012a) p100 phosphorylation is an indicator of non-canonical NF-κB signalling and therefore, the NBD CPPs were assessed for their ability to effect non-canonical NF-κB signalling and inhibit the stimulated phosphorylation of p100 and proteolytic processing of p100 protein to p52, thus raising the question as to whether the disruption of the

IKK complex would have any bearing on IKK α -mediated activation of the non-canonical NF- κ B pathway? PC3 cells were cultured in 12-well plates until 70-80% confluent and rendered quiescent by incubation in serum-free media for 24 hours, to downregulate growth signalling pathways in cells. Cells were then pre-treated with NBD WT or MT CPP (both 100 μ M) for 2 hours and then exposed to the agonist Lymphotoxin- $\alpha_1\beta_2$ (LTX; 20ng/ml), a recognised driver of non-canonical NF- κ B signalling (Paul et al., 2018) for 4 hours. In Figure 3.6, from immunoblotting (A) and subsequent densitometric quantification and analysis (B), there was a significant ($p < 0.05$) decrease in both phosphorylation of p100 ($69.7 \pm 3.4\%$; $n=3$, $p < 0.001$) in the LTX stimulated sample that was pre-treated with 100 μ M of the NBD WT CPP in comparison to the stimulated control in the presence of vehicle. As IKK α is recognised to regulate and control this pathway (Paul et al., 2018) its protein expression was also measured. There was a significant ($p < 0.05$) decrease in IKK α protein expression ($62.8 \pm 6.9\%$; $n=3$, $p < 0.01$) in the LTX stimulated sample that was pre-treated with a 100 μ M concentration of the NBD WT CPP in comparison to the agonist plus vehicle control. A similar related inhibitory effect was observed, at the level of the processing of p100 to p52 (LTX+WT100 μ M) with observed significant reduction ($70.8\% \pm 12.1\%$; $n=3$, $p < 0.01$) compared to the agonist plus vehicle control. Although the NBD peptide had a significant effect on LTX-stimulated processing of p100 to p52, it didn't cause any significant accumulation of p100 protein. That said this represents the first indication that the NBD WT CPP can inhibit agonist-stimulated non-canonical NF- κ B activation.

(A)



(B)

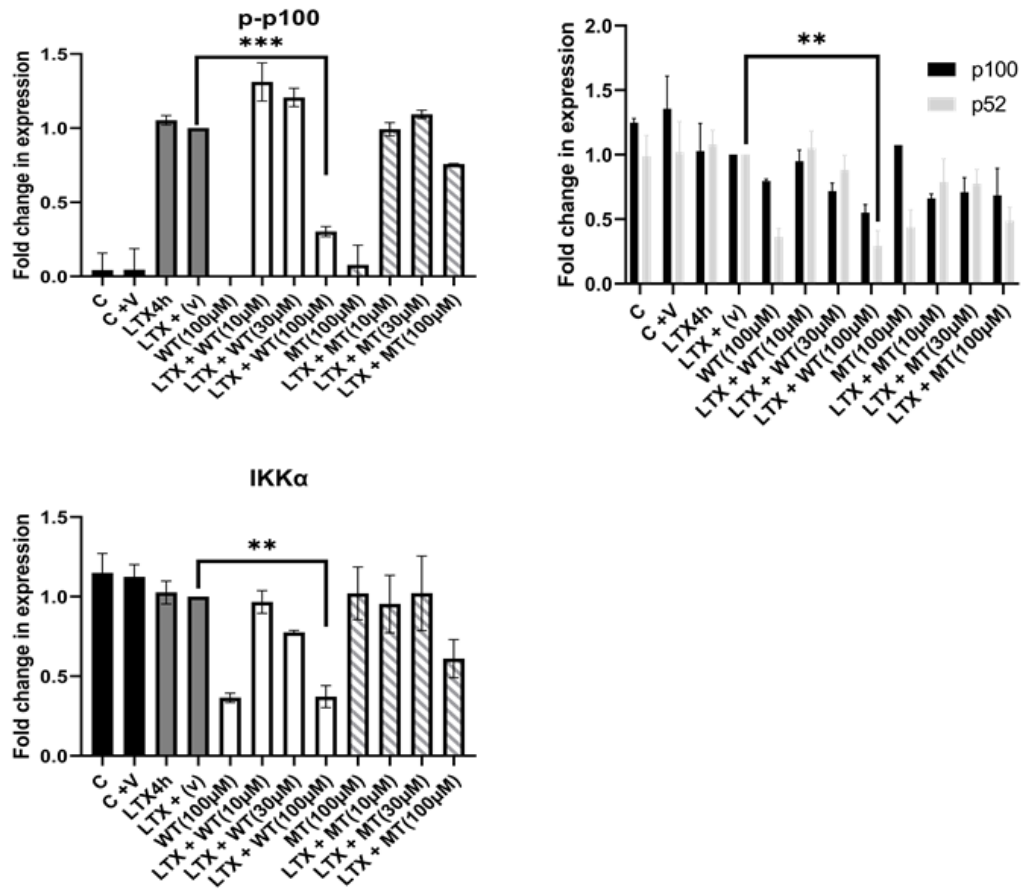


Figure 3.6. Impact of NBD WT CPP on non-canonical NF-κB markers in PC3 cells.

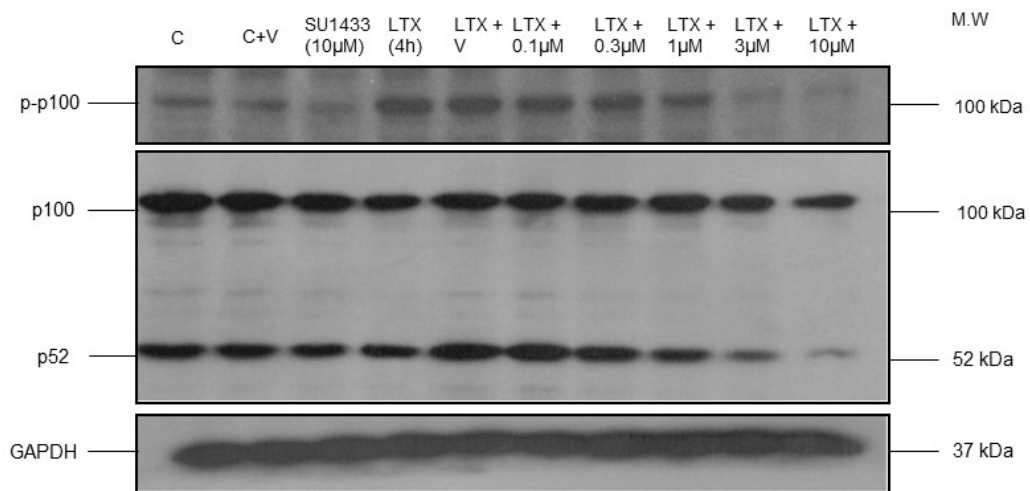
PC3 cells were grown in 12-well plates and serum starved for 24h prior to treatment. After serum starvation, cells were pre-treated with vehicle (0.5% (v/v) DMSO; V) or NBD mutant-type (MT)/ wild-type (WT) CPPs (100μM, 30μM and 10μM) for 2 hours prior to stimulation with LTX (20ng/ml) for 4 hours (LTX4h). (C) and (C + V) represents the non-treated and vehicle treated control respectively in non-stimulated cells. **(A)** Whole cell lysates were prepared for separation using SDS-PAGE and analysis by Western Blotting using the above antibodies (n=3). GAPDH was used as a loading control. **(B)** Data was normalised to the vehicle treated stimulated control (LTX+(v)) and represents mean ± S.E.M. One-way ANOVA with post-hoc Dunnet's test was used to determine statistical significance ($p < 0.05$) of observed changes in agonist-stimulated non-canonical NF-κB activation induced by the mutant-type (LTX + MT) or wild-type (LTX + WT) NBD peptide, relative to the agonist-stimulated vehicle control (LTX + v) (*= $p < 0.05$, **= $p < 0.01$, ***= $p < 0.001$).

3.3.4 Effects of small molecule IKK-kinase inhibitors on agonist-stimulated NF- κ B signalling.

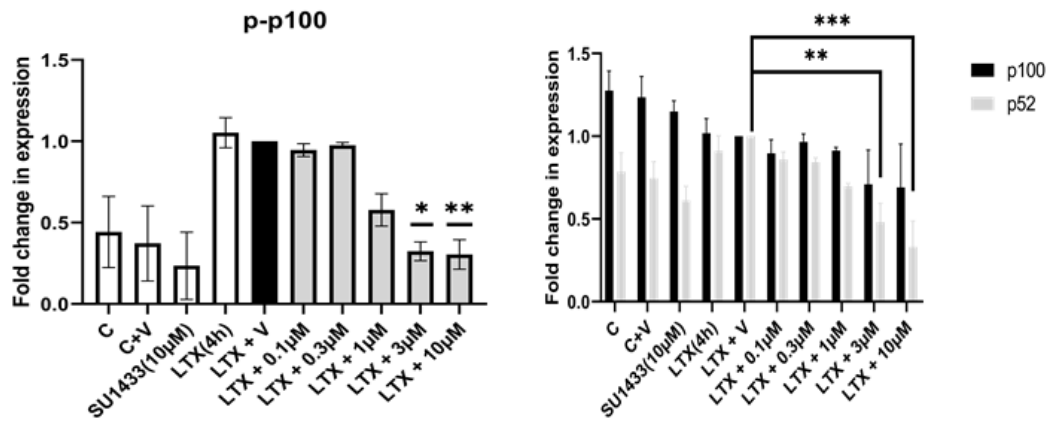
Given that the NBD WT CPP displayed significant impact on the status of AURKA-TPX2 and related mitotic proteins and that it also displayed impact on both canonical and non-canonical NF- κ B activation (see Figures above) it raised the question as to whether impact on the mitotic markers was a consequence of direct targeting of AURKA-TPX2 or as an indirect effect, namely a downstream consequence of IKK α/β perturbation by means of disrupting protein-protein interactions of the IKK complex(es). Therefore, to elucidate the mechanistic regulation further and consider any potential IKK-mediated regulation, alternative strategies to targeting IKK isoform activity and/or expression were considered. Small molecule isoform selective IKK inhibitors when then considered as an alternative pharmacological means of targeting IKK activity. ATP-competitive kinase inhibitors were then used to target the kinase domains (KD) of each isoform and challenge theoretically their intrinsic catalytic activities. Therefore, prior to applying this approach to the examination of AURKA status/phosphorylation/expression etc., preliminary experiments were constructed to investigate and confirm the ability of said kinase inhibitors to target IKK α and IKK β selectively and inhibit NF- κ B signalling mediated by each isoform; non-canonical and canonical NF- κ B respectively (see Section 3.3.4). An “in-house” proprietary IKK α -selective small molecule kinase inhibitor – SU1433 (IC_{50} IKK α vs. IKK β = 0.011 μ M vs. 2.25 μ M) and a commercially available IKK β – selective inhibitor, BMS-345541 (Bristol Myers Squibb Pharmaceuticals; IC_{50} IKK β vs. IKK α = 0.3 μ M vs. 4 μ M; (Burke et al., 2003)), were utilised to test their ability to inhibit NF- κ B signalling, as described by (Gamble et al., 2012b). To assess impact of these molecules, key cellular markers of NF- κ B activation were again measured following agonist stimulation in the absence and presence of increasing concentration of each inhibitor, as described previously in Section 3.3.3. Effective inhibition of IKK α -mediated non-canonical activation would be indicated by inhibition of LTX-stimulated p100 phosphorylation (S866/870) and processing of p100 to p52, whilst inhibition of TNF-stimulated canonical NF- κ B signalling gauged by the effective reversal of agonist-stimulated I κ B degradation and inhibition of p65 (S536) phosphorylation. From Figure 3.7 there was a noticeable significant concentration-dependent inhibition of LTX-stimulated p100 phosphorylation mediated by the “in-house” IKK α -selective inhibitor (SU1433), observed in the immunoblotting (A) and this is further confirmed in the associated densitometric quantification (B). Here there was a significant decrease in LTX-stimulated phosphorylation of p100 at 3 μ M ($67.5 \pm 5.8\%$; $n=3$, $p<0.05$) and 10 μ M ($69.5 \pm 9.1\%$; $n=3$, $p<0.01$) compared to the agonist plus vehicle control (LTX + V). There was also a concentration-dependent decrease in p52 formation relative to the agonist-stimulated vehicle control, which was shown to be significant

at 3 μ M (52.0 \pm 11.6%; n=3, p<0.01) and 10 μ M (67.0 \pm 15.9%; n=3, p<0.001) concentrations. These both are indicative of inhibition of LTX-stimulated non-canonical NF- κ B signalling. In Figure 3.7 (C), from immunoblotting, an IKK β -selective inhibitor (BMS-345541) demonstrated a noticeable reversal of the TNF α -stimulated degradation of I κ B α , which is a hallmark of inhibition of agonist-stimulated canonical NF- κ B signalling. This was further analysed and in Figure 3.7 (D), there was a significant TNF α -mediated degradation of I κ B α (T 30 min) and a significant reversal of TNF α -stimulated I κ B α degradation following pre-treatment with BMS-345541 at 10 μ M (53.8 \pm 7.5%; n=3, p<0.01), 20 μ M (47.8 \pm 5.7%; n=3, p<0.01), 40 μ M (54.0 \pm 5.1%; n=3, p<0.01) and 50 μ M (58.2 \pm 10.8%; n=3, p<0.001). There was also a significant decrease in TNF α -stimulated phosphorylation of p65 (Ser536) following pre-treatment with 50 μ M (50.2 \pm 18.8%; n=3, p<0.05) and this was also indicative of inhibition of agonist-stimulated canonical NF- κ B pathway. Collectively, these experiments confirmed the ability of isoform-selective IKK α or IKK β kinase inhibitors to target non-canonical and canonical NF- κ B signalling pathways respectively.

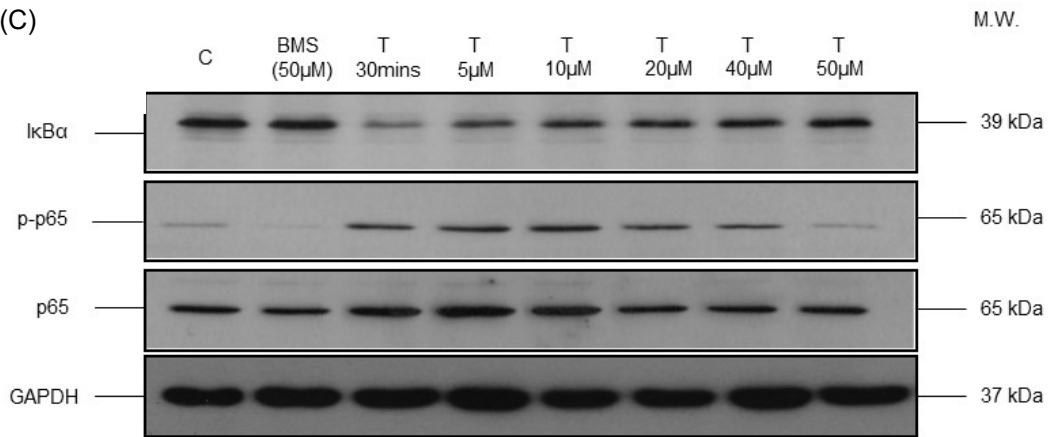
(A)



(B)



(C)



(D)

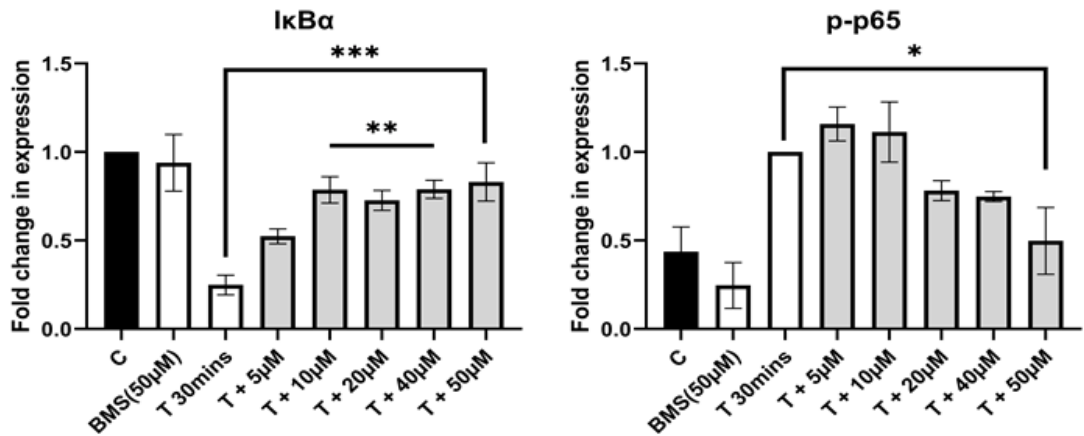


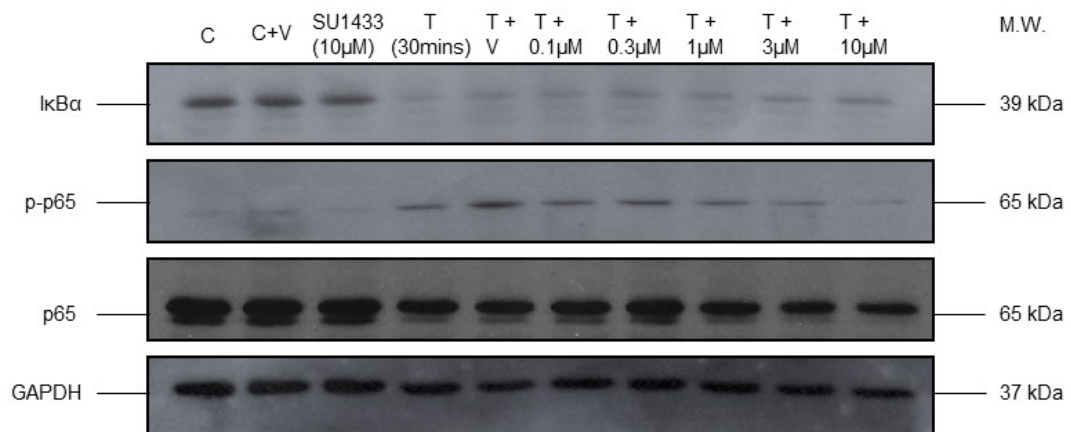
Figure 3.7. Impact of small molecule isoform-selective IKK α and IKK β kinase inhibitors on non-canonical and canonical NF- κ B markers in PC3 cells.

PC3 cells were grown in 12-well plates and serum starved for 24 h prior to stimulation. (A + B) - Validation of IKK α kinase inhibitors effect on non-canonical NF- κ B signalling. After serum starvation, cells were pre-treated with vehicle (DMSO 0.05% (v/v)) or increasing concentrations (0.1-10 μ M) of an "in-house" IKK α inhibitor (SU1433) for 1 h prior to stimulation with LTX (20ng/ml) for 4 hours. GAPDH was used as a loading control (n=3). (C + D) -Validation of IKK β kinase inhibitors effect on canonical NF- κ B signalling. After serum starvation, cells were treated for 1 h with increasing concentrations (5-50 μ M) of the IKK β -selective inhibitor (BMS-34551) prior to exposure to TNF- α (T) (20ng/ml) for 30min. GAPDH was used as a loading control (n=3). Data was normalised to the control (C) or stimulated samples and represents mean \pm S.E.M. One-way ANOVA with post-hoc Dunnet's test was used to determine statistical significance ($p < 0.05$) of observed changes in agonist-stimulated non-canonical/ canonical NF- κ B activation caused by the BMS-34551 or SU1433 kinase inhibitor respectively, relative to the agonist-stimulated vehicle or control (LTX + V / T30). Non-canonical: p-p100: LTX + 3 μ M vs LTX + v, * $p < 0.05$; LTX + 10 μ M vs LTX + v, ** $p < 0.01$. p52: LTX + 3 μ M vs LTX + v, ** $p < 0.01$; LTX + 10 μ M vs LTX + v, *** $p < 0.001$. Canonical: IkB α : T + 10 μ M, T + 20 μ M, T + 40 μ M vs T30, ** $p < 0.01$; T + 50 μ M vs T30, *** $p < 0.001$. p-p65: T + 50 μ M vs T30, * $p < 0.05$.

3.3.5. Effect of a small molecule IKK α -selective kinase inhibitor on agonist-stimulated canonical NF- κ B signalling.

Having demonstrated the ability of the described IKK α and IKK β inhibitors to display their expected pharmacological selectivity for inhibition of LTX-stimulated non-canonical NF- κ B activation (IKK α -mediated; SU1433 sensitive) and TNF α -stimulated canonical NF- κ B activation (IKK β -mediated; BMS-345541 sensitive) respectively, experiments were then constructed to determine whether this selectivity was robust i.e. could either molecule target the alternative NF- κ B signalling events to display 'off-target' effects? Therefore, cells were serum starved for 24 hours and then pre-treated with an "in-house" developed IKK α -selective small molecule kinase inhibitor (SU1433) prior to stimulation with TNF α (20ng/ml) for 30 min to assess the effects of the IKK α inhibitor on agonist-stimulated canonical NF- κ B signalling. In Figure 3.8 (A) and (B) there was no significant ($p > 0.05$) reversal of TNF α -induced I κ B α degradation nor any decrease in TNF α -stimulated Ser536 phosphorylation of p65 caused by pre-treatment of cells with the IKK α -selective compound SU1433. As there was no significant effect on agonist stimulation of the canonical NF- κ B pathway, which is largely IKK β regulated, it highlighted and confirmed the selectivity of the "in-house" IKK α -selective inhibitor, SU1433.

(A)



(B)

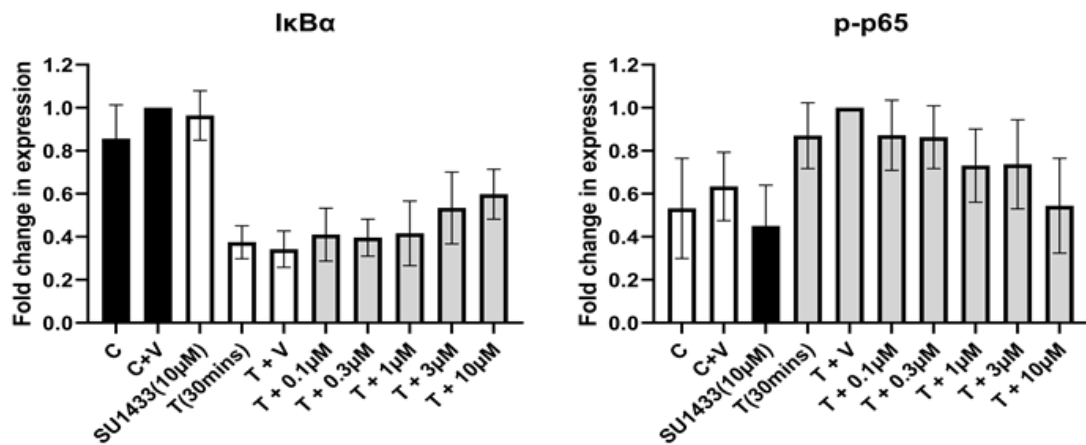


Figure 3.8. Impact of an IKK α -selective kinase inhibitor on canonical NF- κ B cellular markers.

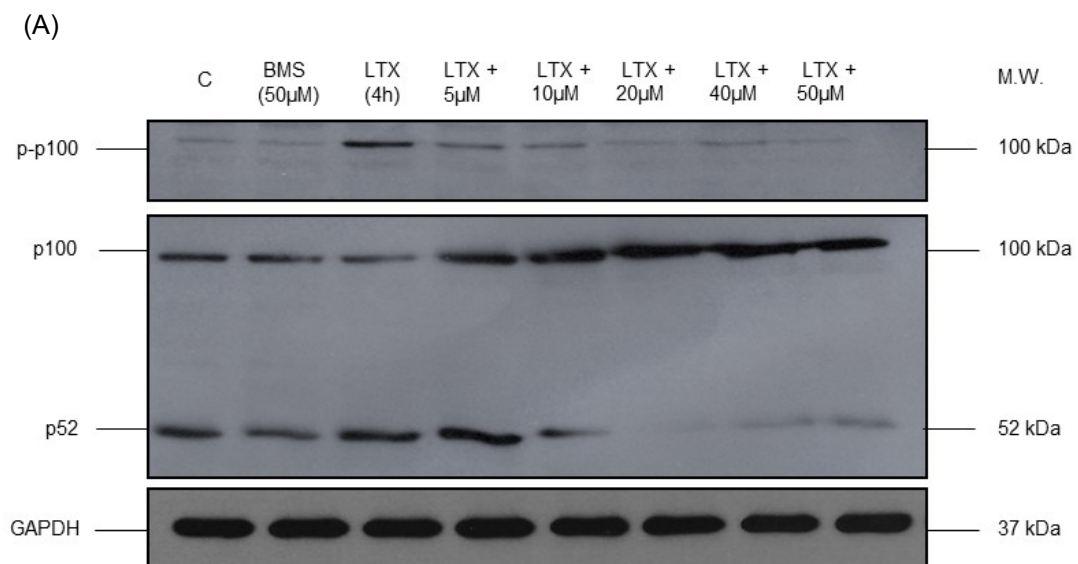
PC3 cells were grown in 12-well plates and serum starved for 24h prior to stimulation. Investigating effect of IKK α -selective kinase inhibitor on canonical NF- κ B signalling. Cells were incubated with vehicle (0.05% (v/v) DMSO) or with increasing concentrations (0.1-10 μ M) of an “in-house” IKK α inhibitor (SU1433) for 1 hour prior to exposure to TNF- α (T) (20ng/ml) for 30min (T30min). (C) and (C + V) represents the non-treated and vehicle treated control respectively in non-stimulated cells. (A) Whole cell lysates were prepared for separation using SDS-PAGE and analysis by Western Blotting using the above antibodies (n=3). GAPDH was used as a loading control. (B) Data was normalised to the vehicle or vehicle-stimulated sample (T + V) and represents mean \pm S.E.M. One-way ANOVA with post-hoc Dunnet’s test was used to determine statistical significance ($p < 0.05$) of observed changes in agonist-stimulated canonical NF- κ B activation brought about by the SU1433 kinase inhibitor, relative to the agonist-stimulated vehicle control (T + v). I κ B α and p-p65: T + 0.1 – 10 μ M vs T + v, * $p > 0.05$.

3.3.6. Effect of a small molecule IKK β -selective kinase inhibitor on agonist-stimulated non-canonical NF- κ B signalling.

Extending the studies of Section 3.3.5 above, the potential effect of the IKK β inhibitor, BMS-345541 on regulation of agonist-stimulated non-canonical NF- κ B signalling was also investigated. Cells were again serum starved for 24 hours and then pre-treated with increasing concentrations of the BMS-345541 compound for 1 hour prior to exposure to LTX (20ng/ml) for 4 hours to then assess the potential effects of the IKK β inhibitor on cellular markers of agonist-stimulated non-canonical NF- κ B signalling.

In Figure 3.9, LTX stimulated a 5-fold increase in phosphorylation of p100 (Ser860/868) which was noticeably reversed by IKK β -selective inhibitor, BMS-345541. This was observed in the immunoblotting (A) and further confirmed in the associated quantification (B). Here there was a significant decrease in LTX-stimulated phosphorylation of p100 at 5 μ M (50.6 \pm 6.5%; n=3, $p < 0.001$), 10 μ M (57.9 \pm 8.7%; n=3, $p < 0.001$), 20 μ M (79.9 \pm 4.5%; n=3,

$p < 0.001$), $40\mu\text{M}$ ($78.3 \pm 1.7\%$; $n=3$, $p < 0.001$) and $50\mu\text{M}$ ($73.5 \pm 7.1\%$; $n=3$, $p < 0.001$) compared to the agonist stimulated sample (LTX 4h). There was also a significant reduction in LTX-stimulated p52 formation relative to the agonist stimulated sample, which was shown to be significant at $20\mu\text{M}$ ($56.8 \pm 21.3\%$; $n=3$, $p < 0.05$), $40\mu\text{M}$ ($54.8 \pm 16.4\%$; $n=3$, $p < 0.05$) and $50\mu\text{M}$ ($59.9 \pm 8.0\%$; $n=3$, $p < 0.05$) concentrations. These both indicated that pre-treatment of cells with the BMS compound resulted in effective concentration-dependent inhibition of LTX-stimulated non-canonical NF- κB signalling. Although the BMS-345541 compound is recognised primarily as an IKK β inhibitor, it is worth noting that whilst this inhibitor is indeed IKK β -selective it does possess IKK α inhibitory action (Burke et al., 2003); its potency against IKK β being 10-fold greater than that against IKK α (IC_{50} IKK β vs. IKK α = $0.3\mu\text{M}$ vs. $4\mu\text{M}$; (Burke et al., 2003)). This ability to target IKK α may account for the significant inhibitory effects on markers of agonist-stimulated non-canonical NF- κB signalling.



(B)

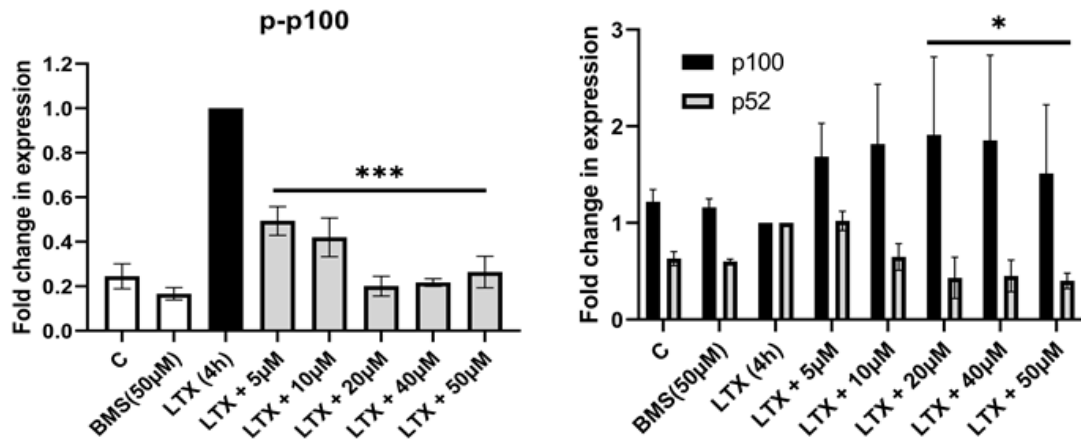


Figure 3.9. Impact of a small molecule IKK β -selective kinase inhibitor on non-canonical NF- κ B cellular markers in PC3 cells.

PC3 cells were grown in 12-well plates and serum starved for 24h prior to stimulation. After serum starvation, cells were pre-treated with increasing concentrations (5-50 μ M) of IKK β inhibitor (BMS-34551) for 1 hour prior to exposure to LTX (20ng/ml) for 4 hours (LTX4h). (C) represents the non-treated control in non-stimulated cells. GAPDH was used as a loading control (n=3). (A) Whole cell lysates were prepared for separation using SDS-PAGE and analysed by Western Blotting using the above antibodies (n=3). GAPDH was used as a loading control. (B) Data was normalised to the stimulated sample (LTX (4h)) and represents mean \pm S.E.M. One-way ANOVA with post-hoc Dunnet's test was used to determine statistical significance ($p < 0.05$) of observed changes in agonist-stimulated non-canonical NF- κ B activation brought about by the BMs-34551 kinase inhibitor, relative to the agonist-stimulated control (LTX 4h). p-p100: LTX + 5-50 μ M vs LTX 4h, *** $p < 0.001$. p52: LTX + 20-50 μ M vs LTX 4h, * $p < 0.05$.

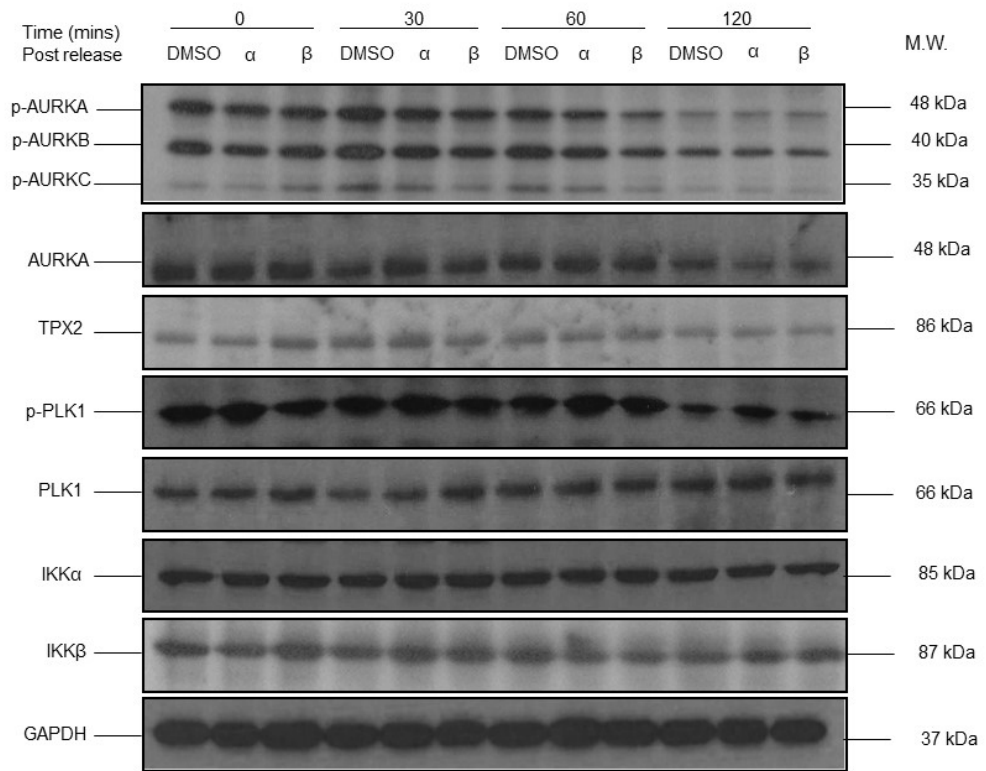
3.3.7. Effects of small molecule IKK α and IKK β inhibitors on the status of AURKA and cell cycle markers in synchronised PC3 cells.

Having confirmed the ability of IKK isoform-selective kinase inhibitors to effectively abrogate IKK-mediated NF- κ B activation, these inhibitors were then applied in experiments using Nocodazole arrested mitotic PC3 prostate cancer cells. Small molecule (SM) kinase inhibitors SU1433 and BMS-345541 were used as pharmacological tools to determine whether targeting IKK α/β catalytic activity had a bearing and influence on the status of AURKA and associated proteins TPX2 and PLK1 during mitosis. Cells were again treated and released from a nocodazole-mediated arrest/trap at pro-metaphase. Expression and/or phosphorylation of AURKs, TPX2 and PLK1 were again examined by Western blotting at 30, 60 and 120 minute time points post release from nocodazole-mediated arrest.

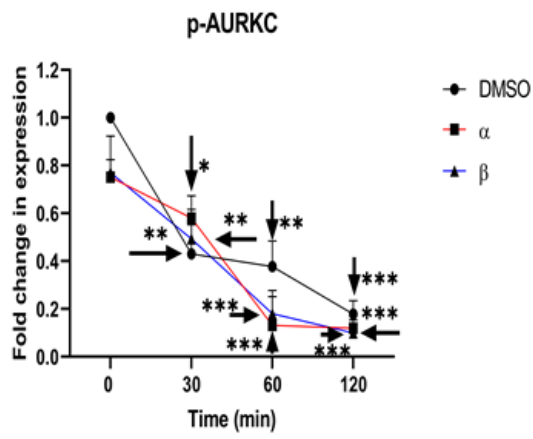
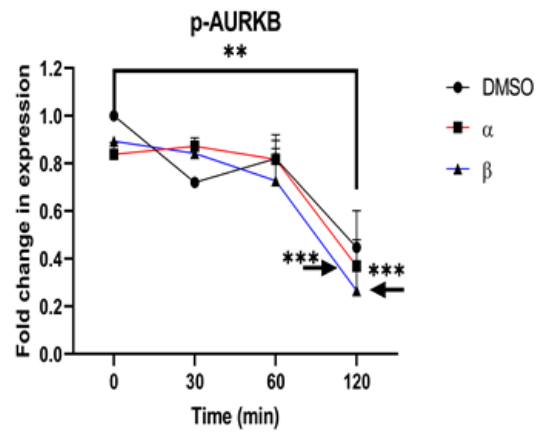
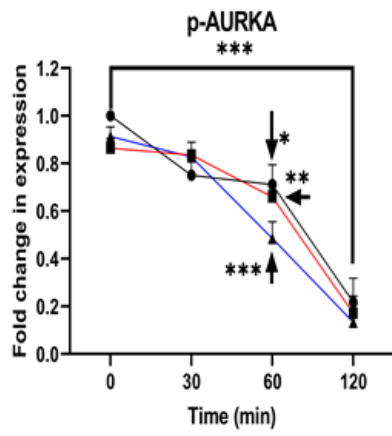
Figure 3.10 shows the effect of the IKK small molecule kinase inhibitors on AURKA signalling post trap and release. After 16-20 hours treatment with nocodazole, cells were washed and released with full RPMI 1640 media before treatment with 3 μ M SU1433 (IKK α -selective inhibitor) or 50 μ M BMS-345541 (IKK β -selective inhibitor). In Figure 3.10, there was

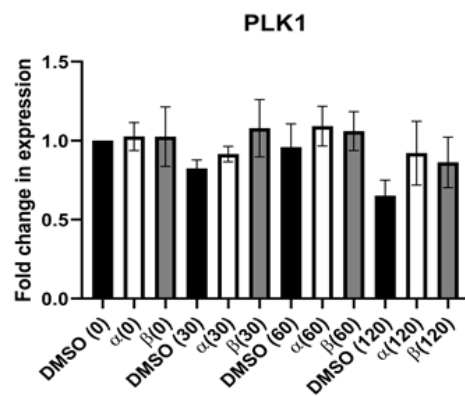
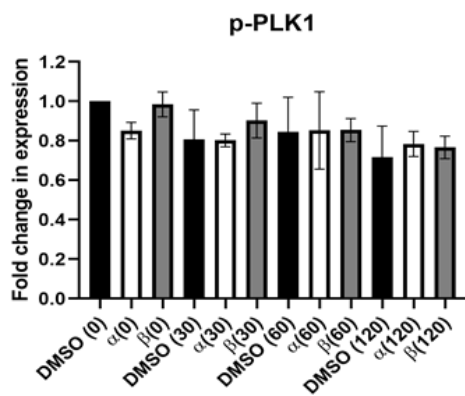
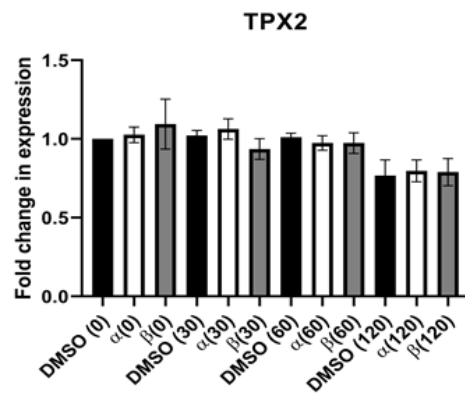
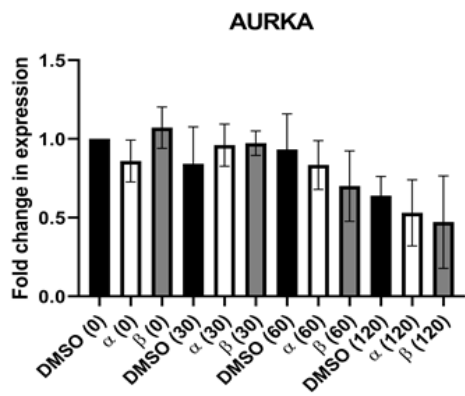
no change in status of AURKA and its related markers in terms of expression and/or phosphorylation in cells treated with either the IKK α or the IKK β small molecule kinase inhibitors relative to the vehicle control at each time point. There was a significant reduction in phosphorylation of AURKA after 60 min, in vehicle ($28.8 \pm 8.3\%$; $n=3$, $p<0.05$), IKK α kinase inhibitor ($34.1 \pm 2.8\%$; $n=3$, $p<0.01$) and IKK β kinase inhibitor ($51.4 \pm 70.0\%$; $n=3$, $p<0.001$) treated samples. A significant decrease was also observed at the 120 minute time point in DMSO ($78.2 \pm 10.1\%$; $n=3$, $p<0.001$), the IKK α kinase inhibitor ($82.8 \pm 7.2\%$; $n=3$, $p<0.001$) and the IKK β kinase inhibitor ($86.6 \pm 7.4\%$; $n=3$, $p<0.001$). Similar was observed for AURKB phosphorylation, in which there was a significant reduction after 120 min in vehicle ($55.3 \pm 15.4\%$; $n=3$, $p<0.01$), IKK α kinase inhibitor ($63.2 \pm 11.1\%$; $n=3$, $p<0.001$) and IKK β kinase inhibitor ($73.4 \pm 12.5\%$; $n=3$, $p<0.001$) treated samples. Lastly, phosphorylation of AURKC was shown to be significantly decreased after 30min in cells treated with DMSO ($56.9 \pm 12.2\%$; $n=3$, $p<0.01$), IKK α kinase inhibitor ($41.9 \pm 9.3\%$; $n=3$, $p<0.05$) and IKK β kinase inhibitor ($50.7 \pm 12.3\%$; $n=3$, $p<0.01$). It was also significantly reduced after 60 minutes in cells treated with DMSO ($62.3 \pm 10.7\%$; $n=3$, $p<0.01$), IKK α kinase inhibitor ($86.8 \pm 12.0\%$; $n=3$, $p<0.001$) and IKK β kinase inhibitor ($81.9 \pm 9.7\%$; $n=3$, $p<0.001$). Lastly, there was also a significant decrease observed after 120 minutes in samples treated with; DMSO ($82.1 \pm 5.6\%$; $n=3$, $p<0.001$), IKK α kinase inhibitor ($88.0 \pm 3.4\%$; $n=3$, $p<0.001$) and IKK β kinase inhibitor ($90.1 \pm 2.9\%$; $n=3$, $p<0.001$). As there was no difference between the vehicle-treated sample at each time point compared to that for the cells treated with inhibitory IKK α -selective or IKK β -selective kinase inhibitors at each time point, this suggested that the abrogation of IKK α/β kinase activity had no bearing on the phosphorylation of each AURK subtype. They decreased naturally following release from nocodazole arrest as the cells progressed through the cell cycle to completion of mitosis. Furthermore, there were no significant differences observed in the status of other AURK-associated cell cycle markers; TPX2 expression and PLK1 total protein expression and phosphorylation (Thr215), which all again decreased naturally over this time course. Expression and/or phosphorylation of AURKs, TPX2, PLK1 decreased naturally over time and this decrease was not accelerated as a result of treatment with the IKK α - or IKK β -selective kinase inhibitors. The expression of the IKK proteins remained constant throughout the time frames of the experiment, consistent with the previous experimental outcomes as described in Section 3.2.1.1 – they were not cell cycle regulated.

(A)



(B)





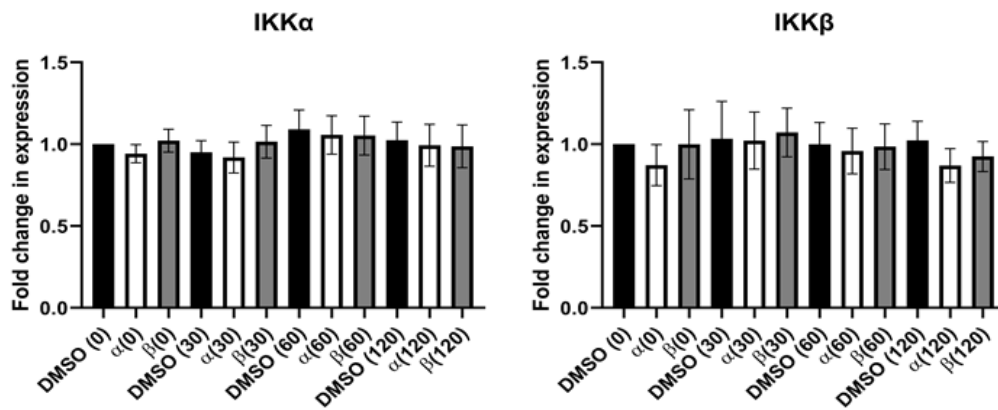


Figure 3.10. Impact of small molecule isoform-selective IKK inhibitors on AURKs and related protein markers of mitosis and IKK proteins in PC3 cells.

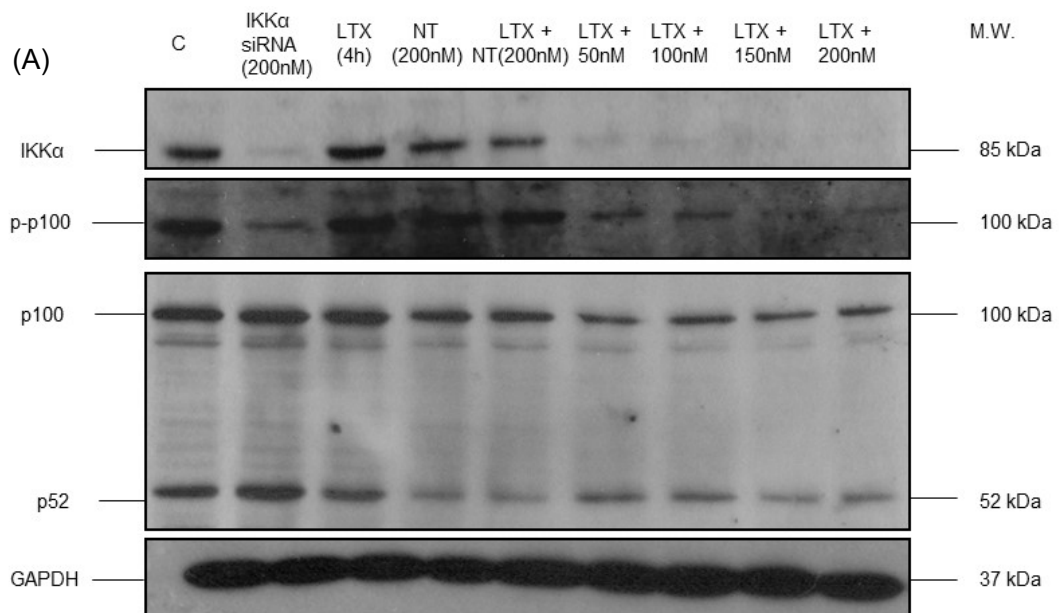
PC3 cells were grown on 10mm dishes and treated with 50ng/ml Nocodazole (16-20 hours) prior to treatment with vehicle (0.05% (v/v) DMSO), an IKK α -inhibitor (SU1433) - 3 μ M or an IKK β -inhibitor (BMS-345541) - 50 μ M upon release from trap at 30min, 60min and 120min. (A) Whole cell lysates were prepared for separation using SDS-PAGE and analysed by Western Blotting using the above antibodies (n=3). GAPDH was used as a loading control. (B) Data was normalised to the control (DMSO 0) and represents mean \pm S.E.M. One-way ANOVA with post-hoc Dunnett's test was used to determine statistical significance ($p < 0.05$) of observed changes relative to vehicle control at 0 min. (*= $p < 0.05$, **= $p < 0.01$, ***= $p < 0.001$). p-AURKA: DMSO(60) vs DMSO(0), * $p < 0.05$; α (60) vs DMSO(0), ** $p < 0.01$; β (60) vs DMSO(0), *** $p < 0.001$; DMSO(120) vs DMSO(0), *** $p < 0.001$; α (120) vs DMSO(0), *** $p < 0.001$; β (120) vs DMSO(0), *** $p < 0.001$. p-AURKB DMSO(120) vs DMSO(0), ** $p < 0.01$; α (120) vs DMSO(0), *** $p < 0.001$; β (120) vs DMSO(0), *** $p < 0.001$. p-AURKC: DMSO(30) vs DMSO(0), ** $p < 0.01$; α (30) vs DMSO(0), * $p < 0.05$; β (30) vs DMSO(0), ** $p < 0.01$; DMSO(60) vs DMSO(0), ** $p < 0.01$; α (60) vs DMSO(0), *** $p < 0.001$; β (60) vs DMSO(0), *** $p < 0.001$; DMSO(120) vs DMSO(0), *** $p < 0.001$; α (120) vs DMSO(0), *** $p < 0.001$; β (120) vs DMSO(0), *** $p < 0.001$. For changes relative to vehicle control at each time point vs SU1433 or BMS-345541 at the same timepoint, one-way ANOVA with post-hoc Dunnett's test was used to determine statistical significance ($p < 0.05$) of observed changes relative to vehicle control at the appropriate time point.

3.3.8. Effects of siRNA IKK α and IKK β on agonist-stimulated NF- κ B signalling.

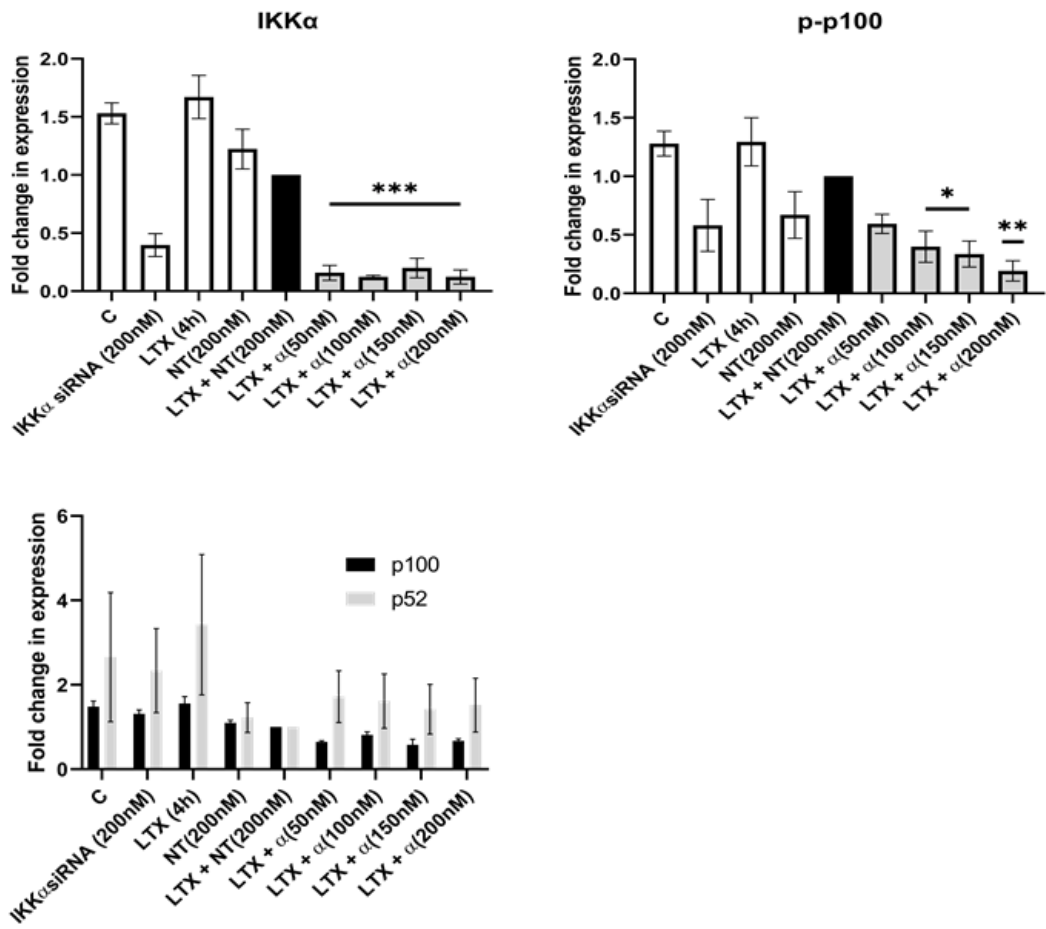
Small-interfering RNA (siRNA) targeting both IKK proteins, IKK α - and IKK β , and a scrambled non-targeting sequence (NT), were utilised to target 'run-down' of the total protein expression of each IKK protein at the transcriptional level to test IKK-Aurora signalling. This enabled the construction of experiments aimed at elucidating whether the regulatory mechanism of the AURKA-TPX2 modulation was reliant on cellular IKK protein expression/interaction. This represented an alternative molecular strategy of targeting IKK expression/activity distinct from the previously utilised pharmacological approach using IKK-selective kinase inhibitors. Use of siRNA would target the protein of interest at the transcriptional level and cause a synthetic gene 'knock-down' of each isoform which would prevent the protein being translated.

Therefore, prior to applying this approach to the examination of AURKA etc., preliminary experiments were constructed to investigate and confirm the ability of targeted siRNA to downregulate IKK α and IKK β selectively and inhibit NF- κ B signalling mediated by each isoform; non-canonical and canonical NF- κ B respectively (see Section 3.3.8). To establish optimal conditions for siRNA transfection, PC3 cells were treated with various concentrations of lipofectamine RNAiMAX and then analysed (data not shown). Following on from this initial optimisation, a volume of 5 μ l of lipofectamine was determined as appropriate for transfection. PC3 cells were transfected with a concentration range of siRNA targeting the IKK proteins as well as a single concentration of a NT control sequence (equal to the highest concentration of siRNA targeting the protein of interest), as described in Section 2.2.5.3 of the materials and methods. This was followed by serum starvation for 24 hours prior to stimulation with the appropriate agonist. As mentioned previously in Section 3.3.3, reversal of LTX-stimulated p100 phosphorylation (S866/870) is an indicator of non-canonical pathway inhibition, as inhibition of p65 (S536) phosphorylation and reversal of I κ B α degradation is an indicator of canonical NF- κ B pathway inhibition. Therefore, the IKK siRNA used here will be assessed on their ability to affect these respective pathways and reverse the effect on each marker after stimulation. In Figure 3.11 (A) and (B) there was a substantial and significant decrease in total protein expression of IKK α at 50nM ($84.2 \pm 6.6\%$; n=3, p<0.001), 100nM ($87.6 \pm 1.4\%$; n=3, p<0.001), 150nM ($80.0 \pm 8.4\%$; n=3, p<0.001) and 200nM ($87.7 \pm 6.1\%$; n=3, p<0.001). This was coupled with a noticeable concentration dependent inhibition of LTX-stimulated p100 phosphorylation which was shown to be significant at 100nM ($60.1 \pm 13.3\%$; n=3, p<0.05), 150nM ($66.4 \pm 11.1\%$; n=3, p<0.05) and 200nM ($80.8 \pm 8.7\%$; n=3, p<0.01)

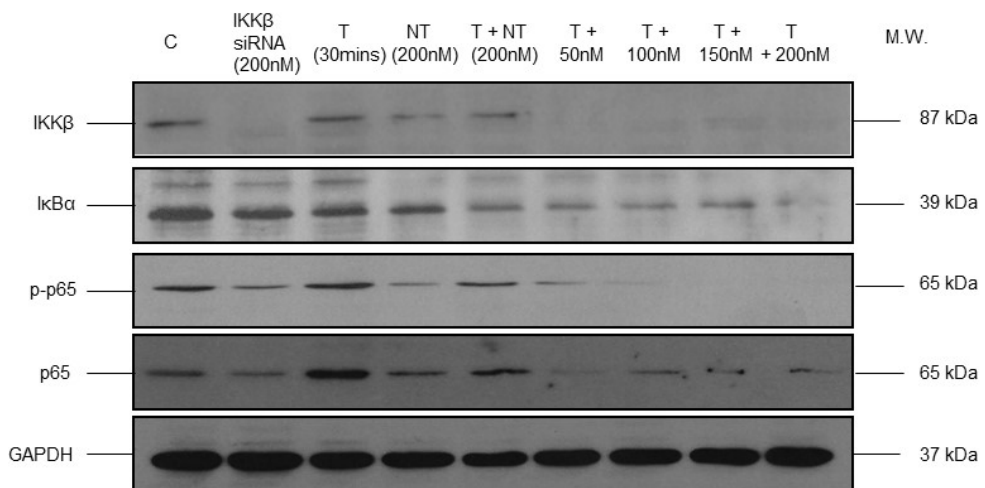
compared to the agonist-stimulated sample treated with Non-targeting (NT) siRNA. Hence, this highlighted the ability of the IKK α siRNA to run down total protein expression and affect agonist-stimulated non-canonical NF- κ B pathway signalling. However, treatment with IKK α siRNA failed to inhibit processing of p100 and subsequent accumulation of p52 (another hallmark of LTX-stimulated non-canonical NF- κ B signalling). In Figure 3.11 (C and D), from quantitative immunoblotting and the subsequent quantification there was a concentration-dependent decrease in TNF α -stimulated p65 phosphorylation (Ser536) relative to the agonist-stimulated sample treated with non-targeting siRNA. This was determined to be significant at 100nM ($39.2 \pm 3.3\%$; n=3, p<0.05), 150nM ($55.6 \pm 10.5\%$; n=3, p<0.01) and 200nM ($86.6 \pm 4.3\%$; n=3, p<0.001). This correlated with a significant decrease in total protein expression of IKK β across the concentration range; 50nM ($91.1 \pm 2.4\%$; n=3, p<0.001), 100nM ($95.5 \pm 8.5\%$; n=3, p<0.001), 150nM ($90.0 \pm 5.2\%$; n=3, p<0.001) and 200nM ($86.4 \pm 9.8\%$; n=3, p<0.001). Hence, this indicated that IKK β siRNA can be used to run down total IKK β protein expression and indicative of inhibition of agonist-stimulated canonical NF- κ B signalling. However, IKK β siRNA failed to elicit a reversal of I κ B α degradation. Collectively, these experiments confirmed the ability of IKK α/β siRNA to target the non-canonical and canonical NF- κ B signalling pathways respectively.



(B)



(C)



(D)

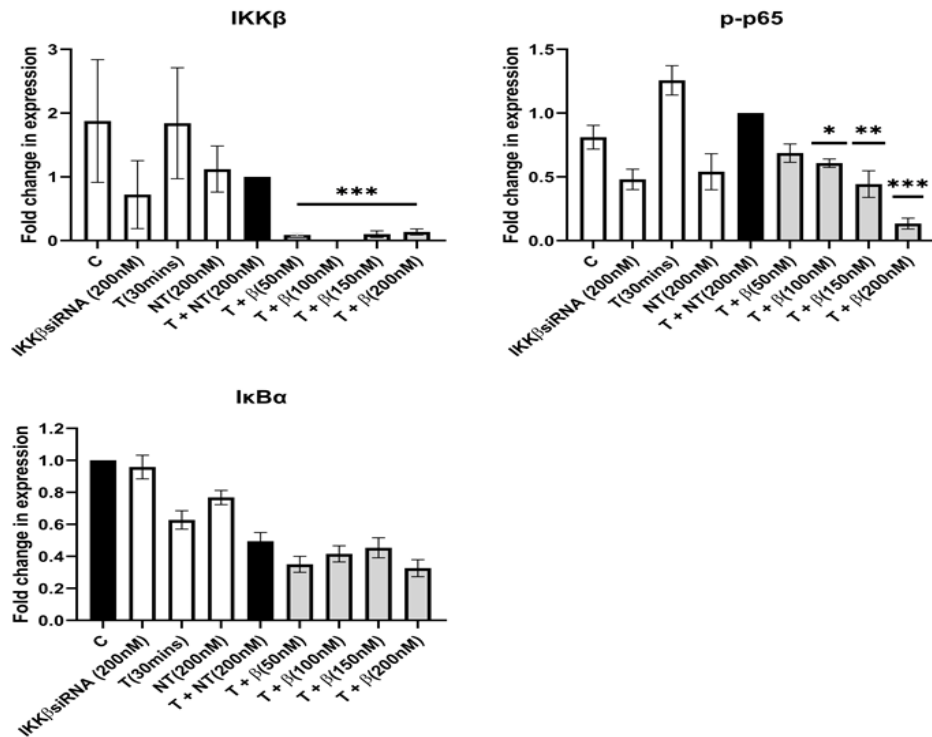


Figure 3.11. Impact of isoform-selective IKK α and IKK β siRNA on non-canonical and canonical NF- κ B markers in PC3 cells.

PC3 cells were grown in 12-well plates and treated with IKK α /IKK β siRNA (50nM, 100nM, 150nM and 200nM) or Non-targeting (NT) siRNA as a control (200nM) and 5 μ l of lipofectamine for transfection overnight before changing to full media for 16 hours. Cells were then serum starved for 24h prior to stimulation. **(A)** - Validation of siRNA IKK α effect on non-canonical NF- κ B signalling. After serum starvation, siRNA IKK α treated cells were treated with Lymphotoxin- β 2 (LTX) (20ng/ml) for 4h (LTX4h) prior to preparation of whole cell lysates for separation using SDS-PAGE and analysis by Western Blotting using the above antibodies (n=3). GAPDH was used as a loading control. **(C)** - Validation of siRNA IKK β effects on canonical NF- κ B signalling. After serum starvation, siRNA IKK β treated cells were exposed to TNF- α (T) (20ng/ml) for 30min (T30min) before preparation of whole cell lysates for separation using SDS-PAGE and analysis by Western Blotting using the above antibodies (n=3). GAPDH was used as a loading control. (B and D) - Data was normalised to the control (C) or stimulated sample treated with NT siRNA (LTX + NT or T + NT (200nM)) and represents mean \pm S.E.M. One-way ANOVA with post-hoc Dunnett's test was used to determine statistical significance ($p < 0.05$) of observed changes in agonist-stimulated non-canonical/canonical NF- κ B activation caused by siRNA IKK α or IKK β respectively, relative to the agonist-stimulated non-targeting control (LTX + NT 200nM / T + NT (200nM) to reverse non-canonical or canonical NF- κ B stimulation. Non-canonical: IKK α : LTX + siRNA IKK α (50 – 200nM) vs LTX + NT (200nM), *** $p < 0.001$. p-p100: LTX + siRNA IKK α (100nM), LTX + siRNA IKK α (150nM) vs LTX + NT (200nM), * $p < 0.05$; LTX + siRNA IKK α (200nM) vs LTX + NT (200nM), ** $p < 0.01$. Canonical: IKK β : T + siRNA IKK β (50 – 200nM) vs T + NT (200nM), *** $p < 0.001$. p-p65: T + siRNA IKK β (100nM) vs T + NT (200nM), * $p < 0.05$; T + siRNA IKK β (150nM) vs T + NT (200nM), ** $p < 0.01$; T + siRNA IKK β (200nM) vs T + NT (200nM), *** $p < 0.001$.

3.3.9. Effects of siRNA run-down of IKKs on AURKA and cell cycle markers status following nocodazole trap and release in PC3 cells.

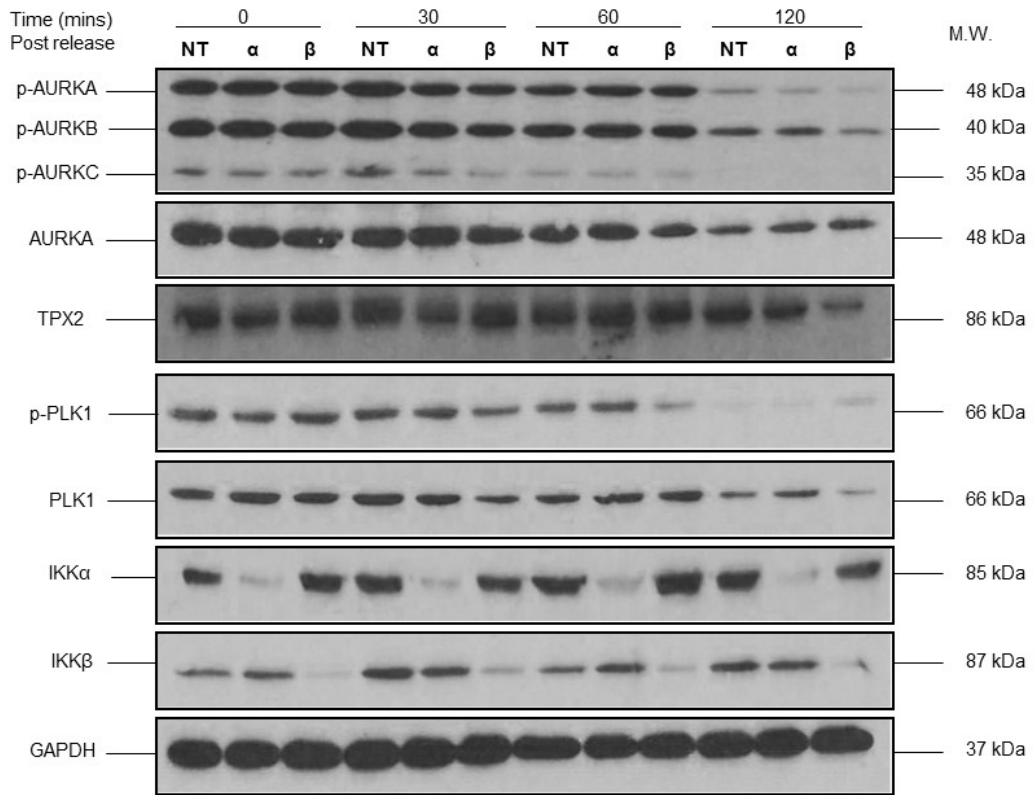
Having confirmed the ability of IKK targeting siRNAs to effectively abrogate IKK isoform expression and aspects of IKK-mediated NF- κ B activation, these siRNAs were then applied in experiments using Nocodazole arrested mitotic PC3 prostate cancer cells. Small-interfering RNA (siRNA) that targeted both IKK α and IKK β were used as a molecular tool to determine the influence of the IKKs on AURKA and the status of cell cycle markers throughout mitosis. By targeting the IKK proteins at the transcriptional level, this helped to determine if IKK protein expression had any role in regulating the status of AURKA and associated proteins TPX2 and PLK1 during mitosis. A scrambled non-targeting (NT) sequence that didn't target any of the IKKs was used as a control. To investigate the effect of the siRNA on AURKA and its markers status after release from nocodazole trap at pro-metaphase, their expression and/or phosphorylation were examined by Western blotting at 30, 60 and 120 minute time points.

Figure 3.12 shows the effect of siRNA on AURKA signalling post trap and release. Cells were initially transfected for the appropriate transfection time period as detailed in Section 2.2.5.3 - with 100nM IKK α siRNA, 100nM IKK β siRNA or a non-targeting scrambled RNA sequence. For this experiment, all cells were transfected with siRNA using 5 μ l of lipofectamine RNAiMAX as a transfection reagent. In Figure 3.12 (A and B), again, over time post release from Nocodazole arrest there was a natural time course of AURK dephosphorylation and AURKA protein degradation apparent in the cells treated with the NT control. For the first three time points of the kinetic analysis (0, 30, 60 min) there was no significant impact of prior siRNA treatment on any of the markers measured. There was also significant decrease in AURKA phosphorylation at the 120 minute time point post-release from nocodazole compared to the vehicle control at 0 min, in all of the treatment groups; for both siRNA IKK α ($75.4 \pm 6.1\%$; n=3, p<0.01) and siRNA IKK β ($84.4 \pm 4.1\%$; n=3, p<0.001) treated cells, this was significantly greater than when cells were treated with the non-targeting control ($50.8 \pm 16.4\%$; n=3, p<0.05). This indicated that the levels of AURKA phosphorylation decreased naturally over time, but was potentially enhanced slightly by treatment with siRNA IKK α/β . However, this was not significantly different from the non-targeting treated control at this time point. A similar profile was observed for phosphorylation of AURKB at the 120 minute time point; siRNA IKK α ($53.9 \pm 4.7\%$; n=3, p<0.001), siRNA IKK β ($67.8\% \pm 8.7\%$; n=3, p<0.001) and non-targeting ($40.1 \pm 4.1\%$; n=3, p<0.05). This was also true for phosphorylation of AURKC at the 120 minute time point; siRNA IKK α ($94.5 \pm 2.7\%$; n=3, p<0.01), siRNA IKK β ($95.8 \pm 1.3\%$; n=3, p<0.01) and non-targeting ($87.3 \pm 7.1\%$; n=3, p<0.01). Also, in Figure 3.12 (A) and (B) the total expression of AURKA was measured to conclude if the reduction in

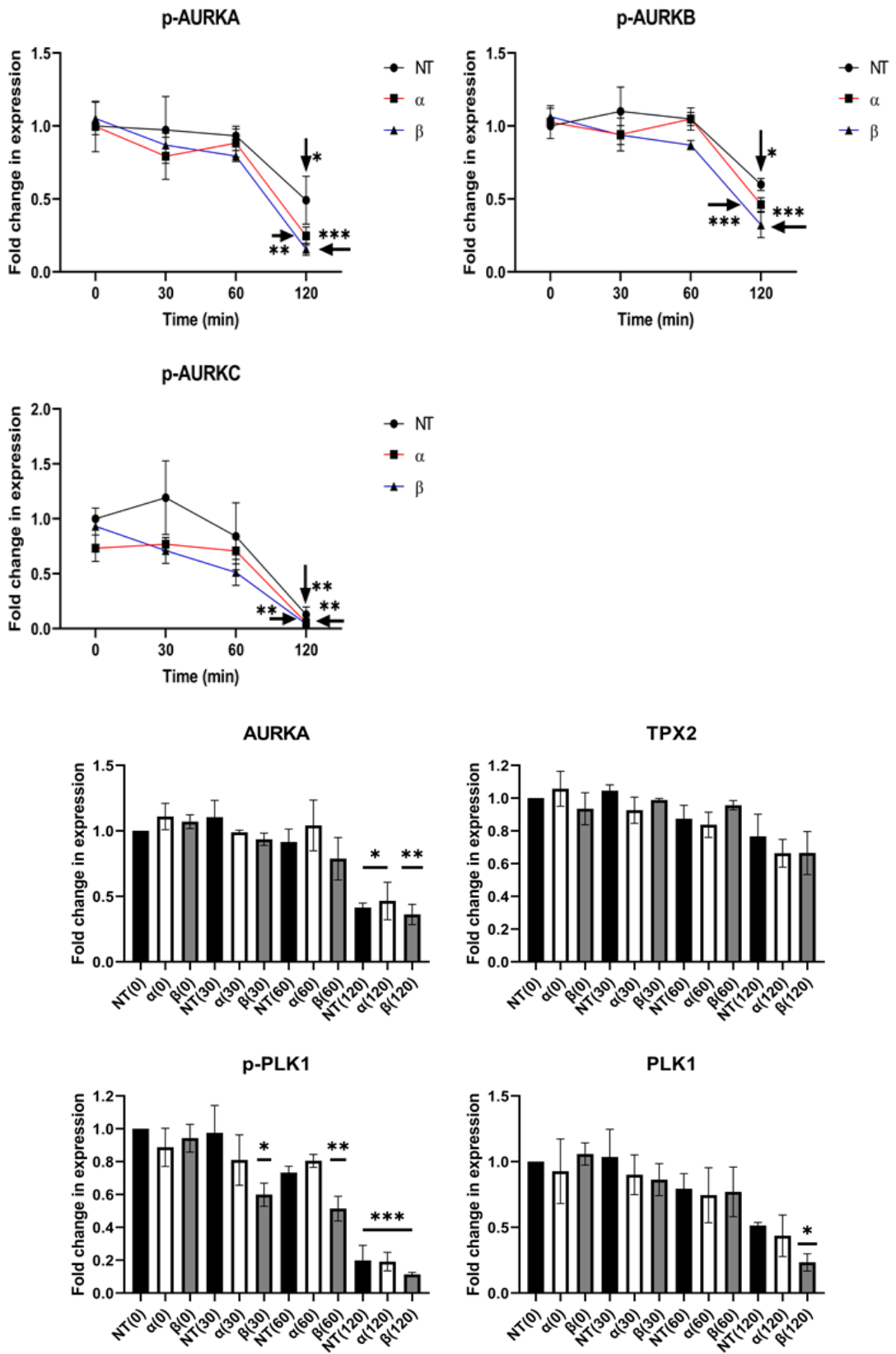
phosphorylation was linked to a comparable loss of AURKA at the protein level or as a result of dephosphorylation following treatment with either siRNA IKK α or IKK β . There was a significant reduction in total AURKA expression in cells treated with siRNA IKK α ($53.5 \pm 14.3\%$; $n=3$, $p<0.05$), siRNA IKK β ($63.8 \pm 7.7\%$; $n=3$, $p<0.01$) and NT siRNA ($58.5 \pm 3.4\%$; $n=3$, $p<0.05$) at the 120 minute time point. This suggested that AURKA phosphorylation correlates with the expression and as it decreased over time was substantially affected by siRNA rundown. Over the time course carried out, the levels of total AURKA and phosphorylation were both reduced in the non-targeting control and the siRNA treated cells which suggested that the levels of AURKA and its phosphorylation reduced naturally over time. In Figure 3.12, from quantitative immunoblotting (A) and the resultant quantification, the expression of the critical AURKA co-activator TPX2 was also measured. The expression of TPX2 was not significantly ($p>0.05$) decreased by any of the treatment groups compared to control NT treatments at each time point and its expression decreased naturally with time as the cells moved through mitosis. In Figure 3.12 (B) there was a significant reduction in phosphorylation of PLK1, most notably in cells treated with siRNA IKK β vs control NT cells. At 30 min the phosphorylation of PLK was reduced in siRNA IKK β treated cells by ($40.1 \pm 7.1\%$; $n=3$, $p<0.05$) and 60 min ($48.5 \pm 7.5\%$; $n=3$, $p<0.01$) however not significantly different for the control NT treated cells. At 120 minute after release from Nocodazole arrest the reduction in PLK1 phosphorylation was also present and statistically reduced ($p<0.01$) in the non-targeting control, siRNA IKK α and siRNA IKK β treated cells. The reduction in phosphorylation of PLK1 in these samples was ($80.1 \pm 9.1\%$; $n=3$, $p<0.001$) for the non-targeting control, ($80.8 \pm 5.6\%$; $n=3$, $p<0.001$) for siRNA IKK α treated cells and ($88.6 \pm 1.3\%$; $n=3$, $p<0.001$) for siRNA IKK β treated cells respectively. Crucially, there was no significant difference between all these treatment groups at these time points. Phosphorylation of PLK1 was reduced naturally as time progressed, especially at the 120-minute time-point but this seemed to be increased particularly in siRNA IKK β treated cells at the earlier time points. Total PLK1 expression was assessed next to see if it correlated with the loss of phosphorylation. Figure 3.12 (A) and (B) shows there was a significant loss of total PLK expression in siRNA IKK β treated cells at the 120-minute time point ($76.6 \pm 6.5\%$; $n=3$, $p<0.05$) but no significant difference when compared to the non-targeting treated control at this time point. Lastly, the expression of IKK α and IKK β was measured to check for rundown of the total protein expression. There was an average decrease in expression of 60% and 77% for IKK α and IKK β respectively, which was induced by the siRNA targeting each subtype. This difference in expression levels compared to the previous section could be because cells were serum starved in that experiment and hence more sensitive to downregulation and even cell death which may contribute to the decrease in expression in that setting. As there was no difference between the non-targeting treated

samples at each time point compared to that for the cells treated with siRNA IKK α or siRNA IKK β at each time point, this suggested that downregulation of IKK α/β protein expression and associated activity had no bearing on the expression and/or phosphorylation of AURKs, TPX2 and PLK1. These decreased naturally over time and this decrease was not significantly ($p>0.05$) accelerated as a result of treatment with the IKK α - or IKK β -targeting siRNA. Although, the phosphorylation and total expression of PLK1 was significantly decreased by siRNA IKK β , a study by Higashimoto et al. (2008) indicated that PLK is involved in regulation of the IKK complex through phosphorylation of IKK β . Thus, further experiments are needed to investigate this. Following on from this section, the established siRNA conditions were harnessed and utilised/adapted to enable experiments treating cells with NBD CPPs with a background of reduced /depleted cellular IKK expression.

(A)



(B)



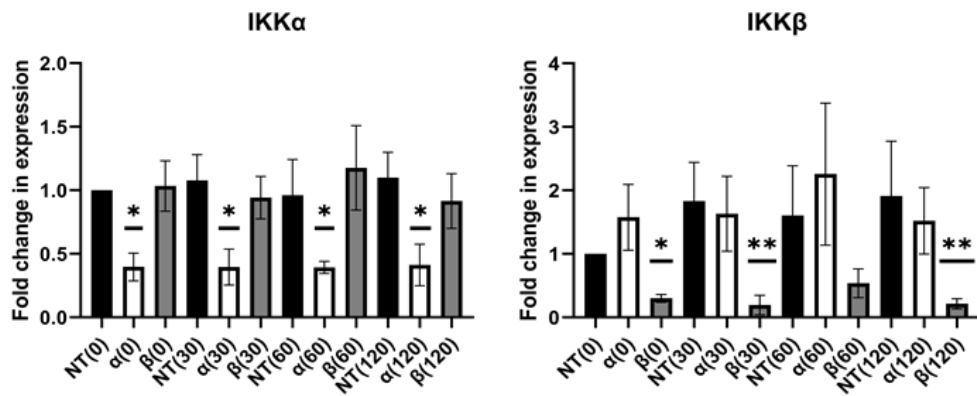


Figure 3.12. Impact of isoform-selective siRNA targeting of IKKs on AURKs and related protein markers of mitosis and IKK proteins in PC3 cells.

PC3 cells were grown on 10mm dishes and treated with IKKα/IKKβ siRNA (100nM) or Non-targeting (NT) siRNA as a control (100nM) and transfected with 5μl of lipofectamine for 16 hours before addition of fresh full RPMI 1640 media for a further 12-16 hours prior to treatment with 50ng/ml Nocodazole (16-20 hours) and subsequent release from trap at 30min, 60min and 120min. (A) Whole cell lysates were prepared for separation using SDS-PAGE and analysed by Western Blotting using the above antibodies (n=3). GAPDH was used as a loading control. (B) Data was normalised to the control (NT0) and represents mean ± S.E.M. One-way ANOVA with post-hoc Dunnett's test was used to determine statistical significance ($p < 0.05$) of observed changes relative to Non-targeting control (NT0) at 0 min. (*= $p < 0.05$, **= $p < 0.01$, ***= $p < 0.001$). p-AURKA: NT(120) vs NT(0), * $p < 0.05$; α(120) vs NT(0), ** $p < 0.01$; β(120) vs NT(0), *** $p < 0.001$. p-AURKB NT(120) vs NT(0), * $p < 0.05$; α(120) vs NT(0), *** $p < 0.001$; β(120) vs NT(0), *** $p < 0.001$. p-AURKC: NT(120) vs NT(0), ** $p < 0.01$; α(120) vs NT(0), ** $p < 0.01$; β(120) vs NT(0), ** $p < 0.01$. For changes relative to non-targeting control at each time point vs siRNA IKKα or IKKβ at the relevant time point, one-way ANOVA with post-hoc Dunnett's test was used to determine statistical significance ($p < 0.05$) of observed changes relative to the non-targeting control at the appropriate time point.

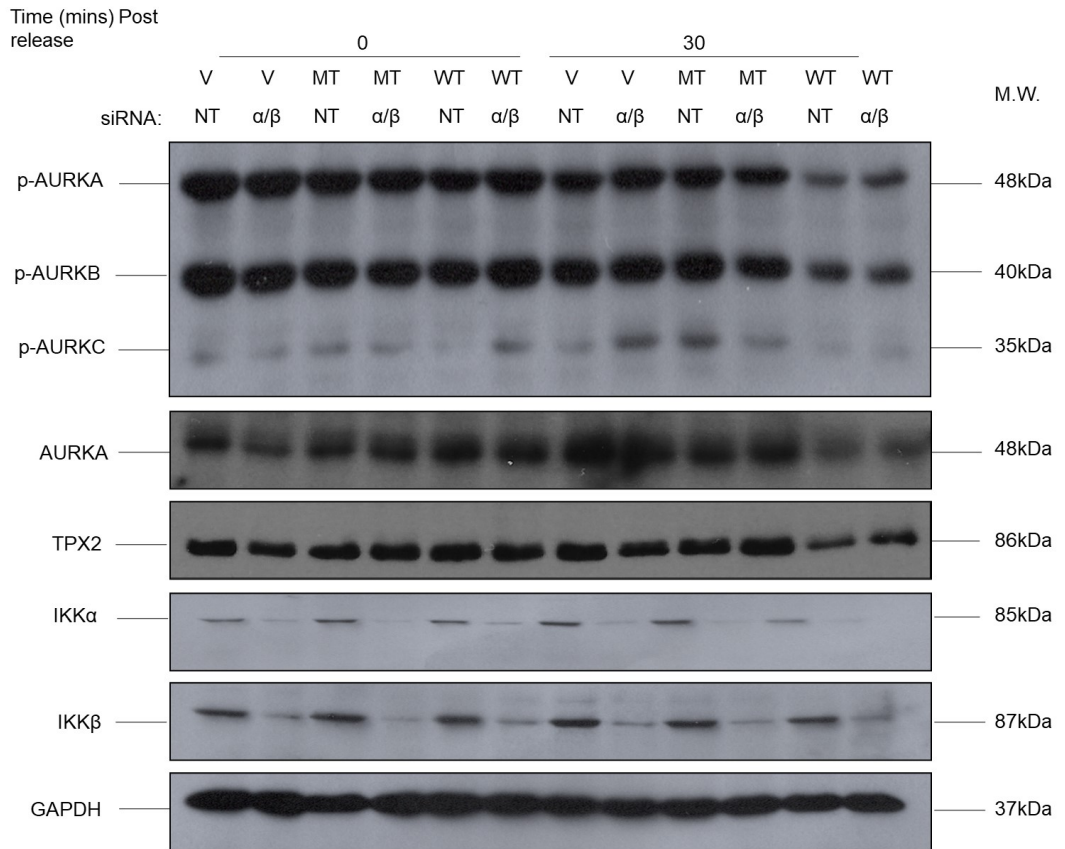
3.3.10. Effects of NBD CPPs in the absence and presence of siRNA IKKs on the status of AURKA and cell cycle markers in synchronised PC3 cells.

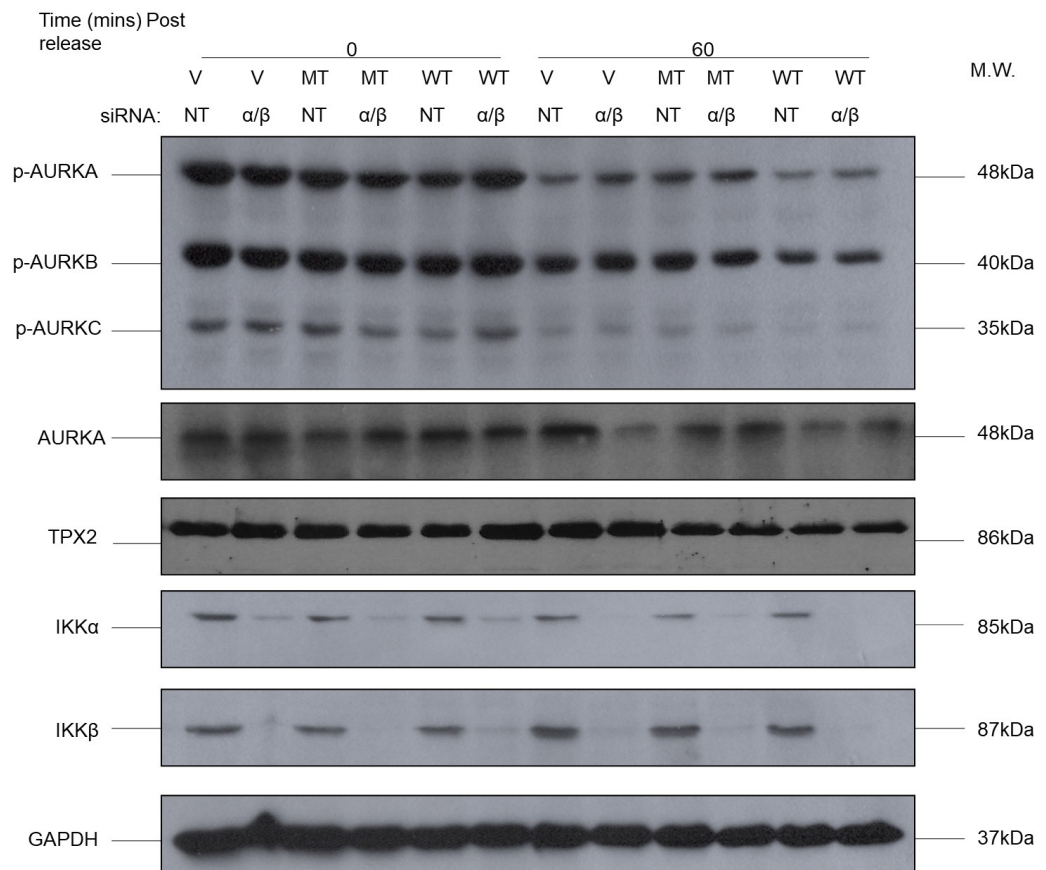
Following on from the confirmation that single-targeting of IKKα or IKKβ could effectively run-down each IKK isoform in terms of protein expression as well as abrogating the signalling of the IKK-mediated NF-κB pathways, dual-targeting of IKKα and IKKβ simultaneously with siRNA run-down was utilised to create a molecularly induced "null IKK" background (with no catalytic IKK proteins present) to then incorporate the NBD CPPs into experiments and test their potential effects on the IKK-AURKA dynamics. A scrambled sequence that didn't target either of the IKKs was used as a control, again a non-targeting (NT) sequence. Cells were again treated and released from a nocodazole-mediated arrest/trap at pro-metaphase and

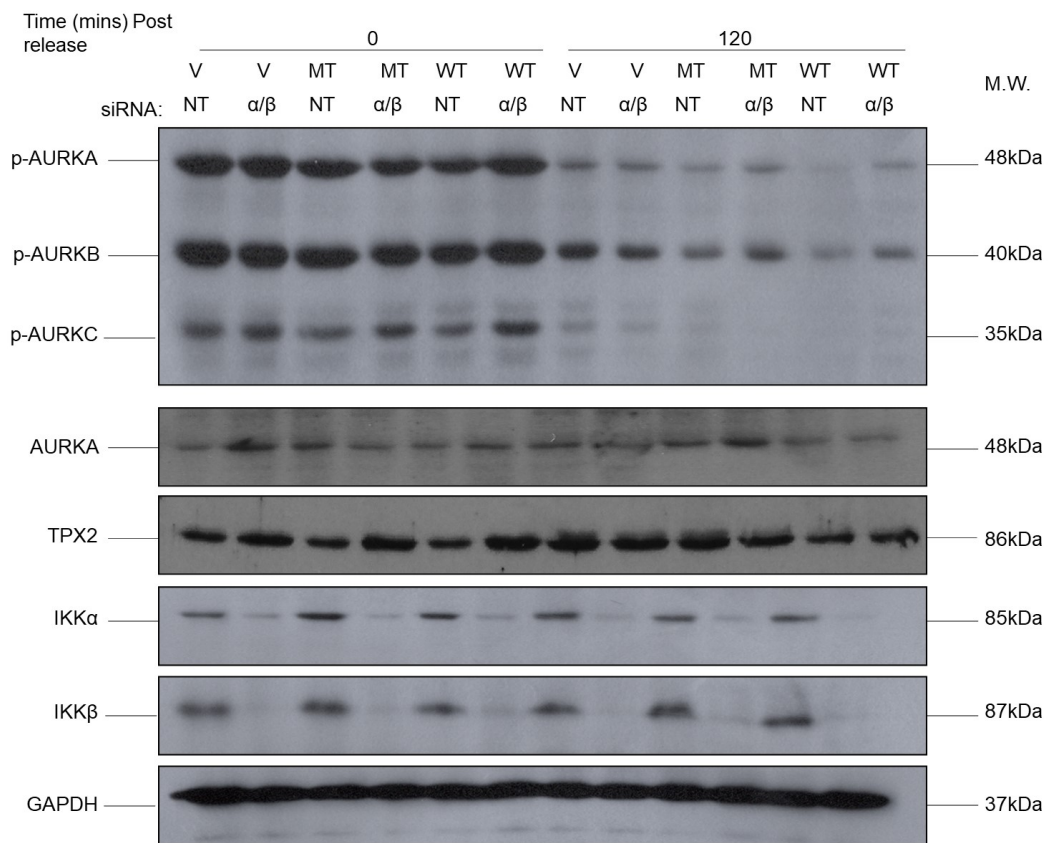
then treated with the NBD CPPs after release from nocodazole trap at 30, 60 and 120 minute time points. Expression and/or phosphorylation of AURKs, TPX2 and PLK1 were again examined by Western blotting at 30, 60 and 120 minute time points post-release from nocodazole-mediated arrest.

Figure 3.13 shows the effect of the NBD CPPs in the absence and presence of siRNA targeted run-down of IKKs on AURKA signalling post-trap and release from nocodazole (n=2). Cells were transfected for the appropriate transfection time period as detailed in Section 2.2.5.3 with 50nM IKK α siRNA and 50nM IKK β siRNA at the same time or a non-targeting (NT) scrambled RNA sequence (100nM). IKK α and IKK β siRNA were transfected with 2.5 μ l of lipofectamine RNAiMAX each (5 μ l total) and as such NT siRNA was transfected with 5 μ l lipofectamine RNAiMAX to parallel this. The expression of IKK α and IKK β was measured in order to check for run-down of the total protein. There was an average decrease in expression of 87% and 82% for IKK α and IKK β respectively taken across all time points, which was induced by the siRNA targeting each subtype. As can be observed from the quantitative immunoblotting (A) and parallel quantification (B), there was a noticeable accelerated decrease in phosphorylation of the three AURK subtypes, total expression of AURKA and the critical AURKA co-activator TPX2 in the samples treated with the NBD WT CPP in comparison to the vehicle and NBD MT CPP treated samples, across all time points. TPX2 showed a reduction in expression at 30 min in the DMSO treated NT siRNA ($83.5 \pm 13.4\%$ vs $61.8 \pm 11.4\%$) and IKK α/β ($67.8 \pm 10.0\%$ vs $59.8 \pm 5.9\%$) samples versus the same siRNA samples treated with the NBD WT CPP at this time point. TPX2 also showed a reduction in expression at 120 min in the DMSO treated NT siRNA ($67.0 \pm 15.9\%$ vs $24.1 \pm 10.8\%$) and IKK α/β ($62.1 \pm 15.7\%$ vs $31.3 \pm 2.3\%$) samples versus the same siRNA samples treated with the NBD WT CPP at this time point. Also, to be noted was the fact that there was no noticeable difference in expression of these proteins between the sample treated with the NT siRNA and the NBD WT CPP in combination compared to the siRNA IKK α and IKK β with the NBD WT CPP. This suggests that the IKK proteins aren't involved in the effect that the NBD WT CPP is exerting on AURKA total expression and phosphorylation and expression of TPX2. These experiments suggest that the NBD WT CPP can exert its effect on AURKA/TPX2 signalling when both IKK α and IKK β have been downregulated. Following on from this, the demonstration of the effects NBD WT CPP in a cellular model deficient of the IKK proteins (i.e. a genetic 'knockout' model) could potentially confirm that the NBD WT peptide could directly impact IKK/AURKA/TPX2 signalling independent of the classical IKK isoforms.

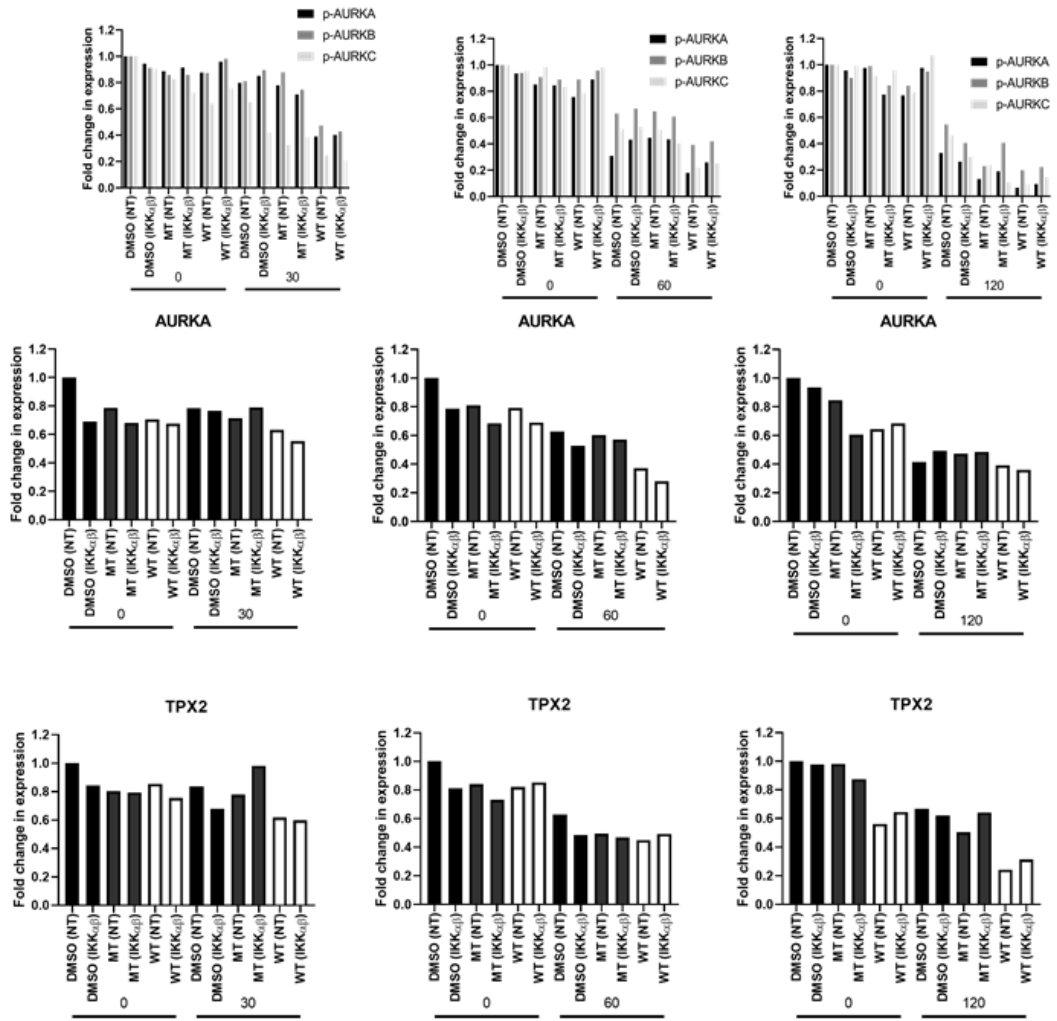
(A)







(B)



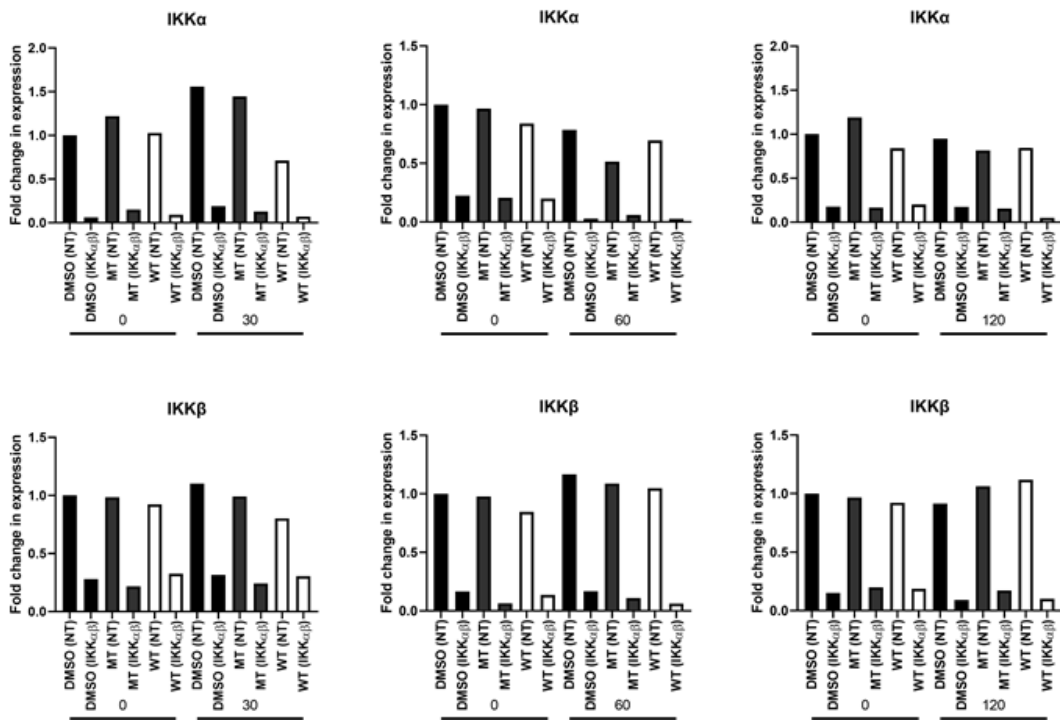


Figure 3.13. Impact of siRNA targeting IKKs and NBD CPPs alone or in combination on AURKs and related markers in synchronised PC3 cells.

PC3 cells were grown on 10mm dishes and treated with IKK α (50nM) and IKK β siRNA (50nM) simultaneously (total 100nM) or Non-targeting (NT) siRNA as a control (100nM) and 5 μ l total volume of lipofectamine for 16h and grown in fresh full media for a further 12-16h prior to treatment with 50ng/ml Nocodazole (16-20h). This was followed by treatment with either NBD WT or MT (100 μ M) or DMSO as a vehicle control (0.5% (v/v)) upon release from trap and incubated for 30min, 60min and 120min. **(A)** Whole cell lysates were prepared for separation using SDS-PAGE and analysed by Western Blotting using the above antibodies (n=2). GAPDH was used as a loading control. **(B)** Data was normalised to the vehicle treated NT siRNA sample (DMSO (NT)) at 0 min.

3.4. Examining the status of AURKs and related markers in MEF cells through mitosis.

3.4.1. Assessment of the status of AURKA and cell cycle components following Nocodazole mediated cell cycle arrest/trap and release in Double-knockout (DKO) MEF cells.

Having demonstrated in the previous experiments that the NBD WT CPP can continue to exert its effect on AURKA/TPX2 signalling in a background where the expression of IKK α and IKK β had been knocked down, *ikka*^{-/-}/*ikkb*^{-/-} double Knockout (DKO) Mouse Embryonic fibroblast (MEF) cell line with both catalytic IKK proteins (IKK α and IKK β) absent were used to represent a null background of IKK proteins in which to test the NBD WT CPP and see if it had a similar effect to that shown in the PC3 cell line. This was viewed as model system to aid determining whether the mechanistic effect of the peptide on AURKA and related markers was IKK-independent, given IKK α and IKK β are absent from this cell line.

To establish optimal conditions for cell synchronisation in DKO MEFs, cells were treated with various concentrations of nocodazole for 16-20 hours and examined for phosphorylation of AURKA, AURKB and AURKC in synchronised vs non-synchronised cells via immunoblotting (data not shown). Following on from this an optimal treatment concentration was determined as 100ng/ml and in preparation for experiments cells were treated routinely for 16-20 hours to establish cell cycle arrest or 'trap'. In Figure 3.14 (A) immunoblotting was used to assess the cell cycle status of total AURKA and its phosphorylation, as well as the outcome of important cell cycle markers (TPX2, p-PLK1, PLK1) in relation to AURKA following nocodazole trap and release at the appropriate time points (up to 6 hours). These markers were subsequently quantified (B). DKO MEF cells were treated for 16-20 hours with nocodazole (100ng/ml). The phosphorylation of the AURKs (A, B and C) were expressed at an elevated and maximum level at the 0 hour time point (TR₀), which compared consistently with the positive control (TR_{NR}) in which the cells had been trapped with nocodazole and not released while incubated for 6 hours.

In Figure 3.14 (A) and (B) there was a significant ($p < 0.05$) decrease in phosphorylation of AURKA (T288) following release at 1h ($47.4 \pm 17.3\%$; $n=3$, $p < 0.05$), 2h ($55.4 \pm 6.6\%$; $n=3$, $p < 0.05$), 4h ($73.5 \pm 9.0\%$; $n=3$, $p < 0.01$) and 6h ($78.5 \pm 3.3\%$; $n=3$, $p < 0.001$) respectively, in comparison to the samples from synchronised cells at the 0 time point (TR₀). On the other hand, the phosphorylation of AURKB (T232) was more highly expressed in terms of phosphorylation than AURKA in DKO MEF cells and the phosphorylation remained elevated for a longer period within the time-frame examined. The phosphorylation of AURKB wasn't significantly reduced until the 6h time point ($57.5 \pm 6.5\%$; $n=3$, $p < 0.05$). The phosphorylation

of AURKC (T198) was also measured but was expressed at such low levels that analysis gave no significant difference across the sample set ($p > 0.05$).

The total expression of AURKA was also analysed and was shown to be significantly reduced compared to basal levels after 1h post-release from nocodazole synchronisation ($57.1 \pm 13.5\%$; $n=3$, $p < 0.01$) and this remained at a constant level at 2h ($49.1 \pm 7.7\%$; $n=3$, $p < 0.01$), 4h ($47.8 \pm 11.8\%$; $n=3$, $p < 0.05$) and 6h ($57.8 \pm 3.9\%$; $n=3$, $p < 0.01$) respectively. As the cells were released and progressed through mitosis, AURKA expression and phosphorylation (T288) were reduced to basal levels after the 2 h time point as compared to the negative controls (NT₀ and NT₆) – which were cells which were not trapped with nocodazole at 0 and 6h time points. By the quantification indicated in Figure 3.14 (B), the detected phosphorylation of AURKA decreased faster kinetically than the total AURKA protein expression which remained at a constant level for longer. This was perhaps not unexpected given the phosphorylation of the protein, an indicator of catalytic activity, would firstly need to be ‘switched off’ prior to degradation of the protein. Phosphorylation of AURKB (T232) declined significantly after 6h and this may have reflected the role of AURKB as being later in the cell cycle and into cytokinesis compared to AURKA. As was the case in PC3 cells, total expression of AURKB and AURKC weren’t measured in this study due to time constraints. Understanding the relationship between phosphorylation and total protein expression for each of these isoforms would require further work.

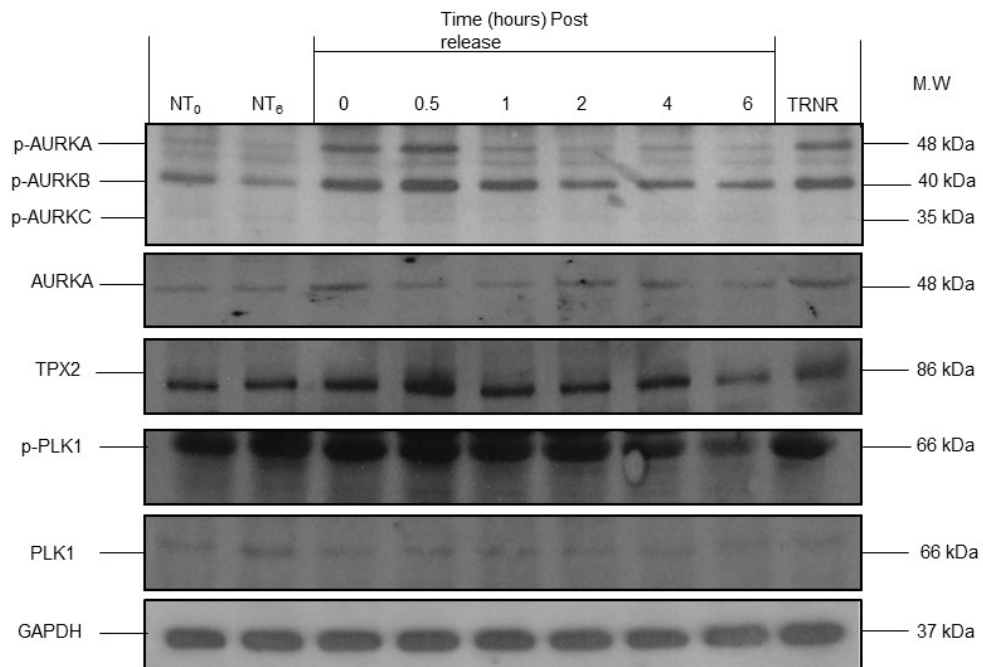
As before, the expression pattern of the crucial AURKA co-activator TPX2 was also measured. This followed a different pattern to AURKA in which the expression of TPX2 remained elevated for longer and wasn’t significantly reduced until the 6h time point ($60.5 \pm 9.4\%$; $n=3$, $p < 0.05$) post release from the nocodazole-mediated trap, compared to the TR0 sample. Again, as expression of TPX2 remained higher for longer than AURKA, this could suggest that TPX2 could be dissociated from AURKA but not necessarily degraded in the cell. Finally, the phosphorylation and total expression of the key mitotic marker PLK1 was also measured. PLK1 was also shown to not be significantly reduced until 6 hours following release from nocodazole trap, both in terms of phosphorylation ($59.5 \pm 14.8\%$; $n=3$, $p < 0.05$) and total expression ($47.2 \pm 21.4\%$; $n=3$, $p < 0.05$), relative to the TR0 sample. The elevated levels of TPX2 and PLK1 (total and phosphorylation) up to 6 hours post-release from nocodazole synchronisation could suggest a different role for these protein in this cell type versus the prostate cancer cell line.

In Figure 3.14 (C) deletion of IKKs in MEF cells were assessed using quantitative immunoblotting to validate that they were indeed ‘Knock-out’ models and did not express the catalytic IKK proteins. The models used were as follows; wild-type MEFs (WT MEFs) – IKK α and IKK β present, IKK α knockout (*ikka*^{-/-}) MEFs – IKK α absent and IKK β present, IKK β

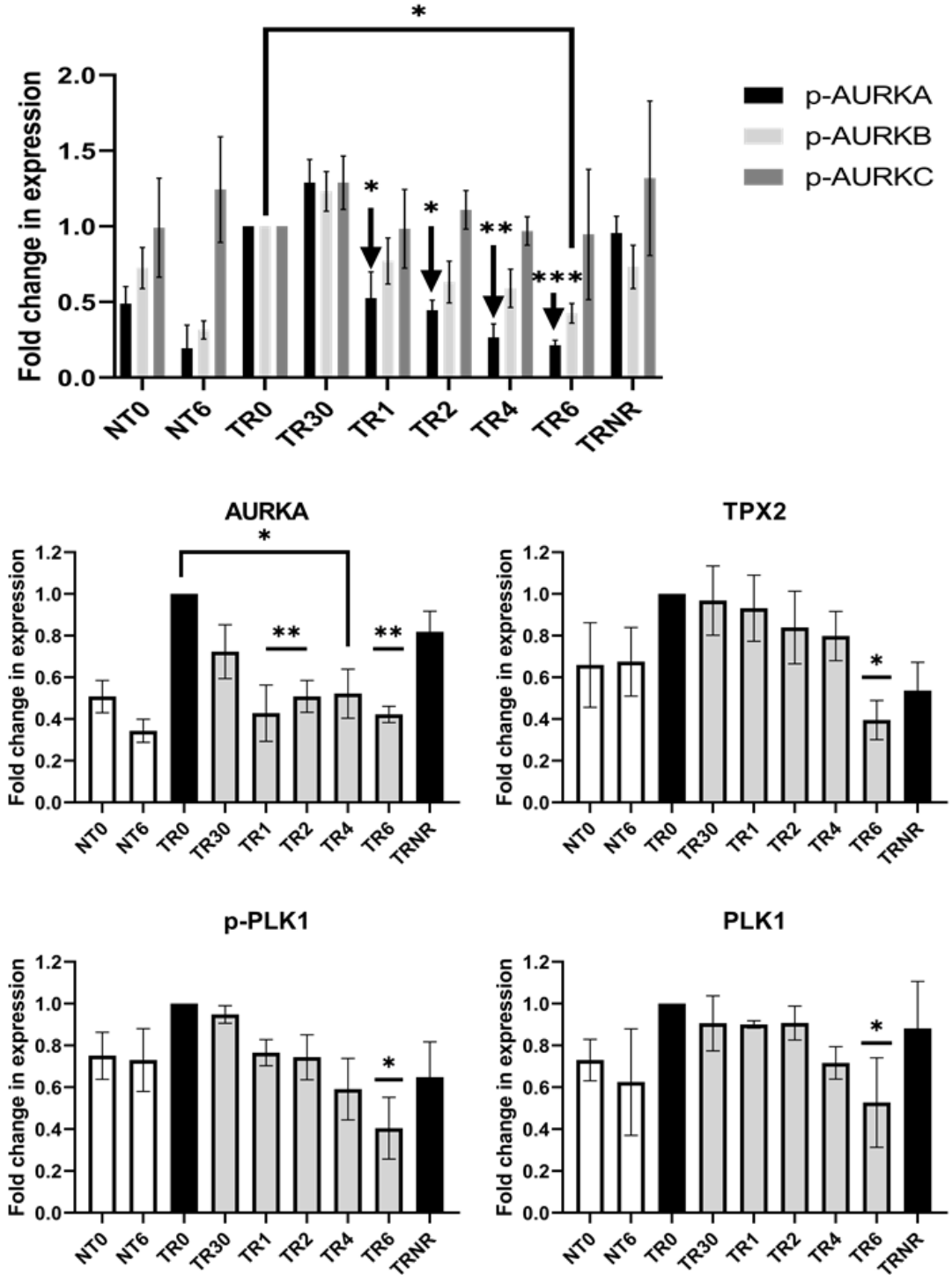
knockout (*ikkb^{-/-}*) MEFs – IKK α present and IKK β absent and double knockout (DKO) MEFs – IKK α and IKK β absent (*ikka^{-/-}ikkb^{-/-}*). In Figure 3.14 (D) there was a reduction in IKK α expression in both IKK α ^{-/-} MEFs and DKO MEFs in comparison to the WT MEFs model. In Figure 3.14 (D) there was also a reduction in IKK β expression in both *ikkb^{-/-}* MEFs and DKO MEFs compared to the WT MEFs model. There was also a decrease in IKK β expression present in the IKK α ^{-/-} MEF sample. This may just be that expression of IKK β was lower in *ikka^{-/-}* MEFs compared to the WT MEFs. Any low level of expression observed for IKK protein in their relevant knockout MEF models, reflected background readings within the densitometric quantification process.

Collectively, these experimental outcomes demonstrated that nocodazole treatment of DKO MEF cells resulted in the arrest of cells and a similar pattern in expression of mitotic markers to that observed previously in PC3 cells (Section 3.2.1). This could be used in future experimental work when assessing cellular interventions examining the potential effects of the NBD WT CPP on IKK-AURKA signalling following nocodazole trap and release of the DKO MEFs, as a ‘null IKK’ cellular model.

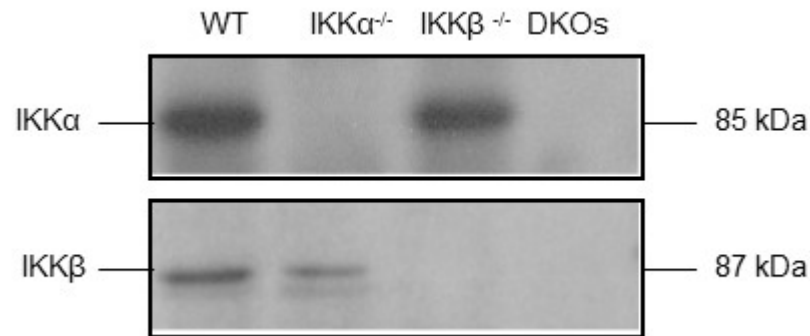
(A)



(B)



(C)



(D)

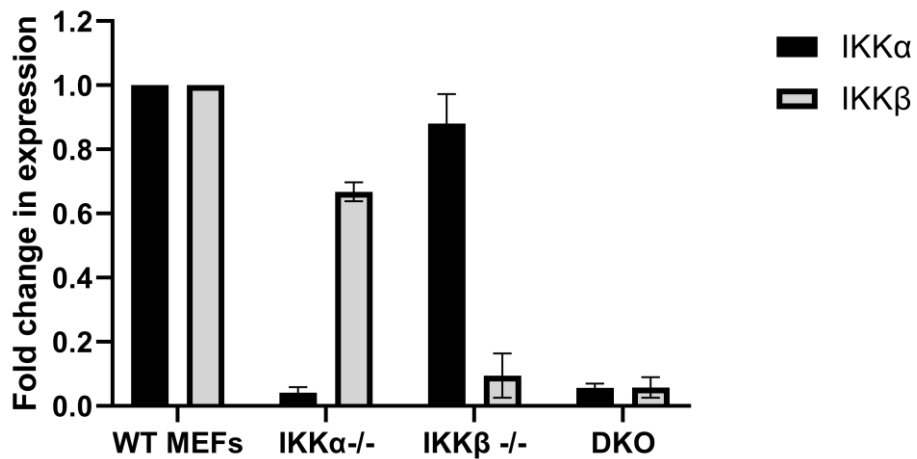


Figure 3.14. Effect of Nocodazole trap and release on AURKs and related protein markers of mitosis in DKO MEFs.

DKO MEFs were grown on 10mm dishes and treated with 100ng/ml Nocodazole (16-20 hours) and these were then released by washing twice with fresh media, times indicated as hours post-release from Nocodazole trap. Non-trapped cells at 0 and 6h (NT0 and NT6) represent the negative control. Cells treated with Nocodazole and then not washed and released represented the positive control (Trap and non-released, TRNR). (A) Whole cell lysates were prepared for separation using SDS-PAGE and analysis by Western Blotting using the above antibodies (n=3). GAPDH was used as a loading control. (B) Data was normalised to synchronised sample before release at the zero time-point (TR0) and represents mean \pm S.E.M. One-way ANOVA with post-hoc Dunnett's test was used to determine statistical significance ($p < 0.05$) of observed changes relative to TR0 synchronised sample at 0 min. (*= $p < 0.05$, **= $p < 0.01$, ***= $p < 0.001$). All results indicated on graphs represent fold change in expression post-release from mitotic arrest compared to the TR0 sample. (C) Whole cell extracts of cultured MEFs with varying genetic backgrounds were prepared and the presence/absence of IKK α and IKK β determined by Western Blotting using the antibodies indicated. WT = WT MEFs, *ikka*^{-/-} = IKK α Knockout, *ikkb*^{-/-} = IKK β knockout, DKOs = double knockout. (D) Data was normalised to the WT MEFs sample and represents mean \pm S.E.M (n=3).

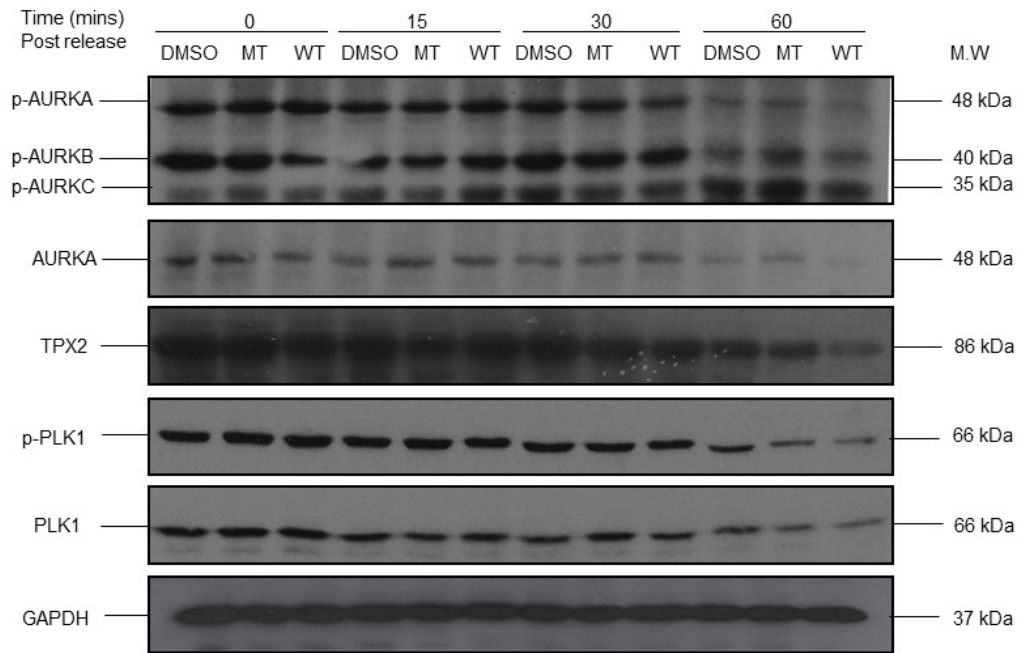
3.4.2. Effects of NBD WT CPP on the status of AURKA and cell cycle markers following nocodazole trap and release in DKO MEF cells.

Following on from and related to experiments in Section 3.3.10, the next stage of investigation was to test whether the NBD WT CPP was able to modulate the status of AURKs, AURKA and the associated mitotic markers described previously in a cellular double knockout model of the catalytic IKK proteins. Therefore, the effect of the NBD WT CPP on AURKA and related protein markers after release from nocodazole arrest at pro-metaphase in DKO MEF cells were investigated. Cells were treated with nocodazole (100ng/mL) for 16-20 hours prior to being washed and released as described previously – Section 2.2.2.1, before NBD MT or NBD WT CPPs (100µM) were added upon release as described previously and samples prepared thereafter at appropriate time points.

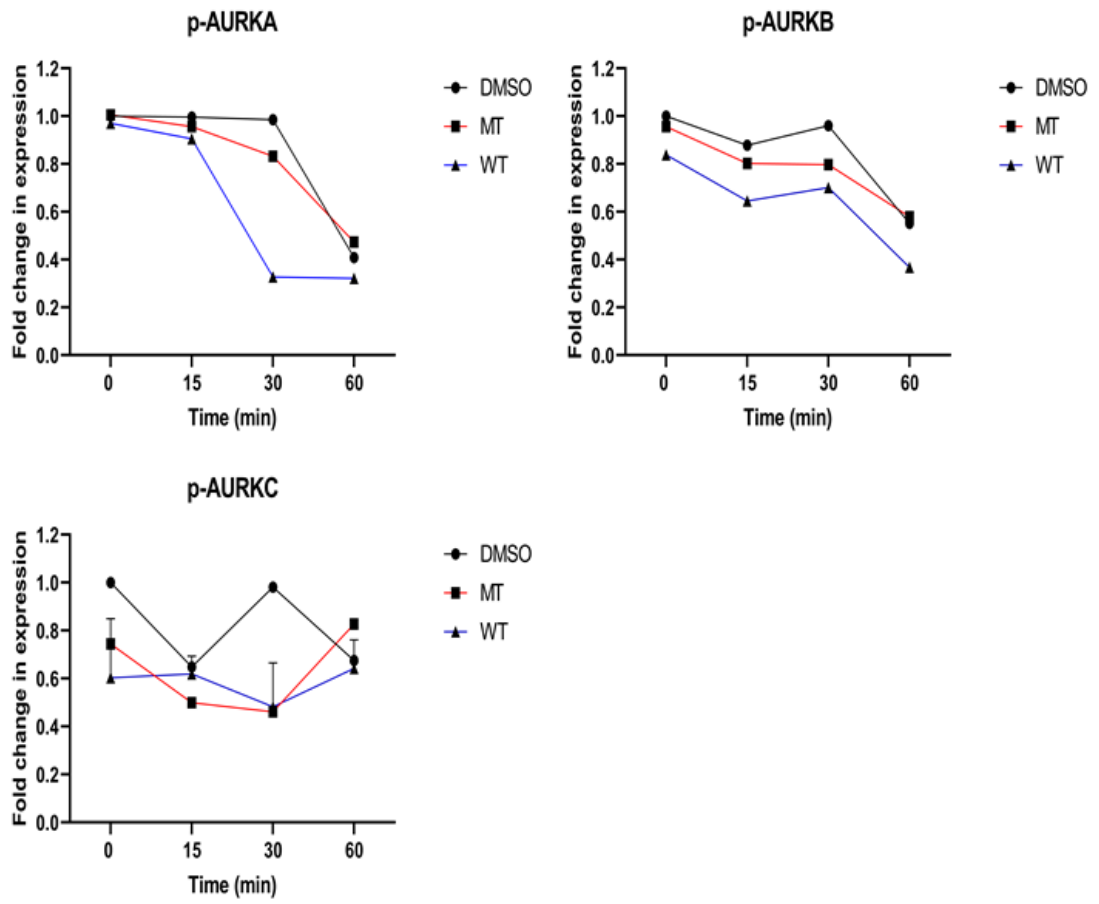
Figure 3.15 (A) showed by immunoblotting, the effect of MT and WT NBD CPP on the status of p-AURKs, AURKA, TPX2 and p-PLK1/PLK1 post-trap and release in DKO MEF cells lacking the catalytic IKK proteins (n=2). In Figure 3.15, the immunoblotting (A) and associated quantification (B) indicated that the NBD WT CPP kinetically accelerated the natural decrease in phosphorylation of AURKA and AURKB as well as total expression of AURKA and these were particularly reduced at the 60 minutes post-release, compared to the vehicle treated control at this time point. As mentioned in the previous Section (3.4.2), the levels of AURKC phosphorylation were low and hence resulted in immeasurable changes in expression levels across the different sample sets. This pattern was also observed in the expression of TPX2, where there was a noticeable decrease in expression after 60 min in the sample treated with the NBD WT CPP compared to the MT and DMSO treated sample at this time point. Also, it was observed that there was no noticeable effect of the NBD WT CPP on total expression and phosphorylation of PLK1 across the time course. That said, it is important to note that the results here were collated from only two experimental repeats (n = 2) and as such further replications will be needed to determine if the results were statistically significant or not.

In summary, the NBD WT CPP demonstrated the ability to inhibit the AURKs and TPX2 signalling even in the absence of the IKK proteins, but further experimental repeats are needed to determine if this is statistically significant and further investigation is needed to determine mechanistically whether this is a direct impact of the peptide on AURKs and TPX2 which causes these proteins to be dephosphorylated and/or degraded.

(A)



(B)



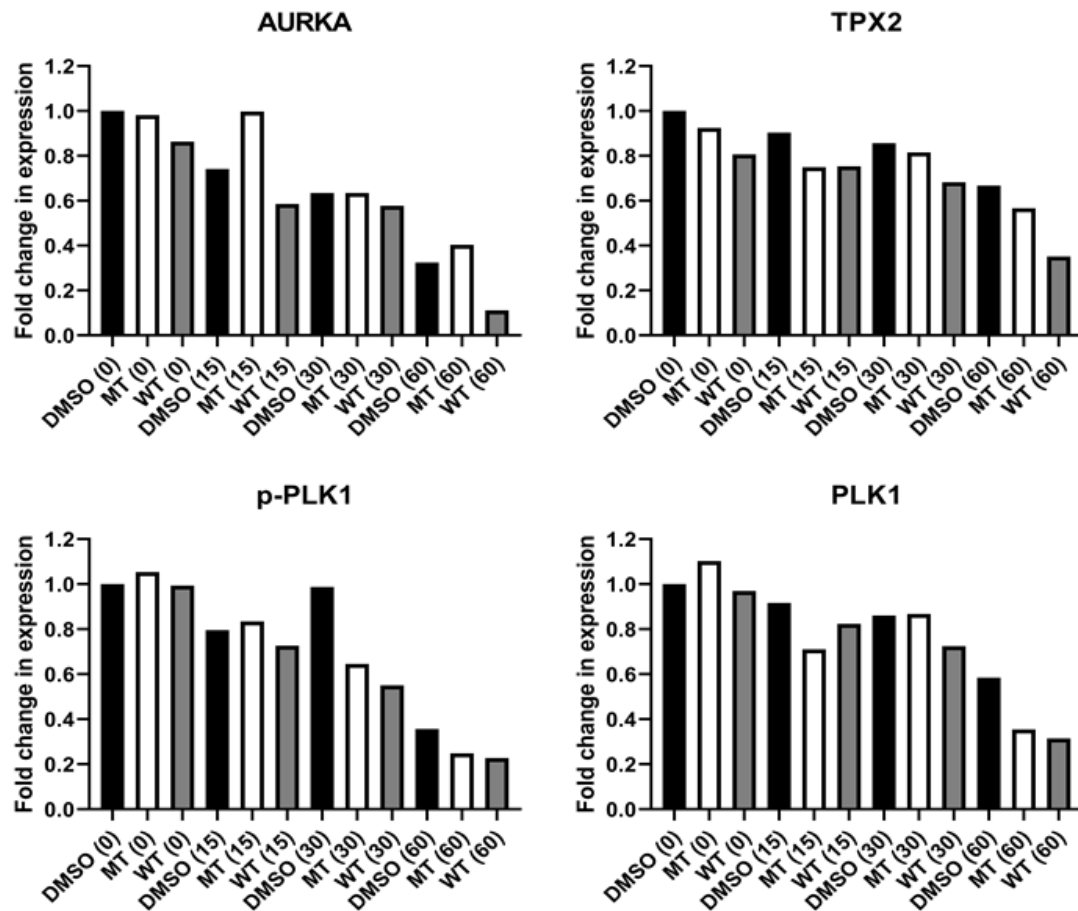


Figure 3.15. Impact of NBD CPPs on AURKs and related protein markers of mitosis in DKO MEF cells.

DKO MEF cells were grown on 10mm dishes and treated with 100ng/ml nocodazole (16-20 hours) prior to treatment with either NBD WT or MT (100 μ M) or DMSO as a vehicle control (0.5% (v/v)) upon release from trap at 15min, 30min and 60min. **(A)** Whole cell lysates were prepared for separation using SDS-PAGE and analysed by Western Blotting using the above antibodies (n=2). GAPDH was used as a loading control. **(B)** Data was normalised to the vehicle treated control (DMSO 0).

3.4.3. Assessment of the status of AURKA and cell cycle components following Nocodazole mediated cell cycle arrest/trap and release in Wild-type (WT) MEF cells.

Having previously demonstrated the successful nocodazole-mediated arrest of the DKO MEF cellular model, a parallel approach was established in Wild-type (WT) MEFs which expressed IKK α and IKK β . This enabled analysis in a normal MEF genetic background and served as a relevant comparator for the previously examined DKO MEFs i.e. was the effect of the NBD WT CPP the same, similar or different in these cells?

To establish optimal conditions for cell synchronisation in WT MEFs, cells were treated with various concentrations of Nocodazole for 16-20 hours and examined for phosphorylation of AURKA, AURKB and AURKC in synchronised vs non-synchronised cells via immunoblotting (data not shown). Following on from this an optimal treatment concentration was determined as 100ng/ml and in preparation for experiments cells were treated routinely for 16-20 hours to establish cell cycle arrest or 'trap'. In Figure 3.16 (A) immunoblotting was used in order to assess the cell cycle status of total AURKA and its phosphorylation, as well as the outcome of important cell cycle markers (TPX2, p-PLK1, PLK1) in relation to following nocodazole trap and release at the appropriate time points (up to 6 hours) and these markers were subsequently quantified (B). WT MEF cells were treated for 16-20 hours with Nocodazole (100ng/ml). The phosphorylation of the AURKs (A, B and C) were expressed at an elevated and maximum level at the 0 hour time point (TR0), which compared consistently with the positive control (TRNR) in which the cells had been trapped with nocodazole and not released while incubated for 6 hours.

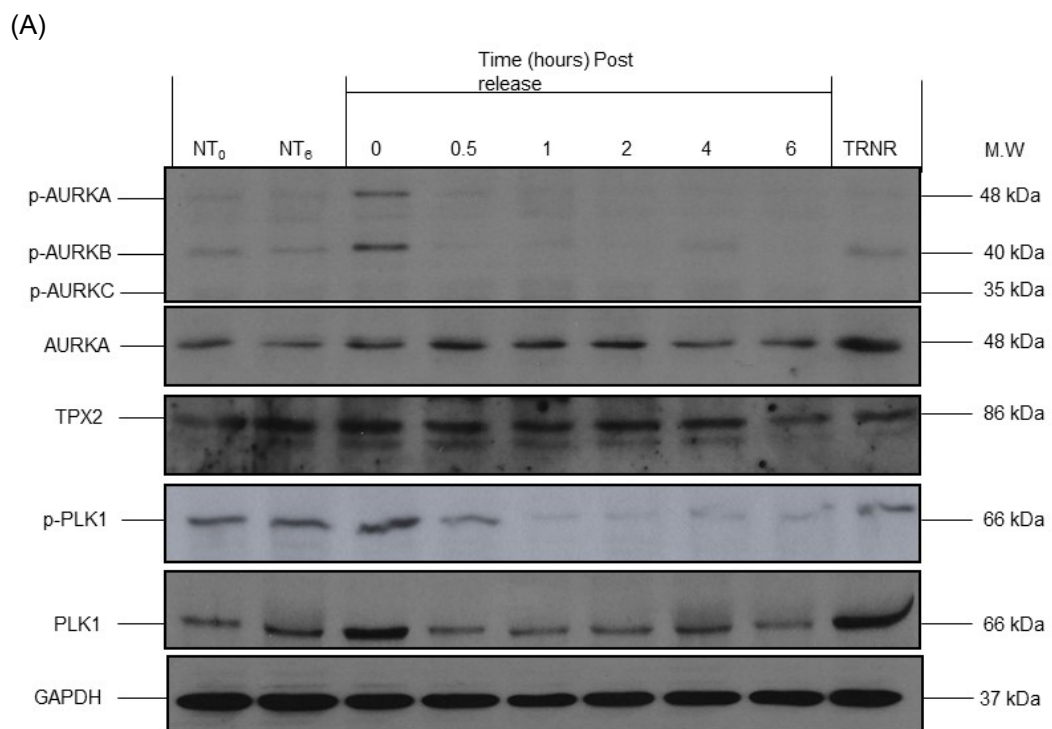
In Figure 3.16 (A) and (B) there was a significant ($p < 0.05$) decrease in phosphorylation of AURKA following release at 30min ($68.2 \pm 2.8\%$; $n=3$, $p < 0.001$) 1h, ($79.5 \pm 4.3\%$; $n=3$, $p < 0.001$), 2h ($75.2 \pm 7.5\%$; $n=3$, $p < 0.001$), 4h ($77.6 \pm 6.1\%$; $n=3$, $p < 0.001$) and 6h ($81.5 \pm 0.2\%$; $n=3$, $p < 0.001$) respectively, compared to the synchronised sample at the 0 time point (TR0). The phosphorylation of AURKB was also significantly ($p < 0.05$) reduced after 1h ($72.0 \pm 20.8\%$; $n=3$, $p < 0.05$), 2h ($74.7 \pm 17.4\%$; $n=3$, $p < 0.05$), 4h ($71.8 \pm 9.9\%$; $n=3$, $p < 0.05$) and 6h (TR6) ($81.6 \pm 11.2\%$; $n=3$, $p < 0.05$) relative to the normalised TR0 sample. The phosphorylation of AURKC was also measured but as was the case in the DKO model, the expression levels were very low and this made quantifying the results difficult and unable to determine any significant values.

The total expression of AURKA was also analysed and in contrast to its phosphorylation, wasn't significantly reduced until the 6-hour time point (55.4 ± 14.3 ; $n=3$, $p < 0.05$) relative to the TR0 sample. This was perhaps not wholly unexpected given the phosphorylation of the protein, an indicator of catalytic activity, would firstly need to be 'switched off' prior to degradation of the protein.

As well as the phosphorylation of the AURKs and total expression of AURKA, the expression of the critical AURKA co-activator, TPX2 was also measured. The expression levels of TPX2 followed a similar pattern to that in the DKO MEFs and remained elevated until a significant reduction was observed at the 6 hour time point ($40.9 \pm 8.3\%$; $n=3$, $p < 0.05$) compared to the TR0 sample. As expression of TPX2 remains higher for longer than AURKA, this could suggest that TPX2 could be dissociated from AURKA but not necessarily degraded in the cell. Lastly, the phosphorylation and total expression of PLK was measured both these

significantly decreased from the 30 minute time point. Firstly, with regards to the phosphorylation of PLK1, it was found to be significantly decreased after 30 min ($47.6 \pm 0.9\%$; $n=3$, $p<0.001$), 1h ($90.8 \pm 3.7\%$; $n=3$, $p<0.001$), 2h ($86.8 \pm 2.7\%$; $n=3$, $p<0.001$), 4h ($79.5 \pm 1.2\%$; $n=3$, $p<0.001$) and 6h ($85.6 \pm 2.8\%$; $n=3$, $p<0.001$) following release from nocodazole arrest, relative to the TR0 sample. This was mirrored in the total expression of PLK1 which was also significantly reduced after 30 min ($58.9 \pm 3.8\%$; $n=3$, $p<0.001$), 1h ($43.9 \pm 11.1\%$; $n=3$, $p<0.05$), 2h ($54.7 \pm 5.7\%$; $n=3$, $p<0.01$), 4h ($50.1 \pm 4.2\%$; $n=3$, $p<0.01$) and 6h ($55.9 \pm 7.7\%$; $n=3$, $p<0.01$) relative to the TR0 sample.

Collectively, these experimental outcomes demonstrated that nocodazole treatment of WT MEF cells resulted in the arrest of cells and a similar pattern in expression of mitotic markers to that observed previously in PC3 cells (Section 3.2.1) and more closely to the DKO MEF cells (Section 3.4.1), though the kinetics of dephosphorylation of AURKA were much more rapid than in the DKO MEF cells. That said, the conditions and characteristics detailed could be used in future experimental work when assessing cellular interventions examining the potential effects of the NBD WT CPP on IKK-AURK signalling following trap and release in WT MEF cells.



(B)

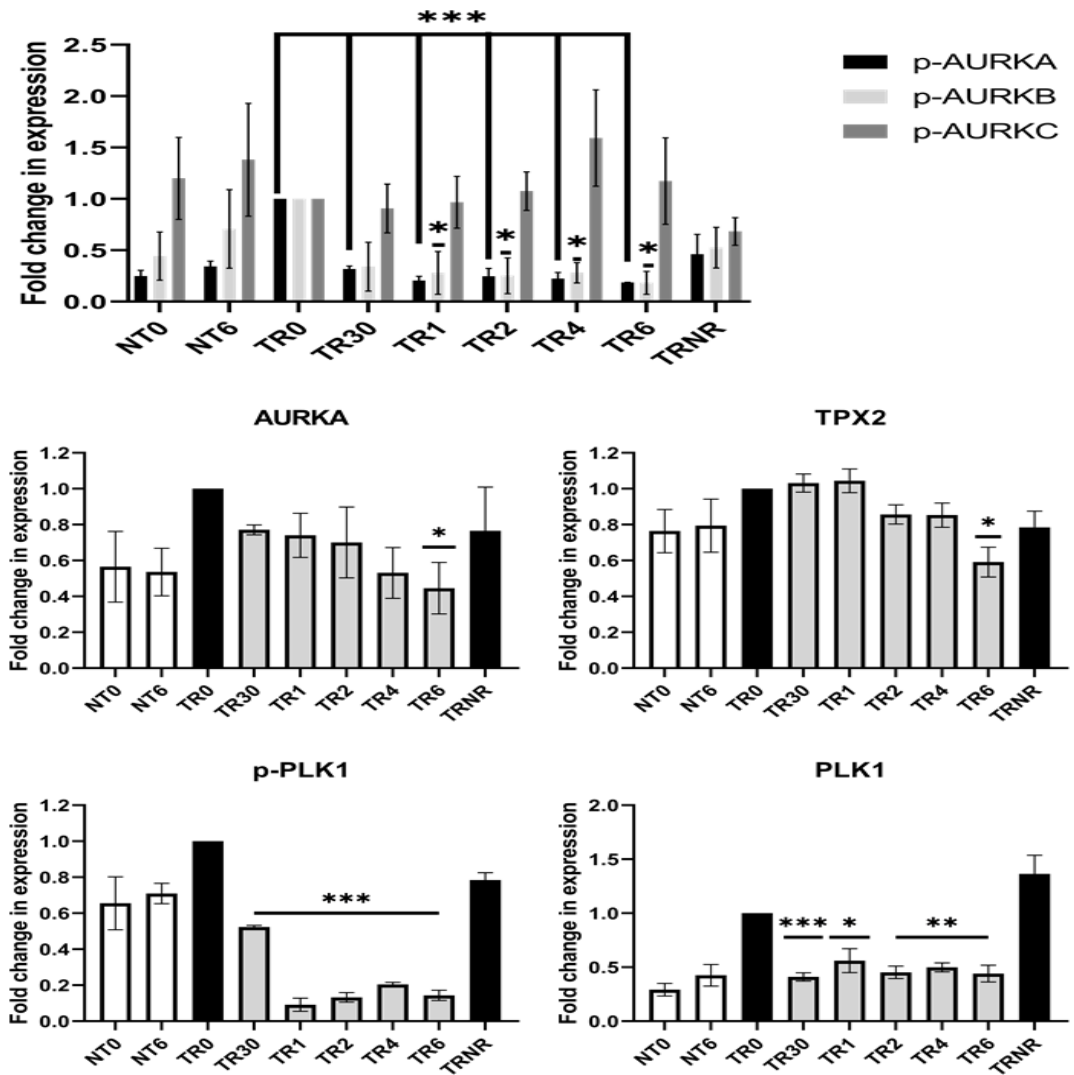


Figure 3.16. Effect of Nocodazole trap and release on AURKs and related protein markers of mitosis in WT MEF cells.

WT MEFs were grown on 10mm dishes and treated with 100ng/ml Nocodazole (16-20 hours) and these were then released by washing twice with fresh media; times indicated as hours post-release from Nocodazole trap. Non-trapped cells at 0 and 6h (NT0 and NT6) represent the negative control. Cells treated with Nocodazole and then not washed and released represented the positive control (Trap and release non-release, TRNR). (A) Whole cell lysates were prepared for separation using SDS-PAGE and analysis by Western Blotting using the above antibodies (n=3). GAPDH was used as a loading control. (B) Data was normalised to synchronised sample before release at the zero time point (TR0) and represents mean \pm S.E.M. One-way ANOVA with post-hoc Dunnett's test was used to determine statistical significance ($p < 0.05$) of observed changes relative to TR0 synchronised sample at 0 min. (*= $p < 0.05$, **= $p < 0.01$, ***= $p < 0.001$).

3.4.4. Effects of NBD WT CPP on the status of AURKA and cell cycle markers following nocodazole trap and release in WT MEF cells.

Having previously demonstrated the ability of the NBD WT CPP to 'accelerate' the decrease in AURKA phosphorylation and total expression as well as expression of key related mitotic markers in DKO MEFs (Figure 3.14) experiments were then constructed that sought to examine the effect of the peptides in WT MEFs which expressed IKK α and IKK β .

Therefore, the effect of the NBD WT CPP on AURKA and related protein markers after release from nocodazole arrest at pro-metaphase in WT MEF cells were investigated. WT MEFs were treated with nocodazole (100ng/mL) for 16-20 hours prior to being washed and released as described previously – Section 2.2.2.1, before NBD MT or NBD WT peptides (100 μ M) were added upon release as described previously and samples prepared thereafter at appropriate time points.

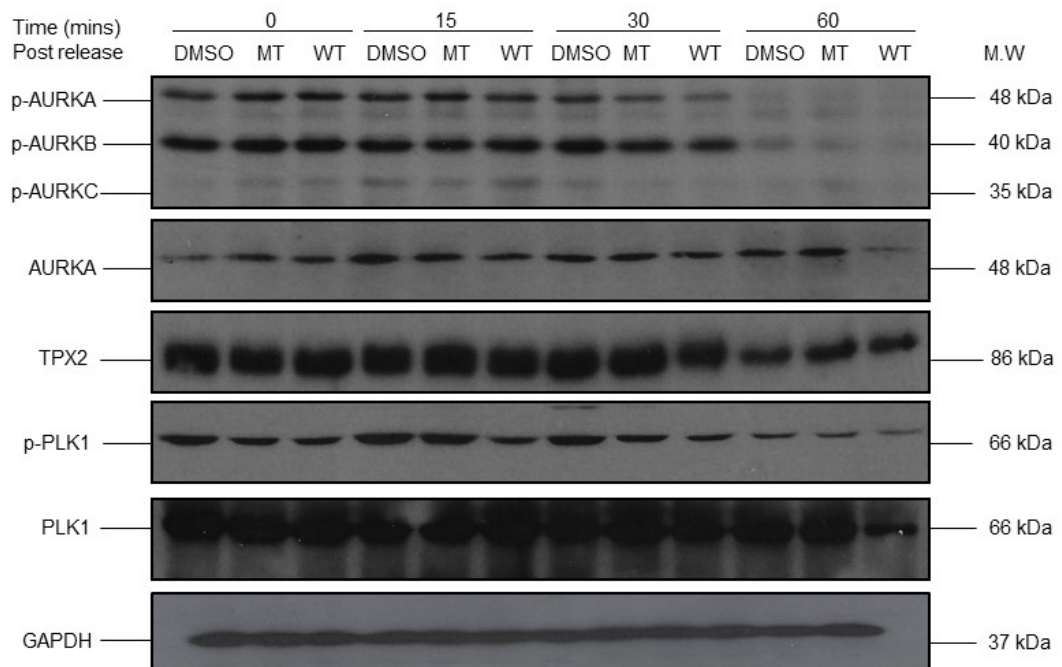
Figure 3.17 (A) indicated via immunoblotting the effect of the MT and WT NBD CPP on the status of p-AURKs, AURKA, TPX2 and p-PLK1/PLK1 post-trap and release. In Figure 3.17, from immunoblotting (A) and the associated quantification (B), the NBD WT CPP caused a significant ($p < 0.05$) decrease in phosphorylation of AURKA relative to the vehicle control at 0 min (DMSO 0). Phosphorylation of AURKA was reduced after treatment with the NBD WT CPP at 30 min ($45.9 \pm 12.7\%$; $n=3$, $p < 0.05$) and 60 min ($73.0 \pm 11.6\%$; $n=3$, $p < 0.001$) respectively. At the 60 minute time point, this decrease was significant ($p < 0.05$) but there was also a statistically significant decrease measured in cells treated with the vehicle control ($45.4 \pm 11.2\%$; $n=3$, $p < 0.05$) and NBD MT CPP ($46.4 \pm 9.7\%$; $n=3$, $p < 0.05$). There was also a significant reduction in phosphorylation of AURKA at 60 min post-release from nocodazole-mediated arrest, relative to the vehicle treated control at this time point ($81.9 \pm 8.7\%$ vs $47.5 \pm 6.1\%$; $n=3$, $p < 0.05$). This indicated that AURKA phosphorylation decreased naturally over time and this decrease in phosphorylation was accelerated by the NBD WT CPP. In Figure 3.17 (B), the NBD WT CPP also caused a significant reduction in AURKB phosphorylation at 30 min ($87.5 \pm 3.4\%$ vs $48.3 \pm 2.4\%$; $n=3$, $p < 0.05$) and 60 min ($59.0 \pm 16.4\%$ vs $23.1 \pm 6.0\%$; $n=3$, $p < 0.05$) relative to the vehicle treated control at these time points. Phosphorylation of AURKC was also measured but as mentioned before, it was expressed at low levels and this made quantifying the results difficult and unable to determine any significant values. The reduction in total AURKA expression was also assessed to determine whether the kinetics of protein degradation were comparable to the NBD WT CPPs effect on AURKA phosphorylation. In Figure 3.17 (B), the NBD WT CPP caused a significant reduction in expression of total AURKA at 60 min compared to the vehicle control at this time point ($83.0 \pm 7.6\%$ vs $36.1 \pm 10.4\%$; $n=3$, $p < 0.01$). Expression of total AURKB and C were not measured and therefore it

remains to be seen if the NBD WT CPP has an inhibitory effect on total protein expression across all AURKs in WT MEF cells.

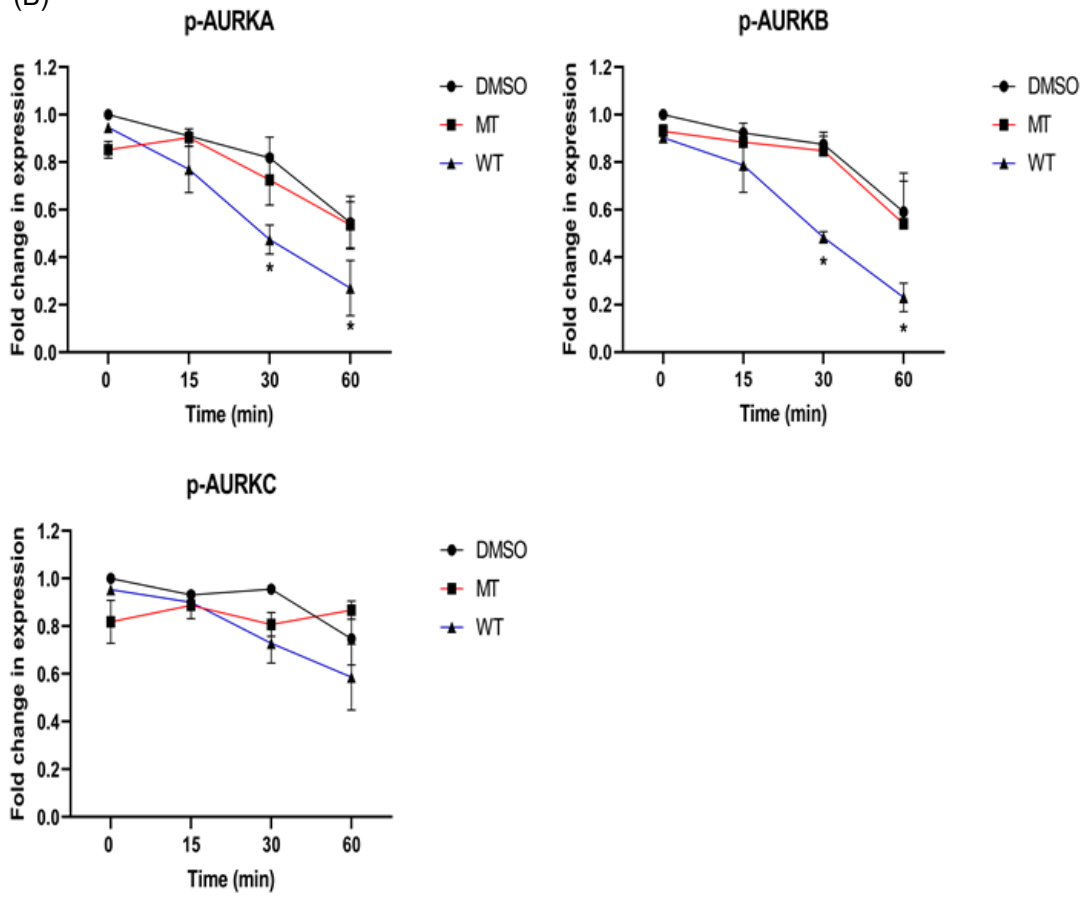
In Figure 3.17 (B), the NBD WT CPP also caused a significant reduction in expression of TPX2 after 60 min relative to the vehicle treated control at this time point ($76.2 \pm 1.7\%$ vs $41.1 \pm 5.8\%$; $n=3$, $p<0.01$). Lastly, the effects of the NBD WT CPP on the phosphorylation and total expression of PLK1 in WT MEF cells were examined. The NBD WT CPP significantly downregulated phosphorylation of PLK1 at the 60 minute time point compared to the vehicle control at this time point ($67.3 \pm 13.0\%$ vs $27.7 \pm 0.6\%$; $n=3$, $p<0.05$). Similarly, this was also observed in the terms of reduced total expression of PLK1 relative to the vehicle control at this time point ($78.0 \pm 7.8\%$ vs $37.9 \pm 3.3\%$; $n=3$, $p<0.05$).

These experimental outcomes again highlighted the ability of the NBD CPP to target IKK-AURK signalling in a comparable way to that observed in the DKO MEFs and further suggested that mechanistically the impact of the NBD CPP was in targeting AURKs and related proteins irrespective of IKK genetic background.

(A)



(B)



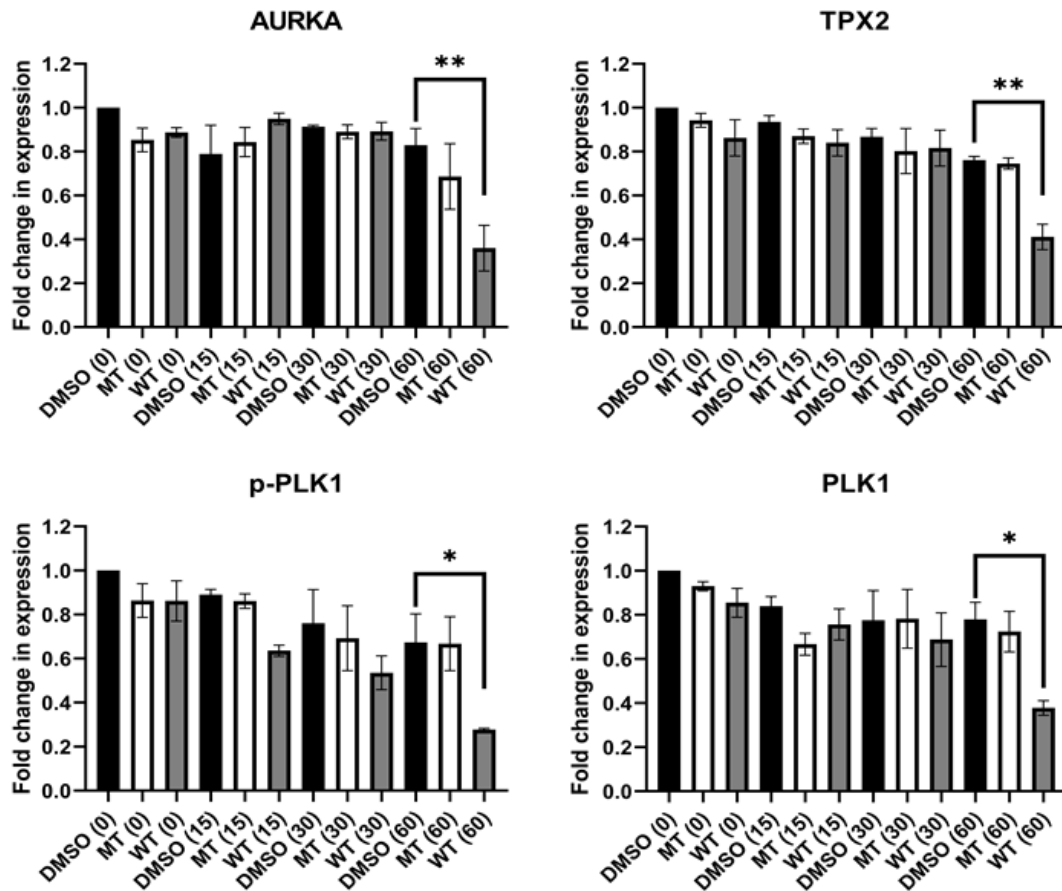


Figure 3.17. Impact of NBD WT CPP on AURKA and related protein markers of mitosis in WT MEF cells.

WT MEF cells were grown on 10mm dishes and treated with 100ng/ml Nocodazole (16-20 hours) prior to treatment with either NBD CPP WT or MT (100 μ M) or DMSO as a vehicle control (0.5% (v/v)) upon release from trap at 15min, 30min and 60min. (A) Whole cell lysates were prepared for separation using SDS-PAGE and analysed by Western Blotting using the above antibodies (n=3). GAPDH was used as a loading control. (B) Data was normalised to the vehicle treated control at 0 min (DMSO 0) and represents mean \pm S.E.M. One-way ANOVA with post-hoc Dunnett's test was used to determine statistical significance ($p < 0.05$) of observed changes relative to vehicle control at 0 min. (*= $p < 0.05$, **= $p < 0.01$, ***= $p < 0.001$). p-AURKA: WT (30) vs DMSO (30), * $p < 0.05$; WT (60) vs DMSO (60), * $p < 0.05$. p-AURKB: WT (30) vs DMSO (30), * $p < 0.05$; WT (60) vs DMSO (60), * $p < 0.05$.

3.5. Discussion.

The IKK complex is recognised to regulate both the canonical and non-canonical NF- κ B pathways, dependent on which dimeric structure is formed between the two catalytic IKK proteins (see Figure 1.2) (Gamble et al., 2012b, Perkins, 2007). It is now emerging that the IKK complex is shown to be involved in the regulation of multiple substrates outside NF- κ B signalling including; ER α , β -catenin, SMRT, Cyclin D1 and interestingly the AURKs (Gamble et al., 2012b, Perkins, 2007). Therefore, understanding the ways in which the IKK complex regulates and/or interacts with these proteins in the cell could be of importance for cell cycle regulation. The cell cycle protein AURKA is a more recently identified substrate of the IKK complex which has been demonstrated to be regulated by both IKK α (phosphorylation of AURKA by IKK α) and IKK β in the cell cycle (Irelan et al., 2007, Prajapati et al., 2006). More recently, work in the Paul lab has shown that AURKA interacts with the IKKs at both the kinase domain (where AURKA acts as a potential substrate or the IKKs act in a regulatory manner) or at the NEMO binding domain (NBD), which acts as a multi-docking site for different proteins and is of importance in this context (Wilson 2013). We have an established cell-permeable peptide (CPP) molecule derived from the structure of IKK β with an identified primary function of disrupting canonical NF- κ B activation (May et al., 2000b) via perturbation of IKK protein-protein interactions. Previous work in the Paul lab has also proposed it to competitively interfere with IKK-Aurora binding at the NBD as it is demonstrated to have a novel effect in causing AURKA degradation whilst also remaining effective at inhibiting TNF α -mediated p65 phosphorylation described previously (Wilson 2013) and as confirmed in Section 3.3.2. The aims of this chapter were to utilise the NBD peptide to confirm the perturbation of AURKA, TPX2 and p-PLK1/PLK1 status and then construct molecular/pharmacological experiments to identify whether these effects occurred in an IKK dependent (post-disruption of IKK-NEMO complex interactions) or independent mechanism (potentially by targeting AURKA directly).

3.5.1. IKK/Aurora signalling in the cell cycle.

AURKA is required for G₂-M transition in the cell cycle and peaks at anaphase during mitosis to then be targeted for degradation by the APC/C-Cdh1 complex at the end of mitosis, more specifically through cytokinesis (Giubettini et al., 2011, Marumoto et al., 2002). In this study nocodazole was used to trap PC3 cells at G₂/M phase and it was observed that both the expression of AURKA and its phosphorylation (T288) peaked once cells were arrested and then significantly ($p < 0.05$) decreased as they were released from nocodazole trap (Figure 3.2 A and B). This was consistent with the idea that, as mentioned earlier AURKA peaks at G₂/M phase as shown by Giubettini et al. (2011), before ubiquitination and degradation by the APC/C complex. Also, the AURKA co-activator TPX2 displays a similar pattern of expression

to AURKA as the cells move through the different stages of the cell cycle ($p < 0.05$). This is expected as TPX2 has been demonstrated to play a protective role in preventing p-AURKA (Thr288) from de-phosphorylation and subsequent inactivation by the phosphatase, PP1a, leading to degradation, as was demonstrated in studies by both Briassouli et al. (2007) and Giubettini et al. (2011). In a related manner PLK1 that functions downstream of AURKA, and its phosphorylation followed a similar pattern consistent with that shown by AURKA and TPX2 (Figure 3.2). This is because PLK1 is firstly phosphorylated (T210) by AURKA dependent on Bora (co-activator of AURKA known as aurora borealis) at the start of G₂ and its activity increases until it peaks at G₂/M phase (Bruinsma et al., 2014). As the peak of activity in mitosis passes there is then a sequence of dephosphorylation events that helps prepare cells for division and subsequent re-entry in to G₁. This outcome is supported when TPX2 is dephosphorylated, followed by AURKA and this then leads to PLK1 dephosphorylation and subsequent degradation by the APC/C complex (Bruinsma et al., 2014). Interestingly, as shown in Figure 3.3, the NF- κ B components which have been analysed under the same conditions of arrest at prometaphase and subsequent release as demonstrated in the previous Figures (3.1 and 3.2), were relatively unchanged in terms of expression and this was to be expected as they are not cell cycle regulated but are involved in cell growth and regulation of the cell (Perkins, 2007). These initial experiments to establish 'trap' and 'release' conditions and whether nocodazole-mediated cell synchronisation treatment was an appropriate approach to arrest cells was carried out in coordination with Fluorescence-Activated Cell Sorting (FACS) analysis (Figure 3.1A) to establish that the technique was effective and the majority of cells were positioned at the G₂/M phase of the cell cycle. In Figure 3.1 (A), FACS analysis indicated the proportion of cells following nocodazole arrest in each phase of the cell cycle based on DNA content; and this confirmed that the nocodazole-mediated cell synchronisation technique had been successful as most of the synchronised cells were positioned at the G₂/M phase compared to non-synchronised cells.

As mentioned above, AURKA and its related cell cycle markers in PC3 cells followed a similar pattern of peaking in expression once arrested at prometaphase. Both expression and phosphorylation decreased over time as they were released from the 'trap', washed and released back into the cell cycle – this was almost completely abolished after 4 hours. These patterns were consistent with the work of Briassouli et al. (2007), Bruinsma et al. (2014) and Giubettini et al. (2011) who showed similar phosphorylation and expression patterns for AURKA and related protein markers of mitosis (e.g. PLK1, TPX2 etc.) in human breast cancer and human osteosarcoma U2OS cells respectively.

3.5.2. Pharmacologically challenging the IKK-Aurora interaction.

Based on previous peptide array mapping of the IKK β -AURKA interaction, a cell permeable short length peptide that mimicked 11aa of the C-terminal NBD of IKK β was used to challenge IKK-AURKA signalling and its effects on AURKA status and its related protein markers of mitosis, TPX2 and PLK1 were assessed (Figure 3.4). In the presence of the NBD WT CPP, both AURKA expression and phosphorylation decreased more rapidly in comparison to the vehicle treated control at the same/parallel time point as the cells progressed through the cell cycle ($p < 0.05$). Given previous work in the lab (Wilson 2013), involving mapping AURKA binding to IKK $\alpha/\beta/\gamma$ peptide arrays indicated IKK β binding, it was hypothesised that the NBD WT CPP may be competing with TPX2 and allowing the critical phosphothreonine residue (p-T288) to become exposed and be dephosphorylated by PP1a, thus leading to the accelerated degradation of AURKA. To confirm this hypothesis further experimental studies incorporating molecular modelling and structural biology will need to be pursued. A similar pattern of expression was observed for TPX2 and PLK1 in which both were significantly reduced when PC3 cells were exposed to the NBD WT CPP ($p < 0.05$). The accelerated degradation and inhibition of phosphorylation of PLK1 could be as a consequence of this proposed mechanism of TPX2 competition and subsequent exposure of AURKA to PP1a and degradation. As PLK1 was phosphorylated (Thr210) and activated by AURKA, if AURKA is degraded quicker then PLK1 may have become dephosphorylated and degraded quicker (Asteriti et al., 2015).

The NBD peptide was also examined to validate its primary function of inhibiting canonical NF κ B activation as originally shown by May et al. (2000b). This was confirmed in Figure 3.5 in that the NBD WT CPP (100 μ M) inhibited significantly ($p < 0.05$) TNF α -induced phosphorylation of p65, a key indicator of inhibition of canonical NF- κ B signalling pathway activation. Interestingly, a potentially novel finding around NF- κ B signalling was also identified in this study in that the treatment of PC3 cells with NBD WT CPP inhibited LTX-stimulated non-canonical NF- κ B activation. In Figure 3.6, the NBD WT CPP (100 μ M) inhibited significantly the LTX-induced phosphorylation of p100 ($p < 0.05$) and formation of p52 ($p < 0.05$). The NBD WT CPP was also shown to cause a significant decrease in expression of IKK α which regulates the non-canonical NF- κ B signalling pathway ($p < 0.05$). The effects of the NBD WT peptide, derived from IKK β , on non-canonical NF- κ B signalling hasn't been demonstrated in the literature. Solt et al. (2009) confirmed that ablation of the NBD in IKK α had no effect on non-canonical NF- κ B signalling and therefore the association of IKK α and NEMO wasn't involved in this pathway. Could the NBD WT peptide possibly be disrupting the binding between IKK α and NIK and disrupting this protein-protein interaction or alternatively causing

general disruption of IKK complexes? These concepts will need to be examined with further studies.

We sought to elucidate the relationship between IKKs and AURK signalling using different methods of intervention, initially pharmacological, to target different domains within the two catalytic IKK proteins (IKK α and IKK β). Initially, small molecule kinase inhibitors of both IKK α and IKK β were used to target the kinase domain of each IKK isoform as both proteins have been reported to act in a regulatory manner by means of phosphorylating AURKA (Irelan et al., 2007, Prajapati et al., 2006). The pharmacological selectivity of these molecules were first validated to ensure they effectively inhibited agonist driven non-canonical and canonical NF- κ B signalling respectively. The “in-house” IKK α kinase inhibitor (SU1433) caused a concentration dependent inhibition of LTX-induced p100 phosphorylation, which was significant at concentrations of 3 μ M ($p < 0.05$) and 10 μ M ($p < 0.01$). SU1433 also caused a significant decrease in the formation of p52 when used at concentrations of 3 μ M ($p < 0.01$) and 10 μ M ($p < 0.001$). Both results were indicative of non-canonical NF- κ B pathway inhibition (Figure 3.7 A and B). The IKK α kinase inhibitor SU1433 was also tested to see if selectivity was robust, could it modulate NF- κ B markers mediated by the alternative IKK isoform? In this instance, the canonical NF- κ B pathway in which IKK α isn't the main regulatory IKK protein (Figure 3.8). The IKK α kinase inhibitor showed no significant effect on any key markers of canonical NF- κ B signalling and this therefore emphasised the selectivity and potency of the “in-house” kinase inhibitor for causing inhibition of non-canonical NF- κ B signalling. The IKK β kinase inhibitor BMS-34551 caused a reversal of TNF- α -stimulated I κ B α degradation which was significant at concentrations of 10-50 μ M ($p < 0.01$, $p < 0.001$). BMS-34551 also caused a significant reduction in the phosphorylation of p65 at a concentration of 50 μ M ($p < 0.05$). These are both indicative of the inhibition of the canonical NF- κ B pathway (Figure 3.7 C + D). The BMS-34551 inhibitor was also tested on the parallel NF- κ B signalling pathway, i.e. the non-canonical NF- κ B pathway in which IKK β isn't involved in (Gamble et al., 2012b, Paul et al., 2018). The IKK β -selective kinase inhibitor showed a significant decrease in phosphorylation of p100 across all concentrations ($p < 0.001$) and displayed a significant reduction in the formation of p52 at concentrations of 20-50 μ M ($p < 0.05$). This is not completely surprising as Burke et al. (2003) suggested that BMS-34551 inhibited IKK β ($IC_{50} = 0.3\mu$ M) and IKK α ($IC_{50} = 4\mu$ M) and this could vary in different cell types. These results show that both inhibitors were effective at targeting the kinase domain of each IKK protein and successfully inhibited non-canonical (SU1433) and non-canonical/canonical (BMS-34551) NF- κ B signalling respectively. Following on from the validation of the effect of these inhibitors on the relevant NF- κ B signalling pathways, their effects on p-AURKs, AURKA, TPX2, p-PLK/PLK1 were assessed. As can be observed from the quantitative immunoblotting in Figure 3.10 (A) and associated quantification

(B), the addition of the IKK kinase inhibitors had no significant impact on the kinetics of change through mitosis and modulation of p-AURKs/ AURKA status. The significant ($p < 0.05$, $p < 0.01$, $p < 0.001$) decrease in phosphorylation of AURKA, B and C was determined to be as a result of the natural decrease in expression/phosphorylation as cells progressed through the cell cycle. There was no significant ($p > 0.05$) changes in total expression and/or phosphorylation of the other cell cycle markers (TPX2 and PLK1) in the different treatment groups across the different time points relative to the vehicle treated control at each time point. Any decrease in expression observed was again deemed to be due to the progression of the cells through mitosis. Inhibition of IKK catalytic activity played no role in the modulation of mitotic markers. This conclusion could have been further confirmed by the infection of cells with adenovirus constructs that express dominant negative (DN), catalytically inactive forms of IKK α or IKK β however despite efforts to construct such experiments to examine agonist-stimulated NF- κ B activation, effective consistent overexpression of DN-IKK α protein could not be established to test this hypothesis.

The potential impact of down-regulating IKK protein expression on IKK-Aurora signalling/interactions was also examined by targeting IKK α and IKK β at the transcriptional level using siRNA. Previous literature suggested conflicting effects of targeting the IKK proteins on AURKA cell cycle status. In a study by Prajapati et al. (2006) it was shown that siRNA treatment had no effect on cellular AURKA status, whereas it was shown by Ireland et al. (2007) that siRNA treatment caused a delay in cell cycle progression. Again, this molecular intervention was assessed to see if it interfered with non-canonical and canonical NF- κ B signalling and to see if it successfully “knocked down” total protein levels of the catalytic IKK proteins. In Figure 3.11 (A) siRNA IKK α was observed, from immunoblotting and subsequent quantification (B), to inhibit significantly ($p < 0.05$, $p < 0.01$) the LTX-induced phosphorylation of p100 that is associated with non-canonical NF- κ B pathway activation at concentrations of 100-200nM and also successfully resulted in the significant ($p < 0.001$) knock-down of total IKK α protein expression across the concentration range (50-200nM). In Figure 3.11 (C) it was observed from immunoblotting that siRNA IKK β inhibited TNF α -induced phosphorylation of p65 and the quantification (D) confirmed that this was significant ($p < 0.05$, $p < 0.01$, $p < 0.001$) at concentrations of 100-200nM, this outcome is a hallmark of inhibition of the canonical NF- κ B signalling. It was also demonstrated to significantly ($p < 0.001$) knock-down total IKK β protein expression across the concentration range (50-200nM). However, there was no observed reversal of I κ B α degradation. This could possibly be as result of the incomplete rundown of both IKK isoforms following siRNA treatment. Given that there was approximately 15% IKK β protein expression remaining, this may have been sufficient to transduce a signal in the already stimulated pathways and therefore still drive an effective I κ B α degradation. siRNA

rundown didn't affect the standard kinetics already recognised for each of the markers measured. Perhaps the most interesting finding was that siRNA IKK β caused a significant decrease in phosphorylation of PLK1 after 30 min ($p < 0.05$) and 60 min ($p < 0.01$) as well as a significant decrease in total expression after 120 min ($p < 0.05$) there was no significant differences between samples that were treated with either siRNA IKK α or IKK β compared to the vehicle-treated control at the relative time point. As mentioned previously, the reason or significance of this findings would need further investigation but it was shown by (Higashimoto et al., 2008) that PLK1 is involved in the regulation of the IKK complex by phosphorylating IKK β . PLK1 phosphorylated IKK β *in vitro* at residues Ser733, Ser740 and Ser750 in the NBD (Higashimoto et al., 2008). It was demonstrated by Higashimoto et al. (2008), using phosphoantibodies that targeted Ser740, that the NBD is phosphorylated *in vivo*. It was also shown that constitutive activation of PLK1 in cells TNF α -induced IKK activation, decreased phosphorylation of I κ B α and reduction in NF- κ B activation (Higashimoto et al., 2008). Hence, PLK1 was found to negatively regulate TNF α -induced IKK activation by phosphorylating the NBD of IKK β and decreasing its affinity for NEMO.

In the two main studies considered here, reporting on the relationship between IKKs and AURKA, (Irelan et al., 2007) and (Prajapati et al., 2006), there were two main differences in their siRNA targeting of the IKK proteins to investigate the resulting effect on AURKA compared to the siRNA rundown technique here. This study used cells synchronised with nocodazole following treatment with siRNA (closest to mimicking this was a double-thymidine synchronisation treatment in the Prajapati paper) and targeted simultaneously both IKK α and IKK β . To move toward being able to examine the impact of the NBD CPP on AURKs etc. in the absence of IKK protein expression a dual siRNA targeting strategy was then adopted. Both catalytic IKK proteins were targeted at the same time to generate, in theory, a molecularly induced "null IKK" background. The impact of NBD CPPs on mitotic markers were then reappraised in this setting. Outputs from this approach (Figure 3.13) involving the simultaneous targeting of both IKK α and IKK β whilst incorporating the NBD CPPs, identified that there was no significant change to the impact of the NBD WT CPP on mitotic markers in these cells with (almost) no IKK protein expression.

3.5.3. Determining the impact of the NBD CPPs on IKK-AURK signalling in a 'double knock-out' model.

The next series of experiments examining the impact of the NBD CPPs on AURK and associated proteins utilised MEF cells deficient for both IKK α and IKK β , a genetic 'double knock-out'. This was a true null cellular background with no endogenous IKK α and IKK β . Both

Lanni and Jacks (1998) and Pitto et al. (2009) used knock-out and wild-type MEFs models that had been trapped with nocodazole but there are very few examples in the literature of studies that use DKO models as used here, i.e. lacking IKK α and IKK β . In Figure 3.14 (A) and subsequent quantification (B), DKO MEF cells followed a similar pattern of expression of mitotic markers to that observed in PC3 cells in Figure 3.1. Phosphorylation of AURKA and B peaked following nocodazole-mediated arrest and AURKA phosphorylation was significantly ($p < 0.05$, $p < 0.01$, $p < 0.001$) reduced from 1-6 hours, whereas AURKB phosphorylation wasn't significantly ($p < 0.05$) reduced until after 6 hours. AURKB is recognised to be involved later in the cell cycle (Katayama H, 2003) and the experimental result reported here may reflect this or AURKB may be expressed a lot more highly than AURKA in this cell type. The total expression of AURKA followed a similar pattern to its phosphorylation in that it was significantly ($p < 0.05$, $p < 0.01$) reduced from 1-6 hours. It was also observed from the immunoblotting (A) and specifically the quantification (B) that other key related mitotic markers such as TPX2 and PLK1 (total expression and phosphorylation) are not significantly ($p < 0.05$) reduced until 6 hours post-release from nocodazole-mediated arrest, suggesting a possible later role for these proteins in the cell cycle in DKO MEF cells. In Figure 3.14 (C) and (D) it can be seen from immunoblotting and subsequent quantification of the IKK protein expression in the different MEF models (WT, $ikka^{-/-}$, $ikkb^{-/-}$ and DKO) and the subsequent quantification produced from these which showed there were no IKKs present in the DKO model ($p < 0.001$) and confirmed these cells were appropriate for further experiments. These experiments established conditions for nocodazole-mediated arrest of DKO MEF cells. Following this, the NBD WT CPP was incorporated into DKO MEF cells to assess the effect of the NBD WT CPP without the presence of IKKs on the status of AURKA and related mitotic markers.

In Figure 3.15 the NBD CPPs were incorporated into the DKO MEF cellular model to demonstrate the effect of the IKK β -derived NBD WT CPP on AURKA phosphorylation/degradation and its related protein markers status when there are no catalytic IKK proteins present. In this setting, the NBD WT CPP caused an "accelerated" decrease in phosphorylation of AURKA and B as well as total expression of AURKA and TPX2. Phosphorylation and total expression of the mitotic kinase PLK1 was also measured and there seemed to be no noticeable change in these markers when treated with NBD WT CPP compared to the DMSO and NBD MT CPP across the time points. This could suggest that PLK1 is regulated differently in this cellular background compared to in PC3 prostate cancer cells. This suggests that the NBD WT CPP could be affecting AURKA and B phosphorylation status as well as TPX2 expression and perhaps disrupting the AURKA/TPX2 interaction. Whether these findings are significant or not will need to be qualified with further experimental repeats. The NBD WT CPP derived from IKK β still influences AURKs signalling in the absence

of the IKK proteins and hence this gives more solid evidence to support a hypothesis that the impact of the NBD upon AURKs and associated proteins in a cellular setting is mediated in an IKK-independent manner, independent of protein expression and/or catalytic activity.

Following on from preliminary demonstrated impact of the NBD peptide in DKO the MEFs cellular model that was lacking the IKK α and IKK β proteins, we mirrored the experiments with the exact same treatment conditions in wild-type (WT) MEFs, which are normal fibroblasts derived from the murine setting and crucially they have the two catalytic IKK proteins present. This model was used as a comparison to the DKO MEF model to make sure any experimental outcome wasn't as a result of the cell type and is solely due to actions of the NBD WT CPP. In Figure 3.16 (A), immunoblotting and the subsequent quantification (B), showed that the status of p-AURKs, AURKA, TPX2 and p-PLK1/PLK1 demonstrated a similar pattern of expression post-release from nocodazole-mediated arrest to that observed in DKO MEF cells in Figure 3.14. Although, the kinetics were slower in the DKOs compared to the WT MEFs. This suggested that the IKK proteins do have some role in regulating the kinetics of progress through the cell cycle and exit from mitosis. AURK dephosphorylation was particularly slower in DKO MEFs, where there was a lack of IKK protein expression (less NBD structure present to impact on AURKA). When no IKK proteins present, this could suggest that there are still other regulators to 'switch off' AURKA phosphorylation/catalytic activity in the absence of IKK proteins. Going forward it could be suggested to carry out experiments with IKK proteins with a truncated NBD reintroduced into DKO MEF cells. The phosphorylation of AURKA and B peaked following nocodazole-mediated arrest with AURKA rapidly and significantly ($p < 0.001$) decreasing from 30 min through to 6 hours and phosphorylation of AURKB significantly ($p < 0.05$) decreased from 1 hour through to 6 hours post-release. There was also a significant decrease in total expression of AURKA ($p < 0.05$) and TPX2 ($p < 0.05$), both of which occurred later at 6 hours post-release from nocodazole-mediated arrest. The main difference that was observed from DKO MEF cells was the pattern of total expression and phosphorylation of PLK1 in WT MEF cells. There was a significant and rapid decrease in both the phosphorylation ($p < 0.001$) and total expression ($p < 0.05$, $p < 0.01$, $p < 0.001$) of PLK1 from 30 min right through to the 6 hour time point post-release from nocodazole-mediated arrest. As mentioned previously, Fukuda et al. (2005) noted that as MEF cells grow at an exponential growth rate, AURKA was rapidly turned off following release from the G₂/M phase and there may be a possibility that the total expression of AURKA remained elevated despite downregulation of the phosphorylation, due to potentially being activated by an independent pathway/substrate. It was also shown by Lee et al. (2013) that in WT MEFs, AURKA can interact with and phosphorylate a prolyl isomerase known as Peptidyl-prolyl cis-trans isomerase NIMA-interacting 1 (PIN1). PIN1 is shown to be a negative regulator of G₂ activity and hence prevent

mitotic entry. Suppression of PIN1 through its phosphorylation by AURKA is believed to be linked to the regulation of mitotic entry via the AURKA/Bora complex (Lee et al., 2013).

Lastly, Figure 3.17 incorporated the NBD CPPs into WT MEF cells to mirror the experiment we carried out in Figure 3.15 in DKO MEF cells. The NBD WT CPP caused a significant inhibition of both AURKA ($p < 0.05$, $p < 0.001$) and AURKB ($p < 0.01$) phosphorylation as well as total expression of AURKA ($p < 0.05$). There was also a significant reduction in expression of the AURKA co-activator TPX2 ($p < 0.01$) as well as the phosphorylation ($p < 0.05$) and total expression of PLK1 ($p < 0.05$). This therefore indicated that the NBD WT CPP can exert its mechanism of action in WT MEF cells as well as DKO MEF cells and this modulation of AURKA status and that of related mitotic protein markers weren't due to the presence or absence of IKK α and IKK β in the related MEF cellular models.

3.5.4. Conclusions.

Through this study it has been established that the nocodazole cell synchronisation methodology was effective for arresting PC3 (Section 3.2.1), WT MEF (Section 3.4.3) and DKO MEF cells (Section 3.4.1). They also successfully moved through the cell cycle upon release and have allowed the status of p-AURKs, AURKA, TPX2 and p-PLK1/PLK1 to be observed post-release from nocodazole-mediated cell synchronisation. It has been identified that a recognised short length peptide sequence derived from the NBD of IKK β , previously identified to perturb the protein-protein interactions and signalling of the classical IKK complex, in a cell permeable form now also displays alternative cellular targets; inducing the accelerated dephosphorylation of AURKA (Thr288), its accelerated degradation through mitosis, and with similar patterns of expression and/or dephosphorylation observed for both TPX2 and PLK1 as associated regulators of mitosis. Furthermore, from the results generated here using pharmacological and molecular targeting of IKK expression/activity and cells genetically deficient for IKK α/β protein expression it is also proposed that the impact of the NBD WT CPP upon AURKA and related proteins occurs independently of IKK protein expression and catalytic activity and is not a result of IKK complex disruption.

Taking the data gathered here, collectively, the NBD WT CPP can pharmacologically modulate AURKA phosphorylation/degradation and expression of key markers in different cell types. Whilst this may suggest a route to targeting and modulating key mitotic regulators in prostate cancer PC3 cells it remained to be determined whether the impact of the NBD WT CPP observed here could be translated to other cell types, in particular, other cancer cell types

where AURKs, TPX2, PLKs etc. have been reported to be over expressed and/or constitutively active.

Chapter 4: The effect of NBD CPP-mediated targeting of AURKA and associated proteins and potential impact phenotypically in a variety of solid tumour cell lines.

4.1. Introduction.

As described previously in Chapters 1 and 3, the classical IKK complex and IKK proteins regulate the activation of the NF- κ B signalling pathways (Chen et al., 1996). Furthermore, it is now appreciated that in several disease settings IKK-NF- κ B signalling is perturbed and dysregulated. This is particularly common to a number of solid tumours. This is apparent in prostate cancer, as demonstrated in PC3 cells (Zhang et al., 2016). It was detailed by Gasparian et al. (2002) that increased activation of the IKK complex lead to continued activation of NF- κ B signalling and the survival of androgen-independent LNCaP prostate cancer cells. Furthermore, the IKK complex is implicated in the progression of other cancer cell types, including breast cancer cells and those derived from glioblastoma. It has also been shown by Yeh et al. (2011) that the IKK complex increased stability of the protein Myc and this lead to enhanced progression in MCF7 breast cancer cells whilst a study by Lei et al. (2020) showed that TNFAIP3 Interacting Protein 1(TNIP1) was involved in mediating the upregulation of the IKK complex and this was implicated in T98G glioblastoma cell proliferation.

Interestingly, as well as the perceived consensus that the IKK complex plays a role in aberrant tumour expression, across the different cancer cell types, AURKA has also been reported to be overexpressed and involved in tumour progression. For example, in LNCaP androgen-insensitive (AI) cells, where the androgen receptor (AR) is still present and driving growth but insensitive to androgens, it has been indicated by Shu et al. (2010) that the AR acts as a substrate of AURKA and upregulation of AURKA could be a factor in androgen-independent proliferation through phosphorylation and activation of the AR. Also, in MCF7 cells, Lee et al. (2008) showed that inhibition of AURKA overrides estrogen-induced growth associated chemoresistance. Also, it was shown by Borges et al. (2012) that inhibition of AURKA and AURKB, in T98G Glioblastoma cells, enhances chemosensitivity and sensitivity to radiotherapy and may be used as targets in potential adjuvant therapy. Collectively, across these example tumour types there exists a common theme of IKK and AURK signalling contributing to tumour progression.

As demonstrated in the previous chapter, the utilisation of the short length cell permeable NBD peptide derived from IKK β was able to decrease the phosphorylation and/or total expression of AURKA and its protein markers of mitosis in prostate cancer cells (PC3s), as well as in both a molecularly-induced and a cellular 'double-knockout' model of 'null IKK' backgrounds. Hence, in this chapter experiments sought to explore whether the effects of the NBD WT CPP in PC3 cells were reproducible across other cancer cell lines representative of other solid tumours; in another alternative prostate cancer cell line (LNCaP AI) as well as in a Breast cancer cell line (MCF7) and a Glioblastoma (T98G) cell line. As well as exploring the

mechanistic element of the NBD CPPs in each of these cell types, its effect phenotypically, WT CPP on the status of p-AURKs, AURKA, TPX2 and p-PLK1/PLK1 in a number of other solid tumour cell lines, explore whether the mechanism of action of the peptide demonstrated in Chapter 3 in PC3 prostate cancer cells is transferable across different solid tumour cell lines and consequently then determine the impact of the NBD WT CPP on the cell viability/growth of these different cancer cells.

Therefore, the specific aims of this chapter, towards reproducing the impact of the NBD CPPs both mechanistically and phenotypically in different cancer cell lines, were to:

1. Establish a cell-based assay system in different solid tumour cell lines, to enable the assessment of mitotic signalling proteins, based on the nocodazole-mediated cell synchronisation technique used in prostate cancer cells.
2. Confirm the effect of the NBD CPPs on the AURKs in different solid tumour cell lines (LNCaP AIs, MCF7 and T98G) and examine its potential effect on related regulatory proteins associated with cell cycle progression.
3. Determine the impact of the NBD CPPs phenotypically on cell viability in different solid tumour cells lines (PC3, LNCaP AIs, MCF7 and T98G).

Collectively, these experiments aimed to determine whether the NBD WT CPP impacted on the status of AURKA and related protein markers of mitosis as well as phenotypically on cell viability across different solid tumour settings. This would identify any potential pharmacological utility of the NBD WT CPP in challenging aberrant IKK-AURK signalling in these varying cellular settings representative of different solid tumour types.

4.2. Determining the effect of the NBD WT CPP mechanistically on AURKA signalling and phenotypically on cell viability in solid tumour cell lines.

4.2.1. Optimisation of Nocodazole-mediated cell synchronisation conditions in different cancer cell lines (LNCaP AI, MCF7 and T98G cells).

In order to examine cells at the mitotic phase of the cell cycle a nocodazole based strategy, like the one used throughout Chapter 3 and described previously in Section 2.2.2.1, was instigated to arrest growing cells in mitosis. Based on nocodazole concentrations used in previous studies; the prostate cancer cell line, LNCaP (Amin et al., 2014), the breast cancer cell line, MCF7 (Gully et al., 2012) and the glioblastoma cell line, T98G (Kim et al., 2008) were

treated with various concentrations of nocodazole (25ng/ml, 50ng/ml, 100ng/ml, 200ng/ml, 400ng/ml) for 16-20 hours. Cells were washed and released from the nocodazole trap over 2 hours, similar to that detailed in Section 2.2.2.1. In Figure 4.1, immunoblotting of AURKA, B and C phosphorylation demonstrated that nocodazole successfully arrested LNCaP AI (A), MCF7 (B) and T98G (C) cells across all concentrations. A similar pattern in reduction of phosphorylation of AURKs was seen across the different cancer cell types. It can be observed from the resultant immunoblotting panels that a concentration of 50ng/ml was the optimal concentration for treatment of the different solid tumour cell lines used. It was also observed across the cell types, that at the higher concentrations of nocodazole (i.e. 200ng/ml and 400ng/ml) 2 hours post-release from nocodazole-mediated arrest, the cells failed to release from nocodazole-mediated arrest as can be seen in LNCaP AI (A) and T98G (C) cells.

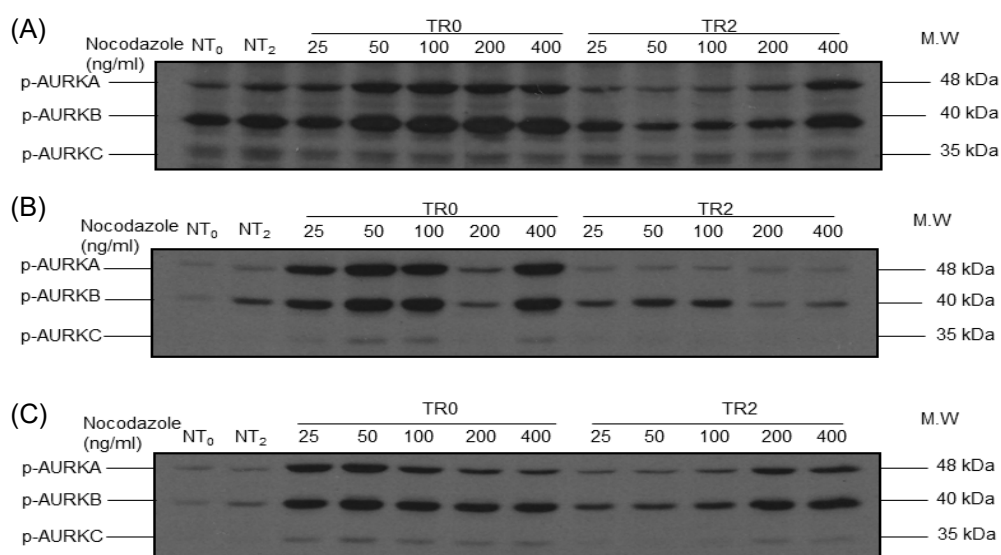


Figure 4.1. Effect of different concentrations of Nocodazole trap and release on p-AURKs in LNCaP AI, MCF7 and T98G cells.

LNCaP AI (A), MCF7 (B) and T98G (C) cells were grown on 10mm dishes and treated with different concentrations of Nocodazole (25ng/ml, 50ng/ml, 100ng/ml, 200ng/ml and 400ng/ml) for 16-20 hours and these were then released by washing twice with fresh media; times indicated as hours post-release from Nocodazole trap. Non-trapped cells at 0 and 2h (NT₀ and NT₂) represent the negative controls. Whole cell lysates were prepared for separation using SDS-PAGE and analysed by Western Blotting using the above antibodies (n=1).

4.2.2. Assessment of the status of AURKA and cell cycle components following Nocodazole mediated cell cycle arrest/trap and release in LNCaP AI, MCF7 and T98G cells.

To establish optimal conditions for nocodazole treatment, LNCaP AI, MCF7 and T98G cells were treated with various concentrations of nocodazole for 16-20 hours and examined for phosphorylation of AURKA, AURKB and AURKC in synchronised vs non-synchronised cells via immunoblotting as detailed in Section 4.2.1. Following on from this an optimal treatment concentration was determined at 50ng/ml and in preparation for experiments cells were treated routinely for 16-20 hours to establish cell cycle arrest or 'trap'.

In Figure 4.2 (A, C and E) immunoblotting was used to assess the cell cycle status of total AURKA and its phosphorylation, as well as the outcome of important cell cycle markers (TPX2, p-PLK1, PLK1) in relation to AURKA following nocodazole trap and release at the appropriate time points (up to 6 hours) in LNCaP AIs, MCF7 and T98G cells respectively and these markers were subsequently quantified (B, D and F). LNCaP AI, MCF7 and T98G cells were treated for 16-20 hours with Nocodazole (50ng/ml). In all cell types, the phosphorylation of the AURKs (A, B and C) were expressed at an elevated and maximum level at the 0 hour time point (TR0), which compared consistently with the positive control (TRNR) in which the cells had been trapped with nocodazole and not released while incubated for 6 hours. In LNCaP AI cells in Figure 4.2 (A) and B, there was a significant decrease in phosphorylation of AURKA following release at 1 hour (TR1) ($46.4 \pm 17.3\%$; $n=3$, $p<0.05$), 2 hours (TR2) ($88.3 \pm 8.9\%$; $n=3$, $p<0.001$), 4 hours (TR4) ($93.0 \pm 2.3\%$; $n=3$, $p<0.001$) and 6 hours (TR6) ($93.7 \pm 1.4\%$; $n=3$, $p<0.001$) respectively, in comparison to the synchronised sample at the 0 time point (TR0). The phosphorylation of AURKB was also significantly reduced after 2 hours (TR2) ($63.8 \pm 22.6\%$; $n=3$, $p<0.05$), 4 hours (TR4) ($78.7 \pm 7.8\%$; $n=3$, $p<0.01$) and 6 hours (TR6) ($94.1 \pm 1.6\%$; $n=3$, $p<0.01$) relative to the TR0 sample. For the last of the AURK family, AURKC, phosphorylation was significantly reduced in a time-dependent manner after 2 hours (TR2) ($77.7 \pm 17.3\%$; $n=3$, $p<0.01$), 4 hours (TR4) ($92.4 \pm 4.7\%$; $n=3$, $p<0.01$) and 6 hours (TR6) ($92.7 \pm 6.5\%$; $n=3$, $p<0.01$) compared to the TR0 sample.

The total expression of AURKA was also analysed and was shown to be significantly reduced after 2 hours (TR2) ($67.5 \pm 4.7\%$; $n=3$, $p<0.001$), 4 hours (TR4) ($65.5 \pm 5.3\%$; $n=3$, $p<0.001$) and 6 hours (TR6) ($67.7 \pm 4.1\%$; $n=3$, $p<0.001$) relative to the TR0 sample. As the cells were released and progressed through mitosis, AURKA expression and phosphorylation (Thr288) was reduced to basal level at the 2 hour time point (also consistent at the 4 and 6 hour time points) as seen when compared to the negative controls (NT₀ and NT₆) – which were cells not treated/trapped with nocodazole and samples prepared at the 0 and 6 hour time

points. By the quantification indicated in Figure 4.2 (B) the detected phosphorylation of AURKA decreased slightly faster kinetically than the total protein expression e.g. significant reduction in phosphorylation after 1 hour compared to 2 hours for total AURKA protein expression but on the other hand the decrease in total expression of AURKA seems to plateau from 2 to 6 hours post-release from nocodazole mediated arrest. This could suggest the phosphorylation of the protein, an indicator of catalytic activity, would firstly need to be 'switched off' before this can lead to degradation of the protein. A similar pattern was also seen in the phosphorylation of AURKB (Thr232), which declined significantly after 2 hours and this may have reflected the role of AURKB as being later in the cell cycle and into cytokinesis compared to AURKA. Phosphorylation of AURKC (Thr198) declined in a similar pattern to AURKB, which may have suggested a different role compared to the more rapid decrease in phosphorylation observed in PC3 cells (Section 3.2.1). Total protein expression of AURKB and C weren't measured in this study and this would need to be carried out to further substantiate the findings based on their phosphorylation.

As well as the phosphorylation of the AURKs and total expression of AURKA, the expression of the critical AURKA co-activator, TPX2, was also measured. The expression levels of TPX2 were not significantly reduced until after 6 hours (TR6) ($53.4 \pm 17.4\%$; $n=3$, $p<0.05$) compared to the TR0 sample. This seems to remain elevated for much longer in this prostate cancer cell line (LNCaP AIs) compared to the PC3 cells in Section 3.2.1. As expression of TPX2 remains higher for longer than AURKA, this could suggest that TPX2 could be dissociated from AURKA but not necessarily degraded in the cell. Lastly, the phosphorylation and total expression of the mitotic marker PLK1, was measured, which is also phosphorylated and regulated by AURKA (Gheghiani et al., 2017). With regards to the phosphorylation of PLK1, it was found to be significantly decreased after 2 hours (TR2) ($85.4 \pm 13.8\%$; $n=3$, $p<0.01$), 4 hours (TR4) ($74.6 \pm 2.4\%$; $n=3$, $p<0.05$) and 6 hours (TR6) ($72.9 \pm 14.5\%$; $n=3$, $p<0.05$) following release from nocodazole arrest relative to the TR0 sample. A similar pattern was observed for the total expression of PLK1 which was also significantly reduced after 2 hours (TR2) ($52.7 \pm 5.8\%$; $n=3$, $p<0.001$), 4 hours (TR4) ($79.9 \pm 3.7\%$; $n=3$, $p<0.001$) and 6 hours ($76.6 \pm 4.9\%$; $n=3$, $p<0.001$) relative to the TR0 sample.

Next, in Figure 4.2 (C) and (D) the same protein markers, as described above, were examined in the MCF7 breast cancer cell line. In this cell line, only the phosphorylation of AURKA and B were measured as phosphorylation of the AURKC isoform was too low to be quantifiable. In Figure 4.2, as shown by the immunoblotting (C) and subsequent quantification (D), there was a rapid, significant decrease in phosphorylation of AURKA following release at 1 hour ($54.0 \pm 10.1\%$; $n=3$, $p<0.05$), 2 hours ($72.8 \pm 20.8\%$; $n=3$, $p<0.01$), 4 hours ($84.1 \pm 12.6\%$; $n=3$, $p<0.01$) and 6 hours ($87.0 \pm 12.8\%$; $n=3$, $p<0.01$) compared to the samples from

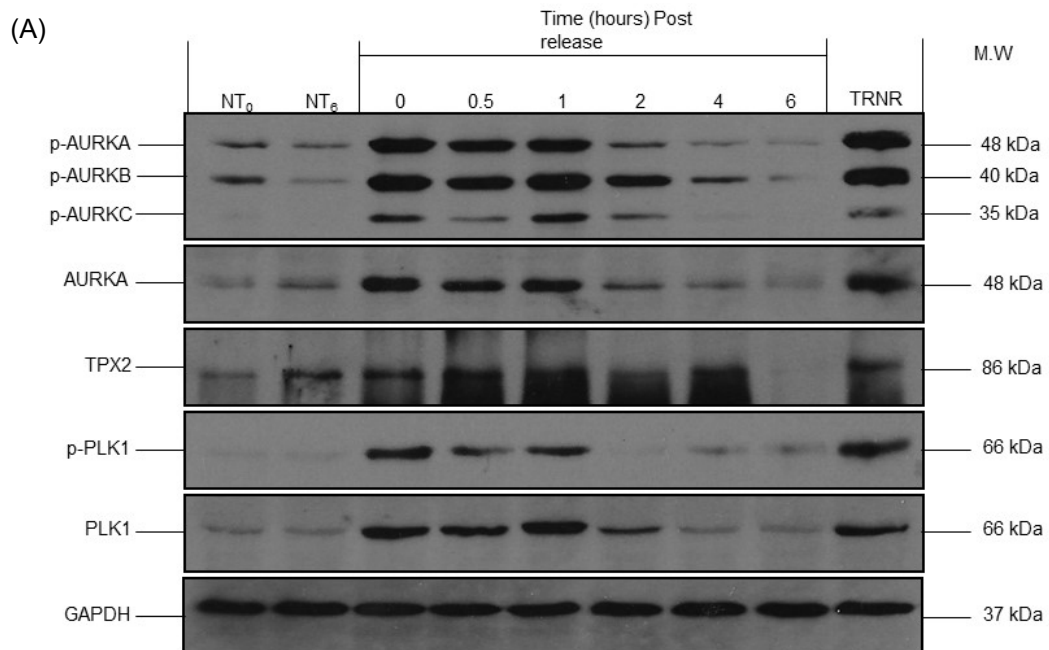
synchronised cells at the 0 time point (TR0). As before, phosphorylation of AURKB declined later post-release from nocodazole-mediated arrest, again reflecting its later role in mitosis. There was significant reduction in phosphorylation after 2 hours ($43.6 \pm 3.1\%$; $n=3$, $p<0.001$), 4 hours ($84.4 \pm 1.3\%$; $n=3$, $p<0.001$) and 6 hours ($93.6 \pm 2.7\%$; $n=3$, $p<0.001$).

The total expression of AURKA was also examined and as before it declined later than phosphorylation. It was significantly reduced after 2 hours ($53.6 \pm 8.6\%$; $n=3$, $p<0.05$), 4 hours ($56.1 \pm 17.1\%$; $n=3$, $p<0.05$) and 6 hours ($54.1 \pm 13.5\%$; $n=3$, $p<0.05$) relative to the TR0 sample. By the quantification indicated in Figure 4.2 (D), the detected phosphorylation of AURKA decreased faster kinetically than the total AURKA protein. Again, this was perhaps not unexpected given the phosphorylation of the protein, an indicator of catalytic activity, would firstly need to be 'switched off' prior to degradation of the protein. The critical AURKA co-activator TPX2 again peaked in mitosis and remained elevated before it was significantly reduced after 4 hours ($56.1 \pm 10.9\%$; $n=3$, $p<0.05$) and 6 hours ($63.0 \pm 11.9\%$; $n=3$, $p<0.01$) post-release compared to the TR0 sample. Lastly the mitotic regulator PLK1 displayed elevated levels of phosphorylation before it was significantly reduced after 4 hours ($59.9 \pm 7.1\%$; $n=3$, $p<0.01$) and 6 hours ($50.5 \pm 13.3\%$; $n=3$, $p<0.05$) following release from nocodazole mediated arrest. This was mirrored in the total expression of PLK1 which was also significantly reduced after 4 hours (39.7 ± 15.3 ; $n=3$, $p<0.05$) and 6 hours ($65.1 \pm 7.4\%$; $n=3$, $p<0.001$) post-release relative to the TR0 sample.

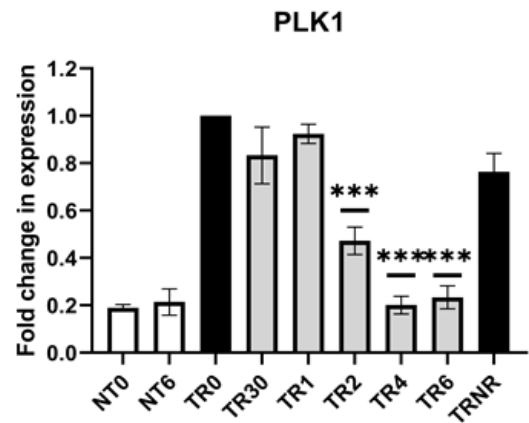
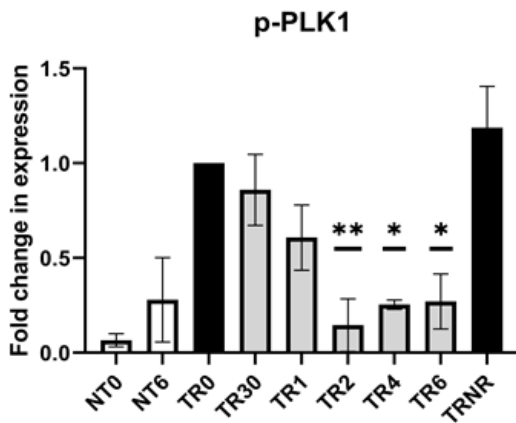
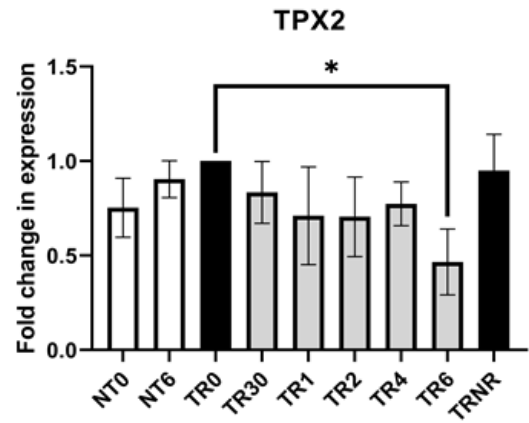
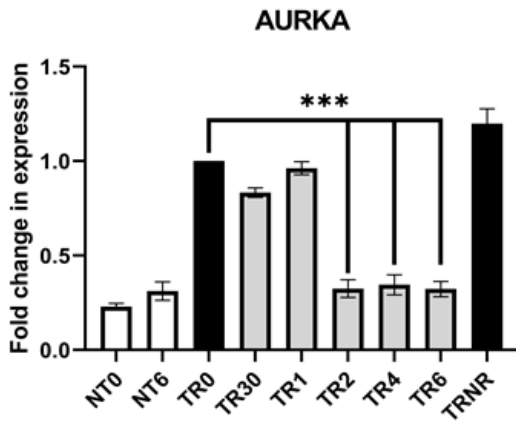
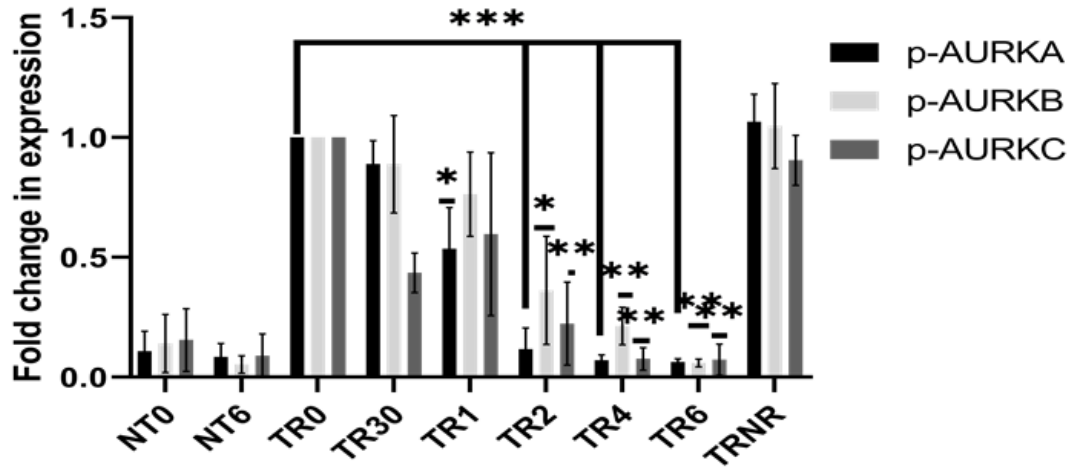
Lastly, in Figure 4.2 (E) and (F) T98G Glioblastoma cells were examined for the relevant markers to mirror those investigated previously in this Section in LNCaP AI and MCF7 cells. The phosphorylation of the AURKs (A, B and C) were expressed at their maximum level at the 0 hour time point, which compared consistently with the positive control (TR_{NR}) in which the cells had been trapped with nocodazole and not released while incubated for 6 hours. To begin with there was a significant decrease in phosphorylation of AURKA following release at 1 hour, TR1 ($35.2 \pm 8.4\%$; $n=3$, $p<0.05$), 2 hours (TR2) ($41.0 \pm 8.6\%$; $n=3$, $p<0.05$), 4 hours (TR4) ($45.3 \pm 5.4\%$; $n=3$, $p<0.01$) and 6 hours (TR6) ($63.3 \pm 8.4\%$; $n=3$, $p<0.001$) respectively, in comparison to the synchronised sample at the 0 time point (TR0). The phosphorylation of AURKB (Thr232) was also significantly reduced after 2 hours (TR2) ($59.7 \pm 4.5\%$; $n=3$, $p<0.05$), 4 hours (TR4) ($56.8 \pm 15.7\%$; $n=3$, $p<0.05$) and 6 hours (TR6) ($57.4 \pm 25.3\%$; $n=3$, $p<0.05$) relative to the normalised TR0 sample. The last of the AURK family, AURKC, was also examined in terms of phosphorylation (Thr198), but the expression was too low to be measured and quantified. The total expression of AURKA was also investigated to see if it mirrored the pattern of phosphorylation. The total expression peaked until it was significantly reduced at 6 hours ($63.1 \pm 11.3\%$; $n=3$, $p<0.05$) post-release from nocodazole-mediated arrest relative to the TR0 sample. This elevated total AURKA status late after release from

nocodazole-mediated arrest perhaps wasn't surprising as the phosphorylation of AURKA decreased faster kinetically than the total AURKA protein expression. Hence, the phosphorylation of the protein would firstly need to be 'switched off' prior to degradation of the protein. As before, TPX2 was also examined and its expression mirrored that of AURKA in that it was not significantly reduced until the 6-hour time point ($48.3 \pm 5.4\%$; $n=3$, $p<0.001$). Finally, the mitotic kinase PLK1 was also investigated. It peaked following arrest and was significantly reduced after 6 hours post-release from nocodazole mediated arrest both in terms of phosphorylation ($42.7 \pm 1.2\%$; $n=3$, $p<0.05$) and total expression ($36.8 \pm 2.2\%$; $n=3$, $p<0.05$).

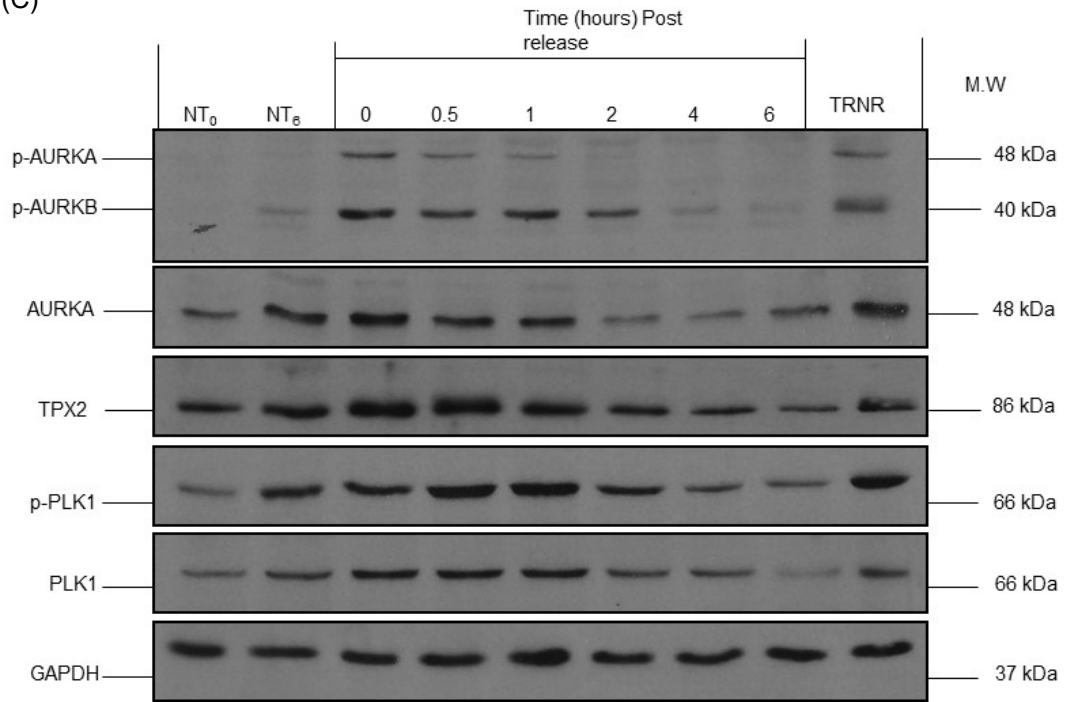
Collectively, these experimental outcomes demonstrated that nocodazole treatment of cells resulted in the arrest of LNCaP AI, MCF7 and T98G cells and could be used in future experimental work examining the potential effects of the NBD WT CPP on the same markers in these mitotic cells following nocodazole-mediated trap and release.



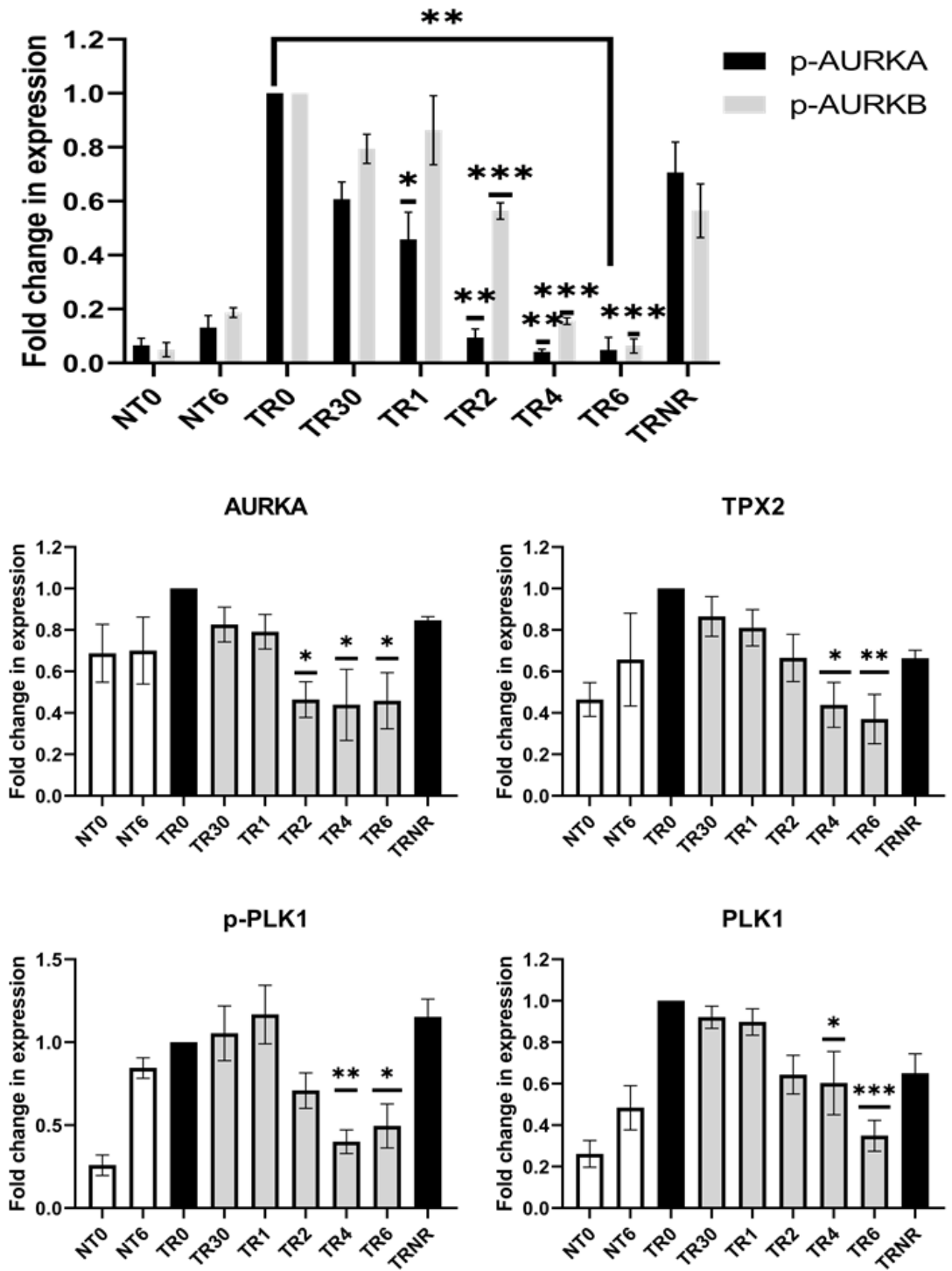
(B)



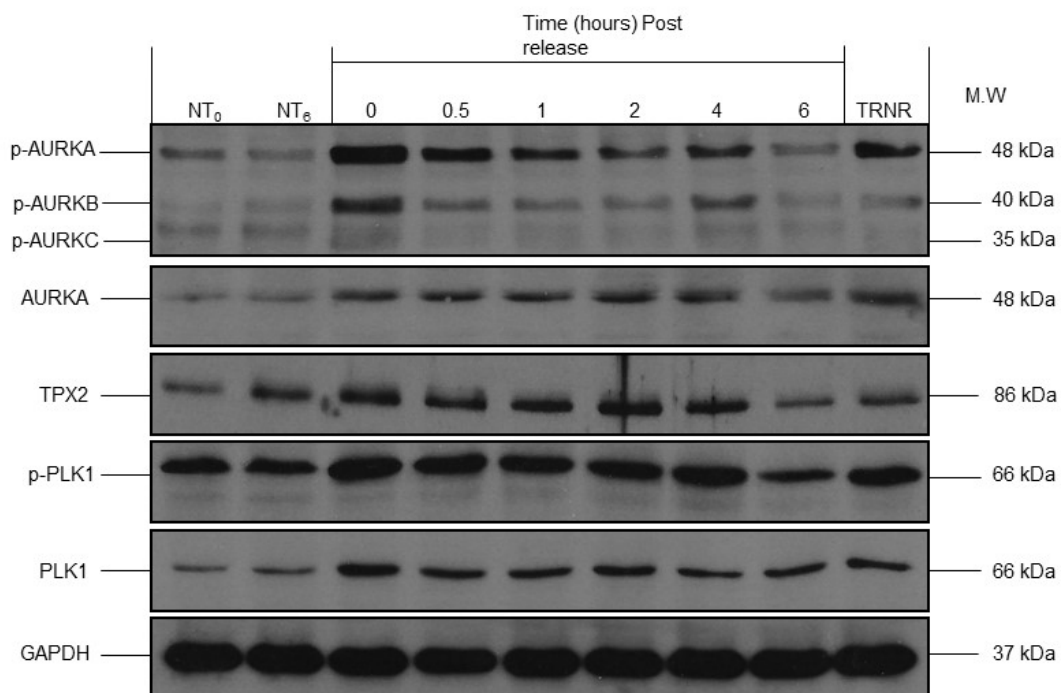
(C)



(D)



(E)



(F)

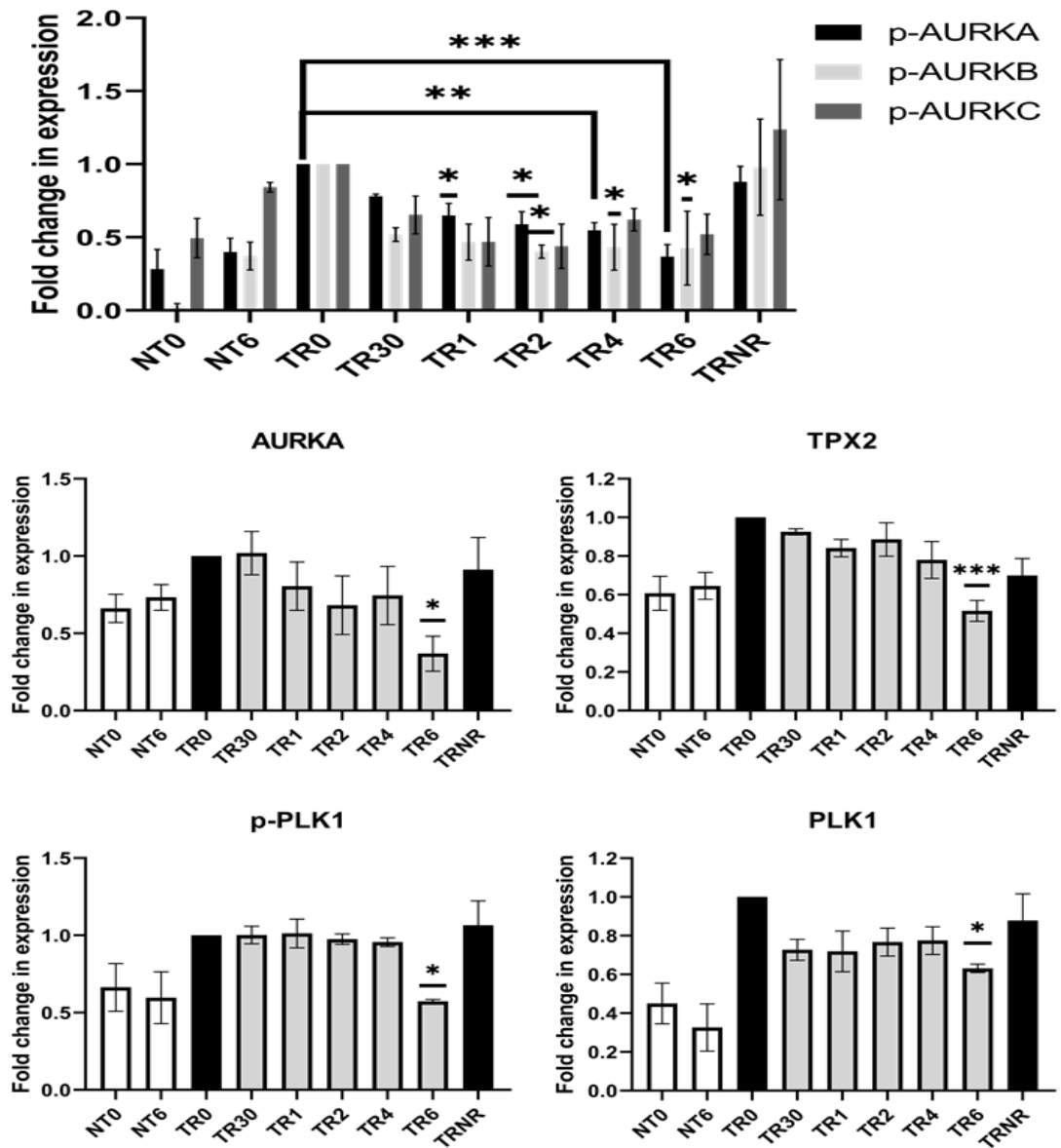


Figure 4.2. Assessment of the status of cell cycle markers following Nocodazole trap and release in LNCaP AI, MCF7 and T98G cells.

LNCaP AI (A + B), MCF7 (C + D) and T98G (E + F) cells were grown on 10mm dishes and treated with 50ng/ml Nocodazole (16-20 hours) and these were then released by washing twice with fresh media; times indicated as hours post-release from Nocodazole trap. Non-trapped cells at 0 and 6h (NT₀ and NT₆) represent the negative controls. Cells treated with Nocodazole but not washed and released represented the positive control (Trap and non-released, TR_{NR}). (A, C, E) whole cell lysates were prepared for separation using SDS-PAGE and analysed by Western Blotting using the above antibodies (n=3). GAPDH was used as a loading control. (B, D, F) Data was normalised to synchronised sample before release at the zero time point (TR₀) and represents mean \pm S.E.M. One-way ANOVA with post-hoc Dunnett's test was used to determine statistical significance ($p < 0.05$) of observed changes relative to TR₀ synchronised sample at 0 min. (*= $p < 0.05$, **= $p < 0.01$, ***= $p < 0.001$). All results indicated on graphs represent fold change in expression post-release from mitotic arrest compared to the TR₀ sample.

4.2.3. Effects of the NBD WT CPP on the status of AURKA and cell cycle markers following nocodazole trap and release in LNCaP AI, MCF7 and T98G cells.

As demonstrated previously in Section 3.3.1, the NBD WT CPP derived from IKK β can be shown to significantly ($p < 0.05$) decrease AURKA phosphorylation and total expression as well as the status of key related markers (TPX2, p-PLK1/PLK1) and therefore suggested to impact on IKK-Aurora signalling in PC3 cells. In this section experiments sought to demonstrate that this effect was transferable to other solid tumour cell lines (LNCaP AI, MCF7 and T98G). Cells were again treated with nocodazole (50ng/mL) for 16-20 hours prior to being washed and released as described previously – Section 2.2.2.1, before NBD MT or NBD WT peptides (100 μ M) were added upon release as described previously and samples prepared thereafter at appropriate time points.

Figure 4.3 (A) shows by immunoblotting the effect of the MT and WT NBD CPP on the status of p-AURKs, AURKA, TPX2 and p-PLK1/PLK1 post-trap and release in LNCaP AI cells. In Figure 4.3, from immunoblotting (A) and the associated quantification (B), the NBD WT CPP caused a significant ($p < 0.05$) reduction in phosphorylation of AURKA relative to the vehicle control at the same time point. The phosphorylation of AURKA post-release was reduced after treatment with the NBD WT CPP at 120 min relative to the vehicle treated sample at this time point ($42.9 \pm 2.8\%$ vs $11.4 \pm 5.8\%$; $n=3$, $p < 0.05$). The AURKA phosphorylation decreased naturally over time and this decrease in phosphorylation was accelerated by the NBD WT CPP. The reduction in total AURKA expression was also assessed to determine whether the kinetics of protein degradation were comparable to the NBD WT CPPs effect on AURKA phosphorylation. In Figure 4.3 (B), the NBD WT CPP caused a significant reduction in expression of total AURKA at 120 min relative to the vehicle treated control at this time point ($62.0 \pm 10.7\%$ vs $17.1 \pm 2.4\%$; $n=3$, $p < 0.001$). This suggested that the total expression of AURKA decreased naturally post-release from nocodazole-mediated arrest and is slightly accelerated by the NBD WT CPP but a wider timeframe may be needed to observe more significant changes in expression as a result of treatment with the NBD WT CPP. There was also a significant reduction in AURKB phosphorylation following treatment with the NBD WT CPP at 120 min in comparison with the vehicle control at the same time point ($47.9 \pm 2.7\%$ vs $8.5 \pm 2.9\%$; $n=3$, $p < 0.05$). This indicated that AURKB phosphorylation decreased naturally over time and this decrease in phosphorylation was accelerated significantly by the NBD WT CPP. Lastly, phosphorylation of AURKC was not significantly reduced ($p > 0.05$) by treatment with the NBD WT CPP relative to vehicle control at each of the individual time points. This could be as a result of its already low levels of expression or it may need a wider time frame

of treatment with the NBD WT CPP in the LNCaP AI cells. Expression of total AURKB and C were not measured and therefore it remains to be seen if the NBD WT CPP has an inhibitory effect on total protein expression across all AURK subtypes in the LNCaP AI cells. Figure 4.3 also showed the effect of the NBD WT CPP on the expression of the critical AURKA co-activator, TPX2. The NBD WT CPP significantly reduced levels of TPX2 at 120 min in comparison to the vehicle treated control at this time point ($79.5 \pm 5.7\%$ vs $31.4 \pm 5.0\%$; $n=3$, $p<0.01$). In Figure 4.3 (B), the NBD WT CPP significantly reduced phosphorylation of PLK1 at the 60 min ($53.4 \pm 14.6\%$; $n=3$, $p<0.05$) and 120 min relative to the vehicle control at 0 min ($78.1 \pm 11.1\%$; $n=3$, $p<0.001$). At the 120-minute time point, this decrease in phosphorylation was significant ($p<0.05$) but there was also a statistically significant decrease in phosphorylation measured in cells treated with the vehicle control ($62.9 \pm 5.5\%$; $n=3$, $p<0.01$) and NBD MT CPP ($67.3 \pm 13.6\%$; $n=3$, $p<0.01$). This indicates that PLK1 phosphorylation decreased naturally over time and this decrease in phosphorylation was accelerated by the NBD WT CPP. Phosphorylation of PLK1 was not significantly reduced ($p>0.05$) by the NBD WT CPP relative to vehicle control at each of the individual time points. This could be as a result of its already low levels of expression or it may need a wider time frame of treatment with the NBD WT CPP in the LNCaP AI cells. Total expression of PLK1 was then assessed to see if the effect of the NBD WT CPP on total protein levels of PLK1 was comparable to its effect on phosphorylation. Figure 4.3 (B) shows that there was a significant reduction in total PLK1 expression induced by the peptide at 120 min in comparison to the vehicle control at this time point ($71.9 \pm 13.1\%$ vs $14.6 \pm 3.1\%$; $n=3$, $p<0.05$). This significant reduction in total expression of PLK1 following treatment with the NBD WT CPP compared to no significant change in phosphorylation could be as a result of shorter differences in time frames needed to observe the NBD WT CPP effect on phosphorylation.

Next, in Figure 4.3 (C) and (D) the exact same markers were examined as above to investigate the impact of the NBD WT CPP in the MCF7 breast cancer cell line. As mentioned before in Section 4.2.2, in this cell line only the phosphorylation of AURKA and B were measured out of the three subtypes as phosphorylation of AURKC was expressed too low to be quantifiable. As shown by the immunoblotting (C) and subsequent quantification (D), phosphorylation of AURKA post-release was reduced after treatment with the NBD WT CPP at 30 min ($90.4 \pm 0.8\%$ vs $63.7 \pm 10.8\%$; $n=3$, $p<0.01$) and 60 min ($75.9 \pm 7.4\%$ vs $44.0 \pm 8.4\%$; $n=3$, $p<0.01$) relative to the vehicle treated sample at these time points. This indicates that AURKA phosphorylation decreased naturally over time and this decrease in phosphorylation was accelerated significantly by the NBD WT CPP. The reduction in total AURKA expression was assessed to determine if it was comparable to the NBD WT CPPs effect on AURKA phosphorylation. In Figure 4.3 (D), the NBD WT CPP caused a significant reduction in

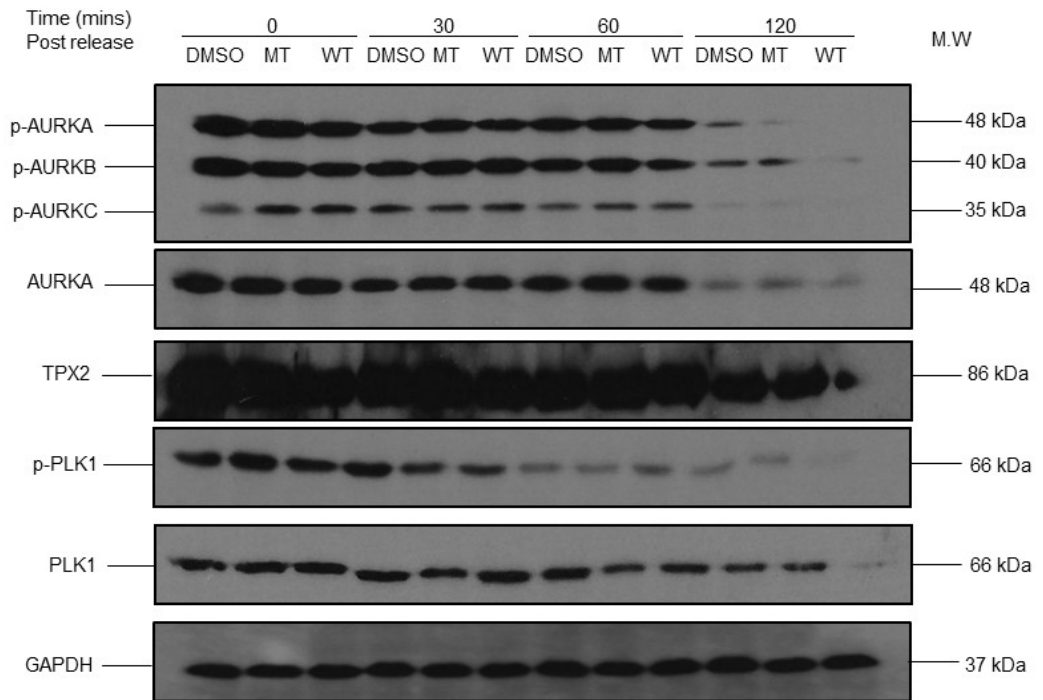
expression of total AURKA at 60 min post-release from nocodazole mediated arrest relative to the vehicle treated sample at this time point ($93.3 \pm 1.3\%$ vs $51.9 \pm 6.9\%$; $n=3$, $p<0.05$). There was also a significant reduction in AURKB at each time point post-release after treatment with the NBD WT CPP at 30 min ($93.9 \pm 2.5\%$ vs $48.9 \pm 7.1\%$; $n=3$, $p<0.001$), 60 min ($91.4 \pm 0.8\%$ vs $43.8 \pm 1.5\%$; $n=3$, $p<0.001$) and 120 min ($71.5 \pm 12.9\%$ vs $36.0 \pm 1.6\%$; $n=3$, $p<0.01$) relative to the vehicle control at these individual time points. As was detailed in LNCaP AI cells, the impact of the NBD CPPs on TPX2 in MCF7 cells was also measured. The expression of TPX2 was significantly reduced in the NBD WT CPP treated sample at 60 min ($92.8 \pm 1.5\%$ vs $66.2 \pm 6.6\%$; $n=3$, $p<0.01$) and 120 min ($79.4 \pm 5.3\%$ vs $30.4 \pm 5.5\%$; $n=3$, $p<0.001$) post-release from nocodazole mediated arrest relative to the vehicle treated sample at these time points. The impact of the NBD peptides on the critical mitotic regulator and G₂/M marker, PLK1 was also investigated, both in terms of total expression and phosphorylation. There was a significant reduction in phosphorylation of PLK1 in the sample treated with the NBD WT CPP and released from nocodazole mediated arrest at 60 min ($92.8 \pm 1.5\%$ vs $60.0 \pm 3.1\%$; $n=3$, $p<0.01$) and 120 min ($68.0 \pm 7.6\%$ vs $34.8 \pm 17.5\%$; $n=3$, $p<0.01$) relative to the vehicle treated control at these time points. Total expression of PLK1 was then assessed to see if impact of the NBD WT CPP was comparable to its effect on phosphorylation. Figure 4.3 (D) shows that there was a significant reduction in total PLK1 expression induced by the WT peptide at 60 min ($81.5 \pm 2.7\%$ vs $36.0 \pm 3.0\%$; $n=3$, $p<0.05$) and 120 min ($55.8 \pm 7.5\%$ vs $12.7 \pm 2.2\%$; $n=3$, $p<0.05$) post-release, relative to the vehicle treated sample at these time points. Total PLK1 expression decreased naturally over time and the decrease in protein expression was accelerated by the NBD WT CPP. This suggest that the NBD WT CPP caused PLK1 to be degraded, as observed in the nocodazole trapped cells (Figure 4.3 C and D) and promoted inhibition of phosphorylation of PLK1. Mechanistically this may have been either as a result of the impact of the NBD WT CPP on upstream AURKA-TPX2 or a direct effect on PLK1 itself.

Lastly, in Figure 4.3 (E) and (F), T98G Glioblastoma cells were examined for the relevant markers to investigate the impact of the NBD CPPs in this cell line as demonstrated previously in LNCaP AI and MCF7 cells. The phosphorylation of the AURK subtypes (A, B and C) were examined as before and as has been the case previously, AURKC phosphorylation was expressed too low to extract any accurate data from and as such all results were shown to be not significant ($p>0.05$). In fact, phosphorylation of AURKA and AURKB were also shown to not be significantly reduced by the NBD WT CPP compared to the vehicle at each time point. This may be due to NBD WT CPP not being as effective in this cell type or may need a wider time frame of treatment than the time points used. The reduction in total AURKA expression was assessed to determine if it was comparable to the NBD WT

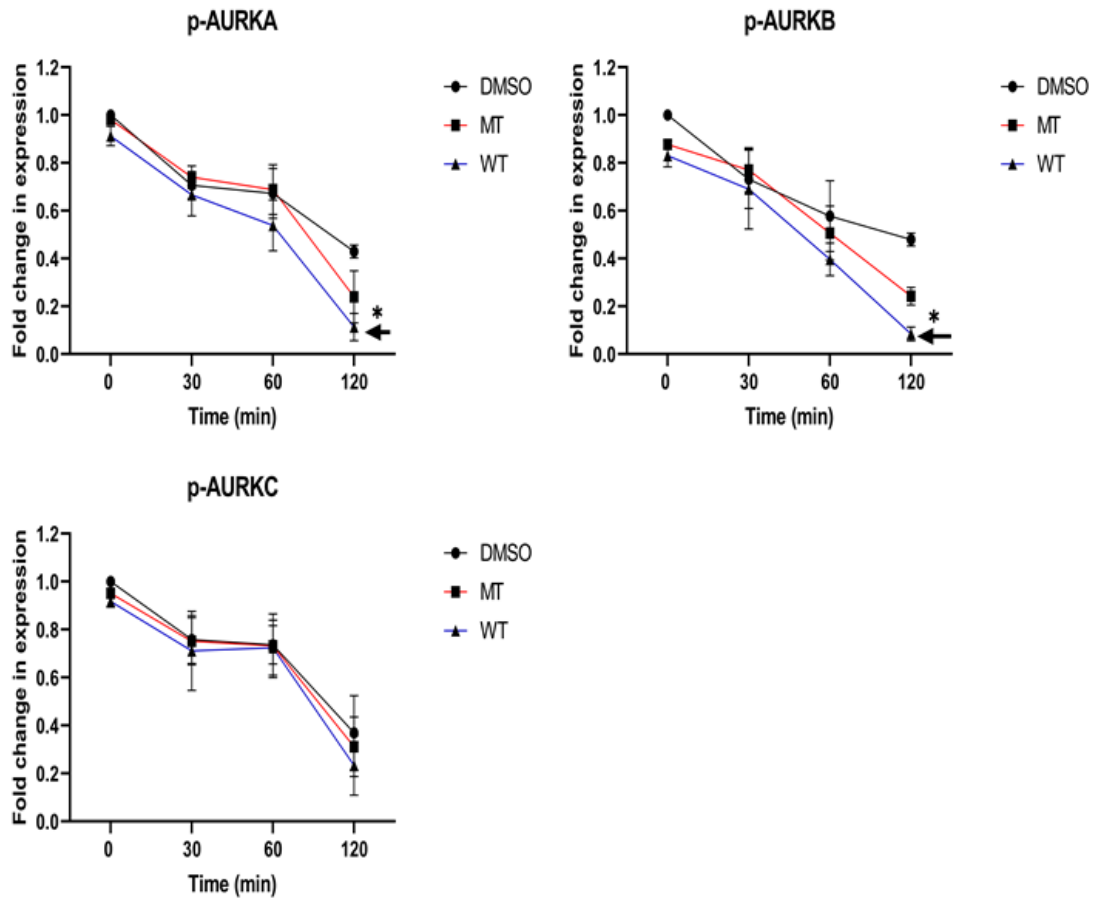
CPPs effect on AURKA phosphorylation. In Figure 4.3 (F), the NBD WT CPP caused a significant reduction in expression of total AURKA at 120 min post-release from nocodazole mediated arrest relative to the vehicle treated sample at this time point ($83.9 \pm 12.9\%$ vs $24.1 \pm 12.4\%$; $n=3$, $p<0.05$). In T98G cells, the NBD WT CPP significantly reduced expression of the essential AURKA co-activator TPX2 at 120 min post-release compared to the vehicle treated sample at this time point ($83.2 \pm 7.6\%$ vs $49.8 \pm 5.6\%$; $n=3$, $p<0.05$). As conducted in the other cell lines, the impact of the NBD WT CPP on PLK1 status was also investigated. The NBD WT CPP significantly reduced both the phosphorylation ($79.9 \pm 5.8\%$ vs $56.1 \pm 8.6\%$; $n=3$, $p<0.05$) and total expression of PLK1 ($77.1 \pm 7.0\%$ vs $26.1 \pm 23.5\%$; $n=3$, $p<0.01$) at 120 min post-release from nocodazole-mediated arrest in comparison to the vehicle treated sample at these time points.

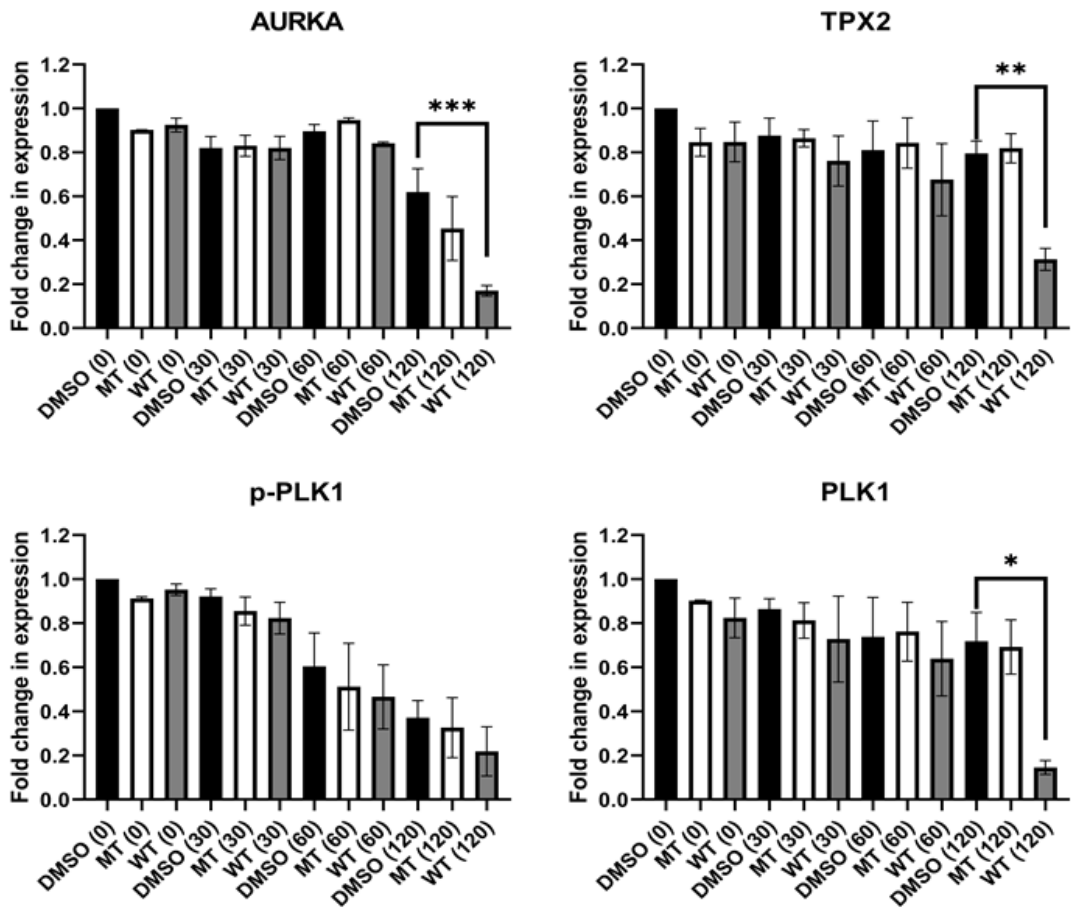
Collectively, these experimental outcomes demonstrated the ability of the NBD WT CPP to impact on the status of AURKA and its related protein markers of mitosis across different solid tumour cell lines (LNCaP AIs, MCF7 and T98G). Whilst the NBD WT CPP was shown to have different effects on these relevant markers across the different cell lines, with varying degrees of impact and kinetics, it commonly 'accelerated' the decrease in phosphorylation/expression of AURKA and related mitotic markers. This may represent and identify a potentially wider ranging utility of the NBD WT CPP for perturbation of AURK-related signalling across different solid tumour types

(A)

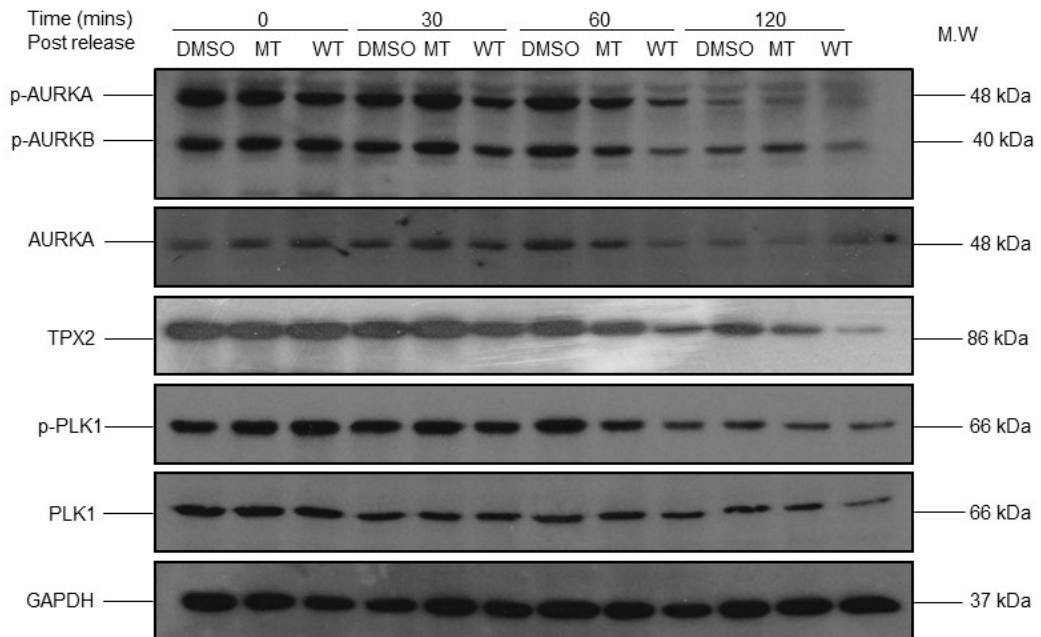


(B)

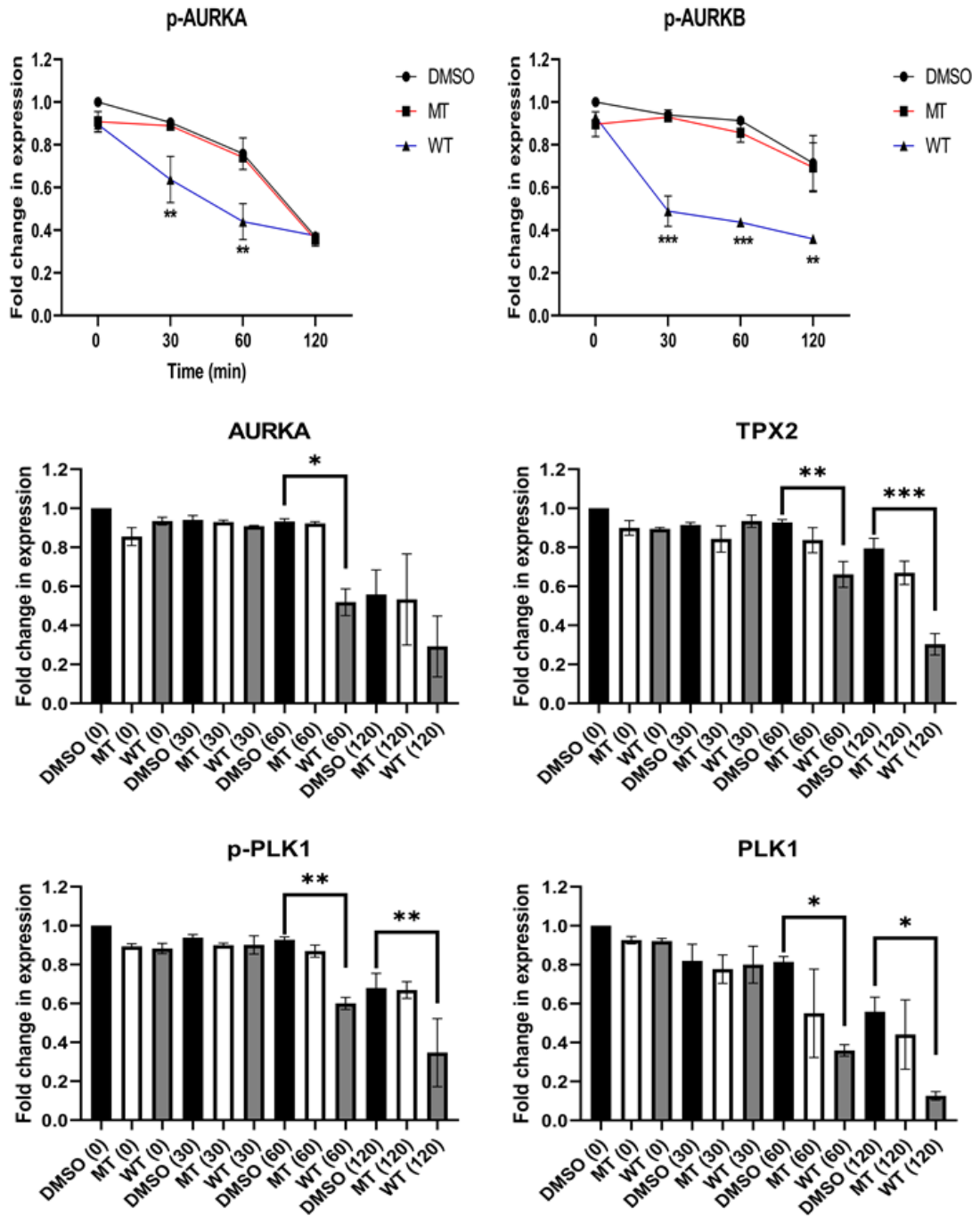




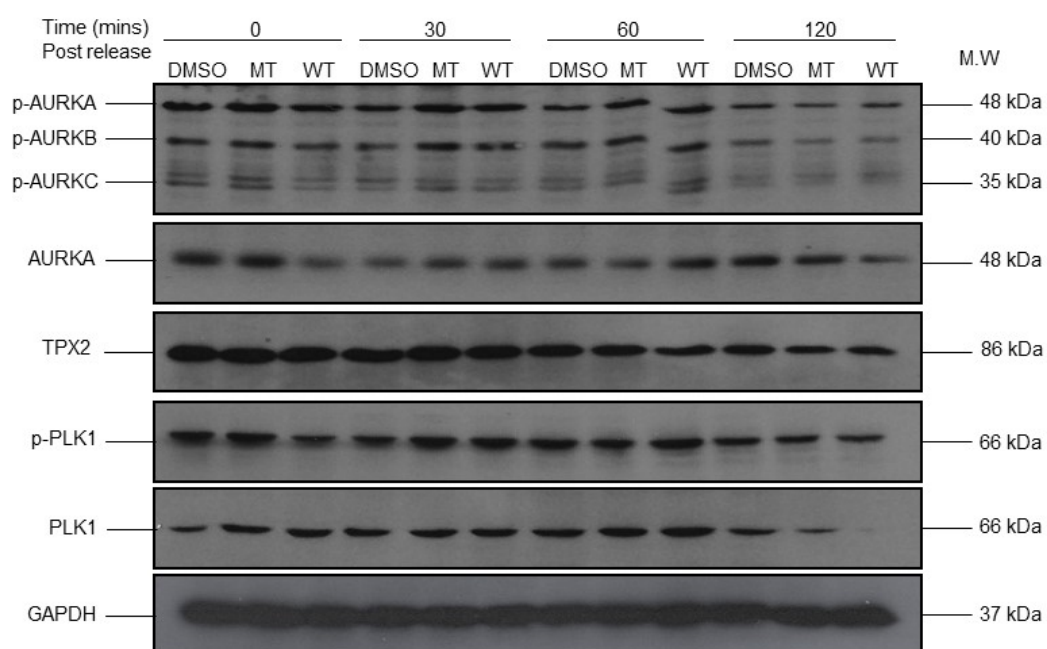
(C)



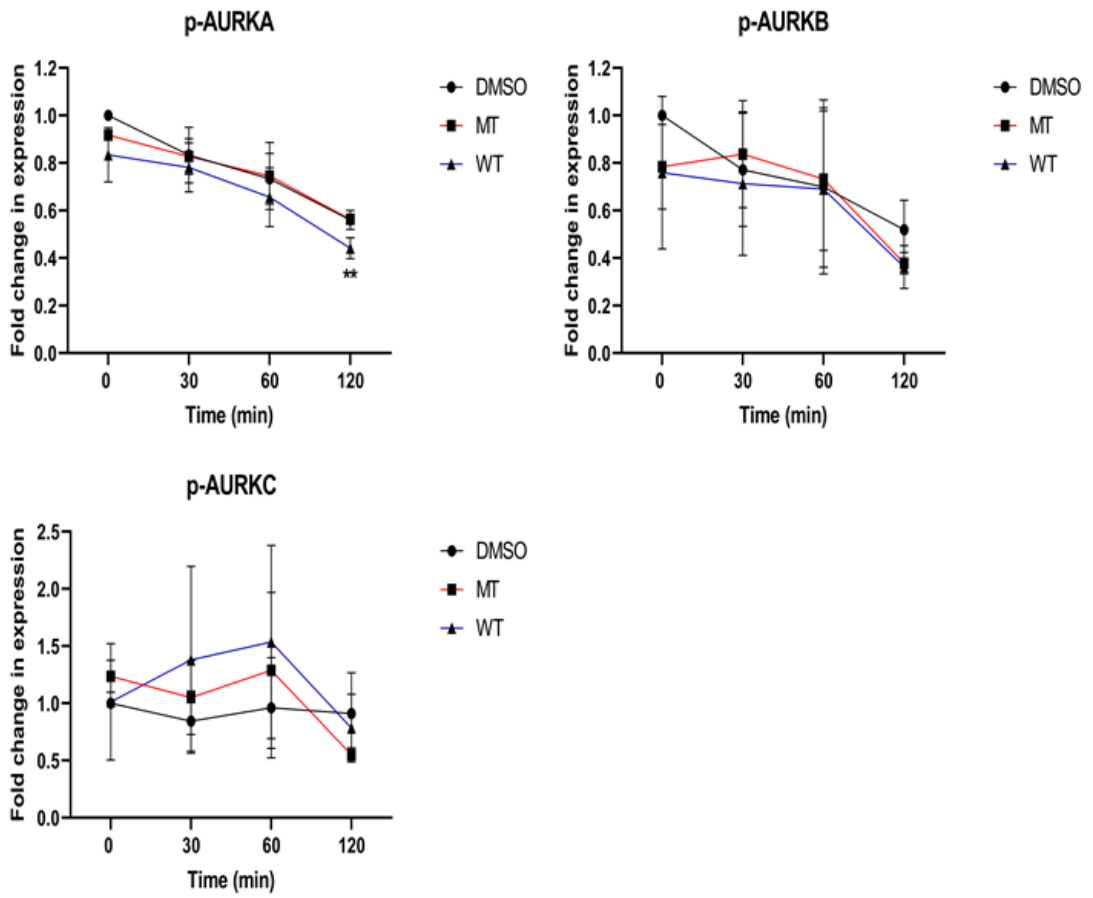
(D)



(E)



(F)



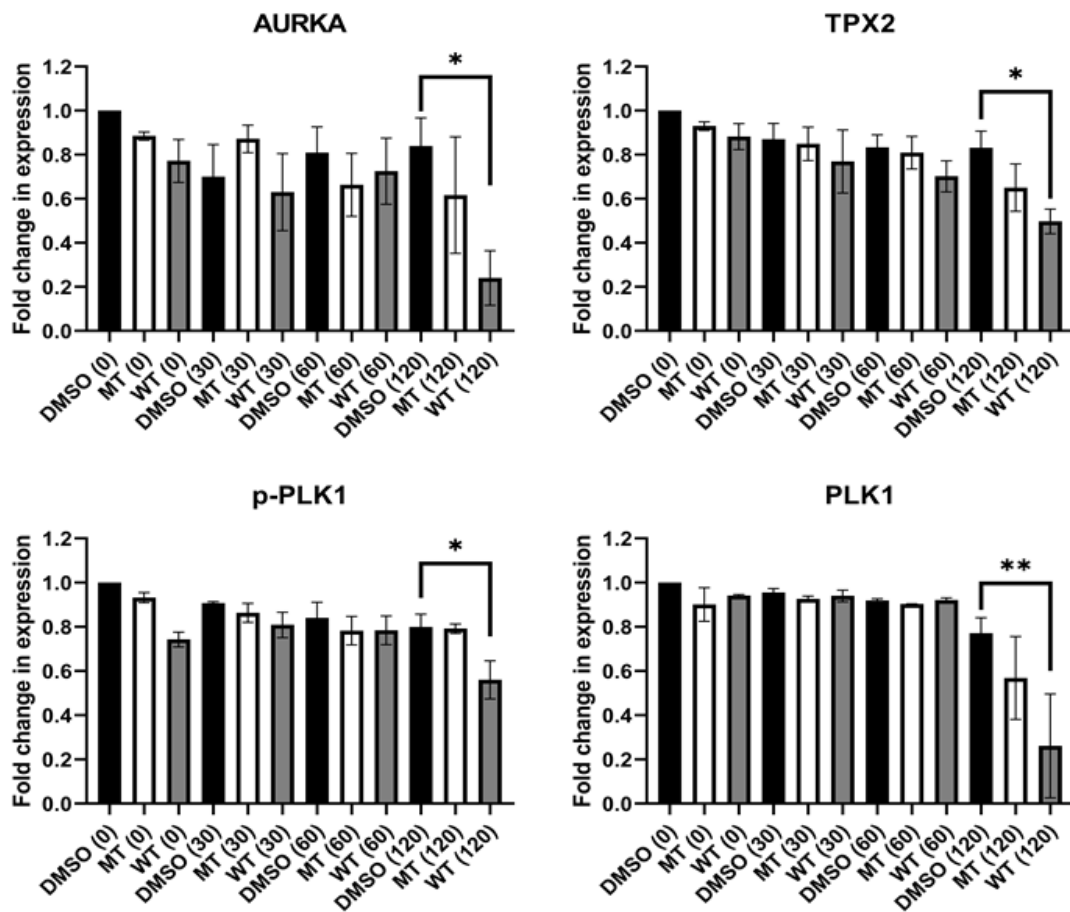


Figure 4.3. Impact of NBD WT CPP on AURKs and related protein markers of mitosis in LNCaP AI, MCF7 and T98G cells.

LNCaP AI (A + B), MCF7 (C + D) and T98G (E + F) cells were grown on 10mm dishes and treated with 50ng/ml Nocodazole (16-20 hours) prior to treatment with either NBD WT or MT (100µM) or DMSO as a vehicle control (0.5% (v/v)) before release from trap for 30min, 60min and 120min. (A, C, E) Whole cell lysates were prepared for separation using SDS-PAGE and analysed by Western Blotting using the above antibodies (n=3). GAPDH was used as a loading control. (B, D, F) Data was normalised to the vehicle treated control at 0 min (DMSO 0) and represents mean ± S.E.M. One-way ANOVA with post-hoc Dunnett's test was used to determine statistical significance (p<0.05) of observed changes induced by the peptides relative to vehicle control at the retrospective time point. (*= p<0.05, **= p<0.01, ***=p<0.001). **LNCaP:** p-AURKA: WT(120) vs DMSO(120), *p<0.05. p-AURKB: WT(120) vs DMSO(120), *p<0.05. **MCF7:** p-AURKA: WT(30) vs DMSO(30), **p<0.01; WT(60) vs DMSO(60), **p<0.01. p-AURKB: WT(30) vs DMSO(30), ***p<0.001; WT(60) vs DMSO(60), ***p<0.001; WT(120) vs DMSO(120), **p<0.01. **T98G:** p-AURKA: WT(120) vs DMSO(120), *p<0.01.

4.2.4. Effects of the NBD CPPs on cell viability in PC3, LNCaP AI, MCF7 and T98G cells.

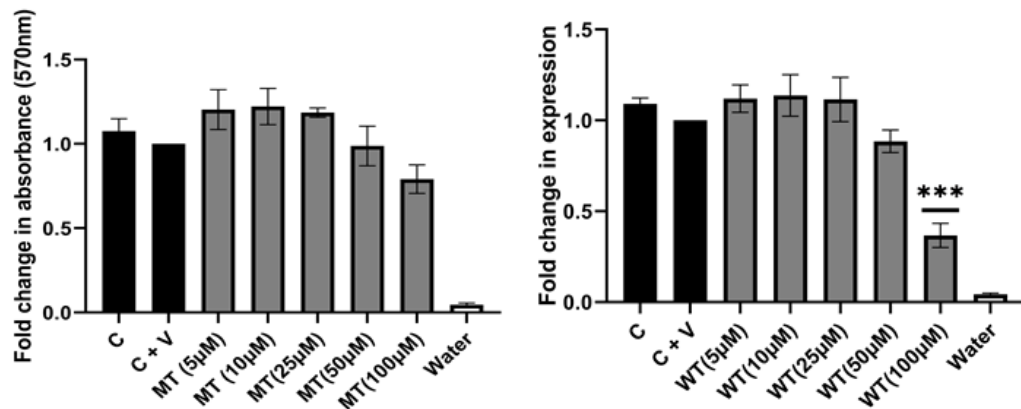
Following on from examining the NBD peptides mechanistically across different solid tumour cell lines in Section 4.2.3, experiments then sought to investigate any potential impact of the NBD WT CPP phenotypically across these cell lines (PC3, LNCaP AI, MCF7 and T98G cells). This allowed a comparison of the selected cell lines (representative of major solid tumour types) with the PC3 cells, in terms of potency against cell viability. This could then be correlated with and related to the impact of the NBD CPPs on AURKs and related markers, as described in the previous section. In order to assess the impact of the NBD WT CPP phenotypically in these different cell lines, the MTT cell viability (i.e. the proportion of live or healthy cells in a sample) assay was carried out based on a method detailed by Zhang et al. (2019) and described in Section 2.2.7.1 of the Materials and Methods.

In Figure 4.4 cells were treated with vehicle (0.5% DMSO (v/v)) or a range of concentrations (5 μ M, 10 μ M, 25 μ M, 50 μ M and 100 μ M) of either the NBD WT CPP or NBD MT CPP for 72h prior to MTT assay and subsequent analysis and quantification. PC3 cells (A) treated with the NBD WT CPP showed a significant reduction in cell viability at a concentration of 100 μ M (63.3 \pm 6.7%; n=3, p<0.001) and when analysed further (E) displayed an IC₅₀ of 51.31 μ M for the impact of the NBD WT CPP on cell viability in PC3 cells. In the other prostate cancer cell line, LNCaP AI's (B), the NBD WT CPP demonstrated a more potent effect as there was a significant reduction in cell viability at 50 μ M (43.6 \pm 4.8%; n=3, p<0.01) and 100 μ M (54.7 \pm 5.1%; n=3, p<0.001). Indeed, further analysis (E) confirmed this and showed an IC₅₀ of 35.76 μ M for the impact of the NBD WT CPP on cell viability in LNCaP AI cells. Conversely, in the MCF7 breast cancer cell line (C), the effect on cell viability was not as potent even though there was a significant reduction at 100 μ M (52.2 \pm 7.9%; n=3, p<0.05) and this was confirmed (E) as the NBD WT CPP produced a much higher IC₅₀ (83.38 μ M) for the impact on cell viability in MCF7 cells. Lastly, in the T98G Glioblastoma cell line, the NBD WT CPP showed a significant decrease in cell viability across all concentrations; 5 μ M (30.0 \pm 1.4%; n=3, p<0.001), 10 μ M (29.3 \pm 3.2%; n=3, p<0.001), 25 μ M (21.1 \pm 4.7%; n=3, p<0.01), 50 μ M (31.0 \pm 5.6%; n=3, p<0.001) and 100 μ M (59.6 \pm 2.9%; n=3, p<0.001) respectively. Further inspection shows that this reduction in cell viability was only 20-30% in concentrations below 100 μ M and this is highlighted in Figure 3.4 (E) which indicates an IC₅₀ of 75.16 μ M for the impact of the NBD WT CPP on cell viability in T98G cells. The NBD MT CPP showed no significant (p>0.05) reduction in cell viability across all concentrations in the different cell types.

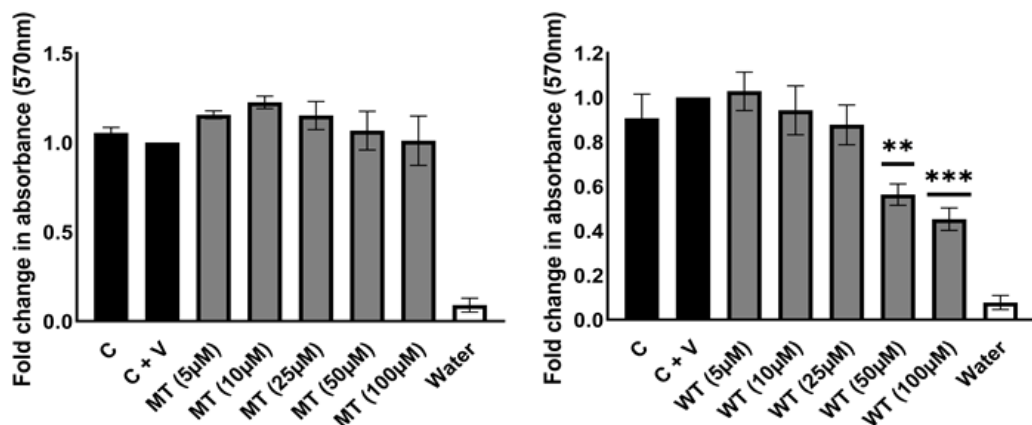
To summarise, these results indicated that the NBD WT CPP can impact phenotypically across the different solid tumour cell types and particularly at the concentration

(100 μ M) that was used routinely in all other cell-based assays. At the 100 μ M concentration used routinely in our cell-based assays there was never a full inhibition across all the cell types used here. Only partial inhibition was observed as there was typically a residual 20-30% viability remaining and therefore may need a higher concentration of the NBD WT CPP to cause full abolition of cell viability or this represents other cellular pathways contributing to the regulation of cell viability and proliferation. Due to its demonstrated effect at targeting the AURKs and related markers across these cell lines, this would suggest that this a plausible pharmacological intervention going forward that could be investigated as a single-agent or a combination approach that targets other aspects of AURK signalling.

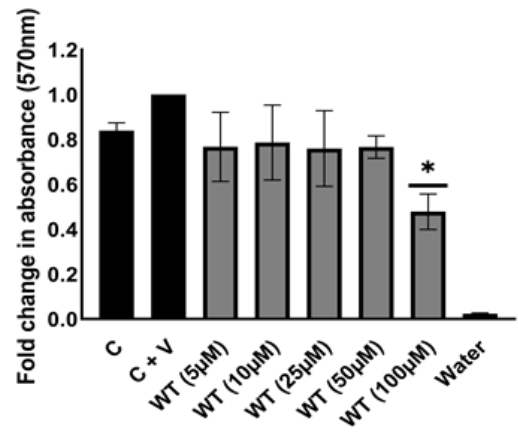
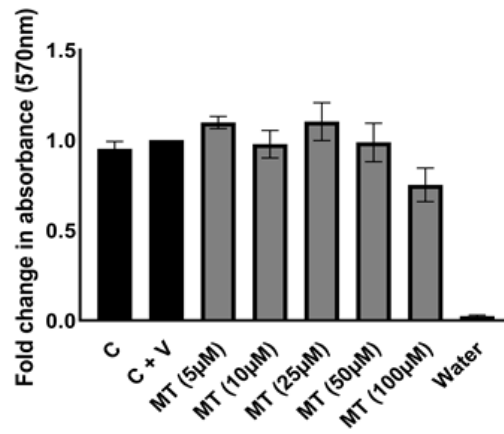
(A)



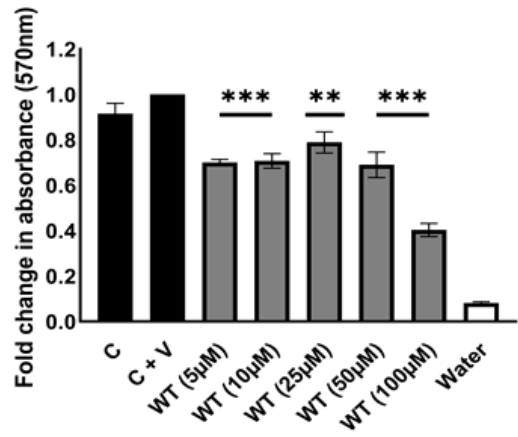
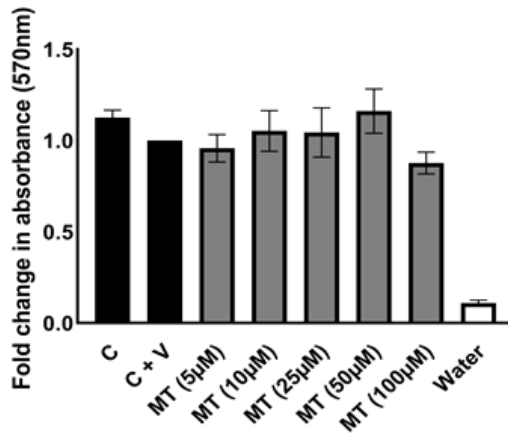
(B)



(C)



(D)



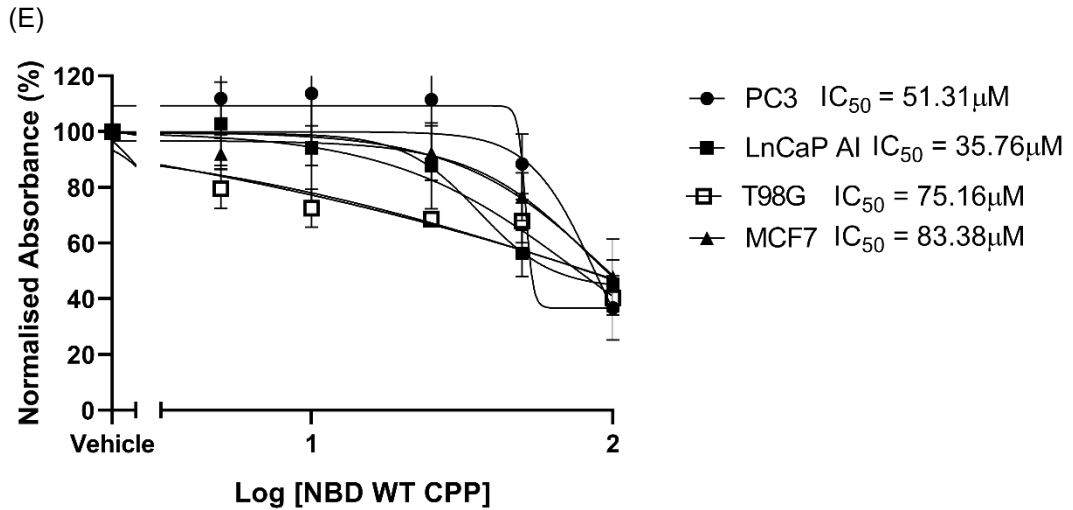


Figure 4.4. Impact of NBD CPPs on cell viability of solid tumour cell lines.

PC3 (A), LNCaP AI (B), MCF7 (C) and T98G (D) cells were seeded into 96-well plates and treated with increasing concentrations (0-100 μM) of NBD MT or WT CPPs for 72h. Cell viability was measured using the MTT assay. DMSO was used as a vehicle (V) control (0.5% (v/v)). Cells cultured in media with no treatment represented the positive control (C). Cells cultured in water represented the negative control (Water). Data was normalised to the vehicle control (C + V) and represents mean \pm S.E.M of fold change in absorbance at 570nm (n=3). Triplicates were averaged for each experiment. One-way ANOVA with post-hoc Dunnet's test was used to determine statistical significance ($p < 0.05$) of observed changes relative to control (C). (*= $p < 0.05$, **= $p < 0.01$, ***= $p < 0.001$). (E) Comparison of the potency of the effect of the NBD WT CPP on cell viability in PC3 (●), LNCaP AI (■), MCF7 (▲) and T98G (□) cells. Cells were treated with a full concentration range of 5 μM , 10 μM , 25 μM , 50 μM and 100 μM of the NBD WT CPP. The results were normalised to vehicle treated control and plotted on a log scale as a percentage of the control relative to absorbance (n=3). The data was fitted with the following equation $Y = \text{Bottom} + (\text{Top} - \text{Bottom}) / (1 + 10^{((\text{Log}IC_{50} - X) * \text{HillSlope}))}$.

4.3. Discussion.

AURKA is recognised to play a pathological role and be upregulated at its chromosome locus (20q13) and at both the transcriptional and translational levels in a number of human cancers and established cultured cells representative of them including; pancreatic, colorectal, breast, ovarian, stomach, cervical and neuroblastoma settings (Briassouli et al., 2007, Kufer et al., 2002). For example, related to breast cancer AURKA acted as a positive regulator of YAP (Yes-associated protein) in the “triple negative” sub-type – where the estrogen receptor, progesterone receptor and HER2 receptor are all not expressed (Chang et al., 2017). Also, in pancreatic adenocarcinomas (a very aggressive cancer with average 5-year survival of only 5% of patients), overexpression of AURKA has been speculated to cause resistance to the taxane family of chemotherapeutics (Anand et al., 2003, Lin et al., 2012). Inhibition of AURKA not only led to reduced tumour cell growth and cell cycle arrest but also increased sensitivity to these aforementioned taxanes (Warner et al., 2006). Thus, it was proposed by Lin et al. (2012) that an inhibitor specific for AURKA in synergism with paclitaxel (taxane chemotherapeutic) could be a possible combination treatment in pancreatic cancer. The studies described above support the consideration of AURKA as a therapeutic target not just in prostate cancer, but in a wide variety of solid tumours.

4.3.1. NBD CPP targeting of AURKA signalling in other solid tumour cell lines.

Prior to the construction of studies designed to test the ability of the NBD WT CPP to impact on the AURKA signalling across the different solid tumour cell lines (LNCaP AI, MCF7 and T98G), the conditions of nocodazole-mediated arrest, in terms of nocodazole concentration had to firstly be optimised and established for each cell line examined (Figure 4.1). The standard ‘wash and release’ procedure that was first utilised in Section 3.2.1 and as described in Section 2.2.2.1 of the Materials and Methods was adapted by optimising the nocodazole concentration used for each cell line. This was utilised to determine the status of each marker (p-AURKs, AURKA, TPX2, p-PLK1/PLK1) as the cells progressed through the cell cycle and to properly assess the impact of the NBD CPPs on each mitotic marker in these different solid tumour cell lines. Unsurprisingly, the cell lines used in this study (PC3, LNCaP AI, MCF7,

T98G) were synchronised successfully. Nocodazole has been used in this context for many years (Zieve et al., 1980). and has been demonstrated to synchronise successfully a number of solid tumour cell types used in this section (prostate, breast and brain) among other cancers (pancreatic, renal, lung etc.) (Amin et al., 2014, Gully et al., 2012, Kim et al., 2008, Yang et al., 2014, Zadra et al., 2014). A study by Martins and Kolega (2012) showed the inability of cells to completely restore motility via microtubule mobilisation following treatment with high concentrations of nocodazole. It was also observed in the MCF7 cells and T98G cells that there was a decrease in proliferation in the samples treated with 200ng/ml and 400ng/ml and both Martins and Kolega (2012) and Signoretto et al. (2016) indicated that high concentrations of nocodazole can lead to toxicity.

In Figure 4.3, the the different solid tumour cell lines (LNCaP AI, MCF7, T98G) were treated with the NBD WT CPP to mirror work carried out previously in Section 3.3.1, to investigate whether the demonstrated effect of NBD WT CPP on the status of p-AURKs, AURKA, TPX2 and p-PLK1/PLK1 in PC3 cells was translatable to other cancer types. Similarly to the PC3 cells, the NBD WT CPP significantly reduced ($p < 0.05$) phosphorylation of AURKA and B (p-AURKC was not significantly reduced) in LNCaP AI cells and phosphorylation of AURKA and B in MCF7 cells (AURKC phosphorylation was not measurable as mentioned before). Interestingly, this was highlighted by Zekri et al. (2012) in that AURKC expression was low at the mRNA level in MCF7 cells but conversely the more aggressive, triple-negative breast cancer cell line MDA-MB-231 showed increased mRNA expression. The NBD WT CPP induced no significant ($p > 0.05$) accelerated reduction in the phosphorylation of any of the AURK subtypes in the T98G cell line. This could have been as a result of a multitude of factors; these cells may have needed to be left for longer incubation times post-release to see an effect or the NBD peptide may not be as potent against certain key markers in this cell type. There was a sub-maximal impact on cell viability exerted by the NBD WT CPP and this could indicate that more than one agent may be needed to target different key markers. Interestingly, when targeting AURKs in cancer, most studies utilised a combination approach as opposed to single agent treatment (Borges et al., 2012). Also, overexpression of AURKA and B have been shown to be involved in the upregulation of the Telomerase Reverse Transcriptase (TERT) promoter which is mutated in the T98G cell line and leads to the overexpression of TERT and resultant tumorigenesis in the Glioblastoma setting (Johanns et al., 2016, Smith et al., 2005, Yang et al., 2004). The TERT gene promotes tumorigenesis by initiating the production of Telomerase, an enzyme which prevents telomeres from shortening and hence allowing the cancer cells to avoid senescence or apoptosis (Johanns et al., 2016). The expression of AURKA and the well-established co-activator TPX2 were significantly ($p < 0.05$) decreased by the NBD WT CPP across all cell types and this was also similarly

observed in the critical mitotic regulator PLK1. PLK1 was significantly ($p < 0.05$) decreased both in terms of total expression and phosphorylation by the NBD WT CPP across all three cell lines (LNCaP AIs, MCF7 and T98G). This indicated that these NBD WT CPP-mediated effects on the status of p-AURKs, AURKA, TPX2 and p-PLK1/PLK1 were translatable to other cancer cell types and may identify a potential means of intervention in solid tumours by off-setting aberrant AURK-related signalling. At that stage the next question, built on these experimental findings, related to whether there was any correlatable impact of the NBD WT CPP phenotypically on the growth and survival of these different solid tumour cell lines (PC3, LNCaP AIs, MCF7 and T98G).

4.3.2. NBD CPP targeting of cell growth in different cancers.

The NBD peptide has been considered extensively in the literature in terms of a potential therapeutic intervention (Dai et al., 2004, Gaurnier-Hausser et al., 2011, Habineza Ndikuyeze et al., 2014, Ianaro et al., 2009). Complimentary to the reports above, this study, has shown the apparent potential for the inhibition of AURKA-TPX2 signalling to be considered as a 'target' in the cancer setting. For instance, the NBD peptide has been demonstrated to inhibit *in vitro* the proliferative activity in both human melanoma and breast cancer cells (Ianaro et al., 2009, Rao Ch et al., 2004). The NBD peptide was also shown to reduce tumour burden in a canine model of relapsed, refractory Diffuse Large B-cell Lymphoma (Gaurnier-Hausser et al., 2011) and also reduced tumorigenesis when continued to a Phase I clinical trial involving dogs with Spontaneous Activated B-cell like Diffuse Large B-cell Lymphoma (Habineza Ndikuyeze et al., 2014). That said, future studies are required to determine the canine candidates that display elevated NF- κ B activity which makes them suitable for NBD peptide treatment and whether this correlates to human studies. In Figure 4.4, the ability of the NBD WT peptide to impact cell viability across different solid tumour cell lines was assessed in two Prostate cancer cell lines (AR negative PC3 cells vs AR positive LNCaP AI cells which are unresponsive to androgens), a Breast cancer (MCF7) and a Glioblastoma cell line (T98G). The NBD WT CPP caused a significant ($p < 0.05$) decrease in cell viability in all the cell lines used in these experiments (PC3, LNCaP AIs, MCF7 and T98G) with a noticeable difference in potency between cell lines. For example, the NBD WT CPP was shown to be more than twice as potent in LNCaP AI cells ($IC_{50} = 35.76\mu\text{M}$) compared to when its impact on cell viability was assessed in MCF7 ($IC_{50} = 83.38\mu\text{M}$) and T98G ($IC_{50} = 75.16\mu\text{M}$) cells. The NBD WT CPP was also assessed in PC3 cells and was shown to be moderately potent ($IC_{50} = 51.31\mu\text{M}$). The key point to highlight across these cell lines was that there was only partial inhibition of cell viability observed, with residual activity still present following treatment with

the maximum concentration of the NBD WT CPP used in this study (100 μ M). This suggested the need to target more than one pathway and perhaps explore other phenotypic outcomes (clonogenics, apoptosis) as viable assay outputs to assess the impact of the NBD WT CPP.

4.3.3. Conclusions.

In this chapter, it was demonstrated that the nocodazole 'trap and release' procedure, first used in Section 3.2.1 in PC3 cells, was as expected transferable to the other solid tumour cell lines used here (Section 4.2.2). These cell lines (LNCaP AIs, MCF7 and T98G) successfully moved through the cell cycle upon release and allowed the status of p-AURKs, AURKA, TPX2 and p-PLK1/PLK1 to be observed post-release from nocodazole-mediated cell synchronisation. The utilisation of the short length peptide derived from the NBD of IKK β , which was identified to accelerate both the dephosphorylation of AURKA (T288) and its degradation as it moved through mitosis, with similar patterns of expression and/or phosphorylation observed for both TPX2 and PLK1 with a similar effect observed across the different solid tumour cell lines. At this preliminary stage, it was suggested that the NBD WT CPP, derived from the IKK β NBD structure, can pharmacologically modulate AURKA, TPX2, PLK1 status, which caused a reduction in expression and/or phosphorylation and accelerated degradation across the different cancer cell lines (PC3, LNCaP AIs, MCF7 and T98G) and also impacted detrimentally cell viability which correlated with this phenotypic outcome. There was a noticeable difference in potency exerted by the NBD WT CPP between the various tumour cell lines, with no reduction in cell viability caused by the control peptide (NBD MT CPP) or the vehicle. Although these experimental outcomes indicated that the NBD WT CPP had an impact both mechanistically and phenotypically across each tumour cell line, the effect was sub-maximal and only caused around 50-60% reduction in cell viability at the highest concentration (100 μ M). It was detailed by Shah et al. (2019) that the use of Epidermal Growth Factor Receptor (EGFR) tyrosine kinase inhibitors (TKIs) – a popular class of 'anti-cancer' therapeutics, often elicits a sub-maximal response in EGFR-mutant non-small-cell lung cancer (NSCLC). Due to this sub-maximal response, residual disease can persist which goes onto acquire resistance and the cancer re-emerges through this means. In this case, the resistance is believed to be through increased AURKA activity and as such AURK inhibitors were shown to suppress this drug-resistance survival and increased the magnitude and duration of the EGFR inhibitor response in a synergistic combination therapy approach (Shah et al., 2019). In the context of this study, the NBD WT CPP could be used alongside existing ATP-competitive AURK KIs to target AURK signalling.

The outcomes above and those in Chapter 3, lead to the question as to whether the

treatment of cells with the NBD WT CPP in conjunction with AURK targeting KIs, as a potential 'two-site' dual targeting strategy, could generate greater AURK inhibition and therefore increased potency against AURKA itself, the other AURK isoforms, associated mitotic markers (e.g. TPX-2 and PLK1) as well as phenotypic outcomes identifiable as hallmarks of tumour cell progression.

**Chapter 5: Characterisation of
pharmacological targeting of AURK
phosphorylation and expression
with small molecule AURK kinase
inhibitors in the absence or
presence of NBD CPPs in PCa cells.**

5.1. Introduction.

Targeting of the AURK proteins with small molecule kinase inhibitors in cancer and particularly in solid tumours has been shown to lack efficacy and a number of reasons have been detailed for this, including; the fact that solid tumours proliferate at a slower rate than haematological tumours and hence the effect of AURKA inhibitors were observed to be more efficacious in blood cancers (Bavetsias and Linardopoulos, 2015a). These solid tumours (gastric, oesophageal and hepatocellular cancer) also display overexpression of the essential AURKA co-activator TPX2 which was associated with poor survival outcome (Wang et al., 2018). Higher or overexpression of TPX2 in these setting then leads to higher AURKA catalytic activity and decreases the efficacy of ATP-competitive inhibitors by reducing the targetability of the AURKA ATP-binding site in the active site of the protein (Anderson et al., 2007). As mentioned in the previous chapter, single-agent targeting of varying kinases often produces a sub-maximal response in cancer treatment and over time drug resistance develops due to remaining cancer cells re-emerging through activation of proteins like the AURKs, which confer resistance (Bavetsias and Linardopoulos, 2015a, Shah et al., 2019). Dual pharmacological targeting which involved incorporating kinase inhibitors that target the AURKs(AURKA, AURKB and AURKC) showed improvement (compared to single agent treatment) to overcome this AURK-associated resistance in cancer and improve the clinical outcome of the disease (Bavetsias and Linardopoulos, 2015a).

In a study by Anderson et al. (2007), examining the structure-activity relationship (SAR) of AURK inhibitors it was found that potency against AURKA activity was impacted in the presence of TPX2; an increased expression of TPX2 protein decreased potency. The presence of TPX2 alters the SAR in such a way that the binding of TPX2 to AURKA decreases the size of hydrophobic 'Y-pocket' adjacent to the ATP binding site and therefore reduces the accessibility of this hydrophobic pocket to AURK inhibitors which bind in it (Anderson et al., 2007). Anderson et al. (2007) highlighted that as the chemical space occupied by any inhibitor increased, more developed interactions with the kinase domain of AURKA were required to achieve potent inhibition and in the presence of elevated TPX2 expression/interaction that reduced accessibility of the 'Y-pocket', the ability of the AURK KIs to effectively target and reduce catalytic activity decreased. Therefore, numerous studies have screened *in silico*, using computational- based approaches to identify inhibitors of the AURKA-TPX2 complex that accounted for the impact of TPX2 on AURKA binding of ATP-competitive small molecule inhibitors. These include studies by Asteriti et al. (2017) and Cole et al. (2017) that both identified (through *in silico* screening) inhibitors of the AURKA-TPX2 complex, rather than of AURKA alone. Cole et al. (2017) demonstrated inhibition of TPX2 binding to AURKA via

fluorescence anisotropy (FA) assay ($K_i = 63\mu\text{M}$) and Asteriti et al. (2017) showed compounds that could not only inhibit AURKA activity *in silico* but also *in vitro* when assessed by their ability to impact the p-AURKA signal (AURKA activation) in osteosarcoma cells.

The NBD WT CPP utilised in this study was hypothesised to target and impact AURKA-TPX2 dynamics. As the peptide wasn't structurally similar to an ATP-competitive molecule, the mechanism of 'switching off' AURKA activity is not wholly clear. PP1a has been reported to be involved in the dephosphorylation of AURKA (T288) but it remains unclear what the mechanism of TPX2 removal is to start the process of AURKA deactivation. Is it IKK-dependent and therefore the terminal NBD domain of the IKKs expressed in cells is involved in the competitive removal of TPX2? Based on results of Chapter 3 it can therefore be suggested that the NBD WT CPP can accelerate dephosphorylation of AURKA. As TPX2 kinetics for degradation are also impacted by the NBD WT CPP, can the peptide, by virtue of its key tryptophan residues (W-S-W) disrupt binding of TPX2 to the 'Y-pocket' on AURKA by competing with the conserved Tyr-Ser-Tyr (Y-S-Y) motif on TPX2 that binds to AURKA and so facilitate its protein degradation also? Therefore, if the 'pocket' can be made more accessible by the NBD WT CPP then this would therefore enable various AURK KIs, of differing chemical space, to engage the active site of AURKA and reduce catalytic activity. To note, is that in this study, the status of AURK phosphorylation (relative to protein expression) and expression, has been used in Western blotting experiments as a surrogate marker of catalytic activity.

Hence in this section of research, experiments sought to demonstrate and confirm the efficacy of commercially available ATP-competitive AURK inhibitors on the status of p-AURKs in a cell-based assay system involving PC3 cells which have been synchronised with nocodazole. Following on from this, once potency of each kinase inhibitor against p-AURKs and AURKA expression was established, experiments were constructed to investigate whether incorporation of the NBD WT CPP in a combination with the ATP-competitive AURK inhibitors as a dual-targeting treatment approach had any capability to improve the efficacy of targeting p-AURKs/AURKA, TPX2 and PLK1.

Therefore, the specific aims of this chapter, were to:

1. Establish a cell-based assay system, using nocodazole arrest/trap and release, to enable the assessment of the ability of different ATP-competitive AURK inhibitors to impact p-AURKs in mitotic PC3 prostate cancer cells.
2. Determine the impact of the ATP-competitive AURK inhibitors alone and in combination with NBD CPPs on the AURKs in mitotic PC3 cells and examine the potential effect on related regulatory proteins associated with cell cycle progression.

Collectively, these experiments aimed to determine whether treatment of mitotic cells with ATP-competitive AURK inhibitors impacted expression/phosphorylation of AURKs and TPX2 and whether this impact could be enhanced by combined treatment of cells with the NBD WT CPP and so potentially improve efficacy beyond that of each used as single-agents.

5.2. Effect of AURK inhibitors and NBD CPPs alone or in combination on the status of p-AURKs, AURKA and TPX2.

5.2.1. Assessment of the efficacy of ATP-competitive AURK inhibitors on AURK signalling following nocodazole trap and release in PC3 cells.

Before proceeding to experiments which incorporate the NBD WT CPP in combination with the commercially available ATP-competitive AURK inhibitors (AURK inhibitor II, AURK inhibitor III, Aurora kinase/CDK inhibitor, VX-680 or ZM 447439), initial experiments were constructed to determine the potency of these inhibitors alone, at varying concentrations, in mitotic PC3 cells.

In order to assess the potency of the AURK inhibitors (AURK inhibitor II, AURK inhibitor III, Aurora kinase/CDK inhibitor, VX-680 or ZM 447439), with varying chemical space, isoform selectivity and potencies in cell-free/cell-based assays, PC3 cells were synchronised with nocodazole (50ng/ml) for 16-20 hours before wash and release procedure were carried out similarly to that described in Section 2.2.2.1 of the Materials and Methods. Following release from nocodazole-mediated cell synchronisation, cells were treated with increasing concentrations of; AURK inhibitor II (1 μ M, 2 μ M, 5 μ M, 10 μ M and 20 μ M), AURK inhibitor III (1 μ M, 2 μ M, 5 μ M, 10 μ M and 20 μ M), Aurora kinase/CDK inhibitor (0.25 μ M, 0.5 μ M, 1 μ M, 2 μ M, 5 μ M), VX-680 (0.1 μ M, 0.3 μ M, 1 μ M, 3 μ M and 10 μ M) or ZM 447439 (0.1 μ M, 0.3 μ M, 1 μ M, 3 μ M and 10 μ M) for 30 min before preparation of WCEs. AURK inhibitors (AURK inhibitor II, AURK inhibitor III, Aurora kinase/CDK inhibitor, VX-680 or ZM 447439) were dissolved initially in 100% DMSO and diluted to appropriate working stock concentrations of 10-20mM. For cell treatments stock solutions were diluted in culture media and added to wells (typical DMSO final concentration 0.0005-0.1% (v/v)) and as a result all experiments involving AURK inhibitors used DMSO (0.0005-0.1% (v/v)) as a vehicle control. The effect of the AURK inhibitors on the phosphorylation of AURKs were examined by Western blotting at a 30 minute time point.

Figure 5.1 (A) shows by immunoblotting the effect of the AURK inhibitor II (All) on the status of p-AURKs post-trap and release. In Figure 5.1 (A), from immunoblotting and the subsequent quantification, the All caused a significant ($p < 0.05$) reduction in phosphorylation

of AURKA relative to the vehicle treated sample at 30 min post-release from nocodazole-mediated arrest. The phosphorylation of AURKA was reduced after treatment with All at a concentration of 20 μ M (34.3 \pm 0.5%; n=3, p<0.05). There was also a significant reduction in the phosphorylation of AURKB caused by treatment with All at a concentration of 20 μ M (54.3 \pm 15.3%; n=3, p<0.01). Finally, All also significantly reduced phosphorylation of AURKC at a concentration of 10 μ M (62.7 \pm 13.4%; n=3, p<0.05) and 20 μ M (82.3 \pm 13.2%; n=3, p<0.01). Further analysis highlighted the potency of the All against phosphorylation of the three AURK subtypes – as a surrogate markers of catalytic activity. It was relatively low in potency across all three isoforms but displayed a higher degree of potency against phosphorylation of AURKB (IC₅₀ = 12.5 μ M) and C (IC₅₀ = 9.73 μ M) compared to AURKA (IC₅₀ = >20 μ M).

Next, experiments examined the effects of AURK inhibitor III (AIII) on the phosphorylation of the three AURK subtypes. Results of immunoblotting, subsequent quantification and further analysis of potency are depicted in Figure 5.1 (B). AIII showed no significant (p>0.05) reduction of phosphorylation of AURKA, B and C and this was mirrored when the potency was quantified, with a low potency (IC₅₀ = >20 μ M) against all three p-AURK subtypes. This was in contrast to the study by Zhang et al. (2006) which demonstrated that the AURK inhibitor III was a potent selective inhibitor of AURKA (IC₅₀ = 42nM) in a cell free assay.

Following on from this, Figure 5.1 (C), shows the effect of the Aurora kinase/CDK inhibitor (AurCDK) on the phosphorylation status of all three AURK subtypes. AurCDK significantly reduced phosphorylation of AURKA at a concentration of 0.5 μ M (36.6 \pm 5.3%; n=3, p<0.01), 1 μ M (57.4 \pm 12.1%; n=3, p<0.001), 2 μ M (90.1 \pm 7.8%; n=3, p<0.001) and 5 μ M (99.2% \pm 0.4%; n=3, p<0.001) respectively, relative to the vehicle treated sample at 30 min post-release from nocodazole-mediated arrest. AurCDK also significantly decreased the phosphorylation of AURKB at a concentration of 2 μ M (93.3 \pm 9.7%; n=3, p<0.001) and 5 μ M (98.5 \pm 4.5%; n=3, p<0.001). Lastly, AurCDK also caused a significant reduction in phosphorylation of AURKC at concentrations of 2 μ M (86.0 \pm 5.0%; n=3, p<0.05) and 5 μ M (96.3 \pm 1.0%; n=3, p<0.05). These results for immunoblotting quantification correlated with the further analysis of potency. The Aurora kinase/CDK inhibitor was slightly more potent against AURKA (IC₅₀ = 0.812 μ M) vs AURKB (IC₅₀ = 1.05 μ M) and C (IC₅₀ = 1.06 μ M).

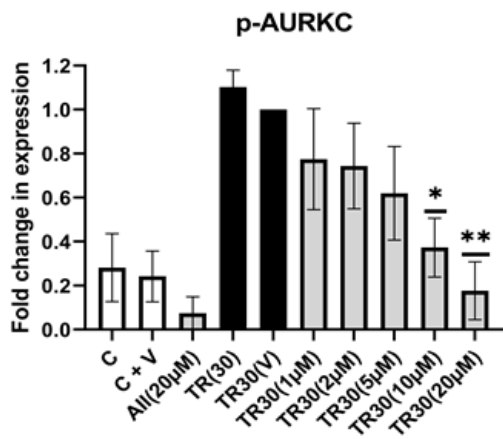
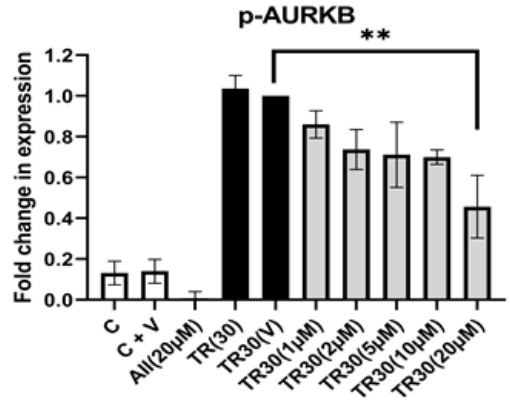
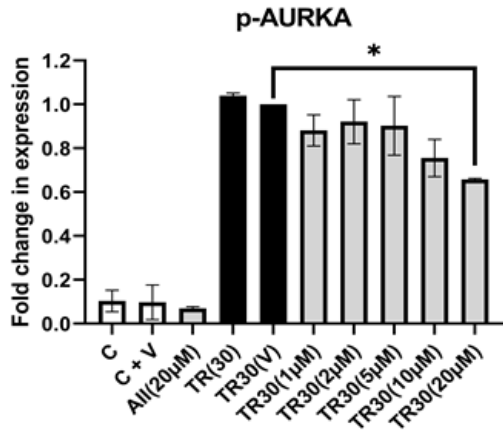
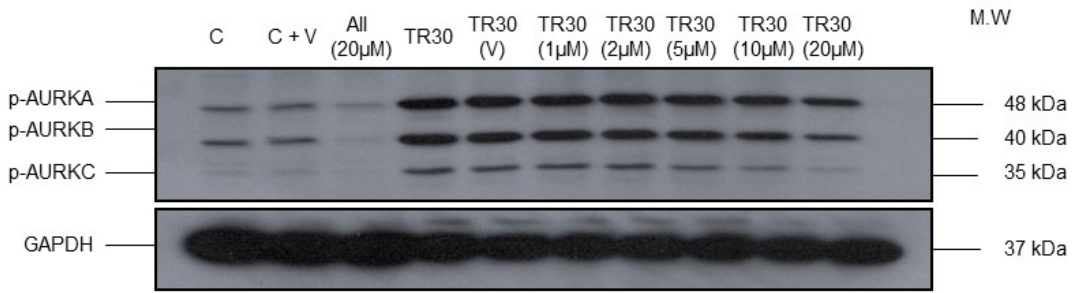
In Figure 5.1 (D), the pan-AURK inhibitor VX-680 with a more restricted chemical space (see Section 2.1.2.2 of Materials and Methods) was utilised. This is one of the most researched AURK inhibitors in the literature and progressed to Phase II of clinical trials before it was terminated due to severe toxicity as a result of one of the patients suffering severe cardiac problems (Baldini et al., 2014). In this study, *in vitro*, VX-680 caused a significant reduction in phosphorylation of AURKA across the concentration range used here; 0.1 μ M

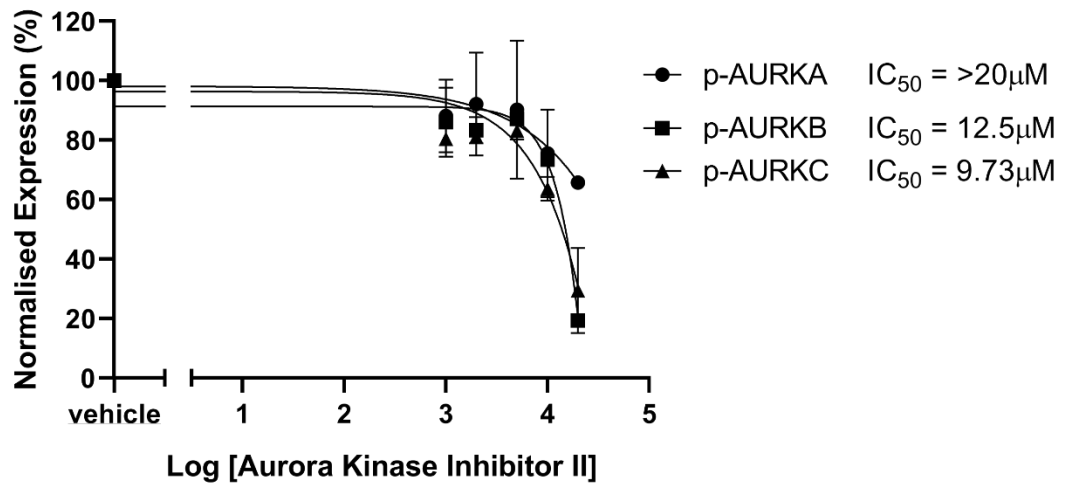
(44.1 ± 8.8%; n=3, p<0.001), 0.3µM (63.2 ± 11.1%; n=3, p<0.001), 1µM (93.8 ± 1.2%; n=3, p<0.001), 3µM (93.8 ± 4.9%; n=3, p<0.001) and 10µM (97.0 ± 4.2%; n=3, p<0.001) respectively. Similarly, VX-680 also significantly decreased phosphorylation of AURKB at concentrations of 1µM (81.3 ± 6.8%; n=3, p<0.001), 3µM (97.8 ± 2.9%; n=3, p<0.001) and 10µM (97.8 ± 1.5%; n=3, p<0.001). The effect of VX-680 in reducing AURKC phosphorylation mirrored the impact on phosphorylation of AURKB at concentrations of; 1µM (85.4 ± 4.6%; n=3, p<0.001), 3µM (94.8 ± 1.9%; n=3, p<0.001) and 10µM (99.4 ± 1.3%; n=3, p<0.001). This quantification correlated with the measure of potency which showed that VX-680 was approximately five times more potent against phosphorylation of AURKA (IC₅₀ = 0.137µM) versus B (IC₅₀ = 0.573µM) and C (0.540µM).

Lastly, this study also investigated the action of the AURK inhibitor ZM 447439 (ZM), a molecule with extended chemical space (see Section 2.1.2.2 of Materials and Methods), on phosphorylation of the three AURK subtypes. ZM caused a significant reduction in phosphorylation of AURKA at concentrations of; 1µM (21.3 ± 5.8%; n=3, p<0.05), 3µM (38.2 ± 4.5%; n=3, p<0.001) and 10µM (59.7 ± 1.4%; n=3, p<0.001). It was apparent by immunoblotting and subsequent quantification that ZM was least potent against AURKA phosphorylation and caused a significant reduction at 1µM (65.2 ± 14.1%; n=3, p<0.001), 3µM (97.8 ± 1.8%; n=3, p<0.001) and 10µM (98.8 ± 1.1%; n=3, p<0.001). In a similar pattern to the effect on phosphorylation of AURKB, ZM also significantly decreased phosphorylation of AURKC at concentrations of 0.3µM (57.8 ± 8.3%; n=3, p<0.01), 1µM (83.4 ± 4.7%; n=3, p<0.001), 3µM (92.6 ± 2.5%; n=3, p<0.001) and 10µM (99.7 ± 2.7%; n=3, p<0.001). Further analysis confirmed these findings as the ZM inhibitor was shown to be ten times less potent against phosphorylation of AURKA and the rank order of potency was; AURKC (IC₅₀ = (0.236µM)) > AURKB (IC₅₀ = 0.624µM) > AURKA IC₅₀ = (6.2µM).

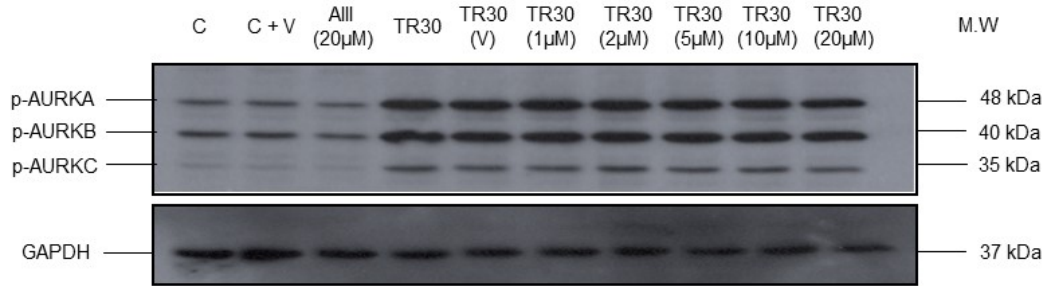
Collectively, treatment with the various ATP-competitive AURK inhibitors (AURK inhibitor II, AURK inhibitor III, Aurora kinase/CDK inhibitor, VX-680 or ZM 447439) allowed the establishment of a concentration gradient and rank order of potency for each inhibitor in a robust cell-based assay system. This could be used in future experimental studies examining the potential effects of the NBD WT CPP and the aforementioned AURK inhibitors in combination against AURKA-TPX2 signalling in mitotic cells.

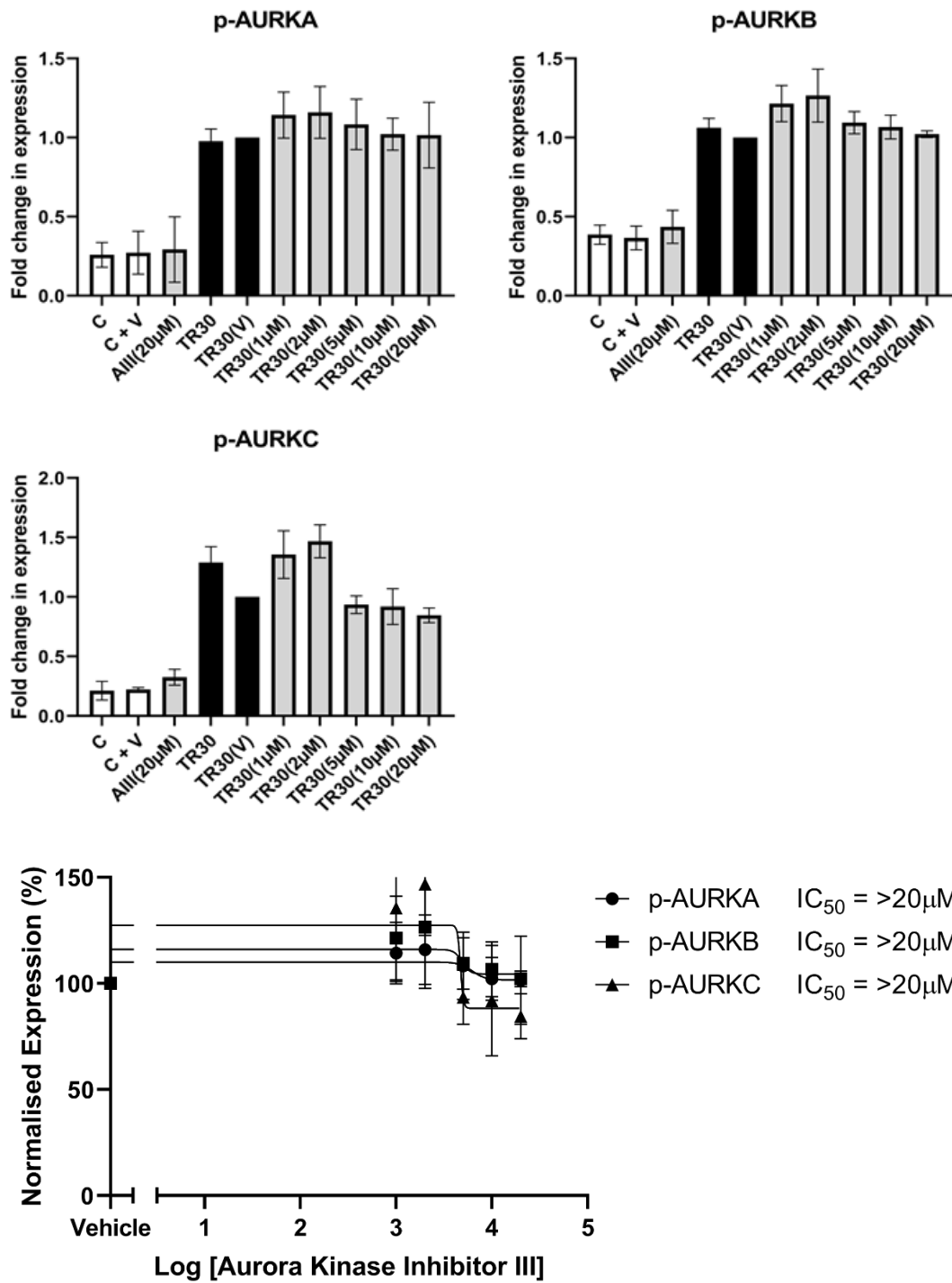
(A)

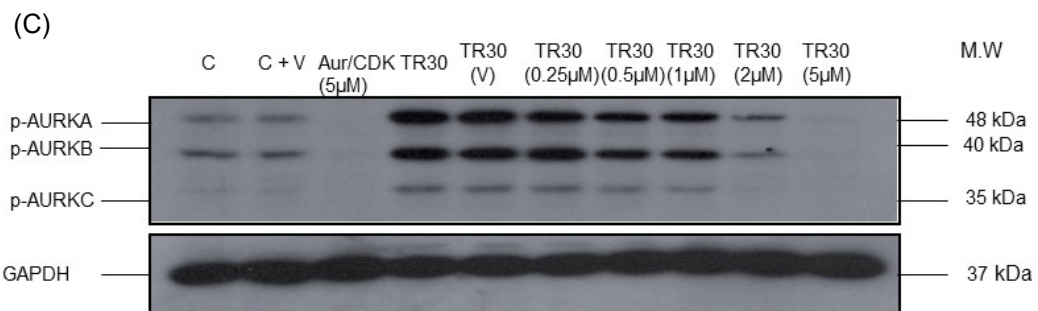


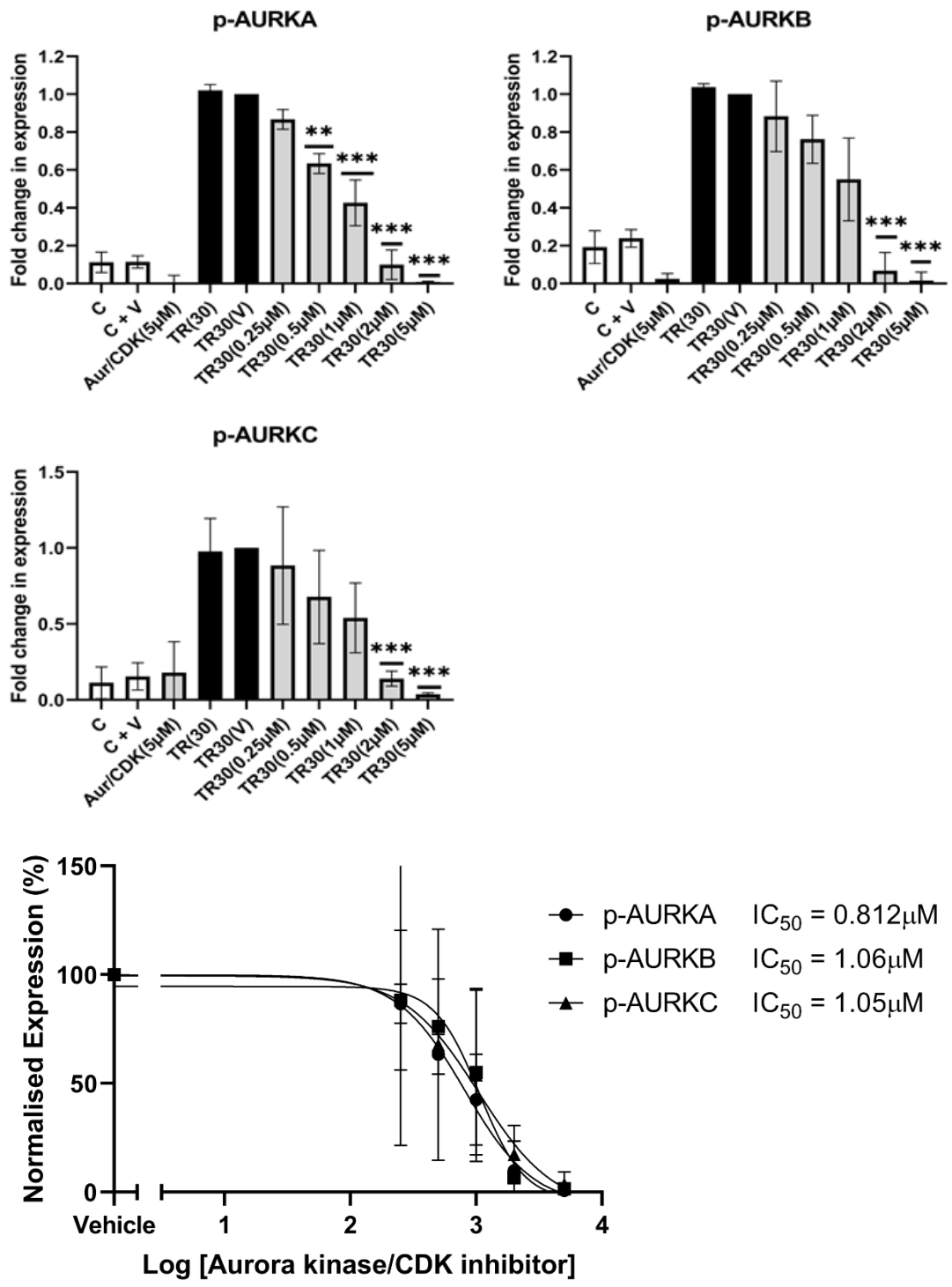


(B)

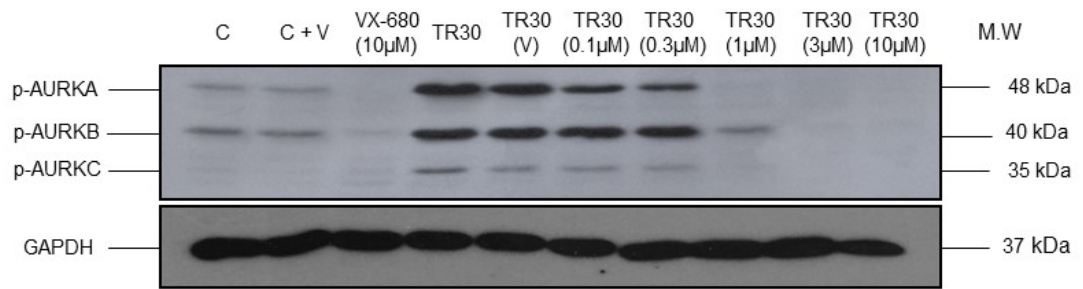


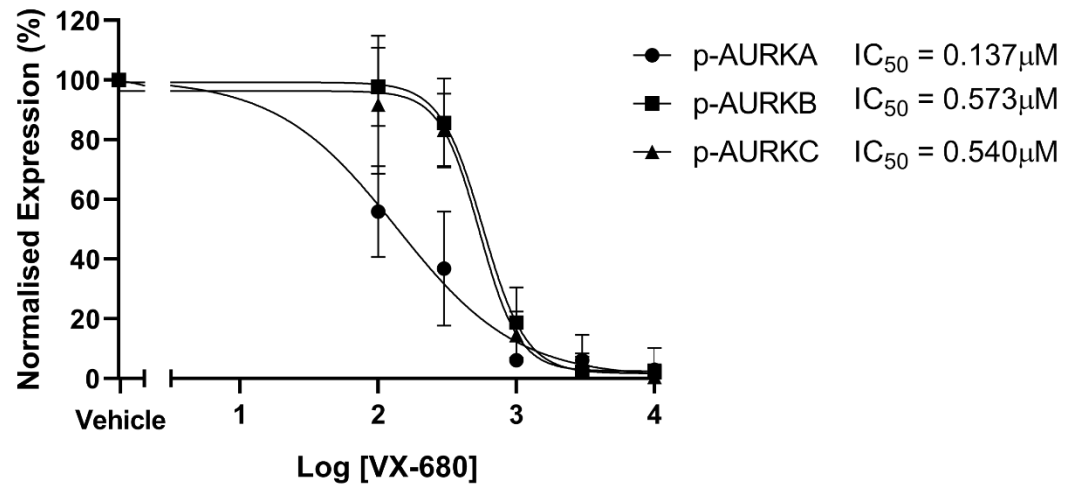
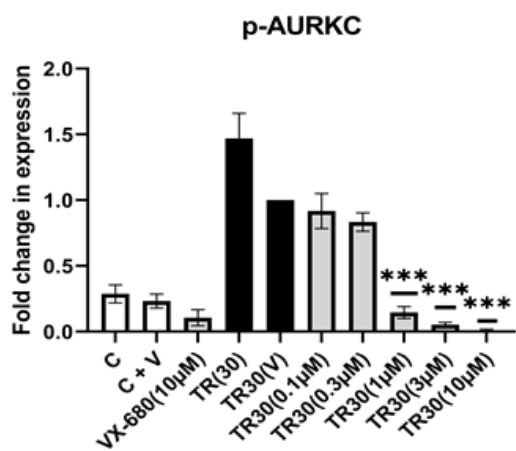
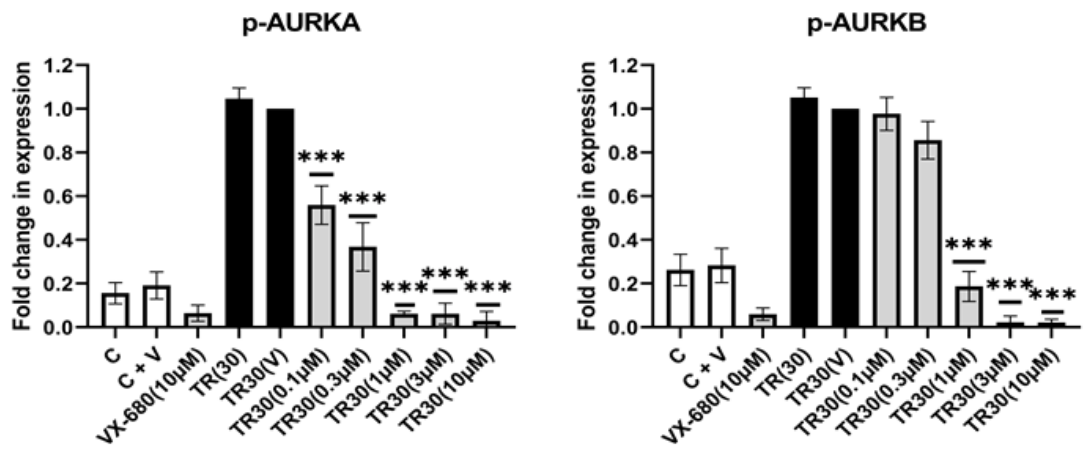




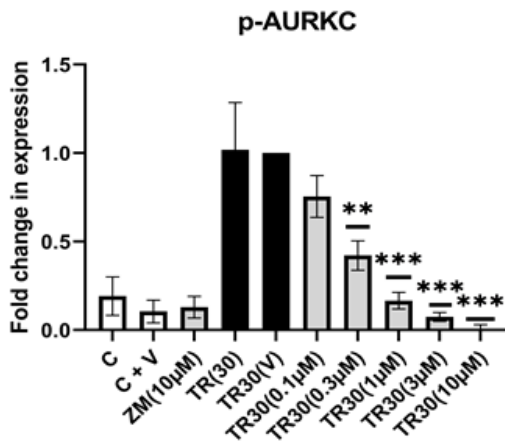
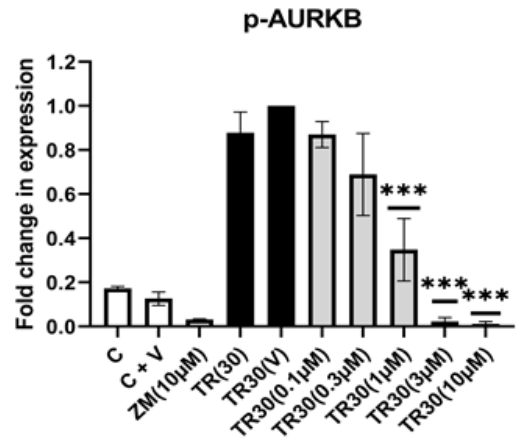
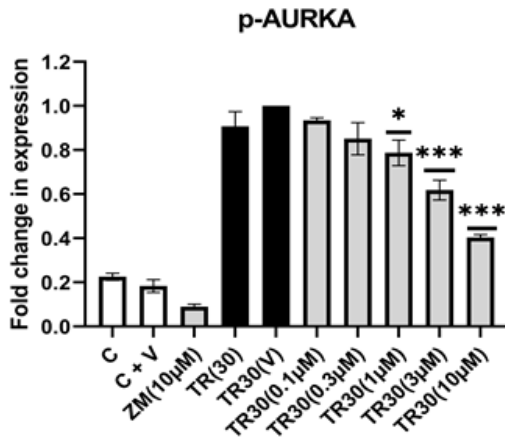
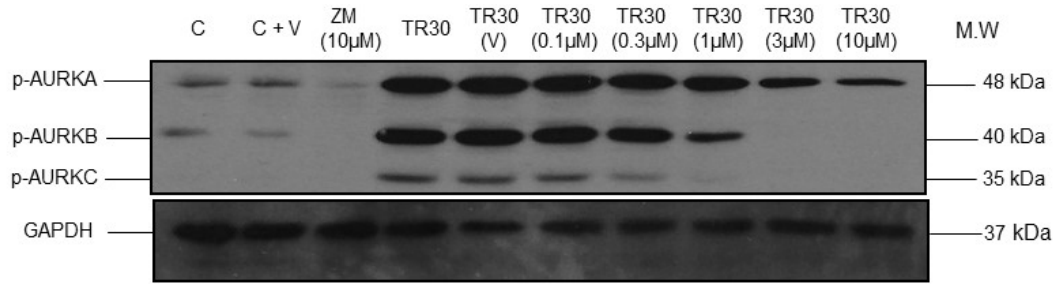


(D)





(E)



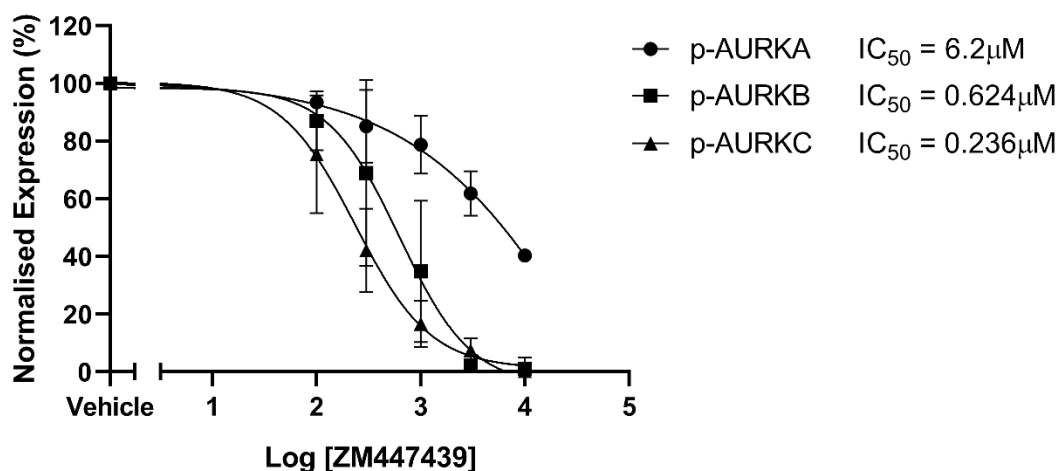


Figure 5.1. Effect of different concentrations of AURK inhibitors (AURK inhibitor II, AURK inhibitor III, Aurora kinase/CDK inhibitor, VX-680 or ZM 447439) on phosphorylation of Aurora kinases.

PC3 cells were grown on 10mm dishes and treated with 50ng/ml Nocodazole (16-20 hours) prior to treatment with AURK inhibitor II (A), AURK inhibitor III (B), Aurora kinase/CDK inhibitor (C), VX-680 (D) or ZM 447439 (E) DMSO as a vehicle control for each inhibitor (0.1%, 0.2%, 0.001%, 0.005% and 0.0005%(v/v) respectively) upon release from trap at 30min. Whole cell lysates were prepared for separation using SDS-PAGE and analysed by Western Blotting using the above antibodies (n=3). (C) and (C + V) represents the non-treated and vehicle treated control respectively in non-synchronised cells. GAPDH was used as a loading control. Data was normalised to synchronised sample treated with DMSO before release from trap at 30min time point (TR30 V) and represents mean \pm S.E.M. One-way ANOVA with post-hoc Dunnett's test was used to determine statistical significance ($p < 0.05$) of observed changes relative to TR30 (V) sample (*= $p < 0.05$, **= $p < 0.01$, ***= $p < 0.001$). Comparison of the potency of ATP-competitive AURK inhibitors on expression of p-AURKA (●), p-AURKB (■), p-AURKC (▲). Cells were treated with a full concentration range for each inhibitor: AURK inhibitor II (1 μ M, 2 μ M, 5 μ M, 10 μ M and 20 μ M), AURK inhibitor III (1 μ M, 2 μ M, 5 μ M, 10 μ M and 20 μ M), Aurora kinase/CDK inhibitor (0.25 μ M, 0.5 μ M, 1 μ M, 2 μ M, 5 μ M), VX-680 (0.1 μ M, 0.3 μ M, 1 μ M, 3 μ M and 10 μ M) and ZM 447439 (0.1 μ M, 0.3 μ M, 1 μ M, 3 μ M and 10 μ M). The results were normalised to the vehicle treated control expression and plotted on a log scale as a percentage of the control with regards to expression (n=3). The data was fitted with the following equation: $Y = \text{Bottom} + (\text{Top} - \text{Bottom}) / (1 + 10^{((\text{LogIC}_{50} - X) * \text{HillSlope})})$.

5.2.2. Effect of AURK inhibitor II alone or in combination with NBD WT CPP on AURKA status/signalling.

As demonstrated previously, the NBD WT CPP derived from IKK β significantly ($p < 0.05$) decreased AURKA phosphorylation and total expression as well as the status of key related markers (TPX2, p-PLK1/PLK1) and therefore suggested to impact on IKK-AURK signalling in PC3 (Section 3.3.1), LNCaP AI, MCF7 and T98G cells respectively. In Section 5.2.1, experiments utilised commercially available ATP-competitive AURK inhibitors (AURK inhibitor II, AURK inhibitor III, Aurora kinase/CDK inhibitor, VX-680 or ZM 447439) in a cell-based assay involving synchronised PC3 cells to demonstrate their efficacy as a single-agent treatment. In this Section and the proceeding Sections, experiments sought to determine, through simultaneous treatment of cells with the NBD WT CPP and AURK inhibitors (AURK inhibitor II, AURK inhibitor III, Aurora kinase/CDK inhibitor, VX-680 or ZM 447439) in combination, the resultant impact on the status of AURKA/TPX2 signalling compared to the single-agent treatments. Cells were again treated with nocodazole (50ng/mL) for 16-20 hours prior to being washed and released as described previously – Section 2.2.2.1, before NBD WT CPP (100 μ M) and/or AURK inhibitor II (10 μ M) were added upon release and samples prepared thereafter at appropriate time points. The WT peptide and the AURK inhibitor II in parallel to vehicle were prepared as described previously. The effect of the NBD WT CPP and/or AURK inhibitor II on AURKA and its related mitotic markers in terms of their expression and/or phosphorylation were examined by Western blotting at 10, 20 and 30 minute time points.

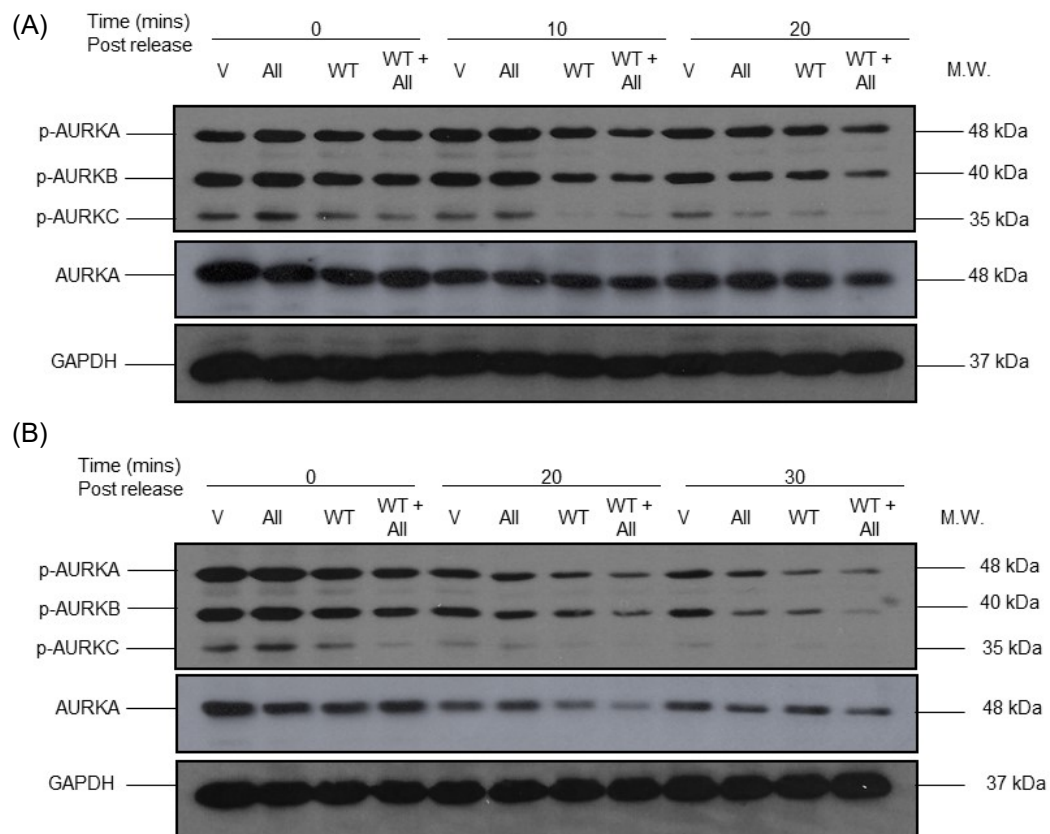
Figure 5.2 showed by immunoblotting the effect of the NBD WT CPP and/or AURK inhibitor II on the status of p-AURKs and AURKA post-trap and release; (A) 0, 10 and 20 min and (B) 0, 20 and 30 min. It was demonstrated in the subsequent quantification (C) at 0, 10 and 20 min and (D) at 0, 20 and 30 min in PC3 cells, the NBD WT CPP in combination with the AURK inhibitor II caused a significantly greater reduction in phosphorylation of AURKA relative to the vehicle control sample, NBD WT CPP alone and AURK inhibitor II alone at each time point in PC3 cells. In Figure 5.2 (A + C), the phosphorylation of AURKA was reduced after treatment with the NBD WT CPP in combination with AURK inhibitor II compared to the vehicle control at 10 min ($96.7 \pm 11.4\%$ vs $55.7 \pm 4.9\%$; $n=3$, $p < 0.05$). In Figure 5.2 (B +D) the NBD WT CPP in combination with AURK inhibitor II caused a significant reduction in phosphorylation of AURKA in comparison to the vehicle treated control after 30 min ($64.3 \pm 8.6\%$ vs $12.4 \pm 1.3\%$; $n=3$, $p < 0.001$). There was also a significant difference in the reduction in AURKA phosphorylation in the sample treated with a combination of the two agents

compared to single-agent treatment with; NBD WT CPP ($50.2 \pm 3.9\%$ vs $12.4 \pm 1.3\%$; $n=3$, $p<0.01$) or AURK inhibitor II ($43.5 \pm 3.1\%$ vs $12.4 \pm 1.3\%$; $n=3$, $p<0.05$) at the 30 minute time-point. There was also a significant reduction in AURKB phosphorylation (Figure 5.2 A + C) caused by treatment with the NBD WT CPP and AURK inhibitor II in combination compared the vehicle control after 10 min ($84.3 \pm 10.0\%$ vs $44.5 \pm 6.4\%$; $n=3$, $p<0.05$) and 20 min ($75.5 \pm 4.7\%$ vs $32.1 \pm 4.8\%$; $n=3$, $p<0.01$) post-release from nocodazole-mediated arrest. In Figure 5.2 (B + D), AURKB phosphorylation was again shown to be significantly reduced in the sample treated with the combination of agents after 20 min ($66.3 \pm 4.4\%$ vs $29.0 \pm 6.0\%$; $n=3$, $p<0.001$) and also after 30 min ($58.4 \pm 2.8\%$ vs $15.1 \pm 1.7\%$; $n=3$, $p<0.001$) compared to the vehicle treated samples at each of these time points. At the 30-minute time point, the sample treated simultaneously with the NBD WT CPP and AURK inhibitor II was also significantly further reduced in comparison to treatment with the NBD WT CPP ($51.9 \pm 4.4\%$ vs $15.1 \pm 1.7\%$; $n=3$, $p<0.001$) or AURK inhibitor II ($39.6 \pm 4.3\%$ vs $15.1 \pm 1.7\%$; $n=3$, $p<0.05$) alone at this time point. Lastly, the phosphorylation of AURKC was also significantly reduced by the combination treatment after 30 min relative to the vehicle treated sample ($46.5 \pm 14.0\%$ vs $5.2 \pm 3.9\%$; $n=3$, $p<0.05$) but was not significantly reduced in comparison to the single agent treatments.

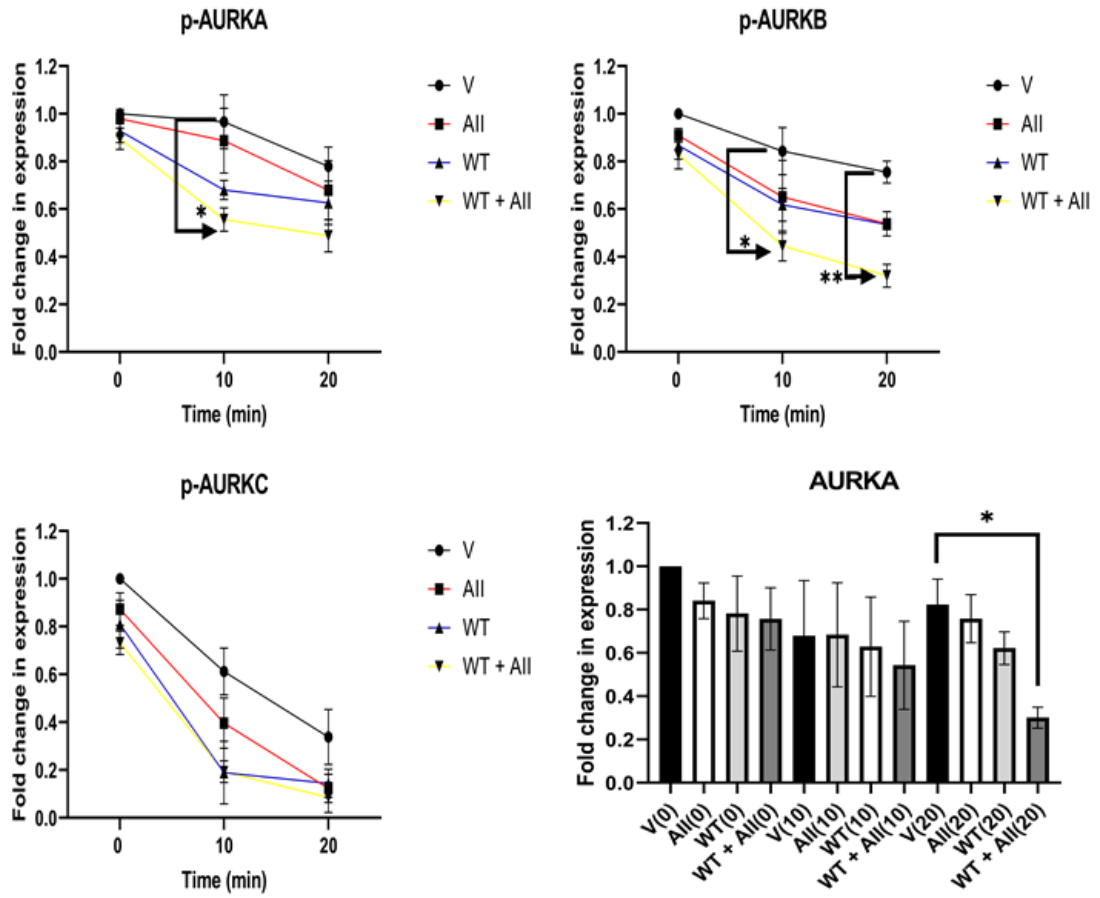
The reduction in total AURKA expression was assessed to determine if it was comparable to the effect of the NBD WT CPP and AURK inhibitor II on AURKA phosphorylation. To begin with, following combination treatment, there was a significant reduction in total AURKA expression at 20 minutes post-release relative to the vehicle treated sample. This was observed in both Figure 5.2 C ($82.3 \pm 6.8\%$ vs $30.1 \pm 2.8\%$; $n=3$, $p<0.05$) and Figure 5.2 D ($69.2 \pm 6.0\%$ vs $32.8 \pm 2.7\%$; $n=3$, $p<0.05$) respectively. Beyond this, there was also a significant reduction in total expression of AURKA caused by the simultaneous treatment of the NBD WT CPP and AURK inhibitor II at the 30 minute time point ($57.2 \pm 3.9\%$ vs $21.8 \pm 5.5\%$; $n=3$, $p<0.05$), compared to the vehicle treated sample. Similarly to the phosphorylation, there was also an enhanced, significant reduction in AURKA total expression in the sample treated with a combination of the two agents compared to single-agent treatment with; NBD WT CPP ($61.1 \pm 3.4\%$ vs $21.8 \pm 5.5\%$; $n=3$, $p<0.05$) or AURK inhibitor II ($63.3 \pm 9.6\%$ vs $21.8 \pm 5.5\%$; $n=3$, $p<0.01$) at the 30 minute time point.

Collectively, these experimental outcomes demonstrated the ability of the NBD WT CPP and AURK inhibitor II, when used in combination, to significantly enhance the reduction of the expression and/or phosphorylation of AURKs in comparison to when these agents were used alone. Whether this enhancement of efficacy and improved ability to impact AURKA and related mitotic markers could be extended to the other ATP-competitive AURK inhibitors (AURK inhibitor III, Aurora kinase/CDK inhibitor, VX-680 or ZM 447439), again with differing

chemical space, selectivity and potencies used in Section 5.2.1, in combination with the NBD WT CPP, was investigated next.



(C)



(D)

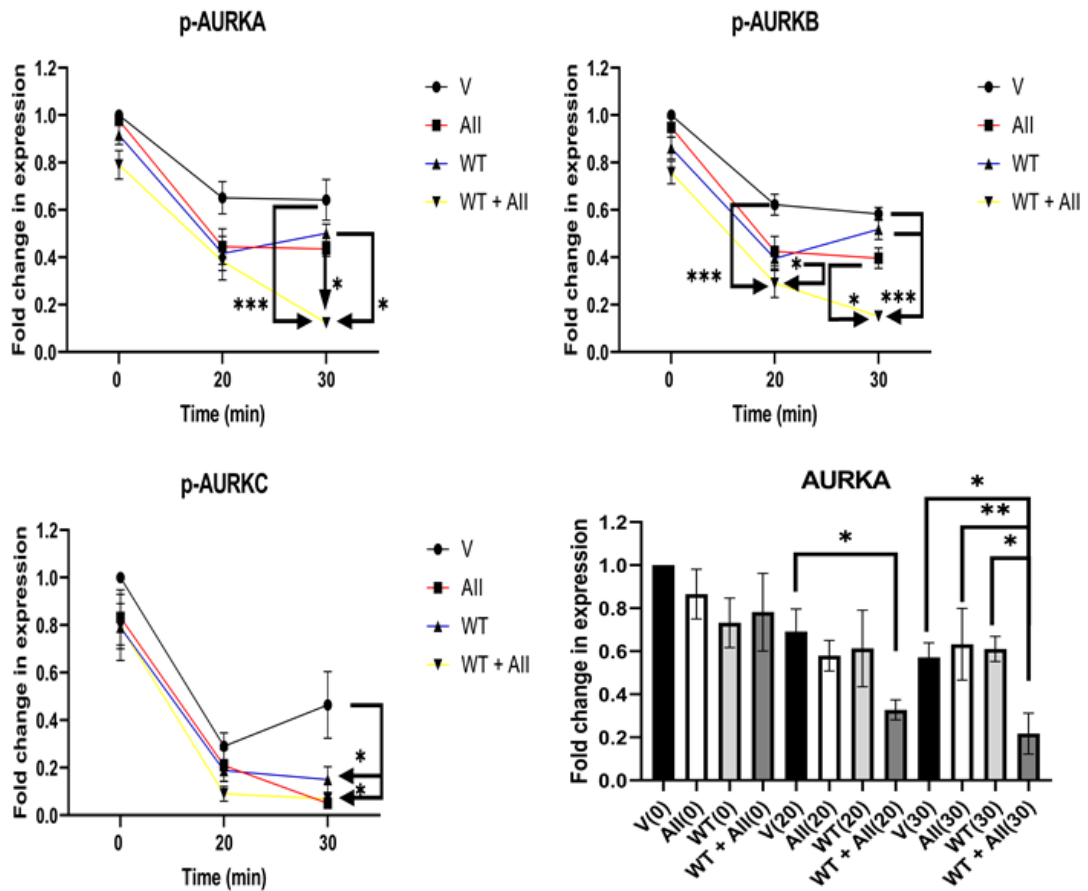


Figure 5.2. Effect of AURK inhibitor II alone or in combination with NBD WT CPP on AURKs and related protein markers of mitosis in PC3 cells.

PC3 cells were grown on 10mm dishes and treated with 50ng/ml Nocodazole (16-20 hours) prior to treatment with AURK inhibitor II (10 μ M), NBD WT CPP (100 μ M), DMSO as a vehicle control (0.5% (v/v)) or NBD WT CPP (WT) and AURK inhibitor II (All) in combination upon release from trap at: (A + C) 0, 10 and 20 min; (B + D) 0, 20 and 30 min. A and B: Whole cell lysates were prepared for separation using SDS-PAGE and analysed by Western Blotting using the above antibodies (n=3). GAPDH was used as a loading control. C and D: Data was normalised to the vehicle treated control at 0 min (V0) and represents mean \pm S.E.M. One-way ANOVA with post-hoc Tukey multiple comparisons test was used to determine statistical significance ($p < 0.05$) of observed changes between the means of the different treatment groups compared to the WT + All at the same time point (*= $p < 0.05$, **= $p < 0.01$, ***= $p < 0.001$). (C): p-AURKA: WT + All (10) vs V(10), * $p < 0.05$. p-AURKB: WT + All (10) vs V (10), * $p < 0.05$; WT + All (20) vs V(20), ** $p < 0.01$. (D): p-AURKB: WT + All (20) vs V(20), *** $p < 0.001$; WT + All (20) vs WT(20), * $p < 0.05$; WT + All (30) vs V(30), *** $p < 0.001$; WT + All (30) vs All(30), * $p < 0.05$; WT + All (30) vs WT(30), *** $p < 0.001$. p-AURKC: WT + All (30) vs V(30), * $p < 0.05$; WT (30) vs V(30), * $p < 0.05$.

5.2.3. Effect of AURK inhibitor III alone and in combination with NBD WT CPP on AURKA signalling.

Following on from the demonstrated impact of the NBD WT CPP and AURK inhibitor II in combination on the status AURKs and AURKA (Section 5.2.2), experiments then sought to determine whether this enhanced efficacy through this combination treatment approach was apparent with other AURK inhibitors (AURK inhibitor III, Aurora kinase/CDK inhibitor, VX-680 or ZM 447439) utilised in this study. To begin with, treatment with the NBD WT CPP and/or Cyclopropane carboxylic acid-(3-(4-(3-trifluoromethyl-phenylamino)-pyrimidin-2-ylamino)-phenyl)-amide (AURK Inhibitor III) and the resultant impact on AURKA signalling compared to treatment with these agents alone or vehicle was investigated. Cells were again treated with nocodazole (50ng/ml) for 16-20 hours prior to being washed and released as described previously – Section 2.2.2.1, before NBD WT CPP (100 μ M) and/or AURK inhibitor III (20 μ M) were added upon release and samples prepared thereafter at appropriate time points. The WT peptide and the AURK inhibitor III in parallel to vehicle were prepared as described previously. The effect of the NBD WT CPP and/or AURK inhibitor III on AURKA and its related mitotic markers in terms of their expression and/or phosphorylation were examined by Western blotting at 10, 20 and 30 minute time points.

Figure 5.3 demonstrated by immunoblotting, the effect of the NBD WT CPP and/or AURK inhibitor III on the status of p-AURKs and AURKA post-trap and release; (A) 0, 10 and 20 min and (B) 0, 20 and 30 min. It was demonstrated in the subsequent quantification (C) at 0, 10 and 20 min and (D) at 0, 20 and 30min in PC3 cells, the NBD WT CPP in combination with the AURK inhibitor III caused a reduction in phosphorylation of AURKA relative to the vehicle, NBD WT CPP alone and AURK inhibitor III alone at each time point in PC3 cells. In Figure 5.3 (A + C), phosphorylation of AURKA was reduced after treatment with the NBD WT CPP and AURK inhibitor III in combination compared to the vehicle control at 10 min ($86.2 \pm 3.7\%$ vs $47.5 \pm 6.5\%$; $n=3$, $p<0.01$) and 20 min ($76.7 \pm 9.8\%$ vs $29.1 \pm 4.6\%$; $n=3$, $p<0.001$). This decrease in phosphorylation of AURKA caused by the combination treatment after 20 minutes was also significantly different from the reduction in phosphorylation caused by the NBD WT CPP ($66.7 \pm 4.6\%$ vs $29.1 \pm 4.6\%$; $n=3$, $p<0.01$) or AURK inhibitor III ($74.6 \pm 3.2\%$ vs $29.1 \pm 4.6\%$; $n=3$, $p<0.001$) alone. Similar was also seen at the 20 minute time point in Figure 5.3 (D), in which there was also a significant reduction in AURKA induced by treatment with the NBD WT CPP and AURK inhibitor III together, relative to the vehicle treated sample ($79.0 \pm 5.9\%$ vs $41.1 \pm 3.9\%$; $n=3$, $p<0.05$). Again, there was a significant difference in the reduction of AURKA phosphorylation between the NBD WT CPP and AURK inhibitor III in combination compared to the single agents alone at the 20 minute time point; NBD WT CPP

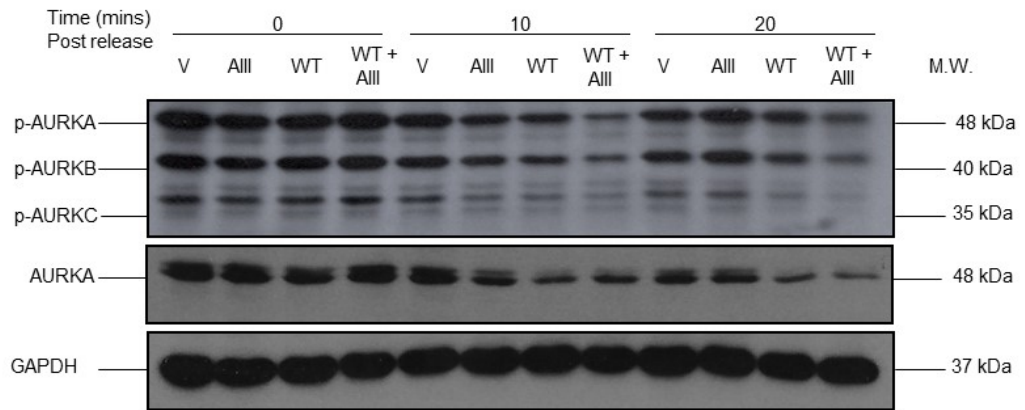
($77.1 \pm 7.8\%$ vs $41.1 \pm 3.9\%$; $n=3$, $p<0.05$) or AURK inhibitor III ($87.2 \pm 2.4\%$ vs $41.1 \pm 3.9\%$; $n=3$, $p<0.01$). In Figure 5.3 (D) the NBD WT CPP in combination with AURK inhibitor III also caused a significant reduction in phosphorylation of AURKA in comparison to the vehicle treated control after 30 min ($77.4 \pm 9.2\%$ vs $15.0 \pm 3.2\%$; $n=3$, $p<0.001$). There was also a significant difference in the reduction in AURKA phosphorylation in the sample treated with a combination of the two agents compared to single-agent treatment with; NBD WT CPP ($50.2 \pm 3.9\%$ vs $12.4 \pm 1.3\%$; $n=3$, $p<0.01$) or AURK inhibitor III ($43.5 \pm 16.7\%$ vs $12.4 \pm 1.3\%$; $n=3$, $p<0.05$) at the 30 minute time-point. There was also a significant reduction in AURKB phosphorylation (Figure 5.3 A + C) caused by treatment with the NBD WT CPP and AURK inhibitor III in combination compared to the vehicle control after 10 min ($80.7 \pm 1.1\%$ vs $49.3 \pm 0.4\%$; $n=3$, $p<0.05$) and 20 min ($82.3 \pm 8.4\%$ vs $42.8 \pm 2.1\%$; $n=3$, $p<0.01$). At the 20 minute time point there was also a significant difference between treatment with AURK inhibitor III alone and treatment with a combination of the NBD WT CPP and AURK inhibitor III ($77.1 \pm 5.9\%$ vs $42.8 \pm 2.1\%$; $n=3$, $p<0.05$). In Figure 5.3 (B + D), AURKB phosphorylation was again shown to be significantly reduced in the sample treated with the combination therapy after 20 min ($79.5 \pm 3.4\%$ vs $49.3 \pm 3.4\%$; $n=3$, $p<0.05$) and after 30 min ($84.2 \pm 6.5\%$ vs $15.8 \pm 6.6\%$; $n=3$, $p<0.001$) compared to the vehicle treated samples at these time points. At the 30 minute time point, the sample treated simultaneously with the NBD WT CPP and AURK inhibitor III was also significantly further reduced in comparison to treatment with the NBD WT CPP ($46.2 \pm 1.8\%$ vs $15.8 \pm 6.6\%$; $n=3$, $p<0.05$) or AURK inhibitor III ($61.1 \pm 10.7\%$ vs $15.8 \pm 6.6\%$; $n=3$, $p<0.001$) alone at this time point. Lastly, in Figure 5.3 (C) the phosphorylation of AURKC was also significantly reduced by the combination treatment after 10 min ($73.6 \pm 6.4\%$ vs $30.8 \pm 2.8\%$; $n=3$, $p<0.001$) relative to the vehicle treated sample at this time point. There was also a significant difference in the reduction in AURKC phosphorylation in the sample treated with a combination of the two agents compared to single-agent treatment with the AURK inhibitor III ($73.8 \pm 6.1\%$ vs $30.8 \pm 2.8\%$; $n=3$, $p<0.001$) at the 10 minute time point. There was also significant reduction in the combination treatment sample at the 20 minute time point relative to the vehicle treated sample ($56.9 \pm 6.1\%$ vs $22.9 \pm 2.8\%$; $n=3$, $p<0.01$). There was also a significant difference between treatment of the AURK inhibitor III on its own and the inhibitor in combination with the NBD WT CPP ($69.6 \pm 7.0\%$ vs $22.9 \pm 2.8\%$; $n=3$, $p<0.01$). Similarly, in Figure 5.3 (D), treatment with the NBD WT CPP and AURK inhibitor III significantly reduced AURKC phosphorylation at the 20 minute time point ($59.1 \pm 1.5\%$ vs $13.9 \pm 8.0\%$; $n=3$, $p<0.01$).

The reduction in total AURKA expression was assessed to determine if it was comparable to the effect of the NBD WT CPP and AURK inhibitor III on AURKA phosphorylation. To begin with, following combination treatment, there was a significant

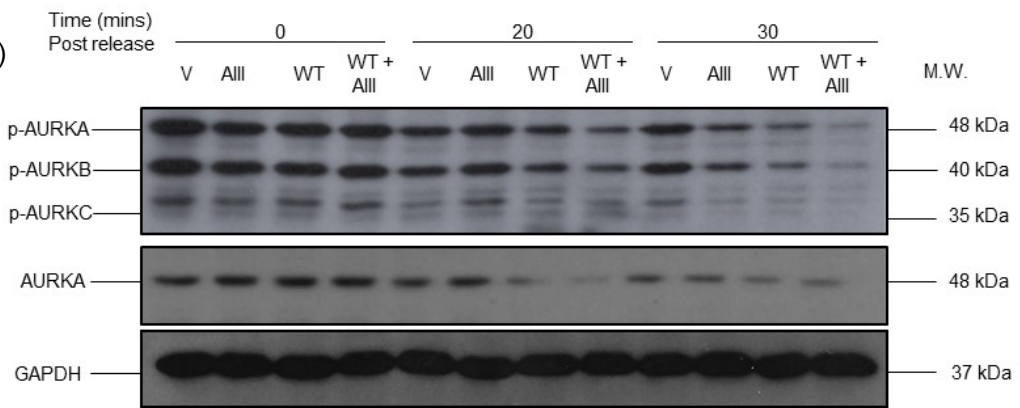
reduction in total AURKA expression at 20 minutes post-release from nocodazole-mediated arrest, relative to the vehicle treated sample. This was observed in both Figure 5.3C ($81.0 \pm 11.1\%$ vs $18.3 \pm 8.4\%$; $n=3$, $p<0.001$) and Figure 5.3D ($81.1 \pm 6.8\%$ vs $33.7 \pm 4.7\%$; $n=3$, $p<0.001$) respectively. Similarly in Figure 5.3C, there was a significant difference in the decrease in phosphorylation brought about by the combination of the two agents compared to the single agents alone after 20 minutes; NBD WT CPP ($67.3 \pm 3.3\%$ vs $18.3 \pm 8.4\%$; $n=3$, $p<0.01$) or AURK inhibitor III ($75.3 \pm 11.5\%$ vs $18.3 \pm 8.4\%$; $n=3$, $p<0.001$). This comparison between the combination treatment and single agents alone was mirrored in Figure 5.3D at the 20 minute time point; NBD WT CPP ($59.1 \pm 2.8\%$ vs $33.7 \pm 4.7\%$; $n=3$, $p<0.001$) or AURK inhibitor III ($72.7 \pm 9.3\%$ vs $33.7 \pm 4.7\%$; $n=3$, $p<0.001$) respectively. There was also a significant reduction in AURKA total expression caused by treatment of the NBD WT CPP and AURK inhibitor III at the 30 minute time point ($68.7 \pm 2.0\%$ vs $21.9 \pm 3.9\%$; $n=3$, $p<0.001$). Similar to the findings observed with AURKA phosphorylation, there was also an enhanced, significant reduction in AURKA total expression in the sample treated with a combination of the two agents compared to single-agent treatment with the AURK inhibitor III ($60.3 \pm 5.9\%$ vs $21.9 \pm 3.9\%$; $n=3$, $p<0.001$) at the 30 minute time point. There was also a significant difference in total AURKA expression observed in the sample treated with the NBD WT CPP compared to the vehicle at the 30 minute time point ($68.7 \pm 2.0\%$ vs $21.9 \pm 5.8\%$; $n=3$, $p<0.001$). This showed that the total expression of AURKA had declined to basal levels by the 30 minute time point as there was no significant difference between treatment with NBD WT CPP alone and the combination treated sample at this time point.

Collectively, these experimental outcomes demonstrated the ability of the NBD WT CPP and AURK inhibitor III, when used in combination, to significantly enhance the reduction of AURKA phosphorylation and expression in comparison to when these agents were used alone. Whether this enhancement of efficacy and improved ability to impact AURKA and related mitotic markers can be extended to the other ATP-competitive AURK inhibitors (Aurora kinase/CDK inhibitor, VX-680 or ZM 447439) again with differing chemical space, selectivity and potencies, used in Section 5.2.1, in combination with the NBD WT CPP, was investigated next.

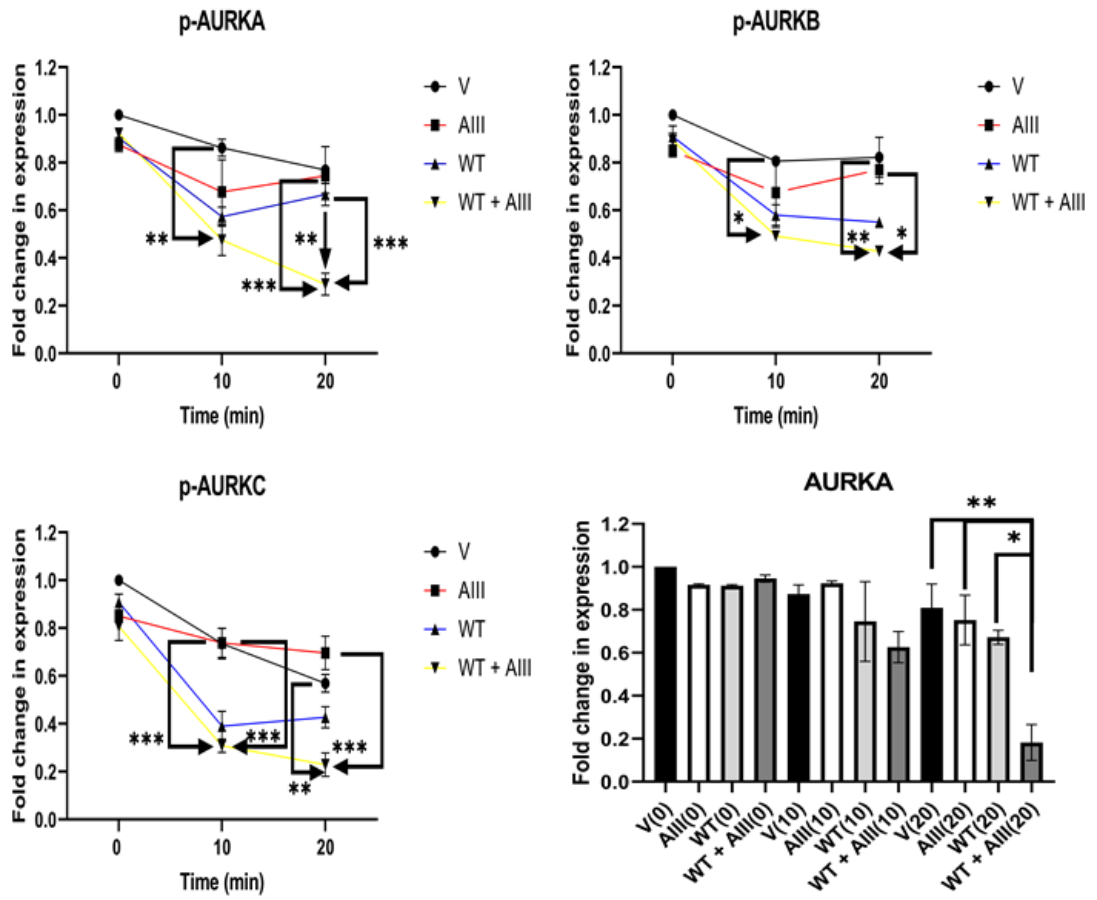
(A)



(B)



(C)



(D)

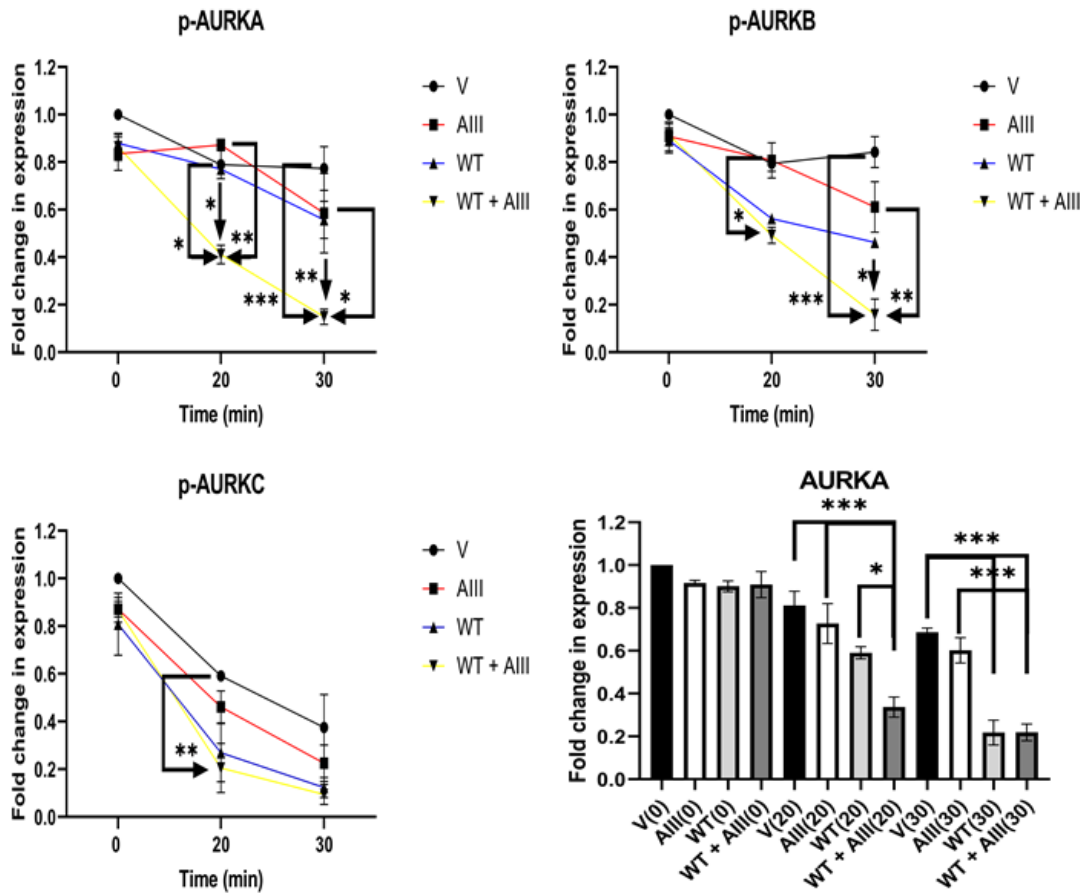


Figure 5.3. Effect of AURK inhibitor III alone or in combination with NBD WT CPP on AURKs and related protein markers of mitosis in PC3 cells.

PC3 cells were grown on 10mm dishes and treated with 50ng/ml Nocodazole (16-20 hours) prior to treatment with AURK inhibitor III (20 μ M), NBD WT CPP (100 μ M), DMSO as a vehicle control (0.5% (v/v)) or NBD WT CPP (WT) and AURK inhibitor III (AIII) in combination upon release from trap at: (A + C) 0, 10 and 20 min (B + D) 0, 20 and 30 min. A and B: Whole cell lysates were prepared for separation using SDS-PAGE and analysed by Western Blotting using the above antibodies (n=3). GAPDH was used as a loading control. C and D: Data was normalised the vehicle treated control at 0 min (V0) and represents mean \pm S.E.M. One-way ANOVA with post-hoc Tukey multiple comparisons test was used to determine statistical significance ($p < 0.05$) of observed changes between the means of the different treatment groups compared to the WT + AIII at the same time point (*= $p < 0.05$, **= $p < 0.01$, ***= $p < 0.001$).
(C): p-AURKA: WT + AIII (10) vs V(10), ** $p < 0.01$; WT + AIII (20) vs V(20), *** $p < 0.001$; WT + AIII (20) vs AIII(20), *** $p < 0.001$; WT + AIII (20) vs WT(20), ** $p < 0.01$. p-AURKB: WT + AIII (10) vs V(10), * $p < 0.05$; WT + AIII (20) vs V(20), ** $p < 0.01$; WT + AIII (20) vs AIII(20), * $p < 0.05$. p-AURKC: WT + AIII (10) vs V(10), *** $p < 0.001$; WT + AIII (10) vs AIII(10), *** $p < 0.001$; WT + AIII (20) vs V(20), ** $p < 0.01$; WT + AIII (20) vs AIII(20), *** $p < 0.001$. (D): p-AURKA: WT + AIII (20) vs V(20), * $p < 0.05$; WT + AIII (20) vs AIII(20), ** $p < 0.01$; WT + AIII (20) vs WT(20), * $p < 0.05$; WT + AIII (30) vs V(30), *** $p < 0.001$; WT + AIII (30) vs AIII(30), * $p < 0.05$; WT + AIII (30) vs WT(30), ** $p < 0.01$. p-AURKB: WT + AIII (20) vs V(20), * $p < 0.05$; WT + AIII (30) vs V(30), *** $p < 0.001$; WT + AIII (30) vs AIII(30), ** $p < 0.01$; WT + AIII (30) vs WT(30), * $p < 0.05$. p-AURKC: WT + AIII (20) vs V(20), ** $p < 0.01$.

5.2.4. Effect of Aurora kinase/CDK inhibitor alone or in combination with NBD WT CPP on AURKA-TPX2 signalling.

Next, treatment with the NBD WT CPP and/or 4-(5-Amino-1-(2,6-difluorobenzoyl)-1H-[1,2,4] triazol-3-ylamino)-benzenesulfonamide (Aurora kinase/CDK inhibitor) and the resultant impact on AURKA/TPX2 signalling compared to treatment with these agents alone or vehicle was explored. Cells were again treated with nocodazole (50ng/ml) for 16-20 hours prior to being washed and released as described previously – Section 2.2.2.1, before NBD WT CPP (100 μ M) and/or Aurora kinase/CDK inhibitor (0.5 μ M) were added upon release and samples prepared thereafter at appropriate time points. The WT peptide and the Aurora kinase/CDK inhibitor were prepared as described previously. The effect of the NBD WT CPP and/or Aurora kinase/CDK inhibitor on AURKA and its related mitotic markers in terms of their expression and/or phosphorylation were examined by Western blotting at 10, 20 and 30 minute time points.

In Figure 5.4, immunoblotting showed the effect of the NBD WT CPP and/or Aurora kinase/CDK inhibitor on the status of p-AURKs, AURKA and TPX2 post-trap and release; (A) 0, 10 and 20 min and (B) 0, 20 and 30 min. It was demonstrated in the subsequent quantification (C) at 0, 10 and 20 min and (D) at 0, 20 and 30 min in PC3 cells, the NBD WT CPP in combination with Aurora kinase/CDK inhibitor caused a reduction in phosphorylation of AURKA relative to the vehicle, NBD WT CPP and Aurora kinase/CDK inhibitor at each time point. In Figure 4.4 (A + C), the phosphorylation of AURKA was reduced after treatment with the NBD WT CPP and Aurora kinase/CDK inhibitor in combination, compared to the vehicle control at 20 min ($78.3 \pm 5.8\%$ vs $20.4 \pm 5.0\%$; $n=3$, $p<0.001$). This decrease in phosphorylation of AURKA caused by the combination treatment was also significantly different from the decrease caused by the NBD WT CPP ($70.5 \pm 0.9\%$ vs $20.4 \pm 5.0\%$; $n=3$, $p<0.001$) or Aurora kinase/CDK inhibitor ($54.5 \pm 4.1\%$ vs $20.4 \pm 5.0\%$; $n=3$, $p<0.001$) alone at the 20 minute time point. This was mirrored in Figure 5.4 (D) in which there was again a significant reduction in AURKA phosphorylation at 20 min post-release from nocodazole-mediated arrest ($81.5 \pm 8.5\%$ vs $21.6 \pm 5.4\%$; $n=3$, $p<0.01$) compared to the vehicle at this time point. As before, this effect exerted by the combination treatment to cause an increased reduction in AURKA phosphorylation was significantly enhanced compared to that induced by the single agent treatments of NBD WT CPP ($63.2 \pm 4.5\%$ vs $21.6 \pm 5.4\%$; $n=3$, $p<0.01$) or Aurora kinase/CDK inhibitor ($65.8 \pm 3.9\%$ vs $21.6 \pm 5.4\%$; $n=3$, $p<0.01$) at the 20 minute time point. Similar results were also seen at the 30 minute time point in Figure 5.4 (D), in which there was also a significant reduction in AURKA phosphorylation induced by treatment with

the NBD WT CPP and Aurora kinase/CDK inhibitor in combination, relative to the vehicle treated sample ($63.3 \pm 10.0\%$ vs $8.5 \pm 0.8\%$; $n=3$, $p<0.001$). Again, there was a significant difference in the reduction of AURKA phosphorylation between the NBD WT CPP and Aurora kinase/CDK inhibitor in combination compared to the single agent treatment with the NBD WT CPP at the 30 minute time point ($40.3 \pm 9.6\%$ vs $8.5 \pm 0.8\%$; $n=3$, $p<0.05$). There was also a significant reduction in AURKB phosphorylation (Figure 5.4 A + C) caused by treatment with the NBD WT CPP and Aurora kinase/CDK inhibitor in combination compared to the vehicle control after 20 min ($85.4 \pm 3.3\%$ vs $18.1 \pm 7.3\%$; $n=3$, $p<0.001$). AURKB phosphorylation was again shown to be significantly reduced in the sample treated with the combination of agents in comparison to the NBD WT CPP ($58.8 \pm 4.4\%$ vs $18.1 \pm 7.3\%$; $n=3$, $p<0.001$) and Aurora kinase/CDK inhibitor ($61.2 \pm 12.4\%$ vs $18.1 \pm 7.3\%$; $n=3$, $p<0.01$) alone at 20 minutes post-release from nocodazole-mediated arrest. This was mirrored in Figure 5.4 (D) in which there was a significant reduction in AURKB phosphorylation caused by treatment with the NBD WT CPP and Aurora kinase/CDK inhibitor in combination compared to the vehicle ($87.1 \pm 1.9\%$ vs $15.8 \pm 6.2\%$; $n=3$, $p<0.001$), NBD WT CPP ($49.3 \pm 7.5\%$ vs $15.8 \pm 6.2\%$; $n=3$, $p<0.01$) or Aurora kinase/CDK inhibitor ($67.3 \pm 6.8\%$ vs $15.8 \pm 6.2\%$; $n=3$, $p<0.001$) at the 20 minute time point. At the 30 minute time point, the sample treated simultaneously with the NBD WT CPP and Aurora kinase/CDK inhibitor was also significantly reduced in comparison to the vehicle treatment ($79.2 \pm 5.8\%$ vs $8.3 \pm 2.1\%$; $n=3$, $p<0.001$). The combination treatment also displayed significant reduction in comparison to treatment with the NBD WT CPP ($50.0 \pm 3.3\%$ vs $8.3 \pm 2.1\%$; $n=3$, $p<0.001$) alone at the 30 minute time point. Lastly, there was no significant difference in reduction of AURKC phosphorylation between treatment groups compared to the NBD WT CPP and Aurora kinase/CDK inhibitor in combination across the different time points. This could be due to the low levels of AURKC phosphorylation observed in the immunoblotting in Figure 5.4 (A and B).

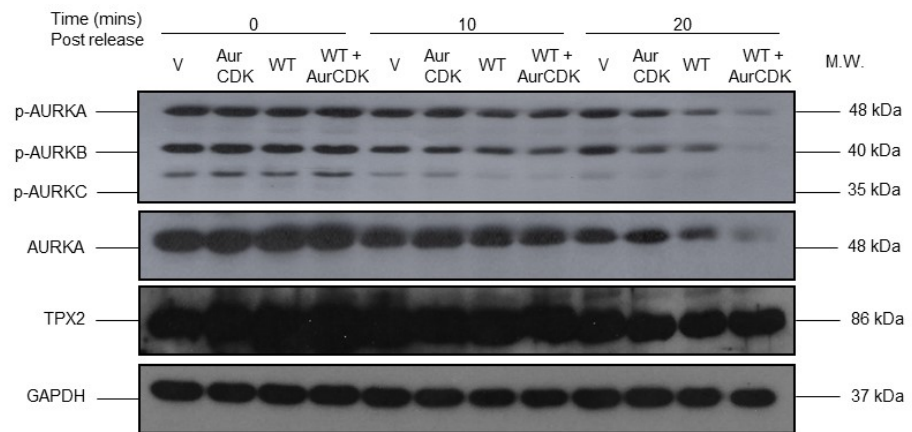
The reduction in total AURKA expression was assessed to determine if it was comparable to the effect of the NBD WT CPP and Aurora kinase/CDK inhibitor on AURKA phosphorylation. To begin with, in Figure 5.4 (C), following combination treatment, there was a significant reduction in total AURKA expression at 20 minutes ($82.0 \pm 6.0\%$ vs $27.3 \pm 5.2\%$; $n=3$, $p<0.001$) post-release relative to the vehicle treated sample at the retrospective time point. At the 20 minute time point there was also a significant difference in the reduction of total AURKA expression caused by the simultaneous treatment with the NBD WT CPP and Aurora kinase/CDK inhibitor compared to single treatment with the Aurora kinase/CDK inhibitor ($72.3 \pm 3.8\%$ vs $27.3 \pm 5.2\%$; $n=3$, $p<0.01$) or NBD WT CPP ($62.9 \pm 13.1\%$ vs $27.3 \pm 5.2\%$; $n=3$, $p<0.05$). In Figure 5.4 (D) there was a significant decrease in total AURKA expression caused by the combination treatment after 20 min ($78.2 \pm 6.9\%$ vs $20.9 \pm 2.3\%$;

n=3, p<0.001) and 30 min ($59.7 \pm 2.5\%$ vs $10.3 \pm 5.0\%$; n=3, p<0.001) post-release compared to the vehicle treated sample. There was also a further, significant reduction in total AURKA expression in the sample treated with a combination of the two agents compared to single-agent treatment with; NBD WT CPP ($56.6 \pm 1.7\%$ vs $20.9 \pm 2.3\%$; n=3, p<0.05) or Aurora kinase/CDK inhibitor ($58.2 \pm 13.6\%$ vs $20.9 \pm 2.3\%$; n=3, p<0.01) at the 20 minute time point. At the 30 minute time point there was also a significant difference in the reduction in total AURKA expression through combination treatment of the NBD WT CPP and Aurora kinase/CDK inhibitor in comparison to the NBD WT CPP alone ($43.6 \pm 6.9\%$ vs $10.3 \pm 5.0\%$; n=3, p<0.05).

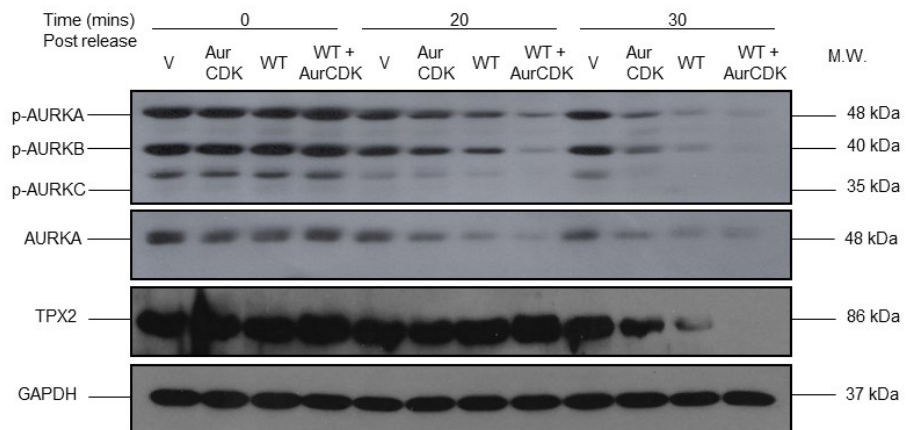
In this section, the effect of the NBD WT CPP and Aurora kinase/CDK inhibitor on the expression of the critical AURKA co-activator TPX2 was also examined. In Figure 5.4 (D), there was a significant reduction in TPX2 expression caused by simultaneous treatment with the NBD WT CPP and the Aurora kinase/CDK inhibitor compared to the vehicle treated sample at the 30 minute time point ($91.8 \pm 3.4\%$ vs $21.3 \pm 10.3\%$; n=3, p<0.001). This decrease in expression of TPX2 caused by the combination treatment was also significantly different from the decrease caused by the NBD WT CPP ($65.3 \pm 4.2\%$ vs $21.3 \pm 10.3\%$; n=3, p<0.001) or Aurora kinase/CDK inhibitor ($85.0 \pm 7.7\%$ vs $21.3 \pm 10.3\%$; n=3, p<0.001) alone at 30 minutes post-release from nocodazole-mediated arrest.

Collectively, these experimental outcomes demonstrated the ability of the NBD WT CPP and Aurora kinase/CDK inhibitor, when used in combination, to significantly enhance the reduction of AURKA phosphorylation and/or expression as well as the expression of TPX2 in comparison to when these agents were used alone.

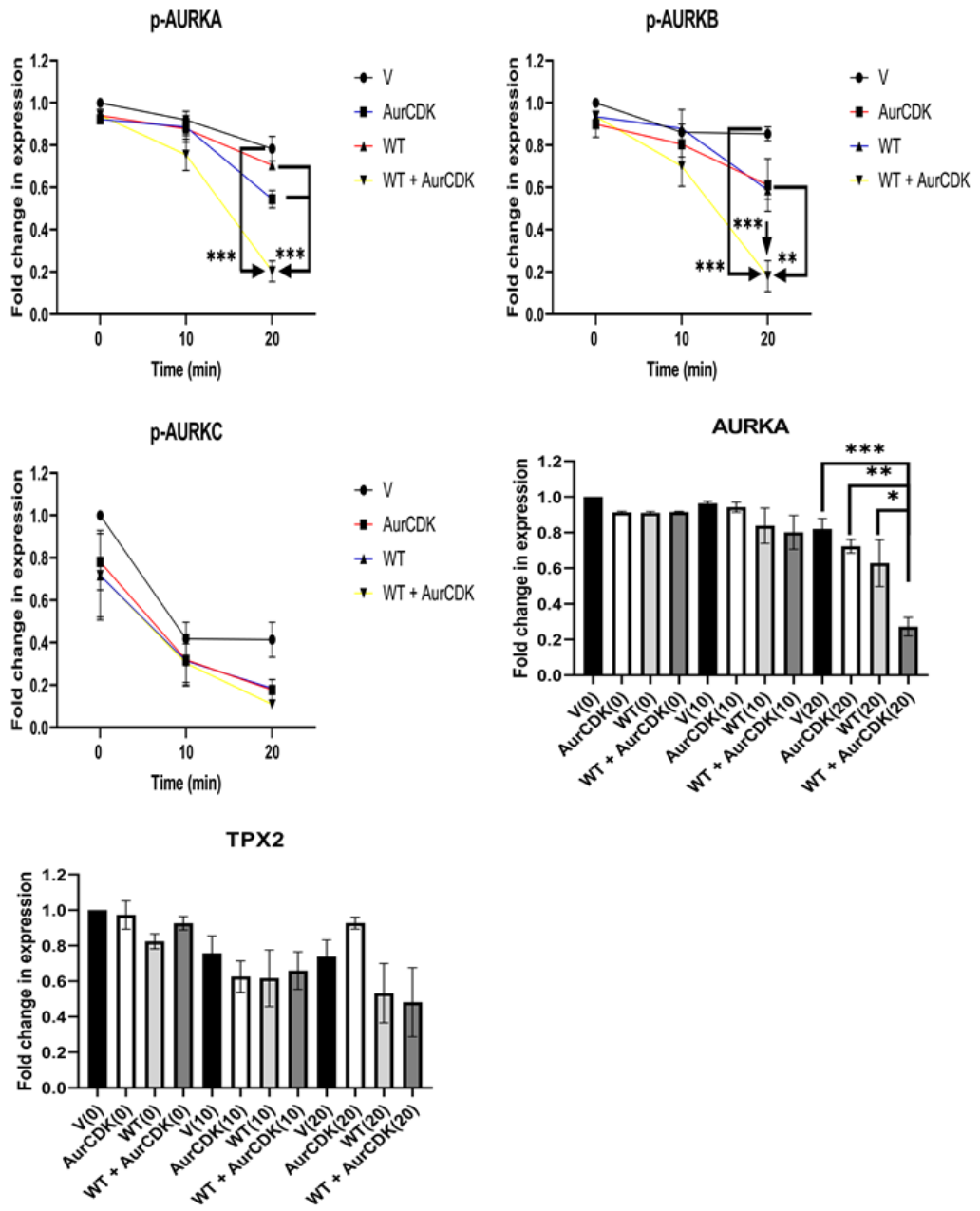
(A)



(B)



(C)



(D)

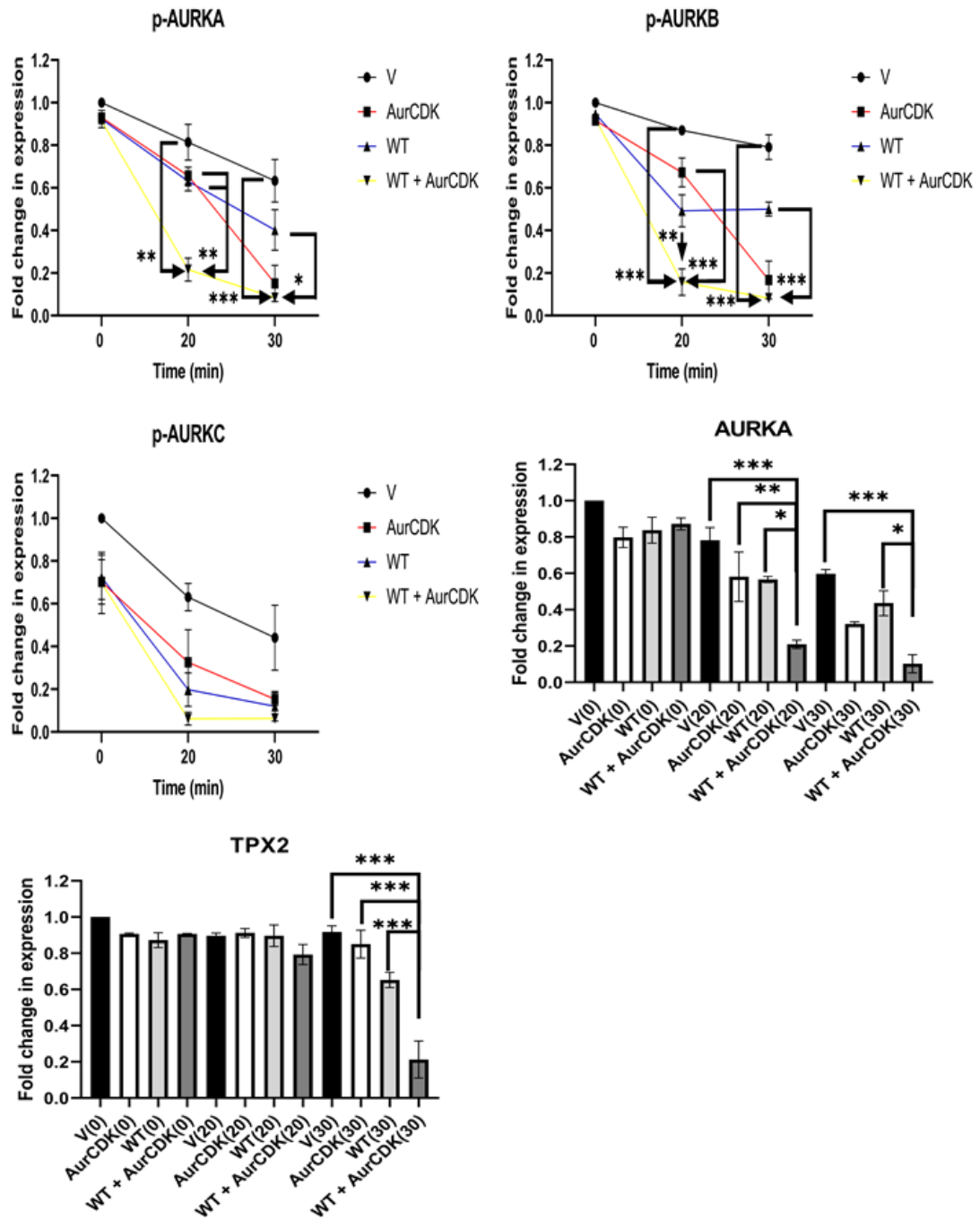


Figure 5.4. Effect of Aurora kinase/CDK inhibitor alone and in combination with NBD WT CPP on AURKs and related protein markers of mitosis in PC3 cells.

PC3 cells were grown on 10mm dishes and treated with 50ng/ml Nocodazole (16-20 hours) prior to treatment with Aurora kinase/CDK inhibitor (0.5 μ M), NBD WT CPP (100 μ M), DMSO as a vehicle control (0.5% (v/v)) or NBD WT CPP (WT) and Aurora kinase/CDK (AurCDK) inhibitor in combination upon release from trap at: **(A + C)** 0, 10 and 20 min **(B + D)** 0, 20 and 30 min. A and B: Whole cell lysates were prepared for separation using SDS-PAGE and analysed by Western Blotting using the above antibodies (n=3). GAPDH was used as a loading control. C and D: Data was

normalised to the vehicle treated control at 0 min (V0) and represents mean \pm S.E.M. One-way ANOVA with post-hoc Tukey multiple comparisons test was used to determine statistical significance ($p < 0.05$) of observed changes between the means of the different treatment groups compared to the WT + AurCDK at the same time point (* = $p < 0.05$, ** = $p < 0.01$, *** = $p < 0.001$). **(C)**: p-AURKA: WT + AurCDK (20) vs V(20), *** $p < 0.001$; WT + AurCDK (20) vs AurCDK (20), *** $p < 0.001$; WT + AurCDK (20) vs WT(20), *** $p < 0.001$. p-AURKB: WT + AurCDK (20) vs V(20), *** $p < 0.001$; WT + AurCDK (20) vs AurCDK (20), ** $p < 0.01$; WT + AurCDK (20) vs WT(20), *** $p < 0.001$. **(D)**: p-AURKA: WT + AurCDK (20) vs V(20), ** $p < 0.01$; WT + AurCDK (20) vs AurCDK (20), ** $p < 0.01$; WT + AurCDK (20) vs WT(20), ** $p < 0.01$; WT + AurCDK (30) vs V(30), *** $p < 0.001$; WT + AurCDK (30) vs WT(30), * $p < 0.05$. p-AURKB: WT + AurCDK (20) vs V(20), *** $p < 0.001$; WT + AurCDK (20) vs AurCDK(20), *** $p < 0.001$; WT + AurCDK (20) vs WT(20), ** $p < 0.01$; WT + AurCDK (30) vs V(30), *** $p < 0.001$; WT + AurCDK (30) vs WT(30), *** $p < 0.001$

5.2.5. Effect of VX-680 alone and in combination with NBD WT CPP on AURKA-TPX2 signalling.

Following on from the demonstrated effect of simultaneous targeting with NBD WT CPP and the Aurora kinase/CDK inhibitor to exert an increased disruption of AURKA/TPX2 signalling, the treatment with the NBD WT CPP and/or N-[4-[[4-(4-Methyl-1-piperazinyl)-6-[(5-methyl-1H-pyrazol-3-yl)amino]-2-pyrimidinyl]thio]phenyl]cyclopropanecarboxamide (VX-680) and the resultant impact on AURKA-TPX2 signalling compared to treatment with these agents alone or vehicle were explored. Cells were again treated with nocodazole (50ng/ml) for 16-20 hours prior to being washed and released as described previously – Section 2.2.2.1, before NBD WT CPP (100 μ M) and/or VX-680 (0.1 μ M) were added upon release and samples prepared thereafter at appropriate time points. The WT peptide and the VX-680 were prepared as described previously. The effect of the NBD WT CPP and/or VX-680 on AURKA and its related mitotic markers in terms of their expression and/or phosphorylation were examined by Western blotting at 10, 20 and 30 minute time points.

Figure 5.5, confirmed by means of immunoblotting the effect of the NBD WT CPP and/or VX-680 on the status of p-AURKs, AURKA and TPX2 post-trap and release; (A) 0, 10 and 20 min and (B) 0, 20 and 30 min. It was demonstrated in the subsequent quantification (C) at 0, 10, and 20 min and (D) at 0, 20 and 30min in PC3 cells, the NBD WT CPP in combination with VX-680 caused a reduction in phosphorylation of AURKA relative to the vehicle, NBD WT CPP and VX-680 at each time point. In Figure 5.5 (A + C), the phosphorylation of AURKA was reduced after treatment with the NBD WT CPP and VX-680 in combination, compared to the vehicle control at 10 min ($79.4 \pm 9.4\%$ vs $46.5 \pm 6.3\%$; $n=3$, $p < 0.001$) and 20 min ($77.5 \pm 3.3\%$ vs $19.4 \pm 1.9\%$; $n=3$, $p < 0.001$). This decrease in phosphorylation of AURKA caused by the combination treatment was also significantly different from the decrease caused by the NBD WT CPP ($73.5 \pm 5.9\%$ vs $46.5 \pm 6.3\%$; $n=3$, $p < 0.01$) or VX-680 ($70.0 \pm 3.8\%$ vs $46.5 \pm 6.3\%$; $n=3$, $p < 0.05$) alone at 10 minutes post-release

from nocodazole-mediated arrest. There was also a significant difference in the reduction in AURKA phosphorylation as a result of the combination treatment compared to single agent treatment with the NBD WT CPP ($68.0 \pm 1.3\%$ vs $19.4 \pm 1.9\%$; $n=3$, $p<0.001$) or VX-680 ($52.7 \pm 5.2\%$ vs $19.4 \pm 1.9\%$; $n=3$, $p<0.001$) alone at the 20 minute time point. This was mirrored in Figure 5.5 (D) in which there was again a significant reduction in AURKA phosphorylation at 20 min post-release ($83.7 \pm 7.7\%$ vs $25.6 \pm 2.5\%$; $n=3$, $p<0.001$) compared to the vehicle. As before, this effect exerted by the combination treatment on AURKA phosphorylation was significantly different from the single agent treatments of NBD WT CPP ($70.4 \pm 12.3\%$ vs $25.6 \pm 2.5\%$; $n=3$, $p<0.001$) or VX-680 ($55.3 \pm 4.2\%$ vs $25.6 \pm 2.5\%$; $n=3$, $p<0.05$) alone at the 20 minute time point. Similar was also seen at the 30 minute time point in Figure 4.5 (D), in which there was also a significant reduction in AURKA phosphorylation induced by simultaneous treatment with the NBD WT CPP and VX-680, relative to the vehicle treated sample ($65.4 \pm 3.4\%$ vs $12.1 \pm 1.9\%$; $n=3$, $p<0.001$) at this time point. Again, there was a significant difference in the reduction of AURKA phosphorylation between the NBD WT CPP and VX-680 in combination compared to the single agent treatment with the NBD WT CPP at the 30 minute time point ($51.8 \pm 7.4\%$ vs $12.1 \pm 1.9\%$; $n=3$, $p<0.01$). There was also a significant reduction in AURKB phosphorylation (Figure 5.5 A + C) caused by treatment with the NBD WT CPP and VX-680 in combination compared to the vehicle control at 20 min post-release ($84.2 \pm 7.3\%$ vs $27.3 \pm 10.7\%$; $n=3$, $p<0.01$). AURKB phosphorylation was again shown to be significantly reduced in the sample treated with the combination therapy in comparison to the NBD WT CPP ($71.4 \pm 1.8\%$ vs $27.3 \pm 10.7\%$; $n=3$, $p<0.05$) and VX-680 ($75.4 \pm 15.5\%$ vs $27.3 \pm 10.7\%$; $n=3$, $p<0.05$) alone at 20 min post-release from nocodazole-mediated arrest. This was mirrored in Figure 5.5 (D) in which there was a significant reduction in AURKB phosphorylation caused by treatment with the NBD WT CPP and VX-680 in combination compared to the vehicle ($88.2 \pm 12.6\%$ vs $28.4 \pm 1.0\%$; $n=3$, $p<0.001$), NBD WT CPP ($71.3 \pm 3.7\%$ vs $28.4 \pm 1.0\%$; $n=3$, $p<0.05$) or VX-680 ($75.8 \pm 12.6\%$ vs $28.4 \pm 1.0\%$; $n=3$, $p<0.01$) alone at the 20 minute time point. At the 30 minute time point, the sample treated simultaneously with the NBD WT CPP and VX-680 was also significantly reduced in comparison to the vehicle treatment ($74.3 \pm 8.2\%$ vs $13.7 \pm 3.9\%$; $n=3$, $p<0.001$). The combination treatment caused a further enhanced reduction which was significantly reduced in comparison to treatment with the NBD WT CPP ($56.4 \pm 2.0\%$ vs $13.7 \pm 3.9\%$; $n=3$, $p<0.05$) or VX-680 ($56.1 \pm 16.1\%$ vs $13.7 \pm 3.9\%$; $n=3$, $p<0.05$) alone at the 30 minute time point post-release. Lastly, there was also a significant difference in the reduction of AURKC phosphorylation in the sample treated with a combination of the NBD WT CPP and VX-680 compared to the vehicle treated sample ($84.9 \pm 6.4\%$ vs $19.4 \pm 7.8\%$; $n=3$, $p<0.001$) or the sample treated with VX-680 ($64.1 \pm 12.9\%$ vs $19.4 \pm 7.8\%$; $n=3$, $p<0.05$) at 10 min post-release. AURKC phosphorylation was also

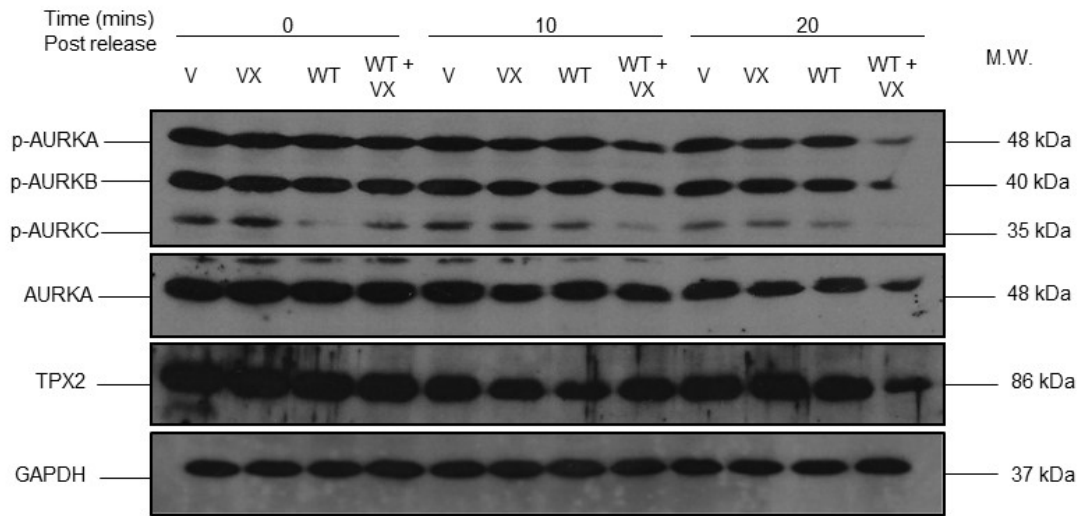
significantly reduced following simultaneous treatment with the NBD WT CPP and VX-680 at the 20 minute time point in both Figure 5.5C ($57.3 \pm 3.2\%$ vs $4.8 \pm 1.1\%$; $n=3$, $p<0.01$) and 5.5D ($70.0 \pm 11.5\%$ vs $12.7 \pm 0.9\%$; $n=3$, $p<0.05$).

The reduction in total AURKA expression was assessed to determine if it was comparable to the effect of the NBD WT CPP and VX-680 in combination on AURKA phosphorylation. In Figure 5.5 (C), following combination treatment with the NBD WT CPP and VX-680, there was a significant reduction in total AURKA expression at 20 minutes ($86.7 \pm 4.2\%$ vs $46.7 \pm 12.7\%$; $n=3$, $p<0.001$) post-release from nocodazole-mediated arrest relative to the vehicle treated sample. At the 20 minute time point there was also a significant difference in the reduction of total AURKA expression caused by the simultaneous treatment of the NBD WT CPP and VX-680 compared to single agent treatment with VX-680 ($72.5 \pm 6.1\%$ vs $46.7 \pm 12.7\%$; $n=3$, $p<0.05$) alone. In Figure 5.5 (D) there was a significant decrease in total AURKA expression caused by the combination treatment after 20 min ($86.4 \pm 2.9\%$ vs $60.5 \pm 4.1\%$; $n=3$, $p<0.01$) and 30 min ($80.1 \pm 5.5\%$ vs $19.5 \pm 2.5\%$; $n=3$, $p<0.001$) post-release compared to the vehicle treated sample. There was also a further, significant reduction in total AURKA expression in the sample treated with a combination of the two agents compared to single-agent treatment with; NBD WT CPP ($52.6 \pm 8.5\%$ vs $19.5 \pm 2.5\%$; $n=3$, $p<0.001$) or VX-680 ($64.3 \pm 2.9\%$ vs $19.5 \pm 2.5\%$; $n=3$, $p<0.001$) at the 30 minute time point.

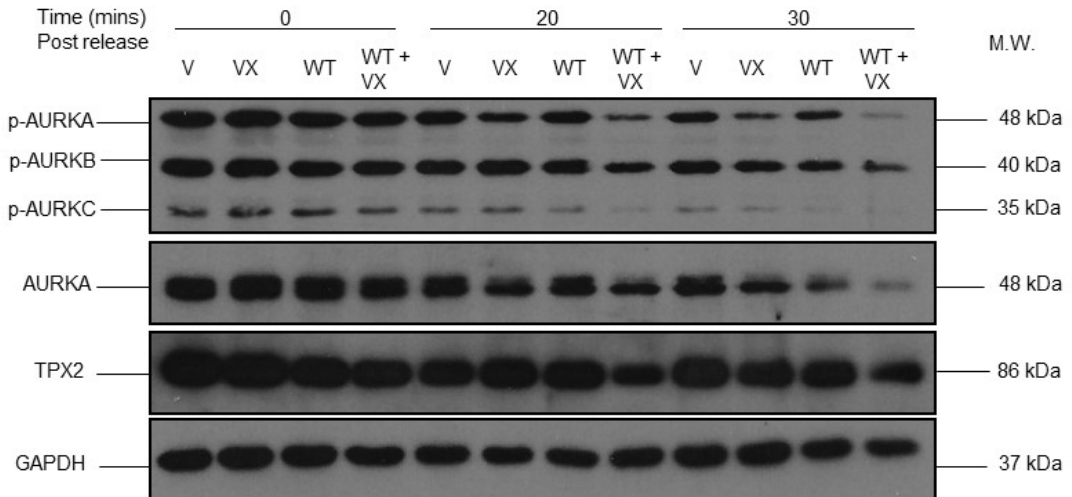
Lastly, we examined the effect of the NBD WT CPP and VX-680 on the expression of the AURKA co-activator TPX2. In Figure 5.5 (D), there was a significant reduction in TPX2 expression caused by simultaneous treatment with the NBD WT CPP and VX-680 in comparison to the vehicle treated sample at the 30 minute time point ($84.5 \pm 3.1\%$ vs $39.3 \pm 9.5\%$; $n=3$, $p<0.01$). This decrease in expression of TPX2 caused by the combination treatment was also significantly different from the decrease caused by the NBD WT CPP ($79.8 \pm 8.3\%$ vs $39.3 \pm 9.5\%$; $n=3$, $p<0.01$) or VX-680 ($78.9 \pm 3.0\%$ vs $21.3 \pm 39.3 \pm 9.5\%$; $n=3$, $p<0.01$) alone at 30 min post-release.

Collectively, these experimental outcomes demonstrated the ability of the NBD WT CPP and VX-680, when used in combination, to significantly enhance the reduction of AURKA phosphorylation and/or expression as well as the expression of TPX2 in comparison to when these agents were used alone.

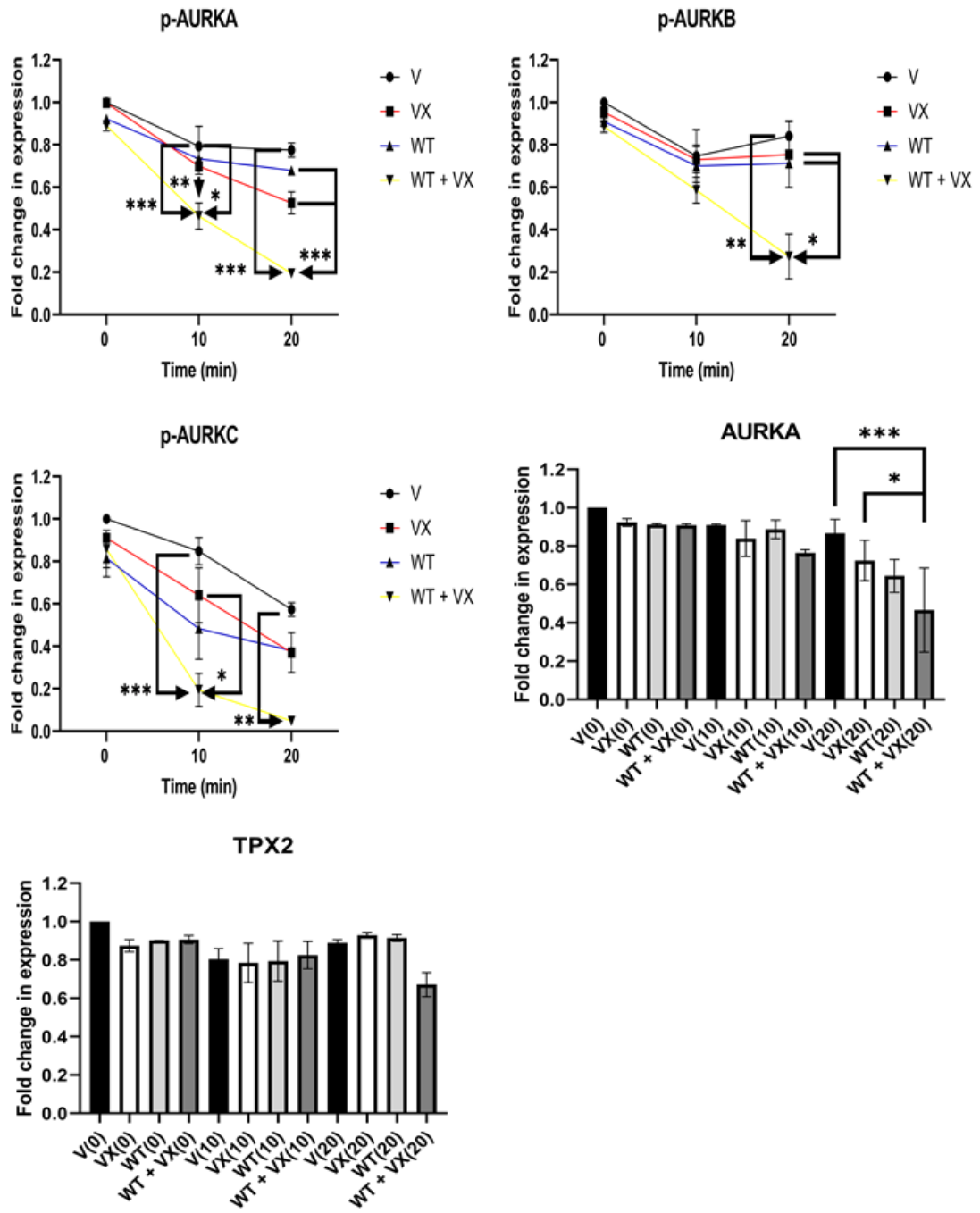
(A)



(B)



(C)



(D)

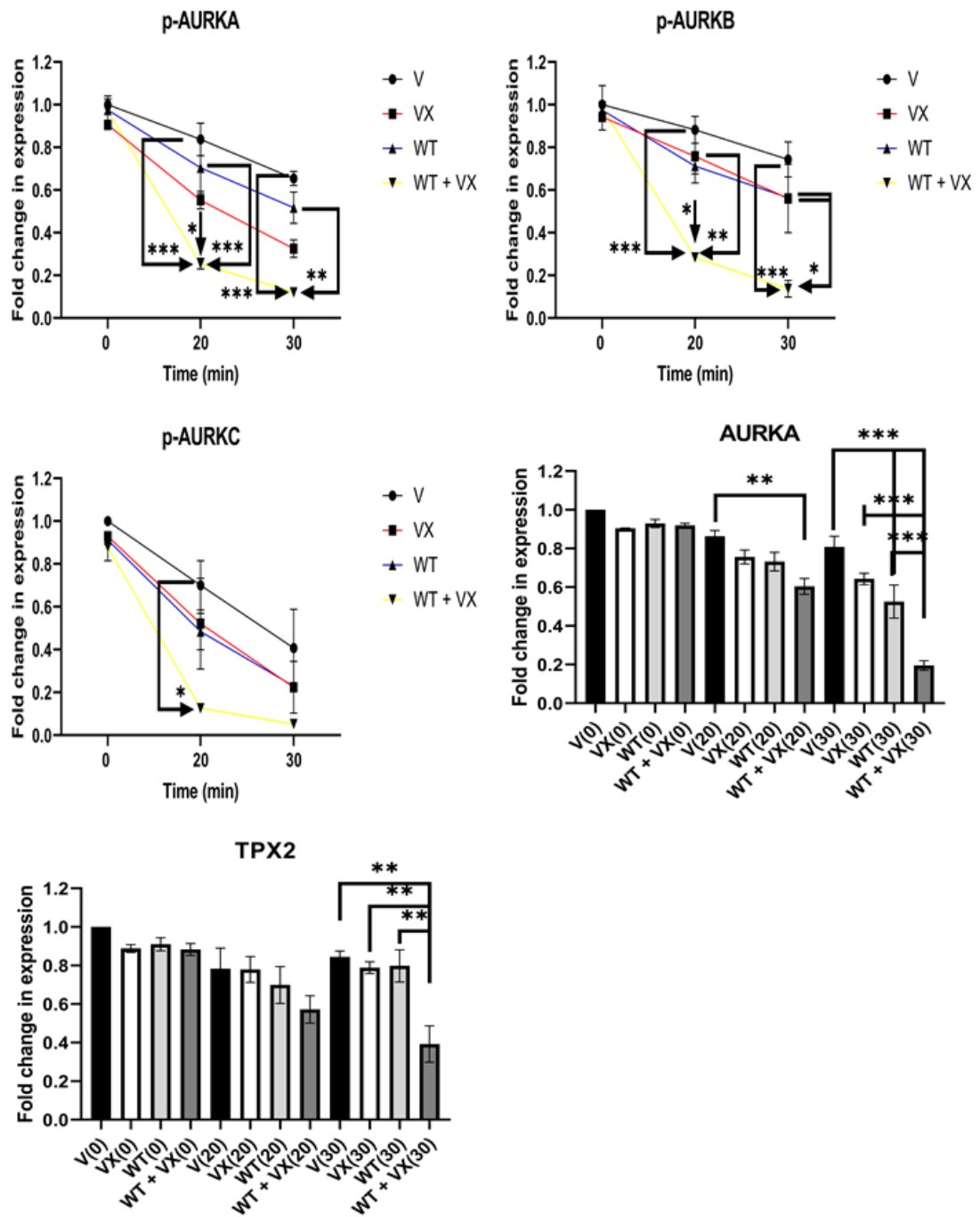


Figure 5.5. Effect of VX-680 alone and in combination with NBD WT CPP on AURKs and related protein markers of mitosis in PC3 cells.

PC3 cells were grown on 10mm dishes and treated with 50ng/ml Nocodazole (16-20 hours) prior to treatment with VX-680 (0.1 μ M), NBD WT CPP (100 μ M), DMSO as a vehicle control (0.5% (v/v)) or NBD WT CPP (WT) and VX-680 (VX) in combination upon release from trap at: (A + C) 0, 10 and 20 min (B + D) 0, 20 and 30 min. A and B: Whole cell lysates were prepared for separation using SDS-PAGE and analysed by Western Blotting using the above antibodies (n=3). GAPDH was used as a loading control. C and D: Data was normalised to the vehicle treated control at 0 min

(V0) and represents mean \pm S.E.M. One-way ANOVA with post-hoc Tukey multiple comparisons test was used to determine statistical significance ($p < 0.05$) of observed changes between the means of the different treatment groups compared to the WT + VX at the same time point (*= $p < 0.05$, **= $p < 0.01$, ***= $p < 0.001$). (C): p-AURKA: WT + VX (10) vs V(10), *** $p < 0.001$; WT + VX (10) vs VX(10), ** $p < 0.01$; WT + VX(10) vs WT(10), * $p < 0.05$; WT + VX(20) vs V(20), *** $p < 0.001$; WT + VX (20) vs VX(20), *** $p < 0.001$; WT + VX (20) vs WT(20), *** $p < 0.001$. p-AURKB: WT + VX (20) vs V(20), ** $p < 0.01$; WT + VX(20) vs VX(20), * $p < 0.05$; WT + VX(20) vs WT(20), * $p < 0.05$. p-AURKC: WT + VX (10) vs V(10), *** $p < 0.001$; WT + VX (10) vs VX(10), * $p < 0.05$; WT + VX (20) vs V(20), ** $p < 0.01$. (D): p-AURKA: WT + VX (20) vs V(20), *** $p < 0.001$; WT + VX (20) vs VX(20), * $p < 0.05$; WT + VX (20) vs WT(20), *** $p < 0.001$; WT + VX (30) vs V(30), *** $p < 0.001$; WT + VX (30) vs WT(30), ** $p < 0.01$. p-AURKB: WT + VX (20) vs V(20), *** $p < 0.001$; WT + VX (20) vs VX(20), ** $p < 0.01$; WT + VX (20) vs WT(20), * $p < 0.05$; WT + VX (30) vs V(30), *** $p < 0.001$; WT + VX (30) vs VX(30), * $p < 0.05$; WT + VX (30) vs WT(30), * $p < 0.05$. p-AURKC: WT + VX (20) vs V(20), * $p < 0.05$.

5.2.6. Effect of ZM 447439 alone and in combination with NBD WT CPP on AURKA signalling.

Lastly, the effect of the NBD WT CPP and/or N-[4-[[6-methoxy-7-[3-(4-morpholinyl)propoxy]-4-quinazoliny]amino]phenyl]-benzamide (ZM 447439) and the resultant impact on AURKA signalling compared to treatment with these agents alone or vehicle was explored. Cells were again treated with nocodazole (50ng/ml) for 16-20 hours prior to being washed and released as described previously – Section 2.2.2.1, before NBD WT CPP (100 μ M) and/or ZM 447439 (0.1 μ M) were added upon release and samples prepared thereafter at appropriate time points. The WT peptide and the ZM 447439 were prepared as described previously. The effect of the NBD WT CPP and/or ZM 447439 on AURKA and its related mitotic markers in terms of their expression and/or phosphorylation were examined by Western blotting at 10, 20 and 30 minute time points.

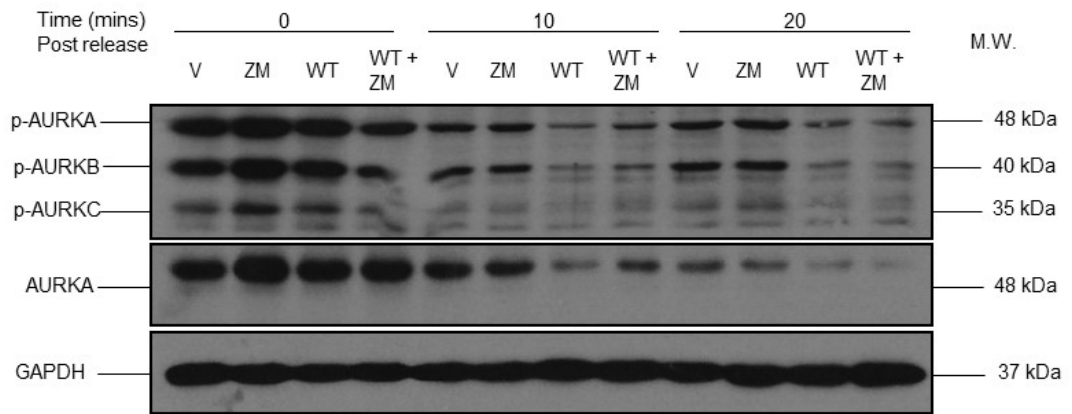
Figure 5.6 indicated by immunoblotting the effect of the NBD WT CPP and/or ZM 447439 on the status of p-AURKs and AURKA post-trap and release; (A) 0, 10 and 20 min and (B) 0, 20 and 30 min. It was demonstrated in the subsequent quantification (C) at 0, 10, and 20 min and (D) at 0, 20 and 30 min in PC3 cells, the NBD WT CPP in combination with ZM 447439 caused a reduction in phosphorylation of AURKA relative to the vehicle, NBD WT CPP and ZM 447439 at each time point. In Figure 5.6 (A + C), the phosphorylation of AURKA was reduced after treatment with the NBD WT CPP and ZM 447439 in combination, compared to the vehicle control at 10 min ($54.1 \pm 1.3\%$ vs $31.1 \pm 3.9\%$; $n=3$, $p < 0.01$) and 20 min ($57.8 \pm 1.2\%$ vs $31.7 \pm 0.3\%$; $n=3$, $p < 0.01$) post-release from nocodazole-mediated arrest. This decrease in phosphorylation of AURKA caused by the combination treatment with the NBD WT CPP and ZM 447439 was also significantly different from the decrease caused by the ZM 447439 alone at 10 min ($52.4 \pm 1.0\%$ vs $31.1 \pm 3.9\%$; $n=3$, $p < 0.05$) and 20 min ($68.1 \pm 1.0\%$

vs $31.7 \pm 0.3\%$;n=3, $p<0.001$) post-release. Similar was also seen at the 20 minute time point in Figure 5.6D, in which there was also a significant reduction in phosphorylation of AURKA induced by treatment with the NBD WT CPP and ZM 447439 in combination, relative to the vehicle treated sample ($56.2 \pm 3.4\%$ vs $27.2 \pm 3.1\%$; n=3, $p<0.01$) at this time point. Again, there was a significant difference in the reduction of AURKA phosphorylation between the NBD WT CPP and ZM 447439 in combination and the single agent treatment with ZM 447439 at the 20 minute time point ($62.2 \pm 4.9\%$ vs $27.2 \pm 3.1\%$; n=3, $p<0.001$). The NBD WT CPP and ZM 447439 combination also caused a significant reduction in phosphorylation of AURKA in comparison to the vehicle treated control at 30 min ($56.5 \pm 5.7\%$ vs $4.1 \pm 2.2\%$; n=3, $p<0.001$) post-release. There was also a significant difference in the reduction in AURKA phosphorylation in the sample treated with a combination of the two agents compared to single-agent treatment with; NBD WT CPP ($26.9 \pm 3.0\%$ vs $4.1 \pm 2.2\%$; n=3, $p<0.05$) or ZM 447439 ($48.6 \pm 4.8\%$ vs $4.1 \pm 2.2\%$; n=3, $p<0.001$) at 30 minutes post-release. There was also a significant reduction in AURKB phosphorylation (Figure 5.6 A + C) caused by treatment with the NBD WT CPP and ZM 447439 in combination compared to the vehicle control at 20 min ($66.5 \pm 4.7\%$ vs $24.5 \pm 2.4\%$; n=3, $p<0.001$) post-release. AURKB phosphorylation was again shown to be significantly reduced in the sample treated with the combination therapy of the NBD WT CPP and ZM 447439 in comparison to the ZM 447439 alone after 20 min ($68.4 \pm 2.4\%$ vs $24.5 \pm 2.4\%$; n=3, $p<0.001$). This was mirrored in Figure 5.6D in which there was a significant reduction in AURKB phosphorylation caused by treatment with the NBD WT CPP and ZM 447439 in combination compared to the vehicle ($61.1 \pm 2.3\%$ vs $15.2 \pm 2.2\%$; n=3, $p<0.001$) and ZM 447439 ($64.6 \pm 3.7\%$ vs $15.2 \pm 2.2\%$; n=3, $p<0.001$) alone at the 20 minute time point post-release. At the 30 minute time point, the sample treated simultaneously with the NBD WT CPP and ZM 447439 was also significantly reduced in comparison to the vehicle treatment ($65.8 \pm 5.2\%$ vs $4.7 \pm 2.0\%$; n=3, $p<0.001$). The combination treatment caused a further significant reduction in comparison to treatment with the NBD WT CPP ($26.2 \pm 3.2\%$ vs $4.7 \pm 2.0\%$; n=3, $p<0.05$) or ZM 447439 ($51.8 \pm 4.2\%$ vs $4.7 \pm 2.0\%$; n=3, $p<0.001$) alone at the 30 minute time point post-release. Lastly, in Figure 5.6D, the phosphorylation of AURKC was also significantly reduced by the combination treatment after 30 min post-release relative to the vehicle treated sample ($75.3 \pm 13.0\%$ vs $4.9 \pm 0.5\%$; n=3, $p<0.001$). There was also a significant reduction in AURKC phosphorylation as a result of simultaneous treatment of the NBD WT CPP and ZM 447439 in comparison to the single agent treatments; NBD WT CPP ($56.9 \pm 5.6\%$ vs $4.9 \pm 0.5\%$; n=3, $p<0.01$) or ZM 447439 ($48.1 \pm 9.1\%$ vs $4.9 \pm 0.5\%$; n=3, $p<0.05$).

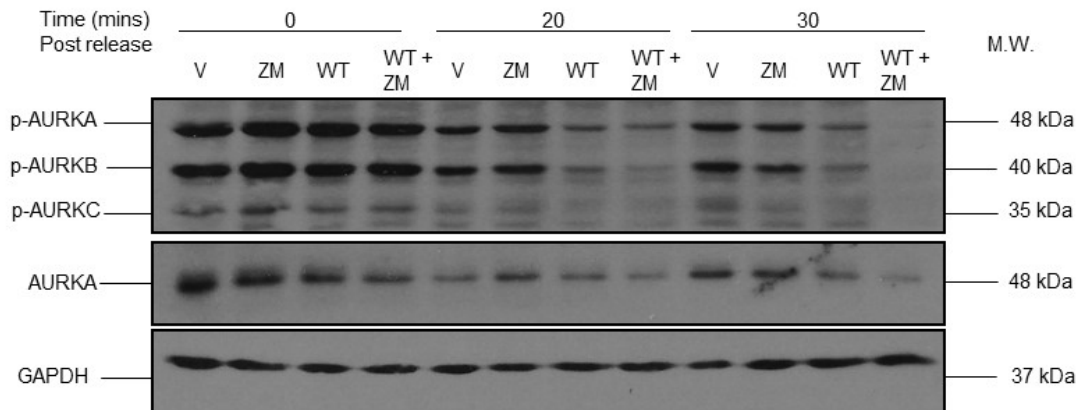
The reduction in total AURKA expression was assessed to determine if it was comparable to the effect of the NBD WT CPP and ZM 447439 on AURKA phosphorylation. In

Figure 5.6 (C) following combination treatment with the NBD WT CPP and the ZM 447439, there was a significant reduction in total AURKA expression at 10 min ($80.8 \pm 5.4\%$ vs $35.1 \pm 7.1\%$; $n=3$, $p<0.01$) and 20 min ($57.1 \pm 11.9\%$ vs $9.7 \pm 2.3\%$; $n=3$, $p<0.001$) post-release relative to the vehicle treated sample. At the 10 minute time point there was also a significant difference in the reduction of total AURKA expression caused by the simultaneous treatment of the NBD WT CPP and ZM 447439 compared to single treatment with ZM 447439 ($77.5 \pm 9.8\%$ vs $35.1 \pm 7.1\%$; $n=3$, $p<0.01$). In Figure 5.6D there was a significant decrease in total AURKA expression caused by the combination treatment after 20 min ($75.8 \pm 7.4\%$ vs $27.7 \pm 5.6\%$; $n=3$, $p<0.05$) and 30 min ($69.4 \pm 6.8\%$ vs $7.9 \pm 4.5\%$; $n=3$, $p<0.001$) post-release compared to the vehicle treated sample. Similarly to the phosphorylation, there was also a further, significant reduction in total AURKA expression in the sample treated with a combination of the two agents compared to single-agent treatment with; NBD WT CPP ($53.0 \pm 3.4\%$ vs $7.9 \pm 4.5\%$; $n=3$, $p<0.05$) or ZM 447439 ($64.3 \pm 7.4\%$ vs $7.9 \pm 4.5\%$; $n=3$, $p<0.01$) at the 30 minute time point. Collectively, these experimental outcomes demonstrated the ability of the NBD WT CPP and ZM 447439, when used in combination, to significantly enhance the reduction of the expression and/or phosphorylation of AURKs in comparison to when these agents were used alone.

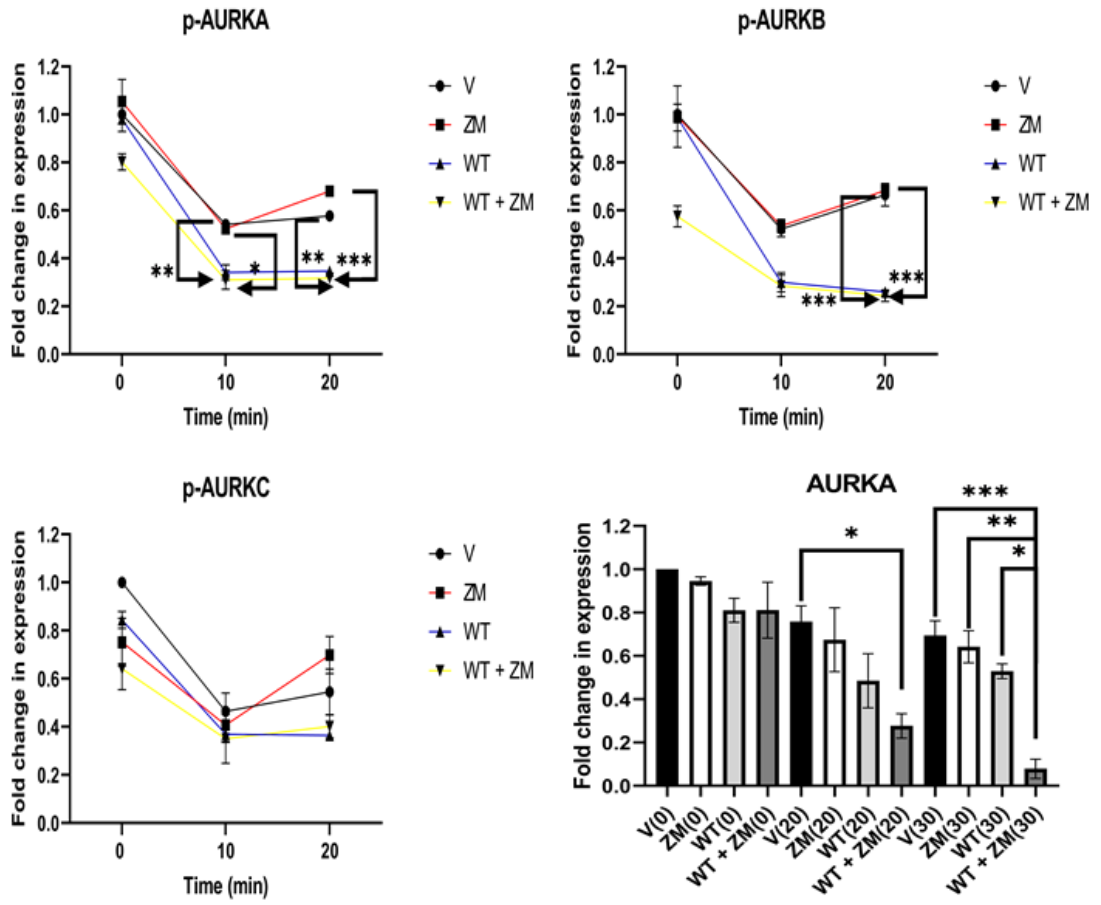
(A)



(B)



(C)



(D)

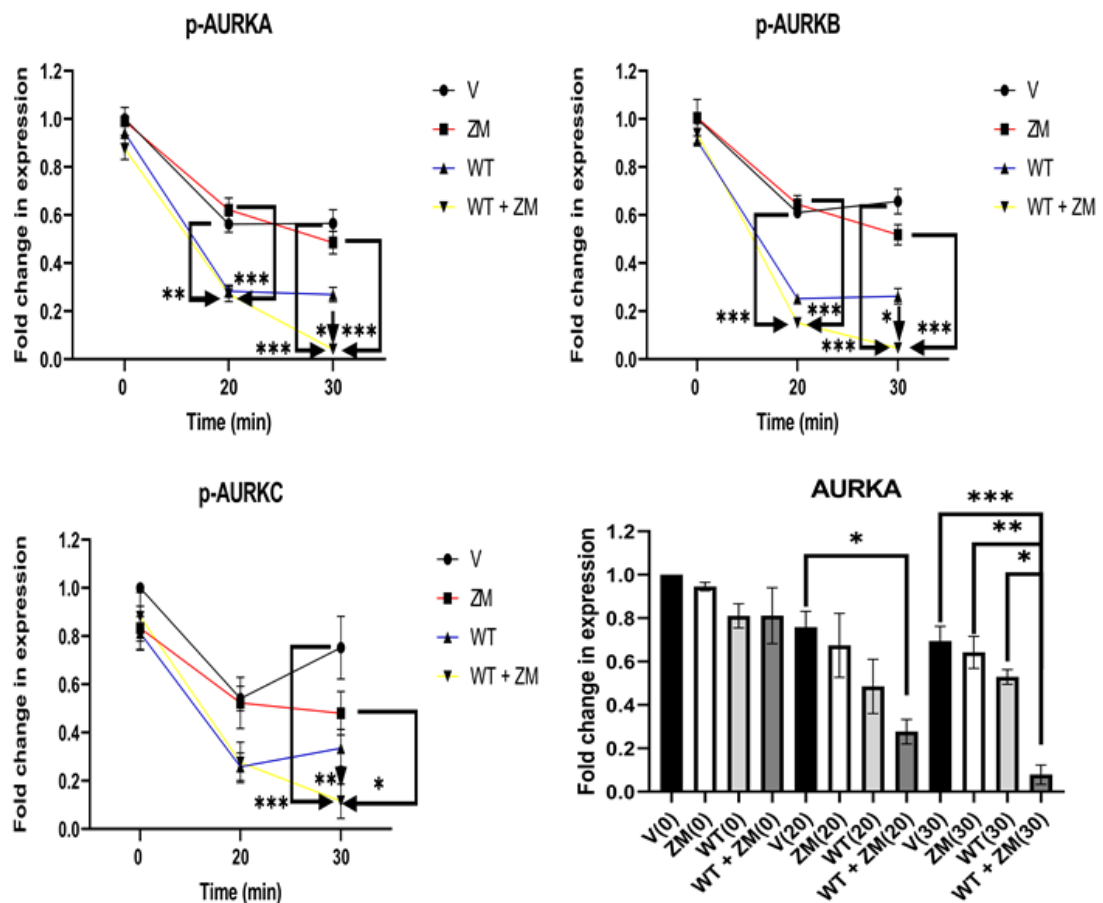


Figure 5.6. Effect of ZM 447439 alone and in combination with NBD WT CPP on AURKs and related protein markers of mitosis in PC3 cells.

PC3 cells were grown on 10mm dishes and treated with 50ng/ml Nocodazole (16-20 hours) prior to treatment with ZM 447439 (0.1 μ M), NBD WT CPP (100 μ M), DMSO as a vehicle control (0.5% (v/v)) or NBD WT CPP (WT) and ZM 447439 (ZM) in combination upon release from trap at: (A + C) 0, 10 and 20 min (B + D) 0, 20 and 30 min. A and B: Whole cell lysates were prepared for separation using SDS-PAGE and analysed by Western Blotting using the above antibodies (n=3). GAPDH was used as a loading control. C and D: Data was normalised to the vehicle treated control at 0 min (V0) and represents mean \pm S.E.M. One-way ANOVA with post-hoc Tukey multiple comparisons test was used to determine statistical significance ($p < 0.05$) of observed changes between the means of the different treatment groups compared to the WT + ZM at the same time point (*= $p < 0.05$, **= $p < 0.01$, ***= $p < 0.001$). (C): p-AURKA: WT + ZM (10) vs V(10), ** $p < 0.01$; WT + ZM (10) vs ZM(10), * $p < 0.05$; WT + ZM (20) vs V(20), ** $p < 0.01$; WT + ZM (20) vs ZM(20), *** $p < 0.001$. p-AURKB: WT + ZM (20) vs V(20), *** $p < 0.001$; WT + ZM(20) vs ZM(20), *** $p < 0.001$. (D): p-AURKA: WT + ZM (20) vs V(20), ** $p < 0.01$; WT + ZM (20) vs ZM(20), *** $p < 0.001$; WT + ZM (30) vs V(30), *** $p < 0.001$; WT + ZM (30) vs ZM(30), *** $p < 0.001$; WT + ZM (30) vs WT(30), * $p < 0.05$. p-AURKB: WT + ZM (20) vs V(20), *** $p < 0.001$; WT + ZM (20) vs ZM(20), *** $p < 0.001$; WT + ZM (30) vs V(30), *** $p < 0.001$; WT + ZM (30) vs ZM(30), *** $p < 0.001$; WT + ZM (30) vs WT(30), * $p < 0.05$. p-AURKC: WT + ZM (30) vs V(30), *** $p < 0.001$; WT + ZM (30) vs ZM(30), * $p < 0.05$; WT + ZM (30) vs WT(30), ** $p < 0.01$.

5.3. Discussion.

AURKA and TPX2 overexpression simultaneously, leads to non-limiting amounts of TPX2 (which is the co-activator for AURKA), which can lead to abnormal AURKA-mediated phosphorylation of downstream targets (Asteriti et al., 2010) which in turn leads to accelerated progression through mitosis and an increased rate of proliferation. The upregulation of this complex of AURKA and TPX2 can cause; deregulation of spindle formation function and chromosome segregation, giving rise to aneuploid daughter cells (Asteriti et al., 2010). This can lead to a proliferative advantage and favour tumorigenesis. Recent studies have shown that a mutant version of AURKA (S155R) displayed low kinase activity due to the inability of TPX2 to bind and cause full activation, as such the AURKA/TPX2 complex has been suggested as a “holoenzyme” (a biochemically active enzyme in which full activation occurs upon binding of a coenzyme) (Asteriti et al., 2010, Bibby et al., 2009). The AURKA-TPX2 complex has therefore emerged as a potential oncogenic target and this has been demonstrated in various cancer studies. AURKA and TPX2 have been shown to act as potential biomarkers in KRAS-driven pancreatic ductal adenocarcinomas (PDACs) and inhibition of the AURKA-TPX2 signalling axis may be a potentially lethal therapeutic intervention in MYC-regulated colon cancers (Gomes-Filho et al., 2020b, Takahashi et al., 2015). Another study by van Gijn et al. (2019) demonstrated that BRCA2-deficient, genomically-unstable cancer cells are more sensitive to AURKA or TPX2 inhibition. Therefore, with these selected examples it is no surprise that the AURKA-TPX2 complex is being considered a potential drug target beyond previous focus on AURKA alone. Thus, the experimental work carried out in this chapter sought to characterise the effects of simultaneously targeting AURKA-TPX2 signalling pharmacologically in prostate cancer cells. Furthermore, this was approached with a hypothesis that the treatment of prostate cancer cells with NBD WT would potentially enable improved targeting of AURKA-TPX2 binding with a range of pharmacological kinase inhibitors. Moreover, with variable pharmacological characteristics determined by varying chemical space it was further hypothesised that the NBD WT CPP would enable those molecules with extended structure that were less potent *in vitro* in cells to display an enhanced efficacy to impact on expression/phosphorylation of AURKs and TPX2.

5.3.1. Single-agent pharmacological targeting of AURK signalling.

Commercially available ATP-competitive AURK inhibitors were tested for their ability to impact AURKs and cause a reduction of phosphorylation of the three AURK isoforms in cell-based

assays with synchronised PCa cells that had undergone nocodazole-mediated arrest (Figure 5.1). This initial experiment was carried out to establish both the potency of each inhibitor in this assay and the robustness of the retrospective assay before proceeding to further studies to investigate their impact on the status of p-AURKs, AURKA and TPX2.

The AURK inhibitor II, which was an early hit compound discovered in a screen of AstraZeneca compounds by Heron et al. (2006), was identified by means of a kinase assay *in vitro* and cell-based assays. This AURK inhibitor produced an IC₅₀ of 310nM against AURKA in this paper vs the assays here in which it produced IC₅₀ values against the phosphorylation status of AURKA, B and C as follows; >20µM, 12.5µM and 9.73µM respectively. The study by Heron et al. (2006) also indicated that the cellular potency of this initial hit could be improved by replacing the methoxy group (O-CH₃) at the C7 position of the quinazoline with a 3-(1-morpholino) propoxy side chain. The AURK inhibitor III was discovered during a high-throughput screening (HTS) of 4,6-Disubstituted Pyrimidines compounds which inhibited kinase activity of the EGFR, it was shown to be ineffective at 10µM but inhibited AURKA activity potently *in vitro* with an IC₅₀ = 42nM (Zhang et al., 2006). This contrasted with the potency observed against phosphorylation of AURKA, B and C in the cell-based assays used here, in which the IC₅₀ value was >20µM across all three subtypes. A [1,2,4]triazole-3,5-diamine dual CDK/AURK inhibitor examined in Figure 5.1 (C) showed nanomolar to low micromolar potency against phosphorylation of the AURK isoforms in the described assays with synchronised cells; AURKA (0.812µM), AURKB (1.06µM) and AURKC (1.05µM) respectively. This correlated relatively well with a study by Emanuel et al. (2005) which showed that the Aurora kinase/CDK inhibitor blocked AURKA (IC₅₀ = 11nM) and AURKB (IC₅₀ = 15nM) activity *in vitro* (i.e. a cell-free assay). It also inhibited cell cycle regulatory proteins (CDK1/B, CDK2/A, CDK2/E, Wee1, Myt1, etc.) at low micromolar concentrations in nocodazole synchronised cells (Emanuel et al., 2005), in a similar manner to the conditions carried out in the assays used here. The pan-AURK inhibitor, VX-680 potently inhibited kinase activity of AURKA, B and C (IC₅₀ = 0.6nM, 18nM and 5nM) (Bebbington et al., 2009). VX-680 was also shown to bind to AURKA in what is known as a “closed, inactive” confirmation, the cyclopropyl group of the amide in the VX-680 inhibitor makes interactions with a lipophilic pocket derived from the F275 of the DFG loop that is not present in the “open, active” confirmation (Bebbington et al., 2009). A similar pattern of potency was seen in the cell-based assay here which examined the effect of VX-680 on phosphorylation of the three AURK isoforms; AURKA (IC₅₀ = 0.137µM), AURKB (IC₅₀ = 0.573µM) and AURKC (IC₅₀ = 0.540µM). The more restricted chemical structure/space of this compound relative to the other compounds used here likely accounts for its selectivity profile for the three AURK isoforms, being a pan-inhibitor and less selective in binding. Lastly, the AURK inhibitor ZM 447439,

which was discovered by Ditchfield et al. (2003) inhibited activity of AURKA ($IC_{50} = 110\text{nM}$) and AURKB ($IC_{50} = 130\text{nM}$). These reported effects were replicated in this study based on its effect on phosphorylation of AURK family members in the trap/release assay - (Figure 5.1E); AURKA ($IC_{50} = 6.2\mu\text{M}$), AURKB ($IC_{50} = 0.624\mu\text{M}$) and AURKC ($IC_{50} = 0.236\mu\text{M}$) respectively. Therefore, the assay used in this section has been robust and consistent enough to allow the quantification of the potency of different ATP-competitive AURK inhibitors (AURK inhibitor II, AURK inhibitor III, Aurora kinase/CDK inhibitor, VX-680 or ZM 447439) to impact on p-AURKs in PCa cells. The substantial discrepancies between IC_{50} values reported in the literature and those reported here is due to; the studies in the literature take place in cell-free assays only, with no other proteins present to compete for binding with the protein of interest or impact the accessibility of the kinase ATP-binding pocket (e.g. TPX2). Also, the assay here used synchronised cells – AURKs are upregulated in the synchronised cells and in the case of AURKA, TPX2 is likely to be upregulated in a cell-cycle dependent manner and also bound with AURKA, making it a more challenging target, less accessible to ATP-competitive AURK inhibitors and therefore less susceptible to inhibition and associated dephosphorylation.

5.3.2. Dual pharmacological targeting of AURKA-TPX2 signalling.

It was shown by Anderson et al. (2007) that the presence of TPX2 in an *in vitro* (i.e. performed in a cell-free assay in a test tube with no other competing proteins except AURKA and TPX2) kinase assay incorporating ATP-competitive AURK inhibitors, reduced the size and the accessibility of a hydrophobic 'Y' pocket (where TPX2 binds to AURKA) to inhibitors that access this allosteric site adjacent to the ATP binding site. As described previously, it was hypothesised that, to improve the efficacy of these ATP-competitive AURK inhibitors (AURK inhibitor II, AURK inhibitor III, Aurora kinase/CDK inhibitor, VX-680 or ZM 447439) when utilised alone (as demonstrated in Figure 5.1) they could be combined with the NBD WT CPP to generate improved and better targeting of markers of AURKA status/activity. This was demonstrated as a significant ($p < 0.05$) improvement in efficacy of ATP-competitive AURK inhibitors (AURK inhibitor II, AURK inhibitor III, Aurora kinase/CDK inhibitor, VX-680 or ZM 447439) at concentrations in which they were previously ineffective (Figure 5.1) when used as single agent treatments. There was a reduction in phosphorylation of AURKs and AURKA total expression which was significantly ($p < 0.05$) enhanced in samples treated with a combination of the NBD WT CPP and AURK inhibitors (AURK inhibitor II, AURK inhibitor III, Aurora kinase/CDK inhibitor, VX-680 and ZM447439) compared to the single agent or vehicle treatment at the same time point post-release from nocodazole mediated arrest. There was

also a similar pattern observed against TPX2 expression following treatment with Aurora kinase/CDK inhibitor or VX-680 in combination with the NBD WT CPP. This enhancement in efficacy was particularly prominent in Figures 5.4, 5.5 and 5.6, which involved combination treatments with the Aurora kinase/CDK inhibitor and VX-680. Interestingly there was rank order of potency, rather a rank order of combined enhancement of potency which was VX-680 > ZM447439 > Aurora kinase/CDK inhibitor > AURK inhibitor II > AURK inhibitor III. It was shown by Anderson et al. (2007) that VX-680 does not fully occupy the hydrophobic 'back pocket', its cyclopropane ring is extended and approaches the pocket. Hence it was hypothesised by Anderson et al. (2007) that inhibitors like VX-680 that interacted with the 'back pocket' were more challenged to bind AURKA when TPX2 was bound due to a reduction in size of the hydrophobic pocket in which they bind. TPX2 would limit access to the deeper sites of interaction within the binding pocket of the kinase domain. Hence, the data reported here supports the suggestion that the NBD WT CPP may be able to compete with TPX2 and prevent its binding to AURKA, improving accessibility to the hydrophobic 'Y-pocket' for the AURK inhibitors (AURK inhibitor II, AURK inhibitor III, Aurora kinase/CDK inhibitor, VX-680 or ZM 447439) to exert their effects on AURKA phosphorylation and status. Future studies involving the use of kinase assays as well as co-immunoprecipitation strategies, where the NBD WT CPP was incorporated alone or in combination with the AURK inhibitors would allow the further assessment of the potential impact on catalytic activity of AURKA and AURKA-TPX2 binding respectively.

5.3.3. Conclusions.

In this chapter, it was firstly demonstrated that the previously utilised trap/release assay approach could be developed to establish a robust assay format for assessing the potency of ATP-competitive AURK inhibitors in challenging/monitoring phosphorylation of AURKA, B and C (Figure 5.1) as PC3 cells moved through the cell cycle upon release from nocodazole-mediated arrest. Following establishment of the potency of AURK inhibitors alone in this cell-based assay, incorporation of the NBD WT CPP in combination with AURK inhibitors demonstrated an improvement in efficacy with regards to impacting AURKA-TPX2 signalling. A study by Lake et al. (2018) suggested a molecular mechanism for AURK inhibitors interacting with AURKA when TPX2 was bound. They suggested that binding of TPX2 to AURKA restrains AURKA in a DFG-in state, causing it to become more resistant to inhibitors which favour the DFG-out confirmation but promotes the binding of inhibitors which favour the DFG-in confirmation (Lake et al., 2018). Thus, any cellular state which favours TPX2 bound to AURKA will be less sensitive to DFG-out inhibitors, for example, in the experimental

conditions used in this study when cells were synchronised with nocodazole at the G₂/M phase in the cell cycle (Lake et al., 2018). More recently it has been shown by Janeček et al. (2016) that in appreciating the impact of TPX2 on the ability to target AURKA they developed a molecule known as AurkinA that inhibited the interaction between AURKA and TPX2, by binding to the hydrophobic 'Y-pocket' which was normally bound by a conserved Tyr8-Ser9-Tyr10 (Y-S-Y) motif of TPX2. Thus, with the observation made through this study, it could be proposed that the NBD WT CPP can compete with TPX2 at the 'Y-pocket' in a similar manner to AurkinA due to the key hexapeptide sequence (LDWSWL) of the NBD WT CPP. The Try-Ser-Try (W-S-W) sequence present in the NBD WT CPP may perhaps mimics that of the critical TPX2 motif (Y-S-Y) which binds AURKA, with the more hydrophobic and bulkier extended side chains of NBD may preferentially compromise TPX2 binding to AURKA via the Y-S-Y motif. Through this hypothesised mechanism it can be suggested that the NBD WT CPP competes with TPX2 and potentially improved accessibility and efficacy of AURK inhibitors to AURKA. Lastly, AURKB and AURKC are activated and regulated in similar pattern by the protein INCENP (Abdul Azeez et al., 2019). AURKA and AURKB share nearly identical active sites and both are dependent on co-activators for full activation, the selectivity of AURK inhibitors against these other AURK family members may also be driven by similar conformational effects and this may be extended to AURKC (Lake et al., 2018). To establish the full effect of the NBD WT CPP on AURKB and AURKC and whether efficacy of AURK inhibitors can be improved in relation to these proteins, their total expression along with that of the critical co-activator protein INCENP and parallel kinase assay *in vitro* will need to be evaluated in future studies to mimic the study carried out here with regards to AURKA and TPX2. Also, reflecting on previous work in the lab, IKK β could also bind to AURKB and AURKC on the scanning peptide arrays. Could the reverse binding be examined and would AURKB and AURKC also interact with the NBD given that they are targetable with the NBD WT CPP?

To conclude, experiments here established a successful and robust assay to quantify the potency of ATP-competitive AURK inhibitors to effect the phosphorylation status of AURKA, B and C. Additionally, incorporation of the NBD WT CPP in combination with the AURK inhibitors improved the efficacy of disruption to AURKA/TPX2 signalling compared to the single agents alone. With this it can be proposed that mechanistically this could be through competition of the NBD WT CPP with TPX2, allowing improved accessibility to the AURKA active site for the AURK inhibitors to then impact AURKA phosphorylation, as a surrogate marker for catalytic activity and expression. Further structural biology studies will need to be carried out to determine this fully, reliant on a protein crystallisation of AURKA in concert with NBD WT-related peptides. Generation of such a peptide-protein co-crystal would allow further

understanding of and insight into the potential interactions developed between the NBD WT peptide and AURKA.

Given the ability of the AURK KIs and NBD WT in combination to target AURKs and AURKA status it remained to be determined whether the observations made here could be translated to impact on phenotypic outcomes associated with tumour development and progression; increased cell proliferation, enhanced replicative potential, avoidance of apoptosis etc, commonly recognised as Hallmarks of cancer.

Chapter 6: Characterising the phenotypic outcomes of disrupting AURKA-TPX2 signalling in PCa cells.

6.1. Introduction.

Inhibition of AURKA or TPX2 through pharmacological and/or molecular targeting also has the potential to impact related downstream phenotypic outcome of cancer cells. The inhibition of AURKA (via targeting with microRNA, siRNA and ATP-competitive AURK inhibitors) has been described to impact phenotypically across a variety of different cancer cells in a multitude of ways including; inhibition of cell proliferation (Min et al., 2016, Ryu et al., 2018), induction of apoptosis (Yuan et al., 2015), inhibition of replicative potential (Zhang et al., 2018) and improving sensitivity to radiotherapy (Hu et al., 2020). Similar phenotypic outcomes were observed when expression of TPX2 was downregulated by means of siRNA targeting in a study by Warner et al. (2009). Through this molecular targeting at the transcriptional level, inhibition of cell proliferation and colony formation as well as the induction of apoptosis were all observed in pancreatic cancer cell lines. Overexpression of TPX2 was also shown to promote proliferation and invasiveness in Glioblastoma cell lines (Gu et al., 2016) as well as metastasis in colon cancer cells (Wei et al., 2013). This highlights how approaches towards development of future cancer therapeutics could incorporate the targeting of AURKA and TPX2 individually as well as the potential of targeting both proteins simultaneously.

The treatment of cancers with two or more therapeutic interventions/agents (so-called combination therapy) is a key foundation of cancer treatments which aims to target vital pathways in a synergistic or additive manner through amalgamation of these anti-cancer therapies, which leads to enhanced efficacy (Bayat Mokhtari et al., 2017). This also reduced the required dose of each individual agent, thus reducing their associated potential side-effects/toxicities (Bayat Mokhtari et al., 2017). This treatment approach has the potential to reduce drug resistance while at the same time providing anti-cancer benefits such as; reducing tumour growth and metastatic potential, arresting mitotically active cells, causing a reduction in cancer stem cell populations and induction of apoptosis (Bayat Mokhtari et al., 2017). Cancer drug discovery has mainly focussed on the search for synergistic combination therapies (interaction of two or more agents to produce a combined effect greater than the sum of their separate effects) due to the perceived enhancement of therapeutic efficacy at lower doses (Saputra et al., 2018). It was suggested by Saputra et al. (2018) that computer simulations indicated that synergistic drug combinations were most effective at delaying resistance onset, through early annihilation of cell numbers versus antagonistic drug combinations (combination which leads to a smaller effect than expected), which were effective at suppressing the expansion of resistant sub-clones in an “anti-resistant” approach.

It was hypothesised, based on results in Chapter 5, that there was potential to target the AURKA-TPX2 complex in two different ways (dual targeting) – NBD peptide disruption at an as yet fully defined allosteric site (that could be the AURKA-TPX2 interface) and at the catalytic site through ATP-competitive AURK inhibitor targeting. Hence in this chapter it was sought to investigate whether targeting alone with each of the ATP-competitive AURK inhibitors utilised in the previous chapter (AURK inhibitor III, AURK inhibitor II, Aurora Kinase/CDK inhibitor, VX-680 and ZM 447439) and the NBD WT CPP can show an enhancement in efficacy and improved ability to impact cell viability and clonogenic survival of PC3 cells when used in combination. Furthermore, this study also explored the potential of the NBD WT CPP in combination with AURK inhibitors (AURK inhibitor III, AURK inhibitor II, Aurora Kinase/CDK inhibitor, VX-680 and ZM 447439) to induce apoptosis.

Therefore, the specific aims of this chapter examining the changes in phenotypic outcomes associated with targeting AURKA-TPX2 signalling, were to:

1. Examine the impact of the NBD CPPs alone on phenotypic outcomes of cell viability and clonogenic survival in PC3 cells.
2. Determine the impact of ATP-competitive AURK inhibitors (AURK inhibitor III, AURK inhibitor II, Aurora Kinase/CDK inhibitor, VX-680 and ZM 447439) alone and in combination with the NBD CPPs on phenotypic outcomes of cell viability and clonogenic survival in PC3 cells and quantify potential outcomes using Combination Index Analysis (CIA).
3. Determine the impact of the AURK inhibitor, VX-680, alone and in combination with the NBD CPPs on phenotypic outcomes of apoptosis in PC3 cells.

Collectively, these experiments aimed to determine whether the ATP-competitive AURK inhibitors (AURK inhibitor III, AURK inhibitor II, AURK/CDK inhibitor, VX-680 and ZM 447439) could impact the phenotypic outcomes (cell viability, clonogenic survival, apoptosis) of PC3 cells and whether this impact could be enhanced quantitatively by using the NBD WT CPP in combination with the individual AURK inhibitors compared to the efficacy of either peptide or inhibitors alone.

6.2. Effect NBD CPPs or AURK inhibitors alone and in combination on phenotypic characteristics of prostate cancer cells.

6.2.1. Effect of NBD WT CPPs on cell viability and clonogenic survival in PC3 cells.

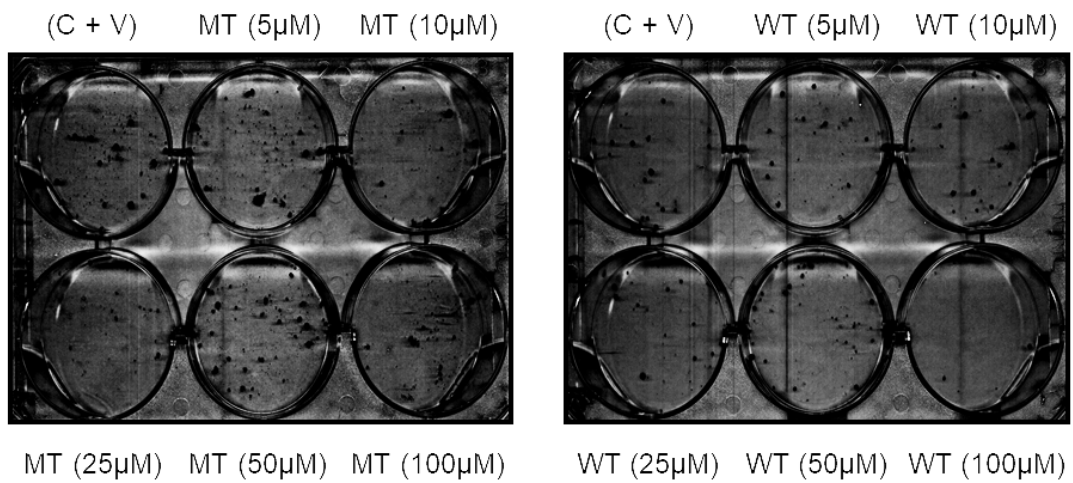
Following on from Chapter 5 that demonstrated the targeted inhibition of AURKA-TPX2 signalling by the NBD WT CPP in combination with ATP-competitive AURK inhibitors (AURK inhibitor II, AURK inhibitor III, AURK/CDK inhibitor, ZM 447439 and VX-680), experiments were constructed that sought to investigate whether AURKA-TPX2 targeting translated to the phenotypic outcomes of PC3 cells. Initial experiments examined the effects of the NBD CPPs alone on the phenotypic characteristics. The effect of the NBD MT CPP and NBD WT CPP on PC3 cell viability was previously demonstrated in Section 4.2.4. This was also investigated and analysed along with each AURKA inhibitor in the combination treatments in the MTT assays carried out in this chapter. Previously, in Figure 4.4, the NBD WT CPP showed a significant reduction in cell viability at a concentration of 100 μ M ($63.3 \pm 6.7\%$; $n=3$, $p<0.001$) and when analysed further displayed an IC_{50} of 51.31 μ M for the impact of the NBD WT CPP on cell viability in PC3 cells.

To assess the impact of the NBD CPPs on the replicative potential of PC3 cells, the clonogenic survival/colony formation assay was carried out based on a method described by Carlin et al. (2000) and detailed in Section 2.2.7.2. In Figure 6.1, PC3 cells were treated with vehicle (0.5% DMSO (v/v)) and increasing concentrations (5 μ M, 10 μ M, 25 μ M, 50 μ M and 100 μ M) of either the NBD WT CPP or NBD MT CPP for 72h prior to clonogenic assay and subsequent analysis and quantification. Following treatment with the NBD WT CPP (Figure 5.1 A + B) PC3 cells showed a significant reduction in clonogenic survival at concentrations of 10 μ M ($26.1 \pm 5.0\%$; $n=3$, $p<0.05$), 25 μ M ($26.3 \pm 2.6\%$; $n=3$, $p<0.05$), 50 μ M ($30.9 \pm 9.5\%$; $n=3$, $p<0.01$) and 100 μ M ($61.6 \pm 1.9\%$; $n=3$, $p<0.001$). When analysed further, in Figure 6.1 (C) the NBD WT CPP displayed an IC_{50} of 59.3 μ M. The NBD MT CPP caused no significant ($p>0.05$) reduction in clonogenic survival across the concentration range in PC3 cells (Figure 6.1 A and B). Inhibition caused by NBD WT CPP was not of the classical sigmoidal concentration-dependent form however there was partial/incomplete inhibition at the highest concentration (100 μ M).

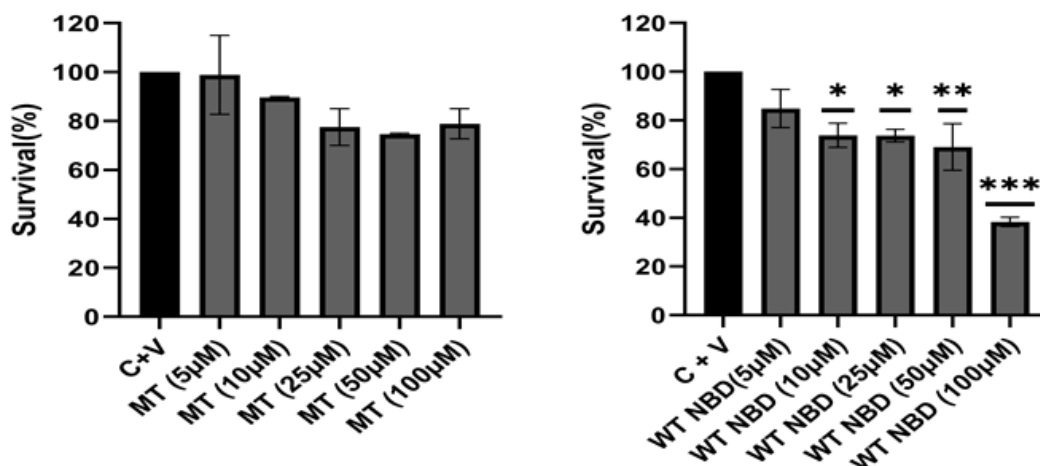
To summarise, these experimental outcomes indicated that the NBD WT CPP can impact phenotypically on both cell viability (Section 4.2.4) and clonogenic survival across different concentrations (10-100 μ M) and correlated well with the concentration (i.e. 100 μ M) that was used to target AURKA-TPX2 signalling in different cell-based assays throughout this

thesis. There was also no significant impact on clonogenic survival caused by the “control” mutated and inactive NBD MT CPP. This suggested that treating cells with NBD WT CPP and targeting potentially AURKA-TPX2 signalling could be a plausible pharmacological intervention to impact on phenotypic outcomes of prostate cancer cells. Therefore, it could potentially be utilised as a component of a combined treatment approach alongside AURK inhibitors (AURK inhibitor II, AURK inhibitor III, AURK/CDK inhibitor, ZM 447439 and VX-680) to further enhance the inhibition of phenotypic characteristics of PCa cells.

(A)



(B)



(C)

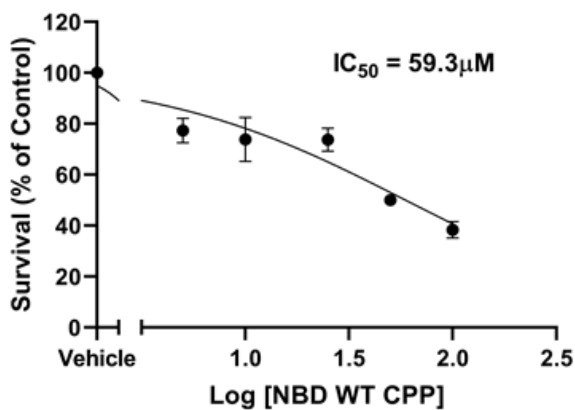


Figure 6.1. Effect of NBD CPPs treatment on clonogenic survival of PC3 cells.

PC3 cells were seeded (300 cells / ml) into 6-well plates and treated with increasing concentrations of NBD MT or WT (5μM, 10μM, 25μM, 50μM and 100μM) for 72h. Replicative potential was measured using the clonogenic survival assay as described in materials and methods and photographed, also in panel A. DMSO was used as a vehicle (C + V) control (0.5% (v/v)). Data was normalised to the vehicle control (C + V) and represents mean ± S.E.M of change in percentage survival (n=3). **(B)** One-way ANOVA with post-hoc Dunnet's test was used to determine statistical significance ($p < 0.05$) of observed changes relative to vehicle treated control (C + V). (*= $p < 0.05$, **= $p < 0.01$, ***= $p < 0.001$). **(C)** Potency of the NBD WT CPP (●) to effect clonogenic survival in PC3 cells. The results were normalised to vehicle treated control and plotted on a log scale as a percentage of the control relative to clonogenic survival (n=3). The data was fitted with the following equation: $Y = \text{Bottom} + (\text{Top} - \text{Bottom}) / (1 + 10^{((\text{LogIC}_{50} - X) * \text{HillSlope}))}$). Broken X-axis was used to represent vehicle treated control.

6.2.2. Effect of AURK inhibitor II and NBD WT CPP alone and in combination on cell viability and clonogenic survival of prostate cancer cells.

As mentioned previously, the NBD WT CPP caused a significant ($p < 0.05$) but incomplete or partial reduction in cell viability (Figure 4.4) and as above impacted clonogenic survival also (Figure 6.1). A similar pattern was observed in terms of the impact of single-agent treatment of the NBD WT CPP, on AURKA-TPX2 signalling, which caused a submaximal reduction in AURKA phosphorylation and protein expression (Figure 3.3). Following on from this, as demonstrated in Chapter 5, treatment of PC3 cells simultaneously with the NBD WT CPP in combination with ATP-competitive AURK inhibitors (AURK inhibitor II, AURK inhibitor III, AURK/CDK inhibitor, ZM 447439 and VX-680), enhanced efficacy of impact on AURKA-TPX2 signalling, again reducing AURKA phosphorylation and protein expression. Hence, this study sought to investigate whether this observed enhanced pharmacological efficacy, against AURKA-TPX2 signalling, displayed by both agents when combined, could be translated to potential synergistic inhibition of cellular phenotypic outcomes.

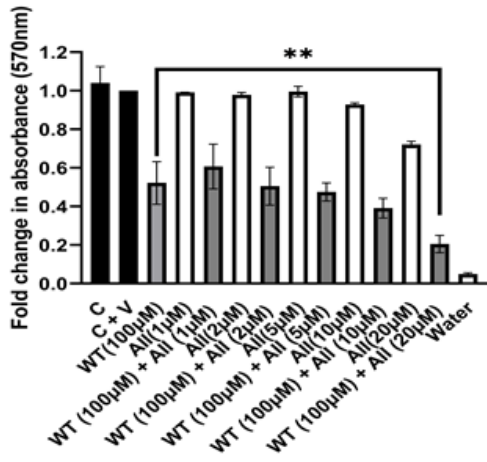
Firstly, in Figure 6.2 (A – C), to assess impact on cell viability, PC3 cells were treated with vehicle, the NBD WT CPP (100 μ M) and/or AURK inhibitor II (1 μ M, 2 μ M, 5 μ M, 10 μ M and 20 μ M), prepared as described previously for 72h prior to MTT assay and subsequently analysed as detailed in Section 2.2.7.1 of the Materials & Methods. Also, in Figure 5.2 (D – H), PC3 cells were treated with the NBD WT / MT CPP (100 μ M) and/or AURK inhibitor II (0.1 μ M, 0.3 μ M, 1 μ M, 3 μ M and 10 μ M) for 72h prior to clonogenic survival assay and associated analysis as detailed in Section 2.2.7.2 of the Materials & Methods.

In Figure 6.2 (A) treatment of cells with AURK inhibitor II in combination with a constant single concentration of NBD WT CPP (100 μ M) (that generated partial inhibition), significantly ($p < 0.05$) enhanced reduction of cell viability compared to single agent treatment with the NBD WT CPP. This enhanced reduction in cell viability caused by the combination treatment approach compared to the NBD WT CPP alone was significant at a AURK inhibitor II concentration of 20 μ M ($52.2 \pm 11.0\%$ vs $20.6 \pm 4.5\%$; $n=3$, $p < 0.01$). Following on from this, in Figure 5.2 (B) the combination of the two agents was analysed to determine the degree of drug interaction based on the calculation of combination index (CI) values (CI < 1 - synergism, CI = 1 – Additivity and CI > 1 – Antagonism) by the methodology detailed in Section 2.8.2. The drug combination between AURK inhibitor II and the NBD WT CPP was characterised as synergistic across the concentration range of AURK inhibitor II; 1 μ M (CI = 0.83), 2 μ M (CI = 0.78), 5 μ M (CI = 0.79), 10 μ M (CI = 0.77) and 20 μ M (CI = 0.76). The data was then further analysed to determine the potency of the AURK inhibitor II as a single agent and in

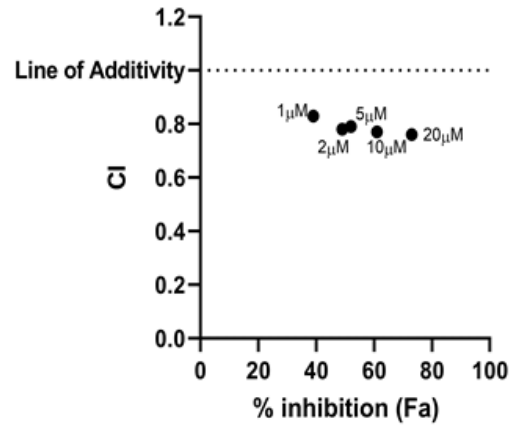
combination with the NBD WT CPP to effect cell viability (Figure 6.2 C), which produced IC_{50} values as follows; AURK inhibitor II ($IC_{50} = >20\mu\text{M}$) and AURK inhibitor II in combination with the NBD WT CPP ($IC_{50} = 2.9\mu\text{M}$). The results above highlighted an estimated 2-fold increase in potency to effect cell viability when the AURK inhibitor II was utilised simultaneously in combination with the NBD WT CPP compared to single agent treatment with the NBD WT CPP.

In Figure 6.2 (D + F), combination treatment with a constant single concentration of NBD WT CPP ($100\mu\text{M}$) and a concentration range of the AURK inhibitor II significantly ($p < 0.05$) enhanced reduction of clonogenic survival. This enhanced reduction in clonogenic survival caused by the combination treatment compared to the NBD WT CPP alone was significant ($p < 0.05$) at a concentrations of; $10\mu\text{M}$ ($38.4 \pm 1.9\%$ vs $0.5 \pm 0.5\%$; $n=3$, $p < 0.001$). The AURK inhibitor II in combination with the 'control' NBD MT CPP caused no significant difference in reduction of clonogenic survival across the concentration range compared to the NBD MT CPP or AURK inhibitor II alone (Figure 6.2 E). Following on from this, in Figure 6.2 (G) the treatment combination was analysed to determine the degree of agent interaction based on the calculation of combination index (CI) values ($CI < 1$ - synergism, $CI = 1$ - Additivity and $CI > 1$ - Antagonism). The combination treatment between AURK inhibitor II and the NBD WT CPP was characterised as synergistic across the concentration range of AURK inhibitor II; $0.1\mu\text{M}$ ($CI = 0.03$), $0.3\mu\text{M}$ ($CI = 0.018$), $1\mu\text{M}$ ($CI = 0.12$), $3\mu\text{M}$ ($CI = 0.16$) and $10\mu\text{M}$ ($CI = 0.17$). Further analysis of the data to determine the potency of the AURK inhibitor II as a single agent and in combination with the NBD WT CPP to effect clonogenic survival (Figure 6.2 H) produced IC_{50} values as follows; AURK inhibitor II ($IC_{50} = 1.04\mu\text{M}$) and AURK inhibitor II + NBD WT CPP ($IC_{50} = 0.02\mu\text{M}$). The results above highlighted an estimated 20 to 30 fold increase in potency to effect clonogenic survival when the AURK inhibitor II was utilised simultaneously in combination with the NBD WT CPP compared to single agent treatment with the NBD WT CPP. The potential of the other AURK inhibitors to manifest similar results was investigated next.

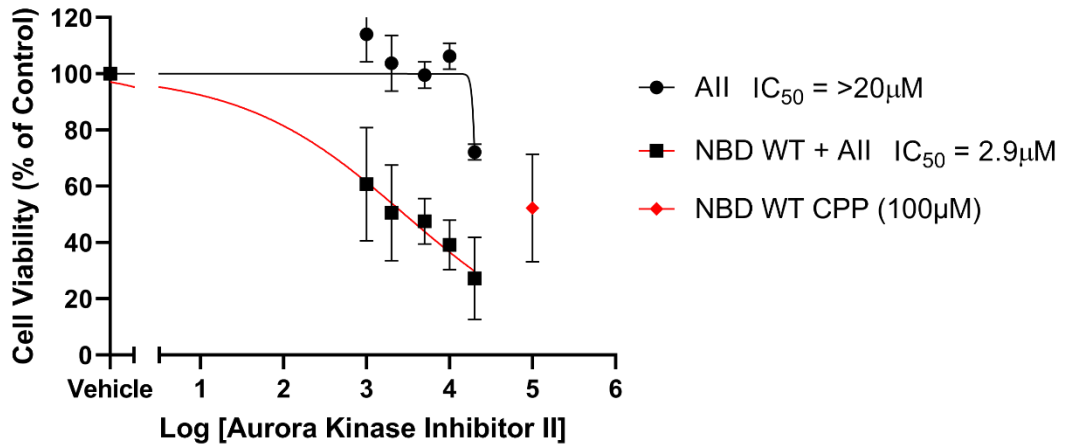
(A)



(B)

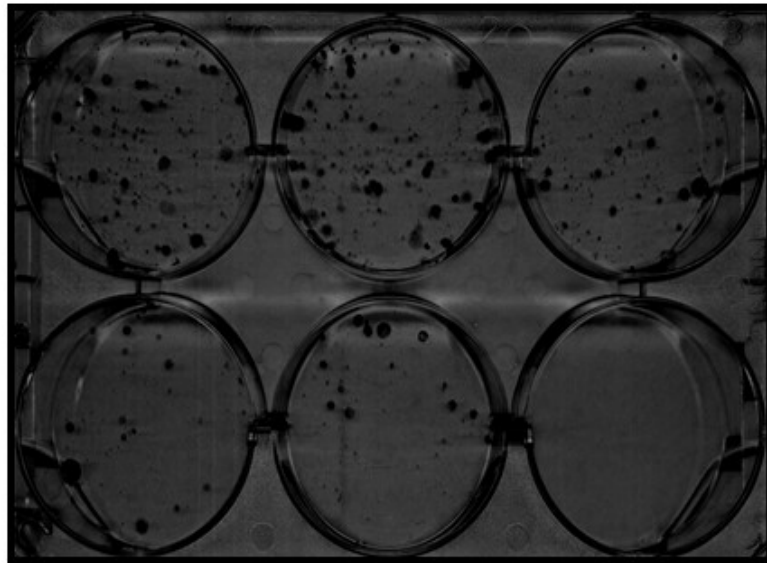


(C)



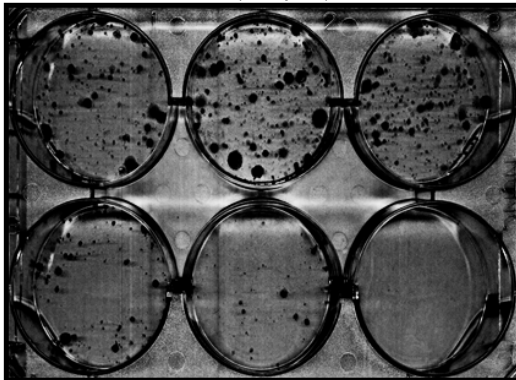
(D)

(C + V) All (0.1 μ M) All (0.3 μ M)

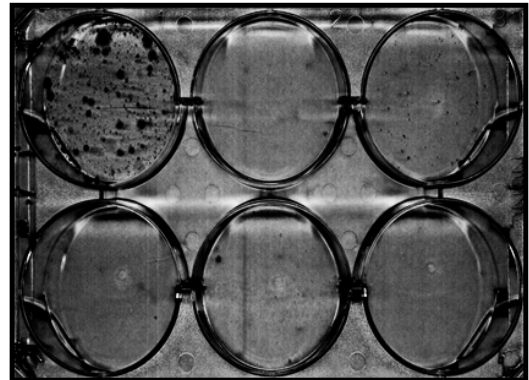


All (1 μ M) All (3 μ M) All (10 μ M)

(C + V) MT + All (0.1 μ M) MT + All (0.3 μ M) (C + V) WT + All (0.1 μ M) WT + All (0.3 μ M)

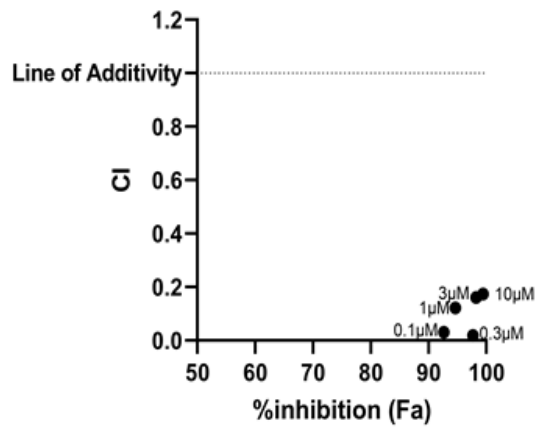
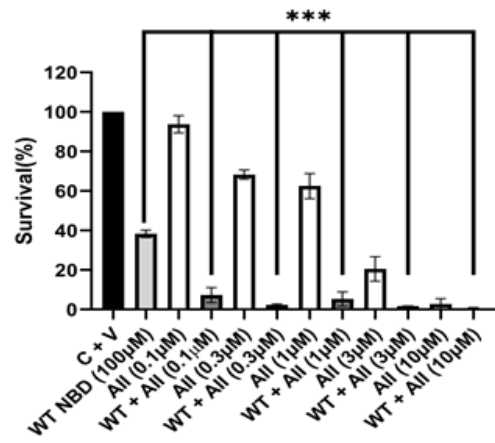
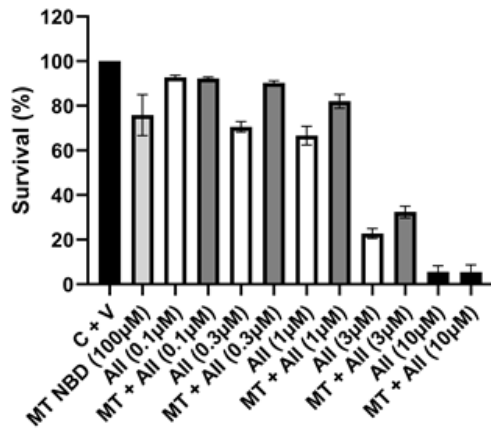


(E) MT + All (1 μ M) MT + All (3 μ M) MT + All (10 μ M)



(F) WT + All (1 μ M) WT + All (3 μ M) WT + All (10 μ M)

(G)



(H)

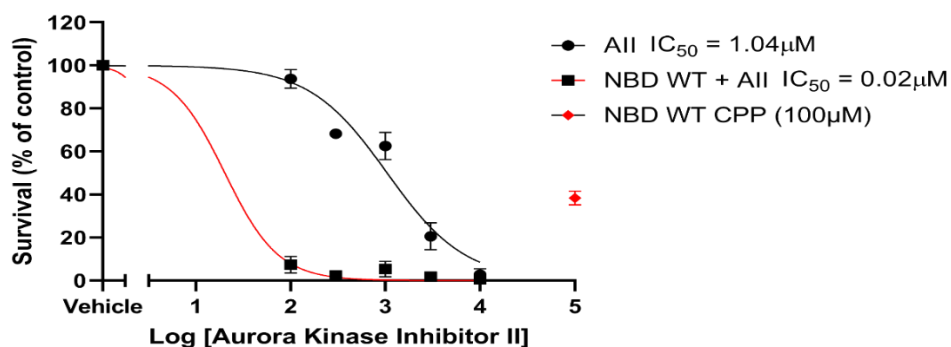


Figure 6.2. Effect of NBD MT/WT CPP and AURK inhibitor II alone or in combination on cell viability and clonogenic survival of PC3 cells.

(A – C) PC3 cells were seeded into 96-well plates and treated with NBD WT (100 μM) and/or increasing concentrations of AURK inhibitor II (1 μM, 2 μM, 5 μM, 10 μM and 20 μM) for 72h. Cell viability was measured using the MTT assay. DMSO was used as a vehicle (C + V) control (0.5% (v/v)). Cells cultured in media with no treatment represented the positive control (C). Cells cultured in water represented the negative control (Water). **(A)** Data was normalised to the vehicle control (C + V) and represents mean ± S.E.M of fold change in absorbance at 570nm (n=3). Triplicates were averaged for each experiment. One-way ANOVA with post-hoc Dunnet's test was used to determine statistical significance ($p < 0.05$) of observed changes between combination treatment and the NBD WT CPP alone to impact on cell viability (*= $p < 0.05$, **= $p < 0.01$, ***= $p < 0.001$). **(B)** Fraction affected-combination index (Fa-CI) plots of combined treatment of NBD WT CPP and AURK inhibitor II in PC3 cells. Combination indices (CI) for drug-interaction determination were indicated as follows; $CI < 1$ (synergism), $CI = 1$ (additivity) and $CI > 1$ (antagonism). The combined effect of NBD WT CPP (100 μM) and AURK inhibitor II (1 μM, 2 μM, 5 μM, 10 μM and 20 μM) on cell viability was determined and plotted (n=3) WT + AII (1 μM) [CI = 0.83], WT + AII (2 μM) [CI = 0.78], WT + AII (5 μM) [CI = 0.79], WT + AII (10 μM) [CI = 0.77], WT + AII (20 μM) [CI = 0.76]. **(C)** Comparison of the potency of the NBD WT CPP (♦), AURK inhibitor II (●) or NBD WT CPP + AURK inhibitor II (■) on cell viability in PC3 cells. The results were normalised to vehicle treated control and plotted on a log scale as a percentage of the control with regards to cell viability (n=3). The data was fitted with the following equation $Y = \text{Bottom} + (\text{Top} - \text{Bottom}) / (1 + 10^{((\text{LogIC}_{50} - X) * \text{HillSlope}))}$. Broken X-axis was used to represent vehicle treated control. **(D – H)** PC3 cells were seeded (300 cells / ml) into 6-well plates and treated with NBD MT or WT (both 100 μM) and/or increasing concentrations of AURK inhibitor II (0.1 μM, 0.3 μM, 1 μM, 3 μM and 10 μM) for 72h. Replicative potential was measured using the clonogenic survival assay as described in M&M and photographed also in panel D. DMSO was used as a vehicle (C + V) control (0.5% (v/v)). **(E + F)** Data was normalised to the vehicle control (C + V) and represents mean ± S.E.M of change in percentage survival (n=3). One-way ANOVA with post-hoc Dunnet's test was used to determine statistical significance ($p < 0.05$) of observed changes between combination treatment and the NBD WT CPP alone to impact on clonogenic survival (*= $p < 0.05$, **= $p < 0.01$, ***= $p < 0.001$). **(G)** Fraction affected-combination index (Fa-CI) plots of combined treatment of NBD WT CPP and AURK inhibitor II in PC3 cells. Combination indices (CI) for drug-interaction determination were indicated as follows; $CI < 1$ (synergism), $CI = 1$ (additivity) and $CI > 1$ (antagonism). The combined anti-proliferative effect of NBD WT CPP (100 μM) and AURK inhibitor II (0.1 μM, 0.3 μM, 1 μM, 3 μM and 10 μM) was determined and plotted (n=3). WT + AII (0.1 μM) [CI = 0.03], WT + AII (0.3 μM) [CI = 0.018], WT + AII (1 μM) [CI = 0.121], WT + AII (3 μM) [CI = 0.16], WT + AII (10 μM) [CI = 0.174]. **(H)** Comparison of the potency of the NBD WT CPP (♦), AURK inhibitor II (●) or NBD WT CPP + AURK inhibitor II (■) on clonogenic survival in PC3 cells. The results were normalised to vehicle treated control and plotted on a log scale as a percentage of the control with regards to clonogenic survival (n=3). The data was fitted with the following equation $Y = \text{Bottom} + (\text{Top} - \text{Bottom}) / (1 + 10^{((\text{LogIC}_{50} - X) * \text{HillSlope}))}$. Broken X-axis was used to represent vehicle treated control.

6.2.3. Effect of AURK inhibitor III and NBD WT CPP alone and in combination on cell viability and clonogenic survival of prostate cancer cells.

Following on from the demonstrated impact of the NBD WT CPP and AURK inhibitor II in combination on cell viability and clonogenic survival (Section 6.2.2), we then sought to determine whether this enhanced efficacy through this combination treatment approach was transferable to other AURK inhibitors (AURK inhibitor III, AURK/CDK inhibitor, VX-680 or ZM 447439) utilised in this study in conjunction with the NBD WT CPP. Similar to the previous section, in Figure 6.3 (A – D), to assess impact on cell viability, PC3 cells were treated with the NBD WT/ MT CPP (100 μ M) and/or AURK inhibitor III (1 μ M, 2 μ M, 5 μ M, 10 μ M and 20 μ M) for 72h prior to MTT assay and subsequently analysed as detailed in Section 2.2.7.1 of the Materials & Methods. Also, in Figure 6.3 (D – I), PC3 cells were treated with the NBD WT/ MT CPP (100 μ M) and/or AURK inhibitor III (1 μ M, 2 μ M, 5 μ M, 10 μ M and 20 μ M) for 72h prior to clonogenic survival assay and retrospective analysis as detailed in Section 2.2.7.2 of the Materials & Methods. The MT/WT peptide and the AURK inhibitor III were dissolved in 100% DMSO as described previously and as a result all experiments involving the NBD CPPs and AURK inhibitor III used DMSO as a vehicle control.

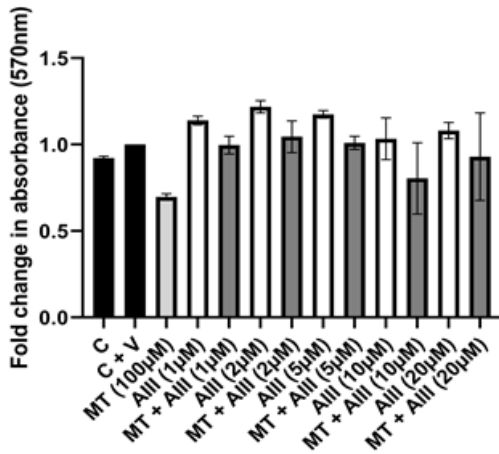
In Figure 6.3 (B) treatment of cells with AURK inhibitor III in combination with a constant single concentration of NBD WT CPP (100 μ M) (that generated partial inhibition), significantly ($p < 0.05$) enhanced reduction of cell viability compared to single agent treatment with the NBD WT CPP. This enhanced reduction in cell viability caused by the combination treatment approach compared to the NBD WT CPP alone was significant at a AURK inhibitor III concentration of 20 μ M ($56.2 \pm 7.8\%$ vs $26.0 \pm 4.1\%$; $n=3$, $p < 0.05$). The AURK inhibitor III in combination with NBD MT CPP 'control' peptide caused no significant difference in reduction of cell viability across the concentration range compared to the NBD MT CPP or AURK inhibitor III alone (Figure 6.3 A). Following on from this, in Figure 6.3 (C) the treatment combination of the NBD WT CPP and AURK inhibitor III was analysed to determine the degree of agent interaction based on the calculation of combination index (CI) values ($CI < 1$ - synergism, $CI = 1$ – Additivity and $CI > 1$ – Antagonism). The combination of AURK inhibitor III with the NBD WT CPP was classified as synergistic across the concentration range of AURK inhibitor III; 1 μ M ($CI = 0.27$), 2 μ M ($CI = 0.30$), 5 μ M ($CI = 0.34$), 10 μ M ($CI = 0.42$) and 20 μ M ($CI = 0.50$). Further analysis of the data to determine the potency of the AURK inhibitor III as a single agent and in combination with the NBD WT CPP to effect cell viability (Figure 6.3 D) produced IC_{50} values as follows; AURK inhibitor III ($IC_{50} = >20\mu$ M) and AURK inhibitor III + NBD WT CPP ($IC_{50} = 7.0\mu$ M). The results above highlighted an estimated 2-fold increase in potency to effect

cell viability when the AURK inhibitor III was utilised simultaneously in combination with the NBD WT CPP compared to single agent treatment with the NBD WT CPP.

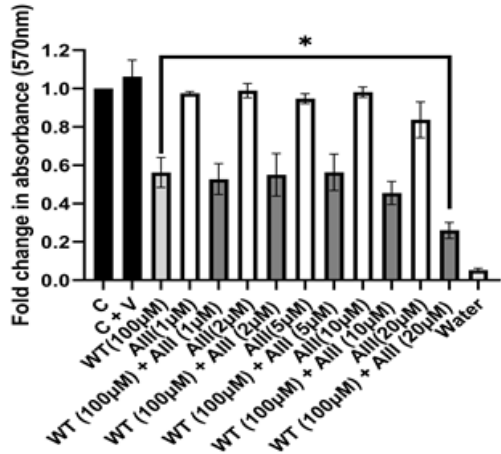
In Figure 6.3 (E + G) combination treatment with a constant single concentration of NBD WT CPP (100 μ M) and a concentration range of the AURK inhibitor III (1-20 μ M) enhanced reduction of clonogenic survival. This enhanced reduction in clonogenic survival caused by the combination treatment was significant ($p < 0.05$) at a concentration of 20 μ M ($38.4 \pm 1.9\%$ vs $4.2 \pm 1.4\%$; $n=3$, $p < 0.001$) in comparison to single agent treatment with the NBD WT CPP. The AURK inhibitor III in combination with NBD MT CPP caused no significant difference in reduction of clonogenic survival across the concentration range compared to the NBD WT CPP or AURK inhibitor III alone (Figure 6.3 F). Following on from this, in Figure 6.3 (H) the treatment combination of the NBD WT CPP and AURK inhibitor III was analysed to determine the degree of agent interaction based on the calculation of combination index (CI) values (CI < 1 - synergism, CI = 1 – Additivity and CI > 1 – Antagonism). The treatment combination between AURK inhibitor III and the NBD WT CPP was characterised as synergistic at the following AURK inhibitor III concentrations: 5 μ M (CI = 0.82), 10 μ M (CI = 0.26) and 20 μ M (CI = 0.08). At the lower concentrations of AURK inhibitor III in combination with the NBD WT CPP the drug interaction was classified as antagonistic; 1 μ M (CI = 2.63) and 2 μ M (CI = 1.71). Further analysis of the data to determine the potency of the AURK inhibitor III as a single agent and in combination with the NBD WT CPP to effect clonogenic survival (Figure 6.3 I) produced IC_{50} values as follows; AURK inhibitor III ($IC_{50} = 19.1\mu$ M) and AURK inhibitor III + NBD WT CPP ($IC_{50} = 2.3\mu$ M). The results above displayed around a 30-fold increase in potency to effect clonogenic survival when the AURK inhibitor III was utilised simultaneously in combination with the NBD WT CPP compared to single agent treatment with the NBD WT CPP.

The potential of the other AURK inhibitors (AURK/CDK inhibitor, VX-680 or ZM 447439) in combination with the NBD WT CPP, will be explored in the proceeding sections of this chapter.

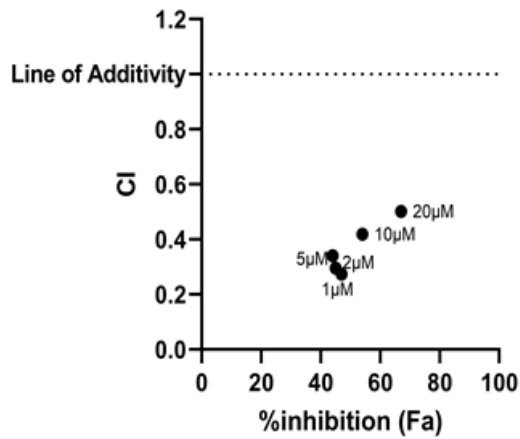
(A)



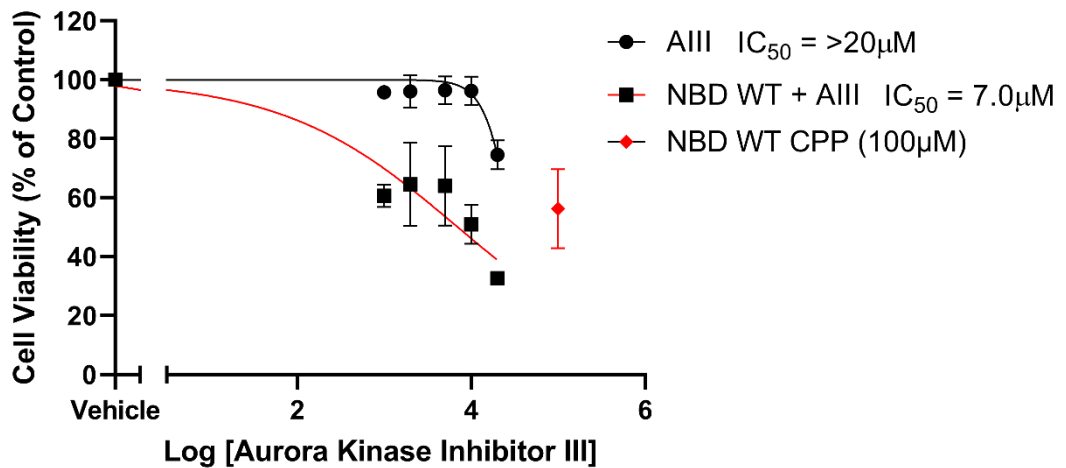
(B)



(C)

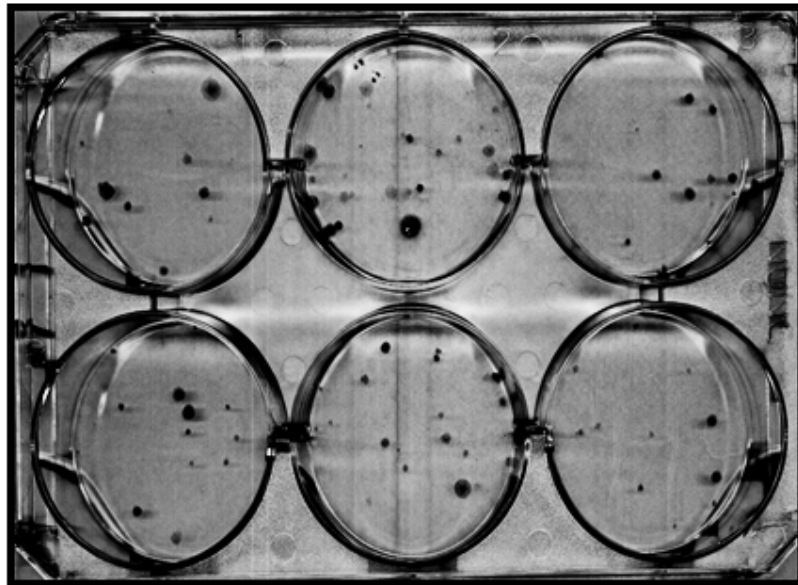


(D)



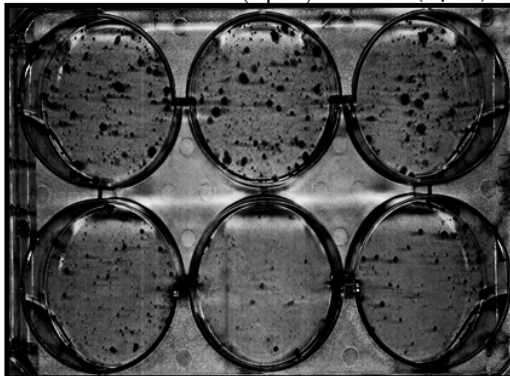
(E)

(C + V) AIII (1 μ M) AIII (2 μ M)

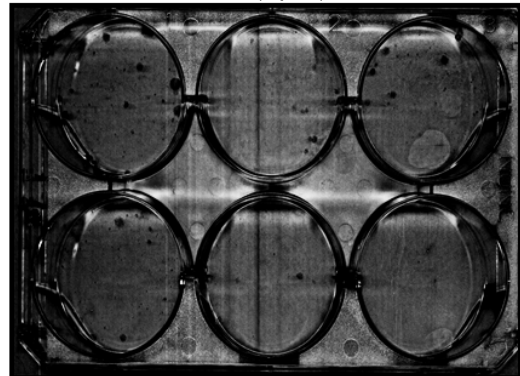


AIII (5 μ M) AIII (10 μ M) AIII (20 μ M)

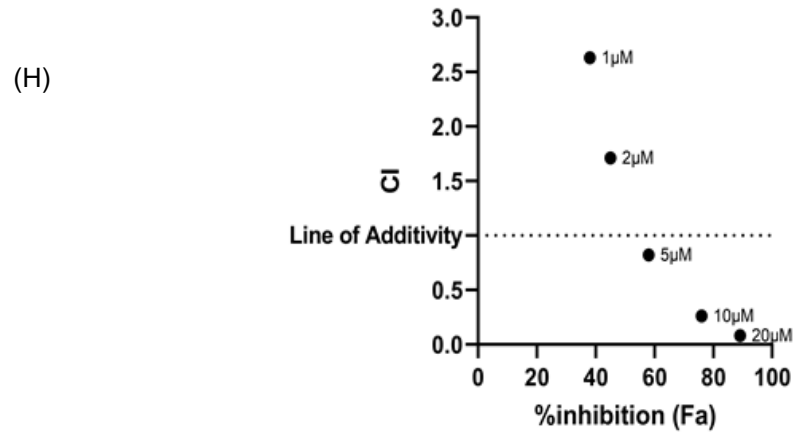
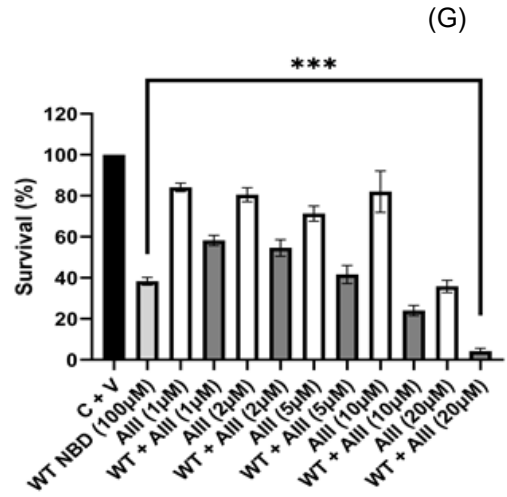
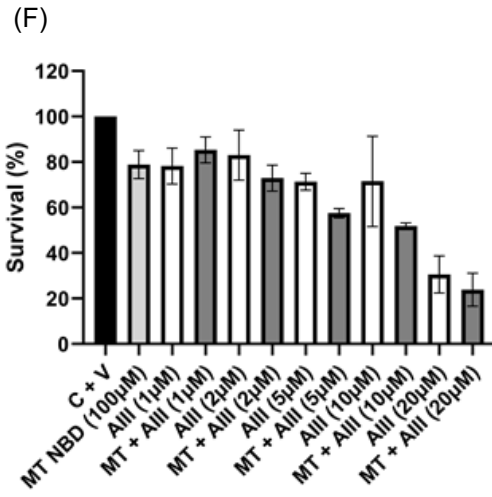
(C + V) MT + AIII (1 μ M) MT + AIII (2 μ M) (C + V) WT + AIII (1 μ M) WT + AIII (2 μ M)



MT + AIII (5 μ M) MT + AIII (10 μ M) MT + AIII (20 μ M)



WT + AIII (5 μ M) WT + AIII (10 μ M) WT + AIII (20 μ M)



(I)

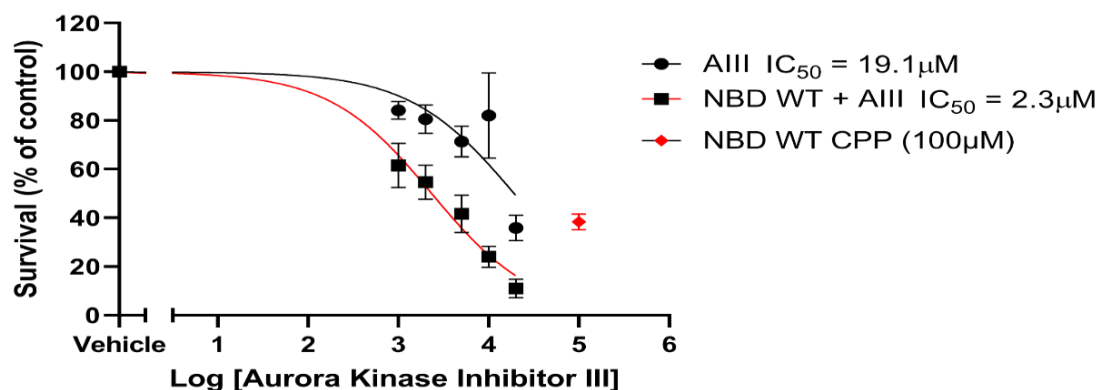


Figure 6.3. Effect of NBD MT/WT CPP and AURK inhibitor III alone or in combination on cell viability and clonogenic survival of PC3 cells.

(A – D) PC3 cells were seeded into 96-well plates and treated with NBD MT (A) or WT (B) (both 100 μM) and/or increasing concentrations of AURK inhibitor III (1 μM, 2 μM, 5 μM, 10 μM and 20 μM) for 72h. Cell viability was measured using the MTT assay. DMSO was used as a vehicle (C + V) control (0.5% (v/v)). Cells cultured in media with no treatment represented the positive control (C). Cells cultured in water represented the negative control (Water). Data was normalised to the vehicle control (C + V) and represents mean ± S.E.M of fold change in absorbance at 570nm (n=3). Triplicates were averaged for each experiment. One-way ANOVA with post-hoc Dunnet's test was used to determine statistical significance (p<0.05) of observed changes between combination treatment and the NBD WT CPP alone to impact on cell viability (*= p<0.05, **= p<0.01, ***=p<0.001). (C) Fraction affected-combination index (Fa-CI) plots of combined treatment of NBD WT CPP and AURK inhibitor III in PC3 cells. Combination indices (CI) for drug-interaction determination were indicated as follows; CI<1 (synergism), CI=1 (additivity) and CI>1 (antagonism). The combined effect of NBD WT CPP (100 μM) and AURK inhibitor III (1 μM, 2 μM, 5 μM, 10 μM and 20 μM) on cell viability was determined and plotted. WT + AIII (1 μM) [CI = 0.273], WT + AIII (2 μM) [CI = 0.295], WT + AIII (5 μM) [CI = 0.34], WT + AIII (10 μM) [CI = 0.418], WT + AIII (20 μM) [CI = 0.501]. (D) Comparison of the potency of the NBD WT CPP (♦), AURK inhibitor III (●) or NBD WT CPP + AURK inhibitor III (■) on cell viability in PC3 cells. The results were normalised to vehicle treated control and plotted on a log scale as a percentage of the control with regards to cell viability (n=3). The data was fitted with the following equation $Y = \text{Bottom} + (\text{Top} - \text{Bottom}) / (1 + 10^{-(\text{LogIC}_{50} - X) \cdot \text{HillSlope}})$. Broken X-axis was used to represent vehicle treated control. (E – I) PC3 cells were seeded (300 cells / ml) into 6-well plates and treated with NBD MT (F) or WT (G) (both 100 μM) and/or increasing concentrations of AURK inhibitor III (1 μM, 2 μM, 5 μM, 10 μM and 20 μM) for 72h. Replicative potential was measured using the clonogenic survival assay as described in M&M and photographed also in panel E. DMSO was used as a vehicle (C + V) control (0.5% (v/v)). Data was normalised to the vehicle control (C + V) and represents mean ± S.E.M of change in percentage survival (n=3). One-way ANOVA with post-hoc Dunnet's test was used to determine statistical significance (p<0.05) of observed changes between combination treatment and the NBD WT CPP alone to impact on clonogenic survival (*= p<0.05, **= p<0.01, ***=p<0.001). (H) Fraction affected-combination index (Fa-CI) plots of combined treatment of NBD WT CPP and AURK inhibitor III in PC3 cells. Combination indices (CI) for drug-interaction were indicated as follows; CI<1 (synergism), CI=1 (additivity) and CI>1 (antagonism). The combined anti-proliferative effect of NBD WT CPP (100 μM) and AURK inhibitor III (1 μM, 2 μM, 5 μM, 10 μM and 20 μM) was determined and plotted. WT + AIII (1 μM) [CI = 2.63], WT + AIII (2 μM) [CI = 1.71], WT + AIII (5 μM) [CI = 0.82], WT + AIII (10 μM) [CI = 0.26], WT + AIII (20 μM) [CI = 0.08]. (I) Comparison of the potency of the NBD WT CPP (♦), AURK inhibitor III (●) or NBD WT CPP + AURK inhibitor III (■) on clonogenic survival in PC3 cells. The results were normalised to vehicle treated control and plotted on a log scale as a percentage of the control with regards to

clonogenic survival (n=3). The data was fitted with the following equation $Y = \text{Bottom} + (\text{Top} - \text{Bottom}) / (1 + 10^{((\text{LogIC}_{50} - X) * \text{HillSlope}))}$. Broken X-axis was used to represent vehicle treated control.

6.2.4. Effect of Aurora kinase/CDK inhibitor and NBD WT CPP alone and in combination on cell viability and clonogenic survival of prostate cancer cells.

Following on from the demonstrated impact of the NBD WT CPP and AURK inhibitor III in combination on cell viability and clonogenic survival (Section 6.2.3), it was then sought to determine in the proceeding sections of this chapter, whether this enhanced efficacy through this combination treatment approach was transferable to other AURK inhibitors (Aurora kinase/CDK inhibitor, VX-680 or ZM 447439) utilised in this study in conjunction with the NBD WT CPP. Firstly, in Figure 6.4 (A – D), to assess impact on cell viability, PC3 cells were treated with the NBD WT/ MT CPP (100µM) and/or Aurora kinase/CDK inhibitor (0.25µM, 0.5µM, 1µM, 2µM and 5µM) for 72h prior to MTT assay and subsequently analysed as detailed in Section 2.2.7.1 of the Materials & Methods. Also, in Figure 6.4 (E – I), PC3 cells were treated with the NBD WT/ MT CPP (100µM) and/or Aurora kinase/CDK inhibitor (10nM, 30nM, 100nM, 300nM and 1µM) for 72h prior to clonogenic survival assay and associated analysis as detailed in Section 2.2.7.2 of the Materials & Methods. The MT/WT peptide and the AURK/CDK inhibitor were dissolved in 100% DMSO as described previously.

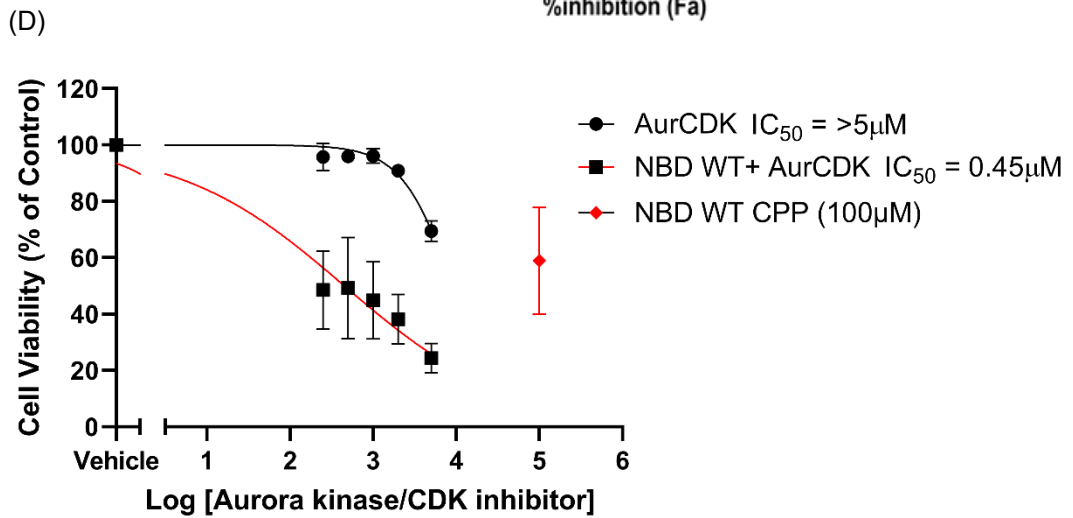
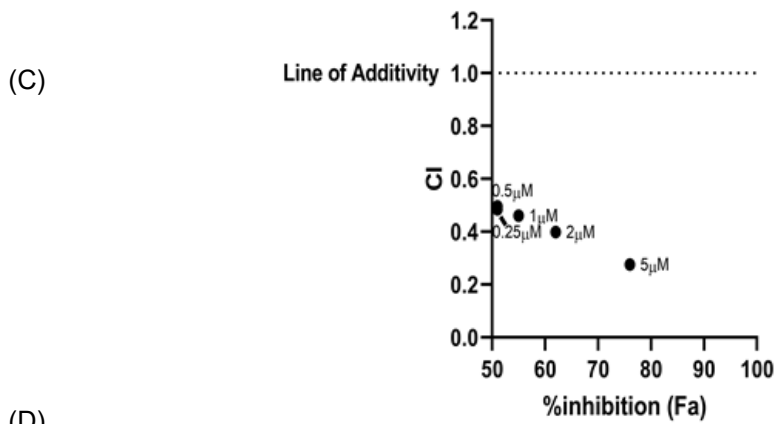
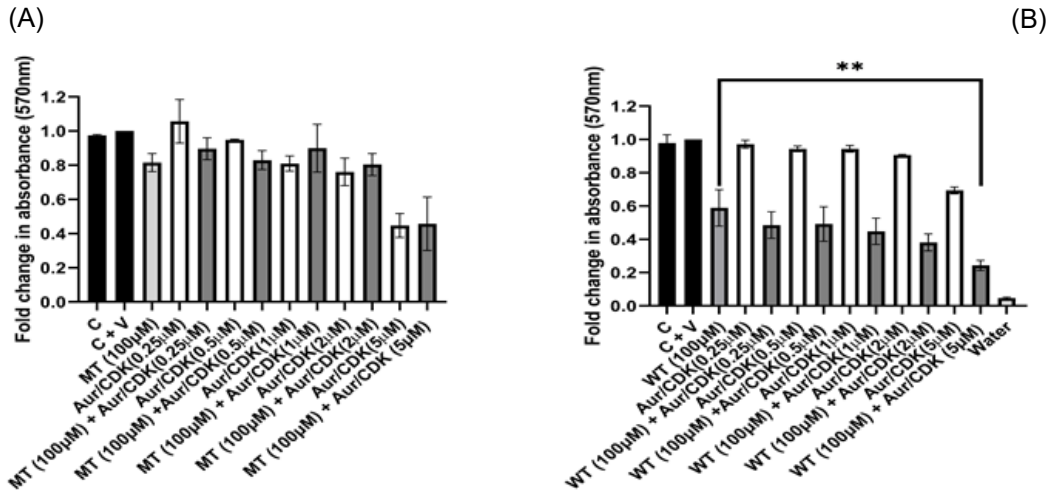
In Figure 6.4 (B), combination treatment of cells with a constant single concentration of NBD WT CPP (100µM) and a concentration range of the Aurora kinase/CDK inhibitor (0.25 - 5µM) significantly ($p < 0.05$) enhanced reduction of cell viability. This enhanced reduction in cell viability caused by the combination treatment compared to the NBD WT CPP alone was significant at an Aurora kinase/CDK inhibitor concentration of 5µM ($58.9 \pm 10.9\%$ vs $24.3 \pm 3.0\%$; $n=3$, $p < 0.01$). The Aurora kinase/CDK inhibitor in combination with NBD MT CPP caused no significant difference in reduction of cell viability across the concentration range compared to the NBD MT CPP or Aurora kinase/CDK inhibitor alone (Figure 6.4 A). Following on from this, in Figure 6.4 (C) the treatment combination of the Aurora kinase/CDK inhibitor and the NBD WT CPP was analysed to determine the degree of agent interaction based on the calculation of combination index (CI) values ($CI < 1$ - synergism, $CI = 1$ – Additivity and $CI > 1$ – Antagonism). The treatment combination between the Aurora kinase/CDK inhibitor and the NBD WT CPP was classified as synergistic across the concentration range of the Aurora kinase/CDK inhibitor; 0.25µM ($CI = 0.48$), 0.5µM ($CI = 0.50$), 1µM ($CI = 0.46$), 2µM ($CI = 0.40$) and 5µM ($CI = 0.28$). Further analysis of the data to determine the potency of the Aurora kinase/CDK inhibitor as a single agent and in combination with the NBD WT CPP to effect cell viability (Figure 6.4 D) produced IC_{50} values as follows; Aurora kinase/CDK inhibitor ($IC_{50} = >5\mu\text{M}$) and Aurora kinase/CDK inhibitor + NBD WT CPP ($IC_{50} = 0.45\mu\text{M}$). The results above

highlighted an almost 3-fold increase in potency to effect cell viability when the Aurora kinase/CDK inhibitor (at a concentration of 5 μ M) was utilised simultaneously in combination with the NBD WT CPP compared to single agent treatment with the NBD WT CPP.

In Figure 6.4 (E + G), combination treatment with a constant single concentration of NBD WT CPP (100 μ M) and a concentration range of the Aurora kinase/CDK inhibitor (10nM - 1 μ M) enhanced reduction of clonogenic survival. This enhanced reduction in clonogenic survival caused by the combination treatment compared to the NBD WT CPP alone was significant ($p < 0.05$) across the concentration range; 10nM (38.4 \pm 1.9% vs 16.1 \pm 3.0%; $n = 3$, $p < 0.05$), 30nM (38.4 \pm 1.9% vs 15.4 \pm 3.5%; $n = 3$, $p < 0.01$), 100nM (38.4 \pm 1.9% vs 11.0 \pm 4.1%; $n = 3$, $p < 0.001$), 300nM (38.4 \pm 1.9% vs 12.6 \pm 3.3%; $n = 3$, $p < 0.001$) and 1 μ M (38.4 \pm 1.9% vs 1.6 \pm 1.6%; $n = 3$, $p < 0.001$). The Aurora kinase/CDK inhibitor in combination with the NBD MT CPP caused no significant difference ($p > 0.05$) in reduction of clonogenic survival across the concentration range compared to the NBD MT CPP or Aurora kinase/CDK inhibitor alone (Figure 6.4 F). Following on from this, in Figure 6.4 (H) the treatment combination was analysed to determine the degree of agent interaction based on the calculation of combination index (CI) values (CI < 1 - synergism, CI = 1 – Additivity and CI > 1 – Antagonism). The combination treatment between the Aurora kinase/CDK inhibitor and the NBD WT CPP was characterised as synergistic across the concentration range of Aurora kinase/CDK inhibitor; 10nM (CI = 0.09), 30nM (CI = 0.11), 100nM (CI = 0.11), 300nM (CI = 0.37) and 1 μ M (CI = 0.02). Further analysis of the data to determine the potency of the Aurora kinase/CDK inhibitor as a single agent and in combination with the NBD WT CPP to effect clonogenic survival (Figure 6.4 I) produced IC₅₀ values as follows; Aurora kinase/CDK inhibitor (IC₅₀ = 28.5nM) and Aurora kinase/CDK inhibitor + NBD WT CPP (IC₅₀ = 6.3nM).

The results above showed an average 5-20 fold increase in potency to effect clonogenic survival across the concentration range of the Aurora kinase/CDK inhibitor, when the Aurora kinase/CDK inhibitor was utilised simultaneously in combination with the NBD WT CPP compared to single agent treatment with the NBD WT CPP.

These results demonstrated the ability of the NBD WT CPP and Aurora kinase/CDK inhibitor, when used in combination, to significantly and synergistically enhance the reduction in cell viability and clonogenic survival in comparison to when these agents were used alone as single-agent treatments.

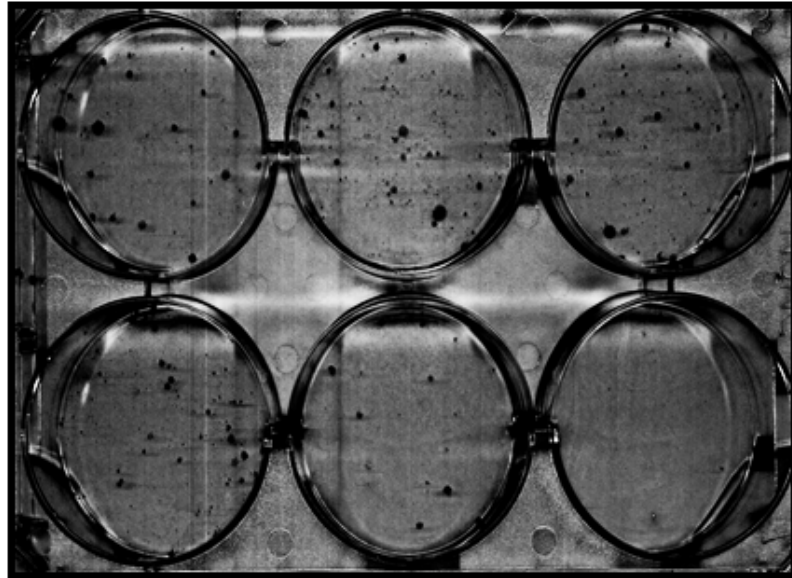


(E)

(C + V)

A/CDK
(10nM)

A/CDK
(30nM)



A/CDK
(100nM)

A/CDK
(300nM)

A/CDK
(1µM)

(C + V)

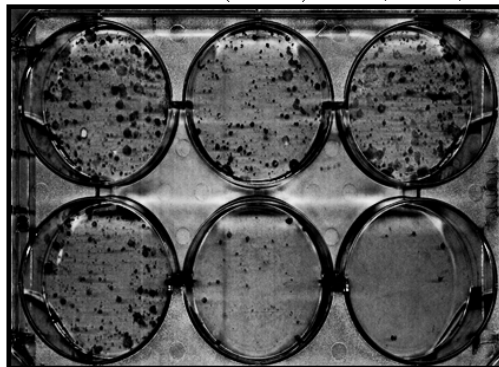
MT +
A/CDK
(10nM)

MT +
A/CDK
(30nM)

(C + V)

WT +
A/CDK
(10nM)

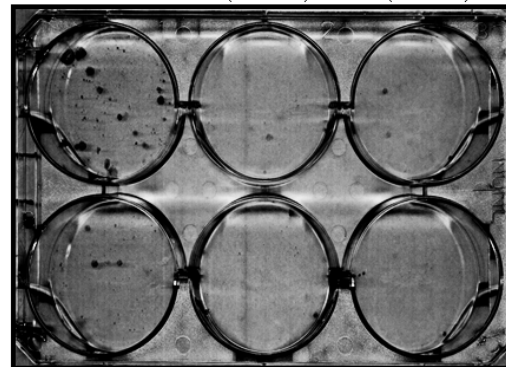
WT +
A/CDK
(30nM)



MT +
A/CDK
(100nM)

MT +
A/CDK
(300nM)

MT +
A/CDK
(1µM)

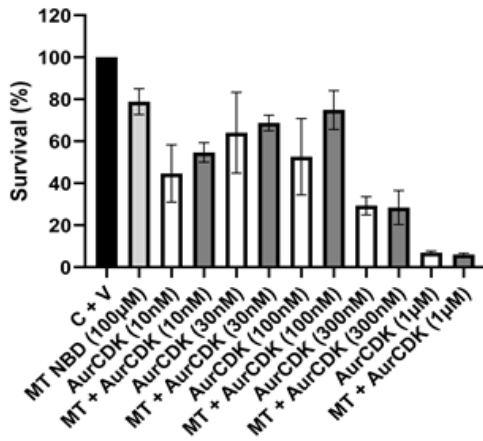


WT +
A/CDK
(100nM)

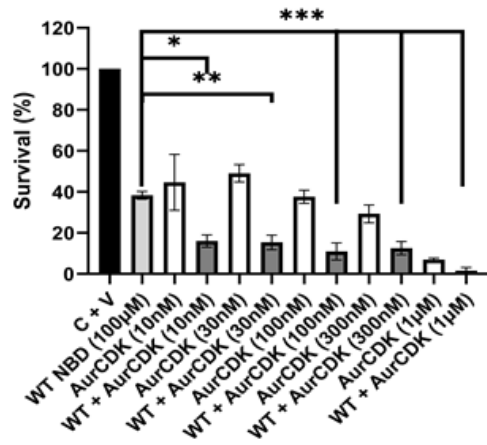
WT +
A/CDK
(300nM)

WT +
A/CDK
(1µM)

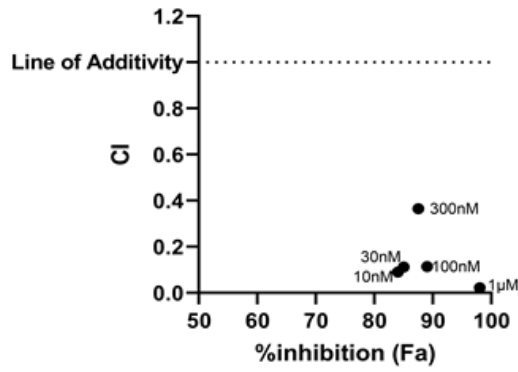
(F)



(G)



(H)



(I)

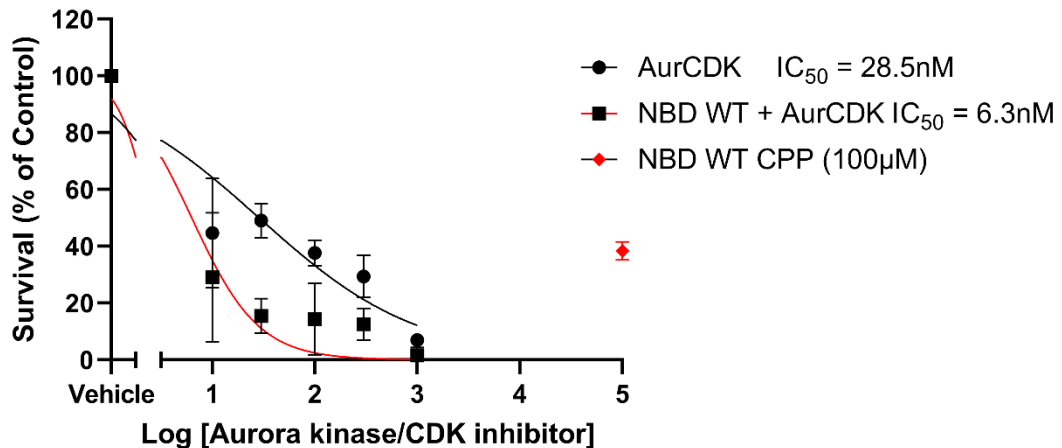


Figure 6.4. Effect of NBD MT/WT CPP and Aurora kinase/CDK inhibitor alone or in combination on cell viability and clonogenic survival of PC3 cells.

(A – D) PC3 cells were seeded into 96-well plates and treated with NBD MT (A) or WT (B) (both 100µM) and/or increasing concentrations of Aurora kinase/CDK inhibitor (0.25µM, 0.5µM, 1µM, 2µM and 5µM) for 72h. Cell viability was measured using the MTT assay. DMSO was used as a vehicle (C + V) control (0.5% (v/v)). Cells cultured in media with no treatment represented the positive control (C). Cells cultured in water represented the negative control (Water). Data was normalised to the vehicle control (C + V) and represents mean ± S.E.M of fold change in absorbance at 570nm (n=3). Triplicates were averaged for each experiment. One-way ANOVA with post-hoc Dunnet's test was used to determine statistical significance ($p < 0.05$) of observed changes between combination treatment and the NBD WT CPP alone to impact on cell viability (*= $p < 0.05$, **= $p < 0.01$, ***= $p < 0.001$). (C) Fraction affected-combination index (Fa-CI) plots of combined treatment of NBD WT CPP and Aurora kinase/CDK inhibitor in PC3 cells. Combination indices (CI) for drug-interaction determination were indicated as follows; $CI < 1$ (synergism), $CI = 1$ (additivity) and $CI > 1$ (antagonism). The combined effect of NBD WT CPP (100µM) and Aurora kinase/CDK inhibitor (0.25µM, 0.5µM, 1µM, 2µM and 5µM) on cell viability was determined and plotted. WT + AurCDK (0.25µM) [$CI = 0.484$], WT + AurCDK (0.5µM) [$CI = 0.495$], WT + AurCDK (1µM) [$CI = 0.46$], WT + AurCDK (2µM) [$CI = 0.398$], WT + AurCDK (5µM) [$CI = 0.275$]. (D) Comparison of the potency of the NBD WT CPP (♦), Aurora kinase/CDK inhibitor (●) or NBD WT CPP + Aurora kinase/CDK inhibitor (■) on cell viability in PC3 cells. The results were normalised to vehicle treated control and plotted on a log scale as a percentage of the control with regards to cell viability (n=3). The data was fitted with the following equation $Y = \text{Bottom} + (\text{Top} - \text{Bottom}) / (1 + 10^{((\text{Log}IC_{50} - X) * \text{HillSlope}))}$. Broken X-axis was used to represent vehicle treated control. (E – I) PC3 cells were seeded (300 cells / ml) into 6-well plates and treated with NBD MT (F) or WT (G) (both 100µM) and/or increasing concentrations of Aurora kinase/CDK inhibitor (10nM, 30nM, 100nM, 300nM and 1µM) for 72h Replicative potential was measured using the clonogenic survival assay as described in M&M and photographed also in panel E. DMSO was used as a vehicle (C + V) control (0.5% (v/v)). Data was normalised to the vehicle control (C + V) and represents mean ± S.E.M of change in percentage survival (n=3). One-way ANOVA with post-hoc Dunnet's test was used to determine statistical significance ($p < 0.05$) of observed changes between combination treatment and the NBD WT CPP alone to impact on clonogenic survival (*= $p < 0.05$, **= $p < 0.01$, ***= $p < 0.001$). (H) Fraction affected-combination index (Fa-CI) plots of combined treatment of NBD WT CPP and Aurora kinase/CDK inhibitor in PC3 cells. Combination indices (CI) for drug-interaction determination were indicated as follows; $CI < 1$ (synergism), $CI = 1$ (additivity) and $CI > 1$ (antagonism). The combined anti-proliferative effect of NBD WT CPP (100µM) and Aurora kinase/CDK inhibitor (10nM, 30nM, 100nM, 300nM and 1µM) was determined and plotted. WT + AurCDK (10nM) [$CI = 0.09$], WT + AurCDK

(30nM) [CI = 0.112], WT + AurCDK (100nM) [CI = 0.114], WT + AurCDK (300nM) [CI = 0.365], WT + AurCDK (1µM) [CI = 0.022], (I) Comparison of the potency of the NBD WT CPP (♦), Aurora kinase/CDK inhibitor (●) or NBD WT CPP + Aurora kinase/CDK inhibitor (■) on clonogenic survival in PC3 cells. The results were normalised to vehicle treated control and plotted on a log scale as a percentage of the control with regards to clonogenic survival (n=3). The data was fitted with the following equation $Y = \text{Bottom} + (\text{Top} - \text{Bottom}) / (1 + 10^{((\text{LogIC}_{50} - X) * \text{HillSlope}))}$. Broken X-axis was used to represent vehicle treated control.

6.2.5. Effect of ZM 447439 and NBD WT CPP alone and in combination on cell viability and clonogenic survival of prostate cancer cells.

In Figure 6.5 (A – D), to assess impact on cell viability, PC3 cells were treated with the NBD WT/ MT CPP (100µM) and/or ZM 447439 (0.1µM, 0.3µM, 1µM, 3µM and 10µM) for 72h prior to MTT assay and subsequently analysed as detailed in Section 2.2.7.1 of the Materials & Methods. Also, in Figure 6.5 (E – I), PC3 cells were treated with the NBD WT/ MT CPP (100µM) and/or ZM 447439 (10nM, 30nM, 100nM, 300nM and 1µM) for 72h prior to clonogenic survival assay and associated analysis as detailed in Section 2.2.7.2 of the Materials & Methods. The MT/WT peptide and the ZM 447439 were dissolved in 100% DMSO as described previously and as a result all experiments involving the NBD CPPs and ZM 447439 used DMSO as a vehicle control.

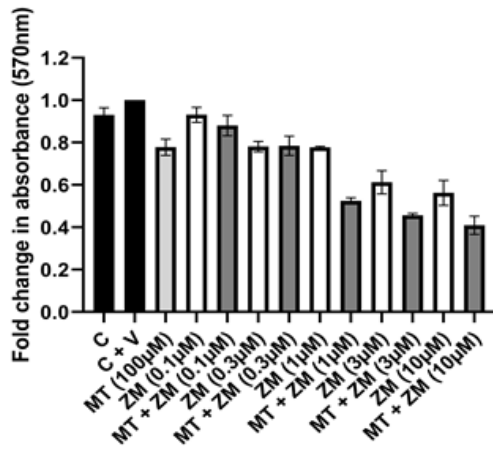
To commence, in Figure 6.5 (B), combination treatment of PC3 cells with a constant single concentration of NBD WT CPP (100µM) and a concentration range of the ZM 447439 (0.1 - 1µM) enhanced reduction of cell viability. This enhanced reduction in cell viability caused by the combination treatment approach compared to the NBD WT CPP alone was significant at the ZM 447439 concentration of 10µM ($58.9 \pm 10.9\%$ vs $32.7 \pm 3.9\%$; n=3, p<0.01). The ZM 447439 in combination with NBD MT CPP caused no significant difference (p>0.05) in reduction of cell viability across the concentration range compared to the NBD MT CPP or ZM 447439 alone (Figure 6.5 A). Following on from this, in Figure 6.5 (C) the combination treatment of ZM 447439 and the NBD WT CPP was analysed to determine the degree of agent interaction based on the calculation of combination index (CI) values (CI < 1 - synergism, CI = 1 – Additivity and CI > 1 – Antagonism). The treatment combination between ZM 447439 and the NBD WT CPP was classified as synergistic across the concentration range of ZM 447439; 0.1µM (CI = 0.56), 0.3µM (CI = 0.41), 1µM (CI = 0.32), 3µM (CI = 0.40) and 10µM (CI = 0.30). The data was then further analysed to determine the potency of the ZM 447439 as a single agent and in combination with the NBD WT CPP to effect cell viability (Figure 6.5 D) produced IC₅₀ values as follows; ZM 447439 (IC₅₀ = 14.1µM) and ZM 447439 + NBD WT CPP (IC₅₀ = 0.836µM). The results above highlighted an around 2-fold increase in potency to effect cell viability when the ZM 447439 (at a concentration of 10µM) was utilised simultaneously in

combination with the NBD WT CPP compared to single agent treatment with the NBD WT CPP.

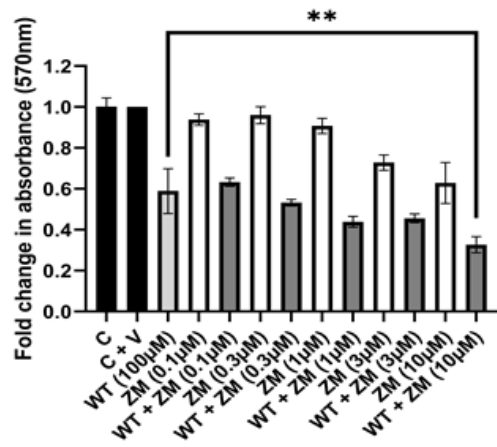
In Figure 6.5 (E + G), combination treatment with a constant single concentration of NBD WT CPP (100 μ M) and a concentration range of the ZM 447439 enhanced reduction of clonogenic survival. This enhanced reduction in clonogenic survival caused by the combination treatment compared to the NBD WT CPP alone was significant ($p < 0.05$) at concentrations of; 100nM ($38.4 \pm 1.9\%$ vs $6.4 \pm 1.8\%$; $n=3$, $p < 0.05$), 300nM ($38.4 \pm 1.9\%$ vs $2.9 \pm 0.9\%$; $n=3$, $p < 0.05$) and 1 μ M ($38.4 \pm 1.9\%$ vs $0.7 \pm 0.2\%$; $n=3$, $p < 0.05$). The ZM 447439 compound in combination with the NBD MT CPP caused no significant difference in reduction of clonogenic survival across the concentration range compared to the NBD MT CPP or ZM 447439 alone (Figure 6.5 F). Following on from this, in Figure 6.5 (H) the combination treatment of ZM 447439 and the NBD WT CPP was analysed to determine the degree of agent interaction based on the calculation of combination index (CI) values (CI < 1 - synergism, CI = 1 – Additivity and CI > 1 – Antagonism). The treatment combination between ZM 447439 and the NBD WT CPP was characterised as synergistic at the following ZM 447439 concentrations: 10nM (CI = 0.24), 30nM (CI = 0.39) and 100nM (CI = 0.61). At the higher concentrations of ZM 447439 in combination with the NBD WT CPP the agent interaction was classified as slightly antagonistic; 300nM (CI = 1.34) and 1 μ M (CI = 1.19). The data was further analysed to determine the potency of the ZM 447439 as a single agent and in combination with the NBD WT CPP to effect clonogenic survival (Figure 6.5 I) and produced IC₅₀ values as follows; ZM 447439 (IC₅₀ = 417nM) and ZM 447439 + NBD WT CPP (IC₅₀ = 27.5nM). The results above highlighted an almost 20-30 fold increase in potency to effect clonogenic survival when the higher concentrations of ZM 447439 (100nM, 300nM and 1 μ M) were utilised simultaneously in combination with the NBD WT CPP compared to single agent treatment with the NBD WT CPP.

These outcomes demonstrated the ability of the NBD WT CPP and ZM 447439, when used in combination, to significantly and synergistically enhance the reduction in cell viability and clonogenic survival in comparison to when these agents were used alone as single-agent treatments.

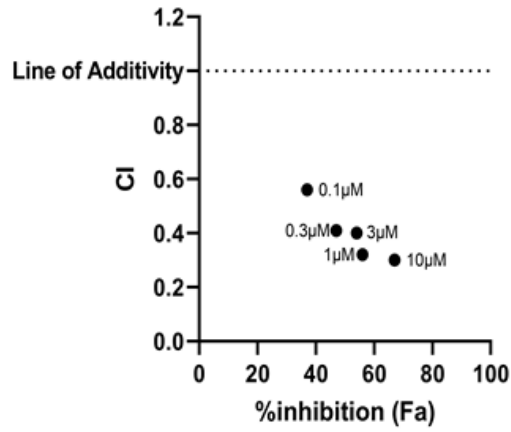
(A)



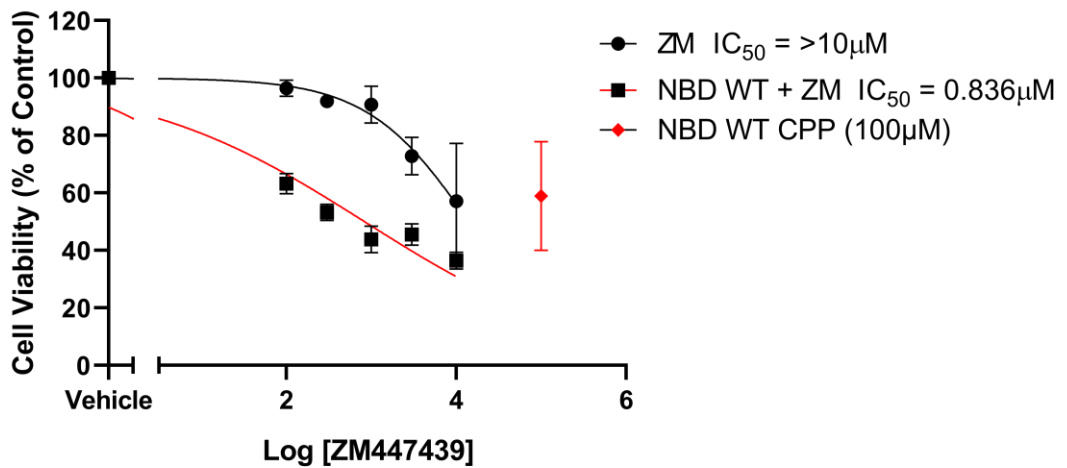
(B)



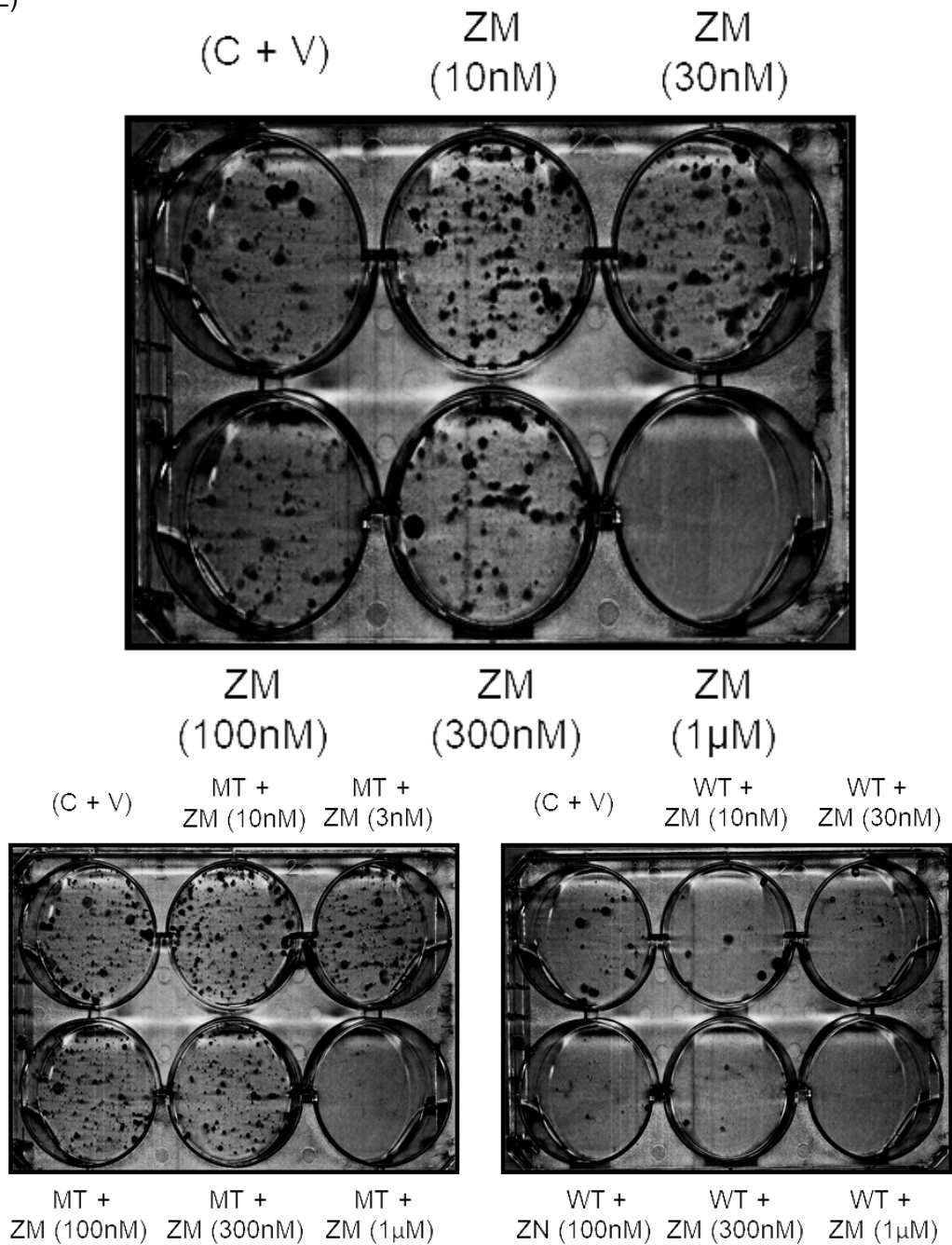
(C)



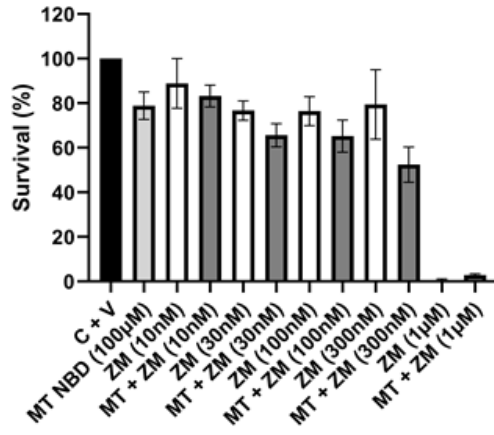
(D)



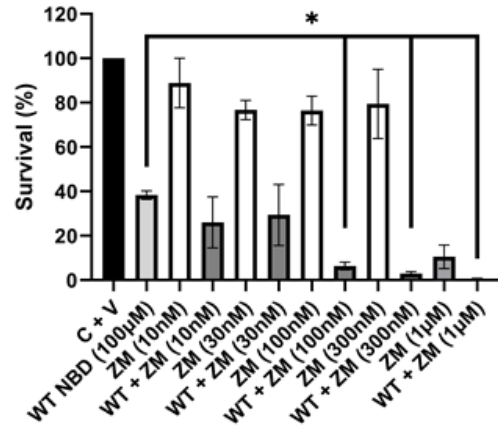
(E)



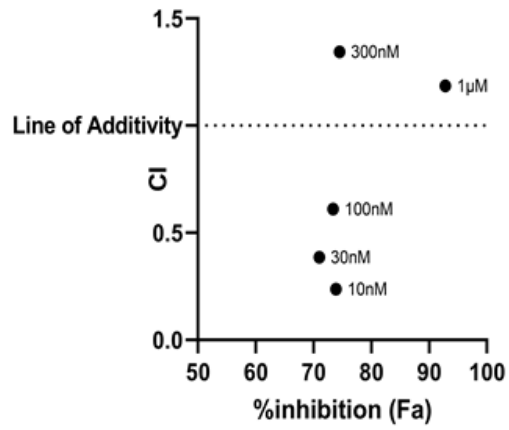
(F)



(G)



(H)



(I)

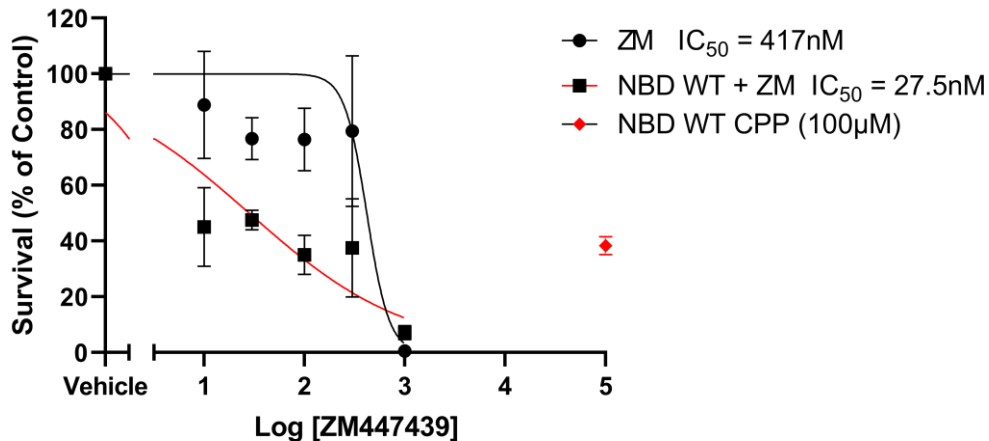


Figure 6.5. Effect of NBD MT/WT CPP and ZM447439 alone or in combination on cell viability and clonogenic survival of PC3 cells.

(A – D) PC3 cells were seeded into 96-well plates and treated with NBD MT (A) or WT (B) (both 100µM) and/or increasing concentrations of ZM 447439 (0.1µM, 0.3µM, 1µM, 3µM and 10µM) for 72h. Cell viability was measured using the MTT assay. DMSO was used as a vehicle (C + V) control (0.5% (v/v)). Cells cultured in media with no treatment represented the positive control (C). Cells cultured in water represented the negative control (Water). Data was normalised to the vehicle control (C + V) and represents mean ± S.E.M of fold change in absorbance at 570nm (n=3). Triplicates were averaged for each experiment. One-way ANOVA with post-hoc Dunnet's test was used to determine statistical significance ($p < 0.05$) of observed changes between combination treatment and the NBD WT CPP alone to impact on cell viability (*= $p < 0.05$, **= $p < 0.01$, ***= $p < 0.001$). (C) Fraction affected-combination index (Fa-CI) plots of combined treatment of NBD WT CPP and ZM 447439 in PC3 cells. Combination indices (CI) for drug-interaction determination were indicated as follows; $CI < 1$ (synergism), $CI = 1$ (additivity) and $CI > 1$ (antagonism). The combined effect of NBD WT CPP (100µM) and ZM 447439 (0.1µM, 0.3µM, 1µM, 3µM and 10µM) on cell viability was determined and plotted. WT + ZM (0.1µM) [$CI = 0.56$], WT + ZM (0.3µM) [$CI = 0.41$], WT + ZM (1µM) [$CI = 0.32$], WT + ZM (3µM) [$CI = 0.4$], WT + ZM (10µM) [$CI = 0.3$], (D) Comparison of the potency of the NBD WT CPP (♦), ZM 447439 (●) or NBD WT CPP + ZM 447439 (■) on cell viability in PC3 cells. The results were normalised to vehicle treated control and plotted on a log scale as a percentage of the control with regards to cell viability (n=3). The data was fitted with the following equation $Y = \text{Bottom} + (\text{Top} - \text{Bottom}) / (1 + 10^{-(\text{LogIC}_{50} - X) * \text{HillSlope}})$. Broken X-axis was used to represent vehicle treated control. (E – I) PC3 cells were seeded (300 cells / ml) into 6-well plates and treated with NBD MT (F) or WT (G) (both 100µM) and/or increasing concentrations of ZM 447439 (10nM, 30nM, 100nM, 300nM and 1µM) for 72h. Replicative potential was measured using the clonogenic survival assay as described in M&M and photographed also in panel E. DMSO was used as a vehicle (C + V) control (0.5% (v/v)). Data was normalised to the vehicle control (C + V) and represents mean ± S.E.M of change in percentage survival (n=3). One-way ANOVA with post-hoc Dunnet's test was used to determine statistical significance ($p < 0.05$) of observed changes between combination treatment and the NBD WT CPP alone to impact on clonogenic survival (*= $p < 0.05$, **= $p < 0.01$, ***= $p < 0.001$). (H) Fraction affected-combination index (Fa-CI) plots of combined treatment of NBD WT CPP and ZM 447439 in PC3 cells. Combination indices (CI) for drug-interaction determination were indicated as follows; $CI < 1$ (synergism), $CI = 1$ (additivity) and $CI > 1$ (antagonism). The combined anti-proliferative effect of NBD WT CPP (100µM) and ZM 447439 (10nM, 30nM, 100nM, 300nM and 1µM) was determined and plotted. WT + ZM (10nM) [$CI = 0.237$], WT + ZM (30nM) [$CI = 0.385$], WT + ZM (100nM) [$CI = 0.61$], WT + ZM (300nM) [$CI = 1.344$], WT + ZM (1µM) [$CI = 1.185$], (I) Comparison of the potency of the NBD WT CPP (♦), ZM 447439 (●) or NBD WT CPP + ZM 447439 (■) on clonogenic survival in PC3 cells. The results were normalised to vehicle treated control and plotted on a log scale as

a percentage of the control with regards to clonogenic survival (n=3). The data was fitted with the following equation $Y = \text{Bottom} + (\text{Top} - \text{Bottom}) / (1 + 10^{((\text{LogIC}_{50} - X) * \text{HillSlope}))}$. Broken X-axis was used to represent vehicle treated control.

6.2.6. Effect of VX-680 and NBD WT CPP alone and in combination on cell viability and clonogenic survival of prostate cancer cells.

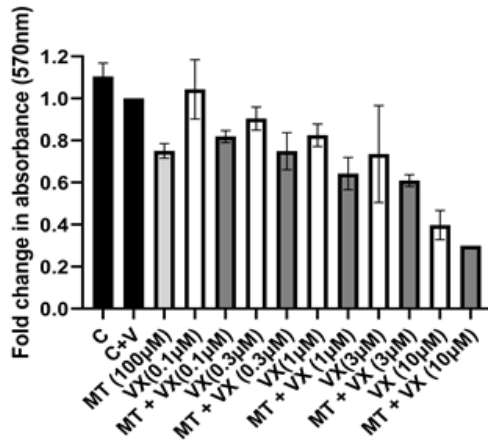
Lastly, in Figure 6.6 (A– D), to assess impact on cell viability, PC3 cells were treated with the NBD WT/ MT CPP (100 μ M) and/or VX-680 (0.1 μ M, 0.3 μ M, 1 μ M, 3 μ M and 10 μ M) for 72h prior to MTT assay and subsequently analysed as detailed in Section 2.2.7.1 of the Materials & Methods. Also, in Figure 6.6 (E – I), PC3 cells were treated with the NBD WT/ MT CPP (100 μ M) and/or VX-680 (1nM, 3nM, 10nM, 30nM and 100nM) for 72h prior to clonogenic survival assay and associated quantitative analysis as detailed in Section 2.2.7.2 of the Materials & Methods. The MT/WT peptide and the VX-680 were dissolved in 100% DMSO as described previously and as a result all experiments involving the NBD CPPs and VX-680 used DMSO as a vehicle control.

To start, in Figure 6.6 (B) combination treatment with a constant single concentration of NBD WT CPP (100 μ M) and a concentration range of VX-680 (0.1 - 10 μ M) enhanced reduction of cell viability. This enhanced reduction in cell viability caused by the combination treatment approach compared to the NBD WT CPP was significant ($p < 0.05$) at a concentration of 10 μ M ($46.8 \pm 2.5\%$ vs $16.7 \pm 1.5\%$; $n=3$, $p < 0.05$). The VX-680 in combination with NBD MT CPP caused no significant difference ($p > 0.05$) in reduction of cell viability across the concentration range compared to the NBD MT CPP or VX-680 alone (Figure 6.6 A). Following on from this, in Figure 6.6 (C) the combination treatment was analysed to determine the degree of agent interaction based on the calculation of combination index (CI) values (CI < 1 - synergism, CI = 1 – Additivity and CI > 1 – Antagonism). The treatment combination between VX-680 and the NBD WT CPP was characterised as synergistic at the following VX-680 concentrations; 0.3 μ M (CI = 0.95), 1 μ M (CI = 0.91), 3 μ M (CI = 0.37) and 10 μ M (CI = 0.27). At the lowest concentration of VX-680 in combination with the NBD WT CPP the drug interaction was classified as slightly antagonistic; 0.1 μ M (CI = 1.11). The data was further analysed to determine the potency of the VX-680 as a single agent and in combination with the NBD WT CPP to cause a reduction in cell viability (Figure 6.6 D) and produced IC₅₀ values as follows; VX-680 (IC₅₀ = 17.1 μ M) and VX-680 + NBD WT CPP (IC₅₀ = 2.2 μ M). The results above highlighted an around 3-fold increase in potency to effect cell viability when the VX-680 (at a concentration of 10 μ M) was utilised simultaneously in combination with the NBD WT CPP compared to single agent treatment with the NBD WT CPP.

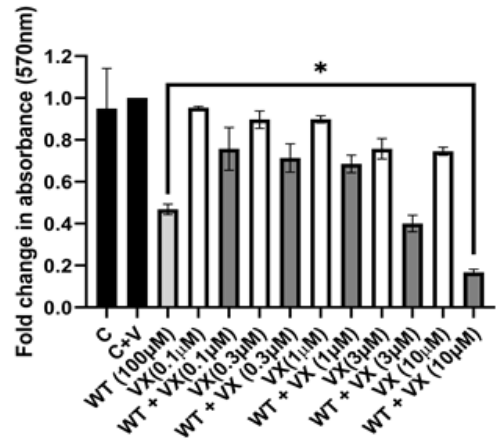
In Figure 6.6 (E + G), combination treatment with a constant single concentration of NBD WT CPP (100 μ M) and a concentration range of the VX-680 (1-100nM) enhanced reduction of clonogenic survival. In comparison to treatment with the NBD WT CPP alone, this enhanced reduction in clonogenic survival caused by the combination treatment approach was significant ($p < 0.05$) at concentrations of; 30nM ($38.4 \pm 1.9\%$ vs $7.9 \pm 4.3\%$; $n=3$, $p < 0.05$) and 100nM ($38.4 \pm 1.9\%$ vs $1.7 \pm 1.7\%$; $n=3$, $p < 0.01$). The VX-680 in combination with the NBD MT CPP caused no significant difference ($p > 0.05$) in reduction of clonogenic survival across the concentration range compared to the NBD MT CPP or VX-680 alone (Figure 5.6 F). Following on from this, in Figure 6.6 (H) the combination treatment was analysed to determine the degree of agent interaction based on the calculation of combination index (CI) values (CI < 1 - synergism, CI = 1 – Additivity and CI > 1 – Antagonism). The treatment combination between VX-680 and the NBD WT CPP was characterised as synergistic across the concentration range of VX-680; 1nM (CI = 0.30), 3nM (CI = 0.19), 10nM (CI = 0.64), 30nM (CI = 0.86) and 100nM (CI = 0.23). The data was further analysed to determine the potency of the VX-680 as a single agent and in combination with the NBD WT CPP to effect clonogenic survival (Figure 6.6 I) and produced IC₅₀ values as follows; VX-680 (IC₅₀ = 7.2nM) and VX-680 + NBD WT CPP (IC₅₀ = 0.23nM). The results above highlighted an average 5 to 30 fold increase in potency to effect clonogenic survival when the higher concentrations of VX-680 (30nM and 100nM) were utilised simultaneously in combination with the NBD WT CPP compared to single agent treatment with the NBD WT CPP.

These results demonstrated the ability of the NBD WT CPP and VX-680, when used in combination, to significantly and synergistically enhance the reduction in cell viability and clonogenic survival in comparison to when these agents were used alone as single-agent treatments. Overall, this was common to all the AURK inhibitors (AURK inhibitor II, AURK inhibitor III, Aurora kinase/CDK inhibitor, ZM 447439 and VX-680) used in this study in that there was a significant improvement in efficacy to impact on cell viability and clonogenic survival when used in combination with the NBD WT CPP compared to single-agent treatment. The impact of the VX-680 alone and in combination with the NBD WT CPP to effect other phenotypic outcomes (induction of apoptosis) will be focussed on for the remainder of this chapter.

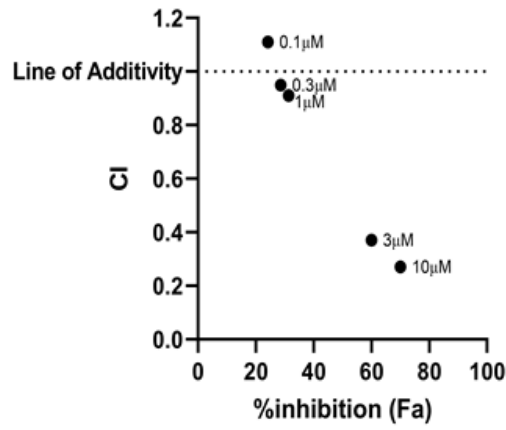
(A)



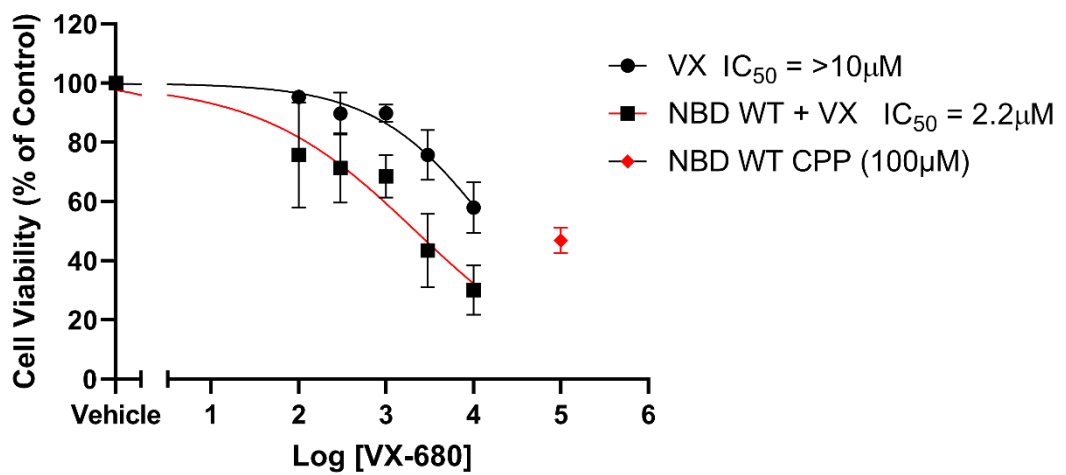
(B)



(C)

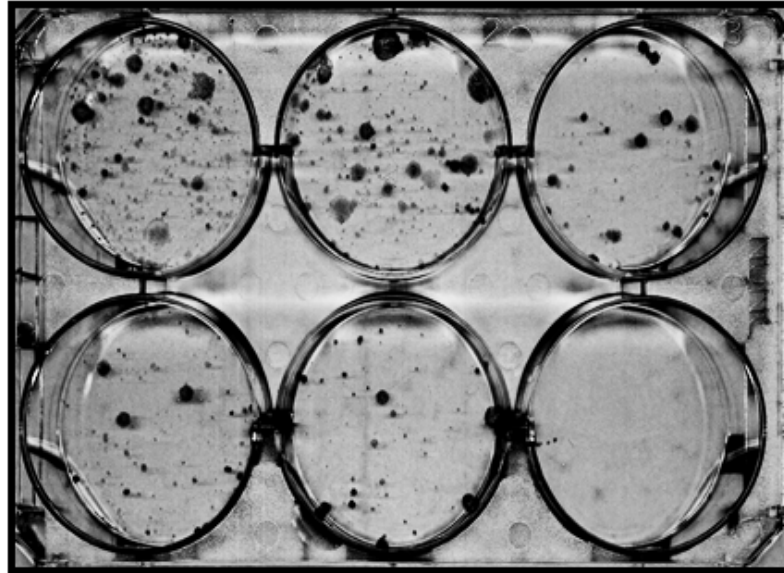


(D)



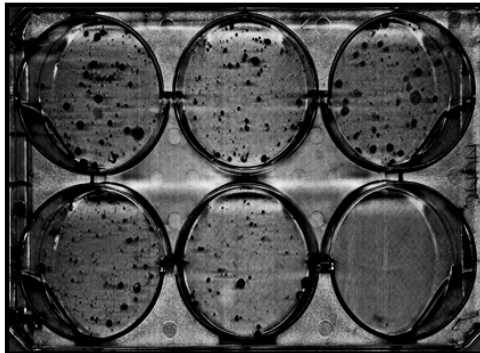
(E)

(C + V) VX (1nM) VX (3nM)



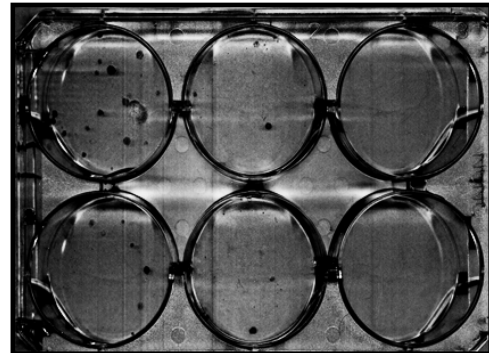
VX (10nM) VX (30nM) VX (100nM)

(C + V) MT + MT +
 VX (1nM) VX (3nM)

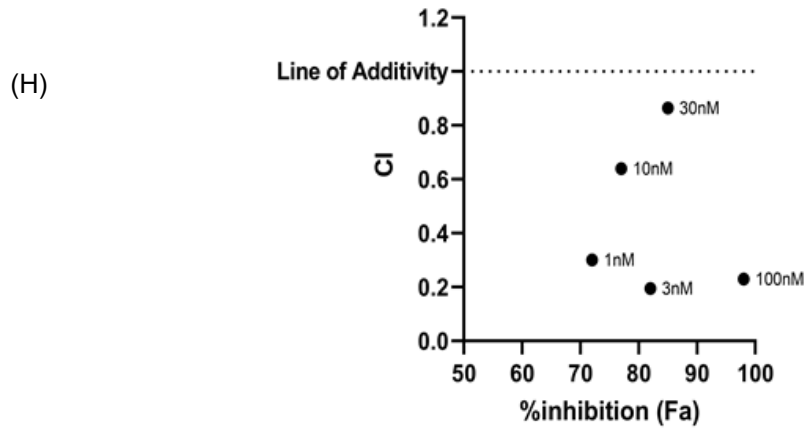
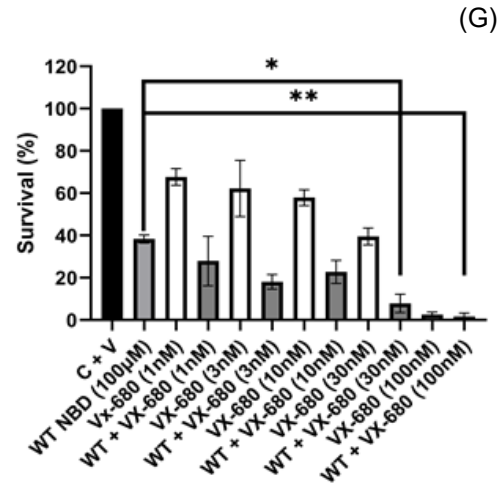
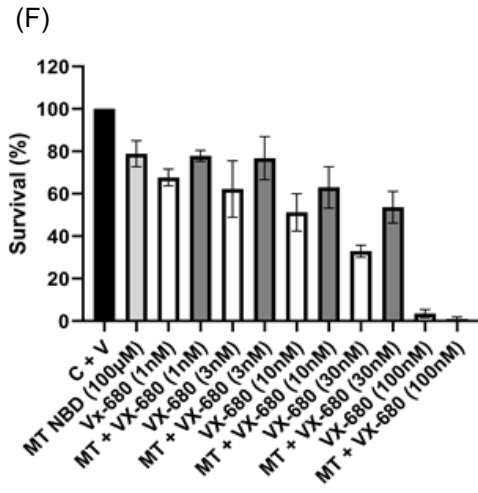


MT + MT + MT +
VX (10nM) VX (30nM) VX (100nM)

(C + V) WT + WT +
 VX (1nM) VX (3nM)



WT + WT + WT +
VX (10nM) VX (30nM) VX (100nM)



(I)

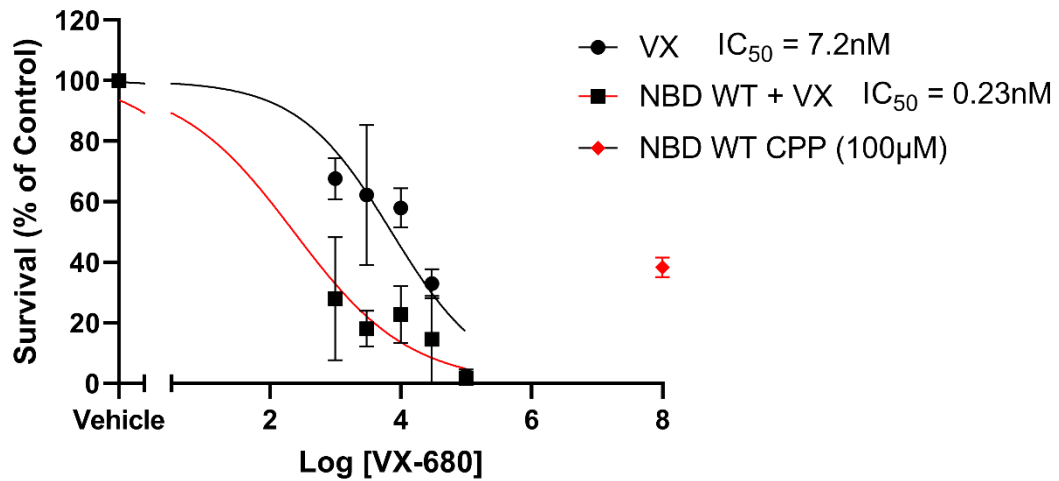


Figure 6.6. Effect of NBD MT/WT CPP and VX-680 alone or in combination on cell viability and clonogenic survival of PC3 cells.

(A – D) PC3 cells were seeded into 96-well plates and treated with NBD MT (A) or WT (B) (both 100µM) and/or increasing concentrations of VX-680 (0.1µM, 0.3µM, 1µM, 3µM and 10µM) for 72h. Cell viability was measured using the MTT assay. DMSO was used as a vehicle (C + V) control (0.5% (v/v)). Cells cultured in media with no treatment represented the positive control (C). Cells cultured in water represented the negative control (Water). Data was normalised to the vehicle control (C + V) and represents mean ± S.E.M of fold change in absorbance at 570nm (n=3). Triplicates were averaged for each experiment. One-way ANOVA with post-hoc Dunnet's test was used to determine statistical significance ($p < 0.05$) of observed changes between combination treatment and the NBD WT CPP alone to impact on cell viability (*= $p < 0.05$, **= $p < 0.01$, ***= $p < 0.001$). (C) Fraction affected-combination index (Fa-CI) plots of combined treatment of NBD WT CPP and VX-680 in PC3 cells. Combination indices (CI) for drug-interaction determination were indicated as follows; $CI < 1$ (synergism), $CI = 1$ (additivity) and $CI > 1$ (antagonism). The combined effect of NBD WT CPP (100µM) and VX-680 (0.1µM, 0.3µM, 1µM, 3µM and 10µM) on cell viability was determined and plotted. WT + VX (0.1µM) [$CI = 1.11$], WT + VX (0.3µM) [$CI = 0.95$], WT + VX (1µM) [$CI = 0.91$], WT + VX (3µM) [$CI = 0.37$], WT + VX (10µM) [$CI = 0.27$], (D) Comparison of the potency of the NBD WT CPP (◆), VX-680 (●) or NBD WT CPP + VX-680 (■) on cell viability in PC3 cells. The results were normalised to vehicle treated control and plotted on a log scale as a percentage of the control with regards to cell viability (n=3). The data was fitted with the following equation $Y = \text{Bottom} + (\text{Top} - \text{Bottom}) / (1 + 10^{((\text{Log}IC_{50} - X) * \text{HillSlope}))}$). Broken X-axis was used to represent vehicle treated control. (E – I) PC3 cells were seeded (300 cells / ml) into 6-well plates and treated with NBD MT or WT (both 100µM) and/or increasing concentrations of VX-680 (1nM, 3nM, 10nM, 30nM and 100nM) for 72h. Replicative potential was measured using the clonogenic survival assay as described in M&M and photographed also in panel E. DMSO was used as a vehicle (C + V) control (0.5% (v/v)). Data was normalised to the vehicle control (C + V) and represents mean ± S.E.M of change in percentage survival (n=3). One-way ANOVA with post-hoc Dunnet's test was used to determine statistical significance ($p < 0.05$) of observed changes between combination treatment and the NBD WT CPP alone to impact on clonogenic survival (*= $p < 0.05$, **= $p < 0.01$, ***= $p < 0.001$). (H) Fraction affected-combination index (Fa-CI) plots of combined treatment of NBD WT CPP and VX-680 in PC3 cells. Combination indices (CI) for drug-interaction determination were indicated as follows; $CI < 1$ (synergism), $CI = 1$ (additivity) and $CI > 1$ (antagonism). The combined anti-proliferative effect of NBD WT CPP (100µM) and VX-680 (1nM, 3nM, 10nM, 30nM and 100nM) was determined and plotted. WT + VX (1nM) [$CI = 0.3$], WT + VX (3nM) [$CI = 0.194$], WT + VX (10nM) [$CI = 0.639$], WT + VX (30nM) [$CI = 0.864$], WT + VX (100nM) [$CI = 0.229$], (I) Comparison of the potency of the NBD

WT CPP (◆), VX-680 (●) or NBD WT CPP + VX-680 (■) on clonogenic survival in PC3 cells. The results were normalised to vehicle treated control and plotted on a log scale as a percentage of the control with regards to clonogenic survival (n=3). The data was fitted with the following equation $Y = \text{Bottom} + (\text{Top} - \text{Bottom}) / (1 + 10^{((\text{LogIC50} - X) * \text{HillSlope}))}$. Broken X-axis was used to represent vehicle treated control.

6.2.7. Effect of VX-680 and NBD WT CPP alone and in combination on the induction of apoptosis in prostate cancer cells.

Following on from the demonstration of the effect of the NBD WT CPP in combination with ATP-competitive AURK inhibitors (AURK inhibitor II, AURK inhibitor III, AURK/CDK inhibitor, ZM 447439 and VX-680) to impact clonogenic survival and cell viability, in this section, this study investigated the ability of VX-680 to induce apoptosis as demonstrated in the literature (Gizatullin et al., 2006) and whether it's efficacy could be enhanced in combination with the NBD WT CPP, to cause an accelerated initiation of cell death in comparison to the single agents alone.

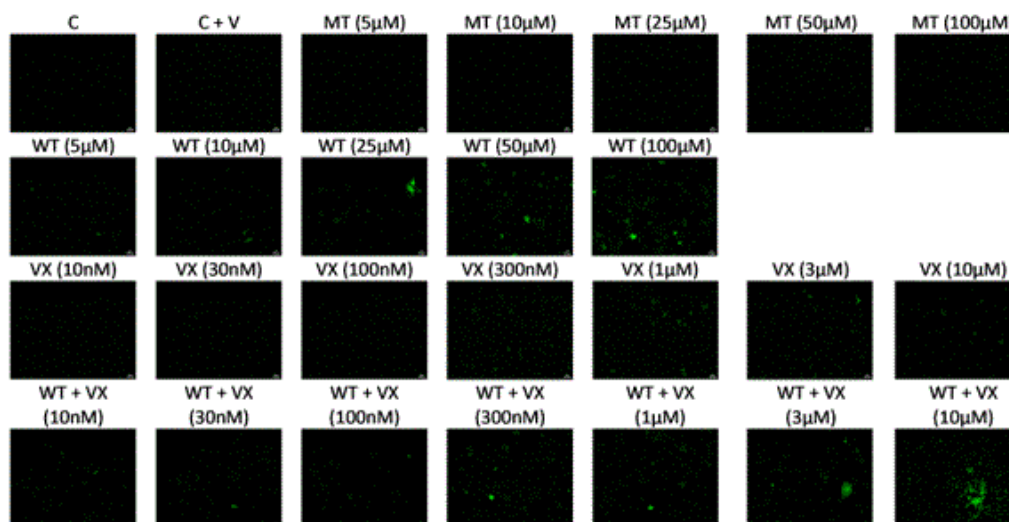
In Figure 6.7 (A + B), to assess the impact on the induction of apoptosis, PC3 cells were treated with the NBD WT/ MT CPP (100µM) as agents alone or in combination with VX-680 (10nM, 30nM, 100nM, 300nM, 1µM, 3µM and 10µM) for 72h prior to NucView® 488 caspase-3/7 substrate assay and associated analysis as detailed in Section 2.2.7.3 of the Materials & Methods. The MT/WT peptide and the VX-680 were dissolved in 100% DMSO as described previously and as a result all experiments involving the NBD CPPs and VX-680 used DMSO as a vehicle control.

It can be observed in Figure 6.7 from the representative images (A) and subsequent quantification (B) that there was no change in Corrected Total Cell Fluorescence (CTCF) and hence no induction of apoptosis across the concentration range of the NBD MT CPP compared to the vehicle treated control. In comparison there was a substantial concentration-dependent increase in CTCF, which translated to an increased induction of apoptosis, following treatment with the NBD WT CPP. There was also an increase in the induction of apoptosis following treatment with the VX-680 alone, which peaked at around a 5-fold change in CTCF. When the NBD WT CPP was used in combination with the VX-680, this substantially enhanced the induction of apoptosis compared to single agent treatment and this was particularly apparent at the higher concentrations of VX-680 (3µM and 10µM) which produced a fold change in CTCF of around 10- and 15-times respectively.

Collectively, these results highlighted the ability of the NBD WT CPP and VX-680 to accelerate the induction of apoptosis when used in combination in a similar manner to the effect both agents had on cell viability and clonogenic survival (Figure 6.6). Whether these

results translate to be statistically significant or not, further repeats will need to be carried out to determine this.

(A)



(B)

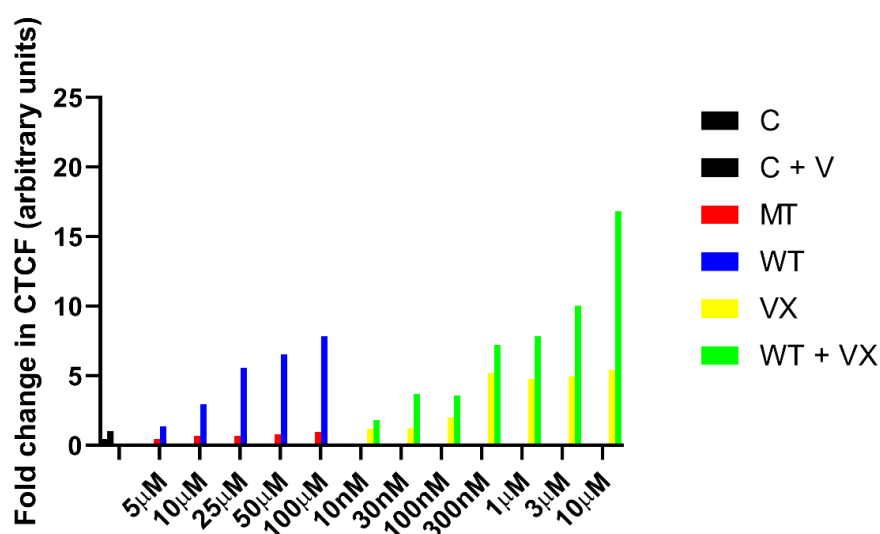


Figure 6.7. Effect of NBD MT/WT CPP and VX-680 alone or in combination on induction of apoptosis in PC3 cells.

(A + B) PC3 cells were seeded (5×10^4 cells / well) into 96-well plates and treated with NBD MT or WT (both $100 \mu\text{M}$) and/or increasing concentrations of VX-680 (10nM, 30nM, 100nM, 300nM, $1 \mu\text{M}$, $3 \mu\text{M}$ and $10 \mu\text{M}$) for 72h. **(A)** Apoptosis was measured using the NUCVIEW® 488 Caspase-3/7 substrate assay (green fluorescent cells). DMSO was used as a vehicle (C + V) control (0.5% (v/v)). Cells cultured in media with no treatment represented a negative control (C). **(B)** Data was normalised to the vehicle treated control (C + V) and represents mean of fold change in Corrected Total Cell Fluorescence (CTCF) ($n=2$). Duplicates were averaged for each treatment group. Scale bar, $500 \mu\text{m}$.

6.3. Discussion.

As detailed previously in this thesis, overexpression of AURKA and TPX2 are key targets in a variety of different cancers. These are associated with most of the hallmarks of cancer (Hanahan and Weinberg, 2011) and this manifests to make these drug targets at a molecular and phenotypic level. AURKA upregulation is linked to; cell proliferation (Min et al., 2016), cell survival (Willems et al., 2019) and inhibition of apoptosis (Katayama et al., 2012) among other phenotypic characteristics. Targeting of TPX2 has been demonstrated to result in inhibition of cell proliferation, cell survival and apoptosis (Zou et al., 2018b) as well as invasion/migration (Yang et al., 2015b) of cancerous cells.

The NBD WT CPP which formed basis of the research carried out in this thesis had been previously demonstrated to inhibit cell proliferation and survival (Ianaro et al., 2009) as well as accelerated the induction of apoptosis (Choi et al., 2003). This inhibition of cell viability following treatment with the NBD WT CPP was also demonstrated in different solid tumour cell lines in Figure 4.4. In this chapter the NBD WT CPP was utilised in combination with ATP-competitive AURK inhibitors (AURK inhibitor III, AURK inhibitor II, Aurora kinase/CDK inhibitor, VX-680 and ZM 447439), as used in previous chapters throughout this thesis, to investigate a potential synergistic effect through targeting of AURKA (ATP competitive AURK inhibitors) and TPX2 (NBD WT CPP – based on our hypothesis that it disrupts AURKA/TPX2 interaction) and whether this correlated to an enhanced efficacy to impact on phenotypic outcomes (cell viability, clonogenic survival and apoptosis).

6.3.1. Dual pharmacological targeting and the impact on cancer cell viability and survival.

Firstly, in Figures 6.2 – 6.6, commercially available ATP-competitive AURK inhibitors (AURK inhibitor II, AURK inhibitor III, Aurora kinase/CDK inhibitor, VX-680 and ZM 447439) and the NBD WT CPP as single agents or in combination were tested on their ability to impact on clonogenic survival and cell viability. Tumours often confer resistance through AURKs, especially in terms of resistance to radiotherapy and chemotherapy (Tang et al., 2017b). Therefore, combination therapies utilising small-molecule kinase inhibitors that target AURKs along with therapies that inhibit other drug targets are popular therapeutic interventions that leads to anti-tumourigenic, anti-proliferative and anti-apoptotic activity in cancer cells (Liu et al., 2019, Mattei et al., 2020, Paller et al., 2014, Sehdev et al., 2013).

In this study, in Figure 6.2, the AURK inhibitor II in combination with the NBD WT CPP synergistically ($CI < 1$) impacted on cell viability and clonogenic survival with a significantly

($p < 0.05$) enhanced efficacy compared to the NBD WT CPP or AURK inhibitor II as a single agent; cell viability ($IC_{50} = 2.9\mu\text{M}$ vs $>20\mu\text{M}$) and clonogenic survival ($IC_{50} = 0.02\mu\text{M}$ vs $1.04\mu\text{M}$). The AURK inhibitor II was used in study by Epis et al. (2017) in combination with miR-331-3p to synergistically inhibit the proliferation and cause a decrease in cell viability of prostate cancer cells through the potential targeting of the Ras-RALA pathway. A possible reason for the large difference in IC_{50} values between cell viability and clonogenic survival could be that AURK inhibitors are cytostatic agents (Gong et al., 2019). Cytostatic agents are thought to have less of an effect in a “live/dead” cell viability assay compared to a clonogenic survival assay which measures the ability of colonies to grow and replicate following treatment.

There was no real evidence of AURK inhibitor III being used in cell-based assays to investigate its effect on phenotypic outcomes. In Figure 6.3, the AURK inhibitor III in combination with the NBD WT CPP synergistically ($CI < 1$) inhibited cell viability across all concentrations and clonogenic survival at the higher concentrations of AURK inhibitor III in PCa cells. The combination treatment significantly ($p < 0.05$) enhanced efficacy compared to the NBD WT CPP or AURK inhibitor III as a single agent; cell viability ($IC_{50} = 7.0\mu\text{M}$ vs $>20\mu\text{M}$) and clonogenic survival ($IC_{50} = 2.3\mu\text{M}$ vs $19.1\mu\text{M}$). The combination therapy was described as antagonistic (combining the two treatments leads to a smaller effect than expected) at the two lower concentrations of $1\mu\text{M}$ ($CI = 2.63$) and $2\mu\text{M}$ ($CI = 1.71$) in the clonogenic survival assay.

In this study, in Figure 6.4, the AURK/CDK inhibitor in combination with the NBD WT CPP synergistically ($CI < 1$) caused a reduction in cell viability and clonogenic survival with a significantly ($p < 0.05$) enhanced efficacy compared to the NBD WT CPP or Aurora kinase/CDK inhibitor as a single agent; cell viability ($IC_{50} = 0.45\mu\text{M}$ vs $>5\mu\text{M}$) and clonogenic survival ($IC_{50} = 6.3\text{nM}$ vs 28.5nM). Next, the AURK/CDK inhibitor was shown in a study by Emanuel et al. (2005) to potently inhibit the proliferation of a variety of different human cancer cell lines ($IC_{50} = 112\text{nM}$ to 514nM). The AURK/CDK inhibitor synergistically inhibited viability in Leukemia cells when used in combination with radiotherapy at concentrations ranging from 100nM to $10\mu\text{M}$ (Rodland et al., 2019).

In Figure 6.5, the ZM447439 in combination with the NBD WT CPP synergistically ($CI < 1$) inhibited cell viability across all concentrations and clonogenic survival at the higher concentrations of ZM447439 in prostate cancer cells. Treatment of cells with the two agents in combination significantly ($p < 0.05$) enhanced efficacy compared to the NBD WT CPP or ZM447439 as a single agent; cell viability ($IC_{50} = 0.836\mu\text{M}$ vs $>10\mu\text{M}$) and clonogenic survival ($IC_{50} = 27.5\text{nM}$ vs 417nM). The combination treatment was described as antagonistic at the two highest concentrations of 300nM ($CI = 2.63$) and $1\mu\text{M}$ ($CI = 1.71$) when exploring the impact on clonogenic survival. ZM447439 significantly inhibited cell proliferation and cell viability at a concentration of $2\mu\text{M}$ in HEK293 cells and also inhibited cell viability in the GL-1

(4.77 μ M) and EMA (8.03 μ M) Canine lymphoid cell lines (Girdler et al., 2006, Shiomitsu et al., 2013).

In this study, in Figure 6.6, VX-680 used in a combination treatment with the NBD WT CPP synergistically (CI < 1) caused a reduction in cell viability at all concentrations except the lowest concentration of VX-680 and clonogenic survival across all concentrations of VX-680 in PCa cells. Both agents in combination significantly ($p < 0.05$) enhanced efficacy compared to the NBD WT CPP or VX-680 as a single agent; cell viability (IC₅₀ = 2.6 μ M vs 19.8 μ M) and clonogenic survival (IC₅₀ = 0.23nM vs 7.2nM). The combination treatment was described as antagonistic at lowest concentrations of 0.1 μ M (CI = 1.11) against cell viability. Lastly, VX-680 had been shown to effect cell survival and viability in various studies. In Renal cell carcinoma (RCC) cell lines, VX-680 exerted an antiproliferative effect on all 11 RCC cell lines studied with IC₅₀ values ranging from 100nM to 10 μ M (Li et al., 2010). Similarly to the other AURK inhibitors already mentioned, VX-680 can enhance the sensitivity of cancer cells to chemotherapeutics. Indeed, in a study by Yao et al. (2014), VX-680 and Cisplatin synergistically inhibited proliferation of the HepG2 hepatocellular carcinoma cell line.

6.3.2. Combination treatment and the impact on the growth of 3D cultures and the induction of cell death.

VX-680 was the sole AURK inhibitor used to investigate the impact of combination treatments with the NBD CPPs on further phenotypic characteristics due to the fact it is probably the best characterised AURK inhibitor in the literature and time constraints in the project prevented further exploration with the other inhibitors. VX-680 was shown to induce apoptosis in human cholangiocarcinoma cell lines (QBC939 and HCCC-9810) and is believed to exert its effect on cell death through a Caspase-3-dependent pathway (Liu and Qin, 2018). As a result, this study utilised a Caspase-3/7 substrate assay to quantify the apoptosis induced by the two single agents and both simultaneously as a combination treatment. The induction of the apoptosis by the NBD WT CPP increased in a concentration-dependent manner, whereas the induction by VX-680 wasn't as substantial. Both agents used in a combination treatment produced a substantial, enhanced induction of apoptosis, especially at the higher concentrations of VX-680, compared to both the single agent treatments alone. This correlated well with a study which showed the use of VX-680 in the same caspase-3 substrate assay in Hepatoblastoma cells and the results were similar in terms of the impact of the VX-680 to induce apoptosis (Dewerth et al., 2012).

6.3.3. Conclusions.

In this chapter, it has been demonstrated that the NBD WT CPP alone could impact clonogenic survival, to parallel the data gathered around its impact on cell viability in different tumour cell line models (Figure 4.4). Following on from this, demonstration of a synergistically significant reduction in cell viability and clonogenic survival was apparent following combination treatment with the NBD WT CPP and each one of the ATP-competitive AURK inhibitors (AURK inhibitor II, AURK inhibitor III, Aurora kinase/CDK inhibitor, ZM 447439 and VX-680). The problem with these inhibitors was that they have not shown clinical efficacy in a patient setting as single agents. For example, a Genome-wide CRISPR screen was performed to pinpoint genes which showed synthetic lethality following treatment with VX-680 (Huang et al., 2020). The top 'Hit' gene was GSG2 (Haspin) and the depleting of Haspin and VX-680 was controlled by inhibition of Haspin with AURKB (Huang et al., 2020). Combination therapy that targets both Haspin and AURKB synergistically enhanced the efficacy in comparison to single agent treatment in head and neck squamous cell carcinoma and non-small cell lung cancer (NSCLC) (Huang et al., 2020). Investigation of VX-680 in combination with the NBD WT CPP to impact on further phenotypic outcomes (apoptosis) was also carried out and the results correlated well with similar studies found in the literature (Dewerth et al., 2012).

In conclusion, the NBD WT CPP in combination with ATP-competitive AURK inhibitors can synergistically enhance the efficacy and ability to impact cell viability and clonogenic survival compared to the NBD WT CPP alone. The NBD WT CPP in combination with VX-680 enhanced the induction of apoptosis; whether this is statistically significant and translates to the other AURK inhibitors will need to be confirmed by further studies. In conclusion, the work presented in this chapter, has suggested that the impact on phenotypic outcomes detailed above can be correlated with the synergistic targeting of AURKA and the disruption of AURKA-TPX2 signalling as presented in Chapter 5.

Chapter 7: GENERAL DISCUSSION.

There were five main aims driving the experimental work presented in this study and thesis. Firstly, to characterise the impact of the IKK β -derived NBD WT CPP on IKK-AURKA signalling and determine the impact of this targeting upon other related markers of AURK signalling linked to cellular migration; TPX-2 as a critical regulator of AURKA activation and deactivation, PLK1 as a downstream substrate for AURKA activated via phosphorylation to support further progression through cell division. Thereafter, the second aim was to determine the mechanism of IKK β -mediated targeting of AURKA-TPX2 status and by comparative analysis using both molecular (siRNA 'run-down') and pharmacological (small molecule kinase inhibitors) methods, better understand whether changes in AURKA/TPX2/PLK1 status were mediated in an IKK-dependent or IKK-independent manner, seeking to identify whether this was as a result of and downstream from IKK complex disruption or a potentially direct effect independent of the IKK complex. Thirdly, the reproducibility of the NBD WT peptide-mediated impact on AURKA-TPX2 signalling was examined in a variety of other established cancer lines representative of major solid tumour types with the aim of determining whether this targeting had utility across multiple cancer types. In the context of pharmacological targeting and taking into account of the experimental outcomes described earlier (Chapter 3), the dual pharmacological targeting of AURKA (and potentially TPX2) with the NBD WT CPP and ATP-competitive AURK inhibitors (AURK inhibitor II, AURK inhibitor III, Aurora kinase/CDK inhibitor, VX-680 or ZM 447439) was pursued to identify whether combination strategies could enhance impact on AURKA-TPX2 signalling. Lastly, experiments sought to determine whether the observed outcomes of dual targeting could be translated to impact PCa cells phenotypically.

7.1. Targeting IKK-AURKA interactions.

At the initiation of this study there were numerous studies in the literature that reported interactions between the IKK proteins and AURKA but the role of each IKK isoform protein in these interactions and the consequences functionally of these interactions remained fully uncharacterised. Apparent was contradictory experimental data. IKK β has been suggested to be an antagonist for AURKA and targeted it for degradation by the cellular ubiquitin ligase β TRCP, which is also involved in normal mitotic progression and the maintenance of spindle bipolarity (Irelan et al., 2007). In contrast, Prajapati et al. (2006) showed that IKK α was associated with AURKA in the centrosome and regulated AURKA via phosphorylation at Thr288. This modulation of AURKA phosphorylation by IKK α was described to lead to regulation of the mitotic (M) phase of the cell cycle in HeLa and COS7 cells (Prajapati et al., 2006). AURKA and the IKK proteins (IKK α and IKK β) have also been reported to interact with

the Pro-survival signalling protein, TNF-related apoptosis-inducing ligand (TRAIL), which supports cell survival by increasing the phosphorylation state of both AURKA and the IKK proteins (Mazzera et al., 2013b). Aside of these studies identifying potential mechanisms of regulation of AURKA dependent on phosphorylation, previous work in the Paul lab, and the basis to this project, demonstrated that recombinant AURKA protein bound to scanning peptide arrays representing both IKK α and IKK β proteins. AURKA binding was observed to occur with sequences representing/encompassing the kinase domain (KD) and the NEMO binding domain (NBD) (Wilson 2013). The interactions of the IKK proteins with AURKA were also mapped using peptide arrays and identified that IKK β interacted with a region of the kinase domain of AURKA (and similar sites in AURKB/C) which corresponded to the identified binding sites for TPX2 in AURKA (Wilson 2013). There were numerous potential alignments of both IKK α and IKK β interactions with AURKA binding closely to the TPX2 binding sites and mutational and truncation analysis identified the NBD to be key. Moreover, the two key Tryptophans (Trp739 and Trp741) within the hexapeptide sequence (L-D-W-S-W-L) of the NBD were essential for binding. Hence, a peptide derived from the structure of the IKK β NBD could be used as a potential competitive disruptor and was then shown to be effective in preliminary experiments (Wilson 2013). This was taken forward in this study and developed further by analysis of additional protein regulators and substrates (as 'markers') associated with AURKA activation and progression through mitosis to add credence to initial result and highlight potentially the mechanism of disrupting AURKA-TPX2 binding by the NBD WT CPP.

The process of AURKA being deactivated/'switched-off' in cells is not fully understood. It is well characterised that TPX2 is removed from AURKA to allow dephosphorylation of the critical phospho-threonine residue (Thr288) and subsequent deactivation of AURKA activity (Giubettini et al., 2011). The mechanism of TPX2 removal to start the process of AURKA deactivation is unclear. So, it can be hypothesised, based on the results gathered in this thesis, that as cells go through mitosis, IKK β is localised to the centrosome and interacts with AURKA and/or TPX2 and competitively removes TPX2. Concurrently, is TPX2 removed to allow PP1a access to the AURKA kinase domain and catalytic site to dephosphorylate the critical phosphothreonine residue (Thr288) of AURKA?

Following on from previous work in Paul lab demonstrating IKK-AURKA interactions in an *in vitro* recombinant protein-based assay system, experimental strategies to understand these interactions better were translated to a cell-based setting using pharmacological techniques targeting the kinase domains with IKK isoform selective ATP-competitive kinase inhibitors and molecular siRNA targeted run-down of total IKK protein expression. This enabled the impact of these strategies to be compared to that of the NBD WT CPP on IKK-AURKA signalling (Figure 7.1). Inhibition of IKK catalytic activity played no role in the

modulation of mitotic markers. This questioned different aspects of IKK-AURKA structure-function (Figure 7.1) and allowed further establishment of the mechanism by which the NBD WT CPP modulated IKK/AURKA/IKK-AURKA function. The NBD peptides were recognised as IKK disruptors in the study by May et al. (2000b) where it was shown that the use of a NBD

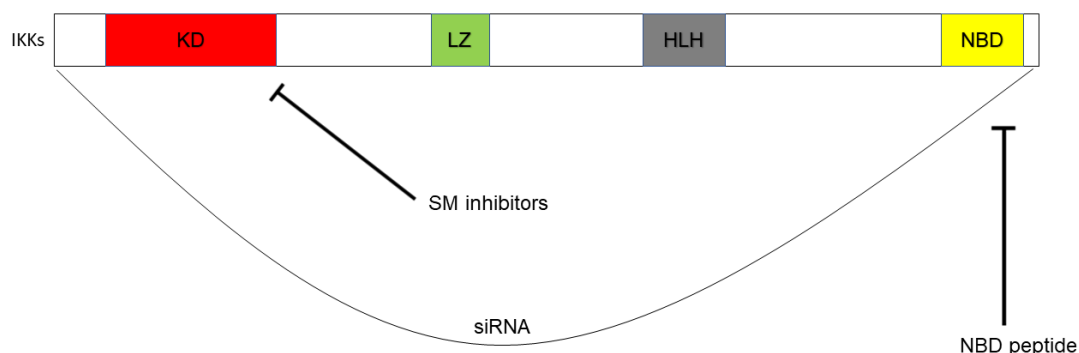


Figure 7.1. Molecular and Pharmacological techniques to investigate mechanisms of IKK-AURKA through different features of the IKK proteins.

Techniques to investigate and target the mechanism of IKK-AURKA interaction: small molecule (SM) IKK α/β inhibitors, IKK α/β siRNA and the NBD peptide (LZ – Leucine Zipper, Helix Loop Helix, NBD – NEMO binding domain).

CPP can disrupt the binding between NEMO and IKK α/β and cause inhibition of cytokine-induced activation of NF- κ B signalling. Therefore, here, a novel unreported effect of the NBD WT CPP has been identified. This is first report of an alternative outcome for NBD peptides in terms of cellular targets and associated cellular outcomes - namely on phosphorylation of AURKA/B/C but also developed to show impact on total protein expression of AURKA, expression of the key AURKA co-activator TPX2 and expression/phosphorylation of the key AURKA-regulated protein substrate, the mitotic kinase PLK1. Perturbation of AURK signalling by the NBD peptide was apparent but the key question of whether it was either IKK-dependent (i.e. dependent on IKK complex disruption) or IKK-independent (i.e. direct effects of NBD WT CPP on AURKA-TPX2 binding) remained. Through siRNA depletion of IKK α and IKK β at the transcriptional level and the use of KIs to inhibit catalytic activity, it was determined that neither the kinase domain nor the expression of IKK proteins was required for the NBD WT CPP to show its impact on AURKA and related markers. This contrasted with results shown by Ireland et al. (2007) and Prajapati et al. (2006) who both showed that siRNA rundown of the IKK proteins caused inhibition of cell cycle progression in HeLa cells via FACS analysis. Ireland et al. (2007) also showed that rundown of IKK β in mitotic cells maintained an increased expression of AURKA, suggesting a model in which IKK β acts as an antagonist of AURKA during mitosis. On the other hand, Prajapati et al. (2006) showed that IKK α has a potential role in the regulation of M phase regulatory factors, including regulation of the phosphorylation

and activation of AURKA. Following individual targeting of IKK proteins for rundown with siRNA, simultaneously 'knock-down' of both IKK α and IKK β to create a synthetic null IKK background was pursued and this showed that the NBD WT CPP could still impact on phosphorylation and total expression of AURKA and TPX2 expression in a background of significantly reduced cellular IKK protein expression. This supported the rationale that the NBD WT CPP exerted its effect on AURKA signalling with a mechanism of action that is IKK-independent. Although, this wasn't a complete run down (with some IKK proteins expression remaining that may mediate signalling), to substantiate this theory, the NBD WT CPP was utilised in a true cellular knockout model, MEFs genetically deficient for IKK α and IKK β . In this setting, the NBD WT CPP remained able to impact the status of p-AURKs, AURKA and TPX2 despite no IKK proteins being present. Beyond this, future work would likely consist of co-immunostaining of both AURKA and TPX2, looking at potential co-localisation kinetics following use of the approach of mitotic arrest and release and determining whether the NBD WT CPP could impact on the localisation of these proteins as they progress through the cell cycle. It would also be beneficial to the project to carry out assays to assess the catalytic activity of AURKA following Nocodazole trap and release and furthermore assess any potential impact the NBD WT CPP could have on AURKA activity as cells progress through mitosis.

This study also showed that the effects of the NBD WT CPP to impact on the status of AURKA and related protein markers of mitosis (p-AURKS, AURKA, TPX2 and PLK1) was reproducible across different solid tumour cell lines (AR positive and negative prostate, breast and brain cancer). Hence, this all suggested that the NBD WT CPP may exert its effect on AURKA in these different cellular settings via an IKK-independent mechanism, i.e. potentially a direct impact on AURKA-TPX2 binding across different cancer subtypes and so demonstrate its potential utility in targeting this signalling axis in a variety of cancers. Going forward, similar studies to those carried out in Chapters 5 and 6 in which the NBD WT CPP and AURK inhibitors were used as combination treatments would ideally be investigated in these different cellular systems to identify any subtleties in terms of impact on AURKA signalling and phenotypic outcomes. Possible future work could involve treatment with the NBD WT CPP in combination with the Gold standard treatments for each of these cancer types; breast (Tamoxifen), brain (temozolomide in combination with radiation) and prostate (ADT alone or in combination with radiation) (Crawford et al., 2019, Hu et al., 2015, Ozdemir-Kaynak et al., 2018). This would allow assessment of more clinically relevant combination treatments in different *in vitro* cancer cell lines before progressing to *in vivo* tumour models of these cancer types.

7.2. Targeting IKK-AURKA-TPX2 signalling.

AURKA and the binding of its essential co-activator TPX2 is a well-established phenomenon in the literature that is required for the complete activation of AURKA kinase activity. Bayliss et al. (2003) developed a crystal structure of a 43-amino acid (residues 1-43 that are required for AURKA binding) TPX2 peptide bound to the catalytic domain of AURKA. Upon binding, the activation loop of AURKA undergoes a 'twisting motion' and AURKA is auto-phosphorylated and auto-activated to become an "activated kinase" (Bayliss et al., 2003, Evers et al., 2005). This twisting of the activation loop also caused the phosphorylated threonine residue (Thr288) to tuck in towards the protein and become inaccessible to dephosphorylation by protein phosphatases and so hinders subsequent inactivation (Bayliss et al., 2003, Evers et al., 2005). It was also demonstrated by Evers et al. (2005) that a single amino acid difference in the binding regions between AURKA and AURKB was responsible for TPX2 binding AURKA and not AURKB. Similarly, in another study by Fu et al. (2009) it was shown that changing the Gly-198 residue in AURKA to an equivalent Asn-142 residue in AURKB caused AURKA to form a complex with the AURKB binding partner INCENP and to recruit to subcellular localisations that were normally occupied by AURKB. Several studies have reported that the following residues of TPX2 were in contact with the large lobe of AURKA and essential for binding; Y8, Y10 and D11, mutation of these to alanine abolished activation by TPX2 (Asteriti et al., 2017, Evers et al., 2005, Janeček et al., 2016). Crucially, in relationship to this study, Janeček et al. (2016) showed that they could use a small molecule, AurkinA, to block the AURKA-TPX2 interaction through its binding to a hydrophobic 'Y-pocket' which was usually occupied by a conserved Tyr8-Ser9-Tyr10 (Y-S-Y) motif from TPX2. This motif is distinctively like that which is present in the hexapeptide sequence (L-D-**W-S-W**-L) of the NBD WT CPP and it is this Try-Ser-Try (W-S-W) motif which could be the means by which the NBD WT CPP disrupts AURKA-TPX2 binding. Taking this forward, potential future experiments could have a structural biology focus and incorporate crystallisation and co-crystallisation approaches to examine the potential direct interaction of the NBD peptide with AURKA, identification of the binding site (if it binds) and how it correlates with TPX2 binding. Ultimately from this could we gain insight into the chemical space around peptide-protein binding towards the development of NBD-based disruptors/mimetics that potentially make the active site more accessible to dual targeting with kinase inhibitors? A study by Anderson et al. (2007) indicated that when TPX2 was present, the binding of TPX2 to AURKA decreased the size of the hydrophobic 'Y-pocket' and reduced the ability of AURK inhibitors to access it. From this study, the NBD WT CPP in combination with commercially available ATP-competitive AURK inhibitors (AURK inhibitor II, AURK inhibitor III, Aurora kinase/CDK inhibitor, VX-680 or ZM 447439) improved efficacy of the said AURK inhibitors against AURKA-TPX2 signalling and it

was hypothesised that this was as result of a direct effect of the NBD WT CPP disrupting AURKA-TPX2 binding. Indeed, so-called allosteric inhibitors or proteins-protein interaction (PPI) mimetics that disrupt the binding between AURKA and TPX2 as alternatives to small-molecule ATP-competitive AURK inhibitors make for an attractive proposition. Kinase inhibitors, although initially promising pre-clinically, have displayed only moderate effects once in clinical trials and showed incomplete selectivity, either against the other AURK family members or other kinases (Asteriti et al., 2017). To date in the literature, there have only been two physical compounds that disrupt AURKA-TPX2 binding, the rest are computational-based libraries or 'hits'. The first is the aforementioned AurkinA compound which binds in the micromolar range to the hydrophobic 'Y-pocket' normally occupied by the conserved Tyr-Ser-Tyr motif of TPX2 (Janeček et al., 2016). The second is a naturally occurring, cancer cell killing compound known as Withanone, which was shown to disrupt AURKA-TPX2 binding at the so-called 'W-pocket', disrupting binding at residue Trp34 and these are two of three "druggable hotspots" between AURKA and TPX2, the other being the 'F-pocket' (Grover et al., 2012, McIntyre et al., 2017). The 'W pocket' is of interest as it favours binding of tryptophan (W) and phenylalanine (F) residues (McIntyre et al., 2017), both of which are present in the 11mer NBD WT CPP and involved in its blockade of NF- κ B signalling and potential disruption of AURKA-TPX2 binding. To conclude, there are limited means of targeting AURKA-TPX2 signalling in the literature and this study suggested that dual targeting enhanced the efficacy of commercially available AURK inhibitors compared to single agent treatment. Future work would involve comparative pharmacological assays which would compare the NBD WT CPP with AurkinA and Withanone as single agents or in combination studies to see if the effect is similar to the impact observed with the NBD WT CPP. This could then be extended to crystallisation of AURKA with one of the agents or a combination with the AURK inhibitors to investigate their different modes of binding.

As another aspect of AURK signalling, AURKs have been increasingly linked to resistance of cancer cells to treatment with existing chemotherapeutics and radiotherapy (Tang et al., 2017b). Indeed, AURKA was shown to confer chemoresistance in; colorectal (Cammarelli et al., 2010), breast (Lee et al., 2008) and NSCLC (Xu et al., 2014) among other cancer subtypes. Also, aberrant expression of AURKB was linked to resistance to the chemotherapeutic tamoxifen in breast cancer and was also responsible for cancer cell resistance to TRAIL-induced apoptosis through phosphorylation of survivin (Larsen et al., 2015, Yoon et al., 2012, Zhang et al., 2015). As mentioned before and as carried out in this thesis, synergistically targeting different proteins of interest can enhance the efficacy of anti-tumour effects and this can also be correlated to overcoming drug resistance (Tang et al., 2017b). For example, it was shown by Yuan et al. (2012) that in Chronic myeloid leukemia

(CML) patients with BCR-ABL mutation and resistance to second generation TKIs, that inhibition of AURKA with AURK inhibitors can sensitise mutant CML cells to TKIs. It was also shown by Opyrchal et al. (2014) that the SMAD5 oncogenic signalling pathway was activated by AURKA and this down-regulated estrogen receptor α (ER α), resulting in estrogen resistance in ER α ⁺ breast cancers. Combination therapy with tamoxifen (chemotherapeutic) and the AURK inhibitor MLN8327 alleviated this resistance to estrogen (Opyrchal et al., 2014). Another factor which may have contributed towards the link between AURKs and drug resistance in cancer was that AURKA has been implicated in the functioning of cancer stem cells (CSCs), which possess the characteristic of self-renewal (Chefetz et al., 2011). It was shown that AURKA could activate the wnt signalling pathway in Glioma-initiating cells (GIC) through interacting with AXIN and stabilising β -catenin, promoting the ability of GICs to self-renew (Xia et al., 2013). To conclude, the observed enhanced efficacy (both phenotypic and signalling outcomes) of the combined use of NBD WT CPP and AURK inhibitors could be extended to the above disease settings in that the NBD WT CPP plus an AURKA inhibitor plus another selected kinase inhibitor could be used as a potential adjuvant therapy to overcome disease resistance and improve the therapeutic potential of chemotherapeutics.

Translating the NBD WT CPP plus AURK inhibitors targeting approach to phenotypic outcomes demonstrated enhancement in efficacy also and was shown to cause a synergistically enhanced efficacy with regards to the impact on cell viability, clonogenic survival and apoptosis (VX-680). This combination approach with AURK inhibitors which caused enhanced efficacy against phenotypic outcomes has been observed widely in the literature. Indeed, AURK inhibitors in combination with EGFR and PI3K inhibitors synergistically inhibited the proliferation of oral tumour cell lines (Furqan et al., 2019). Furthermore, pharmacologically targeted inhibition of AURKA and p21-activated kinase 1 (PAK1) synergistically decreased the survival of multiple breast cancer cell lines (Korobeynikov et al., 2019). This highlights that the NBD WT CPP could be further harnessed as a pharmacological tool to broaden our knowledge of the AURKA-TPX2 protein-protein interaction and impact on the growth and survival of cancer cells. These combination approaches will need to be further explored in animal models of prostate cancer *in vivo* (Xenograft and genetic models) before being considered for potential progressing to patient studies.

7.3. Additional future work.

A longer term end goal related to harnessing the pharmacological impact of the NBD WT CPP is the development of peptidomimetic molecules, built on the key structural features of the

NBD, that could be progressed through 'hit-to-lead' and 'lead optimisation' strategies to develop 'drug-like' molecules relevant for clinical intervention in cancer. These, again, can only be based on the outcomes from key structural biology studies described above (Section 7. 2). In the shorter term, there is additional scope to develop cell-based studies of IKK-AURK-TPX2 signalling further and to better understand the cellular dynamic of the relationship between these proteins individually and collectively. Continuation of the previous work conducted in the Paul lab co-immunoprecipitating (co-IP) IKK β and AURKA (Wilson 2013) could be extended to consider co-IP of AURKA and TPX2. This would be utilised firstly to confirm what is widely known in the literature in that TPX2 binds to AURKA to form a complex as it is activated at the G₂/M transition before showing that both proteins are no longer co-immunoprecipitated (i.e. dissociated) as the cells enter and subsequently progress through mitosis. Secondly this co-IP model would also be exploited to use the NBD WT CPP to potentially disrupt the binding between AURKA and TPX2 and hence the decreased presence of one, the other or both proteins in the co-immunoprecipitation. In short, this would provide an alternative insight into the binding interactions of the AURKA-TPX2 complex and confirm the impact on the NBD WT CPP on the AURKA-TPX2 complex

Additional validation studies could also be constructed, for example, utilising targeted siRNA rundown of AURKA and/or TPX2, similar to previously reported studies, (Zhong et al., 2016) (Liu et al., 2014a) to show that rundown of these protein alone or in combination ablated the effect of the NBD WT CPP the previously assessed markers of mitosis and phenotypic outcomes. A study by Solt et al. (2009) truncated the NBD of IKK α and IKK β individually to show the effects on IKK complex disruption. A comparative study with both IKK α and IKK β in NBD-truncated forms simultaneously could be carried out to further substantiate the hypothesis that the NBD WT CPP has a direct impact on AURKA signalling. On the other hand, the use of a different molecular biology technique could be exploited which gives a more rapid removal and selectivity of target protein in comparison to use of siRNA to rundown protein expression. This involved use of the degradation tag (dTAG) system discovered by Nabet et al. (2018) and loosely based on the technique of targeted protein degradation using hetero-bifunctional 'small-molecule degraders' or proteolysis targeting chimera (PROTAC) which was pioneered by Sakamoto et al. (2001). This dTAG system involved the use of clustered regularly interspaced short palindromic repeats (CRISPR)-mediated 'knock in' of a mutant FKBP12^{F36V} tag on the protein of interest (POI) and this resulted in the formation of a tertiary complex between the tagged POI, a FKBP12^{F36V} degrader (dTAG molecule) and the ubiquitin proteasome machinery through the binding with cereblon (E3 ubiquitin ligase), this resulted in rapid targeted degradation (Nabet et al., 2018). This could be a means by which to create a more definitive molecular model (potential to be used *in vivo*) to show the impact

that depleting the IKK proteins ($\alpha/\beta/\gamma$) has on the mechanistic action of the peptide. Conversely, it could also be used to target AURKA and/or TPX2 for degradation and investigate whether the NBD WT CPP can still impact on the individual proteins of interest still present in each model (p-AURKs, AURKA, TPX2, p-PLK1/PLK1) and what impact degrading these proteins both individually and simultaneously had phenotypically as well as pharmacologically.

Another alternative approach would be to create CRISPR-cas9 knockout models in a PCa background. CRISPR-cas9 is a technique discovered in bacteria which can allow researchers to introduce double-stranded breaks in the target DNA sequence by using short guide RNA (gRNA) that bind to the specific target DNA sequence and direct the cas9 enzyme to introduce these double-stranded breaks at sites complementary to the gRNA sequence, the cell's own DNA machinery is then used to "knock-in" or "knock-out" target genes (Jinek et al., 2012). The advantage of this is that it confers similar benefits to those shown using the dTAG technique but also would allow us to create a true knockout cell line. Although we utilised a DKO IKK α/β model in MEF cells, this isn't representative of the cancer setting in which the AURKs are overexpressed and have been implicated as a potential oncogene (Yan et al., 2016). So, it would be beneficial if a similar DKO IKK α/β model was established in PC3 prostate cancer cells which would be more a representative model with regards to this thesis as a whole and examining IKK-AURKA signalling in the cancer setting. Lastly, if time had permitted, it would have been beneficial to carry out some kinase profiling experiments to investigate any potential off-target effects of AURK inhibitors (AURK inhibitor II, AURK inhibitor III, Aurora kinase/CDK inhibitor, VX-680 or ZM 447439) and the NBD WT CPP at the concentrations used in the various assays in this study, as off-target effects are common amongst all kinase inhibitors (Wynn et al., 2011). It would also be beneficial to complete the analysis of the phenotypic outcomes section by exploring the effect of combination treatments across all inhibitors on apoptosis and exploring the effects of the NBD WT CPP alone and the combination treatments on the cell cycle via FACS analysis.

7.4. Conclusions.

AURKA and its essential co-activator TPX2 have both been implicated to be aberrantly expressed in a variety of different cancers, both in solid and haematological tumours but targeting with conventional ATP-competitive AURK inhibitors has been particularly problematic in solid tumours. Studies are now exploring the targeting of the AURKA-TPX2 PPI directly with PPI mimetics or so-called allosteric inhibitors that disrupt the TPX2 binding

pockets on AURKA and impact on the interaction between AURKA and TPX2. This method of targeting has the benefit that PPI interactions are less evolutionary conserved compared to the ATP-binding sites on kinases and hence confer a greater degree of selectivity. That said, developing an allosteric inhibitor with appropriate 'drug-like' physicochemical characteristics can be challenging.

This study utilised a CPP derived from the NBD of the IKK β protein, a catalytic component of the NF- κ B pathway, as this domain was demonstrated from previous preliminary data to bind AURKA (Wilson 2013). The resultant NBD WT CPP was shown in this current study to cause a reduction in the phosphorylation of the three AURK isoforms (A, B and C) as well as the total expression of AURKA, TPX2 and p-PLK1/PLK1 in prostate, breast and glioblastoma cells lines. In prostate cancer cells and MEFs this occurred via an IKK-independent mechanism which may be as a result of a direct impact on AURKA-TPX2 binding. Further work must be carried be out to understand fully and determine whether this is a direct disruption of the interaction between AURKA and TPX2. In prostate cells, combination treatments with ATP-competitive AURK inhibitors (AURK inhibitor II, AURK inhibitor III, Aurora kinase/CDK inhibitor, ZM 447439 and VX-680) and the NBD WT CPP resulted in an enhancement of efficacy against AURKA and TPX2 status compared to any single agent treatment. This translated to impact synergistically on cell viability and clonogenic survival in prostate cells. The NBD WT CPP in combination with VX-680 displayed an enhanced efficacy to impact prostate cancer cell apoptosis in comparison to single agent treatment but was inconclusive when assessed for its ability to enhance the efficacy and effect changes in volume of prostate cancer cell spheroids (data not shown). This suggested that further investigation is needed to determine whether the significantly enhanced efficacy conveyed by the combination treatments to effect AURKA-TPX2 status translated to impact on apoptosis and spheroid growth. Collectively, from this study, the NBD WT CPP derived from the IKK β protein can be put forward as potential 'lead' for the development of pharmacological agents that target AURKA-TPX2 status and signalling via an alternative mechanism to that delivered by recognised ATP-competitive AURK inhibitors. This approach in the longer term may also be relevant to therapeutic intervention in multiple tumour types.

References

- ABDUL AZEEZ, K. R., CHATTERJEE, S., YU, C., GOLUB, T. R., SOBOTT, F. & ELKINS, J. M. 2019. Structural mechanism of synergistic activation of Aurora kinase B/C by phosphorylated INCENP. *Nat Commun*, 10, 3166.
- ABDULGHANI, J., GU, L., DAGVADORJ, A., LUTZ, J., LEIBY, B., BONUCCELLI, G., LISANTI, M. P., ZELLWEGER, T., ALANEN, K., MIRTTI, T., VISAKORPI, T., BUBENDORF, L. & NEVALAINEN, M. T. 2008. Stat3 promotes metastatic progression of prostate cancer. *The American journal of pathology*, 172, 1717-28.
- ALFARO-ACO, R., THAWANI, A. & PETRY, S. 2017. Structural analysis of the role of TPX2 in branching microtubule nucleation. *J Cell Biol*, 216, 983-997.
- ALGABA, F., TRIAS, I. & ARCE, Y. 2007. Natural history of prostatic carcinoma: the pathologist's perspective. *ReFortschritte der Krebsforschung. Progres dans les recherches sur le cancercent results in cancer research.*, 175, 9-24.
- ALLART-VORELLI, P., PORRO, B., BAGUET, F., MICHEL, A. & COUSSON-GÉLIE, F. 2015. Haematological cancer and quality of life: A systematic literature review.
- AMIN, K. S., JAGADEESH, S., BAISHYA, G., RAO, P. G., BARUA, N. C., BHATTACHARYA, S. & BANERJEE, P. P. 2014. A naturally derived small molecule disrupts ligand-dependent and ligand-independent androgen receptor signaling in human prostate cancer cells. *Mol Cancer Ther*, 13, 341-52.
- AMMIRANTE, M., LUO, J. L., GRIVENNIKOV, S., NEDOSPASOV, S. & KARIN, M. 2010. B-cell-derived lymphotoxin promotes castration-resistant prostate cancer. *Nature*, 464, 302-305.
- ANAND, S., PENRHYN-LOWE, S. & VENKITARAMAN, A. R. 2003. AURORA-A amplification overrides the mitotic spindle assembly checkpoint, inducing resistance to Taxol. *Cancer Cell*, 3, 51-62.
- ANDERSON, K., YANG, J., KORETKE, K., NURSE, K., CALAMARI, A., KIRKPATRICK, R. B., PATRICK, D., SILVA, D., TUMMINO, P. J., COPELAND, R. A. & LAI, Z. 2007. Binding of TPX2 to Aurora A alters substrate and inhibitor interactions. *Biochemistry*, 46, 10287-10295.
- ANTHONY, N. G., BAIGET, J., BERRETTA, G., BOYD, M., BREEN, D., EDWARDS, J., GAMBLE, C., GRAY, A. I., HARVEY, A. L., HATZIIEREMIA, S., HO, K. H., HUGGAN, J. K., LANG, S., LLONA-MINGUEZ, S., LUO, J. L., MCINTOSH, K., PAUL, A., PLEVIN, R. J., ROBERTSON, M. N., SCOTT, R., SUCKLING, C. J., SUTCLIFFE, O. B., YOUNG, L. C. & MACKAY, S. P. 2017a. Inhibitory Kappa B Kinase alpha

- (IKK α) Inhibitors That Recapitulate Their Selectivity in Cells against Isoform-Related Biomarkers. *J Med Chem*, 60, 7043-7066.
- ANTHONY, N. G., BAIGET, J., BERRETTA, G., BOYD, M., BREEN, D., EDWARDS, J., GAMBLE, C., GRAY, A. I., HARVEY, A. L., HATZIEREMIA, S., HO, K. H., HUGGAN, J. K., LANG, S., LLONA-MINGUEZ, S., LUO, J. L., MCINTOSH, K., PAUL, A., PLEVIN, R. J., ROBERTSON, M. N., SCOTT, R., SUCKLING, C. J., SUTCLIFFE, O. B., YOUNG, L. C. & MACKAY, S. P. 2017b. Inhibitory Kappa B Kinase α (IKK α) Inhibitors That Recapitulate Their Selectivity in Cells against Isoform-Related Biomarkers. *Journal of Medicinal Chemistry*, 60, 7043-7066.
- ANTONARAKIS, E. S., PIULATS, J. M., GROSS-GOUPIL, M., GOH, J., OJAMAA, K., HOIMES, C. J., VAISHAMPAYAN, U., BERGER, R., SEZER, A., ALANKO, T., DE WIT, R., LI, C., OMLIN, A., PROCOPIO, G., FUKASAWA, S., TABATA, K. I., PARK, S. H., FEYERABEND, S., DRAKE, C. G., WU, H., QIU, P., KIM, J., POEHLEIN, C. & DE BONO, J. S. 2020. Pembrolizumab for Treatment-Refractory Metastatic Castration-Resistant Prostate Cancer: Multicohort, Open-Label Phase II KEYNOTE-199 Study. *J Clin Oncol*, 38, 395-405.
- ASTERITI, I. A., DAIDONE, F., COLOTTI, G., RINALDO, S., LAVIA, P., GUARGUAGLINI, G. & PAIARDINI, A. 2017. Identification of small molecule inhibitors of the Aurora-A/TPX2 complex. *Oncotarget*.
- ASTERITI, I. A., RENSEN, W. M., LINDON, C., LAVIA, P. & GUARGUAGLINI, G. 2010. The Aurora-A/TPX2 complex: a novel oncogenic holoenzyme? *Biochim Biophys Acta*, 1806, 230-9.
- AUGELLO, M. A., DEN, R. B. & KNUDSEN, K. E. 2014. AR function in promoting metastatic prostate cancer. *Cancer and Metastasis Reviews*, 33, 399-411.
- AUS, G. 2008. Cryosurgery for Prostate Cancer. *Journal of Urology*.
- BALCHAND, S. K., MANN, B. J., TITUS, J., ROSS, J. L. & WADSWORTH, P. 2015. TPX2 Inhibits Eg5 by Interactions with Both Motor and Microtubule. *J Biol Chem*, 290, 17367-79.
- BALDINI, E., D'ARMIENTO, M. & ULISSE, S. 2014. A new aurora in anaplastic thyroid cancer therapy. *Int J Endocrinol*, 2014, 816430.
- BANSAL, A., SINGH, M. P. & RAI, B. 2016. Human papillomavirus-associated cancers: A growing global problem. *Int J Appl Basic Med Res*, 6, 84-9.
- BASSÈRES, D. S. & BALDWIN, A. S. 2006. Nuclear factor- κ B and inhibitor of κ B kinase pathways in oncogenic initiation and progression. *Oncogene*, 25, 6817-6830.

- BAUMAN, G., RUMBLE, R. B., CHEN, J., LOBLAW, A. & WARDE, P. 2012. Intensity-modulated Radiotherapy in the Treatment of Prostate Cancer. *Clinical Oncology*, 24, 461-473.
- BAVETSIAS, V. & LINARDOPOULOS, S. 2015a. Aurora Kinase Inhibitors: Current Status and Outlook. *Frontiers in Oncology*, 5.
- BAVETSIAS, V. & LINARDOPOULOS, S. 2015b. Aurora Kinase Inhibitors: Current Status and Outlook. *Front Oncol*, 5, 278.
- BAYAT MOKHTARI, R., HOMAYOUNI, T. S., BALUCH, N., MORGATSKAYA, E., KUMAR, S., DAS, B. & YEGER, H. 2017. Combination therapy in combating cancer. *Oncotarget*, 8, 38022-38043.
- BAYLISS, R., BURGESS, S. G. & MCINTYRE, P. J. 2017. Switching Aurora-A kinase on and off at an allosteric site. *FEBS J*, 284, 2947-2954.
- BAYLISS, R., SARDON, T., VERNOS, I. & CONTI, E. 2003. Structural basis of Aurora-A activation by TPX2 at the mitotic spindle. *Molecular Cell*, 12, 851-862.
- BEBBINGTON, D., BINCH, H., CHARRIER, J. D., EVERITT, S., FRAYSSE, D., GOLEC, J., KAY, D., KNEGTEL, R., MAK, C., MAZZEI, F., MILLER, A., MORTIMORE, M., O'DONNELL, M., PATEL, S., PIERARD, F., PINDER, J., POLLARD, J., RAMAYA, S., ROBINSON, D., RUTHERFORD, A., STUDLEY, J. & WESTCOTT, J. 2009. The discovery of the potent aurora inhibitor MK-0457 (VX-680). *Bioorg Med Chem Lett*, 19, 3586-92.
- BEG, A. A., SHA, W. C., BRONSON, R. T., GHOSH, S. & BALTIMORE, D. 1995. Embryonic lethality and liver degeneration in mice lacking the RelA component of NF-kappa B.
- BELTRAN, H., OROMENDIA, C., DANILA, D. C., MONTGOMERY, B., HOIMES, C., SZMULEWITZ, R. Z., VAISHAMPAYAN, U., ARMSTRONG, A. J., STEIN, M., PINSKI, J., MOSQUERA, J. M., SAILER, V., BAREJA, R., ROMANEL, A., GUMPENI, N., SBONER, A., DARDENNE, E., PUCA, L., PRANDI, D., RUBIN, M. A., SCHER, H. I., RICKMAN, D. S., DEMICHELIS, F., NANUS, D. M., BALLMAN, K. V. & TAGAWA, S. T. 2019. A Phase II Trial of the Aurora Kinase A Inhibitor Alisertib for Patients with Castration-resistant and Neuroendocrine Prostate Cancer: Efficacy and Biomarkers. *Clin Cancer Res*, 25, 43-51.
- BIBBY, R. A., TANG, C., FAISAL, A., DROSOPOULOS, K., LUBBE, S., HOULSTON, R., BAYLISS, R. & LINARDOPOULOS, S. 2009. A cancer-associated aurora A mutant is mislocalized and misregulated due to loss of interaction with TPX2. *J Biol Chem*, 284, 33177-84.
- BILL-AXELSON, A., HOLMBERG, L., RUUTU, M., HAGGMAN, M., ANDERSSON, S. O., BRATELL, S., SPANGBERG, A., BUSCH, C., NORDLING, S., GARMO, H.,

- PALMGREN, J., ADAMI, H. O., NORLEN, B. J., JOHANSSON, J. E. & SCANDINAVIAN PROSTATE CANCER GROUP STUDY, N. 2005. Radical prostatectomy versus watchful waiting in early prostate cancer. *N Engl J Med*, 352, 1977-1984.
- BISCHOFF, J. R., ANDERSON, L., ZHU, Y., MOSSIE, K., NG, L., SOUZA, B., SCHRYVER, B., FLANAGAN, P., CLAIRVOYANT, F., GINTHER, C., CHAN, C. S. M., NOVOTNY, M., SLAMON, D. J. & PLOWMAN, G. D. 1998. A homologue of *Drosophila aurora* kinase is oncogenic and amplified in human colorectal cancers. *EMBO Journal*, 17, 3052-3065.
- BOHMER, D., WIRTH, M., MILLER, K., BUDACH, V., HEIDENREICH, A. & WIEGEL, T. 2016. Radiotherapy and Hormone Treatment in Prostate Cancer. *Dtsch Arztebl Int*, 113, 235-41.
- BOLANOS-GARCIA, V. M. 2005. Aurora kinases.
- BORGES, K. S., CASTRO-GAMERO, A. M., MORENO, D. A., DA SILVA SILVEIRA, V., BRASSESCO, M. S., DE PAULA QUEIROZ, R. G., DE OLIVEIRA, H. F., CARLOTTI, C. G., JR., SCRIDELI, C. A. & TONE, L. G. 2012. Inhibition of Aurora kinases enhances chemosensitivity to temozolomide and causes radiosensitization in glioblastoma cells. *J Cancer Res Clin Oncol*, 138, 405-14.
- BORTHAKUR, G., DOMBRET, H., SCHAFHAUSEN, P., BRUMMENDORF, T. H., BOISSEL, N., JABBOUR, E., MARIANI, M., CAPOLONGO, L., CARPINELLI, P., DAVITE, C., KANTARJIAN, H. & CORTES, J. E. 2015. A phase I study of danusertib (PHA-739358) in adult patients with accelerated or blastic phase chronic myeloid leukemia and Philadelphia chromosome-positive acute lymphoblastic leukemia resistant or intolerant to imatinib and/or other second generation c-ABL therapy. *Haematologica*, 100, 898-904.
- BRASIER, A. R. 2006. The NF- κ B Regulatory Network. *Cardiovascular Toxicology*, 6, 111-130.
- BRAUN, P. & GINGRAS, A. C. 2012. History of protein-protein interactions: from egg-white to complex networks. *Proteomics*, 12, 1478-98.
- BRAY, F., FERLAY, J., SOERJOMATARAM, I., SIEGEL, R. L., TORRE, L. A. & JEMAL, A. 2018. Global cancer statistics 2018: GLOBOCAN estimates of incidence and mortality worldwide for 36 cancers in 185 countries. *CA Cancer J Clin*, 68, 394-424.
- BRIASSOULI, P., CHAN, F., SAVAGE, K., REIS-FILHO, J. S. & LINARDOPOULOS, S. 2007. Aurora-A Regulation of Nuclear Factor-kappaB Signaling by Phosphorylation of I κ B α . *Cancer Research*, 67, 1689-1695.

- BROWN, J. R., KORETKE, K. K., BIRKELAND, M. L., SANSEAU, P. & PATRICK, D. R. 2004. Evolutionary relationships of Aurora kinases: implications for model organism studies and the development of anti-cancer drugs. *BMC evolutionary biology*, 4, 39-39.
- BRUINSMA, W., MACÛREK, L., FREIRE, R., LINDQVIST, A. & MEDEMA, R. H. 2014. Bora and Aurora-A continue to activate Plk1 in mitosis. *Journal of Cell Science*, 127, 801-811.
- BRUNET, S., SARDON, T., ZIMMERMAN, T., WITTMANN, T., PEPPERKOK, R., KARSENTI, E. & VERNOS, I. 2004. Characterization of the TPX2 domains involved in microtubule nucleation and spindle assembly in *Xenopus* egg extracts. *Mol Biol Cell*, 15, 5318-28.
- BURGESS, S. G., OLEKSY, A., CAVAZZA, T., RICHARDS, M. W., VERNOS, I., MATTHEWS, D. & BAYLISS, R. 2016. Allosteric inhibition of Aurora-A kinase by a synthetic vNAR domain. *Open Biol*, 6.
- BURKE, J. R., PATTOLI, M. A., GREGOR, K. R., BRASSIL, P. J., MACMASTER, J. F., MCINTYRE, K. W., YANG, X., IOTZOVA, V. S., CLARKE, W., STRNAD, J., QIU, Y. & ZUSI, F. C. 2003. BMS-345541 is a highly selective inhibitor of I kappa B kinase that binds at an allosteric site of the enzyme and blocks NF-kappa B-dependent transcription in mice. *J Biol Chem*, 278, 1450-6.
- BURUM-AUENSEN, E., DE ANGELIS, P. M., SCHJØLBERG, A. R., KRAVIK, K. L., AURE, M. & CLAUSEN, O. P. F. 2007. Subcellular localization of the spindle proteins Aurora A, Mad2, and BUBR1 assessed by immunohistochemistry. *The journal of histochemistry and cytochemistry : official journal of the Histochemistry Society*, 55, 477-486.
- BUSCHHORN, H. M. K., KLEIN, R. R., CHAMBERS, S. M., HARDY, M. C., GREEN, S., BEARSS, D. & NAGLE, R. B. 2005. Aurora-A over-expression in high-grade PIN lesions and prostate cancer. *Prostate*, 64, 341-346.
- BUTZ, K., WHITAKER, N., DENK, C., ULLMANN, A., GEISEN, C. & HOPPE-SEYLER, F. 1999. Induction of the p53-target gene GADD45 in HPV-positive cancer cells. *Oncogene*, 18, 2381-6.
- CAMMARERI, P., SCOPELLITI, A., TODARO, M., ETERNO, V., FRANCESCANGELI, F., MOYER, M. P., AGRUSA, A., DIELI, F., ZEUNER, A. & STASSI, G. 2010. Aurora-a is essential for the tumorigenic capacity and chemoresistance of colorectal cancer stem cells. *Cancer Res*, 70, 4655-65.
- CAO, Y., LUO, J.-L. & KARIN, M. 2007. I kappa B kinase alpha kinase activity is required for self-renewal of ErbB2/Her2-transformed mammary tumor-initiating cells. *Proceedings of the National Academy of Sciences of the United States of America*, 104, 15852-7.

- CARDUCCI, M., SHAHEEN, M., MARKMAN, B., HURVITZ, S., MAHADEVAN, D., KOTASEK, D., GOODMAN, O. B., JR., RASMUSSEN, E., CHOW, V., JUAN, G., FRIBERG, G. R., GAMELIN, E., VOGL, F. D. & DESAI, J. 2018. A phase 1, first-in-human study of AMG 900, an orally administered pan-Aurora kinase inhibitor, in adult patients with advanced solid tumors. *Invest New Drugs*, 36, 1060-1071.
- CARLIN, S., CUNNINGHAM, S. H., BOYD, M., MCCLUSKEY, A. G. & MAIRS, R. J. 2000. Experimental targeted radioiodide therapy following transfection of the sodium iodide symporter gene: Effect on clonogenicity in both two-and three-dimensional models. *Cancer Gene Therapy*.
- CARMENA, M. & EARNSHAW, W. C. 2003. The cellular geography of aurora kinases. *Nature Reviews Molecular Cell Biology*, 4, 842-854.
- CARMENA, M., RUCHAUD, S. & EARNSHAW, W. C. 2009. Making the Auroras glow: regulation of Aurora A and B kinase function by interacting proteins.
- CARMENA, M., WHEELLOCK, M., FUNABIKI, H. & EARNSHAW, W. C. 2012. The chromosomal passenger complex (CPC): from easy rider to the godfather of mitosis. *Nature Reviews Molecular Cell Biology*, 13, 789-803.
- CHALLAPALLI, A., JONES, E., HARVEY, C., HELLAWEEL, G. O. & MANGAR, S. A. 2012. High dose rate prostate brachytherapy: An overview of the rationale, experience and emerging applications in the treatment of prostate cancer.
- CHAN, E. H. Y., SANTAMARIA, A., SILLJÉ, H. H. W. & NIGG, E. A. 2008. Plk1 regulates mitotic Aurora A function through β TrCP-dependent degradation of hBora. *Chromosoma*, 117, 457-469.
- CHANG, S. S., YAMAGUCHI, H., XIA, W., LIM, S. O., KHOTSKAYA, Y., WU, Y., CHANG, W. C., LIU, Q. & HUNG, M. C. 2017. Aurora A kinase activates YAP signaling in triple-negative breast cancer. *Oncogene*, 36, 1265-1275.
- CHAO, M. W., GRIMM, P., YAXLEY, J., JAGAVKAR, R., NG, M. & LAWRENTSCHUK, N. 2015. Brachytherapy: state-of-the-art radiotherapy in prostate cancer. *BJU Int*, 116 Suppl 3, 80-8.
- CHEFETZ, I., HOLMBERG, J. C., ALVERO, A. B., VISINTIN, I. & MOR, G. 2011. Inhibition of Aurora-A kinase induces cell cycle arrest in epithelial ovarian cancer stem cells by affecting NF κ B pathway. *Cell Cycle*, 10, 2206-14.
- CHEN, W., LI, Z., BAI, L. & LIN, Y. 2011. NF-kappaB, a mediator for lung carcinogenesis and a target for lung cancer prevention and therapy.
- CHEN, Z. J., PARENT, L. & MANIATIS, T. 1996. Site-specific phosphorylation of I κ B α by a novel ubiquitination-dependent protein kinase activity. *Cell*, 84, 853-62.

- CHIAL, B. H., WRITE, P. D., RIGHT, S. & EDUCATION, N. 2008. *RE: Proto-oncogenes to Oncogenes to Cancer.*
- CHO, S. & KANG, S. H. 2014. Current status of cryotherapy for prostate and kidney cancer.
- CHODAK, G. W. 2005. Maximum androgen blockade: a clinical update. *Reviews in urology*, 7 Suppl 5, S13-7.
- CHOI, M., ROLLE, S., WELLNER, M., CARDOSO, M. C., SCHEIDEREIT, C., LUFT, F. C. & KETTRITZ, R. 2003. Inhibition of NF-kappaB by a TAT-NEMO-binding domain peptide accelerates constitutive apoptosis and abrogates LPS-delayed neutrophil apoptosis. *Blood*, 102, 2259-67.
- CHOU, T. C., MOTZER, R. J., TONG, Y. & BOSL, G. J. 1994. Computerized quantitation of synergism and antagonism of taxol, topotecan, and cisplatin against human teratocarcinoma cell growth: a rational approach to clinical protocol design. *J Natl Cancer Inst*, 86, 1517-24.
- COLE, D. J., JANECEK, M., STOKES, J. E., ROSSMANN, M., FAVER, J. C., MCKENZIE, G. J., VENKITARAMAN, A. R., HYVONEN, M., SPRING, D. R., HUGGINS, D. J. & JORGENSEN, W. L. 2017. Computationally-guided optimization of small-molecule inhibitors of the Aurora A kinase-TPX2 protein-protein interaction. *Chem Commun (Camb)*, 53, 9372-9375.
- COLLINS, P. E., GRASSIA, G., COLLERAN, A., KIELY, P. A., IALENTI, A., MAFFIA, P. & CARMODY, R. J. 2015. Mapping the Interaction of B Cell Leukemia 3 (BCL-3) and Nuclear Factor kappaB (NF-kappaB) p50 Identifies a BCL-3-mimetic Anti-inflammatory Peptide. *J Biol Chem*, 290, 15687-96.
- COLLINS, T., READ, M. A., NEISH, A. S., WHITLEY, M. Z., THANOS, D. & MANIATIS, T. 1995. Transcriptional regulation of endothelial cell adhesion molecules: NF-kappa B and cytokine-inducible enhancers. *FASEB journal : official publication of the Federation of American Societies for Experimental Biology*, 9, 899-909.
- CRAWFORD, E. D., HEIDENREICH, A., LAWRENTSCHUK, N., TOMBAL, B., POMPEO, A. C. L., MENDOZA-VALDES, A., MILLER, K., DEBRUYNE, F. M. J. & KLOTZ, L. 2019. Androgen-targeted therapy in men with prostate cancer: evolving practice and future considerations. *Prostate Cancer Prostatic Dis*, 22, 24-38.
- CRISPI, S., FAGLIARONE, C., BIROCCIO, A., D'ANGELO, C., GALATI, R., SACCHI, A., VINCENZI, B., BALDI, A. & VERDINA, A. 2010. Antiproliferative effect of Aurora kinase targeting in mesothelioma. *Lung Cancer*, 70, 271-9.
- CUZICK, J., THORAT, M. A., ANDRIOLE, G., BRAWLEY, O. W., BROWN, P. H., CULIG, Z., EELES, R. A., FORD, L. G., HAMDY, F. C., HOLMBERG, L., ILIC, D., KEY, T. J., LA VECCHIA, C., LILJA, H., MARBERGER, M., MEYSKENS, F. L., MINASIAN, L. M.,

- PARKER, C., PARNES, H. L., PERNER, S., RITTENHOUSE, H., SCHALKEN, J., SCHMID, H. P., SCHMITZ-DRAGER, B. J., SCHRODER, F. H., STENZL, A., TOMBAL, B., WILT, T. J. & WOLK, A. 2014. Prevention and early detection of prostate cancer. *Lancet Oncol*, 15, e484-92.
- DAI, S., HIRAYAMA, T., ABBAS, S. & ABU-AMER, Y. 2004. The IkappaB kinase (IKK) inhibitor, NEMO-binding domain peptide, blocks osteoclastogenesis and bone erosion in inflammatory arthritis. *J Biol Chem*, 279, 37219-22.
- DALL'ERA, M. A., COOPERBERG, M. R., CHAN, J. M., DAVIES, B. J., ALBERTSEN, P. C., KLOTZ, L. H., WARLICK, C. A., HOLMBERG, L., BAILEY, D. E., WALLACE, M. E., KANTOFF, P. W. & CARROLL, P. R. 2008. Active surveillance for early-stage prostate cancer: Review of the current literature. *Cancer*, 112, 1650-1659.
- DALVA-AYDEMIR, S., AKYERLI, C. B., YUKSEL, S. K., KESKIN, H. & YAKICIER, M. C. 2019. Toward In Vitro Epigenetic Drug Design for Thyroid Cancer: The Promise of PF-03814735, an Aurora Kinase Inhibitor. *OMICS*, 23, 486-495.
- DAVE, S. H., TILSTRA, J. S., MATSUOKA, K., LI, F., KARRASCH, T., UNO, J. K., SEPULVEDA, A. R., JOBIN, C., BALDWIN, A. S., ROBBINS, P. D. & PLEVY, S. E. 2007. Amelioration of chronic murine colitis by peptide-mediated transduction of the IkappaB kinase inhibitor NEMO binding domain peptide. *J Immunol*, 179, 7852-9.
- DE BRUIN, M. L., SPARIDANS, J., VAN'T VEER, M. B., NOORDIJK, E. M., LOUWMAN, M. W. J., ZIJLSTRA, J. M., VAN DEN BERG, H., RUSSELL, N. S., BROEKS, A., BAAIJENS, M. H. A., ALEMAN, B. M. P. & VAN LEEUWEN, F. E. 2009. Breast cancer risk in female survivors of Hodgkin's lymphoma: lower risk after smaller radiation volumes. *Journal of clinical oncology : official journal of the American Society of Clinical Oncology*, 27, 4239-46.
- DEHM, S. M. & TINDALL, D. J. 2006. Molecular regulation of androgen action in prostate cancer. *Journal of cellular biochemistry*, 99, 333-44.
- DEWERTH, A., WONNER, T., LIEBER, J., ELLERKAMP, V., WARMANN, S. W., FUCHS, J. & ARMEANU-EBINGER, S. 2012. In vitro evaluation of the Aurora kinase inhibitor VX-680 for Hepatoblastoma. *Pediatr Surg Int*, 28, 579-89.
- DIELI, F., VERMIJLEN, D., FULFARO, F., CACCAMO, N., MERAVIGLIA, S., CICERO, G., ROBERTS, A., BUCCHERI, S., D'ASARO, M., GEBBIA, N., SALERNO, A., EBERL, M. & HAYDAY, A. C. 2007. Targeting human {gamma}delta T cells with zoledronate and interleukin-2 for immunotherapy of hormone-refractory prostate cancer. *Cancer Res*, 67, 7450-7.
- DITCHFIELD, C., JOHNSON, V. L., TIGHE, A., ELLSTON, R., HAWORTH, C., JOHNSON, T., MORTLOCK, A., KEEN, N. & TAYLOR, S. S. 2003. Aurora B couples chromosome

- alignment with anaphase by targeting BubR1, Mad2, and Cenp-E to kinetochores. *J Cell Biol*, 161, 267-80.
- DOLCET, X., LLOBET, D., PALLARES, J. & MATIAS-GUIU, X. 2005. NF- κ B in development and progression of human cancer.
- DONG, T., LI, C., WANG, X., DIAN, L., ZHANG, X., LI, L., CHEN, S., CAO, R., LI, L., HUANG, N., HE, S. & LEI, X. 2015. Ainsliadimer A selectively inhibits IKK α /beta by covalently binding a conserved cysteine. *Nat Commun*, 6, 6522.
- DOUST, J., MILLER, E., DUCHESNE, G., KITCHENER, M. & WELLER, D. 2004. A systematic review of brachytherapy: Is it an effective and safe treatment for localised prostate cancer?
- DRAKE, C. G. 2011. Update on prostate cancer vaccines. *Cancer J*, 17, 294-9.
- EL-DEIRY, W. S., GOLDBERG, R. M., LENZ, H. J., SHIELDS, A. F., GIBNEY, G. T., TAN, A. R., BROWN, J., EISENBERG, B., HEATH, E. I., PHUPHANICH, S., KIM, E., BRENNER, A. J. & MARSHALL, J. L. 2019. The current state of molecular testing in the treatment of patients with solid tumors, 2019. *CA: A Cancer Journal for Clinicians*.
- ELINAV, E., NOWARSKI, R., THAISS, C. A., HU, B., JIN, C. & FLAVELL, R. A. 2013. Inflammation-induced cancer: crosstalk between tumours, immune cells and microorganisms. *Nat Rev Cancer*, 13, 759-71.
- ELKAMHAWY, A., KIM, N. Y., HASSAN, A. H. E., PARK, J. E., PAIK, S., YANG, J. E., OH, K. S., LEE, B. H., LEE, M. Y., SHIN, K. J., PAE, A. N., LEE, K. T. & ROH, E. J. 2020. Thiazolidine-2,4-dione-based irreversible allosteric IKK-beta kinase inhibitors: Optimization into in vivo active anti-inflammatory agents. *Eur J Med Chem*, 188, 111955.
- ELMORE, S. 2007. Apoptosis: A Review of Programmed Cell Death. *Toxicologic Pathology*, 35, 495-516.
- EMANUEL, S., RUGG, C. A., GRUNINGER, R. H., LIN, R., FUENTES-PESQUERA, A., CONNOLLY, P. J., WETTER, S. K., HOLLISTER, B., KRUGER, W. W., NAPIER, C., JOLLIFFE, L. & MIDDLETON, S. A. 2005. The in vitro and in vivo effects of JNJ-7706621: a dual inhibitor of cyclin-dependent kinases and aurora kinases. *Cancer Res*, 65, 9038-46.
- EPIS, M. R., GILES, K. M., BEVERIDGE, D. J., RICHARDSON, K. L., CANDY, P. A., STUART, L. M., BENTEL, J., COHEN, R. J. & LEEDMAN, P. J. 2017. miR-331-3p and Aurora Kinase inhibitor II co-treatment suppresses prostate cancer tumorigenesis and progression. *Oncotarget*, 8, 55116-55134.

- EYERS, P. A., CHURCHILL, M. E. & MALLER, J. L. 2005. The Aurora A and Aurora B protein kinases: a single amino acid difference controls intrinsic activity and activation by TPX2. *Cell Cycle*, 4, 784-9.
- EYERS, P. A. & MALLER, J. L. 2004. Regulation of Xenopus Aurora A Activation by TPX2. *Journal of Biological Chemistry*, 279, 9008-9015.
- FARRUGGIO, D. C., TOWNSLEY, F. M. & RUDERMAN, J. V. 1999. Cdc20 associates with the kinase aurora2/Aik. *Proc Natl Acad Sci U S A*, 96, 7306-7311.
- FELDMAN, B. J. & FELDMAN, D. 2001. The development of androgen-independent prostate cancer. *Nature reviews. Cancer*, 1, 34-45.
- FIELDING, A. B., DOBREVA, I., MCDONALD, P. C., FOSTER, L. J. & DEDHAR, S. 2008. Integrin-linked kinase localizes to the centrosome and regulates mitotic spindle organization. *Journal of Cell Biology*, 180, 681-689.
- FIELER, V. K. 1997. Side effects and quality of life in patients receiving high-dose rate brachytherapy. *Oncol Nurs Forum*, 24, 545-553.
- FRANK, S. J., PISTERS, L. L., DAVIS, J., LEE, A. K., BASSETT, R. & KUBAN, D. A. 2007. An assessment of quality of life following radical prostatectomy, high dose external beam radiation therapy and brachytherapy iodine implantation as monotherapies for localized prostate cancer. *J Urol*, 177, 2151-6; discussion 2156.
- FU, J., BIAN, M., LIU, J., JIANG, Q. & ZHANG, C. 2009. A single amino acid change converts Aurora-A into Aurora-B-like kinase in terms of partner specificity and cellular function. *Proc Natl Acad Sci U S A*, 106, 6939-44.
- FUKUDA, T., MISHINA, Y., WALKER, M. P. & DIAUGUSTINE, R. P. 2005. Conditional transgenic system for mouse aurora a kinase: degradation by the ubiquitin proteasome pathway controls the level of the transgenic protein. *Mol Cell Biol*, 25, 5270-81.
- FURQAN, M., HUMA, Z., ASHFAQ, Z., NASIR, A., ULLAH, R., BILAL, A., IQBAL, M., KHALID, M. H., HUSSAIN, I. & FAISAL, A. 2019. Identification and evaluation of novel drug combinations of Aurora kinase inhibitor CCT137690 for enhanced efficacy in oral cancer cells. *Cell Cycle*, 18, 2281-2292.
- GABILLARD, J. C., ULISSE, S., BALDINI, E., SORRENTI, S., CREMET, J. Y., COCCARO, C., PRIGENT, C., D'ARMIENTO, M. & ARLOT-BONNEMAINS, Y. 2011. Aurora-C interacts with and phosphorylates the transforming acidic coiled-coil 1 protein. *Biochemical and Biophysical Research Communications*, 408, 647-653.
- GAMBLE, C., MCINTOSH, K., SCOTT, R., HO, K. H., PLEVIN, R. & PAUL, A. 2012a. Inhibitory kappa B Kinases as targets for pharmacological regulation. *Br J Pharmacol*, 165, 802-19.

- GAMBLE, C., MCINTOSH, K., SCOTT, R., HO, K. H., PLEVIN, R. & PAUL, A. 2012b. Inhibitory kappa B Kinases as targets for pharmacological regulation. *British journal of pharmacology*, 165, 802-19.
- GAO, C.-F., XIE, Q., SU, Y.-L., KOEMAN, J., KHOO, S. K., GUSTAFSON, M., KNUDSEN, B. S., HAY, R., SHINOMIYA, N. & VANDE WOUDE, G. F. 2005. Proliferation and invasion: plasticity in tumor cells. *Proceedings of the National Academy of Sciences of the United States of America*, 102, 10528-10533.
- GARBER, K. 2006. The second wave in kinase cancer drugs. *Nat Biotechnol*, 24, 127-30.
- GASPARIAN, A. V., YAO, Y. J., KOWALCZYK, D., LYAKH, L. A., KARSELADZE, A., SLAGA, T. J. & BUDUNOVA, I. V. 2002. The role of IKK in constitutive activation of NF-kappaB transcription factor in prostate carcinoma cells. *J Cell Sci*, 115, 141-51.
- GAURNIER-HAUSSER, A., PATEL, R., BALDWIN, A. S., MAY, M. J. & MASON, N. J. 2011. NEMO-binding domain peptide inhibits constitutive NF-kappaB activity and reduces tumor burden in a canine model of relapsed, refractory diffuse large B-cell lymphoma. *Clin Cancer Res*, 17, 4661-71.
- GEORGIEVA, I., KOYCHEV, D., WANG, Y., HOLSTEIN, J., HOPFENMULLER, W., ZEITZ, M. & GRABOWSKI, P. 2010. ZM447439, a novel promising aurora kinase inhibitor, provokes antiproliferative and proapoptotic effects alone and in combination with bio- and chemotherapeutic agents in gastroenteropancreatic neuroendocrine tumor cell lines. *Neuroendocrinology*, 91, 121-30.
- GHEGHIANI, L., LOEW, D., LOMBARD, B., MANSFELD, J. & GAVET, O. 2017. PLK1 Activation in Late G2 Sets Up Commitment to Mitosis. *Cell Rep*, 19, 2060-2073.
- GHOSH, P. M., MALIK, S. N., BEDOLLA, R. G., WANG, Y., MIKHAILOVA, M., PRIHODA, T. J., TROYER, D. A. & KREISBERG, J. I. 2005. Signal transduction pathways in androgen-dependent and -independent prostate cancer cell proliferation. *Endocrine-related cancer*, 12, 119-34.
- GIET, R., MCLEAN, D., DESCAMPS, S., LEE, M. J., RAFF, J. W., PRIGENT, C. & GLOVER, D. M. 2002. Drosophila Aurora A kinase is required to localize D-TACC to centrosomes and to regulate astral microtubules. *Journal of Cell Biology*, 156, 437-451.
- GILBERT, E. S. 2009. Ionizing Radiation and Cancer Risks: What Have We Learned From Epidemiology? *Int J Radiat Biol.*, 85, 467-482.
- GIRDLER, F., GASCOIGNE, K. E., EYERS, P. A., HARTMUTH, S., CRAFTER, C., FOOTE, K. M., KEEN, N. J. & TAYLOR, S. S. 2006. Validating Aurora B as an anti-cancer drug target. *J Cell Sci*, 119, 3664-75.

- GIRLING, J. S., WHITAKER, H. C., MILLS, I. G. & NEAL, D. E. 2007. Pathogenesis of prostate cancer and hormone refractory prostate cancer. *Indian Journal of Urology*, 23, 35-42.
- GIUBETTINI, M., ASTERITI, I. A., SCROFANI, J., DE LUCA, M., LINDON, C., LAVIA, P. & GUARGUAGLINI, G. 2011. Control of Aurora-A stability through interaction with TPX2. *Journal of Cell Science*, 124, 113-122.
- GIZATULLIN, F., YAO, Y., KUNG, V., HARDING, M. W., LODA, M. & SHAPIRO, G. I. 2006. The Aurora kinase inhibitor VX-680 induces endoreduplication and apoptosis preferentially in cells with compromised p53-dependent postmitotic checkpoint function. *Cancer Res*, 66, 7668-77.
- GOMES-FILHO, S. M., DOS SANTOS, E. O., BERTOLDI, E. R. M., SCALABRINI, L. C., HEIDRICH, V., DAZZANI, B., LEVANTINI, E., REIS, E. M. & BASSERES, D. S. 2020a. Aurora A kinase and its activator TPX2 are potential therapeutic targets in KRAS-induced pancreatic cancer. *Cell Oncol (Dordr)*.
- GOMES-FILHO, S. M., DOS SANTOS, E. O., BERTOLDI, E. R. M., SCALABRINI, L. C., HEIDRICH, V., DAZZANI, B., LEVANTINI, E., REIS, E. M. & BASSERES, D. S. 2020b. Aurora A kinase and its activator TPX2 are potential therapeutic targets in KRAS-induced pancreatic cancer. *Cell Oncol (Dordr)*, 43, 445-460.
- GONG, X., DU, J., PARSONS, S. H., MERZOUG, F. F., WEBSTER, Y., IVERSEN, P. W., CHIO, L. C., VAN HORN, R. D., LIN, X., BLOSSER, W., HAN, B., JIN, S., YAO, S., BIAN, H., FICKLIN, C., FAN, L., KAPOOR, A., ANTONYSAMY, S., MC NULTY, A. M., FRONING, K., MANGLICMOT, D., PUSTILNIK, A., WEICHERT, K., WASSERMAN, S. R., DOWLESS, M., MARUGAN, C., BAQUERO, C., LALLENA, M. J., EASTMAN, S. W., HUI, Y. H., DIETER, M. Z., DOMAN, T., CHU, S., QIAN, H. R., YE, X. S., BARDA, D. A., PLOWMAN, G. D., REINHARD, C., CAMPBELL, R. M., HENRY, J. R. & BUCHANAN, S. G. 2019. Aurora A Kinase Inhibition Is Synthetic Lethal with Loss of the RB1 Tumor Suppressor Gene. *Cancer Discov*, 9, 248-263.
- GRAY, C. M., REMOUCHAMPS, C., MCCORKELL, K. A., SOLT, L. A., DEJARDIN, E., ORANGE, J. S. & MAY, M. J. 2014. Noncanonical NF-kappaB signaling is limited by classical NF-kappaB activity. *Sci Signal*, 7, ra13.
- GROVER, A., SINGH, R., SHANDILYA, A., PRIYANDOKO, D., AGRAWAL, V., BISARIA, V. S., WADHWA, R., KAUL, S. C. & SUNDAR, D. 2012. Ashwagandha derived withanone targets TPX2-Aurora A complex: computational and experimental evidence to its anticancer activity. *PLoS One*, 7, e30890.
- GU, J. J., ZHANG, J. H., CHEN, H. J. & WANG, S. S. 2016. TPX2 promotes glioma cell proliferation and invasion via activation of the AKT signaling pathway. *Oncol Lett*, 12, 5015-5022.

- GULLY, C. P., VELAZQUEZ-TORRES, G., SHIN, J. H., FUENTES-MATTEI, E., WANG, E., CARLOCK, C., CHEN, J., ROTHENBERG, D., ADAMS, H. P., CHOI, H. H., GUMA, S., PHAN, L., CHOU, P. C., SU, C. H., ZHANG, F., CHEN, J. S., YANG, T. Y., YEUNG, S. C. & LEE, M. H. 2012. Aurora B kinase phosphorylates and instigates degradation of p53. *Proc Natl Acad Sci U S A*, 109, E1513-22.
- HABINEZA NDIKUYEZE, G., GAURNIER-HAUSSER, A., PATEL, R., BALDWIN, A. S., MAY, M. J., FLOOD, P., KRICK, E., PROPERT, K. J. & MASON, N. J. 2014. A phase I clinical trial of systemically delivered NEMO binding domain peptide in dogs with spontaneous activated B-cell like diffuse large B-cell lymphoma. *PLoS One*, 9, e95404.
- HACKER, H. & KARIN, M. 2006. Regulation and Function of IKK and IKK-Related Kinases. *Sci. STKE*, 2006, re13--re13-.
- HAGEMANN, T., LAWRENCE, T., MCNEISH, I., CHARLES, K. A., KULBE, H., THOMPSON, R. G., ROBINSON, S. C. & BALKWILL, F. R. 2008. "Re-educating" tumor-associated macrophages by targeting NF-kappaB. *J Exp Med*, 205, 1261-8.
- HANAHAH, D. & WEINBERG, R. A. 2000. The hallmarks of cancer. *Cell*, 100, 57-70.
- HANAHAH, D. & WEINBERG, R. A. 2011. Hallmarks of cancer: the next generation. *Cell*, 144, 646-74.
- HAYDEN, M. S. & GHOSH, S. 2012. NF- κ B, the first quarter-century: Remarkable progress and outstanding questions. *Genes and Development*, 26, 203-234.
- HAYES, J. H. & BARRY, M. J. 2014. Screening for Prostate Cancer With the Prostate-Specific Antigen Test. *Jama*, 311, 1143-1143.
- HE, W., ZHANG, M. G., WANG, X. J., ZHONG, S., SHAO, Y., ZHU, Y. & SHEN, Z. J. 2013. AURKA suppression induces DU145 apoptosis and sensitizes DU145 to docetaxel treatment. *Am J Transl Res*, 5, 359-67.
- HELFRICH, B. A., KIM, J., GAO, D., CHAN, D. C., ZHANG, Z., TAN, A. C. & BUNN, P. A., JR. 2016. Barasertib (AZD1152), a Small Molecule Aurora B Inhibitor, Inhibits the Growth of SCLC Cell Lines In Vitro and In Vivo. *Mol Cancer Ther*, 15, 2314-2322.
- HERON, N. M., ANDERSON, M., BLOWERS, D. P., BREED, J., EDEN, J. M., GREEN, S., HILL, G. B., JOHNSON, T., JUNG, F. H., MCMIKEN, H. H., MORTLOCK, A. A., PANNIFER, A. D., PAUPTIT, R. A., PINK, J., ROBERTS, N. J. & ROWSELL, S. 2006. SAR and inhibitor complex structure determination of a novel class of potent and specific Aurora kinase inhibitors. *Bioorg Med Chem Lett*, 16, 1320-3.
- HIGANO, C., VOLGELZANG, N. J., SOSMAN, J. A., FENG, A., CARON, D. & SMALL, E. J. 2004. Safety and Biological Activity of Repeated Doses of Recombinant Human Flt3 Ligand in Patients with Bone Scan-Negative Hormone Refractory Prostate Cancer.

Clinical cancer research : an official journal of the American Association for Cancer Research, 10, 1219-1225.

- HIGASHIMOTO, T., CHAN, N., LEE, Y. K. & ZANDI, E. 2008. Regulation of I(kappa)B kinase complex by phosphorylation of (gamma)-binding domain of I(kappa)B kinase (beta) by Polo-like kinase 1. *J Biol Chem*, 283, 35354-67.
- HINZ, M. & SCHEIDEREIT, C. 2014. The IkappaB kinase complex in NF-kappaB regulation and beyond. *EMBO Rep*, 15, 46-61.
- HIROTA, T., KUNITOKU, N., SASAYAMA, T., MARUMOTO, T., ZHANG, D., NITTA, M., HATAKEYAMA, K. & SAYA, H. 2003. Aurora-A and an interacting activator, the LIM protein Ajuba, are required for mitotic commitment in human cells. *Cell*, 114, 585-598.
- HOESEL, B. & SCHMID, J. A. 2013. The complexity of NF-kB signaling in inflammation and cancer. *Molecular cancer*, 12, 86-86.
- HORIKAWA, T., YANG, J., KONDO, S., YOSHIZAKI, T., JOAB, I., FURUKAWA, M. & PAGANO, J. S. 2007. Twist and epithelial-mesenchymal transition are induced by the EBV oncoprotein latent membrane protein 1 and are associated with metastatic nasopharyngeal carcinoma. *Cancer Research*, 67, 1970-1978.
- HOTTE, S. J. & SAAD, F. 2010. Current management of castrate-resistant prostate cancer. *Current oncology (Toronto, Ont.)*, 17 Suppl 2, S72-9.
- HSU, C. W., CHEN, Y. C., SU, H. H., HUANG, G. J., SHU, C. W., WU, T. T. & PAN, H. W. 2017. Targeting TPX2 Suppresses the Tumorigenesis of Hepatocellular Carcinoma Cells Resulting in Arrested Mitotic Phase Progression and Increased Genomic Instability. *J Cancer*, 8, 1378-1394.
- HU, J. C., LAVIANA, A. & SEDRAKYAN, A. 2016. High-Intensity Focused Ultrasound for Prostate Cancer: Novelty or Innovation? *JAMA*, 315, 2659-60.
- HU, Q., LUO, T., ZHONG, X., HE, P., TIAN, T. & ZHENG, H. 2015. Application status of tamoxifen in endocrine therapy for early breast cancer. *Exp Ther Med*, 9, 2207-2212.
- HU, S., CAO, M., HE, Y., ZHANG, G., LIU, Y., DU, Y., YANG, C. & GAO, F. 2020. CD44v6 Targeted by miR-193b-5p in the Coding Region Modulates the Migration and Invasion of Breast Cancer Cells. *J Cancer*, 11, 260-271.
- HUANG, M., FENG, X., SU, D., WANG, G., WANG, C., TANG, M., PAULUCCI-HOLTHAUZEN, A., HART, T. & CHEN, J. 2020. Genome-wide CRISPR screen uncovers a synergistic effect of combining Haspin and Aurora kinase B inhibition. *Oncogene*, 39, 4312-4322.
- HUANG, S., PETTAWAY, C. A., UEHARA, H., BUCANA, C. D. & FIDLER, I. J. 2001. Blockade of NF-kappaB activity in human prostate cancer cells is associated with suppression of angiogenesis, invasion, and metastasis. *Oncogene*, 20, 4188-97.

- HUANG, Y. C., LEE, C. T., LEE, J. C., LIU, Y. W., CHEN, Y. J., TSENG, J. T., KANG, J. W., SHEU, B. S., LIN, B. W. & HUNG, L. Y. 2016. Epigenetic silencing of miR-137 contributes to early colorectal carcinogenesis by impaired Aurora-A inhibition. *Oncotarget*, 7, 76852-76866.
- HUBER, M. A., AZOITEI, N., BAUMANN, B., GRÜNERT, S., SOMMER, A., PEHAMBERGER, H., KRAUT, N., BEUG, H. & WIRTH, T. 2004. NF-kappaB is essential for epithelial-mesenchymal transition and metastasis in a model of breast cancer progression. *The Journal of clinical investigation*, 114, 569-81.
- HUGGINS, C., STEVENS, R. E. & HODGES, C. V. 1941. The effects of castration on advanced carcinoma of the prostate gland. *JAMA: Surgery*, 43, 209-223.
- HUTTERER, A., BERDNIK, D., WIRTZ-PEITZ, F., ŽIGMAN, M., SCHLEIFFER, A. & KNOBLICH, J. A. 2006. Mitotic Activation of the Kinase Aurora-A Requires Its Binding Partner Bora. *Developmental Cell*, 11, 147-157.
- IANARO, A., TERSIGNI, M., BELARDO, G., DI MARTINO, S., NAPOLITANO, M., PALMIERI, G., SINI, M., DE MAIO, A., OMBRA, M., GENTILCORE, G., CAPONE, M., ASCIERTO, M., SATRIANO, R. A., FARINA, B., FARAONE-MENNELLA, M., ASCIERTO, P. A. & IALENTI, A. 2009. NEMO-binding domain peptide inhibits proliferation of human melanoma cells. *Cancer Lett*, 274, 331-6.
- INOUE, J. I., GOHDA, J., AKIYAMA, T. & SEMBA, K. 2007. NF- κ B activation in development and progression of cancer.
- IRELAN, J. T., MURPHY, T. J., DEJESUS, P. D., TEO, H., XU, D., GOMEZ-FERRERIA, M. A., ZHOU, Y., MIRAGLIA, L. J., RINES, D. R., VERMA, I. M., SHARP, D. J., TERGAONKAR, V. & CHANDA, S. K. 2007. A role for IkappaB kinase 2 in bipolar spindle assembly. Irelan, J.T. et al., 2007. A role for IkappaB kinase 2 in bipolar spindle assembly. *Proceedings of the National Academy of Sciences of the United States of America*, 104(43), pp.16940–5. *Proceedings of the National Academy of Sciences of the United States of America*, 104, 16940-5.
- ISRAEL, A. 2010. The IKK complex, a central regulator of NF-kappaB activation. *Cold Spring Harb Perspect Biol*, 2, a000158.
- JAIN, G., VOOGDT, C., TOBIAS, A., SPINDLER, K. D., MOLLER, P., CRONAUER, M. V. & MARIENFELD, R. B. 2012. IkappaB kinases modulate the activity of the androgen receptor in prostate carcinoma cell lines. *Neoplasia*, 14, 178-89.
- JAMASPIHVILI, T., BERMAN, D. M., ROSS, A. E., SCHER, H. I., DE MARZO, A. M., SQUIRE, J. A. & LOTAN, T. L. 2018. Clinical implications of PTEN loss in prostate cancer. *Nat Rev Urol*, 15, 222-234.

- JANECEK, M., ROSSMANN, M., SHARMA, P., EMERY, A., HUGGINS, D. J., STOCKWELL, S. R., STOKES, J. E., TAN, Y. S., ALMEIDA, E. G., HARDWICK, B., NARVAEZ, A. J., HYVONEN, M., SPRING, D. R., MCKENZIE, G. J. & VENKITARAMAN, A. R. 2016. Allosteric modulation of AURKA kinase activity by a small-molecule inhibitor of its protein-protein interaction with TPX2. *Sci Rep*, 6, 28528.
- JANEČEK, M., ROSSMANN, M., SHARMA, P., EMERY, A., HUGGINS, D. J., STOCKWELL, S. R., STOKES, J. E., TAN, Y. S., ALMEIDA, E. G., HARDWICK, B., NARVAEZ, A. J., HYVÖNEN, M., SPRING, D. R., MCKENZIE, G. J. & VENKITARAMAN, A. R. 2016. Allosteric modulation of AURKA kinase activity by a small-molecule inhibitor of its protein-protein interaction with TPX2. *Scientific Reports*, 6, 28528-28528.
- JELLUMA, N., BRENKMAN, A. B., VAN DEN BROEK, N. J. F., CRUIJSEN, C. W. A., VAN OSCH, M. H. J., LENS, S. M. A., MEDEMA, R. H. & KOPS, G. J. P. L. 2008. Mps1 Phosphorylates Borealin to Control Aurora B Activity and Chromosome Alignment. *Cell*, 132, 233-246.
- JEYAPRAKASH, A. A., KLEIN, U. R., LINDNER, D., EBERT, J., NIGG, E. A. & CONTI, E. 2007. Structure of a Survivin-Borealin-INCENP Core Complex Reveals How Chromosomal Passengers Travel Together. *Cell*, 131, 271-285.
- JIANG, Y., LIU, Y., TAN, X., YU, S. & LUO, J. 2019. TPX2 as a Novel Prognostic Indicator and Promising Therapeutic Target in Triple-negative Breast Cancer. *Clin Breast Cancer*, 19, 450-455.
- JIN, R., STERLING, J. A., EDWARDS, J. R., DEGRAFF, D. J., LEE, C., PARK, S. I. & MATUSIK, R. J. 2013. Activation of NF-kappa B Signaling Promotes Growth of Prostate Cancer Cells in Bone. *PLoS ONE*, 8.
- JIN, R. J., LHO, Y., CONNELLY, L., WANG, Y., YU, X., JEAN, L. S., CASE, T. C., ELLWOOD-YEN, K., SAWYERS, C. L., BHOWMICK, N. A., BLACKWELL, T. S., YULL, F. E. & MATUSIK, R. J. 2008. The nuclear factor- κ B pathway controls the progression of prostate cancer to androgen-independent growth. *Cancer Research*, 68, 6762-6769.
- JINEK, M., CHYLINSKI, K., FONFARA, I., HAUER, M., DOUDNA, J. A. & CHARPENTIER, E. 2012. A programmable dual-RNA-guided DNA endonuclease in adaptive bacterial immunity. *Science*, 337, 816-21.
- JOHANNIS, T. M., FU, Y., KOBAYASHI, D. K., MEI, Y., DUNN, I. F., MAO, D. D., KIM, A. H. & DUNN, G. P. 2016. High incidence of TERT mutation in brain tumor cell lines. *Brain Tumor Pathol*, 33, 222-7.
- JONES, D., NOBLE, M., WEDGE, S. R., ROBSON, C. N. & GAUGHAN, L. 2017. Aurora A regulates expression of AR-V7 in models of castrate resistant prostate cancer. *Sci Rep*, 7, 40957.

- JOST, P. J. & RULAND, J. 2007. Aberrant NF- κ B signaling in lymphoma: Mechanisms, consequences, and therapeutic implications.
- KADARA, H., LACROIX, L., BEHRENS, C., SOLIS, L., GU, X., LEE, J. J., TAHARA, E., LOTAN, D., HONG, W. K., WISTUBA, II & LOTAN, R. 2009. Identification of gene signatures and molecular markers for human lung cancer prognosis using an in vitro lung carcinogenesis system. *Cancer Prev Res (Phila)*, 2, 702-11.
- KALLAS, A., POOK, M., MAIMETS, M., ZIMMERMANN, K. & MAIMETS, T. 2011. Nocodazole treatment decreases expression of pluripotency markers nanog and Oct4 in human embryonic stem cells. *PLoS ONE*, 6.
- KANG, Y. & MASSAGUÉ, J. 2004. Epithelial-mesenchymal transitions: Twist in development and metastasis.
- KARANTANOS, T., CORN, P. G. & THOMPSON, T. C. 2013. Prostate cancer progression after androgen deprivation therapy: mechanisms of castrate resistance and novel therapeutic approaches. *Oncogene*, 32, 5501-11.
- KARIN, M. 2006. Nuclear factor-kappaB in cancer development and progression. *Nature*, 441, 431-6.
- KATAYAMA H, B. W. R. S. S. 2003. The Aurora kinases: role in cell transformation and tumorigenesis. *Cancer Met. Rev.*, 22, 451-464.
- KATAYAMA, H., SASAI, K., KAWAI, H., YUAN, Z.-M., BONDARUK, J., SUZUKI, F., FUJII, S., ARLINGHAUS, R. B., CZERNIAK, B. A. & SEN, S. 2004. Phosphorylation by aurora kinase A induces Mdm2-mediated destabilization and inhibition of p53. *Nature Genetics*, 36, 55-62.
- KATAYAMA, H., WANG, J., TREEKITKARNMONGKOL, W., KAWAI, H., SASAI, K., ZHANG, H., WANG, H., ADAMS, H. P., JIANG, S., CHAKRABORTY, S. N., SUZUKI, F., ARLINGHAUS, R. B., LIU, J., MOBLEY, J. A., GRIZZLE, W. E., WANG, H. & SEN, S. 2012. Aurora kinase-A inactivates DNA damage-induced apoptosis and spindle assembly checkpoint response functions of p73. *Cancer Cell*, 21, 196-211.
- KATSHA, A., BELKHIRI, A., GOFF, L. & EL-RIFAI, W. 2015. Aurora kinase A in gastrointestinal cancers: time to target. *Mol Cancer*, 14, 106.
- KATSHA, A., SOUTTO, M., SEHDEV, V., PENG, D., WASHINGTON, M. K., PIAZUELO, M. B., TANTAWY, M. N., MANNING, H. C., LU, P., SHYR, Y., ECSEDY, J., BELKHIRI, A. & EL-RIFAI, W. 2013. Aurora kinase A promotes inflammation and tumorigenesis in mice and human gastric neoplasia. *Gastroenterology*, 145, 1312-22 e1-8.
- KIM, M., LIAO, J., DOWLING, M. L., VOONG, K. R., PARKER, S. E., WANG, S., EL-DEIRY, W. S. & KAO, G. D. 2008. TRAIL inactivates the mitotic checkpoint and potentiates

- death induced by microtubule-targeting agents in human cancer cells. *Cancer Res*, 68, 3440-9.
- KIMURA, M., MATSUDA, Y., YOSHIOKA, T. & OKANO, Y. 1999. Cell cycle-dependent expression and centrosome localization of a third human Aurora/Ipl1-related protein kinase, AIK3. *Journal of Biological Chemistry*, 274, 7334-7340.
- KING, M.-C., MARKS, J. H. & MANDELL, J. B. 2003. Breast and ovarian cancer risks due to inherited mutations in BRCA1 and BRCA2. *Science (New York, N.Y.)*, 302, 643-646.
- KISHORE, N., SOMMERS, C., MATHIALAGAN, S., GUZOVA, J., YAO, M., HAUSER, S., HUYNH, K., BONAR, S., MIELKE, C., ALBEE, L., WEIER, R., GRANETO, M., HANAU, C., PERRY, T. & TRIPP, C. S. 2003. A selective IKK-2 inhibitor blocks NF-kappa B-dependent gene expression in interleukin-1 beta-stimulated synovial fibroblasts. *J Biol Chem*, 278, 32861-71.
- KIVINUMMI, K., URBANUCCI, A., LEINONEN, K., TAMMELA, T. L. J., ANNALA, M., ISAACS, W. B., BOVA, G. S., NYKTER, M. & VISAKORPI, T. 2017. The expression of AURKA is androgen regulated in castration-resistant prostate cancer. *Sci Rep*, 7, 17978.
- KOLLAREDDY, M., DZUBAK, P., ZHELEVA, D. & HAJDUCH, M. 2008. Aurora kinases: structure, functions and their association with cancer.
- KOROBAYNIKOV, V., BORAKOVE, M., FENG, Y., WUEST, W. M., KOVAL, A. B., NIKONOVA, A. S., SEREBRIISKII, I., CHERNOFF, J., BORGES, V. F., GOLEMIS, E. A. & SHAGISULTANOVA, E. 2019. Combined inhibition of Aurora A and p21-activated kinase 1 as a new treatment strategy in breast cancer. *Breast Cancer Res Treat*, 177, 369-382.
- KUFER, T. A., SILLJ, H. H. W., K??RNER, R., GRUSS, O. J., MERALDI, P. & NIGG, E. A. 2002. Human TPX2 is required for targeting Aurora-A kinase to the spindle. *Journal of Cell Biology*, 158, 617-623.
- KUMAR, R. J., BARQAWI, A. & CRAWFORD, E. D. 2005. Adverse events associated with hormonal therapy for prostate cancer. *Rev Urol*, 7 Suppl 5, S37-43.
- LAEMMLI, U. K. 1970. Cleavage of structural proteins during the assembly of the head of bacteriophage T4. *Nature*, 227, 680-5.
- LAKE, E. W., MURETTA, J. M., THOMPSON, A. R., RASMUSSEN, D. M., MAJUMDAR, A., FABER, E. B., RUFF, E. F., THOMAS, D. D. & LEVINSON, N. M. 2018. Quantitative conformational profiling of kinase inhibitors reveals origins of selectivity for Aurora kinase activation states. *Proc Natl Acad Sci U S A*, 115, E11894-E11903.
- LANNI, J. S. & JACKS, T. 1998. Characterization of the p53-dependent postmitotic checkpoint following spindle disruption. *Molecular and cellular biology*, 18, 1055-64.

- LARA, P. N., JR., CHEE, K. G., LONGMATE, J., RUEL, C., MEYERS, F. J., GRAY, C. R., EDWARDS, R. G., GUMERLOCK, P. H., TWARDOWSKI, P., DOROSHOW, J. H. & GANDARA, D. R. 2004. Trastuzumab plus docetaxel in HER-2/neu-positive prostate carcinoma: final results from the California Cancer Consortium Screening and Phase II Trial. *Cancer*, 100, 2125-31.
- LARSEN, S. L., YDE, C. W., LAENKHOLM, A. V., RASMUSSEN, B. B., DUUN-HENRIKSEN, A. K., BAK, M., LYKKESFELDT, A. E. & KIRKEGAARD, T. 2015. Aurora kinase B is important for antiestrogen resistant cell growth and a potential biomarker for tamoxifen resistant breast cancer. *BMC Cancer*, 15, 239.
- LEE, D. F. & HUNG, M. C. 2008. Advances in targeting IKK and IKK-related kinases for cancer therapy. *Clin Cancer Res*, 14, 5656-62.
- LEE, H. H., ZHU, Y., GOVINDASAMY, K. M. & GOPALAN, G. 2008. Downregulation of Aurora-A overrides estrogen-mediated growth and chemoresistance in breast cancer cells. *Endocr Relat Cancer*, 15, 765-75.
- LEE, Y. C., QUE, J., CHEN, Y. C., LIN, J. T., LIOU, Y. C., LIAO, P. C., LIU, Y. P., LEE, K. H., LIN, L. C., HSIAO, M., HUNG, L. Y., HUANG, C. Y. & LU, P. J. 2013. Pin1 acts as a negative regulator of the G2/M transition by interacting with the Aurora-A-Bora complex. *J Cell Sci*, 126, 4862-72.
- LEI, Q., GU, H., LI, L., WU, T., XIE, W., LI, M. & ZHAO, N. 2020. TNIP1-mediated TNF- α /NF- κ B signalling cascade sustains glioma cell proliferation. *J Cell Mol Med*, 24, 530-538.
- LI, X., SAKASHITA, G., MATSUZAKI, H., SUGIMOTO, K., KIMURA, K., HANAOKA, F., TANIGUCHI, H., FURUKAWA, K. & URANO, T. 2004. Direct association with inner centromere protein (INCENP) activates the novel chromosomal passenger protein, Aurora-C. *Journal of Biological Chemistry*, 279, 47201-47211.
- LI, Y., ZHANG, Z. F., CHEN, J., HUANG, D., DING, Y., TAN, M. H., QIAN, C. N., RESAU, J. H., KIM, H. & TEH, B. T. 2010. VX680/MK-0457, a potent and selective Aurora kinase inhibitor, targets both tumor and endothelial cells in clear cell renal cell carcinoma. *Am J Transl Res*, 2, 296-308.
- LIANG, B., ZHENG, W., FANG, L., WU, L., ZHOU, F., YIN, X., YU, X. & ZOU, Z. 2016. Overexpressed targeting protein for Xklp2 (TPX2) serves as a promising prognostic marker and therapeutic target for gastric cancer. *Cancer Biol Ther*, 17, 824-32.
- LIAO, J. B. 2006. Viruses and human cancer. *The Yale Journal of bBology and Medicine*, 79, 115-122.
- LIN, Y., RICHARDS, F. M., KRIPPENDORFF, B. F., BRAMHALL, J. L., HARRINGTON, J. A., BAPIRO, T. E., ROBERTSON, A., ZHELEVA, D. & JODRELL, D. I. 2012. Paclitaxel

- and CYC3, an aurora kinase A inhibitor, synergise in pancreatic cancer cells but not bone marrow precursor cells. *British Journal of Cancer*, 107, 1692-1701.
- LIU, F., XIA, Y., PARKER, A. S. & VERMA, I. M. 2012. IKK biology.
- LIU, H., LIANG, H., MENG, H., DENG, X., ZHANG, X. & LAI, L. 2018. A novel allosteric inhibitor that prevents IKKbeta activation. *Medchemcomm*, 9, 239-243.
- LIU, H. C., ZHANG, G. H., LIU, Y. H., WANG, P., MA, J. F., SU, L. S., LI, S. L., ZHANG, L. & LIU, J. W. 2014a. TPX2 siRNA regulates growth and invasion of esophageal cancer cells. *Biomed Pharmacother*, 68, 833-9.
- LIU, J. & QIN, C. Y. 2018. VX-680 induces p53-mediated apoptosis in human cholangiocarcinoma cells. *Anticancer Drugs*, 29, 1004-1010.
- LIU, N., WANG, Y. A., SUN, Y., ECSEDY, J., SUN, J., LI, X. & WANG, P. 2019. Inhibition of Aurora A enhances radiosensitivity in selected lung cancer cell lines. *Respir Res*, 20, 230.
- LIU, Q., WU, H., CHIM, S. M., ZHOU, L., ZHAO, J., FENG, H., WEI, Q., WANG, Q., ZHENG, M. H., TAN, R. X., GU, Q., XU, J., PAVLOS, N., TICKNER, J. & XU, J. 2013. SC-514, a selective inhibitor of IKKbeta attenuates RANKL-induced osteoclastogenesis and NF-kappaB activation. *Biochem Pharmacol*, 86, 1775-83.
- LIU, Q., YANG, P., TU, K., ZHANG, H., ZHENG, X., YAO, Y. & LIU, Q. 2014b. TPX2 knockdown suppressed hepatocellular carcinoma cell invasion via inactivating AKT signaling and inhibiting MMP2 and MMP9 expression. *Chin J Cancer Res*, 26, 410-7.
- LIU, T., ZHANG, L., JOO, D. & SUN, S. C. 2017. NF-kappaB signaling in inflammation. *Signal Transduct Target Ther*, 2.
- LIU, X., LI, Z., SONG, Y., WANG, R., HAN, L., WANG, Q., JIANG, K., KANG, C. & ZHANG, Q. 2016. AURKA induces EMT by regulating histone modification through Wnt/ β -catenin and PI3K/Akt signaling pathway in gastric cancer. *Oncotarget*, 7, 33152-64.
- LIU, Z., HAZAN-HALEVY, I., HARRIS, D. M., LI, P., FERRAJOLI, A., FADERL, S., KEATING, M. J. & ESTROV, Z. 2011. STAT-3 activates NF-kappaB in chronic lymphocytic leukemia cells. *Molecular cancer research : MCR*, 9, 507-515.
- LO IACONO, M., MONICA, V., SAVIOZZI, S., CEPPI, P., BRACCO, E., PAPOTTI, M. & SCAGLIOTTI, G. V. 2011. Aurora Kinase A expression is associated with lung cancer histological-subtypes and with tumor de-differentiation. *J Transl Med*, 9, 100.
- LONDHE, P., YU, P. Y., IJIRI, Y., LADNER, K. J., FENGER, J. M., LONDON, C., HOUGHTON, P. J. & GUTTRIDGE, D. C. 2018. Classical NF-kappaB Metabolically Reprograms Sarcoma Cells Through Regulation of Hexokinase 2. *Front Oncol*, 8, 104.

- LU, S., TSAI, S. Y. & TSAI, M. J. 1997. Regulation of androgen-dependent prostatic cancer cell growth: androgen regulation of CDK2, CDK4, and CKI p16 genes. *Cancer research*, 4511-4516.
- MA, N., TITUS, J., GABLE, A., ROSS, J. L. & WADSWORTH, P. 2011. TPX2 regulates the localization and activity of Eg5 in the mammalian mitotic spindle. *J Cell Biol*, 195, 87-98.
- MAHATO, R., QIN, B. & CHENG, K. 2011. Blocking IKK α expression inhibits prostate cancer invasiveness. *Pharmaceutical research*, 28, 1357-69.
- MARQUES, R. B., DITS, N. F., ERKENS-SCHULZE, S., VAN WEERDEN, W. M. & JENSTER, G. 2010. Bypass mechanisms of the androgen receptor pathway in therapy-resistant prostate cancer cell models. *PloS one*, 5, e13500-e13500.
- MARUMOTO, T., HIROTA, T., MORISAKI, T., KUNITOKU, N., ZHANG, D., ICHIKAWA, Y., SASAYAMA, T., KUNINAKA, S., MIMORI, T., TAMAKI, N., KIMURA, M., OKANO, Y. & SAYA, H. 2002. Roles of aurora-A kinase in mitotic entry and G2 checkpoint in mammalian cells. *Genes to Cells*, 7, 1173-1182.
- MATSUMOTO, Y., MARUSAWA, H., KINOSHITA, K., ENDO, Y., KOU, T., MORISAWA, T., AZUMA, T., OKAZAKI, I. M., HONJO, T. & CHIBA, T. 2007. Helicobacter pylori infection triggers aberrant expression of activation-induced cytidine deaminase in gastric epithelium. *Nat Med*, 13, 470-6.
- MATTEI, J. C., BOUVIER-LABIT, C., BARETS, D., MACAGNO, N., CHOCRY, M., CHIBON, F., MORANDO, P., ROCHWERGER, R. A., DUFFAUD, F., OLSCHWANG, S., SALAS, S. & JIGUET-JIGLAIRE, C. 2020. Pan Aurora Kinase Inhibitor: A Promising Targeted-Therapy in Dedifferentiated Liposarcomas With Differential Efficiency Depending on Sarcoma Molecular Profile. *Cancers (Basel)*, 12.
- MAY, M. J., D'ACQUISTO, F., MADGE, L. A., GLOCKNER, J., POBER, J. S. & GHOSH, S. 2000a. Selective inhibition of NF-kappaB activation by a peptide that blocks the interaction of NEMO with the IkappaB kinase complex. *Science*, 289, 1550-4.
- MAY, M. J., D'ACQUISTO, F., MADGE, L. A., GLÖCKNER, J., POBER, J. S. & GHOSH, S. 2000b. Selective {Inhibition} of {NF}- κ {B} {Activation} by a {Peptide} {That} {Blocks} the {Interaction} of {NEMO} with the {IkB} {Kinase} {Complex}. *Science*, 289, 1550-1554.
- MAZUR, P. 1984. Freezing of living cells: mechanisms and implications. *The American journal of physiology*, 247, C125-C142.
- MAZZERA, L., LOMBARDI, G., ABELTINO, M., RICCA, M., DONOFRIO, G., GIULIANI, N., CANTONI, A. M., CORRADI, A., BONATI, A. & LUNGI, P. 2013a. Aurora and IKK

- kinases cooperatively interact to protect multiple myeloma cells from Apo2L/TRAIL. *Blood*, 122, 2641-2653.
- MAZZERA, L., LOMBARDI, G., ABELTINO, M., RICCA, M., DONOFRIO, G., GIULIANI, N., CANTONI, A. M., CORRADI, A., BONATI, A. & LUNGHI, P. 2013b. Aurora and IKK kinases cooperatively interact to protect multiple myeloma cells from Apo2L/TRAIL. *Blood*, 122, 2641-53.
- MCCULLOUGH, A. R. 2005. Sexual dysfunction after radical prostatectomy. *Reviews in urology*, 7 Suppl 2, S3-S10.
- MCINTYRE, P. J., COLLINS, P. M., VRZAL, L., BIRCHALL, K., ARNOLD, L. H., MPAMHANGA, C., COOMBS, P. J., BURGESS, S. G., RICHARDS, M. W., WINTER, A., VEVERKA, V., DELFT, F. V., MERRITT, A. & BAYLISS, R. 2017. Characterization of Three Druggable Hot-Spots in the Aurora-A/TPX2 Interaction Using Biochemical, Biophysical, and Fragment-Based Approaches. *ACS Chem Biol*, 12, 2906-2914.
- MERCURIO, F., ZHU, H., MURRAY, B. W., SHEVCHENKO, A., BENNETT, B. L., LI, J., YOUNG, D. B., BARBOSA, M., MANN, M., MANNING, A. & RAO, A. 1997. IKK-1 and IKK-2: cytokine-activated I κ B kinases essential for NF- κ B activation. *Science (New York, N.Y.)*, 278, 860-6.
- MIN, Y. H., KIM, W. & KIM, J. E. 2016. The Aurora kinase A inhibitor TC-A2317 disrupts mitotic progression and inhibits cancer cell proliferation. *Oncotarget*, 7, 84718-84735.
- MINNELLI, C., LAUDADIO, E., MOBBILI, G. & GALEAZZI, R. 2020. Conformational Insight on WT- and Mutated-EGFR Receptor Activation and Inhibition by Epigallocatechin-3-Gallate: Over a Rational Basis for the Design of Selective Non-Small-Cell Lung Anticancer Agents. *Int J Mol Sci*, 21.
- NABET, B., ROBERTS, J. M., BUCKLEY, D. L., PAULK, J., DASTJERDI, S., YANG, A., LEGGETT, A. L., ERB, M. A., LAWLOR, M. A., SOUZA, A., SCOTT, T. G., VITTORI, S., PERRY, J. A., QI, J., WINTER, G. E., WONG, K. K., GRAY, N. S. & BRADNER, J. E. 2018. The dTAG system for immediate and target-specific protein degradation. *Nat Chem Biol*, 14, 431-441.
- NARAYANAN, D. L., SALADI, R. N. & FOX, J. L. 2010. Ultraviolet radiation and skin cancer. *Int J Dermatol*, 49, 978-86.
- NAUGLER, W. E. & KARIN, M. 2008. The wolf in sheep's clothing: the role of interleukin-6 in immunity, inflammation and cancer. *Trends Mol Med*, 14, 109-19.
- NISHIDA, N., YANO, H., NISHIDA, T., KAMURA, T. & KOJIRO, M. 2006. Angiogenesis in cancer.

- NOH, E. M., LEE, Y. R., HONG, O. Y., JUNG, S. H., YOUN, H. J. & KIM, J. S. 2015. Aurora kinases are essential for PKC-induced invasion and matrix metalloproteinase-9 expression in MCF-7 breast cancer cells. *Oncology Reports*, 34, 803-810.
- NOOREN, I. M. & THORNTON, J. M. 2003. Diversity of protein-protein interactions. *EMBO J*, 22, 3486-92.
- OPYRCHAL, M., SALISBURY, J. L., ZHANG, S., MCCUBREY, J., HAWSE, J., GOETZ, M. P., LOMBERK, G. A., HADDAD, T., DEGNIM, A., LANGE, C., INGLE, J. N., GALANIS, E. & D'ASSORO, A. B. 2014. Aurora-A mitotic kinase induces endocrine resistance through down-regulation of ERalpha expression in initially ERalpha+ breast cancer cells. *PLoS One*, 9, e96995.
- OZDEMIR-KAYNAK, E., QUTUB, A. A. & YESIL-CELIKTAS, O. 2018. Advances in Glioblastoma Multiforme Treatment: New Models for Nanoparticle Therapy. *Front Physiol*, 9, 170.
- PALLER, C. J., WISSING, M. D., MENDONCA, J., SHARMA, A., KIM, E., KIM, H. S., KORTENHORST, M. S., GERBER, S., ROSEN, M., SHAIKH, F., ZAHURAK, M. L., RUDEK, M. A., HAMMERS, H., RUDIN, C. M., CARDUCCI, M. A. & KACHHAP, S. K. 2014. Combining the pan-aurora kinase inhibitor AMG 900 with histone deacetylase inhibitors enhances antitumor activity in prostate cancer. *Cancer Med*, 3, 1322-35.
- PAN, H. W., SU, H. H., HSU, C. W., HUANG, G. J. & WU, T. T. 2017. Targeted TPX2 increases chromosome missegregation and suppresses tumor cell growth in human prostate cancer. *Onco Targets Ther*, 10, 3531-3543.
- PAUL, A., EDWARDS, J., PEPPER, C. & MACKAY, S. 2018. Inhibitory-kappaB Kinase (IKK) alpha and Nuclear Factor-kappaB (NFkappaB)-Inducing Kinase (NIK) as Anti-Cancer Drug Targets. *Cells*, 7.
- PEDAMALLU, C. S. & POSFAI, J. 2010. Open source tool for prediction of genome wide protein-protein interaction network based on ortholog information. *Source Code Biol Med*, 5, 8.
- PERAMBAKAM, S., HALLMEYER, S., REDDY, S., MAHMUD, N., BRESSLER, L., DECHRISTOPHER, P., MAHMUD, D., NUNEZ, R., SOSMAN, J. A. & PEACE, D. J. 2006. Induction of specific T cell immunity in patients with prostate cancer by vaccination with PSA146-154 peptide. *Cancer Immunol Immunother*, 55, 1033-42.
- PERKINS, N. D. 2007. Integrating cell-signalling pathways with NF-kappaB and IKK function. *Nature reviews. Molecular cell biology*, 8, 49-62.
- PERLMUTTER, M. A. & LEPOR, H. 2007. Androgen deprivation therapy in the treatment of advanced prostate cancer. *Reviews in urology*, 9 Suppl 1, S3-8.

- PIETERS, B. R., DE BACK, D. Z., KONING, C. C. E. & ZWINDERMAN, A. H. 2009. Comparison of three radiotherapy modalities on biochemical control and overall survival for the treatment of prostate cancer: A systematic review.
- PITTO, L., RIZZO, M., SIMILI, M., COLLIGIANI, D., EVANGELISTA, M., MERCATANTI, A., MARIANI, L., CREMISI, F. & RAINALDI, G. 2009. miR-290 acts as a physiological effector of senescence in mouse embryo fibroblasts. *Physiological Genomics*, 39, 210-218.
- PORTA, C., RIMOLDI, M., RAES, G., BRYNS, L., GHEZZI, P., DI LIBERTO, D., DIELI, F., GHISLETTI, S., NATOLI, G., DE BAETSELIER, P., MANTOVANI, A. & SICA, A. 2009. Tolerance and M2 (alternative) macrophage polarization are related processes orchestrated by p50 nuclear factor kappaB. *Proc Natl Acad Sci U S A*, 106, 14978-83.
- PRAJAPATI, S., TU, Z., YAMAMOTO, Y. & GAYNOR, R. B. 2006. IKK β regulates the mitotic phase of the cell cycle by modulating Aurora A phosphorylation. *Cell Cycle*, 5, 2371-2380.
- PRESCOTT, J. A. & COOK, S. J. 2018. Targeting IKK β in Cancer: Challenges and Opportunities for the Therapeutic Utilisation of IKK β Inhibitors. *Cells*, 7.
- PRIESTLEY, P., BABER, J., LOLKEMA, M. P., STEEGHS, N., DE BRUIJN, E., SHALE, C., DUYVESTYEN, K., HAIDARI, S., VAN HOECK, A., ONSTENK, W., ROEPMAN, P., VODA, M., BLOEMENDAL, H. J., TJAN-HEIJNEN, V. C. G., VAN HERPEN, C. M. L., LABOTS, M., WITTEVEEN, P. O., SMIT, E. F., SLEIJFER, S., VOEST, E. E. & CUPPEN, E. 2019. Pan-cancer whole-genome analyses of metastatic solid tumours. *Nature*.
- PUGACHEVA, E. N., JABLONSKI, S. A., HARTMAN, T. R., HENSKE, E. P. & GOLEMIS, E. A. 2007. HEF1-Dependent Aurora A Activation Induces Disassembly of the Primary Cilium. *Cell*, 129, 1351-1363.
- RADOSEVICH, J. A. 2012. *HPV and cancer*.
- RAO CH, V., LI, X., MANNA, S. K., LEI, Z. M. & AGGARWAL, B. B. 2004. Human chorionic gonadotropin decreases proliferation and invasion of breast cancer MCF-7 cells by inhibiting NF-kappaB and AP-1 activation. *J Biol Chem*, 279, 25503-10.
- RAO, V. S., SRINIVAS, K., SUJINI, G. N. & KUMAR, G. N. 2014. Protein-protein interaction detection: methods and analysis. *Int J Proteomics*, 2014, 147648.
- REBELLO, R. J., PEARSON, R. B., HANNAN, R. D. & FURIC, L. 2017. Therapeutic Approaches Targeting MYC-Driven Prostate Cancer. *Genes (Basel)*, 8.
- RENNIE, Y. K., MCINTYRE, P. J., AKINDELE, T., BAYLISS, R. & JAMIESON, A. G. 2016. A TPX2 Proteomimetic Has Enhanced Affinity for Aurora-A Due to Hydrocarbon Stapling of a Helix. *ACS Chem Biol*, 11, 3383-3390.

- RISK, M. & CORMAN, J. M. 2009. The role of immunotherapy in prostate cancer: an overview of current approaches in development. *Rev Urol*, 11, 16-27.
- RODLAND, G. E., MELHUS, K., GENERALOV, R., GILANI, S., BERTONI, F., DAHLE, J., SYLJUASEN, R. G. & PATZKE, S. 2019. The Dual Cell Cycle Kinase Inhibitor JNJ-7706621 Reverses Resistance to CD37-Targeted Radioimmunotherapy in Activated B Cell Like Diffuse Large B Cell Lymphoma Cell Lines. *Front Oncol*, 9, 1301.
- RONG, R., JIANG, L. Y., SHEIKH, M. S. & HUANG, Y. 2007. Mitotic kinase Aurora-A phosphorylates RASSF1A and modulates RASSF1A-mediated microtubule interaction and M-phase cell cycle regulation. *Oncogene*, 26, 7700-7708.
- RUSHE, M., SILVIAN, L., BIXLER, S., CHEN, L. L., CHEUNG, A., BOWES, S., CUERVO, H., BERKOWITZ, S., ZHENG, T., GUCKIAN, K., PELLEGRINI, M. & LUGOVSKOY, A. 2008. Structure of a NEMO/IKK-Associating Domain Reveals Architecture of the Interaction Site. *Structure*, 16, 798-808.
- RYU, J., PYO, J., LEE, C. W. & KIM, J. E. 2018. An Aurora kinase inhibitor, AMG900, inhibits glioblastoma cell proliferation by disrupting mitotic progression. *Cancer Med*, 7, 5589-5603.
- SAKAMOTO, K. M., KIM, K. B., KUMAGAI, A., MERCURIO, F., CREWS, C. M. & DESHAIES, R. J. 2001. Protacs: chimeric molecules that target proteins to the Skp1-Cullin-F box complex for ubiquitination and degradation. *Proc Natl Acad Sci U S A*, 98, 8554-9.
- SANCHEZ-PULIDO, L., PEREZ, L., KUHN, S., VERNOS, I. & ANDRADE-NAVARRO, M. A. 2016. The C-terminal domain of TPX2 is made of alpha-helical tandem repeats. *BMC Struct Biol*, 16, 17.
- SAPUTRA, E. C., HUANG, L., CHEN, Y. & TUCKER-KELLOGG, L. 2018. Combination Therapy and the Evolution of Resistance: The Theoretical Merits of Synergism and Antagonism in Cancer. *Cancer Res*, 78, 2419-2431.
- SARKAR, S., BRAUTIGAN, D. L. & LARNER, J. M. 2017. Aurora Kinase A Promotes AR Degradation via the E3 Ligase CHIP. *Mol Cancer Res*, 15, 1063-1072.
- SASAI, K., KATAYAMA, H., STENOIEN, D. L., FUJII, S., HONDA, R., KIMURA, M., OKANO, Y., TATSUKA, M., SUZUKI, F., NIGG, E. A., EARNSHAW, W. C., BRINKLEY, W. R. & SEN, S. Aurora-C kinase is a novel chromosomal passenger protein that can complement Aurora-B kinase function in mitotic cells. 2004 2004. 249-263.
- SASCO, A. J., SECRETAN, M. B. & STRAIF, K. 2004. Tobacco smoking and cancer: a brief review of recent epidemiological evidence. *Lung Cancer*, 45 Suppl 2, S3-9.
- SCHARER, C. D., LAYCOCK, N., OSUNKOYA, A. O., LOGANI, S., MCDONALD, J. F., BENIGNO, B. B. & MORENO, C. S. 2008. Aurora kinase inhibitors synergize with paclitaxel to induce apoptosis in ovarian cancer cells. *J Transl Med*, 6, 79.

- SCHMID, J. A. & BIRBACH, A. 2008. I κ B kinase beta (IKK β /IKK2/IKKB) β --a key molecule in signaling to the transcription factor NF- κ B. *Cytokine Growth Factor Rev*, 19, 157-65.
- SCHRIJVERS, D. 2007. Androgen-independent prostate cancer. *Prostate Cancer*, 1, 34-45.
- SEHDEV, V., KATSHA, A., ECSEDY, J., ZAIKA, A., BELKHIRI, A. & EL-RIFAI, W. 2013. The combination of alisertib, an investigational Aurora kinase A inhibitor, and docetaxel promotes cell death and reduces tumor growth in preclinical cell models of upper gastrointestinal adenocarcinomas. *Cancer*, 119, 904-14.
- SEKI, A., COPPINGER, J. A., JANG, C. Y., YATES, J. R. & FANG, G. 2008. Bora and the Kinase Aurora A Cooperatively Activate the Kinase Plk1 and Control Mitotic Entry. *Science*, 320, 1655-1658.
- SEN, S., ZHOU, H. & WHITE, R. A. 1997. A putative serine/threonine kinase encoding gene BTAK on chromosome 20q13 is amplified and overexpressed in human breast cancer cell lines. *Oncogene*, 14, 2195-2200.
- SENGLE, G., TSUTSUI, K., KEENE, D. R., TUFA, S. F., CARLSON, E. J., CHARBONNEAU, N. L., ONO, R. N., SASAKI, T., WIRTZ, M. K., SAMPLES, J. R., FESSLER, L. I., FESSLER, J. H., SEKIGUCHI, K., HAYFLICK, S. J. & SAKAI, L. Y. 2012. Microenvironmental regulation by fibrillin-1. *PLoS Genetics*, 8.
- SESSA, F., MAPELLI, M., CIFERRI, C., TARRICONE, C., ARECES, L. B., SCHNEIDER, T. R., STUKENBERG, P. T. & MUSACCHIO, A. 2005. Mechanism of Aurora B activation by INCENP and inhibition by hesperadin. *Molecular Cell*, 18, 379-391.
- SEYMOUR, J. F., KIM, D. W., RUBIN, E., HAREGEWOIN, A., CLARK, J., WATSON, P., HUGHES, T., DUFVA, I., JIMENEZ, J. L., MAHON, F. X., ROUSSELOT, P., CORTES, J., MARTINELLI, G., PAPAYANNIDIS, C., NAGLER, A. & GILES, F. J. 2014. A phase 2 study of MK-0457 in patients with BCR-ABL T315I mutant chronic myelogenous leukemia and philadelphia chromosome-positive acute lymphoblastic leukemia. *Blood Cancer J*, 4, e238.
- SHAFI, A. A., YEN, A. E. & WEIGEL, N. L. 2013. Androgen receptors in hormone-dependent and castration-resistant prostate cancer. *Pharmacology & therapeutics*, 140, 223-38.
- SHAH, K. N., BHATT, R., ROTOW, J., ROHRBERG, J., OLIVAS, V., WANG, V. E., HEMMATI, G., MARTINS, M. M., MAYNARD, A., KUHN, J., GALEAS, J., DONNELLA, H. J., KAUSHIK, S., KU, A., DUMONT, S., KRINGS, G., HARINGSMA, H. J., ROBILLARD, L., SIMMONS, A. D., HARDING, T. C., MCCORMICK, F., GOGA, A., BLAKELY, C. M., BIVONA, T. G. & BANDYOPADHYAY, S. 2019. Aurora kinase A drives the evolution of resistance to third-generation EGFR inhibitors in lung cancer. *Nat Med*, 25, 111-118.

- SHARIFI, N. 2013. Mechanisms of androgen receptor activation in castration-resistant prostate cancer. *Endocrinology*, 154, 4010-4017.
- SHARIFI, N., GULLEY, J. L. & DAHUT, W. L. 2005. Androgen deprivation therapy for prostate cancer. *JAMA : the journal of the American Medical Association*, 294, 238-244.
- SHEN, H. & MAKI, C. G. 2011. Pharmacologic activation of p53 by small-molecule MDM2 antagonists. *Curr Pharm Des*, 17, 560-8.
- SHEPPARD, K. A., ROSE, D. W., HAQUE, Z. K., KUROKAWA, R., MCINERNEY, E., WESTIN, S., THANOS, D., ROSENFELD, M. G., GLASS, C. K. & COLLINS, T. 1999. Transcriptional activation by NF- κ B requires multiple coactivators. *Mol Cell Biol*, 19, 6367-6378.
- SHIOMITSU, K., XIA, X., WAITE, K., SEHGAL, I. & LI, S. 2013. Evaluation of the Aurora Kinase Inhibitor, ZM447439, in Canine Malignant Lymphoid Cells <i>in Vitro&/i>. *Open Journal of Veterinary Medicine*, 03, 29-38.
- SHORE, N. 2014. Management of early-stage prostate cancer. *The American journal of managed care*, 20, s260-72.
- SHU, S. K., LIU, Q., COPPOLA, D. & CHENG, J. Q. 2010. Phosphorylation and activation of androgen receptor by Aurora-A. *Journal of Biological Chemistry*, 285, 33045-33053.
- SIMONS, J. W., MIKHAK, B., CHANG, J. F., DEMARZO, A. M., CARDUCCI, M. A., LIM, M., WEBER, C. E., BACCALA, A. A., GOEMANN, M. A., CLIFT, S. M., ANDO, D. G., LEVITSKY, H. I., COHEN, L. K., SANDA, M. G., MULLIGAN, R. C., PARTIN, A. W., CARTER, H. B., PIANTADOSI, S., MARSHALL, F. F. & NELSON, W. G. 1999. Induction of immunity to prostate cancer antigens: results of a clinical trial of vaccination with irradiated autologous prostate tumor cells engineered to secrete granulocyte-macrophage colony-stimulating factor using ex vivo gene transfer. *Cancer Res*, 59, 5160-8.
- SMALL, E. J., REESE, D. M., UM, B., WHISENANT, S., DIXON, S. C. & FIGG, W. D. 1999. Therapy of advanced prostate cancer with granulocyte macrophage colony-stimulating factor. *Clin Cancer Res*, 5, 1738-44.
- SMALL, E. J., TCHEKMEDYIAN, N. S., RINI, B. I., FONG, L., LOWY, I. & ALLISON, J. P. 2007. A pilot trial of CTLA-4 blockade with human anti-CTLA-4 in patients with hormone-refractory prostate cancer. *Clin Cancer Res*, 13, 1810-5.
- SMITH, S. L., BOWERS, N. L., BETTICHER, D. C., GAUTSCHI, O., RATSCHILLER, D., HOBAN, P. R., BOOTON, R., SANTIBANEZ-KOREF, M. F. & HEIGHWAY, J. 2005. Overexpression of aurora B kinase (AURKB) in primary non-small cell lung carcinoma is frequent, generally driven from one allele, and correlates with the level of genetic instability. *Br J Cancer*, 93, 719-29.

- SMITH, S. M., LYU, Y. L. & CAI, L. 2014. NF- κ B affects proliferation and invasiveness of breast cancer cells by regulating CD44 expression. *PLoS ONE*, 9.
- SOLT, L. A., MADGE, L. A. & MAY, M. J. 2009. NEMO-binding domains of both IKK α and IKK β regulate I κ B kinase complex assembly and classical NF- κ B activation. *J Biol Chem*, 284, 27596-608.
- SOLT, L. A., MADGE, L. A., ORANGE, J. S. & MAY, M. J. 2007. Interleukin-1-induced NF- κ B activation is NEMO-dependent but does not require IKK β . *J Biol Chem*, 282, 8724-33.
- SOORIAKUMARAN, P., NYBERG, T., AKRE, O., HAENDLER, L., HEUS, I., OLSSON, M., CARLSSON, S., ROOBOL, M. J., STEINECK, G. & WIKLUND, P. 2014. Comparative effectiveness of radical prostatectomy and radiotherapy in prostate cancer: observational study of mortality outcomes. *BMJ*, 348, g1502-g1502.
- SORENSEN, C. S., LUKAS, C., KRAMER, E. R., PETERS, J. M., BARTEK, J. & LUKAS, J. 2000. Nonperiodic Activity of the Human Anaphase-Promoting Complex-Cdh1 Ubiquitin Ligase Results in Continuous DNA Synthesis Uncoupled from Mitosis. *Molecular and Cellular Biology*, 20, 7613-7623.
- SOUCEK, L., LAWLOR, E. R., SOTO, D., SHCHORS, K., SWIGART, L. B. & EVAN, G. I. 2007. Mast cells are required for angiogenesis and macroscopic expansion of Myc-induced pancreatic islet tumors. *Nature medicine*, 13, 1211-1218.
- SPARMANN, A. & BAR-SAGI, D. 2004. Ras-induced interleukin-8 expression plays a critical role in tumor growth and angiogenesis. *Cancer Cell*, 6, 447-458.
- SRIDHAR, S. S., FREEDLAND, S. J., GLEAVE, M. E., HIGANO, C., MULDER, P., PARKER, C., SARTOR, O. & SAAD, F. 2014. Castration-resistant prostate cancer: From new pathophysiology to new treatment. *European Urology*, 65, 289-299.
- STEWART, S. & FANG, G. 2005. Anaphase-promoting complex/cyclosome controls the stability of TPX2 during mitotic exit. *Mol Cell Biol*, 25, 10516-27.
- SUH, J., PAYVANDI, F., EDELSTEIN, L. C., AMENTA, P. S., ZONG, W. X., GELINAS, C. & RABSON, A. B. 2002. Mechanisms of constitutive NF- κ B activation in human prostate cancer cells. *Prostate*, 52, 183-200.
- SUMAN, S. & MISHRA, A. 2018. Network analysis revealed aurora kinase dysregulation in five gynecological types of cancer. *Oncol Lett*, 15, 1125-1132.
- SUN, X., NIU, S., ZHANG, Z., WANG, A., YANG, C., GUO, Z., HAO, Y., LI, X. & WANG, X. 2019. Aurora kinase inhibitor VX680 suppresses the proliferation and migration of HUVECs and angiogenesis. *Mol Med Rep*, 19, 3841-3847.
- SUNDARARAJAN, S. & VOGELZANG, N. 2014. Chemotherapy in the Treatment of Prostate Cancer — The Past, the Present, and the Future. *chemotherapy*, 10, 14-21.

- TAKAHASHI, Y., SHERIDAN, P., NIIDA, A., SAWADA, G., UCHI, R., MIZUNO, H., KURASHIGE, J., SUGIMACHI, K., SASAKI, S., SHIMADA, Y., HASE, K., KUSUNOKI, M., KUDO, S., WATANABE, M., YAMADA, K., SUGIHARA, K., YAMAMOTO, H., SUZUKI, A., DOKI, Y., MIYANO, S., MORI, M. & MIMORI, K. 2015. The AURKA/TPX2 axis drives colon tumorigenesis cooperatively with MYC. *Ann Oncol*, 26, 935-42.
- TANG, A., GAO, K., CHU, L., ZHANG, R., YANG, J. & ZHENG, J. 2017a. Aurora kinases: novel therapy targets in cancers. *Oncotarget*, 10.18632/oncotarget.14893-10.18632/oncotarget.14893.
- TANG, A., GAO, K., CHU, L., ZHANG, R., YANG, J. & ZHENG, J. 2017b. Aurora kinases: novel therapy targets in cancers. *Oncotarget*, 8, 23937-23954.
- THEODORESCU, D. 2004. Cancer cryotherapy: evolution and biology. *Reviews in urology*, 6 Suppl 4, S9-S19.
- TOMII, C., INOKUCHI, M., TAKAGI, Y., ISHIKAWA, T., OTSUKI, S., UETAKE, H., KOJIMA, K. & KAWANO, T. 2017. TPX2 expression is associated with poor survival in gastric cancer. *World J Surg Oncol*, 15, 14.
- TRAYNOR, A. M., HEWITT, M., LIU, G., FLAHERTY, K. T., CLARK, J., FREEDMAN, S. J., SCOTT, B. B., LEIGHTON, A. M., WATSON, P. A., ZHAO, B., O'DWYER, P. J. & WILDING, G. 2011. Phase I dose escalation study of MK-0457, a novel Aurora kinase inhibitor, in adult patients with advanced solid tumors. *Cancer Chemother Pharmacol*, 67, 305-14.
- TRINO, S., IACOBUCCI, I., ERRIQUEZ, D., LAURENZANA, I., DE LUCA, L., FERRARI, A., GHELLI LUSERNA DI RORA, A., PAPAYANNIDIS, C., DERENZINI, E., SIMONETTI, G., LONETTI, A., VENTURI, C., CATTINA, F., OTTAVIANI, E., ABBENANTE, M. C., RUSSO, D., PERINI, G., MUSTO, P. & MARTINELLI, G. 2016. Targeting the p53-MDM2 interaction by the small-molecule MDM2 antagonist Nutlin-3a: a new challenged target therapy in adult Philadelphia positive acute lymphoblastic leukemia patients. *Oncotarget*, 7, 12951-61.
- TSE, A. K., CHEN, Y. J., FU, X. Q., SU, T., LI, T., GUO, H., ZHU, P. L., KWAN, H. Y., CHENG, B. C., CAO, H. H., LEE, S. K., FONG, W. F. & YU, Z. L. 2017. Sensitization of melanoma cells to alkylating agent-induced DNA damage and cell death via orchestrating oxidative stress and IKKbeta inhibition. *Redox Biol*, 11, 562-576.
- VADER, G., KAUW, J. J. W., MEDEMA, R. H. & LENS, S. M. A. 2006. Survivin mediates targeting of the chromosomal passenger complex to the centromere and midbody. *EMBO reports*, 7, 85-92.

- VAN ANTWERP, D. J., MARTIN, S. J., KAFRI, T., GREEN, D. R. & VERMA, I. M. 1996. Suppression of TNF-alpha-induced apoptosis by NF-kappaB. *Science (New York, N.Y.)*, 274, 787-9.
- VAN GIJN, S. E., WIERENGA, E., VAN DEN TEMPEL, N., KOK, Y. P., HEIJINK, A. M., SPIERINGS, D. C. J., FOIJER, F., VAN VUGT, M. & FEHRMANN, R. S. N. 2019. TPX2/Aurora kinase A signaling as a potential therapeutic target in genomically unstable cancer cells. *Oncogene*, 38, 852-867.
- VAN LEEUWEN, I. M., RAO, B., SACHWEH, M. C. & LAIN, S. 2012. An evaluation of small-molecule p53 activators as chemoprotectants ameliorating adverse effects of anticancer drugs in normal cells. *Cell Cycle*, 11, 1851-61.
- VOGELSTEIN, B., LANE, D. & LEVINE, A. J. 2000. p53: The most frequently altered gene in human cancers. *Nature*, 408, 307-310.
- VOS, J. W., PIEUCHOT, L., EVRARD, J. L., JANSKI, N., BERGDOLL, M., DE RONDE, D., PEREZ, L. H., SARDON, T., VERNOS, I. & SCHMIT, A. C. 2008. The plant TPX2 protein regulates prospindle assembly before nuclear envelope breakdown. *Plant Cell*, 20, 2783-97.
- WADSWORTH, P. 2015. Tpx2. *Curr Biol*, 25, R1156-8.
- WALLIS, C. J. & NAM, R. K. 2015. Prostate Cancer Genetics: A Review. *EJIFCC*, 26, 79-91.
- WALSH, A. L., CONSIDINE, S. W., THOMAS, A. Z., LYNCH, T. H. & MANECKSHA, R. P. 2014. Digital rectal examination in primary care is important for early detection of prostate cancer: A retrospective cohort analysis study. *British Journal of General Practice*, 64, e783-e787.
- WANG, Q., CHEN, Q., ZHU, L., CHEN, M., XU, W., PANDAY, S., WANG, Z., LI, A., ROE, O. D., CHEN, R., WANG, S., ZHANG, R. & ZHOU, J. 2017. JWA regulates TRAIL-induced apoptosis via MARCH8-mediated DR4 ubiquitination in cisplatin-resistant gastric cancer cells. *Oncogenesis*, 6, e353.
- WANG, S., CHEN, Y. & CHAI, Y. 2018. Prognostic role of targeting protein for Xklp2 in solid tumors: A PRISMA-compliant systematic review and meta-analysis. *Medicine (Baltimore)*, 97, e13018.
- WANG, S., LIU, Z., WANG, L. & ZHANG, X. 2009. NF-kappaB signaling pathway, inflammation and colorectal cancer. *Cellular & molecular immunology*, 6, 327-34.
- WARNER, S. L., MUNOZ, R. M., STAFFORD, P., KOLLER, E., HURLEY, L. H., VON HOFF, D. D. & HAN, H. 2006. Comparing Aurora A and Aurora B as molecular targets for growth inhibition of pancreatic cancer cells. *Molecular cancer therapeutics*, 5, 2450-2458.

- WARNER, S. L., STEPHENS, B. J., NWOKENKWO, S., HOSTETTER, G., SUGENG, A., HIDALGO, M., TRENT, J. M., HAN, H. & VON HOFF, D. D. 2009. Validation of TPX2 as a potential therapeutic target in pancreatic cancer cells. *Clin Cancer Res*, 15, 6519-28.
- WEI, P., ZHANG, N., XU, Y., LI, X., SHI, D., WANG, Y., LI, D. & CAI, S. 2013. TPX2 is a novel prognostic marker for the growth and metastasis of colon cancer. *J Transl Med*, 11, 313.
- WEN, D., NONG, Y., MORGAN, J. G., GANGURDE, P., BIELECKI, A., DASILVA, J., KEAVENEY, M., CHENG, H., FRASER, C., SCHOPF, L., HEPPELLE, M., HARRIMAN, G., JAFFEE, B. D., OCAIN, T. D. & XU, Y. 2006. A selective small molecule I κ B Kinase beta inhibitor blocks nuclear factor kappaB-mediated inflammatory responses in human fibroblast-like synoviocytes, chondrocytes, and mast cells. *J Pharmacol Exp Ther*, 317, 989-1001.
- WIDODO, N., PRIYANDOKO, D., SHAH, N., WADHWA, R. & KAUL, S. C. 2010. Selective killing of cancer cells by Ashwagandha leaf extract and its component Withanone involves ROS signaling. *PLoS One*, 5, e13536.
- WILLEMS, E., DEBOBELEER, M., DIGREGORIO, M., LOMBARD, A., GOFFART, N., LUMAPAT, P. N., LAMBERT, J., VAN DEN ACKERVEKEN, P., SZPAKOWSKA, M., CHEVIGNE, A., SCHOLTES, F. & ROGISTER, B. 2019. Aurora A plays a dual role in migration and survival of human glioblastoma cells according to the CXCL12 concentration. *Oncogene*, 38, 73-87.
- WILT, T. J., BRAWER, M. K., JONES, K. M., BARRY, M. J., ARONSON, W. J., FOX, S., GINGRICH, J. R., WEI, J. T., GILHOOLY, P., GROB, B. M., NSOULI, I., IYER, P., CARTAGENA, R., SNIDER, G., ROEHRBORN, C., SHARIFI, R., BLANK, W., PANDYA, P., ANDRIOLE, G. L., CULKIN, D., WHEELER, T. & PROSTATE CANCER INTERVENTION VERSUS OBSERVATION TRIAL STUDY, G. 2012. Radical prostatectomy versus observation for localized prostate cancer. *The New England journal of medicine*, 367, 203-13.
- Wilson, A 2013, *Disrupting the Inhibitory Kappa B kinase (IKK) – Aurora A Axis in Cancer*, University of Strathclyde, Glasgow.
- WOGAN, G. N., HECHT, S. S., FELTON, J. S., CONNEY, A. H. & LOEB, L. A. 2004. Environmental and chemical carcinogenesis. *Semin Cancer Biol*, 14, 473-86.
- WYNN, M. L., VENTURA, A. C., SEPULCHRE, J. A., GARCIA, H. J. & MERAJVER, S. D. 2011. Kinase inhibitors can produce off-target effects and activate linked pathways by retroactivity. *BMC Syst Biol*, 5, 156.

- XIA, J., TROCK, B. J., COOPERBERG, M. R., GULATI, R., ZELIADT, S. B., GORE, J. L., LIN, D. W., CARROLL, P. R., CARTER, H. B. & ETZIONI, R. 2012. Prostate Cancer Mortality following Active Surveillance versus Immediate Radical Prostatectomy. *Clinical cancer research : an official journal of the American Association for Cancer Research*, 18, 5471-5478.
- XIA, Y., SHEN, S. & VERMA, I. M. 2014. NF- κ B, an active player in human cancers. *Cancer immunology research*, 2, 823-30.
- XIA, Z., WEI, P., ZHANG, H., DING, Z., YANG, L., HUANG, Z. & ZHANG, N. 2013. AURKA governs self-renewal capacity in glioma-initiating cells via stabilization/activation of beta-catenin/Wnt signaling. *Mol Cancer Res*, 11, 1101-11.
- XU, J., YUE, C. F., ZHOU, W. H., QIAN, Y. M., ZHANG, Y., WANG, S. W., LIU, A. W. & LIU, Q. 2014. Aurora-A contributes to cisplatin resistance and lymphatic metastasis in non-small cell lung cancer and predicts poor prognosis. *J Transl Med*, 12, 200.
- XU, X., WANG, X., XIAO, Z., LI, Y. & WANG, Y. 2011. Two TPX2-dependent switches control the activity of Aurora A. *PLoS One*, 6, e16757.
- YAN, M., WANG, C., HE, B., YANG, M., TONG, M., LONG, Z., LIU, B., PENG, F., XU, L., ZHANG, Y., LIANG, D., LEI, H., SUBRATA, S., KELLEY, K. W., LAM, E. W., JIN, B. & LIU, Q. 2016. Aurora-A Kinase: A Potent Oncogene and Target for Cancer Therapy. *Med Res Rev*, 36, 1036-1079.
- YANG, D., SUN, Y. Y., LIN, X., BAUMANN, J. M., DUNN, R. S., LINDQUIST, D. M. & KUAN, C. Y. 2013. Intranasal delivery of cell-penetrating anti-NF-kappaB peptides (Tat-NBD) alleviates infection-sensitized hypoxic-ischemic brain injury. *Exp Neurol*, 247, 447-455.
- YANG, H., LAWRENCE, H. R., KAZI, A., GEVARIYA, H., PATEL, R., LUO, Y., RIX, U., SCHONBRUNN, E., LAWRENCE, N. J. & SEBTI, S. M. 2014. Dual Aurora A and JAK2 kinase blockade effectively suppresses malignant transformation. *Oncotarget*, 5, 2947-61.
- YANG, H., OU, C. C., FELDMAN, R. I., NICOSIA, S. V., KRUK, P. A. & CHENG, J. Q. 2004. Aurora-A kinase regulates telomerase activity through c-Myc in human ovarian and breast epithelial cells. *Cancer Res*, 64, 463-7.
- YANG, K.-T., TANG, C.-J. C. & TANG, T. K. 2015a. Possible Role of Aurora-C in Meiosis. *Frontiers in Oncology*, 5.
- YANG, Y., LI, D. P., SHEN, N., YU, X. C., LI, J. B., SONG, Q. & ZHANG, J. H. 2015b. TPX2 promotes migration and invasion of human breast cancer cells. *Asian Pac J Trop Med*, 8, 1064-1070.

- YAO, R., ZHENG, J., ZHENG, W., GONG, Y., LIU, W. & XING, R. 2014. VX680 suppresses the growth of HepG2 cells and enhances the chemosensitivity to cisplatin. *Oncol Lett*, 7, 121-124.
- YEH, P. Y., LU, Y. S., OU, D. L. & CHENG, A. L. 2011. I κ B kinases increase Myc protein stability and enhance progression of breast cancer cells. *Mol Cancer*, 10, 53.
- YEMELYANOV, A., GASPARIAN, A., LINDHOLM, P., DANG, L., PIERCE, J. W., KISSELJOV, F., KARSELADZE, A. & BUDUNOVA, I. 2006. Effects of IKK inhibitor PS1145 on NF- κ B function, proliferation, apoptosis and invasion activity in prostate carcinoma cells. *Oncogene*, 25, 387-98.
- YOON, M. J., PARK, S. S., KANG, Y. J., KIM, I. Y., LEE, J. A., LEE, J. S., KIM, E. G., LEE, C. W. & CHOI, K. S. 2012. Aurora B confers cancer cell resistance to TRAIL-induced apoptosis via phosphorylation of survivin. *Carcinogenesis*, 33, 492-500.
- YUAN, C. X., ZHOU, Z. W., YANG, Y. X., HE, Z. X., ZHANG, X., WANG, D., YANG, T., WANG, N. J., ZHAO, R. J. & ZHOU, S. F. 2015. Inhibition of mitotic Aurora kinase A by alisertib induces apoptosis and autophagy of human gastric cancer AGS and NCI-N78 cells. *Drug Des Devel Ther*, 9, 487-508.
- YUAN, H., WANG, Z., ZHANG, H., ROTH, M., BHATIA, R. & CHEN, W. Y. 2012. Overcoming CML acquired resistance by specific inhibition of Aurora A kinase in the KCL-22 cell model. *Carcinogenesis*, 33, 285-93.
- YUN, C. H., MENGWASSER, K. E., TOMS, A. V., WOO, M. S., GREULICH, H., WONG, K. K., MEYERSON, M. & ECK, M. J. 2008. The T790M mutation in EGFR kinase causes drug resistance by increasing the affinity for ATP. *Proc Natl Acad Sci U S A*, 105, 2070-5.
- ZADRA, G., PHOTOPOULOS, C., TYEKUCHEVA, S., HEIDARI, P., WENG, Q. P., FEDELE, G., LIU, H., SCAGLIA, N., PRIOLO, C., SICINSKA, E., MAHMOOD, U., SIGNORETTI, S., BIRNBERG, N. & LODA, M. 2014. A novel direct activator of AMPK inhibits prostate cancer growth by blocking lipogenesis. *EMBO Mol Med*, 6, 519-38.
- ZANDI, E., ROTHWARF, D. M., DELHASE, M., HAYAKAWA, M. & KARIN, M. 1997. The I κ B kinase complex (IKK) contains two kinase subunits, IKK α and IKK β , necessary for I κ B phosphorylation and NF- κ B activation. *Cell*, 91, 243-252.
- ZEITLIN, S. G., SHELBY, R. D. & SULLIVAN, K. F. 2001. CENP-A is phosphorylated by Aurora B kinase and plays an unexpected role in completion of cytokinesis. *Journal of Cell Biology*, 155, 1147-1157.
- ZHANG, K., WANG, T., ZHOU, H., FENG, B., CHEN, Y., ZHI, Y. & WANG, R. 2018. A Novel Aurora-A Inhibitor (MLN8237) Synergistically Enhances the Antitumor Activity of Sorafenib in Hepatocellular Carcinoma. *Mol Ther Nucleic Acids*, 13, 176-188.

- ZHANG, Q., LIU, Y., GAO, F., DING, Q., CHO, C., HUR, W., JIN, Y., UNO, T., JOAZEIRO, C. A. & GRAY, N. 2006. Discovery of EGFR selective 4,6-disubstituted pyrimidines from a combinatorial kinase-directed heterocycle library. *J Am Chem Soc*, 128, 2182-3.
- ZHANG, X., SUN, Y., WANG, P., YANG, C. & LI, S. 2019. Reduced pim-1 expression increases chemotherapeutic drug sensitivity in human androgen-independent prostate cancer cells by inducing apoptosis. *Experimental and Therapeutic Medicine*, 2731-2738.
- ZHANG, Y., HOLLENBECK, B. K., SCHROECK, F. R. & JACOBS, B. L. 2014. Managed Care and the Dissemination of Robotic Prostatectomy. *Surgical Innovation*, 21, 566-571.
- ZHANG, Y., JIANG, C., LI, H., LV, F., LI, X., QIAN, X., FU, L., XU, B. & GUO, X. 2015. Elevated Aurora B expression contributes to chemoresistance and poor prognosis in breast cancer. *Int J Clin Exp Pathol*, 8, 751-7.
- ZHANG, Y., LAPIDUS, R. G., LIU, P., CHOI, E. Y., ADEDIRAN, S., HUSSAIN, A., WANG, X., LIU, X. & DAN, H. C. 2016. Targeting I κ B Kinase beta/NF- κ B Signaling in Human Prostate Cancer by a Novel I κ B Kinase beta Inhibitor CmpdA. *Mol Cancer Ther*, 15, 1504-14.
- ZHAO, J., ZHANG, L., MU, X., DOEBELIN, C., NGUYEN, W., WALLACE, C., REAY, D. P., MCGOWAN, S. J., CORBO, L., CLEMENS, P. R., WILSON, G. M., WATKINS, S. C., SOLT, L. A., CAMERON, M. D., HUARD, J., NIEDERNHOFER, L. J., KAMENECKA, T. M. & ROBBINS, P. D. 2018a. Development of novel NEMO-binding domain mimetics for inhibiting IKK/NF- κ B activation. *PLoS Biol*, 16, e2004663.
- ZHAO, J., ZHANG, L., MU, X., DOEBELIN, C., NGUYEN, W., WALLACE, C., REAY, D. P., MCGOWAN, S. J., CORBO, L., CLEMENS, P. R., WILSON, G. M., WATKINS, S. C., SOLT, L. A., CAMERON, M. D., HUARD, J., NIEDERNHOFER, L. J., KAMENECKA, T. M. & ROBBINS, P. D. 2018b. Development of novel NEMO-binding domain mimetics for inhibiting IKK/NF- κ B activation. *PLoS Biology*, 16, 1-27.
- ZHAO, Z. S., LIM, J. P., NG, Y. W., LIM, L. & MANSER, E. 2005. The GIT-associated kinase PAK targets to the centrosome and regulates Aurora-A. *Molecular Cell*, 20, 237-249.
- ZHONG, N., SHI, S., WANG, H., WU, G., WANG, Y., MA, Q., WANG, H., LIU, Y. & WANG, J. 2016. Silencing Aurora-A with siRNA inhibits cell proliferation in human lung adenocarcinoma cells. *Int J Oncol*, 49, 1028-38.
- ZHOU, F., GAO, S., HAN, D., HAN, W., CHEN, S., PATALANO, S., MACOSKA, J. A., HE, H. H. & CAI, C. 2019. TMPRSS2-ERG activates NO-cGMP signaling in prostate cancer cells. *Oncogene*, 38, 4397-4411.
- ZIADA, A., BARQAWI, A., GLODE, L. M., VARELLA-GARCIA, M., CRIGHTON, F., MAJESKI, S., ROSENBLUM, M., KANE, M., CHEN, L. & CRAWFORD, E. D. 2004. The use of

- trastuzumab in the treatment of hormone refractory prostate cancer; phase II trial. *Prostate*, 60, 332-7.
- ZIEGELBAUER, K., GANTNER, F., LUKACS, N. W., BERLIN, A., FUCHIKAMI, K., NIKI, T., SAKAI, K., INBE, H., TAKESHITA, K., ISHIMORI, M., KOMURA, H., MURATA, T., LOWINGER, T. & BACON, K. B. 2005. A selective novel low-molecular-weight inhibitor of I κ B kinase-beta (IKK-beta) prevents pulmonary inflammation and shows broad anti-inflammatory activity. *Br J Pharmacol*, 145, 178-92.
- ZIEVE, G. W., TURNBULL, D., MULLINS, J. M. & MCINTOSH, J. R. 1980. Production of large numbers of mitotic mammalian cells by use of the reversible microtubule inhibitor nocodazole. Nocodazole accumulated mitotic cells. *Exp Cell Res*, 126, 397-405.
- ZORBA, A., NGUYEN, V., KOIDE, A., HOEMBERGER, M., ZHENG, Y., KUTTER, S., KIM, C., KOIDE, S. & KERN, D. 2019. Allosteric modulation of a human protein kinase with monobodies. *Proc Natl Acad Sci U S A*, 116, 13937-13942.
- ZOU, J., HUANG, R. Y., JIANG, F. N., CHEN, D. X., WANG, C., HAN, Z. D., LIANG, Y. X. & ZHONG, W. D. 2018a. Overexpression of TPX2 is associated with progression and prognosis of prostate cancer. *Oncol Lett*, 16, 2823-2832.
- ZOU, Z., YUAN, Z., ZHANG, Q., LONG, Z., CHEN, J., TANG, Z., ZHU, Y., CHEN, S., XU, J., YAN, M., WANG, J. & LIU, Q. 2012. Aurora kinase A inhibition-induced autophagy triggers drug resistance in breast cancer cells. *Autophagy*, 8, 1798-1810.
- ZOU, Z., ZHENG, B., LI, J., LV, X., ZHANG, H., YU, F., KONG, L., LI, Y., YU, M., FANG, L. & LIANG, B. 2018b. TPX2 level correlates with cholangiocarcinoma cell proliferation, apoptosis, and EMT. *Biomed Pharmacother*, 107, 1286-1293.

